RGIA INSTITUTE OF TECHNOLOGY — OFFICE OF CONTRACT ADMINISTRATION

PROJECT ADMINISTRATION DATA SHEET

ISED INFORMATION ONLY ☐ ORIGINAL ☒ REVISION NO. ____

ct No. E-20-605 GTRI/~~GTL~~ DATE 10 / 25 / 84

ct Director: S. N. Atluri School/~~Lab~~ CE

sor: NASA - Lewis Research Center Cleveland, OH

Agreement: Grant No. NAG3-346 Supplements No. 2 and No. 3.

rd Period: From _____ To 10/15/85 (Performance) 10/15/85 (Reports)

sor Amount: This Change Total to Date

Estimated: $ 50,345 $ 170,528

Funded: $ 50,345 $ 170,528

Sharing Amount: $ 11,998 ($29,229 Total to Date) Cost Sharing No: E-20-314

:

INISTRATIVE DATA OCA Contact Dennis Farmer x4820

onsor Technical Contact: 2) Sponsor Admin/Contractual Matters:

nse Priority Rating: _____ Military Security Classification: _____

(or) Company/Industrial Proprietary: _____

TRICTIONS

Attached _____ Supplemental Information Sheet for Additional Requirements.

el: Foreign travel must have prior approval — Contact OCA in each case. Domestic travel requires sponsor approval where total will exceed greater of $500 or 125% of approved proposal budget category.

pment: Title vests with _____

MMENTS:

pplement No. 2 extends completion date to 10/15/84.

pplement No. 3 adds $50,345 in new funds and extends period of performance through 10/15/85.

IES TO:

ct Director
arch Administrative Network
arch Property Management
unting
Procurement/EES Supply Services
Research Security Services
Reports Coordinator (OCA)
Research Communications (2)
GTRI
Library
Project File
Other

GEORGIA INSTITUTE OF TECHNOLOGY
OFFICE OF CONTRACT ADMINISTRATION

NOTICE OF PROJECT CLOSEOUT

Closeout Notice Date 05/02/90

t No. E-20-605 Center No. R5112-2A0

t Director ATLURI S N School/Lab CE

r NASA/LEWIS RESEARCH CTR, OH

ct/Grant No. NAG 3-346 Contract Entity GTRC

Contract No.

GENERALIZED VARIATIONAL PRINCIPES (TOPICS IN ANALY OF INELASTIC BEHAVIOR)

ive Completion Date 851010 (Performance) 851010 (Reports)

---

ut Actions Required:	Y/N	Date Submitted
nal Invoice or Copy of Final Invoice	Y	
nal Report of Inventions and/or Subcontracts	Y	860103
vernment Property Inventory & Related Certificate	Y	
assified Material Certificate	N	
lease and Assignment	N	
her	N	

mments

---

ject Under Main Project No.

ues Project No.

bution Required:

oject Director	Y
ministrative Network Representative	Y
RI Accounting/Grants and Contracts	Y
ocurement/Supply Services	Y
search Property Managment	Y
search Security Services	N
ports Coordinator (OCA)	Y
RC	Y
oject File	Y
her	N
	N

Final Patent Questionnaire sent to PDPI.

Generalized Variational Principles
(Topics in Analysis of Inelastic Behavior of Structures at Elevated Temperature)

A Renewal Research Proposal

Prepared by
Satya N. Atluri
Regents' Professor of Mechanics
Center for the Advancement of Computational Mechanics
Georgia Institute of Technology, Atlanta, Georgia 30332

Abstract:

The original proposal, containing a description of the proposed research during the three-year period 12/82 to 12/85, was submitted in June 1982.

In the following, a brief summary of research accomplishments to date under the current grant is first given. This is followed by a brief description of the research proposed to be undertaken during the period 12/10/83 to 12/9/84, and this forms a part of the overall research originally proposed for the three-year period (and included here as Appendix I).

Research Accomplishments to Date:

Some salient accomplishments to date are briefly summarized:

(i) Stability of Time Integration for Rate-Dependent Inelastic Stress Analysis:

In inelastic stress analysis, it can happen that a small change in the initial condition or time step size leads to a very large change

in the numerical approximation to an otherwise stable mathematical solution of the initial value/boundary value problem. Problems involving materials with a relaxation time (or spectrum of relaxation times) are the most susceptible to such numerical instabilities, so attention has been focused, under the present research grant efforts, on such problems. Since a direct analysis of the present assumed-stress based finite element initial value problem is more intractable, attention has been focused on the related initial-value problem:

$$\dot{\underset{\sim}{\sigma}}^{*} = \underset{\approx}{\nu}:\underset{\sim}{\varepsilon} + \underset{\sim}{\Sigma} \quad ; \quad \underset{\sim}{\tau}(o) = \underset{\sim}{\tau}_{o} \tag{1}$$

where $\dot{\underset{\sim}{\sigma}}^{*}$ is the co-rotational stress-rate, $\underset{\sim}{\varepsilon}$ the strain rate, and $\underset{\sim}{\Sigma}$ the contribution due to inelasticity; $\underset{\approx}{\nu}$ and $\underset{\sim}{\Sigma}$ depend on time. It has been shown [1] that the time step (h) in an Euler scheme must be chosen so that:

$$\left| (1 - h\dot{J}) + h\rho\left\{\partial_{\underset{\sim}{\tau}}(\underset{\approx}{\nu}:\underset{\sim}{\varepsilon} + \underset{\sim}{\Sigma}) \Big|_{\underset{\sim}{\tau} = \underset{\sim}{\tau}_{N}}\right\}\right| \leq 1 \tag{2}$$

where $\dot{J} = \mathrm{tr}\underset{\sim}{\varepsilon}$. The time-step bound in (2) is rather stringent. As a means of improving these bounds, several linear finite approximation schemes have been explored. One of these consists in replacing the term $\underset{\sim}{\Sigma}$ in (1) by $\underset{\sim}{\Sigma} + \theta h(\partial_{\underset{\sim}{\tau}}\underset{\sim}{\Sigma}):\dot{\underset{\sim}{\sigma}}^{*}$ to obtain:

$$\dot{\underset{\sim}{\sigma}}^{*} = [\underset{\sim}{I} - \theta h\partial_{\underset{\sim}{\tau}}\underset{\sim}{\Sigma}]^{-1}:(\underset{\approx}{\nu}:\underset{\sim}{\varepsilon} + \underset{\sim}{\Sigma}) \tag{3}$$

where $0 < \theta < 1$. An interesting effect of this scheme has been found to be to lengthen all of the characteristic times so that the time step exceeds the least of them by no more than a factor of $(1/\theta)$. Other linear finite approximations have been explored by introducing the notion of inelastic stretching, $\underset{\sim}{\varepsilon}^{i} = -\underset{\approx}{v}^{-1}:\underset{\sim}{\varepsilon}$ and by introducing the intermediate stress $\underset{\sim}{\tau}_{\theta}$ defined by:

$$\underset{\sim}{\tau}_{\theta} = (1 - \theta)\underset{\sim}{\tau}_{N} + \theta\underset{\sim}{\tau}_{N+1} \tag{4}$$

It is assumed that a function $\underset{\sim}{g}(\underset{\sim}{\tau})$ may be defined such that $\underset{\sim}{\varepsilon}^{i} = \underset{\approx}{g}:\underset{\sim}{\tau}$, and write $\underset{\approx}{G}$ for $\partial_{\underset{\sim}{\tau}}\underset{\sim}{\varepsilon}^{i}$, $\underset{\approx}{g}_{\theta} = \underset{\approx}{g}(\underset{\sim}{\tau}_{\theta})$, and $\underset{\sim}{G}_{\theta} = \underset{\approx}{G}(\underset{\sim}{\tau}_{\theta})$. In the schemes to improve stability, $\underset{\approx}{V}$ has been replaced by:

$$\underset{\approx}{V}'_{\theta} \equiv [\underset{\approx}{V}^{-1} + \theta h \underset{\approx}{G}_{\theta}]^{-1} = [\underset{\approx}{I} + \theta h \underset{\approx}{V}:\underset{\approx}{G}_{\theta}]^{-1}:\underset{\approx}{V} \tag{5}$$

or $$\underset{\approx}{V}''_{\theta} = [\underset{\approx}{I} + \theta h \underset{\approx}{V}:\underset{\approx}{g}_{\theta}] \tag{6}$$

The results of these stability investigations have been discussed, along with numerical illustrations, in [1-3], for finite as well as infinitesimal deformation inelastic stress analysis.

(ii) Objectivity of Numerical Integration of Inelastic Initial Value Problems

In order to be called objective, a numerically integrated physical entity, such as stress, must transform between frames according

to the same rule as the entity itself. An algorithm which produces an objective approximation will itself be called objective. Research has been focused in algorithms for numerical integration of inelastic initial value problems which produce objective approximations, and significant results have been obtained, as reported in detail in [2,4].

The general results on objective numerical integration given in [2,4] apply to tensors of all orders of physical interest, such as displacement, strain, and stress. Consider, for instance, the stress in an inleastic problem. It is well-known that the material rate of stress is an non-objective quantity. According to the algorithms presented in [2,4], the true stress at any time t in the inelastic solid is given by:

$$\underset{\sim}{\tau}(t) = J_{\tau}^{-1}\underset{\sim}{Q}^{T}(t)\cdot\underset{\sim}{\tau}(t)\cdot\underset{\sim}{Q}(t) + \int_{\tau}^{t} J_{t}(\zeta)\underset{\sim}{Q}^{T}(t)\cdot\underset{\sim}{Q}(\zeta)\cdot\dot{\underset{\sim}{\sigma}}^{*}(\zeta)\cdot\underset{\sim}{Q}^{T}(\zeta)\cdot\underset{\sim}{Q}(t)\,d\zeta \tag{7}$$

where $\dot{\underset{\sim}{\sigma}}^{*}$ is the objective co-rotational rate of stress, and $\underset{\sim}{Q}(t)$ is defined as the solution of

$$\dot{\underset{\sim}{Q}}(t) = -\underset{\sim}{Q}(t)\cdot\underset{\sim}{\omega}(t) \quad \underset{\sim}{Q}(\tau) = \underset{\sim}{I} \tag{8}$$

Eq. (7) is numerically approximated as:

$$\underset{\sim}{\tau}_{N+1} = J_{N}^{-1}(t_{N+1})\underset{\sim}{Q}^{T}(t_{N+1})\cdot\underset{\sim}{\tau}_{N}\cdot\underset{\sim}{Q}(t_{N+1})$$

$$+ hJ_{N+1}(t_{N} + \theta)\underset{\sim}{Q}^{T}(t_{N+1})\cdot\underset{\sim}{Q}(t_{N+\theta})\cdot\underset{\sim}{\sigma}^{*}_{N+\theta}\cdot\underset{\sim}{Q}^{T}(t_{N+\theta})\cdot\underset{\sim}{Q}(t_{N+1}) \tag{9}$$

An exact representation for $Q(t_{N+\theta})$, i.e., the solution of Eq. (8), has also been derived [2,4]. The above algorithm has been demonstrated to be very efficient in a large set of numerical examples [1,3,5].

(iii) Constitutive Modeling in Anisotropic Hardening Plasticity:

The question of generalization to finite deformations of the constitutive relations of classical infinitesimal strain theories of elasticity and classical elastoplasticity with isotropic or anisotropic (kinematic) hardening plasticity, has been critically examined. Valid generalizations which lead to physically plausible metallic behavior are presented [6,7]. A significant contribution has been that the current controversies in literature surrounding (i) the choice of stress-rate in the above mentioned generalizations and (ii) the anamoly of oscillatory shear stresses in kinematic hardening plasticity in simple finite shear (that have been presented by several authors) have been resolved. Nagtegaal et al. [Nagtegaal, J. C. and de Jong, J. E., "Some Aspects of Non-Isotropic Workhardening in Finite Strain Plasticity" in Plasticity of Metals at Finite Strain: Theory, Experiment, and Computation (Eds. E. H. Lee et al.), Div. of Appl. Mech., Stanford Univ., pp. 65-102, 1982] first presented the interesting but spurious result that the computed shear stress in simple finite shear is oscillatory in the case of elastic-plastic and rigid-plastic materials which exhibit anisotropic hardening. In the equation for the rate of change of the back-stress (the current center of the yield surface), they used the Zaremba-Jaumann-Noll rigid body rate of $\underset{\sim}{\alpha}$. The above anamoly has prompted a series of

investigations by Lee and colleagues [E. H. Lee and T. B. Wertheimer, "Deformation Analysis of Simple Shear with Anisotropic Hardening in Finite-Deformation Plasticity" in Computer Methods for Nonlinear Solids and Structural Mechanics (Eds. S. N. Atluri et al.), ASME, pp. 145-155, 1983] who suggested that a complete investigation of the micro-mechanics and the structure of possible macroscopic relations is needed to fully understand this phenomenon. It turns out [6,7] that the anamolies as described above are not peculiar to the anisotropic plasticity alone; similar behavior in finite shear may result even in the case of hypoelasticity and classical isotropic-hardening plasticity theory. In [6,7], a generalized objective stress rate was introduced as:

$$\overset{\cdot}{\underset{\sim}{\sigma}}{}^{*} = \overset{\cdot}{\underset{\sim}{\sigma}}{}^{o} - \gamma_7(\underset{\sim}{\sigma}\cdot\underset{\sim}{\varepsilon}) - \gamma_8(\underset{\sim}{\varepsilon}\cdot\underset{\sim}{\sigma}) \tag{10}$$

where γ_7 and γ_8 are constants. A similar rate was defined for α^o. A significant conclusion in [6,7] was that with the use of these generalized rates, no anamolies arise in any of the constitutive models: hypoelasticity, isotropic hardening rigid plasticity, isotropic hardening elasto-plasticity, or in anisotropic hardening plasticity.

Research is in progress to correctly formulate constitutive models for rate-sensitive inelastic materials (viscoplastic and creep) at finite deformations along lines similar to those in [6,7] for rate-insensitive plasticity.

(iv) Least-Order, Stable, Invariant Stress-Based Finite Elements:

Typical polynomial shape functions employed in the standard isoparametric displacement elements, of the Serendipity or Legendre type, are incomplete and contain parasitic terms in the Pascal triangle representation and lead to deficiencies in stress-states. Consequently, displacement elements are almost always too stiff. While the currently popular artifact of reduced integration sometimes makes these elements flexible, concurrently it introduces the so-called kinematic modes. Consequently, stress-based elements potentially offer greater versatility in three-dimensional analysis of turbine structural components, especially under time varying initial strain fields. In developing such stress-based elements, several criteria must be borne in mind: (i) the cardinal stress states of pure tension, shear, bending, and torsion should be present in the element so that the element can pass the usual as well as higher-order patch tests; (ii) the element should be invariant with respect to the coordinates used in the development of stiffness matrix, etc.; (iii) the element should not have any kinematic mechanisms nor should it develop strains under rigid body translations and rotations; (iv) the element should be robust and preferably be least sensitive to distortion i.e., the aspect ratio of the element size; (v) for economy in element development, the element should give accurate results with the least number of stress polynomials; and (vi) the disparity between the actual stiffness behavior and the computed element stiffness coefficients should be as small as possible without resort to heuristic or arbitrary numerical techniques. Such elements have been named [8] as least-order, stable, invariant, stress-based elements.

Significant strides have been made [8] in the recent months in the use of symmetry group theoretical methods in establishing a range of optimal least-order, stable, invariant stress-spaces for use both in the context of hybrid as well as mixed formulations. Families of both two- and three- dimensional stress-based elements have been developed and tested. In all the cases, the results [8] have been found to be much superior in comparison to the usual displacement elements in terms of accuracy of computed displacements and stresses, robustness, convergence, and distortion sensitivity. Work is in progress in exploiting these concepts in the context of plate and shell elements.

(v) Criteria for Creep Crack-Growth

In Refs. [9,10,11], a new parameter $(\dot{T})_c$, which is a path-independent incremental integral, was introduced as a criterion for the study of creep crack growth in structures operating at elevated temperatures. This parameter was: (i) a measure of crack-tip stress-strain fields; (ii) valid for arbitrary constitutive properties of the materials such as steady-state as well as unsteady creep, elasto-plasticity, viscoplasticity, etc.; and (iii) valid for arbitrary load histories.

In recent months several interesting and novel results have been established [12,13] which are concerned with the possible experimental measurement of the above new path-independent integral. Firstly, it is difficult to measure data near the crack-tip. Experimental measurements are easier to be made at the external boundary of the specimen. Thus, another path-independent integral $(\dot{T})_p$ is created such

that

$$(\dot{T})_p = \int_S -\left\{\Delta t_i\left(\frac{\partial u_i}{\partial x_1} + \tfrac{1}{2}\frac{\partial \Delta u_i}{\partial x_1}\right) + \left(\frac{\partial t_i}{\partial x_1} + \tfrac{1}{2}\frac{\partial \Delta t_i}{\partial x_i}\right)\Delta u_i\right\} ds \tag{11.a}$$

$$= \int_{\Gamma+S_{c\Gamma}} -\left\{\Delta t_i\left(\frac{\partial u_i}{\partial x_1} + \tfrac{1}{2}\frac{\partial \Delta u_i}{\partial x_1}\right) + \left(\frac{\partial t_i}{\partial x_1} + \tfrac{1}{2}\frac{\partial \Delta t_i}{\partial x_1}\right)\Delta u_i\right\} ds$$

$$+ \int_{V-V_\Gamma} [(\sigma_{ij,1} + \tfrac{1}{2}\Delta\sigma_{ij,1})\Delta\varepsilon_{ij} - (\varepsilon_{ij,1} + \tfrac{1}{2}\Delta\varepsilon_{ij,1})\Delta\sigma_{ij}]dv \tag{11.b}$$

$$= \int_{\Gamma+S_{c\Gamma}} \left\{\Delta W n_1 - (t_i + \Delta t_i)\frac{\partial \Delta u_i}{\partial x_i} - \Delta t_i \frac{\partial u_i}{\partial x_i}\right\} ds$$

$$+ \int_{V-V_\Gamma} [(\sigma_{ij,1} + \tfrac{1}{2}\Delta\sigma_{ij,1})\Delta\varepsilon_{ij} - (\varepsilon_{ij,1} + \tfrac{1}{2}\Delta\varepsilon_{ij,1})\Delta\sigma_{ij}]dv \tag{11.c}$$

In the above, S is the external boundary of the cracked body, Γ is any internal contour enclosing the crack-tip, $S_{c\Gamma}$ is the crack surface enclosed by Γ, V is the total volume of the cracked body, and V_Γ is the volume enclosed by Γ. The definition of $(\dot{T})_p$ as in (11.a) makes it convenient to be measured on a test specimen since it involves only data at the external boundary of the specimen. Note that Eq. (11) is valid for creep-brittle as well as creep-ductile materials in general.

Extensive work is underway to test the validity of the above new parameter, by simulating available experimental data on creep crack growth. Some of the above results are documented in preliminary reports [12,13].

All the above studies in (i) to (v) lead to the following Ph.D

dissertations and archival publications:

(a) Ph.D Theses:

(1) Brust, F. W., "Further Studies on Stable Crack Growth in Elastic-Plastic and Creeping Materials" under preparation, to be finished in September 1984.

(2) Punch, E. F., "Stable, Invariant, Least-Order Isoparametric Mixed-Hybrid Stress Elements: Linear Elastic Continua, and Finitely Deformed Plates and Shells", August 1983.

(3) Reed, K. W., "Analysis of Large Quasi-Static Deformations of Inelastic Solids by a New Stress-Based Finite Element Method", April 1982.

(4) Stonesifer, R. B., "Creep Crack Growth, Moving Singularity Finite Element Analysis", December 1981.

(b) Publications:

[1] Reed, K. W. and Atluri, S. N., "Inelastic Stress Analysis at Finite Deformation Through Complementary Energy Approaches" in Computer Methods for Nonlinear Solids and Structural Mechanics (Eds.: S. N. Atluri and N. Perrone), ASME-AMD Vol. 54, pp. 191-227, 1983.

[2] Reed, K. W. and Atluri, S. N., "Analysis of Large Quasi-Static Deformations of Inelastic Bodies by a New Hybrid Stress Finite Element Algorithm", Computer Methods in Applied Mechanics and Engineering , 1983 (In Press).

[3] Reed, K. W. and Atluri, S. N., "Analysis of Large Quasi-Static Deformations of Inelastic Bodies by a New Hybrid Stress Finite Element Algorithm: Applications", Computer Methods in Applied Mechanics and Engineering , 1983 (In Press).

[4] Atluri, S. N., "Inelastic and Dynamic Fracture and Stress Analyses", Proc. NASA University-Industry Workshop, NASA Lewis Research Center, 19-20 April 1983.

[5] Reed, K. W. and Atluri, S. N., "Hybrid Stress Finite Elements for Large Deformations of Inelastic Solids", Computers and Structures (Professor K. Washizu Memorial Issue), 1983 (In Press).

[6] Atluri, S. N., "On Constitutive Relations at Finite Strain: Hypo-elasticity and Elasto-plasticity with Isotropic and Kinematic Hardening", Computer Methods in Applied Mechanics and Engineering , 1983 (In Press).

[7] Reed, K. W. and Atluri, S. N., "On the Generalization of Certain

Rate-Type Constitutive Equations for Very Large Strains" in Constitutive Laws for Engineering Materials: Theory and Application (Eds.: C. S. Desai and R. H. Gallagher), pp. 71-77, 1983.

[8] Punch, E. F. and Atluri, S. N., "Development and Testing of Least-Order, Stable, Invariant 2- and 3-D Mixed-Hybrid Stress Elements", Computer Methods in Applied Mechanics and Engineering (being submitted), 1983.

[9] Stonesifer, R. B. and Atluri, S. N., "On a Study of the $(\Delta T)_C$ and C* Integrals for Fracture Analysis Under Non-Steady Creep", Engineering Fracture Mechanics , Vol. 16, 5, pp. 625-643, 1982.

[10] Stonesifer, R. B. and Atluri, S. N., "Moving Singularity Creep Crack Growth Analysis with the $(\Delta T)_C$ and C* Integrals", Engineering Fracture Mechanics , Vol. 16, 6, pp. 769-782, 1982.

[11] Atluri, S. N., "Path-Independent Integrals in Finite Elasticity and Inelasticity, with Body Forces, Inertia, and Arbitrary Crack-Face Conditions", Engineering Fracture Mechanics , Vol. 16, 2, pp. 341-364, 1982.

[12] Atluri, S. N., "Recent Developments in Energy Integrals and Their Application", Plenary Lecture, to be delivered at the 6th International Congress on Fracture , 1984, India.

[13] Atluri, S. N., "Energy Approaches in Inelastic Fracture", Chapter in Computational Methods in the Mechanics of Fracture (Ed.: S. N. Atluri), North-Holland Press, to appear.

[14] Reed, K. W., Stonesifer, R. B., and Atluri, S. N., "Stress and Fracture Analyses Under Elastic-Plastic and Creep Conditions: Some Basic Developments and Computational Approaches" in Nonlinear Constitute Relations for High Temperature Applications (Proc. Symp. at University of Akron, 19-20 May 1982), 62 pages.

[15] Stonesifer, R. B. and Atluri, S. N., "Creep Crack-Growth: A New Path-Independent Integral $(\dot{T})_C$ and Computational Studies", NASA-CR-167897, 1982, 109 pages.

[16] Reed, K. W. and Atluri, S. N., "Visco-Plasticity and Creep: A Finite Deformation Analysis Using Stress-Based Finite Elements" in Advances in Aerospace Structures and Materials (Eds.: S. S. Wang et al.), ASME-AMD-01, 1981, pp. 211-221.

Brief Description of Proposed Research (12/10/83-12/9/84):

Continuation of research is proposed in the following areas:

CONSTITUTIVE MODELING OF CYCLIC PLASTICITY AND CREEP, USING AN INTERNAL TIME CONCEPT

O. Watanabe and S. N. Atluri

Center for the Advancement of Computational Mechanics
School of Civil Engineering
Georgia Institute of Technology, Atlanta, Georgia 30332

April 1984

CONSTITUTIVE MODELING OF CYCLIC PLASTICITY AND CREEP, USING AN INTERNAL TIME CONCEPT

O. Watanabe and S. N. Atluri

Center for the Advancement of Computational Mechanics
School of Civil Engineering
Georgia Institute of Technology, Atlanta, Georgia 30332

Abstract:

Based on the concept of an intrinsic time, a differential stress-strain relation for plasticity, which is similar in structure to that of classical plasticity but which possesses certain advantages in describing cyclic plasticity, is derived. Its implementation in computational algorithms is shown to be standard. A new constitutive model for creep and its interaction with plasticity is derived by assuming that the internal time measure is related to both inelastic strain history as well as Newtonian time. The problem of modeling experimental data for plasticity and creep by the present analytical relations, as accurately as possible, is discussed. It is demonstrated that the present constitutive relations for plasticity and creep are simple in form, and the material constants are few in number. Numerical examples, which illustrate the validity of the present differential relations, are presented for the cases of cylic plasticity and creep.

1. Introduction:

The characterization of material behavior at elevated temperatures plays an important role in the design of structures such as in hot-sections of modern jet engines and other power plants. The ASME Code [1] defines acceptable levels of stress and strain in critical components of power plants operating at elevated temperatures. The sevère mechanical environment may

often cause these structures to operate near or beyond the yield limit of the material. Consequently, a unified theory of creep and plasticity, applicable to cyclic loading, is often desirable.

Typical constitutive relations for creep reported and used in literature include: the modified strain hardening rule developed by researchers at the Oak Ridge National Lab [2,3]; dislocation models [4,5] based on metal physics; nonlinear viscoelasticity theory [6]; and the kinematic hardening model [7] using an analogy to plasticity. However, recent efforts in material-constitutive-model development reveal a trend toward unifying creep and plasticity. Some experimental results [3,8] have been reported concerning the interaction between creep and plasticity. These unifying theories may be roughly divided into the three categories of: (i) potential theories, (ii) micro phenomenological theories, and (iii) nonlinear viscoplastic theories. Most studies employ these theories either individually or in combination. In the first category, one may cite the theories using time-dependent parameters [9], the concept of kinematic hardening [10], micromechanical considerations [11], and a combination of viscoplastic theory [12]. The phenomenological theories [13-22] employ certain internal variables to reflect the micromechanics of deformation, such as involving dislocations. Most of these theories assume that the plastic strains are also time-dependent, as are creep strains, and that the creep surface will translate and expand in the stress-space in a manner similar to that of isotropic and kinematic hardening used in classical plasticity theory. The nonlinear viscoplasticity theories have the variations, in which: the coefficients of the linear viscoelastic theory [23] are expressed as a function of stresses and strains, the inelastic strains are divided into viscous and viscoelastic components [24], and the internal time is measured by the strain history [25-32]. Of course, the fundamental aspects of inelastic deformations are also studied [33-35] based on micromechanical

considerations.

The intrinsic time theory, labeled "the endochronic theory" was presented by Valanis [25-26] in 1971. This theory held out the prospect of explaining the experimental phenomena of cross-hardening, cyclic hardening, and initial strain problems -- the situations that classical plasticity theory could not cope with. Bazant [27] also showed that the 'endochronic' theory is effective in dealing with problems of inelasticity and failure in concrete, and that the Maxwell chain model can describe the creep behavior.

In 1980 Valanis [29] presented a new intrinsic time model, in which the internal time is related to the inelastic strain, and which rectified some of the stortcomings of his earlier theory. Later, Valanis and Fan [32] presented an incremental or differential form of the integral relation of stress and strain [29] for plasticity. This differential relation [32] is of a fundamentally different form compared to that of classical plasticity. In Ref. [32], an "initial strain" type of iterative finite element approach was developed to study certain two-dimensional problems of cyclic plasticity. Thus, the computational implementation of the differential relation in [32] is non-standard, in that a "tangent stiffness" finite element formulation is not possible.

In this paper, we present an alternative derivation of the differential stress-strain relation for plasticity, based on the concept of an intrinsic time dependent upon plastic strains [29]. This relation is essentially similar in its structure to that of classical plasticity, thus leading to a convenient computational implementation in an initial stress or a tangent stiffness type of finite element formulation. However, the present relation will be shown to have several novel advantages over the classical plasticity theory, in representing cyclic plastic behavior, etc. The details of

analytically modeling the test data, for monotonic or cyclic plasticity, as accurately as possible through the presently developed relations, are discussed.

This paper also presents a new and simple theory for creep using the concept of intrinsic time. This theory assumes that the intrinsic time is measured by inelastic strain as well as Newtonian time, both of which are irreversible. Further, the present theory makes it possible to incorporate the effect of interaction between creep and plasticity in a simple fashion.

Numerical results are presented for cyclic plasticity and creep, in order to verify the validity of the present theories. It is shown that the present constitutive relations are simple in form, and the material constants involved are few in number. Thus, they may be useful in practical analyses of inelastic behavior.

In Section 2, we present the nomenclature; Section 3 contains theoretical developments for plasticity based on an intrinsic time measure; Section 4 contains discussion of the issues related to the determination of material constants, characterization of monotonic and cyclic hardening plasticity, and certain pertinent numerical results; and Section 5 contains a unified theory for creep and plasticity and pertinent numerical results.

2. Nomenclature:

Considerations in the present work are restricted to small strains and infinitesimal deformations. For simplicity, we use a cartesian system of coordinates x_i, with basis $\underline{e}_i$. The stress and strain tensors are represented by $\underset{\sim}{\sigma} = \sigma_{ij}\underline{e}_i\underline{e}_j$ and $\underset{\sim}{\varepsilon} = \varepsilon_{ij}\underline{e}_i\underline{e}_j$, respectively. The stress and strain deviators are represented by $\underset{\sim}{S} = S_{ij}\underline{e}_i\underline{e}_j$, and $\underset{\sim}{e} = e_{ij}\underline{e}_i\underline{e}_j$, respectively. If $\underset{\sim}{A}(A_{ij}\underline{e}_i\underline{e}_j)$ and $\underset{\sim}{B}(B_{mn}\underline{e}_m\underline{e}_n)$ are two second-order tensors, the notation: $\underset{\sim}{A}\cdot\underset{\sim}{B} = A_{im}B_{mn}\underline{e}_i\underline{e}_n$ and $\underset{\sim}{A}:\underset{\sim}{B} = A_{ij}B_{ij}$ is employed.

3. Plasticity: Theoretical Development:

In 1980 Valanis [29] proposed a modification to his earlier 'endochronic' theory, wherein the intrinsic time was redefined to be related to the inelastic strain. In this section, we concern ourselves mainly with the functinal aspects of this theory, and not so much as its thermodynamic foundations. The main purpose here is to rederive a specific form of the differential stress-strain relations for plasticity, that arises out of this theory, which may be more amenable to numerical implementation in, say, the finite element or boundary element methods. It is also our aim to demonstrate that, when the presently derived differential stress-strain relation is used, it has certin advantages over classical elasto-plastic theories. Thus, recent criticisms [36] of certain aspects of the earlier versions of Valanis' work notwithstanding, the present paper points to certain special features of the presently derived elastic-plastic constitutive laws in modeling observed phenomena in cyclic plasticity of metals, better than classical elasto-plastic constitutive relations.

Henceforth, we restrict ourselves to small deformations and small strains. Let $d\underset{\sim}{\varepsilon}$, the differential strain, be decomposed into:

$$d\underset{\sim}{\varepsilon} = d\underset{\sim}{\varepsilon}^{e} + d\underset{\sim}{\varepsilon}^{p} \tag{3.1}$$

where the superscripts (e) and (p) denote 'elastic' and 'plastic' components, respectively. As in the classical pressure-insensitive plasticity, we assume that the 'deviatoric' and 'mean' parts of stress and strain rates can be treated separately. We write:

$$d\underset{\sim}{\varepsilon} = d\underset{\sim}{e} + d\varepsilon_{m}\underset{\sim}{I} \equiv (d\underset{\sim}{e}^{e} + d\underset{\sim}{e}^{p}) + \underset{\sim}{I}(d\varepsilon_{m}^{e} + d\varepsilon_{m}^{p}) \tag{3.2a}$$

$$d\underset{\sim}{\sigma} = d\underset{\sim}{S} + d\sigma_m \underset{\sim}{I} \tag{3.2b}$$

where ($d\underset{\sim}{e}$ and $d\underset{\sim}{S}$) denote the deviatoric and ($d\varepsilon_m$ and $d\sigma_m$) denote the mean parts of tensors ($d\underset{\sim}{\varepsilon}$ and $d\underset{\sim}{\sigma}$) [note that $d\varepsilon_m = (d\underset{\sim}{\varepsilon}:\underset{\sim}{I})/3$; $d\sigma_m = (d\underset{\sim}{\sigma}:\underset{\sim}{I})/3$]. We assume that $d\varepsilon_m^p = 0$, and hence $d\varepsilon_m \equiv d\varepsilon_m^e$. Following Valanis [29] we define an inelastic-strain-rate-like tensor $d\underset{\sim}{\eta}$ such that:

$$d\underset{\sim}{\eta} = d\underset{\sim}{e} - \frac{\alpha}{2\mu_o} d\underset{\sim}{S} \tag{3.3}$$

where μ_o is the elastic shear modulus and α is a positive scalar such that $0 \leqslant \alpha \leqslant 1$. When $\alpha = 1$, since (for materials that are isotropic in the elastic range)

$$\frac{d\underset{\sim}{S}}{2\mu_o} = d\underset{\sim}{e}^e \tag{3.4}$$

one has,

$$d\underset{\sim}{\eta} \equiv d\underset{\sim}{e}^p \tag{3.5}$$

Henceforth in this paper, we set $\alpha = 1$.

As in [29] we define an intrinsic time measure ζ through the equation:

$$d\zeta = \|d\underset{\sim}{e}^p\| = (d\underset{\sim}{e}^p : d\underset{\sim}{e}^p)^{\frac{1}{2}} = (de_{ij}^p de_{ij}^p)^{\frac{1}{2}} \tag{3.6}$$

Note that $d\zeta$ and hence ζ, like Newtonian time t, are irreversible and non-negative. The differential intrinsic time, dz, is defined as:

$$dz = \frac{d\zeta}{f(\zeta)} \tag{3.7}$$

where $f(\zeta)$ is non-negative and $f(o) = 1$.

With the above definitions of an internal time z, the concept of the "endochonic" theory [25,26] leads to the following integral representations for the deviatoric and mean components of stress:*

$$\underset{\sim}{S} = 2\mu(z)\underset{\sim}{e}^{e}(o) + 2\int_{o}^{z}\mu(z - z')\,\frac{d\underset{\sim}{e}}{dz'}\,dz' \tag{3.8a}$$

and

$$\sigma_m = 3\,K(z)\varepsilon_m^{e}(o) + 3\int_{o}^{z}K(z-z')\,\frac{d\varepsilon_m}{dz'}\,dz' \tag{3.8b}$$

Note that z is related now to <u>inelastic</u> strain; hence at z = 0, $\underset{\sim}{e}(o) = \underset{\sim}{e}^{e}(o)$ and $\varepsilon_m = \varepsilon_m^{e}(o)$ where $\underset{\sim}{e}^{e}(o)$ and $\underset{\sim}{\varepsilon}_m^{e}(o)$ are the deviatoric and mean components of strain at the <u>elastic limit</u>.

Purely elastic hydro-static response implies that $K(z) = K_o H(z)$ where H(z) is a Heaviside step function. On the other hand, a <u>constant Poisson's ratio</u> implies that $K(z) = K_o G(z)$; and $\mu(z) = \mu_o G(z)$ with the definition that G(o) = 1.

Letting $\mu(z) = \mu_o G(z)$ and using Laplace transforms and (3.3 - 3.5), one may rewrite (3.8a) as:

$$\underset{\sim}{S} = 2\mu_o \int_{o}^{z}\rho(z - z')\,\frac{\partial \underset{\sim}{e}^{p}}{\partial z'}\,dz' \tag{3.9}$$

where $\rho(z)$ is the solution of the integral equation:

$$\rho(z) - \int_{o}^{z}\rho(z - z')\,\frac{\partial G}{\partial z'}\,dz' = G(z) \tag{3.10a}$$

---

* These are slightly different from Eqs. (2.8) and (2.9) of Ref. [29], in that the initial conditions at z = 0 are accounted for in the present Eqs. (3.8a,b).

or in the transform domain,

$$\overline{\rho} - \overline{\rho}\,\overline{G}\,p = \overline{G} \tag{3.10b}$$

where p is the Laplace variable, and $(\bar{\ })$ indicates a Laplace transform of ( ).

Assuming a constant Poison's ratio [which implies that K(z) may also be written as $K_o G(z)$] and defining Young's modulus, E_o, to be

$$E_o = (9\,\mu_o\,K_o) \div [3K_o + \mu_o] \ , \tag{3.11}$$

one may derive a uniaxial stress-strain relation (with only $\sigma_{11} \neq 0$; but $\varepsilon_{11} \neq 0$, $\varepsilon_{22} \neq 0$, $\varepsilon_{33} \neq 0$) from (3.8a) and (3.8b), to be:

$$\sigma_{11} = E_o \int_o^z G(z - z')\,\frac{\partial\,\varepsilon_{11}}{\partial z'}\,dz' \tag{3.12a}$$

$$\equiv E_o \int_o^z \rho(z - z')\,\frac{\partial\,\varepsilon^p_{11}}{\partial z'}\,dz' \tag{3.12b}$$

where $\rho(z)$ is as defined in (3.10). Note that in the uniaxial-tension case,

$$d\varepsilon^p_{11} = d\varepsilon_{11} - \frac{d\sigma_{11}}{E_o} \ ; \ de^p_{11} = de_{11} - \frac{d\sigma_{11}}{3\mu_o} \tag{3.13a,b}$$

and $$d\varepsilon_m = (d\sigma_{11}/9K_o) \ . \tag{3.13c}$$

On the other hand, if one assumes a purely elastic hydrostatic response, i.e. instead of $K(z) = K_o G(z)$, one takes $K(z) = K(o)H(z)$, the resulting expression for the σ_{11} vs. ε^p_{11} relation would be quite complex and different from (3.12). However, Eq. (3.12) was used, as an approximation, by Wu & Yip in their studies [30,31] of strain-response under uniaxial tension for materials with an entirely-elastic hydrostatic response.

By considering the derivative of Eq. (3.9) with respect to z, Valanis and Fan [32] recently stated the "rate" or "differential" form of the stress-

strain relation to be:

$$\frac{d\underset{\sim}{S}}{dz} = 2\mu_o\ \rho(o)\ \frac{d\underset{\sim}{e}^p}{dz} + 2\mu_o \int_o^z \frac{d\rho}{dz}\ (z - z')\ \frac{\partial \underset{\sim}{e}^p}{\partial z'}\ dz' \tag{3.14}$$

or $$d\underset{\sim}{S} = 2\mu_o[\rho(o)d\underset{\sim}{e}^p + \underset{\sim}{h}(z)\ dz] \tag{3.15}$$

where $$\rho\ (o) = \rho[z = 0]\ ;\ \underset{\sim}{h} = \int_o^z \frac{\partial \rho}{\partial z}\ (z - z')\frac{\partial \underset{\sim}{e}^p}{\partial z'}\ dz' \tag{3.16a,b}$$

Using (3.6 and.7), one may write (3.15) as:

$$d\underset{\sim}{S} = 2\mu_o \left[\rho(o)d\underset{\sim}{e}^p + h(z)\ \frac{(d\underset{\sim}{e}^p : d\underset{\sim}{e}^p)^{\frac{1}{2}}}{f(\zeta)}\right] \tag{3.17}$$

Using (3.15) [or equivalently (3.17)], Valanis and Fan [32] proceed to develop "initial-strain" type iterative finite element algorithms for solving the rate problem of cyclic plasticity. In their development [32], Valanis and Fan point out that the chosen material function $\rho(z)$ should be weakly singular* at $z = 0$ in order: (i) to obtain closed hysteresis loops in the uniaxial or shear stress-strain space; (ii) to ensure initially elastic unloading.

In the following, we derive an alternate form of the rate type stress-strain relation based on the presently sketched intrinsic time concept. This alternate form may be more easy to implement in a numerical algorithm and, in its essential structure, is very similar to the classical elasto-plasticity theory.

We assume the dependence of the shear modulus on intrinsic time to be of the form:

---

* It is not clear, however, that the three term approximation of $\rho(z)$ [Eq. (3.3) of [32]] that is used in [32] possesses this 'singular' property in an exact sense.

$$G(z) = \sum_{r=1}^{N} G_r \exp(-\alpha_r z) \tag{3.18}$$

The corresponding solution for $\rho(z)$ may be obtained using (3.10) (as shown in [29]) to be:

$$\rho(z) = \rho_0 \delta(z) + \rho_1(z) \tag{3.19}$$

where $\delta(z)$ is a Dirac delta function at $z = 0$, and ρ_0 is the "strength" of this weak singularity in $\rho(z)$ at $z = 0$, and $\rho_1(z)$ is a well-behaved function.

Using (3.19) in (3.9), we obtain:

$$\underset{\sim}{S} = 2\mu_o \rho_o \frac{d\underset{\sim}{e}^p}{dz} + 2\mu_o \int_0^z \rho_1(z - z') \frac{d\underset{\sim}{e}^p}{dz'} \, dz' \tag{3.20}$$

$$= S_y^o \frac{d\underset{\sim}{e}^p}{dz} + \underset{\sim}{r}(z) \tag{3.21}$$

where, by definition,

$$S_y^o = 2\mu_o \rho_o \; ; \quad \underset{\sim}{r} = 2\mu_o \int_0^z \rho_1(z - z') \frac{d\underset{\sim}{e}^p}{dz'} \, dz' \tag{3.22a,b}$$

From (3.21 and .22b) it may be seen that the function $\rho_1(z)$ now characterizes the translation of the yield surface in the stress-space.

We now use (3.21) to derive an alternate form of incremental stress-strain relation. Folowing [29] we may characterize the regions of material behavior as:

(i) if $\|\underset{\sim}{S} - \underset{\sim}{r}\| < S_y^o f(\zeta)$, the material is elastic (3.23a)

(ii) if $\|\underset{\sim}{S} - \underset{\sim}{r}\| = S_y^o f(\zeta)$ and

$(\underset{\sim}{S} - \underset{\sim}{r})$: $d\underset{\sim}{e} \leqslant 0$, then again the material is elastic (3.23b)

(iii) if $\|\underset{\sim}{S} - \underset{\sim}{r}\| = S_y^o f(\zeta)$ and $(\underset{\sim}{S} - \underset{\sim}{r})$: $d\underset{\sim}{e} > 0$

then plastic deformation is admissible (3.23c)

We now consider the above case (iii) in detail. We rewrite Eq. (3.21) as:

$$\underset{\sim}{S} = S_y^o f \frac{d\underset{\sim}{e}^p}{d\zeta} + \underset{\sim}{r} \; ; \quad \text{or} \; \frac{d\underset{\sim}{e}^p}{d\zeta} = \frac{(\underset{\sim}{S} - \underset{\sim}{r})}{f S_y^o} \tag{3.24a,b}$$

Differentiating (3.24a) with respect to ζ, we obtain

$$\frac{d\underset{\sim}{S}}{d\zeta} = S_y^o \left[\frac{d^2\underset{\sim}{e}^p}{d\zeta^2} f + \frac{d\underset{\sim}{e}^p}{d\zeta} f' \right] + \frac{d\underset{\sim}{r}}{d\zeta} \tag{3.25}$$

where $f' = (df/d\zeta)$. From (3.3) we have:

$$\frac{d\underset{\sim}{S}}{d\zeta} = 2\mu_o \left(\frac{d\underset{\sim}{e}}{d\zeta} - \frac{d\underset{\sim}{e}^p}{d\zeta} \right) \tag{3.26}$$

Further, from (3.22b) it is seen that:

$$\frac{d\underset{\sim}{r}}{d\zeta} = \frac{1}{f} \frac{d\underset{\sim}{r}}{dz} = 2\mu_o \left[\rho_1(o) \frac{d\underset{\sim}{\eta}}{d\zeta} + \frac{\underset{\sim}{h}^*}{f} \right] \tag{3.27}$$

where, $$\underset{\sim}{h}^* = \int_o^z \frac{\partial \rho_1}{\partial z} (z - z') \frac{d\underset{\sim}{e}^p}{dz'} dz' \tag{3.28}$$

We draw attention to the differences in the definitions of $\underset{\sim}{h}^*$ (involving ρ_1) in (3.28) and that of $\underset{\sim}{h}$ (involving ρ) in (3.16b), respectively.

Using (3.26 and 3.27) in (3.25), it is easy to obtain:

$$d\underset{\sim}{e} = \left[1 + \rho_1(o) + \frac{S_y^o f'}{2\mu_o} \right] d\underset{\sim}{e}^p + \frac{\underset{\sim}{h}^*}{f} d\zeta + \frac{S_y^o f}{2\mu_o} \left(\frac{d^2\underset{\sim}{e}^p}{d\zeta^2} \right) d\zeta \tag{3.29a}$$

$$= \left\{ \left[1 + \rho_1(o) + \frac{S_y^o f'}{2\mu_o} \right] \frac{(\underset{\sim}{S} - \underset{\sim}{r})}{f S_y^o} + \frac{\underset{\sim}{h}^*}{f} \right\} d\zeta + \frac{S_y^o f}{2\mu_o} \left(\frac{d^2 \underset{\sim}{e}^p}{d\zeta^2} \right) d\zeta \qquad (3.29b)$$

In going from (3.29a) to (3.29b), Eq. (3.24b) has been used. Now, taking the tensor trace of both sides of $(\underset{\sim}{S} - \underset{\sim}{r})$, we see that:

$$d\underset{\sim}{e} : (\underset{\sim}{S} - \underset{\sim}{r}) = \left\{ \left[1 + \rho_1(o) + \frac{S_y^o f'}{2\mu_o} \right] \frac{(\underset{\sim}{S} - \underset{\sim}{r}) : (\underset{\sim}{S} - \underset{\sim}{r})}{f\, S_y^o} + \frac{\underset{\sim}{h}^* : (\underset{\sim}{S} - \underset{\sim}{r})}{f} \right\} d\zeta$$

$$+ \frac{S_y^o f}{2\mu_o} \frac{d^2 \underset{\sim}{e}^p}{d\zeta^2} : (\underset{\sim}{S} - \underset{\sim}{r}) \qquad (3.30)$$

Again, using (3.24b), it is seen that:

$$\frac{d^2 \underset{\sim}{e}^p}{d\zeta^2} : (\underset{\sim}{S} - \underset{\sim}{r}) = f\, S_y^o \left(\frac{d^2 \underset{\sim}{e}^p}{d\zeta^2} : \frac{d\underset{\sim}{e}^p}{d\zeta} \right) \qquad (3.31)$$

However, since, during inelastic (plastic) deformation, by definition,

$$\frac{d\underset{\sim}{e}^p}{d\zeta} : \frac{d\underset{\sim}{e}^p}{d\zeta} = 1 \ , \qquad (3.32a)$$

if follows that

$$\frac{d^2 \underset{\sim}{e}^p}{d\zeta^2} : \frac{d\underset{\sim}{e}^p}{d\zeta} = 0 \qquad (3.32b)$$

Moreover, during plastic deformation,

$$(\underset{\sim}{S} - \underset{\sim}{r}) : (\underset{\sim}{S} - \underset{\sim}{r}) = f^2 (S_y^o)^2 \qquad (3.33)$$

Using (3.31), (3.32b), and (3.33) in (3.30), we have:

$$d\zeta = \frac{d\underset{\sim}{e}:(\underset{\sim}{S} - \underset{\sim}{r})}{C(S_y^o f)} \tag{3.34}$$

where [+]

$$C = 1 + \rho_1(o) + \frac{S_y^o f'}{2\mu_o} + \frac{\underset{\sim}{h}^*:(\underset{\sim}{S} - \underset{\sim}{r})}{f^2 S_y^o} \tag{3.35}$$

In (3.35), $\rho_1(o) = \rho_1(z = 0)$ [for ρ_1 of (3.19)] and $\underset{\sim}{h}^*$ is defined in (3.28). Using (3.34) in (3.24b), we have:

$$d\underset{\sim}{e}^p = \frac{(\underset{\sim}{S} - \underset{\sim}{r})}{Cf^2 S_y^{o2}} [(\underset{\sim}{S} - \underset{\sim}{r}):d\underset{\sim}{e}] \tag{3.36}$$

Using (3.36) in (3.3) [for $\alpha = 1$], we obtain the sought-after incremental (or rate or differential) form of the stress-strain relation, in the presence of plastic deformation, to be:

$$d\underset{\sim}{S} = 2\mu_o \left[d\underset{\sim}{e} - \frac{(\underset{\sim}{S} - \underset{\sim}{r})}{Cf^2 S_y^{o2}} \langle (\underset{\sim}{S} - \underset{\sim}{r}):d\underset{\sim}{e} \rangle \right] \tag{3.37}$$

In component form, Eq. (3.37) may be written as:

$$dS_{ij} = 2\mu_o \left[\delta_{im}\delta_{jn} - \frac{(S_{ij} - r_{ij})}{Cf^2 S_y^{o2}} (S_{mn} - r_{mn}) \right] de_{mn} \tag{3.38}$$

Assuming purely-elastic hydrostatic response, Eq. (3.38) may be written in a

---

[+] We note that Valanis [29] presents an alternate derivation for $d\zeta$, and obtains an equation similar to the present Eq. (3.34). However, his result for C given in his Eq. (3.34) [29], which contains certain, rather inconsequential, algebraic errors, differs from the present Eq. (3.35) given above, even after the algebraic errors in his Eq. (3.34) are corrected. Specifically, the constant C in Valanis' Eq. (3.34) does not contain the term $(S_y f'/2\mu_o)$ as in the present (3.35) shown above. It will be shown later in this paper that the present (3.35) is, in fact, correct.

slightly modified form. Noting that, by definition of 'deviatoric' parts of tensors, one has:

$$d\sigma_{ij} = dS_{ij} + \frac{1}{3}d\sigma_{mm}\delta_{ij} \; ; \quad d\sigma_{mm} = 3K_o d\varepsilon_{mm} = (3\lambda_o + 2\mu_o)d\varepsilon_{mm} \tag{3.39a}$$

$$(S_{mn} - r_{mn})de_{mn} = (S_{mn} - r_{mn})(d\varepsilon_{mn} - \frac{1}{3}\delta_{mn}d\varepsilon_{kk}) = (S_{mn} - r_{mn})\, d\varepsilon_{mn} \tag{3.39b}$$

and $$\delta_{im}\delta_{jn}de_{mn} = \delta_{im}\delta_{jn}d\varepsilon_{mn} - \frac{d\varepsilon_{kk}}{3}\delta_{ij} \; , \tag{3.39c}$$

we obtain, from (3.38), the relation:

$$d\sigma_{ij} = \left[2\mu_o\delta_{im}\delta_{jn} + \lambda_o\delta_{ij}\delta_{mn} - \frac{2\mu_o(S_{ij} - r_{ij})(S_{mn} - r_{mn})}{C(S_y^o)^2 f^2(\zeta)}\right]d\varepsilon_{mn} \tag{3.40}$$

where $d\varepsilon_{mn}$ is the rate of <u>total strain</u>, and $\lambda_o = (3K_o - 2\mu_o)/3$. It may be worth recalling that, in the above,

$$S_y^o = 2\mu_o\rho_o \quad \text{and} \quad C = 1 + \rho_1(o) + \frac{(\underset{\sim}{S} - \underset{\sim}{r}):\underset{\sim}{h}^*}{S_y^o f^2(\zeta)} + \frac{S_y^o f'}{2\mu_o}$$

$$\underset{\sim}{r} = 2\mu_o \int_o^z \rho_1(z - z')\frac{d\underset{\sim}{e}^p}{dz'}\,dz' \; ; \quad \underset{\sim}{h}^* = \int_o^z \frac{\partial \rho_1}{\partial z}(z - z')\frac{\partial \underset{\sim}{e}^p}{\partial z'}\,dz'$$

It is interesting to compare (3.40) to the classical kinematic-hardening plasticity theory of Prager, for which the stress-strain law is [37]:

$$d\sigma_{ij} = \left[2\mu_o\delta_{im}\delta_{jn} + \lambda_o\delta_{ij}\delta_{mn} - \frac{6\mu_o^2}{(\hat{C} + 2\mu_o)(\sigma_y^o)^2}(S_{ij} - \alpha_{ij})(S_{mn} - \alpha_{mn})\right]d\varepsilon_{mn} \tag{3.41a}$$

where $$d\alpha_{mn} = \hat{C}d\varepsilon_{mn}^p \tag{3.41b}$$

and σ_y^o is the yield stress in uniaxial tension, and $\hat{C}$ is a constant. It may

be seen that from the point of view of computational implementation, Eqs. (3.40) and (3.41) are more or less similar.

As noted earlier, the function $\rho_1(z)$ controls the translation of the yield surface. If $\rho_1(z)$ is set to zero, i.e., the yield surface is allowed only to expand as in an isotropic hardening theory, we have:

$$\rho_1(o) = \underset{\sim}{h}^* = 0 \; ; \quad \underset{\sim}{r} = 0 \tag{3.42a}$$

Consequently, the function C in Eq. (3.40) becomes:

$$C = 1 + (S_y^o f'/2\mu_o) \tag{3.42b}$$

On the other hand, the classical Prandtl-Reuss isotropic hardening relations for small deformations are [37]:

$$d\sigma_{ij} = \left\{ 2\mu_o \delta_{im}\delta_{jn} + \lambda_o \delta_{ij}\delta_{mn} - \frac{3\mu_o S_{ij} S_{mn}}{\sigma_o^2(\bar{\varepsilon}^p)\,[1+(1/3\mu o)H]} \right\} d\varepsilon_{mn} \tag{3.43}$$

Where $\sigma_o(\bar{\varepsilon}^p)$ is the uniaxial equivalent stress-equivalent strain relation, and H is the slope of the truss stress vs. logarithmic strain relation in uniaxial tension. Thus, the presently derived relation for isotropic hardening, (3.40) [with (3.42a,b)] is analogous to the classical Prandtl-Reuss relation.

However, it will be shown in the next section that the presence of

$$C[\zeta] f^2[\zeta] = C\left[\int \| d\underset{\sim}{e}^p \| \right] f^2 \left[\int \| d\underset{\sim}{e}^p \| \right] \tag{3.44}$$

in the third term of (3.40), and the evolution equation (3.22b) for the translation of the yield surface, $\underset{\sim}{r}$, lead to certain advantages in modeling plasticity under cyclic hardening. Note that $f^2(\zeta)$ is a non-negative function analogous to w^p, the plastic-work.

4. Determination of Material Constants and Representation of Monotonic and Cyclic Hardening Plasticity:

4.A General Considerations:

We develop here the stress-strain relations for uniaxial tension, so as to be consistent with the presently developed alternative three-dimensional relations given in Eqs. (3.21) and (3.40) in integral and differential forms, respectively. We define the uniaxial tension response through the relations: $\sigma_{11} \neq 0$ otherwise $\sigma_{ij} = 0$; $de^p_{22} = de^p_{33} = -(\frac{1}{2})de^p_{11}$, $de^p_{ij} = 0 (i \neq j)$. Using (3.6) we obtain:

$$d\zeta^2 = \frac{3}{2}(de^p_{11})^2 = \frac{3}{2}(d\varepsilon^p_{11})^2$$

or
$$d\zeta = \sqrt{\frac{3}{2}}\,|d\varepsilon^p_{11}| \quad .. \tag{4.1a}$$

and
$$\zeta = \sqrt{\frac{3}{2}}\int \|d\varepsilon^p_{11}\| . \tag{4.1b}$$

We also introduce:

$$dz = d\zeta/f(\zeta) \; ; \quad f(\zeta) = 1 + \beta\zeta \tag{4.2}$$

$$E_o\rho(z) = E_o\rho_o\delta(z) + E_1 e^{-\alpha_1 z} + E_2 \tag{4.3a}$$

and
$$\mu_o\rho(z) = \mu_o\rho_o\delta(z) + (\frac{\mu_o}{E_o})\,E_1 e^{-\alpha_1 z} + (\frac{\mu_o}{E_o})E_2 \tag{4.3b}$$

The stress-strain relation under uniaxial tension that was used by Wu and Yip [30,31] is, as discussed earlier, the present Eq. (3.12b) which is recalled below:

$$\sigma_{11} = E_o \int_o^z \rho(z - z')\,\frac{de^p_{11}}{dz}\,dz' \quad ; \text{ for } \quad \zeta \gtrless 0^+ \tag{4.4}$$

Using (4.1 to 4.3a,b) in (4.4), we obtain, for monotonic uniaxial tension ($\| d\varepsilon^p_{11}\| = d\varepsilon^p_{11}$),

$$\sigma_{11} = E_o \rho_o \sqrt{\frac{2}{3}} \left(1 + \beta \sqrt{\frac{3}{2}}\ \varepsilon^p_{11}\right) + \sqrt{\frac{2}{3}} \left(\frac{E_1}{n_1 \beta}\right) \left(1 + \beta \sqrt{\frac{3}{2}}\ \varepsilon^p_{11}\right)$$

$$x \left\{1 - \left(1 + \beta \sqrt{\frac{3}{2}}\ \varepsilon^p_{11}\right)^{-n_1}\right\} + E_2 \varepsilon^p_{11}\ ; \quad \text{for} \quad \varepsilon^p_{11} \geqslant 0 \tag{4.5a}$$

where $$n_1 = 1 + (\alpha_1/\beta) \tag{4.5b}$$

It may be worth mentioning that Wu and Yip [30,31] use the definition that $d\zeta = |d\varepsilon^p_{11}|$ instead of the one in (4.1b). Hence the result in [30,31] would agree with the present (4.5) if the constants ρ_0, E_0, E_1, E_2, β_1, and α_1 as used in [30,31] are identified, instead, to be: $(\rho_0\sqrt{2/3})$; E_0; E_1; E_2; $(\beta\sqrt{3/2})$; and $(\alpha_1\sqrt{3/2})$, respectively.

On the other hand, the present three-dimensional integral relation, Eq. (3.21), reduces, for the uniaxial tension case, to:

$$\sigma_{11} = 3\mu_o \rho_o \frac{d\varepsilon^p_{11}}{dz} + 3\mu_o \int_o^z \rho_1(z - z') \frac{d\varepsilon^p_{11}}{dz'}\, dz' \tag{4.6}$$

$$= \sqrt{6}\ \mu_o \rho_o \left(1 + \beta \sqrt{\frac{3}{2}}\ \varepsilon^p_{11}\right) + \sqrt{\frac{2}{3}} \left(\frac{3\mu_o}{E_o}\right) \frac{E_1}{\beta n_1} \left(1 + \beta \sqrt{\frac{3}{2}}\ \varepsilon^p_{11}\right)$$

$$x \left\{1 - \left(1 + \beta \sqrt{\frac{3}{2}}\ \varepsilon^p_{11}\right)^{-n_1}\right\} + \left(\frac{3\mu_o}{E_o}\right) E_2 \varepsilon^p_{11}\ ; \text{ for } \quad \varepsilon^p_{11} \geqslant 0 \tag{4.7}$$

In writing (4.7), monotonic loading has been assumed. By comparing (4.5) and (4.7), it may be seen that the Wu-Yip [30,31] relation agrees with the present, provided $E_0 = 3\mu_0$ i.e., the Poisson's ratio $\nu_0 = 1/2$ even in the elastic region. This is due to the fact that the relation (3.12b), used in [30,31], which results in (4.5) is based on the assumption that the Poisson's ratio is constant throughout deformation.

We shall henceforth use (4.7) to evaluate material properties, for use in conjunction with the three-dimensional relations (3.21) and (3.40). We will

assume that the elastic properties are related as: $\mu_o = E_o/2(1 + \nu_o)$; $\lambda_o = 2\mu_o\nu_o/(1 - 2\nu_o)$; $3k_o = (3\lambda_o + 2\mu_o)$.

For large values of ε^p_{11}, the asymptotic value of stress, denoted as σ^∞_{11}, may be obtained from (4.6) to be:

$$\sigma^\infty_{11} = \sqrt{6}\,\mu_o\rho_o\left(1+\beta\sqrt{\frac{3}{2}}\,\varepsilon^p_{11}\right) + \sqrt{\frac{2}{3}}\left(\frac{E_1}{\beta n_1}\right)\left(1+\beta\sqrt{\frac{3}{2}}\,\varepsilon^p_{11}\right)\left(\frac{3\mu_o}{E_o}\right)$$

$$+ \left(\frac{3\mu_o}{E_o}\right) E_2\varepsilon^p_{11} \tag{4.8}$$

Assuming that the elastic constants (E_o, μ_o) are known for the material, it is seen from (4.7) the stress-plastic strain response of the material, given in (4.7) is governed by the five parameters: ρ_o, β, α_1, E_1, and E_2. We now discuss the determination of these five parameters from given test data for the material under monotonic uniaxial tension. To this end, first note that:

$$\frac{d\sigma_{11}}{d\varepsilon^p_{11}} = 3\mu_o\rho_o\beta + \left(\frac{3\mu_o}{E_o}\right)\frac{E_1}{n_1}\left\{1+(n_1-1)\left(1+\beta\sqrt{\frac{3}{2}}\,\varepsilon^p_{11}\right)^{-n_1}\right\} + \left(\frac{3\mu_o}{E_o}\right)E_2 \tag{4.9}$$

and

$$\frac{d\sigma^\infty_{11}}{d\varepsilon^p_{11}} = 3\mu_o\rho_o\beta + \left(\frac{3\mu_o}{E_o}\right)\frac{E_1}{n_1} + \left(\frac{3\mu_o}{E_o}\right)E_2 \tag{4.10}$$

We now define parameters σ^o_o, E_p, σ^∞_o, and E_t as may be determined[+] from the test data as shown in Fig. (1a), to be:

$$\sigma^o_o = \sigma_{11}\Big|_{\varepsilon^p_{11}=0} = \sqrt{6}\,\mu_o\rho_o \tag{4.11a}$$

$$E_p = (d\sigma_{11}/d\varepsilon^p_{11})\Big|_{\varepsilon^p_{11}=0} = 3\mu_o\rho_o\beta + \left(\frac{3\mu_o}{E_o}\right)E_1 \tag{4.11b}$$

[+] Here, it is to be noted that the 'knee' portion (near the 'elastic' limit point) of the stress-strain test data is approximated by a straight line $\sigma_{11} = \sigma^o_o + E_p\varepsilon^p_{11}$ for $\varepsilon^p_{11} \ll 1$; and for large values of ε^p_{11}, the stress-strain test data is approximated by a straight line $\sigma_{11} = \sigma^\infty_o + E_t\varepsilon^p_{11}$ as shown in Fig. 1a. Thus, the parameters σ^o_o, E_p, σ^∞_o, and E_t are "read-off" from the test data for uniaxial tension.

$$\sigma_o^\infty = \sigma_{11}^\infty \Big|_{\varepsilon_{11}^p=0} = \sqrt{6}\,\mu_o\rho_o + \sqrt{\frac{2}{3}}\left(\frac{3\mu_o}{E_o}\right)\frac{E_1}{\beta n_1} \tag{4.11c}$$

and
$$E_t = \frac{d\sigma_{11}^\infty}{d\varepsilon_{11}^p} = 3\mu_o\rho_o\beta + \left(\frac{3\mu_o}{E_o}\right)\frac{E_1}{n_1} + \left(\frac{3\mu_o}{E_o}\right)E_2 \tag{4.11d}$$

The four equations (4.11a-d) are obviously not sufficient to determine the five constants ρ_o, β, α_1, E_1, and E_2. To uniquely determine these five constants, the missing fifth relation may be arrived at by first noting that $\rho_1(z)$ [involving E_1 and E_2] describes the translation of the yield surface, and $f(\zeta)$ [involving β] describes the enlargement (or contraction, as the case may be) of the yield surface. Specifically, by integrating (4.6) for a loading-unloading-reloading case, assuming that $f(\zeta) = 1 + \beta\zeta$, it may be shown that the stress-drop $\Delta\sigma$ during the elastic part of the first unloading is $2\sigma_o^o(1+\beta\sqrt{\frac{3}{2}}|\,\varepsilon_{11}^p\,|^*)$ (see Fig. 3) where $|\,\varepsilon_{11}^p\,|^*$ is the plastic strain at the beginning of elastic unloading. Thus, material constant β may be determined. Now, Eqs. (4.11a-d) may be solved for the remaining four unknowns, as:

$$n_1 \equiv (1 + \alpha_1/\beta) = 1 + \sqrt{\frac{2}{3}}\left(\frac{E_p - E_t}{\sigma_o^\infty - \sigma_o^o}\right)\frac{1}{\beta} \tag{4.12a}$$

$$\rho_o = (\sigma_o^o/\sqrt{6}\,\mu_o) \tag{4.12b}$$

$$E_1 = \left(\frac{E_o}{3\mu_o}\right)\left[(E_p - E_t) + \sqrt{\frac{3}{2}}\,(\sigma_o^\infty - \sigma_o^o)\beta\right] \tag{4.12c}$$

and
$$E_2 = \left(\frac{E_o}{3\mu_o}\right)\left(E_t - \sqrt{\frac{3}{2}}\,\sigma_o^\infty\,\beta\right) \tag{4.12d}$$

If a more accurate approximation near the 'knee' of the stress-strain curve (at $\varepsilon_{11}^p = 0$) is needed, one may use, instead of (4.3b), the assumption:

$$\mu_o \rho(z) = \mu_o \rho_o' \, \delta(z) + \left(\frac{\mu_o}{E_o}\right) E_1 e^{-\alpha_1 z} + \left(\frac{\mu_o}{E_o}\right) E_2 + \left(\frac{\mu_o}{E_o}\right) E_3 e^{-\alpha_3 z} \qquad (4.13)$$

The corresponding solution becomes:

$$\sigma_{11} = \sqrt{6}\, \mu_o \rho_o' \left(1+\beta\sqrt{\frac{3}{2}}\, \varepsilon_{11}^p\right) + \sqrt{\frac{2}{3}} \left(\frac{3\mu_o}{E_o}\right) \frac{E_1}{\beta n_1} \left(1+\beta\sqrt{\frac{3}{2}}\, \varepsilon_{11}^p\right)\left\{1 - \left(1+\beta\sqrt{\frac{3}{2}}\, \varepsilon_{11}^p\right)^{-n_1}\right\}$$

$$+\sqrt{\frac{2}{3}} \left(\frac{3\mu_o}{E_o}\right) \frac{E_3}{\beta n_3} \left(1+\beta\sqrt{\frac{3}{2}}\, \varepsilon_{11}^p\right)\left\{1 - \left(1+\beta\sqrt{\frac{3}{2}}\, \varepsilon_{11}^p\right)^{-n_3}\right\} + \left(\frac{3\mu_o}{E_o}\right) E_2 \varepsilon_{11}^p$$

where $\quad n_3 = 1 + (\alpha_3/\beta) \qquad (4.14)$

The parameters from the test data[+], as shown in Fig. 1(b) are now related as:

$$E_t = 3\mu_o \rho_o' \beta + \left(\frac{3\mu_o}{E_o}\right) \frac{E_1}{n_1} + \left(\frac{3\mu_o}{E_o}\right) \frac{E_3}{n_3} + \left(\frac{3\mu_o}{E_o}\right) E_2 \qquad (4.15a)$$

$$\sigma_o^\infty = \sqrt{6}\, \mu_o \rho_o' + \sqrt{\frac{2}{3}} \left(\frac{3\mu_o}{E_o}\right) \frac{E_1}{\beta n_1} + \sqrt{\frac{2}{3}} \left(\frac{3\mu_o}{E_o}\right) \frac{E_3}{\beta n_3} \qquad (4.15b)$$

$$(\sigma_o^o)' = \sqrt{6}\, \mu_o \rho_o' \qquad (4.15c)$$

$$(E_p)' = 3\mu_o \rho_o' \beta + \left(\frac{3\mu_o}{E_o}\right) E_1 + \left(\frac{3\mu_o}{E_o}\right) E_3 \qquad (4.15d)$$

With β, E_1, and E_2 being as before, the additional constants in the improved approximation are determined as:

[+] In this improved representation, the 'knee' portion of the test data is approximated by a straight line $\sigma_{11} = (\sigma_o^o)' + (E_p)' \varepsilon_{11}^p$ for $\varepsilon_{11}^p \ll 1$, as shown in Fig. 1(b). However, for large values of ε_{11}^p, the test data is approximated by the same straight line as in the earlier representation (shown in Fig. 1a), i.e., $\sigma_{11} = \sigma_o^\infty + E_t \varepsilon_{11}^p$. Note also that the definitions of (σ_o^o) and (E_p), shown in Fig. 1b, remain the same as before, i.e., $\sigma_o^o = \sqrt{6}\, \mu_o \rho_o$, and $E_p = 3\mu_o \rho_o \beta + (3\mu_o/E_o) E_1$.

$$n_3 = \sqrt{\frac{2}{3}}\,\frac{1}{\beta}\left(\frac{E_p' - E_p}{\sigma_o^o - (\sigma_o^o)'}\right) + 1 \tag{4.16a}$$

and

$$E_3 = \left(\frac{E_o}{3\mu_o}\right)\left[(E_p' - E_p) + \sqrt{\frac{3}{2}}\,(\sigma_o^o - \sigma_o^{o\prime})\beta\right] \tag{4.16b}$$

Similar procedures may be employed when an arbitrary number of terms are used in the expansion,

$$E_o\rho(z) = E_o\rho_o\delta(z) + \sum_i E_i e^{-\alpha_i z} \tag{4.17}$$

which makes it possible to represent the knee portion more and more accurately.

We now consider the presently derived differential form of the stress-strain relation, (3.38) or (3.40). For the uniaxial tension problem, Eq. (3.38) becomes:

$$dS_{11} = 2\mu_o\left\{de_{11} - \frac{(S_{11}-r_{11})^2}{Cf^2S_y^{o2}}\,de_{11} - \frac{(S_{11}-r_{11})(S_{22}-r_{22})}{Cf^2S_y^{o2}}\,de_{22} - \frac{(S_{11}-r_{11})(S_{33}-r_{33})}{Cf^2S_y^{o2}}\,de_{33}\right\} \tag{4.18}$$

For uniaxial tension,

$$S_{11} = \frac{2}{3}\,\sigma_{11}\ ;\quad S_{22} = S_{33} = -\frac{1}{3}\,\sigma_{11}\ ;\quad r_{22} = r_{33} = -\frac{1}{2}\,r_{11}$$

$$de_{11} = d\varepsilon_{11} - \frac{d\sigma_{11}}{9K_o}\ ;\quad de_{22} = -\frac{1}{2}\,d\varepsilon_{11} + \frac{d\sigma_{11}}{18K_o} = de_{33}$$

$$r_{11} = 2\mu_o\int_o^z \rho_1(z-z')\,\frac{de_{11}^p}{dz'}\,dz' \tag{4.19}$$

Use of (4.19) in (4.18) results, for the <u>monotonic</u> uniaxial tension problem,

in:

$$d\sigma_{11} = \frac{2\mu_o[1 - (1/C)]}{(2/3) + (2\mu_o/9K_o)[1 - (1/C)]}\, d\varepsilon_{11} \tag{4.20}$$

where, $$C = 1 + \rho_1(o) + \frac{S^o_y f'}{2\mu_o} + \sqrt{\frac{3}{2}}\,\frac{h^*_{11}}{f} \tag{4.22}$$

For the presently assumed $\rho_1(z)$ and f, as in (4.3a) and (4.2) respectively, we have:

$$\rho_1(o) = \left(\frac{E_1}{E_o}\right) + \left(\frac{E_2}{E_o}\right); \tag{4.23a}$$

$$\frac{h^*_{11}}{f} = \frac{1}{f}\int_o^z \frac{\partial \rho_1}{\partial z}(z - z')\,\frac{de^p_{11}}{dz'}\,dz' = -\sqrt{\frac{2}{3}}\left(\frac{E_1}{E_o}\right)\left(\frac{n_1 - 1}{n_1}\right)\left\{1 - f^{-n_1}\right\} \tag{4.23b}$$

and $$C = 1 + \left(\frac{E_2}{E_o}\right) + \left(\frac{E_1}{E_o}\right)\frac{1}{n_1}\left[1 + (n_1 - 1)f^{-n_1}\right] + \rho_o\beta \tag{4.23c}$$

Since, $$d\varepsilon_{11} = d\varepsilon^p_{11} + \frac{d\sigma_{11}}{E_o}\ , \tag{4.24}$$

it may be easily shown, by using (4.24) in (4.20), that:

$$\frac{d\sigma_{11}}{d\varepsilon^p_{11}} = 3\mu_o(C - 1)$$

$$= 3\mu_o\rho_o\beta + \left(\frac{3\mu_o}{E_o}\right)\frac{E_1}{n_1}\left[1 + (n_1 - 1)f^{-n_1}\right] + \left(\frac{3\mu_o}{E_o}\right)E_2\ , \tag{4.25}$$

which agrees with (4.9) derived from the integral relation. This agreement of (4.25) with (4.9) is then a confirmation of the validity of the differential stress-strain relations (3.38) and (3.40), as well as the correctness of the presently derived expression for C as in (3.35).

4.B Numerical Results

4.B.1 Plasticity: monotonic loading:

The applications that we address here pertain to inelastic deformation at elevated temperatures. In this subsection, we will consider plasticity; and later in this paper, we deal with the problem of plasticity-creep interaction. Here we make use of experimental data for type 304 stainless steel at high temperatures, produced by the Power Reactor and Nuclear Fuel Development Corporation (hereafter denoted as PNC) in Japan [38]. First we study the monotonic stress-strain curve at 550°C, for which the PNC data [38] is shown in Fig. 2. The constitutive equation adopted by PNC [38] may be considered to be a modified version of Blackburn's [39] equation, in which an increment of plastic strain is expressed by a power law in terms of stress. This makes the 'knee' portion of the stress vs. plastic strain curve have a very steep initial slope, as shown in Fig. 2.

We now approximate the above PNC data by three different types of the present "intrinsic-time-plasticity" models, Eqs. (4.6) or (4.18). These three modes are designated as Cases A, B, and C, respectively, in Tables 1 and 2. In Case A, a two-term approximation for $\rho_1(z)$ as in (4.36) is used, and the yield-stress (in this case, $\sigma_y^o = \sigma_o^o$) is the highest among all the cases. In Cases B and C, a three-term approximation for $\rho_1(z)$ as in (4.13) is used. The yield stress σ_y^o is now equal to $(\sigma_o^o)'$ in Cases B and C. Note that $(\sigma_o^o)'$ in Case B is chosen to be higher than that in Case C. Material constants (σ_o^o), $(\sigma_o^o)'$, (σ_o^∞), E_t, E_p, and E', as inferred from the test data are given in Table 1. Modeling parameters E_1, E_2, E_3, α_1, α_3, and β as calculated from Eqs. (4.12a-d) and (4.16a,b) are given in Table 2. The value $\beta = 5$ is taken from Wu and Yip [30] who base it on their analysis of experimental data for type 304 stainless steel at room temperature.

Fig. 2 shows the comparison between the PNC data and the present modeling through Eqs. (4.6) or (4.18). The present results for each of the Cases A, B, and C may be seen to agree excellently with experimental data, with the only differences between the three cases being in the knee region, as anticipated.

We briefly touch upon certain aspects of the present numerical calculation. The present theory has a memory of history of inelastic straining, and the entire history of deformation is needed to determine the current state of stress. The terms $\underset{\sim}{r}$ [see (3.22b) or (4.19)] and $\underset{\sim}{h}^*$ [see (3.28) or (4.23b)] need to be integrated numerically. In the present series of numerical studies, including those for creep and plasticity-creep interactions to be discussed in subsection 5.B, it has been found necessary to control the increment Δz in the numerical integration. A trapezoidal rule with a constant value of Δz, i.e., $\Delta z = 0.5 \times 10^{-4}$ has been found to be adequate.

4.B.2. Plasticity: Cyclic Loading:

A typical cyclic loading, under tension-compression straining, is sketched in Fig. 3. The stress under this cyclic history of loading is calculated by using the differential stress-strain relation, (4.18). Note that now, $d\zeta = \sqrt{\frac{3}{2}} |d\varepsilon^p_{11}|$; $\zeta = \sqrt{\frac{3}{2}} \int |d\varepsilon^p_{11}|$; $dz = d\zeta / f(\zeta)$. Note also that the procedure for the present calculation using (4.18) or (4.20) is operationally very similar to that in classical plasticity theory, in that (3.23a,b, and c) apply. Referring to Fig. 3, the stress and strain are increased elastically from the 'free state' point 0 to the yield point denoted by 1. From point 1 the material is subject to plastic deformation, and until the strain of magnitude $\bar{\varepsilon}_{11}$ (see Fig. 3) the yield surface translates and expands. At point 2, the material is unloaded. During unloading the material behaves elastically, and the stress-state reaches a point on the opposite side of the yield surface. The stress drop,

$\Delta\sigma$ in Fig. 3, from point 2 to the elastic limit point 3 is given by $2\sigma_y^o f_2$ where f_2 is the value of f at point 2. Note that the increments of $\Delta\varepsilon_{11}$ between various points in the strain-path, defined, for instance, as $\Delta\zeta_{11}^{P24} = \int_2^4 \|d\varepsilon_{11}^P\|$, are as shown in Fig. 3. We now discuss the quantitative features of the hysterisis loops under cyclic loading for two different-types of functions $f(\zeta)$.

(i) $f(\zeta) = (1 + \beta\zeta)$; $\zeta = \sqrt{\frac{3}{2}} \int |d\varepsilon_{11}^P|$

The analysis of cyclic loading is carried out for material data designated as Case B in Tables 1 and 2, along with the linear function $f(\zeta) = (1 + \beta\zeta)$. Fig. 4 shows the calculated results for the σ-ε relation for the strain range of $\bar{\varepsilon} = \pm 0.5\%$. Peak stresses at the loading-unloading points are denoted by σ_N^t and σ_N^c, where the superscripts t and c imply tension and compression, respectively, while the subscript N implies the Nth cycle of loading. It is observed from Fig. 4 that these peak stresses increase monotonically with N, and do not reach a stable value as is normally observed in experiments. An examination of Fig. 3 clearly shows that the reason for this monotonic increase of the peak stress is the linearity of f with respect to ζ.

(ii) $f(\zeta) = \{a + (1 - a) \exp(-\gamma\zeta)\}$; a and γ constants

Instead of a linear function, the above saturated function f will be employed, wherein a and γ are appropriate material parameters. Note that such an f has also been used by Wu and Yip [30] so as to obtain certain analytical solutions in explicit form. In the above, the parameter 'a' represents a saturated magnitude of the yield surface. If the initial slope at $\zeta = 0$ is equated for both the linear and saturated functions, the following relation is obtained:

$$(a - 1)\nu = \beta \tag{4.26}$$

Even if a saturated function f is used, we may determine the other material parameter $\rho_1(z)$ as if using a linear f, because a saturated function $f(\zeta)$ can be expected to have an influence only for large values of $\zeta(=\sqrt{\frac{3}{2}}\int|d\dot{\epsilon}^p_{11}|)$ such as in cyclic loading.

Appropriate experimental data for plasticity for cyclic loading of Type 304 stainless steel at elevated temperatures does not appear to be readily available. However, as far as room temperature cyclic loading is concerned, data exists [38] for saturated peak stress σ^t_∞ and initial yield stress σ^o_y for Type 304 stainless steel, as:

$$\sigma^o_y \simeq 196 \text{ MPa} \; ; \quad 265 \text{ MPa}$$

Ignoring the kinematic hardening for the time being, one may obtain the following rough <u>over</u> estimation, a_o for a:

$$a_o \simeq \sigma^t_\infty/\sigma^o_y \simeq 1.35$$

We will henceforth assume that a = 1.2. We estimate γ from (4.26) to be:

$$\nu = 5/(.2) = 25$$

Of course, if one can easily identify the point of departure from unloading to reloading, such as point 3 in Fig. 3, in the experimental data, one may estimate the values of a and γ more accurately. However, in general, point 3 cannot be so unambiguously identified from experimental data.

Figure 5 shows the presently computed results using the saturated function f. As may be seen, the hysteris loops saturate after a few cycles of loading. The peak stresses σ^t_N and σ^c_N converge to stable values as shown in Fig. 6. Fig. 7 shows the enlargement of the yield surface, i.e., $f(\zeta)$, as a function

of $\zeta = \int |d\varepsilon_{11}^{p}|$. The corresponding values at each peak of the tension-compression loading-cycles are also depicted in Fig. 7. The increment between the peak of tension and the peak of compression points can be seen, from Fig. 7, to be almost the same regardless of the number of cycles of loading.

The results in Figs. 4 - 7 clearly show the advantageous features of the present rate-type stress-strain relation [(3.38) or (3.40)] for plasticity based on an internal variable theory, over that based on a classical plasticity theory.

5. Creep and Plasticity

5.A Theoretical Development

In Section 3, we employed an intrinsic time measure related, in a differential sense, to the norm of the differential plastic strain, to describe rate-independent plasticity. To characterize the creep and plasticity-creep interaction behavior, we now employ an intrinsic time measure as well as Newtonian time, both of which are nonnegative and irreversible quantities. Specifically, we assume that the internal time increment, dz, is expressible as:

$$(dz)^2 = \frac{(d\zeta)^2}{f^2(\zeta)} + \frac{(dt)^2}{g^2} \tag{5.1}$$

where: $d\zeta^2 = d\underset{\sim}{\eta} : d\underset{\sim}{\eta}$ (5.2a)

$d\underset{\sim}{\eta}$ = inelastic strain differential (5.2b)

(plastic as well as creep, i.e., $d\underset{\sim}{\eta} = d\underset{\sim}{\eta}^{c} + d\underset{\sim}{\eta}^{p}$)

and g = a scaling function (5.2c)

As before, assuming elastic isotropy, we have:

$$d\underset{\sim}{\eta} = \left(d\underset{\sim}{e} - \alpha \frac{d\underset{\sim}{s}}{2\mu_o} \right) \tag{5.3}$$

We will henceforth consider $\alpha = 1$. We assume that the governing equation for creep (and plasticity) is the same as (3.21), i.e.,

$$\underset{\sim}{S} = S_y^o \frac{d\underset{\sim}{\eta}}{dz} + \underset{\sim}{r}(z) \; ; \quad \underset{\sim}{r}(z) = \int_o^z \rho_1(z - z') \frac{d\underset{\sim}{\eta}}{dz'} \, dz' \tag{5.4a,b}$$

From (5.4a) it follows that:

$$\frac{\|\underset{\sim}{S} - \underset{\sim}{r}\|^2}{(S_y^o)^2} dz^2 = d\underset{\sim}{\eta} : d\underset{\sim}{\eta} = d\zeta^2 \tag{5.5}$$

$$\text{i.e.,} \quad \frac{\|\underset{\sim}{S} - \underset{\sim}{r}\|^2}{(S_y^o)^2 f^2(\zeta)} = \frac{1}{f^2(\zeta)} \frac{(d\zeta)^2}{(dz)^2} + \frac{(dt)^2}{(dz)^2} \frac{1}{f^2(\zeta) g^2} \tag{5.6}$$

Using (5.5) in (5.1), we have:

$$dz = \frac{1}{\sqrt{1 - \left\{ \frac{\|\underset{\sim}{S} - \underset{\sim}{r}\|}{S_y^o f(\zeta)} \right\}^2}} \left(\frac{dt}{g} \right) \tag{5.7}$$

The total inelastic strain-increment, $d\underset{\sim}{\eta}$, is given from (5.4a) and (5.7) as:

$$d\underset{\sim}{\eta} = \frac{(\underset{\sim}{S} - \underset{\sim}{r})}{S_y^o} \frac{1}{\sqrt{1 - \left\{ \frac{\|\underset{\sim}{S} - \underset{\sim}{r}\|}{S_y^o f(\zeta)} \right\}^2}} \left(\frac{dt}{g} \right) \tag{5.8}$$

Finally we obtain the differential stress-strain relation in the presence of creep, by using (5.8) in (5.3), as:

$$d\underset{\sim}{S} = 2\mu_o \left\{ d\underset{\sim}{e} - \frac{(\underset{\sim}{S} - \underset{\sim}{r})}{S_y^o} \frac{1}{\sqrt{1 - \left\{ \frac{\|\underset{\sim}{S} - \underset{\sim}{r}\|}{S_y^o f(\zeta)} \right\}^2}} \left(\frac{dt}{g} \right) \right\} \tag{5.9}$$

We will postulate, as did Bazant [28] and Schapery [40] in different

contexts, that the scaling function g is a function of stress σ and the intrinsic time variable ζ, i.e., $g = g(\sigma,\zeta)$. Specifically, we assume here that:

$$g = \frac{f(\zeta)}{B}\left(\frac{\|\underset{\sim}{S} - \underset{\sim}{r}\|}{S_y^o\, f(\zeta)}\right)^{1-m} \tag{5.10}$$

where B and m are constants, so that (5.9) becomes:

$$d\underset{\sim}{S} = 2\mu_o\left\{d\underset{\sim}{e} - B\left(\frac{\|\underset{\sim}{S} - \underset{\sim}{r}\|}{S_y^o f(\zeta)}\right)^m \frac{(\underset{\sim}{S} - \underset{\sim}{r})}{\|\underset{\sim}{S} - \underset{\sim}{r}\|}\,\frac{dt}{\sqrt{1 - \left\{\frac{\|\underset{\sim}{S} - \underset{\sim}{r}\|}{S_y^o f(\zeta)}\right\}^2}}\right\} \tag{5.11}$$

When the magnitude of stress is small compared to the yield stress, we have:

$$\sqrt{1 - \left\{\frac{\|\underset{\sim}{S} - \underset{\sim}{r}\|}{S_y^o f(\zeta)}\right\}^2} \simeq 1 \tag{5.12}$$

Then, Eq. (5.11) becomes:

$$d\underset{\sim}{S} = 2\mu_o\left\{d\underset{\sim}{e} - B\left(\frac{\|\underset{\sim}{S} - \underset{\sim}{r}\|}{S_y^o f(\zeta)}\right)^m \frac{(\underset{\sim}{S} - \underset{\sim}{r})}{\|\underset{\sim}{S} - \underset{\sim}{r}\|}\, dt\right\} \tag{5.13}$$

5.B Determination of Material Constants and Numerical Results:

Following the details in section 4, for uniaxial tension, Eq. (5.11) becomes:

$$d\sigma_{11} = E_o\left\{d\varepsilon_{11} - \sqrt{\frac{2}{3}}\, B\left(\frac{|\sigma_{11} - \frac{3}{2} r_{11}|}{\sigma_y^o f}\right)^m \frac{dt}{\sqrt{1 - \left(\frac{\sigma_{11} - \frac{3}{2} r_{11}}{\sigma_y^o f}\right)^2}}\right. \tag{5.14}$$

Under constant external load, i.e., $d\sigma_{11} = 0$, the creep strain rate is thus given by:

$$\frac{d\varepsilon_{11}}{dt}=B\sqrt{\frac{2}{3}}\left(\frac{\left|\sigma_{11}-\frac{3}{2}r_{11}\right|}{\sigma_y^o f}\right)^m \frac{1}{\sqrt{1-\left(\frac{\sigma_{11}-\frac{3}{2}r_{11}}{\sigma_y^o f}\right)^2}} \tag{5.15}$$

For small values of σ_{11} as compared to σ_y^o, (5.15) may be approximated as:

$$\frac{d\varepsilon_{11}}{dt} \simeq B\sqrt{\frac{2}{3}}\left(\frac{\left|\sigma_{11}-\frac{3}{2}r_{11}\right|}{\sigma_y^o f}\right)^m \tag{5.16}$$

which is similar to the well-known Norton's power law for steady-state creep.

We assume that material parameters E_o, E_1, E_2, ρ_o (or σ_y^o) and β are determined as discussed in section 4. We now discuss ways of determining material constants B and m. When $\sigma_{11} < \sigma_y^o$, the yield surface retains its initial shape at t = 0, which implies that f = 1 and r_{11} = 0. More specifically, if (5.15) is evaluated at t = 0, we obtain:

$$\dot{\varepsilon}_{11}^o = \left.\frac{d\varepsilon_{11}}{dt}\right|_{t=o} = \sqrt{\frac{2}{3}}\,B\left(\frac{\sigma_{11}}{\sigma_y^o}\right)^m \frac{1}{\sqrt{1-\left(\frac{\sigma_{11}}{\sigma_y^o}\right)^2}} \tag{5.17}$$

Thus , we obtain:

$$\log\left[\dot{\varepsilon}_{11}^o\sqrt{1-\left(\frac{\sigma_{11}}{\sigma_y^o}\right)^2}\right] = \log\sqrt{\frac{2}{3}}\,B + m\,\log\left(\frac{\sigma_{11}}{\sigma_y^o}\right) \tag{5.18}$$

Experimental data for $\dot{\varepsilon}_{11}^o[1-(\sigma_{11}/\sigma_y^o)^2]^{\frac{1}{2}}$ versus (σ_{11}/σ_y) may be plotted in a logarithmic scale. A straight line may be used to represent the test data in a least-square sense; and from this, B and m may be determined.

We will henceforth refer to the equation of PNC [38] for the elevated

temperature (550°C) behavior of type 304 stainless steel, as a basis for comparison of the present creep relation (5.15) under constant load. As mentioned earlier, the PNC equation [38] is based on Blackburn's equation [39] and is capable of representing test data over a wide range of stress; however, the equations of [38, 39] do not consider the interaction between creep and plasticity.

We first choose material parameters B and m at 550°C, according to (5.18). Fig. 8 shows the $\dot{\varepsilon}^{o}_{11}$ vs. σ_{11} data in logarithmic scale, where the initial rate of creep strain, $\dot{\varepsilon}^{o}_{11}$ is taken according to the PNC equation [38]. The results obtained, by a straightline curve fitting, for B and m for the cases A, B, and C [with σ^{o}_{y} = 112.8, 103.0, and 92.1 MPa, respectively, as shown in Table 1] are recorded here in Table 3.

We now present results for creep behavior under constant uniaxial loading. When the prescribed stress is less than the yield stress σ^{o}_{y}, the creep analysis is carried out after first raising the stress elastically to the given value. A linear function for f, viz., $f(\zeta) = 1 + \beta\zeta$, is employed, and the increment of internal time , Δz, is assumed to be 0.5×10^{-4}. Fig. 9 shows the presently computed results for creep strain for values of σ_{11}, in each of the cases A, B, and C, respectively, along with PNC's results [38]. A good agreement may be noted between the present and PNC results for σ = 58.8 MPa. However, for larger magnitudes of σ_{11} and for longer times, the results for case A overestimate and those for C underestimate the creep strain as compared to the PNC equation.

When the prescribed stress level in uniaxial tension is higher than the yield stress, a plasticity analysis is first performed prior to a creep analysis. The steady state as observed in creep experiments may then be regarded as the case when the yield-surface ceases to translate and enlarge.

Figure 10 shows the presently computed creep strain variation with time,

along with PNC [38] data, for two values of $\sigma_{11} > \sigma_y^o$, for cases A, B, and C, respectively. In this set of results, a linear function f is used. The present results are lower than the PNC data, and the discrepancy becomes larger as σ_{11} increases. Next, we consider the effect of using a saturated function f as discussed in subsection [4.B.2.(ii)]. Fig. 11 shows the presently computed results for Case A, when the parameter 'a' in the saturated function f is assigned two different values, a = 1.2 and 1.1, respectively. It is observed that the smaller is the value of 'a', the larger is the creep strain as σ_{11} becomes higher. This is due to the fact that even a small difference between the linear and saturated yield functions f will be magnified due to the power law as in Norton's equation, or Eq. (5.15). It may also be noted that a saturated function f has little or no effect on creep strain for lower values of σ_{11}, since the saturated function f is almost identical to the linear f_1 for small values of ζ.

Figure 12 shows the calculated results for creep strain for Case A, with the value of 'a' being assigned 1.1, for various levels of σ_{11} (from 117.7 - 176.5 MPa. The experimental results as well as those from the PNC equation [38] are also shown in Fig. 12. Reasonably good agreement is noted between the three sets of data for all stress levels. It is seen that the discrepancies in analytical modeling are somewhat pronounced in the primary stages of creep, while the discrepancies tend to vanish in the steady state. It may be seem that the yield surface in the present theory tends to translate and expand from the initial state to the steady state more rapidly than it should, but the yield surface in the steady-state is modeled rather accurately.

Conclusion:

This paper presents a differential stress-strain relation for plasticity,

based on an intrinsic-time theory, which is analogous to the classical plasticity relation. Therefore, the present relation may be incorporated readily into existing numerical algorithms. The presently derived equation can approximate the test data for stress-strain curve as accurately as desired. Further, it can very accurately represent, both qualitatively as well as quantitatively, the hardening/softening behavior under cyclic plasticity.

This paper also presents a simple theory for creep based also on an 'internal time' concept. The present theory for creep assumes that the 'internal time' is characterized by both the inelastic strain and Newtonian time. The thus-derived equation employs the concept of a yield surface for plasticity, and makes it possible to incorporate the effects of interaction between creep and plasticity. The presently obtained numerical results may be considered to be reasonable, if the scarcity of available experimental data is kept in mind.

The unified theory presented herein results in constitutive relations that are simple in form; the material constants are few in number and can be easily determined as shown in the paper. It is, therefore, hoped that the present theory may become one of the useful constitutive equations for a practical estimation of inelastic material behavior.

Acknowledgements:

This work was supported by the National Aeronautics & Space Administration, Lewis Research Center, under a grant, No. NAG-346 to Georgia Institute of Technology. The authors acknowledge this support as well as the encouragement of Drs. L. Berke and C. Chamis. It is a pleasure to record here our thanks to Ms. J. Webb for her careful assistance in the preparation of this paper.

References

1. ASME Boiler and Pressure Vessel Code, Sec. III, Case Interpretations, Code Case N-47-17, ASME, 1974.

2. Pugh, C. E., Corum, J. M., Lin, K. C., and Greenstreet, W. L., "Currently Recommended Constitutive Equations for Inelastic Design Analysis of FFTF Components", ORNL TM-3602, Oak Ridge National Lab., Sept. 1972.

3. Corum, J. M., Greenstreet, W. L., Liu, K. C., Pugh, C. E., and Swindeman, R. W., "Interim Guidelines for Detailed Inelastic Analysis of High-Temperature Reactor System Components", ORNL-5014, 1974.

4. Lagneborg, R., "A Theoretical Approach to Creep Deformation During Intermittent Load", Journal of Basic Engineering, Trans. ASME, Vol. 93, No. 2, 1971, pp. 205-210.

5. Gittus, J. H., "Development of Constitutive Relation for Plastic Deformation from a Dislocation Model", Journal of Engineering Materials and Technology, Trans ASME, Vol 98, No. 1, 1976, pp. 52-59.

6. Besseling, J. F., "Theory of Elastic, Plastic, and Creep Deformations of an Initially Isotropic Material Showing Anisotropic Strain-Hardening, Creep Recovery, and Secondary Creep", Journal of Applied Mechanics, Vol. 25, 1958, pp. 529-536.

7. Malinin, N. N. and Khadjinsky, G. M., "Theory of Creep with Anisotropic Hardening", International Journal of Mechanical Science, Vol. 14, No. 4, 1972, pp. 235-246.

8. Jaske, C. E., Leis, B. N., and Pugh, C. E., "Monotonic and Cyclic Stress-Strain Response of Annealed 2 1/4 Cr-1Mo Steel", Symposium on Structural Materials for Service at Elevated Temperatures in Nuclear Power Generation, (Ed. Schaefer), ASME Winter Annual Meeting, 1975, pp. 191-212.

9. Kratochvil, J. and Dillon, O. W. Jr., "Thermodynamics of Crystalline Elastic-Visco-Plastic Materials", Journal of Applied Physics, Vol. 41, No. 4, 1970, pp, 1470-1479.

10. Kujawski, D. and Mroz, Z., "A Viscoplastic Material Model and Its Application to Cyclic Loading", Acta Mechanica, Vol. 36, No. 3-4, 1980, pp. 213-230.

11. Ponter, A. R. S. and Leckie, F. A., "Constitutive Relations for the Time Dependent Deformation of Metals", Journal of Engineering Materials and Technology, Trans. ASME, Vol. 98, No. 1, 1976, pp. 47-51.

12. Chaboche, J. L., "Viscoplastic Constitutive Equations for the Description of Cyclic and Anisotropic Behavior of Metals", Bulletin de L'Academie Polonaise des Sciences, Serie des Sciences Techniques, Vol. XXV, No. 1, 1977, pp. 33-42.

13. Bodner, S. R. and Partom, Y., "Constitutive Equations for Elastic-Viscoplastic Strain-Hardening Materials", Journal of Applied Mechanics, Trans. ASME, Vol. 42, No. 2, 1975, pp. 385-389.

14. Hart, E. W., "Constitutive Relations for the Nonelastic Deformation of Metals", Journal of Engineering Materials and Technology, Trans. ASME, Vol 98, No. 3, 1976, pp. 193-202.

15. Hart, E. W., Li, C. Y., Yamada, H., and Wire, G. L., "Phenomenological Theory: A Guide to Constitutive Relations and Fundamental Deformation Properties", Constitutive Equations in Plasticity, (Ed. Argon, A.S.), M.I.T. Press, 1976, pp. 149-197.

16. Miller, A., "An Inelastic Constitutive Model for Monotonic, Cyclic and Creep Deformation: Part I - Equations Development and Analytical Procedures", Journal of Engineering Materials and Technology, Trans. ASME, Vol. 98, No. 2, 1976, pp. 97-105.

17. Miller, A., "An Inelastic Constitutive Model for Monotonic, Cyclic and Creep Deformation: Part II - Application to Type 304 Stainless Steel", Journal of Engineering Materials and Technology, Trans. ASME, Vol. 98, No. 2, 1976, pp. 106-113.

18. Krieg, R. D., Swearengen, J. C. and Rohde, R. W., "A Physically-Based Internal Variable Model for Rate-Dependent Plasticity", Inelastic Behavior of Pressure Vessel and Piping Components, ASME PVP-PB-028, (Ed. Chang, T. Y., and Kremple, E.), 1978, pp. 15-28.

19. Robinson, D.N., "A Unified Creep-Plasticity Model for Structural Metals at High Temperatures", ORNL TM-5969, October 1978.

20. Lee, D. and Zaverl, F. Jr., "A Generalized Strain Rate Dependent Constitutive Equation for Anisotropic Metals", Acta Metallurgica, Vol. 26, No. 11, 1978, pp. 1771-1780.

21. Stouffer, D. C. and Bodner, S. R., "A Constitutive Model for the Deformation Induced Anisotropic Plastic Flow of Metals", International Journal of Engineering Science, Vol. 17, 1979, pp. 757-764.

22. Bodner, S. R., Partom, I., and Partom, Y., "Uniaxial Cyclic Loading of Elastic-Viscoplastic Materials", Journal of Applied Mechanics, Trans. ASME, Vol. 46, No. 4, 1979, pp. 805-810.

23. Cernocky, E. P. and Kremple, E., "A Theory of Viscoplasticity Based on Infinitesimal Total Strain", Acta Mechanica, Vol. 36, 1980, pp. 263-289.

24. Findley, W. N. and Lai, J. S., "Creep and Recovery of 2618 Aluminum Alloy Under Combined Stress with a Representation by a Viscous-Viscoelastic Model", Journal of Applied Mechanics, Trans. ASME, Vol. 45, No. 3, 1978, pp. 507-514.

25. Valanis, K. C., "A Theory of Viscoplasticity without a Yield Surface, Part I. General Theory', Archives of Mechanics, Vol. 23, No. 4, 1971, pp. 517- 533.

26. Valanis, K. C., "A Theory of Viscoplasticity without a Yield Surface, Part II. Application to Mechanical Behavior of Metals", Archives of Mechanics, Vol. 23, No. 4, 1971, pp. 535-551.

27. Bazant, Z. P. and Bhat, P. D., "Endochronic Theory of Inelasticity and Failure of Concrete", Journal of the Engineering Mechanics Division, ASCE, Vol. 102, No. EM4, 1976, pp. 701-722.

28. Bazant, Z. P., "Endochronic Inelasticity and Incremental Plasticity", International Journal of Solids and Structures, Vol. 14, No. 9, 1978, pp. 691-714.

29. Valanis, K. C., "Fundamental Consequence of a New Intrinsic Time Measure-Plasticity as a Limit of the Endochronic Theory", Archives of Mechanics, Vol. 32, No. 2, 1980, pp. 171-191.

30. Wu, H. C. and Yip, M. C., "Endochronic Description of Cyclic Hardening Behavior for Metallic Materials", Journal of Engineering Materials and Technology, Trans. ASME, Vol. 103, No. 3, 1981, pp. 212-217.

31. Wu, H. C. and Yip, M. C., "Strain Rate and Strain Rate History Effects on the Dynamic Behavior of Metallic Materials", International Journal of Solids and Structures, Vol. 16, No. 6, 1980, pp. 515-536.

32. Valanis, K. C. and Fan, J., "Endochronic Analysis of Cyclic Elastoplastic Strain Fields in a Notched Plate", Journal of Applied Mechanics, Trans. ASME, Vol. 50, No. 4a, 1983, pp. 789-794.

33. Rice, J. R., "On the Structure of Stress-Strain Relations for Time-Dependent Plastic Deformation in Metals", Journal of Applied Mechanics, Trans. ASME, Vol. 37, No. 3, 1970, pp. 728-737.

34. Hill, R. and Rice, J. R., "Constitutive Analysis of Elastic-Plastic Crystals at Arbitrary Strain", Journal of Mechanics and Physics of Solids, Vol. 20, 1972, pp. 401-413.

35. Rice, J. R., "Continuum Mechanics and Thermodynamics of Plasticity in Relation to Microscale Deformation Mechanics", Constitutive Equations in Plasticity, (Ed. Argon, A.S.), M.I.T. Press, 1975, pp. 23-79.

36. Rivlin, R. S., "Some Comments on the Endochronic Theory of Plasticity", International Journal of Solids and Structures, Vol. 17, 1981, pp. 231-248.

37. Atluri, S. N., "On Constitutive Relations at Finite Strain: Hypo-Elasticity and Elastoplasticity with Isotropic or Kinematic Hardening", Computer Methods in Applied Mechanics and Engineering, 1984 (In Press).

38. Report of Research Cooperation Subcommittee 55 on Design Application Procedure of Inelastic Analysis (II), (Chairman, Yamada, Y.), Japan Society of Mechanical Engineers, 1981 (In Japanese).

39. Blackburn, L. D., "Isochronous Stress-Strain Curves for Austenitic Stainless Steels", The Generation of Isochronous Stress-Strain Curves (Ed. Schaefer, A.O.), ASME Winter Annual Meeting, ASME, 1972, pp. 15-48.

40. Schapery, R. A., "On a Thermodynamic Constitutive Theory and Its Application to Various Nonlinear Materials", IUTAM Symposium on Thermoinelasticity, East Kilbride, June 1968, (Ed. Boley, B.A.), Springer-Verlag, pp. 259-285.

Table 1. Material Constants "Read-off" from Test Data

	σ_o^o (MPa)	E_p (GPA)	σ_o^∞ (MPa)	E_t (GPa)	$\sigma_o^{o'}$ (MPa)	E_p' (GPa)	E_o (GPa)
Case A	112.8	17.8	155.0	1.57	-----	----	153.8
Case B	112.8	17.8	155.0	1.57	103.0	44.4	153.8
Case C	112.8	17.8	155.0	1.57	92.1	49.0	153.8

Table 2. Material Constants "Derived" for Present Analytical Modeling

	E_1 (GPa)	α_1	E_2 (GPa)	E_3 (GPa)	α_3	β	σ_y^o (MPa)
Case A	14.3	314	.054	----	----	5	112.8
Case B	14.3	314	.054	23.1	2212	5	103.0
Case C	14.3	314	.054	27.2	2212	5	92.1

Table 3. Material Constants B, m Derived for Present Analytical Modeling of Creep

	B	m
Case A	4.87×10^{-6}	5.2
Case B	2.74×10^{-6}	5.16
Case C	1.23×10^{-6}	4.9

List of Figures

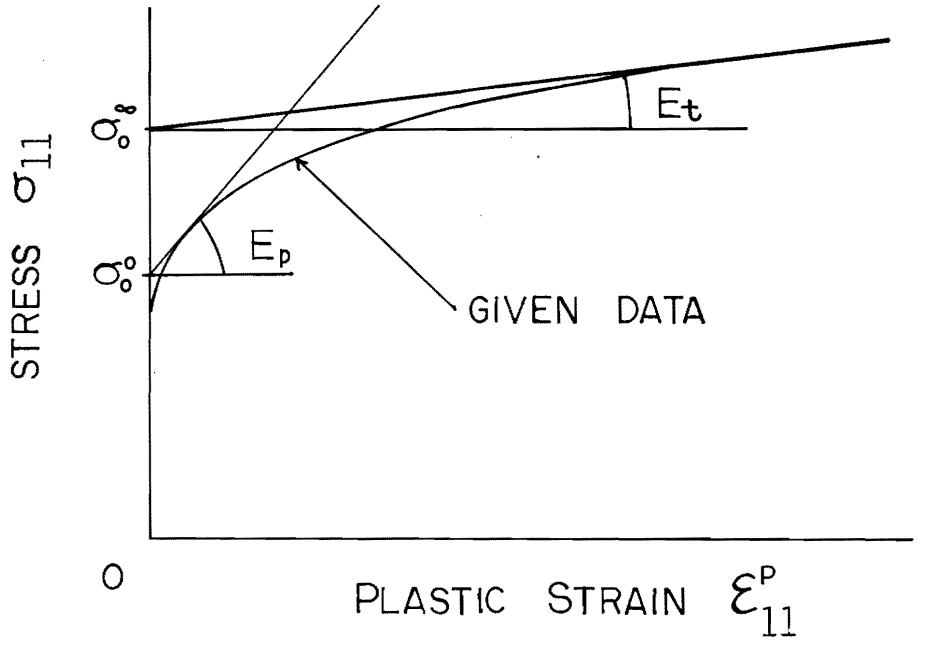

(A) TWO-TERM APPROXIMATION

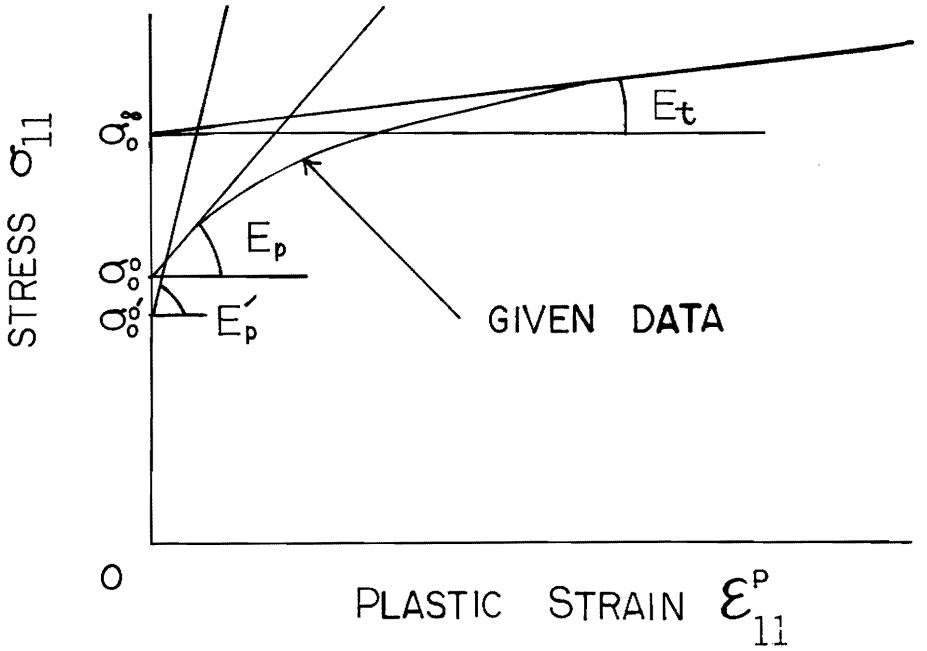

(B) THREE-TERM APPROXIMATION

FIGURE 1

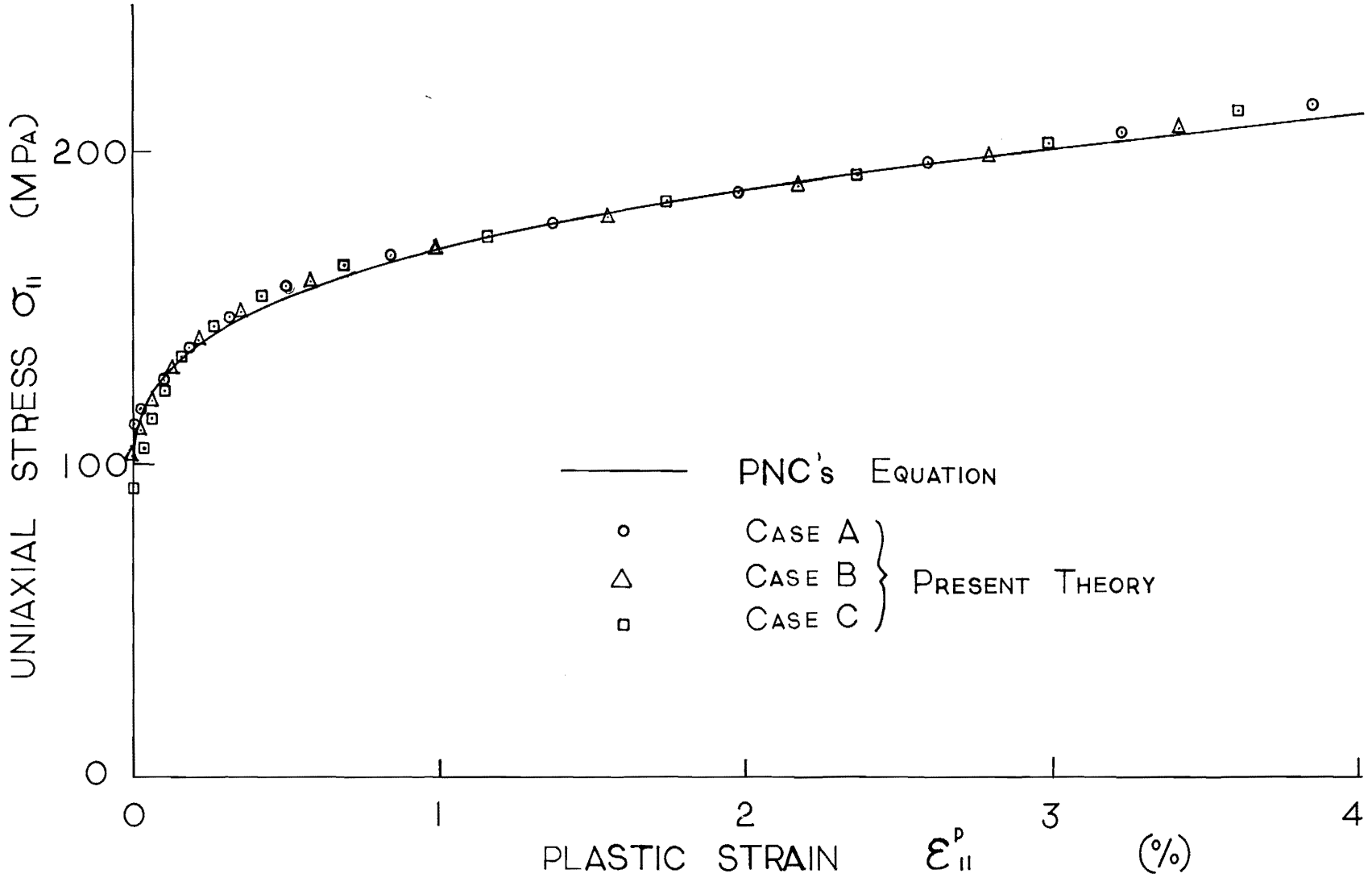
UNIAXIAL STRESS σ_{11} (MPA)
200
100
0
0
1
2
3
4
PLASTIC STRAIN ε^p_{11} (%)
PNC's EQUATION
CASE A
CASE B
CASE C
PRESENT THEORY

FIGURE 2

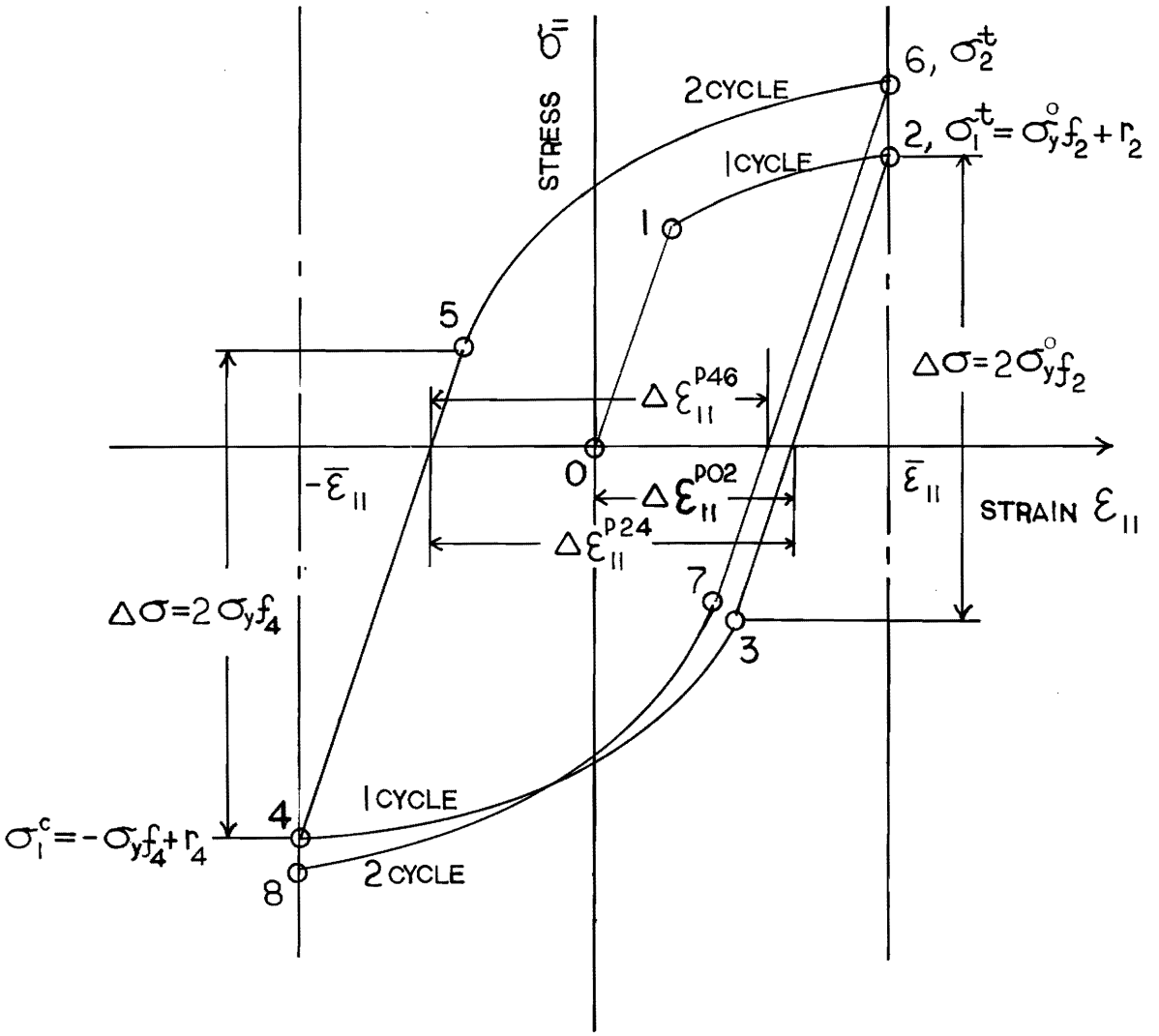
STRESS σ_{11}
STRAIN ε_{11}
6, σ_2^t
2CYCLE
2, $\sigma_1^t = \sigma_y^o f_2 + r_2$
1CYCLE
1
5
$\Delta\sigma = 2\sigma_y^o f_2$
$\Delta\varepsilon_{11}^{p46}$
$-\bar{\varepsilon}_{11}$
0
$\Delta\varepsilon_{11}^{p02}$
$\bar{\varepsilon}_{11}$
$\Delta\varepsilon_{11}^{p24}$
7
3
$\Delta\sigma = 2\sigma_y f_4$
1CYCLE
$\sigma_1^c = -\sigma_y f_4 + r_4$
4
2CYCLE
8

FIGURE 3

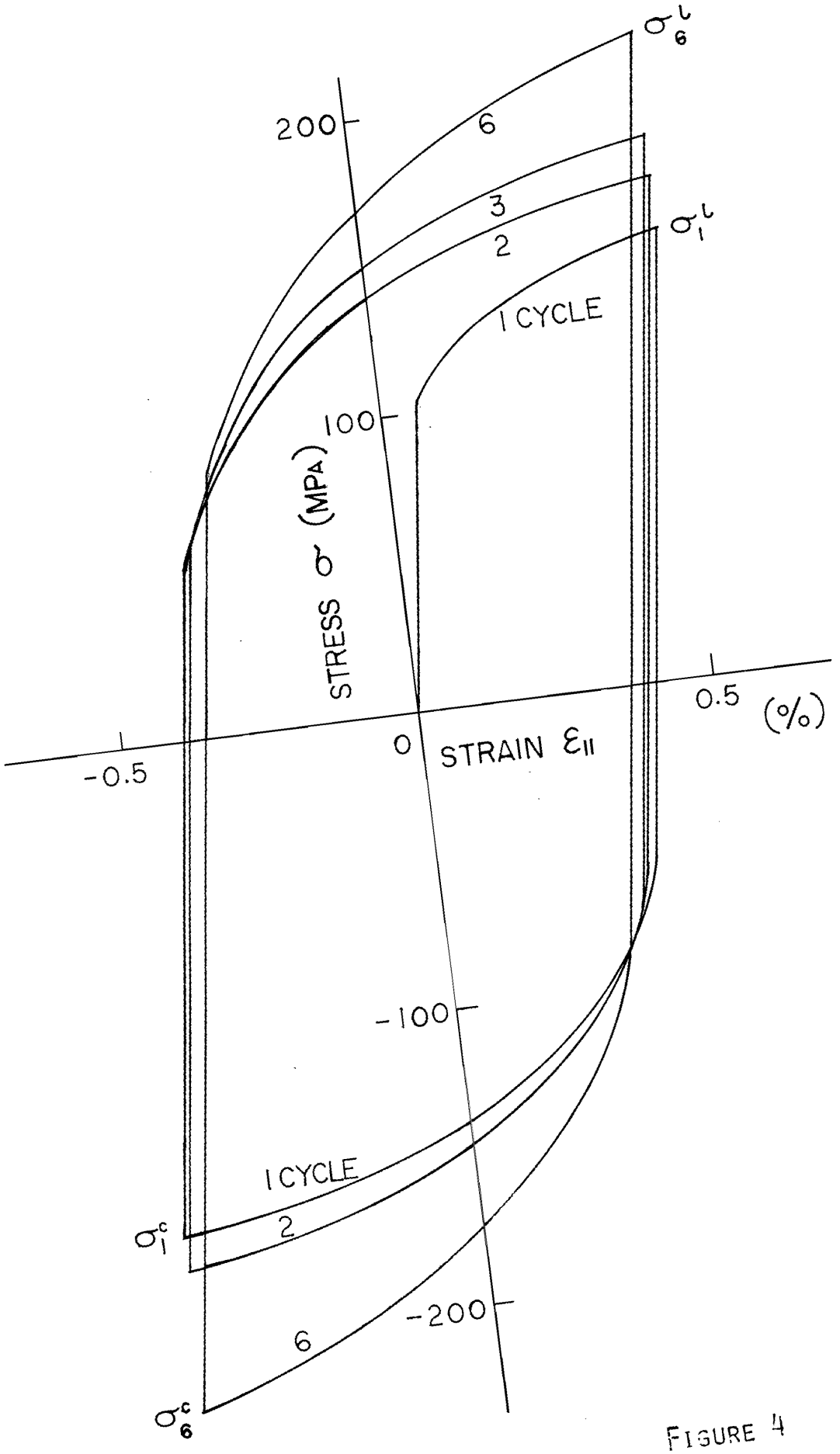
σ_6^t
200
6
3
2
σ_1^t
1 CYCLE
100
STRESS σ (MPA)
0.5
(%)
-0.5
0
STRAIN ε_{11}
-100
1 CYCLE
2
σ_1^c
-200
6
σ_6^c

FIGURE 4

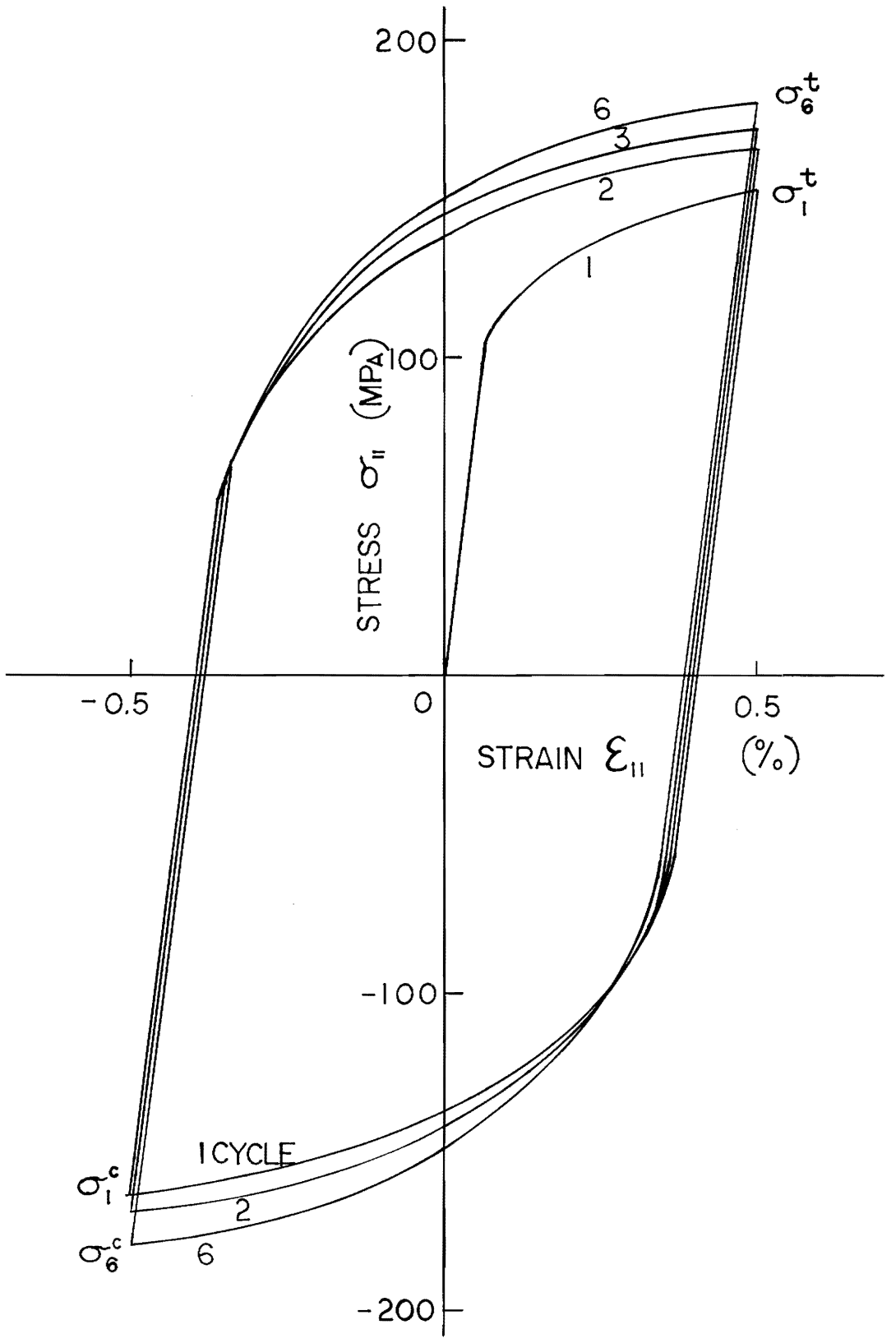
200
100
-100
-200
-0.5
0
0.5
(%)
STRESS σ_{11} (MPA)
STRAIN ε_{11}
σ_6^t
σ_1^t
6
3
2
1
1CYCLE
σ_1^c
σ_6^c
2
6

FIGURE 5

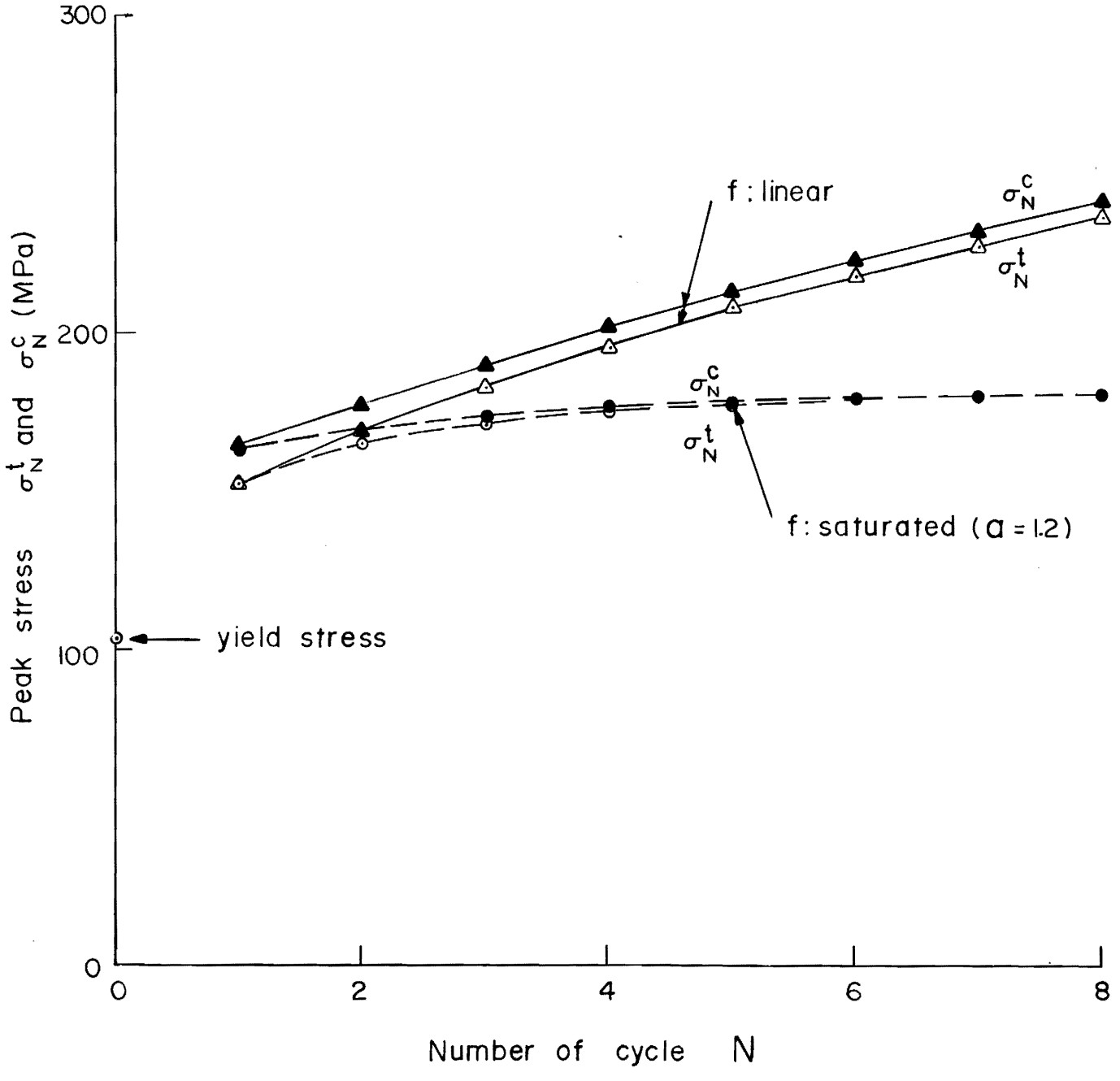
300
200
100
0
0
2
4
6
8
Peak stress σ_N^t and σ_N^c (MPa)
Number of cycle N
f : linear
σ_N^c
σ_N^t
σ_N^c
σ_N^t
f : saturated (α = 1.2)
yield stress

FIGURE 6

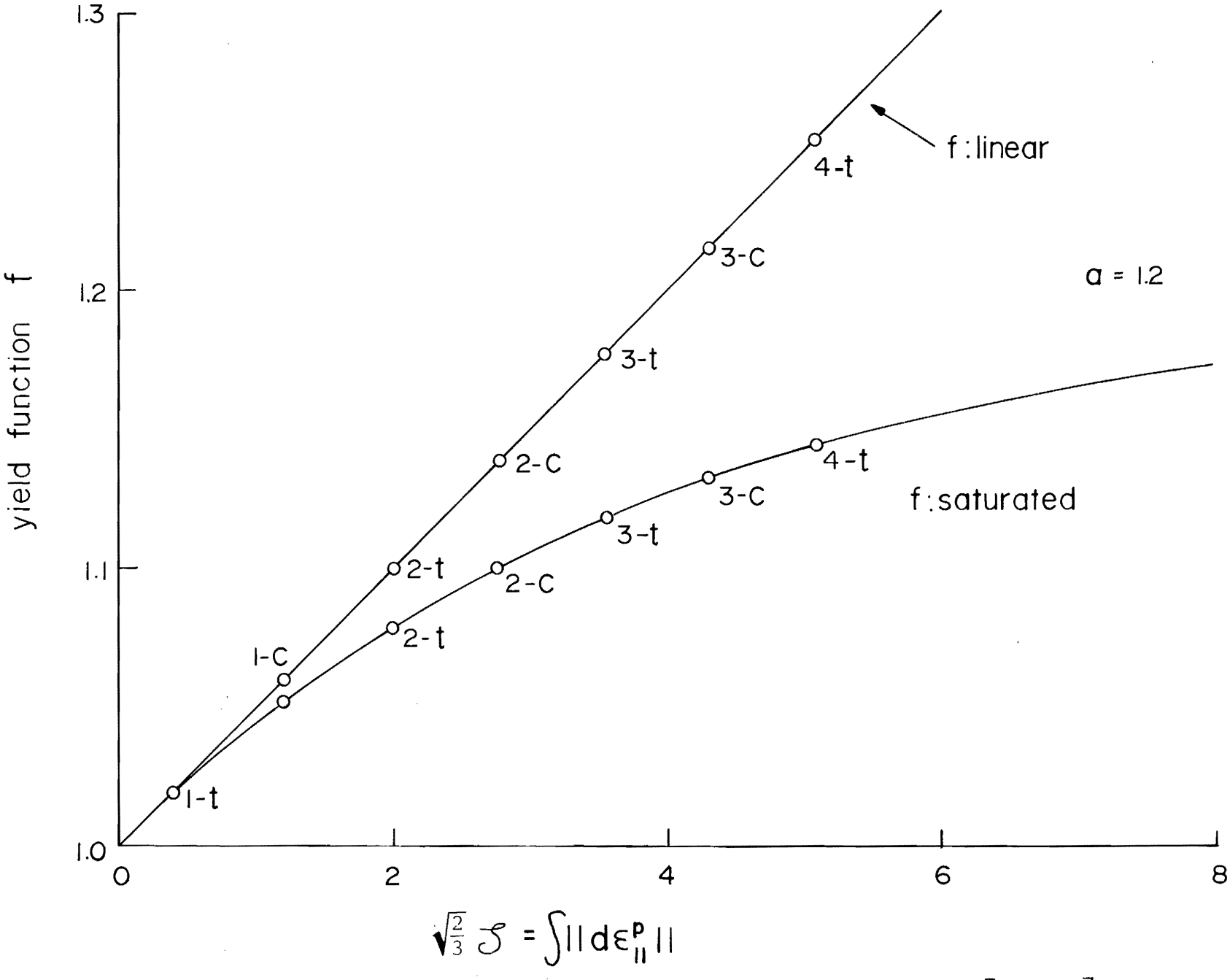
1.3
1.2
1.1
1.0
yield function f
0
2
4
6
8
$\sqrt{\frac{2}{3}}\,\mathcal{S} = \int \| d\varepsilon^{p}_{11} \|$
f : linear
f : saturated
a = 1.2
1-t
1-c
2-t
2-c
3-t
3-c
4-t

FIGURE 7

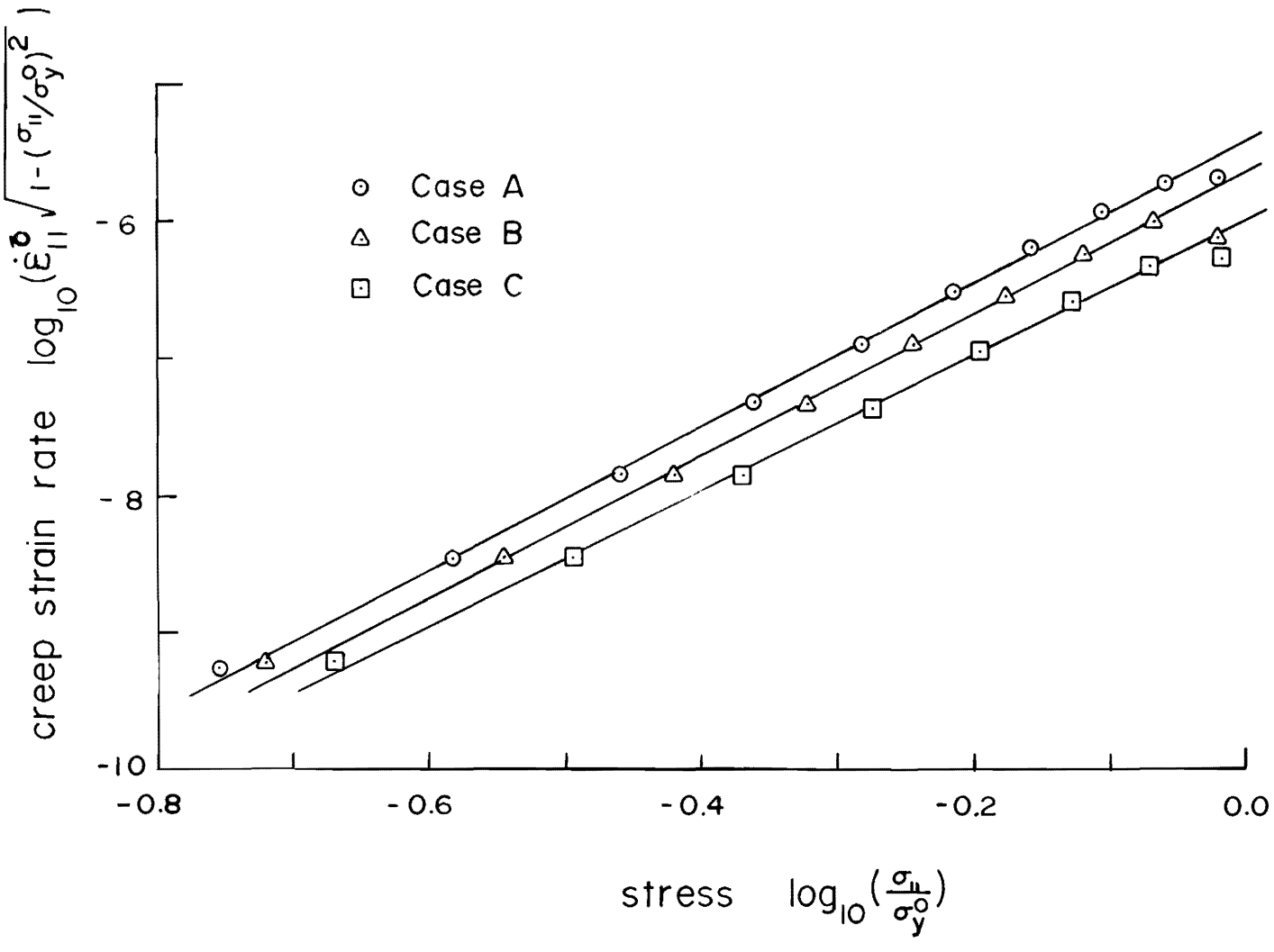
creep strain rate $\log_{10}(\dot{\varepsilon}^{o}_{11}\sqrt{1-(\sigma_{11}/\sigma^{o}_{y})^{2}})$
-6
-8
-10
-0.8
-0.6
-0.4
-0.2
0.0
Case A
Case B
Case C
stress $\log_{10}(\frac{\sigma_E}{\sigma^{o}_{y}})$

FIGURE 3

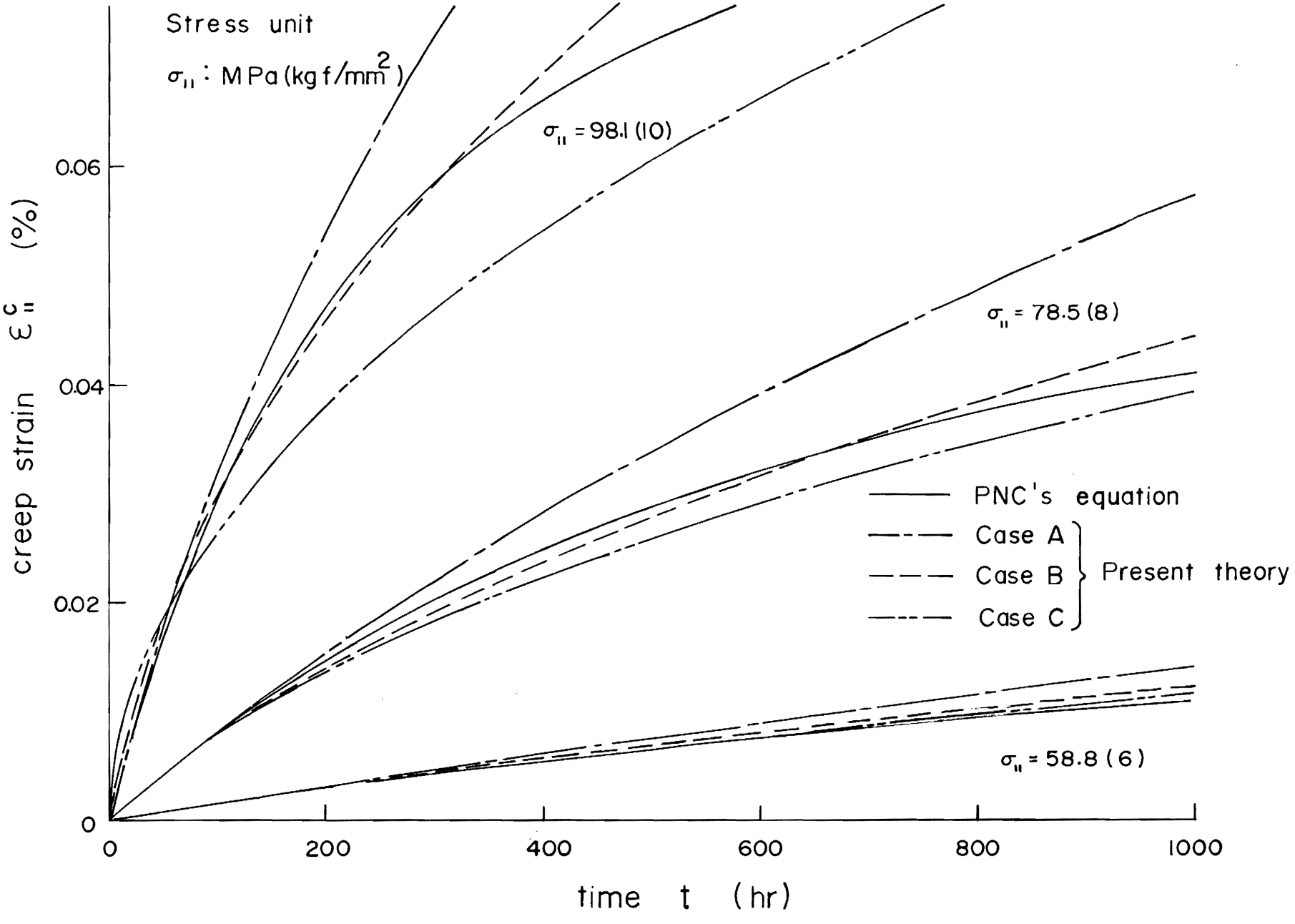
Stress unit
σ_{11} : MPa (kg f/mm^2)
σ_{11} = 98.1 (10)
σ_{11} = 78.5 (8)
σ_{11} = 58.8 (6)
PNC's equation
Case A
Case B
Case C
Present theory
creep strain ε_{11}^c (%)
0.06
0.04
0.02
0
0
200
400
600
800
1000
time t (hr)

FIGURE 9

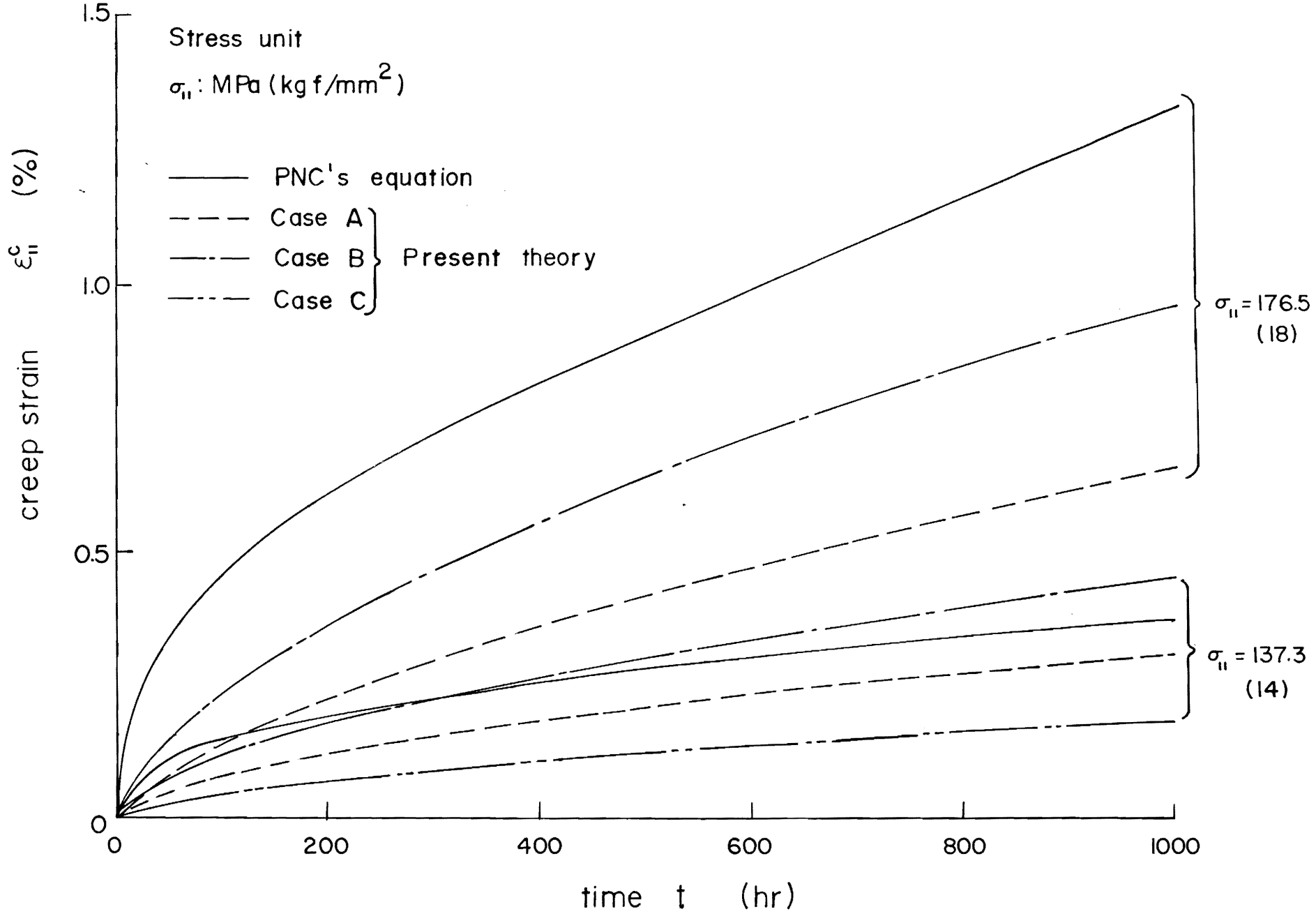
Stress unit
σ_{11} : MPa (kg f/mm^2)
PNC's equation
Case A
Case B
Case C
Present theory
σ_{11} = 176.5
(18)
σ_{11} = 137.3
(14)
creep strain ε^c_{11} (%)
time t (hr)
0
0.5
1.0
1.5
200
400
600
800
1000

FIGURE 10

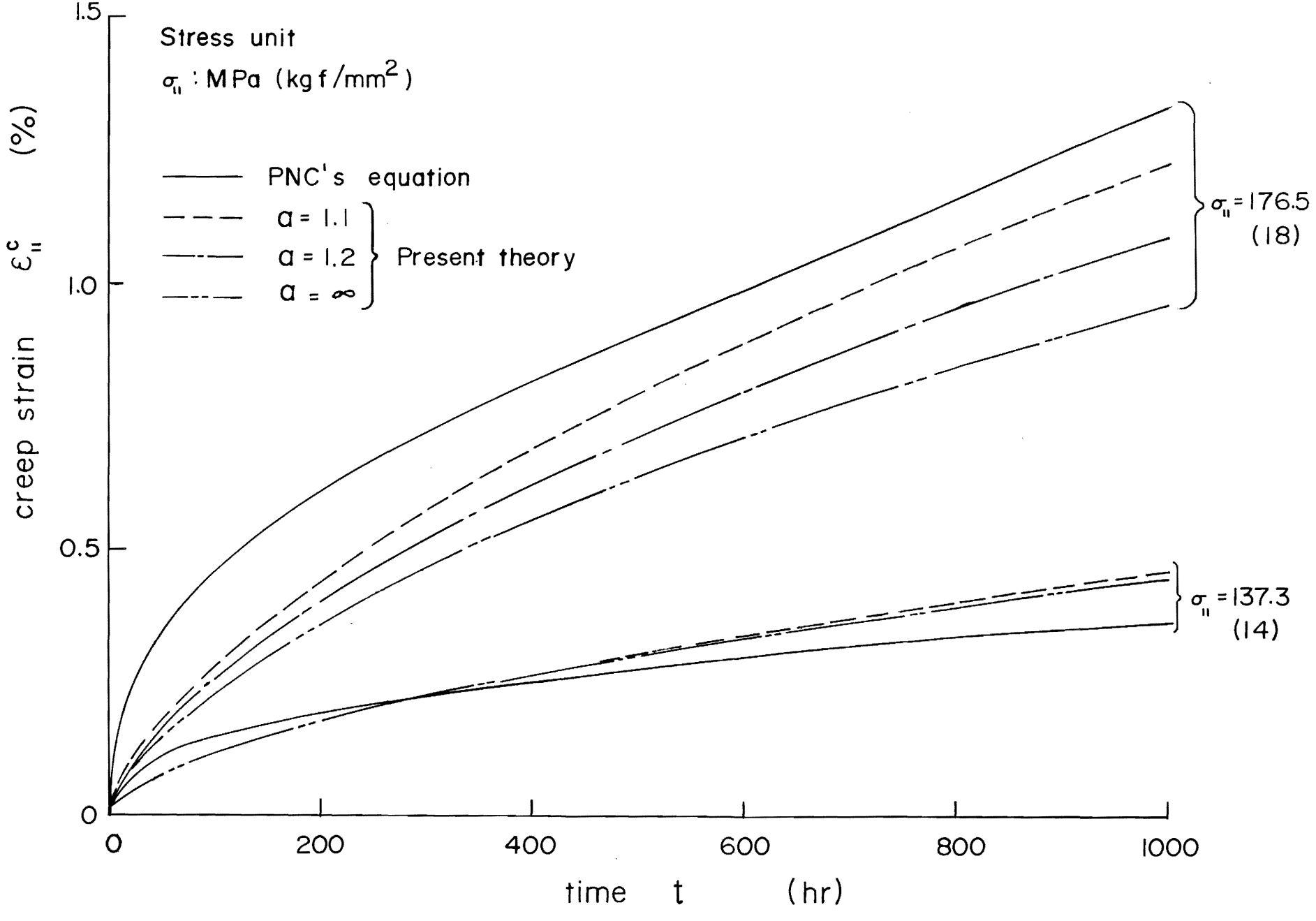
Stress unit
σ_{11} : MPa (kgf/mm^2)
PNC's equation
a = 1.1
a = 1.2
a = ∞
Present theory
σ_{11} = 176.5
(18)
σ_{11} = 137.3
(14)
creep strain ε^c_{11} (%)
1.5
1.0
0.5
0
0
200
400
600
800
1000
time t (hr)

FIGURE 11

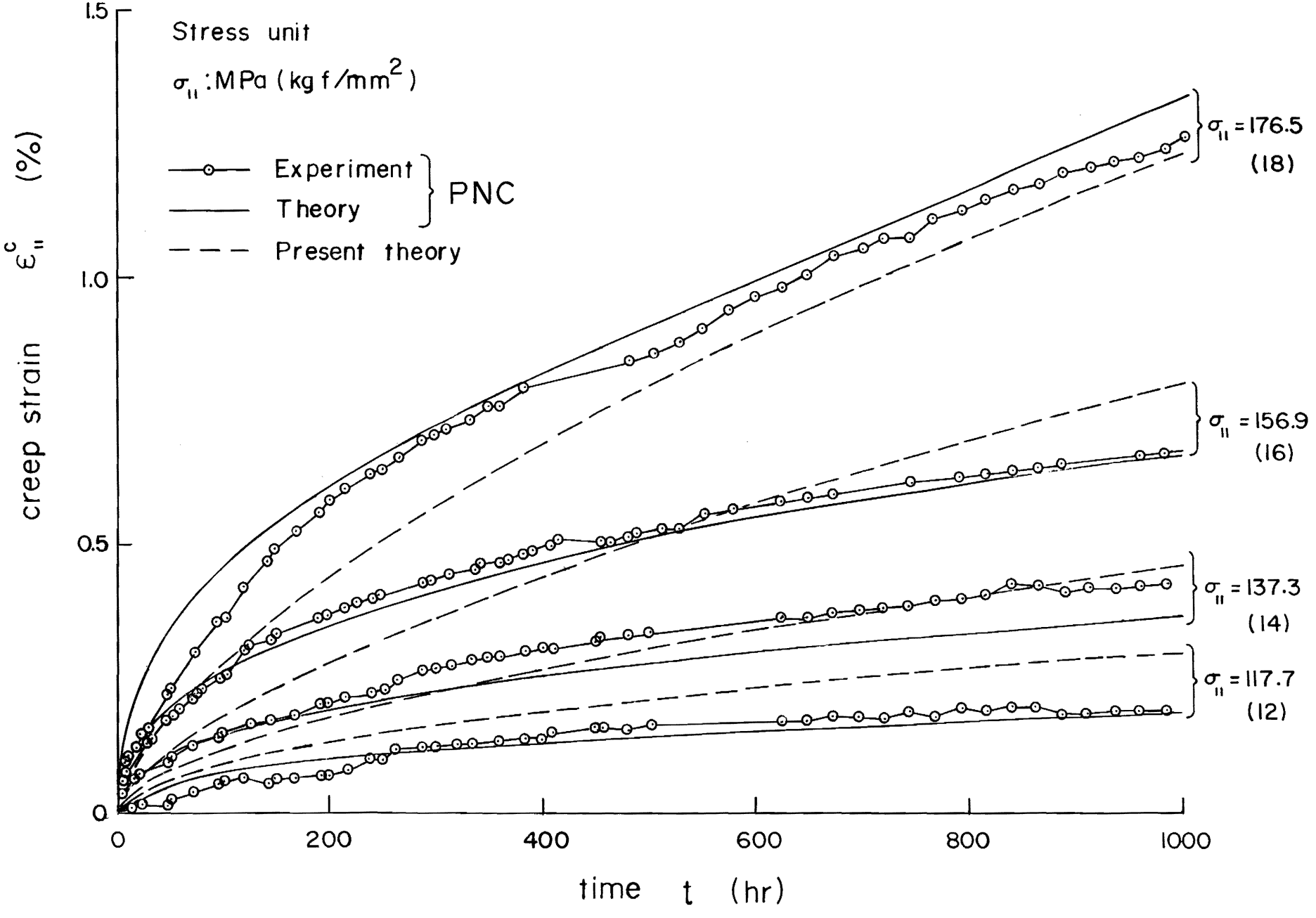
Stress unit
σ_{11} : MPa (kg f/mm^2)
Experiment
Theory
PNC
Present theory
σ_{11} = 176.5
(18)
σ_{11} = 156.9
(16)
σ_{11} = 137.3
(14)
σ_{11} = 117.7
(12)
creep strain ε^c_{11} (%)
1.5
1.0
0.5
0
0
200
400
600
800
1000
time t (hr)

Final Technical Report

on

National Aeronautics & Space Administration

Lewis Research Center

Grant Nos. NAG-346 & NAG-338

(Georgia Tech Project No: E-20-605)

Prepared by

Satya N. Atluri
Regents' Professor & Director
Computational Mechanics Center
Georgia Institute of Technology
Atlanta, GA 30332-0356

Tele: (404)894-2758

Fax: (404)894-2299

COMPUTER METHODS IN APPLIED MECHANICS AND ENGINEERING 43 (1984) 137–171
NORTH-HOLLAND

ON CONSTITUTIVE RELATIONS AT FINITE STRAIN: HYPO-ELASTICITY AND ELASTO-PLASTICITY WITH ISOTROPIC OR KINEMATIC HARDENING*

Satya N. ATLURI
Center for the Advancement of Computational Mechanics, Georgia Institute of Technology, Atlanta, GA 30332, U.S.A.

Received 22 March 1983

The question of 'generalization' to finite strains of the constitutive relations of infinitesimal strain theory of elasticity, and classical elasto-plasticity with isotropic and kinematic hardening, is critically examined. Simple generalizations, which lead to physically plausible material behaviour, are presented.

The current controversies surrounding (i) the choice of stress-rate in the above generalization and (ii) the 'anomaly' of oscillatory stresses in kinematic hardening plasticity, as discussed by E.H. Lee and others, are analyzed. It is found that these 'controversies' are easily resolvable.

0. Introduction

Nagtegaal and de Jong [1] presented in 1981 some interesting results for stresses generated by simple finite shear of elastic-plastic and rigid-plastic materials which exhibit anisotropic hardening. In the equation for the rate of change of the shift tensor $\boldsymbol{\alpha}$ (the current center of the yield surface), they used the Zaremba–Jaumann–Noll rigid body rate of $\boldsymbol{\alpha}$. They found the rather spurious result that the shear stress is oscillatory in time.

The above 'anomaly' has prompted a series of investigations by Lee and his associates [2, 3]. As a 'remedy', Lee et al. [2, 3] suggest the use of a 'modified' Jaumann derivative of $\boldsymbol{\alpha}$ in the evolution equation for $\boldsymbol{\alpha}$. While the use of such a modified derivative in the specific problem of simple shear has been illustrated [2], its generalization to the three-dimensional non-homogeneous case is not yet fully developed. It has been suggested [2] that "a complete investigation of the micro-mechanics and the structures of possible macroscopic constitutive relations will no doubt be needed to fully understand this phenomenon and to generate a fully tested theory".

It turns out that the anomalies as described above are not peculiar to anisotropic plasticity alone; similar behaviour in finite shear may result even in the case of hypo-elasticity and classical isotropic hardening plasticity theory.

Thus, we go back to the central problem of 'generalizing' to the finite strain case, of the constitutive relations of infinitesimal strain theories of classical plasticity with isotropic or kinematic hardening. We discuss the problem of hypo-elasticity as well.

*The author presents this paper to his good friend and colleague, Professor J. Edmund Fitzgerald, on the occasion of his sixtieth birthday.

We show that the current controversies surrounding the choice of stress rate in the finite-strain generalizations of the constitutive relations and the anomalies surrounding kinematic hardening plasticity theory are easily resolvable.

The contents of the paper in the order of their appearance are: (i) preliminaries concerning various 'objective' stress-rates; (ii) some anomalies that may arise even in *elasticity* due to 'simple generalizations' of constitutive relations of infinitesimal strain to finite strain, and (iii) '*proper generalizations*' which lead to physically 'plausible' material behaviour in the case of (iv) hypo-elasticity, (v) classical elasto-plasticity with isotropic hardening, and (vi) classical elasto-plasticity with kinematic hardening.

Notation: Let $\boldsymbol{a}$ be a vector and $\boldsymbol{A}$ a tensor, then

$$\boldsymbol{a} = a_i \boldsymbol{g}^i, \qquad \boldsymbol{A} = A_{ij}\boldsymbol{g}^i\boldsymbol{g}^j, \qquad \boldsymbol{A}\cdot\boldsymbol{a} = A_{ij}a^j\boldsymbol{g}^i,$$
$$\boldsymbol{A}\cdot\boldsymbol{B} = A^{m}_{\cdot n}B^{nk}\boldsymbol{g}_m\boldsymbol{g}_k, \qquad \boldsymbol{A}:\boldsymbol{B} = A^{ij}B_{ij},$$
$$\boldsymbol{A}' = \boldsymbol{A} - \tfrac{1}{3}(\boldsymbol{A}:\boldsymbol{I})\boldsymbol{I} = \text{deviatoric part of tensor } \boldsymbol{A}.$$

1. Preliminaries

Let P be a point, with a position vector $\boldsymbol{R}$, in the undeformed body B. Let p be the map of P in the deformed configuration b, and let the position vector of p be $\boldsymbol{r}$. In general $\boldsymbol{R}$ and $\boldsymbol{r}$ may be measured in arbitrary coordinate frames. Let

$$\mathrm{d}\boldsymbol{R} = \boldsymbol{G}_J\,\mathrm{d}\xi^J \tag{1.1}$$

where ξ^J are arbitrary curvilinear coordinates in B. Then let

$$\mathrm{d}\boldsymbol{r} = \boldsymbol{g}_i\,\mathrm{d}\eta^i = \boldsymbol{g}_J\,\mathrm{d}\xi^J \tag{1.2}$$

where η^i are another set of curvilinear coordinates in b, while ξ^J in b are the 'convected' or 'intrinsic' coordinates. For instance, ξ^J in B as well as η^i in b can both be Cartesian, while ξ^J in b will in general be curvilinear.

Now, the true or Cauchy stress at p in b, denoted here by $\boldsymbol{\tau}$, can be represented as:

$$\boldsymbol{\tau} = \tau^{mn}\boldsymbol{g}_m\boldsymbol{g}_n = \tau^{M^*N^*}\boldsymbol{g}_M\boldsymbol{g}_N \tag{1.3}$$

where the superscripts (M^*N^*) identify the components of $\boldsymbol{\tau}$ in the convected basis $\boldsymbol{g}_M$ at p, as opposed to $\boldsymbol{G}_M$ at P.

Likewise, the Kirchhoff stress tensor denoted here as $\boldsymbol{\sigma}$, can be represented as:

$$\boldsymbol{\sigma} = J\boldsymbol{\tau} = \sigma^{mn}\boldsymbol{g}_m\boldsymbol{g}_n = \sigma^{M^*N^*}\boldsymbol{g}_M\boldsymbol{g}_N, \tag{1.4}$$
$$\sigma^{mn} = J\tau^{mn}, \qquad \sigma^{M^*N^*} = J\tau^{M^*N^*}$$

where J is the determinant of the deformation gradient $\boldsymbol{F}$.

Let v be the instantaneous (at time t) velocity of the material particle at p. Let

$$v = v^m g_m = v^{M^*} g_M . \tag{1.5}$$

Let the velocity gradient e be defined as

$$e = v_{m|n} g^m g^n = v^{J^*}_{:M^*} g_J g^M \tag{1.6}$$

where $(\ )_{|n}$ and $(\ )_{:M^*}$ denote covariant derivatives w.r.t η^n and ξ^M, respectively, using the metric at p. We use the decomposition

$$e = \varepsilon + \omega \tag{1.7}$$

where ε is the strain-rate and ω the spin.

It can be shown [4] that the time rates of change of bases g_M, g^N, g_m, g^n are:

$$\frac{\mathrm{d}(g_M)}{\mathrm{d}t} = e \cdot g_M, \qquad \left(\frac{\mathrm{d}g^N}{\mathrm{d}t}\right) = -e^t \cdot g^N , \tag{1.8}$$

$$\frac{\mathrm{d}g_m}{\mathrm{d}t} = \Gamma^l_{mj} v^j g_l, \qquad \frac{\mathrm{d}g^n}{\mathrm{d}t} = -\Gamma^n_{mj} v^j g^m \tag{1.9}$$

where Γ^l_{mj} are the Christoffel symbols for spatial coordinates η^i at p. If the time rate of change of convecting bases due to a rigid spin of magnitude ω is identified as $(\hat{\mathrm{d}}/\mathrm{d}t)$, it can be shown [4] that

$$\frac{\hat{\mathrm{d}}g_M}{\mathrm{d}t} = \omega \cdot g_M , \qquad \frac{\hat{\mathrm{d}}g^N}{\mathrm{d}t} = \omega \cdot g^N . \tag{1.10}$$

Further, it is easy [4] to verify that

$$\frac{\mathrm{d}}{\mathrm{d}t}(g_{ML}) = 2\varepsilon_{ML} , \qquad \frac{\hat{\mathrm{d}}}{\mathrm{d}t}(g_{ML}) = 0 . \tag{1.11a,b}$$

We now consider the time rate of change of τ for a fixed material particle identified by ξ^J. Thus we define, from (1.3) and (1.9), the material derivative of τ as:

$$\left.\frac{\mathrm{d}\tau}{\mathrm{d}t}\right|_{\xi^J} = \frac{\mathrm{D}\tau}{\mathrm{D}t} = \frac{\mathrm{D}\tau^{mn}}{\mathrm{D}t} g_m g_n = \left[\left(\frac{\partial \tau^{mn}}{\partial t}\right)\Big|_{\eta^l} + v^l \tau^{mn}\Big|_{l}\right] g_m g_n . \tag{1.12}$$

It can be verified that all the four types of derivatives, $\mathrm{D}\tau^{mn}/\mathrm{D}t$, $\mathrm{D}\tau_{mn}/\mathrm{D}t$, ..., $\mathrm{D}\tau^{n}_{m}/\mathrm{D}t$ form the components of one and the same tensor $(\mathrm{D}\tau/\mathrm{D}t)$.

Suppose that $(\hat{\mathrm{d}}\tau_{M^*N^*}/\mathrm{d}t)$ is the rate of change of the stress components relative to the bases $\hat{g}_M$ that *spin* rigidly with the material element at the rate ω. Then due to (1.11b), it is seen [4] that all the four types of components, $(\hat{\mathrm{d}}\tau_{M^*N^*}/\mathrm{d}t)$, $(\hat{\mathrm{d}}\tau^{M^*N^*}/\mathrm{d}t)$, ..., $(\hat{\mathrm{d}}\tau^{N^*}_{M^*}/\mathrm{d}t)$ form the components of one and the same tensor, denoted here as $(\hat{\mathrm{d}}\tau/\mathrm{d}t)$. It can be shown [4] from (1.3) and (1.10) that

$$\frac{\hat{\mathrm{d}}\boldsymbol{\tau}}{\mathrm{d}t} = \frac{\mathrm{D}\boldsymbol{\tau}}{\mathrm{D}t} + \boldsymbol{\tau}\cdot\boldsymbol{\omega} - \boldsymbol{\omega}\cdot\boldsymbol{\tau} \tag{1.13}$$

which can be labeled [4] as the Zaremba–Jaumann–Noll rigid body derivative. Let the quantities[1]

$$\frac{\mathrm{D}^1\tau^{M^\bullet N^\bullet}}{\mathrm{D}t}, \quad \frac{\mathrm{D}^2\tau_{M^\bullet N^\bullet}}{\mathrm{D}t}, \quad \frac{\mathrm{D}^3\tau^{M^\bullet}_{\ \cdot N^\bullet}}{\mathrm{D}t}, \quad \frac{\mathrm{D}^4\tau^{\ N^\bullet}_{M^\bullet\ \cdot}}{\mathrm{D}t} \tag{1.14}$$

identify, respectively, the time rates of change of $\tau^{M^\bullet N^\bullet}$, $\tau_{M^\bullet N^\bullet}$, $\tau^{M^\bullet}_{\ \cdot N^\bullet}$, and $\tau^{\ N^\bullet}_{M^\bullet\ \cdot}$ relative to the *convecting* bases $\boldsymbol{g}_M$. Because of (1.11a), each of the above derivatives form the components of a distinctly differing tensor, $\mathrm{D}^i\boldsymbol{\tau}/\mathrm{D}t$, $i = 1, \ldots, 4$, as follows:

$$\begin{aligned} \frac{\mathrm{D}^1\boldsymbol{\tau}}{\mathrm{D}t} &= \frac{\mathrm{D}^1\tau^{M^\bullet N^\bullet}}{\mathrm{D}t}\boldsymbol{g}_M\boldsymbol{g}_N, & \frac{\mathrm{D}^2\boldsymbol{\tau}}{\mathrm{D}t} &= \frac{\mathrm{D}^2\tau_{M^\bullet N^\bullet}}{\mathrm{D}t}\boldsymbol{g}^M\boldsymbol{g}^N, \\ \frac{\mathrm{D}^3\boldsymbol{\tau}}{\mathrm{D}t} &= \frac{\mathrm{D}^3\tau^{M^\bullet}_{\ \cdot N^\bullet}}{\mathrm{D}t}\boldsymbol{g}_M\boldsymbol{g}^N, & \frac{\mathrm{D}^4\boldsymbol{\tau}}{\mathrm{D}t} &= \frac{\mathrm{D}^4\tau^{\ N^\bullet}_{M^\bullet\ \cdot}}{\mathrm{D}t}\boldsymbol{g}^M\boldsymbol{g}_N. \end{aligned} \tag{1.15}$$

Through the use of (1.8) in (1.3), it can be shown [5] that

$$\frac{\mathrm{D}^1\boldsymbol{\tau}}{\mathrm{D}t} = \frac{\mathrm{D}\boldsymbol{\tau}}{\mathrm{D}t} - \boldsymbol{e}\cdot\boldsymbol{\tau} - \boldsymbol{\tau}\cdot\boldsymbol{e}^{\mathrm{t}}, \tag{1.16}$$

$$\frac{\mathrm{D}^2\boldsymbol{\tau}}{\mathrm{D}t} = \frac{\mathrm{D}\boldsymbol{\tau}}{\mathrm{D}t} + \boldsymbol{e}^{\mathrm{t}}\cdot\boldsymbol{\tau} + \boldsymbol{\tau}\cdot\boldsymbol{e}, \tag{1.17}$$

$$\frac{\mathrm{D}^3\boldsymbol{\tau}}{\mathrm{D}t} = \frac{\mathrm{D}\boldsymbol{\tau}}{\mathrm{D}t} - \boldsymbol{e}\cdot\boldsymbol{\tau} + \boldsymbol{\tau}\cdot\boldsymbol{e}, \tag{1.18}$$

$$\frac{\mathrm{D}^4\boldsymbol{\tau}}{\mathrm{D}t} = \frac{\mathrm{D}\boldsymbol{\tau}}{\mathrm{D}t} + \boldsymbol{e}^{\mathrm{t}}\cdot\boldsymbol{\tau} - \boldsymbol{\tau}\cdot\boldsymbol{e}^{\mathrm{t}}. \tag{1.19}$$

Equation (1.16) can be identified as the 'Truesdell' [6] or 'Oldroyd' [7] rate of $\boldsymbol{\tau}$; (1.17) as the 'Cotter–Rivlin' [8] rate of $\boldsymbol{\tau}$, while (1.18) and (1.19) as the 'mixed-hybrid' (?!) rates of $\boldsymbol{\tau}$.

Likewise, considering the instantaneous rate of $\boldsymbol{\sigma}$ as referred to the current configuration, it is easy to show [5] that

$$\frac{\mathrm{D}\boldsymbol{\sigma}}{\mathrm{D}t} = \frac{\mathrm{D}\boldsymbol{\tau}}{\mathrm{D}t} + \boldsymbol{\tau}(\boldsymbol{\varepsilon}:\boldsymbol{I}), \tag{1.20}$$

$$\frac{\hat{\mathrm{d}}\boldsymbol{\sigma}}{\mathrm{d}t} = \frac{\hat{\mathrm{d}}\boldsymbol{\tau}}{\mathrm{d}t} + \boldsymbol{\tau}(\boldsymbol{\varepsilon}:\boldsymbol{I}), \tag{1.21}$$

[1]The superscripts $1, \ldots, 4$ are used simply as a convenient way of distinguishing the rates of the different types of components of $\boldsymbol{\tau}$.

and

$$\frac{\mathrm{D}^i\boldsymbol{\sigma}}{\mathrm{D}t}=\frac{\mathrm{D}^i\boldsymbol{\tau}}{\mathrm{D}t}+\boldsymbol{\tau}(\boldsymbol{\varepsilon}\cdot\boldsymbol{I}),\quad i=1,\ldots,4. \tag{1.22}$$

It is important to note: (i) $\boldsymbol{\varepsilon}$ is symmetric, (ii) $\boldsymbol{\omega}$ is skew-symmetric, (iii) the eigen-directions of $\boldsymbol{\varepsilon}$ and $\boldsymbol{\tau}$ are in general different, (iv) the material derivative $\mathrm{D}\boldsymbol{\tau}/\mathrm{D}t$ is a symmetric tensor, (v) the Zaremba–Jaumann–Noll derivatives $\hat{\mathrm{d}}\boldsymbol{\tau}/\mathrm{d}t$ and $\hat{\mathrm{d}}\boldsymbol{\sigma}/\mathrm{d}t$ are symmetric, (vi) the derivatives $\mathrm{D}^i\boldsymbol{\tau}/\mathrm{D}t$ and $\mathrm{D}^i\boldsymbol{\sigma}/\mathrm{D}t$, $i=1,2$ are symmetric, while (vii) $\mathrm{D}^i\boldsymbol{\tau}/\mathrm{D}t$ and $\mathrm{D}^i\boldsymbol{\sigma}/\mathrm{D}t$, $i=3,4$ are *unsymmetric.*

The stress-rates in (1.13), (1.16)–(1.19) and (1.21), (1.22) are objective, while the material derivative $\mathrm{D}\boldsymbol{\tau}/\mathrm{D}t$ is *not*, in the following sense. Suppose we introduce a second observer whose reference frame rotates w.r.t that of the first with a time-dependent rigid rotation $\boldsymbol{Q}$. Let the quantities as seen by the second observer be identified by a superposed bar. Then it is seen [5, 9] that

$$\bar{\boldsymbol{\varepsilon}}=\boldsymbol{Q}\cdot\boldsymbol{\varepsilon}\cdot\boldsymbol{Q}^{\mathrm{t}},\qquad \bar{\boldsymbol{\tau}}=\boldsymbol{Q}\cdot\boldsymbol{\tau}\cdot\boldsymbol{Q}^{\mathrm{t}}, \tag{1.23a,b}$$

$$\bar{\boldsymbol{\omega}}=\boldsymbol{Q}\cdot\boldsymbol{\omega}\cdot\boldsymbol{Q}^{\mathrm{t}}+\dot{\boldsymbol{Q}}\cdot\boldsymbol{Q}^{\mathrm{t}},\qquad \bar{\boldsymbol{e}}=\boldsymbol{Q}\cdot\boldsymbol{e}\cdot\boldsymbol{Q}^{\mathrm{t}}+\dot{\boldsymbol{Q}}\cdot\boldsymbol{Q}^{\mathrm{t}}. \tag{1.24a,b}$$

Tensors that transform as in (1.23a,b) under observer transformations are denoted here as being objective. Using (1.23) and (1.24), it is verified that since,

$$\dot{\bar{\boldsymbol{\tau}}}=\mathrm{D}\bar{\boldsymbol{\tau}}/\mathrm{D}t=\boldsymbol{Q}\cdot\dot{\boldsymbol{\tau}}\cdot\boldsymbol{Q}^{\mathrm{t}}+\dot{\boldsymbol{Q}}\cdot\boldsymbol{\tau}\cdot\boldsymbol{Q}^{\mathrm{t}}+\boldsymbol{Q}\cdot\boldsymbol{\tau}\cdot\dot{\boldsymbol{Q}}^{\mathrm{t}},$$

the material rate is *not* an objective rate, while the rates in (1.13), (1.16)–(1.19), (1.21) and (1.22) are *all* objective.

It can be seen that since the change of $\boldsymbol{\omega}$ under observer transformation is of the type (1.24a), the rigid-body rate $\hat{\mathrm{d}}\boldsymbol{\tau}/\mathrm{d}t$ is *objective.* This has recently prompted Dienes [10] to derive a stress-rate that is objective but whose physical meaning is somewhat obscure. Here we present an alternate derivation of the stress-rate of Dienes [10], denoted here as $D^5\boldsymbol{\tau}/\mathrm{D}t$.

The deformation gradient $\boldsymbol{F}$ at the current time (as referred to the time $t=0$) is considered to have the polar-decomposition,

$$\boldsymbol{F}=\boldsymbol{R}\cdot\boldsymbol{U},\qquad \boldsymbol{U}^2=(\boldsymbol{F}^{\mathrm{t}}\cdot\boldsymbol{F}),\qquad \boldsymbol{R}\cdot\boldsymbol{R}^{\mathrm{t}}=\boldsymbol{I} \tag{1.25a,b,c}$$

where $\boldsymbol{R}$ is a rigid-rotation and $\boldsymbol{U}$ is a pure-stretch. Under the above mentioned observer transformations, $\boldsymbol{F}$, $\boldsymbol{R}$, and $\boldsymbol{U}$ transform as

$$\bar{\boldsymbol{F}}=\boldsymbol{Q}\cdot\boldsymbol{F},\qquad \bar{\boldsymbol{R}}=\boldsymbol{Q}\cdot\boldsymbol{R},\qquad \bar{\boldsymbol{U}}=\boldsymbol{U}. \tag{1.26}$$

From (1.25a) we have

$$\dot{\boldsymbol{F}}=\dot{\boldsymbol{R}}\cdot\boldsymbol{U}+\boldsymbol{R}\cdot\dot{\boldsymbol{U}}. \tag{1.27}$$

Since the velocity gradient $\boldsymbol{e}\equiv\dot{\boldsymbol{F}}\cdot\boldsymbol{F}^{-1}$ [4], we have, using (1.25a) and (1.27)

$$\boldsymbol{e} = \dot{\boldsymbol{R}} \cdot \boldsymbol{R}^{\mathrm{t}} + \boldsymbol{R} \cdot \dot{\boldsymbol{U}} \cdot \boldsymbol{U}^{-1} \cdot \boldsymbol{R}^{\mathrm{t}}, \tag{1.28}$$

$$\boldsymbol{e}^{\mathrm{t}} = \boldsymbol{R} \cdot \dot{\boldsymbol{R}}^{\mathrm{t}} + \boldsymbol{R} \cdot \boldsymbol{U}^{-1} \cdot \dot{\boldsymbol{U}} \cdot \boldsymbol{R}^{\mathrm{t}}. \tag{1.29}$$

Note that since $\mathrm{d}(\boldsymbol{R} \cdot \boldsymbol{R}^{\mathrm{t}})/\mathrm{d}t = 0$, $\dot{\boldsymbol{R}} \cdot \boldsymbol{R}^{\mathrm{t}}$ is a skew-symmetric tensor. Designating

$$\dot{\boldsymbol{R}} \cdot \boldsymbol{R}^{\mathrm{t}} = -\boldsymbol{R} \cdot \dot{\boldsymbol{R}}^{\mathrm{t}} = \boldsymbol{\Omega}, \tag{1.30}$$

and subtracting (1.28) from (1.29), we have

$$\boldsymbol{\Omega} = \boldsymbol{\omega} - \tfrac{1}{2}\boldsymbol{R} \cdot (\dot{\boldsymbol{U}} \cdot \boldsymbol{U}^{-1} - \boldsymbol{U}^{-1} \cdot \dot{\boldsymbol{U}}) \cdot \boldsymbol{R}^{\mathrm{t}} \tag{1.31}$$

which, under an observer transformation, becomes

$$\bar{\boldsymbol{\Omega}} = \bar{\boldsymbol{\omega}} - \tfrac{1}{2}\boldsymbol{Q} \cdot \boldsymbol{R} \cdot (\dot{\boldsymbol{U}} \cdot \boldsymbol{U}^{-1} - \boldsymbol{U}^{-1} \cdot \dot{\boldsymbol{U}}) \cdot \boldsymbol{R}^{\mathrm{t}} \cdot \boldsymbol{Q}^{\mathrm{t}}. \tag{1.32}$$

Upon using (1.24a) and rearranging terms, we see

$$\bar{\boldsymbol{\Omega}} = \dot{\boldsymbol{Q}} \cdot \boldsymbol{Q}^{\mathrm{t}} + \boldsymbol{Q} \cdot \boldsymbol{\Omega} \cdot \boldsymbol{Q}^{\mathrm{t}}. \tag{1.33}$$

Thus, under observer transformation, $\boldsymbol{\Omega}$ behaves the same as $\boldsymbol{\omega}$. Thus it may be seen, as noted by Lee et al. [2], that the stress-rate as defined by Dienes [10], namely,

$$\frac{\mathrm{D}^5\boldsymbol{\tau}}{\mathrm{D}t} = \frac{\mathrm{D}\boldsymbol{\tau}}{\mathrm{D}t} + \boldsymbol{\tau} \cdot \boldsymbol{\Omega} - \boldsymbol{\Omega} \cdot \boldsymbol{\tau}, \tag{1.34}$$

is objective and *symmetric*. Note, however, that as opposed to the *current* quantities $\boldsymbol{\omega}$ and $\boldsymbol{\varepsilon}$ which enter $(\hat{\mathrm{d}}/\mathrm{d}t)$ and $\mathrm{D}^i/\mathrm{D}t$ $(i = 1, \ldots, 4)$, the *total* rotation $\boldsymbol{R}$ as obtained from the polar-decomposition of the current deformation gradient $\boldsymbol{F}$, enters the rate $(\mathrm{D}^5\boldsymbol{\tau}/\mathrm{D}t)$.

It is noted that while the above 'objective' rates may be used in postulating constitutive relations, the boundary value rate problem may be stated in other stress-rates (see [11] for details).

2. Some anomalies of simple generalizations of constitutive relations of infinitesimal strain to finite strain

Consider the theory of infinitesimal strain, wherein the strain tensor is $\boldsymbol{\gamma}$. For isotropic linear elastic solids, the relation between the strain $\boldsymbol{\gamma}$ and the stress $\boldsymbol{\sigma}$ may be expressed as

$$\boldsymbol{\sigma} = 2\mu\boldsymbol{\gamma} + \lambda\boldsymbol{I}(\boldsymbol{\gamma} : \boldsymbol{I}) \tag{2.1}$$

where μ and λ are Lamé constants.

The trend, see however [19, 20], in recent '*computational mechanics*' has been to 'generalize' the above relation to finite strains by replacing $\boldsymbol{\sigma}$ by an objective stress-rate, denoted in general by

$\dot{\boldsymbol{\sigma}}^0$, and $\boldsymbol{\gamma}$ by the strain-rate $\boldsymbol{\varepsilon}$. Thus let

$$\dot{\boldsymbol{\sigma}}^0 = 2\mu\boldsymbol{\varepsilon} + \lambda \boldsymbol{I}(\boldsymbol{\varepsilon} : \boldsymbol{I}) \tag{2.2}$$

where $\dot{\boldsymbol{\sigma}}^0$ has most often been taken to be the Zaremba–Jaumann–Noll rate $\hat{\mathrm{d}}\boldsymbol{\sigma}/\mathrm{d}t$, or $\hat{\mathrm{d}}\boldsymbol{\tau}/\mathrm{d}t$ of (1.21) and (1.13), respectively.

We shall examine, in the following, the consequences of such simple generalizations when $\dot{\boldsymbol{\sigma}}^0$ is taken alternatively to be any one of the several choices presented in the previous section, cf. (1.13), (1.16)–(1.19), (1.21), (1.22) or (1.34).

In doing so, we shall consider the example of *finite shear* described in Fig. 1. Here the velocities are specified to be

$$v_1 = 2\omega x_2\,, \qquad v_2 = v_3 = 0\,. \tag{2.3}$$

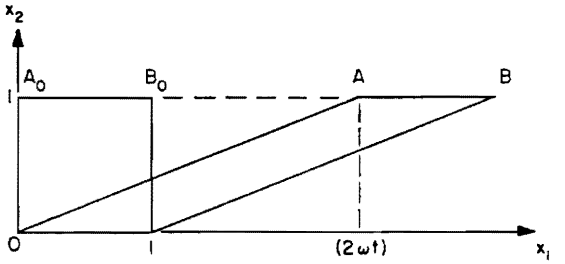

Fig. 1. Simple shear in the x_1 direction.

Hence $\boldsymbol{e}$, $\boldsymbol{\varepsilon}$, and $\boldsymbol{\omega}$ are such that

$$e_{12} = 2\omega, \quad \text{all other components of } \boldsymbol{e} \text{ being zero,} \tag{2.4a}$$

$$\varepsilon_{12} = \varepsilon_{21} = \omega, \quad \text{all other components of } \boldsymbol{\varepsilon} \text{ being zero,} \tag{2.4b}$$

$$\omega_{12} = -\omega_{21} = \omega, \quad \text{all other components of } \boldsymbol{\omega} \text{ being zero.} \tag{2.4c}$$

Note that in the present finite shear case, $(\boldsymbol{\varepsilon} : \boldsymbol{I}) = \varepsilon_{KK} = 0$, hence the Cauchy and Kirchhoff stresses are equivalent to each other. Hence, we may write (2.2) as

$$\dot{\boldsymbol{\tau}}^0 = 2\mu\boldsymbol{\varepsilon}\,. \tag{2.5}$$

Case (i): $\dot{\boldsymbol{\tau}}^0 = \hat{\mathrm{d}}\boldsymbol{\tau}/\mathrm{d}t$ (cf. (1.13)). Thus,

$$\hat{\mathrm{d}}\boldsymbol{\tau}/\mathrm{d}t = 2\mu\boldsymbol{\varepsilon}\,, \tag{2.6}$$

$$\frac{\mathrm{D}\boldsymbol{\tau}}{\mathrm{D}t} = 2\mu\boldsymbol{\varepsilon} + \boldsymbol{\omega}\cdot\boldsymbol{\tau} - \boldsymbol{\tau}\cdot\boldsymbol{\omega}\,, \tag{2.7}$$

i.e.,

$$\frac{D\tau_{11}}{Dt} = 2\omega\tau_{12}\,, \qquad \frac{D\tau_{22}}{Dt} = -2\omega\tau_{12}\,, \tag{2.8a,b}$$

$$\frac{D\tau_{12}}{Dt} = 2\mu\omega - 2\omega\tau_{11}\,. \tag{2.9}$$

We take the initial conditions of the problem to be such that $\boldsymbol{\tau}(t=0) = \mathbf{0}$. The solution of (2.8) and (2.9) for these initial conditions is

$$\tau_{11} = -\tau_{22} = \mu[1-\cos(2\omega t)]\,, \tag{2.10}$$

$$\tau_{12} = \mu \sin(2\omega t)\,. \tag{2.11}$$

That the shear stress oscillates with time is physically unacceptable for any real material.

Case (ii). $\dot{\boldsymbol{\tau}}^0 = D^1\boldsymbol{\tau}/Dt$ (cf. (1.16)).

$$\frac{D\boldsymbol{\tau}}{Dt} = 2\mu\boldsymbol{\varepsilon} + \boldsymbol{e}\cdot\boldsymbol{\tau} + \boldsymbol{\tau}\cdot\boldsymbol{e}^{\mathrm{t}}\,. \tag{2.12}$$

Here the solution can easily be shown to be

$$\tau_{11} = 4\mu(\omega t)^2\,, \qquad \tau_{22} = 0\,, \tag{2.13}$$

$$\tau_{12} = 2\mu(\omega t)\,. \tag{2.14}$$

This appears to be 'plausible'.

Case (iii): $\dot{\boldsymbol{\tau}}^0 = D^2\boldsymbol{\tau}/Dt$ (cf. (1.17)).

$$\frac{D\boldsymbol{\tau}}{Dt} = 2\mu\boldsymbol{\varepsilon} - \boldsymbol{e}^{\mathrm{t}}\cdot\boldsymbol{\tau} - \boldsymbol{\tau}\cdot\boldsymbol{e}\,. \tag{2.15}$$

Here the solution can be shown to be

$$\tau_{11} = 0\,, \qquad \tau_{22} = -4\mu(\omega t)^2\,, \tag{2.16}$$

$$\tau_{12} = 2\mu(\omega t)\,. \tag{2.17}$$

This also appears to be 'plausible'.

Case (iv): $\dot{\boldsymbol{\tau}}^0 = D^3\boldsymbol{\tau}/Dt$ (cf. (1.18)).

$$\frac{D\boldsymbol{\tau}}{Dt} = 2\mu\boldsymbol{\varepsilon} + \boldsymbol{e}\cdot\boldsymbol{\tau} - \boldsymbol{\tau}\cdot\boldsymbol{e}\,. \tag{2.18}$$

Here the solution is

$$\tau_{11} = \mu[1-\cos(2\omega t)]\,, \qquad \tau_{22} = 0\,, \tag{2.19}$$

$$\tau_{12} = \mu \sin(2\omega t)\,, \qquad \tau_{21} = 2\mu(\omega t)\,. \tag{2.20}$$

Of course, this is unacceptable, since the Cauchy stress should be symmetric for the type of continuum considered, viz. the one in which body couples do not exist.

Case (v): $\dot{\boldsymbol{\tau}}^0 = \mathrm{D}^4\boldsymbol{\tau}/\mathrm{D}t$ (cf. (1.19)).

$$\frac{\mathrm{D}\boldsymbol{\tau}}{\mathrm{D}t} = 2\mu\boldsymbol{\varepsilon} - \boldsymbol{e}^{\mathrm{t}}\cdot\boldsymbol{\tau} + \boldsymbol{\tau}\cdot\boldsymbol{e}^{\mathrm{t}}\,. \tag{2.21}$$

Here the solution can be shown to be

$$\tau_{11} = \mu[1-\cos(2\omega t)]\,, \qquad \tau_{22} = 0\,, \tag{2.22}$$

$$\tau_{12} = 2\mu(\omega t)\,, \qquad \tau_{21} = \mu\sin(2\omega t)\,. \tag{2.23}$$

This too is unacceptable.

Case (vi): $\dot{\boldsymbol{\tau}}^0 = \mathrm{D}^5\boldsymbol{\tau}/\mathrm{D}t$ (cf. (1.34)).

Here, Dienes [10] has obtained the solution to be

$$\tau_{11} = 4\mu(\cos 2\beta \ln\cos\beta + \beta\sin 2\beta - \sin^2\beta) = -\tau_{22}\,, \tag{2.24}$$

$$\tau_{12} = 2\mu\cos 2\beta(2\beta - 2\tan^2\beta\ln\cos\beta - \tan\beta)\,, \tag{2.25}$$

where $\tan\beta = \omega$. From [10, Fig. 1], it can be seen that τ_{12} as a function of time is *not* oscillatory.

From the above simple example, are we to conclude that $\hat{\mathrm{d}}\boldsymbol{\tau}/\mathrm{d}t$, $\mathrm{D}^3\boldsymbol{\tau}/\mathrm{D}t$, and $\mathrm{D}^4\boldsymbol{\tau}/\mathrm{D}t$ are bad stress-rates to use in a generalization of a constitutive equation as in (2.2)? Or, as suggested by Dienes [10], is $\hat{\mathrm{d}}\boldsymbol{\tau}/\mathrm{d}t$ "accurate for small strains", but for large strains $\mathrm{D}^5\boldsymbol{\tau}/\mathrm{D}t$ is to be used? Also, even though both $\mathrm{D}^1\boldsymbol{\tau}/\mathrm{D}t$ as well as $\mathrm{D}^2\boldsymbol{\tau}/\mathrm{D}t$ lead to plausible and exactly the same values of τ_{12}, the corresponding solutions for τ_{11} and τ_{22} are entirely different. Which one of the two, $\mathrm{D}^1\boldsymbol{\tau}/\mathrm{D}t$ or $\mathrm{D}^2\boldsymbol{\tau}/\mathrm{D}t$, is to be preferred, if any?

Some of the answers to the above questions that are currently topical in computational mechanics appear to have been provided in the celebrated works of Truesdell [12, 13] and Rivlin [14]. Here we explore further the concepts of [12] and [14], as well as modifications thereof. We find that *all* stress-rates are essentially equivalent when the constitutive equation is *properly posed. Then, not only the anomalies pointed out in this section, but also the paradoxes pointed out by Nagtegaal and de Jong* [1] *and Lee et al.* [2, 3], *largely disappear.* We also see that even though a particular type of constitutive equation can *model* a class of material behaviour, it is ultimately the *experiment* that determines the actual form of the constitutive law.

3. Hypo-elastic materials

As shown by Rivlin [14] and Truesdell [12], an 'objective' stress-strain relation of the 'rate-type' can be postulated as

$$\dot{\boldsymbol{\sigma}}^0 = f(\boldsymbol{\varepsilon}, \boldsymbol{\sigma})\,. \tag{3.1}$$

Here we let $\dot{\boldsymbol{\sigma}}^0$ to be *any one* of the objective stress-rates, $\hat{\mathrm{d}}\boldsymbol{\sigma}/\mathrm{d}t$ or $\mathrm{D}^i\boldsymbol{\sigma}/\mathrm{D}t$ $(i = 1, \ldots, 5)$ or some other. Also, recognizing that $\mathrm{D}^3\boldsymbol{\sigma}/\mathrm{D}t$ and $\mathrm{D}^4\boldsymbol{\sigma}/\mathrm{D}t$ are *unsymmetric*, we let $\dot{\boldsymbol{\sigma}}^0$ be *unsymmetric* in general. Assuming isotropy, an *unsymmetric* function f (unlike the *symmetric* function f introduced by Rivlin [14] and Truesdell [12]) that leads to an objective relation of the type (3.1) can be written as

$$\begin{aligned}\dot{\boldsymbol{\sigma}}^0 = {} & \alpha_0\boldsymbol{I} + \alpha_1\boldsymbol{\sigma} + \alpha_2\boldsymbol{\sigma}^2 + \alpha_3\boldsymbol{\varepsilon} + \alpha_4\boldsymbol{\varepsilon}^2 + \alpha_5\boldsymbol{\sigma}\cdot\boldsymbol{\varepsilon} + \alpha_6\boldsymbol{\varepsilon}\cdot\boldsymbol{\sigma} \\ & + \alpha_7\boldsymbol{\sigma}^2\cdot\boldsymbol{\varepsilon} + \alpha_8\boldsymbol{\varepsilon}\cdot\boldsymbol{\sigma}^2 + \alpha_9\boldsymbol{\sigma}\cdot\boldsymbol{\varepsilon}^2 + \alpha_{10}\boldsymbol{\varepsilon}^2\cdot\boldsymbol{\sigma} + \alpha_{11}\boldsymbol{\varepsilon}^2\cdot\boldsymbol{\sigma}^2 + \alpha_{12}\boldsymbol{\sigma}^2\cdot\boldsymbol{\varepsilon}^2 \\ & + \alpha_{13}\boldsymbol{\sigma}\cdot\boldsymbol{\varepsilon}\cdot\boldsymbol{\sigma}^2 + \alpha_{14}\boldsymbol{\varepsilon}\cdot\boldsymbol{\sigma}\cdot\boldsymbol{\varepsilon}^2 + \alpha_{15}\boldsymbol{\sigma}\cdot\boldsymbol{\varepsilon}^2\cdot\boldsymbol{\sigma}^2 + \alpha_{16}\boldsymbol{\varepsilon}\cdot\boldsymbol{\sigma}^2\cdot\boldsymbol{\varepsilon}^2 \end{aligned} \tag{3.2}$$

where $\alpha_0, \ldots, \alpha_{16}$ are functions of the following *invariants*:

$$I_\sigma = (\boldsymbol{\sigma}:\boldsymbol{I}) = \mathrm{tr}\,\boldsymbol{\sigma}, \qquad II_\sigma = \tfrac{1}{2}[(\mathrm{tr}\,\boldsymbol{\sigma})^2 - (\mathrm{tr}\,\boldsymbol{\sigma}^2)], \qquad III_\sigma = \det\boldsymbol{\sigma}, \tag{3.3}$$

$$\begin{aligned} & M = \boldsymbol{\sigma}:\boldsymbol{\varepsilon}, \qquad N = \boldsymbol{\sigma}^2:\boldsymbol{\varepsilon}, \qquad P = \boldsymbol{\sigma}:\boldsymbol{\varepsilon}^2, \qquad Q = \boldsymbol{\sigma}^2:\boldsymbol{\varepsilon}^2, \\ & R = (\boldsymbol{\sigma}\cdot\boldsymbol{\varepsilon}):(\boldsymbol{\sigma}^2\cdot\boldsymbol{\varepsilon}^2), \qquad V = (\boldsymbol{\varepsilon}\cdot\boldsymbol{\sigma}):(\boldsymbol{\varepsilon}^2\cdot\boldsymbol{\sigma}^2). \end{aligned} \tag{3.4}$$

Following Truesdell's [12] definition of a hypo-elastic material, we restrict f to be a *linear* function of $\boldsymbol{\varepsilon}$. Thus,

$$\alpha_4 = \alpha_9 = \alpha_{10} = \alpha_{11} = \alpha_{12} = \alpha_{14} = \alpha_{15} = \alpha_{16} = 0, \tag{3.5}$$

or

$$\dot{\boldsymbol{\sigma}}^0 = \alpha_0\boldsymbol{I} + \alpha_1\boldsymbol{\sigma} + \alpha_2\boldsymbol{\sigma}^2 + \alpha_3\boldsymbol{\varepsilon} + \alpha_4\boldsymbol{\sigma}\cdot\boldsymbol{\varepsilon} + \alpha_5\boldsymbol{\varepsilon}\cdot\boldsymbol{\sigma} + \alpha_6\boldsymbol{\sigma}^2\cdot\boldsymbol{\varepsilon} + \alpha_7\boldsymbol{\varepsilon}\cdot\boldsymbol{\sigma}^2 + \alpha_8\boldsymbol{\sigma}\cdot\boldsymbol{\varepsilon}\cdot\boldsymbol{\sigma}^2 \tag{3.6}$$

wherein it is seen that α_3, α_4, α_5, α_6, α_7 and α_8 must be independent of $\boldsymbol{\varepsilon}$, while α_0, α_1 and α_2 must be of degree one in $\boldsymbol{\varepsilon}$. Let

$$\delta \equiv I_\varepsilon = (\boldsymbol{\varepsilon}:\boldsymbol{I}).$$

Thus, it is seen that

$$\begin{aligned}\dot{\boldsymbol{\sigma}}^0 = {} & (\delta\beta_0 + M\beta_1 + N\beta_2)\boldsymbol{I} + (\delta\beta_3 + M\beta_4 + N\beta_5)\boldsymbol{\sigma} + (\delta\beta_6 + M\beta_7 + N\beta_8)\boldsymbol{\sigma}^2 \\ & + \beta_9\boldsymbol{\varepsilon} + \beta_{10}\boldsymbol{\sigma}\cdot\boldsymbol{\varepsilon} + \beta_{11}\boldsymbol{\varepsilon}\cdot\boldsymbol{\sigma} + \beta_{12}\boldsymbol{\sigma}^2\cdot\boldsymbol{\varepsilon} + \beta_{13}\boldsymbol{\varepsilon}\cdot\boldsymbol{\sigma}^2 + \beta_{14}\boldsymbol{\sigma}\cdot\boldsymbol{\varepsilon}\cdot\boldsymbol{\sigma}^2 \end{aligned} \tag{3.7}$$

where, now,

$$\beta_i = \beta_i(I_\sigma, II_\sigma, III_\sigma), \quad i = 0, \ldots, 14. \tag{3.8}$$

We impose the second restriction, for the moment, that $\boldsymbol{\sigma}$ enters the constitutive relation only in a *linear* fashion. Thus, we arrive at the relation, for what may be termed as hypo-elastic materials of grade one, that

$$\dot{\boldsymbol{\sigma}}^0 = [\delta(\gamma_1 + \gamma_2 I_\sigma) + \gamma_3 M]\boldsymbol{I} + \delta\gamma_4\boldsymbol{\sigma} + (\gamma_5 + \gamma_6 I_\sigma)\boldsymbol{\varepsilon} + \gamma_7\boldsymbol{\sigma}\cdot\boldsymbol{\varepsilon} + \gamma_8\boldsymbol{\varepsilon}\cdot\boldsymbol{\sigma}. \tag{3.9}$$

Even though $\dot{\boldsymbol{\sigma}}^0$, as noted earlier, may be unsymmetric, the material derivative, $\dot{\boldsymbol{\sigma}}^m \equiv D\boldsymbol{\tau}/Dt$ must be symmetric. Noting this, and substituting for $\dot{\boldsymbol{\sigma}}^0$ any of the objective rates, $\hat{d}\boldsymbol{\tau}/dt$ or $D^i\boldsymbol{\sigma}/Dt$ $(i = 1, \ldots, 4)$, we may postulate the constitutive relation

$$\dot{\boldsymbol{\sigma}}^m = [\delta(\gamma_1 + \gamma_2 I_\sigma) + \gamma_3 M]\boldsymbol{I} + \delta\gamma_4\boldsymbol{\sigma} + (\gamma_5 + \gamma_6 I_\sigma)\boldsymbol{\varepsilon} + \boldsymbol{\omega}\cdot\boldsymbol{\sigma} - \boldsymbol{\sigma}\cdot\boldsymbol{\omega} + \mu_7(\boldsymbol{\sigma}\cdot\boldsymbol{\varepsilon} + \boldsymbol{\varepsilon}\cdot\boldsymbol{\sigma}) \tag{3.10}$$

where

$$\mu_7 = \gamma_7 = \gamma_8 \qquad \text{if } \dot{\boldsymbol{\sigma}}^0 = \hat{d}\boldsymbol{\sigma}/dt, \tag{3.11}$$

$$\mu_7 = (\gamma_7 + 1) = (\gamma_8 + 1) \quad \text{if } \dot{\boldsymbol{\sigma}}^0 = D^1\boldsymbol{\sigma}/Dt, \tag{3.12}$$

$$\mu_7 = (\gamma_7 - 1) = (\gamma_8 - 1) \quad \text{if } \dot{\boldsymbol{\sigma}}^0 = D^2\boldsymbol{\sigma}/Dt, \tag{3.13}$$

$$\mu_7 = (\gamma_7 - 1) = (\gamma_8 + 1) \quad \text{if } \dot{\boldsymbol{\sigma}}^0 = D^3\boldsymbol{\sigma}/Dt, \tag{3.14}$$

$$\mu_7 = (\gamma_8 - 1) = (\gamma_7 + 1) \quad \text{if } \dot{\boldsymbol{\sigma}}^0 = D^4\boldsymbol{\sigma}/Dt. \tag{3.15}$$

Now we study the problem of simple finite shear as described in (2.3), (2.4), when the constitutive law is of the type (3.10).

For finite shear, from (2.4b), $\delta = 0$. First, if (3.10) were to represent the usual linear elastic behaviour at time $t = 0$ (when $\boldsymbol{\sigma} = \boldsymbol{0}$, $I_\sigma = 0$, $M = 0$), we see that

$$\gamma_1 = \lambda \quad \text{and} \quad \gamma_5 = 2\mu \tag{3.16}$$

where λ and μ are Lamé constants. Equation (3.10) can be written, for simple shear, as

$$\dot{\boldsymbol{\sigma}}^m = D\boldsymbol{\sigma}/Dt = \gamma_3 M\boldsymbol{I} + (\gamma_5 + \gamma_6 I_\sigma)\boldsymbol{\varepsilon} + \boldsymbol{\omega}\cdot\boldsymbol{\sigma} - \boldsymbol{\sigma}\cdot\boldsymbol{\omega} + \mu_7(\boldsymbol{\sigma}\cdot\boldsymbol{\varepsilon} + \boldsymbol{\varepsilon}\cdot\boldsymbol{\sigma}). \tag{3.17}$$

Using (2.4b,c) we see that (3.17) becomes

$$\frac{D\sigma_{11}}{Dt} = \dot{\sigma}_{11} = 2\sigma_{12}\omega(1 + \mu_7), \tag{3.18}$$

$$\dot{\sigma}_{12} = \omega[\gamma_5 + \sigma_{11}(\gamma_6 - 1 + \mu_7) + \sigma_{22}(\gamma_6 + 1 + \mu_7)], \tag{3.19}$$

$$\dot{\sigma}_{22} = 2\sigma_{12}\omega(\mu_7 - 1), \tag{3.20}$$

$$\dot{\sigma}_{33} = 2\sigma_{12}\omega\gamma_3. \tag{3.21}$$

Using (3.18) and (3.20) in (3.19), we find

$$\ddot{\sigma}_{12} = 4\omega^2\sigma_{12}\alpha \tag{3.22}$$

where

$$\alpha = \tfrac{1}{2}[3\gamma_3\gamma_6 + 2\gamma_3\mu_7 + 2\mu_7\gamma_6 + 2\mu_7^2 - 2]. \tag{3.23}$$

The solution of (3.22) depends on the value of α. Thus,

$$\sigma_{12} = \begin{cases} At + B & \text{if } \alpha = 0, \quad (3.24) \\ A \sin 2\omega|\alpha|^{1/2}t + B \cos 2\omega|\alpha|^{12}t & \text{if } \alpha < 0, \quad (3.25) \\ A \exp(2\omega\alpha^{1/2}t) + B \exp(-2\omega\alpha^{1/2}t) & \text{if } \alpha > 0. \quad (3.26) \end{cases}$$

Assuming the body to be initially stress-free, the solution becomes

$$\sigma_{12} = \begin{cases} (\omega\gamma_5 t) = 2\mu\omega t, & \alpha = 0, \quad (3.27) \\ (\mu/|\alpha|^{1/2})\sin 2\omega|\alpha|^{1/2}t, & \alpha < 0, \quad (3.28) \\ (\mu/2\alpha^{1/2})[\exp(2\omega\alpha^{1/2}t) - \exp(-2\omega\alpha^{1/2}t)], & \alpha > 0. \quad (3.29) \end{cases}$$

Likewise, the solutions for $\sigma_{11}, \sigma_{22}, \sigma_{33}$ are, respectively,

$$\sigma_{11} = 2\omega(1 + \mu_7) \int_t \sigma_{12}(\tau)\mathrm{d}\tau, \quad (3.30)$$

$$\sigma_{22} = 2\omega(\mu_7 - 1) \int_t \sigma_{12}(\tau)\mathrm{d}\tau, \quad (3.31)$$

$$\sigma_{33} = 2\omega\gamma_3 \int_t \sigma_{12}(\tau)\mathrm{d}\tau. \quad (3.32)$$

Even though it is analogous to that of Truesdell [12, 13], the above analysis differs from that of Truesdell [12, 13] in several ways: (i) only symmetric objective stress-rates are treated in [12, 13], while general unsymmetric objective stress-rates are treated here; (ii) only $\mathrm{D}^1\boldsymbol{\tau}/\mathrm{D}t$ (the now so-called 'Truesdell' rate) is treated in [12, 13], while the present analysis is general for any stress-rate, depending on the values of μ_7, γ_7, and γ_8 as in (3.9), (3.11)–(3.15) (note that the analysis in [12, 13] pertains to the case of (3.12)); (iii) the definitions of the so-called hypo-elastic materials of 'grade zero' and 'grade one' as given in [12] pertain only when $\mathrm{D}^1\boldsymbol{\tau}/\mathrm{D}t$ is used as a stress-rate. Thus, Truesdell's 'grade zero hypo-elastic' material corresponds to the case (cf. (3.12)) when $\mu_7 = 1$, $\gamma_7 = \gamma_8 = 0$. However, the same material may be treated as 'grade one hypo-elastic' when other objective stress-rates are employed (see (3.9), (3.11), (3.13)–(3.15) when $\mu_7 = 1$).

For further simplicity, we consider the case when $\gamma_3 = \gamma_6 = 0$ in (3.17), i.e., we consider the case which represents a valid 'generalization' to finite strains of the elasticity relation (2.1) of infinitesimal theory, for the present *finite shear* problem

$$\dot{\boldsymbol{\sigma}}^0 = \gamma_5\boldsymbol{\varepsilon} + \gamma_7\boldsymbol{\sigma}\cdot\boldsymbol{\varepsilon} + \gamma_8\boldsymbol{\varepsilon}\cdot\boldsymbol{\sigma}, \quad (3.33)$$

$$\dot{\boldsymbol{\sigma}}^{\mathrm{m}} = \gamma_5\boldsymbol{\varepsilon} + \boldsymbol{\omega}\cdot\boldsymbol{\sigma} - \boldsymbol{\sigma}\cdot\boldsymbol{\omega} + \mu_7(\boldsymbol{\sigma}\cdot\boldsymbol{\varepsilon} + \boldsymbol{\varepsilon}\cdot\boldsymbol{\sigma}) \quad (3.34)$$

where μ_7, γ_7, γ_8 are related, for *various stress-rates*, as in (3.11)–(3.15). *Also compare the present generalization* (3.33) *to the more commonly used simple generalization* (2.5).

It is seen that α of (3.23) now reduces to

$$\alpha = (\mu_7^2 - 1). \tag{3.35}$$

Thus, the character of the solution, as indicated in (3.27)–(3.29) depends on μ_7:

$$\sigma_{12} = \begin{cases} 2\mu\omega t, & \mu_7 = \pm 1, \quad (3.36) \\ \mu \sin 2\omega t, & \mu_7 = 0, \quad (3.37) \\ (\mu/2\alpha^{1/2})[\exp(2\omega\alpha^{1/2}t) - \exp(-2\omega\alpha^{1/2}t)], & |\mu_7| > 1. \quad (3.38) \end{cases}$$

It is interesting to note from (3.30)–(3.32) that

$$\sigma_{11} \neq 0, \quad \sigma_{22} = 0, \quad \sigma_{33} = 0, \quad \mu_7 = +1, \tag{3.39a}$$

$$\sigma_{11} = 0, \quad \sigma_{22} \neq 0, \quad \sigma_{33} = 0, \quad \mu_7 = -1, \tag{3.39b}$$

$$\sigma_{11} = -\sigma_{22}, \quad \sigma_{33} = 0, \quad \mu_7 = 0, \tag{3.39c}$$

$$\sigma_{11} \neq 0, \quad \sigma_{22} \neq 0, \quad \sigma_{33} = 0, \quad |\mu_7| > 1. \tag{3.39d}$$

Thus, a generalization of the type (3.33), (3.34) can generate responses of the type (3.36)–(3.39) depending on the value of μ_7.

Of course, an *experiment* must be the ultimate guide to which type of response is correct for a given material. Assuming that a 'linear' variation of σ_{12} with time is the correct one for the given material, an analytical modeling of such a response can be made through an equation of the type (3.33), (3.34) provided $\mu_7 = \pm 1$. The sign of μ_7 (positive or negative) can only be determined from the *experimental* observation of the response functions for σ_{11}, σ_{22} as in (3.39a,b).

Thus, we see that in order to obtain a non-oscillatory variation of σ_{12} with time in simple finite shear, *no one stress-rate is to be preferred* over the others, as the analysis of Section 2 may erroneously lead one to conclude. *The requirement of* $\mu_7 = \pm 1$ *can be met by any one of the stress-rates, provided* γ_7 *and* γ_8 *of* (3.33) *or* (3.9) *are chosen according to* (3.11)–(3.15). Also, even though the stress-rate of Dienes [10] is formally objective, and may lead to a non-oscillatory σ_{12} response in simple shear, its use is not necessary for 'rate-type' materials as demonstrated above.

We also see that the reason for the anomalies shown in Section 2 lies in an improper simple generalization from (2.1) to (2.2), while a correct generalization must be as in (3.9), (3.17) or (3.33).

4. Classical elasto-plasticity: isotropic hardening

We consider the classical 'J_2' plasticity theory, with the 'yield' surface defined by

$$f = \boldsymbol{\sigma}' : \boldsymbol{\sigma}' - \tfrac{2}{3}\bar{\sigma}^2 = 0 \tag{4.1}$$

where

$$\boldsymbol{\sigma}' = \boldsymbol{\sigma} - \tfrac{1}{3}(\boldsymbol{\sigma} : \boldsymbol{I})\boldsymbol{I} \tag{4.2}$$

and $\bar{\sigma}$ is the yield stress in a uniaxial tension test and can be a function of the plastically dissipated energy, i.e. $\bar{\sigma} = \bar{\sigma}(W^{\mathrm{p}})$.

We use an additive decomposition of the strain-rate,

$$\boldsymbol{\varepsilon} = \boldsymbol{\varepsilon}^{\mathrm{e}} + \boldsymbol{\varepsilon}^{\mathrm{p}} \tag{4.3}$$

where (e) and (p) refer to 'elastic' and 'plastic' components, respectively. We use the well-known Drucker's normality rule

$$\boldsymbol{\varepsilon}^{\mathrm{p}} = \lambda \frac{\partial f}{\partial \boldsymbol{\sigma}} . \tag{4.4}$$

Taking an objective rate of f, we find the 'consistency condition' from (4.1) to be

$$\dot{f}^* \equiv \dot{f} = \frac{\partial f}{\partial \boldsymbol{\sigma}} : \dot{\boldsymbol{\sigma}}^* - \tfrac{4}{3}\bar{\sigma}\frac{\mathrm{d}\bar{\sigma}}{\mathrm{d}W^{\mathrm{p}}}\dot{W}^{\mathrm{p}} = 0 \tag{4.5}$$

where

$$\dot{W}^{\mathrm{p}} = \boldsymbol{\sigma} : \boldsymbol{\varepsilon}^{\mathrm{p}} . \tag{4.6}$$

In (4.5), $(\dot{})^*$ denotes a generalized 'objective' rate to be defined momentarily.

Using (4.6) and (4.4) in (4.5), we find

$$\boldsymbol{\varepsilon}^{\mathrm{p}} = \frac{\left[\left(\frac{\partial f}{\partial \boldsymbol{\sigma}}\right) : \dot{\boldsymbol{\sigma}}^*\right]\left(\frac{\partial f}{\partial \boldsymbol{\sigma}}\right)}{\left(\boldsymbol{\sigma} : \frac{\partial f}{\partial \boldsymbol{\sigma}}\right)\left(\frac{\mathrm{d}\bar{\sigma}}{\mathrm{d}W^{\mathrm{p}}}\right)\left(\frac{4}{3}\bar{\sigma}\right)} . \tag{4.7}$$

Noting that during yield (for J_2 theory),

$$\frac{\partial f}{\partial \boldsymbol{\sigma}} = 2\boldsymbol{\sigma}' , \tag{4.8}$$

$$\boldsymbol{\sigma} : \frac{\partial f}{\partial \boldsymbol{\sigma}} = 2\boldsymbol{\sigma} : \boldsymbol{\sigma}' \equiv 2\boldsymbol{\sigma}' : \boldsymbol{\sigma}' = \tfrac{4}{3}\bar{\sigma}^2 , \tag{4.9}$$

we see that

$$\boldsymbol{\varepsilon}^{\mathrm{p}} = \tfrac{9}{4}\frac{(\boldsymbol{\sigma}' : \dot{\boldsymbol{\sigma}}^*)\boldsymbol{\sigma}'}{\bar{\sigma}^3(\mathrm{d}\bar{\sigma}/\mathrm{d}W^{\mathrm{p}})} . \tag{4.10}$$

Now we define 'equivalent stress' and 'equivalent strain' through the relations

$$\sigma_{\mathrm{eq}}^2 = \left(\tfrac{3}{2}\boldsymbol{\sigma}' : \boldsymbol{\sigma}'\right) , \tag{4.11}$$

$$(\varepsilon^{\mathrm{p}}_{\mathrm{eq}})^2 = \tfrac{2}{3}(\boldsymbol{\varepsilon}^{\mathrm{p}})' : (\boldsymbol{\varepsilon}^{\mathrm{p}})' = \tfrac{2}{3}(\boldsymbol{\varepsilon}^{\mathrm{p}} : \boldsymbol{\varepsilon}^{\mathrm{p}}) \tag{4.12}$$

since plastic strain rate is assumed to be 'incompressible' in nature. In terms of these equivalent measures,

$$\dot{W}^{\mathrm{p}} = \boldsymbol{\sigma} : \boldsymbol{\varepsilon}^{\mathrm{p}} \equiv \sigma_{\mathrm{eq}}\varepsilon^{\mathrm{p}}_{\mathrm{eq}} = \bar{\sigma}\varepsilon^{\mathrm{p}}_{\mathrm{eq}} \tag{4.13}$$

since $\sigma_{\mathrm{eq}} = \bar{\sigma}$ during yield.

From (4.11) we find

$$2\sigma_{\mathrm{eq}}\dot{\sigma}^{*}_{\mathrm{eq}} \equiv 2\sigma_{\mathrm{eq}}\dot{\sigma}_{\mathrm{eq}} = 3(\boldsymbol{\sigma}' : \dot{\boldsymbol{\sigma}}'^{*}) \equiv (3\boldsymbol{\sigma}' : \dot{\boldsymbol{\sigma}}^{*})\,. \tag{4.14}$$

Likewise we find

$$\mathrm{d}\bar{\sigma}/\mathrm{d}W^{\mathrm{p}} = \dot{\bar{\sigma}}/\dot{W}^{\mathrm{p}} = (\dot{\bar{\sigma}}/\dot{\varepsilon}^{\mathrm{p}}_{\mathrm{eq}})/\bar{\sigma} = K/\bar{\sigma} \tag{4.15}$$

where K is thus the slope of the 'true stress versus logarithmic plastic strain curve' in a uniaxial tension experiment. Using (4.14), (4.15) in (4.10), we find

$$\boldsymbol{\varepsilon}^{\mathrm{p}} = \tfrac{9}{4}\frac{(\boldsymbol{\sigma}' : \dot{\boldsymbol{\sigma}}^{*})\boldsymbol{\sigma}'}{K\bar{\sigma}^2} = \tfrac{3}{2}\left(\frac{\varepsilon^{\mathrm{p}}_{\mathrm{eq}}}{\bar{\sigma}}\right)\boldsymbol{\sigma}'\,. \tag{4.16}$$

We first consider *finite plane shear* of a *rigid-plastic* material for which $\boldsymbol{\varepsilon}^{\mathrm{e}} = 0$. For this material, *irrespective of the definition for* $\dot{\boldsymbol{\sigma}}^{0}$ *that is used*, we find from (4.16) that

$$\boldsymbol{\sigma}' = \tfrac{2}{3}\left(\frac{\bar{\sigma}}{\varepsilon^{\mathrm{p}}_{\mathrm{eq}}}\right)\boldsymbol{\varepsilon}^{\mathrm{p}}\,. \tag{4.17}$$

For plane-shear of the rigid-plastic material,

$$\boldsymbol{\varepsilon}^{\mathrm{p}} = \begin{bmatrix} 0 & \omega & 0 \\ \omega & 0 & 0 \\ 0 & 0 & 0 \end{bmatrix}, \qquad (\varepsilon^{\mathrm{p}}_{\mathrm{eq}})^2 = \tfrac{2}{3}\cdot 2\omega^2 = \tfrac{4}{3}\omega^2\,. \tag{4.18}$$

Thus from (4.17) we find that

$$\sigma'_{11} = \sigma'_{22} = \sigma'_{33} = \sigma_{13} = \sigma_{23} = 0\,, \tag{4.19}$$

$$\sigma_{12} = \bar{\sigma}/\sqrt{3} \tag{4.20}$$

where $\bar{\sigma}_0$ is the initial yield stress, and the effect of strain hardening in uniaxial tension is expressed by

$$\bar{\sigma} = \bar{\sigma}_0 + \int K\varepsilon^{\mathrm{p}}_{\mathrm{eq}}\,\mathrm{d}t = \bar{\sigma}_0 + (2\omega K t)/\sqrt{3}\,. \tag{4.21}$$

Thus, in isotropic-hardening rigid-plasticity theory, there are no oscillations in the response function $\sigma_{12}(t)$ for any definition of $\dot{\boldsymbol{\sigma}}^0$.

Now we consider elasto-plasticity with isotropic hardening. We assume that until the criterion for initial yield is met, the material behaves linear elastically. Following Section 3, we may define a generalized objective stress-rate to be

$$\dot{\boldsymbol{\sigma}}^* = \dot{\boldsymbol{\sigma}}^0 - \gamma_7(\boldsymbol{\sigma}\cdot\boldsymbol{\varepsilon}) - \gamma_8(\boldsymbol{\varepsilon}\cdot\boldsymbol{\sigma}) \tag{4.22}$$

where γ_7 and γ_8 are defined for various stress-rates $\dot{\boldsymbol{\sigma}}^0$ through (3.11)–(3.15). Thus, a 'correct' generalization of the linear isotropic stress-strain relation, as shown in Section 3, will be

$$\dot{\boldsymbol{\sigma}}^* = \lambda(\boldsymbol{\varepsilon} : \boldsymbol{I})\boldsymbol{I} + 2\mu\boldsymbol{\varepsilon}\,, \quad f<0\,. \tag{4.23}$$

It has already been shown in the case of simple shear that for $\mu_7 = 0$, the solution for σ_{12} is oscillatory in time; for $\mu_7 = \pm 1$, the solution is linear, while for $|\mu_7| > 1$, the solution is exponential.

Equation (4.22) may be written alternatively as

$$(\dot{\boldsymbol{\sigma}}^* : \boldsymbol{I}) = (3\lambda + 2\mu)(\boldsymbol{\varepsilon} : \boldsymbol{I})\,, \tag{4.24}$$

$$(\dot{\boldsymbol{\sigma}}^*)' = 2\mu\boldsymbol{\varepsilon}'\,, \tag{4.25}$$

where

$$(\dot{\boldsymbol{\sigma}}^*)' = \dot{\boldsymbol{\sigma}}^* - \tfrac{1}{3}(\dot{\boldsymbol{\sigma}}^* : \boldsymbol{I})\boldsymbol{I}\,, \qquad \boldsymbol{\varepsilon}' = \boldsymbol{\varepsilon} - \tfrac{1}{3}(\boldsymbol{\varepsilon} : \boldsymbol{I})\boldsymbol{I}\,. \tag{4.26a,b}$$

A generalization of (4.23)–(4.25) may then be made in the case of elasto-plasticity as

$$(\dot{\boldsymbol{\sigma}}^* : \boldsymbol{I}) = (3\lambda + 2\mu)(\boldsymbol{\varepsilon}^e : \boldsymbol{I}) \equiv (3\lambda + 2\mu)(\boldsymbol{\varepsilon} : \boldsymbol{I})\,, \tag{4.27}$$

$$(\dot{\boldsymbol{\sigma}}^*)' = 2\mu(\boldsymbol{\varepsilon}' - \boldsymbol{\varepsilon}^p)\,, \tag{4.28}$$

since $(\boldsymbol{\varepsilon}^p : \boldsymbol{I}) = 0$ and $\boldsymbol{\varepsilon}^p = (\boldsymbol{\varepsilon}^p)'$. Thus, choosing a parameter α such that $\alpha = 1$ when $\boldsymbol{\varepsilon}^p \neq 0$ while $\alpha = 0$ when $\boldsymbol{\varepsilon}^p = 0$, we have

$$(\dot{\boldsymbol{\sigma}}^*)' = 2\mu\left[\boldsymbol{\varepsilon}' - \tfrac{9}{4}\frac{\alpha}{K\bar{\sigma}^2}(\boldsymbol{\sigma}' : \dot{\boldsymbol{\sigma}}^*)\boldsymbol{\sigma}'\right]. \tag{4.29}$$

Note that $(\boldsymbol{\sigma}' : \dot{\boldsymbol{\sigma}}^*) \equiv [\boldsymbol{\sigma}' : (\dot{\boldsymbol{\sigma}}^*)']$. From (4.29) we have (taking the trace product of both sides with $\boldsymbol{\sigma}'$)

$$(\dot{\boldsymbol{\sigma}}^*)' : \boldsymbol{\sigma}' = 2\mu\left[\boldsymbol{\varepsilon}' : \boldsymbol{\sigma}' - \tfrac{3}{2}\frac{\alpha}{K}(\boldsymbol{\sigma}' : \dot{\boldsymbol{\sigma}}^{*\prime})\right]. \tag{4.30}$$

Hence,

$$\boldsymbol{\sigma}' : \dot{\boldsymbol{\sigma}}^* = \left(\frac{2\mu K}{K + 3\mu}\right)(\boldsymbol{\varepsilon}' : \boldsymbol{\sigma}') \quad \text{when } \boldsymbol{\varepsilon}^p > 0\,. \tag{4.31}$$

Note again that $(\boldsymbol{\varepsilon}' : \boldsymbol{\sigma}') = (\boldsymbol{\varepsilon} : \boldsymbol{\sigma}')$. Using (4.31) in (4.29), we have

$$(\dot{\boldsymbol{\sigma}}^*)' = 2\mu\left[\boldsymbol{\varepsilon}' - 2\mu\,\frac{9\alpha}{4(K+3\mu)\bar{\sigma}^2}(\boldsymbol{\varepsilon}:\boldsymbol{\sigma}')\boldsymbol{\sigma}'\right]; \tag{4.32}$$

combining (4.27) and (4.32), we have

$$\dot{\boldsymbol{\sigma}}^* = 2\mu\boldsymbol{\varepsilon} + \lambda(\boldsymbol{\varepsilon}:\boldsymbol{I}) - 2\mu\left[\frac{9\alpha\mu}{(2K+6\mu)\bar{\sigma}^2}(\boldsymbol{\varepsilon}:\boldsymbol{\sigma}')\boldsymbol{\sigma}'\right]. \tag{4.33}$$

It is of interest to note that (4.33), with $\dot{\boldsymbol{\sigma}}^*$ being interpreted as $\hat{\mathrm{d}}\boldsymbol{\sigma}/\mathrm{d}t$, has been widely used in literature with the attribution of such a relation being made to Hill [15] by McMeeking and Rice [16] and others, while it is attributed to Thomas [17] by Truesdell and Noll [9]. For our present purposes, note that $\dot{\boldsymbol{\sigma}}^*$ is defined in (4.22), with γ_7 and γ_8 being defined for any of the rates $\hat{\mathrm{d}}\boldsymbol{\sigma}/\mathrm{d}t$, $\mathrm{D}^i\boldsymbol{\sigma}/\mathrm{D}t$ $(i = 1, \ldots, 4)$, through (3.11)–(3.15). We now see the ramifications of the use of the present relations (4.33) and (4.22) as compared to the relations of [15–17].

From (4.22) and (4.33), we first see that

$$\frac{\mathrm{D}\boldsymbol{\sigma}}{\mathrm{D}t} = \overset{\bullet}{\boldsymbol{\sigma}}{}^{\mathrm{m}} = 2\mu\boldsymbol{\varepsilon} + \lambda(\boldsymbol{\varepsilon}:\boldsymbol{I}) + \boldsymbol{\omega}\cdot\boldsymbol{\sigma} - \boldsymbol{\sigma}\cdot\boldsymbol{\omega} + \mu_7(\boldsymbol{\varepsilon}\cdot\boldsymbol{\sigma} + \boldsymbol{\sigma}\cdot\boldsymbol{\varepsilon}) - 2\mu\left[\frac{9\alpha\mu}{(2K+6\mu)\bar{\sigma}^2}(\boldsymbol{\varepsilon}:\boldsymbol{\sigma}')\boldsymbol{\sigma}'\right] \tag{4.34}$$

with μ_7 being defined for various stress-rates as in (3.11)–(3.15).

We consider the problem of finite simple shear described in (2.3), (2.4). We define scaled variables

$$\tau = 2\omega t, \qquad \boldsymbol{s} = \boldsymbol{\sigma}/2\mu\,. \tag{4.35}$$

Thus, since $(\boldsymbol{\varepsilon}:\boldsymbol{I}) = 0$ for finite shear, we have[2]

$$\frac{\mathrm{D}\boldsymbol{s}}{\mathrm{D}t} = \frac{\mathrm{D}\boldsymbol{\sigma}}{\mathrm{D}t}\left(\frac{1}{2\mu}\right) = \boldsymbol{\varepsilon} + \boldsymbol{\omega}\cdot\boldsymbol{s} - \boldsymbol{s}\cdot\boldsymbol{\omega} + \mu_7(\boldsymbol{\varepsilon}\cdot\boldsymbol{s} + \boldsymbol{s}\cdot\boldsymbol{\varepsilon}) - \frac{1}{c}(\boldsymbol{\varepsilon}:\boldsymbol{s}')\boldsymbol{s}' \tag{4.36}$$

where

$$c = \frac{(2K+6\mu)\bar{\sigma}^2}{36\mu^3}. \tag{4.37}$$

The equations (4.36) can be written, in component form, for the present finite shear case, as

$$\frac{\mathrm{D}s_{11}}{\mathrm{D}\tau} = s_{12}\left[-\frac{s_{11}'}{c} + 1 + \mu_7\right], \tag{4.38}$$

$$\frac{\mathrm{D}s_{22}}{\mathrm{D}\tau} = s_{12}\left[-\frac{s_{22}'}{c} - 1 + \mu_7\right], \tag{4.39}$$

[2]In the remainder of this section, as well as Section 5, we integrate the equations as if they are of 'hypo-elasticity' as done by Truesdell [12, 13]. Thus, the classical plasticity concept of using one set of equations inside the yield surface and another set on the yield surface is ignored for simplicity, as it is not central to our discussion.

$$\frac{Ds_{33}}{D\tau} = s_{12}\left[-\frac{s'_{33}}{c}\right], \tag{4.40}$$

$$\frac{Ds_{12}}{D\tau} = \tfrac{1}{2}\left[1 + s_{11}(\mu_7 - 1) + s_{22}(1+\mu_7) - \frac{2}{c}s_{12}^2\right]. \tag{4.41}$$

Note that, as shown in Section 3, the purely *elastic* relation, namely $c \to \infty$, in (4.36) leads to different types of material response depending on the value of μ_7 (whether (i) $\mu_7 = \pm 1$, (ii) $\mu_7 = 0$, or (iii) $|\mu_7| > 1$). In the elastic-plastic case, viz. (4.36)–(4.41), the response can be seen to depend on not only μ_7 but also c.

In this case it may be noted that Truesdell [13] and Truesdell and Noll [9] presented results for the case, in which (i) $\dot{\sigma}^0 \equiv \hat{\mathrm{d}}\sigma/\mathrm{d}t$ in (4.22); (ii) $\mu_7 = 0$ and hence $\gamma_7 = \gamma_8 = 0$ in (3.11); (iii), due to (ii), $\dot{\sigma}^* = \hat{\mathrm{d}}\sigma/\mathrm{d}t$ in (4.22). Thus, the results in [13] and [9] correspond to the case when $\mu_7 = 0.0$ in (4.38)–(4.41).

Note that for an elastic-plastic structural metal, from (4.37) it may be noted that $c \ll 1$. However, for comparison purposes, (4.38)–(4.41) have been integrated in the present work for the cases: (a) $c = 4, \frac{1}{2}, \frac{1}{4}$, and $\frac{1}{100}$; and (b) $\mu_7 = 0, +1, -1$. The results for the case $|\mu_7| > 1$ have also been obtained but are not included since they do not have any particularly interesting features for the purposes of the present discussion.

Figs. 2–5 show the results for $s_{11}, s_{22}, s_{12}, s_{13}$ for the cases (i) $c = 4$, $\mu_7 = 0$; (ii) $c = \frac{1}{2}$, $\mu_7 = 0$; (iii) $c = \frac{1}{4}$, $\mu_7 = 0$, and (iv) $c = \frac{1}{100}$ and $\mu_7 = 0$, respectively. Note that the solution for s_{12} is oscillatory in time except for very small values of c. Further, it is seen that $s_{11} = -s_{22}$, while $s_{33} = 0$. It may be seen that Figs. 2–5 are identical to those of Truesdell and Noll [9] except they plot the results against arctan τ rather than τ.[3]

Figs. 6–9 show the results for s_{11}, s_{22}, s_{12}, and s_{33} for the cases (i) $c = 4$, $\mu_7 = 1$; (ii) $c = \frac{1}{2}$, $\mu_7 = 1$; (iii) $c = \frac{1}{4}$, $\mu_7 = 1$, and (iv) $c = \frac{1}{100}$ and $\mu_7 = 1$, respectively. It may be noted that in each case, each of the stresses is *non-oscillatory* with respect to time. Thus, Figs. 6–9 may represent a more realistic response of common metallic materials. However, in Figs. 2–5, s_{11} is positive while s_{22} is negative; while in Figs. 5–8, both s_{11} and s_{22} are positive and s_{33} is also non-zero.

Figs. 10–13 show the results for s_{11}, s_{22}, s_{12}, and s_{33} for the cases (i) $c = 4$, $\mu_7 = -1$; (ii) $c = \frac{1}{2}$, $\mu_7 = -1$; (iii) $c = \frac{1}{4}$, $\mu_7 = -1$, and (iv) $c = \frac{1}{100}$ and $\mu_7 = -1$, respectively. For these cases as well, each of the stresses is *non-oscillatory* with respect to time. However, as opposed to the earlier cases, here all the three stresses s_{11}, s_{22} and s_{33} are *compressive*.

Thus, the values of $\mu_7 = (+1)$ or (-1) both produce non-oscillatory results for each case of c while $\mu_7 = 0$ produces oscillatory results. In an analytical modeling of a material behaviour, whether $\mu_7 = +1$ or -1 or $|\mu_7| > 1$ must be decided only from an experiment on the material in question.

Since it has been shown that there are no oscillations in the *rigid-plastic* case irrespective of the definition of the stress-rate that is used, it may be concluded that the oscillations in the *elastic-plastic* case as present in Figs. 2–5 may be attributed to the modeling of the *elastic* portion of the constitutive law.

[3]For reasons left unexplained, Truesdell and Noll [9], for the case $c = 4$, present results only for values of time up to $\tau \simeq 1.75$ or arctan $\tau \simeq 60$ degrees. It may be seen that the results of [9] would be oscillatory even when plotted against arctan τ for values of this angle greater than 60 degrees.

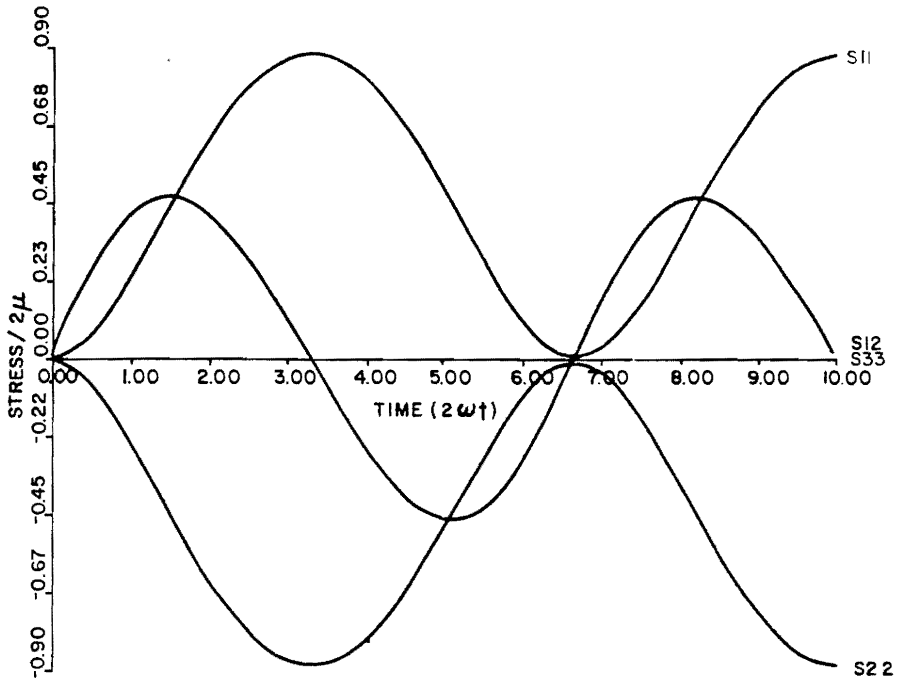

Fig. 2. Stress variations in simple shear: elasto-plastic isotropic-hardening material ($c = 4$, $\mu_7 = 0$).

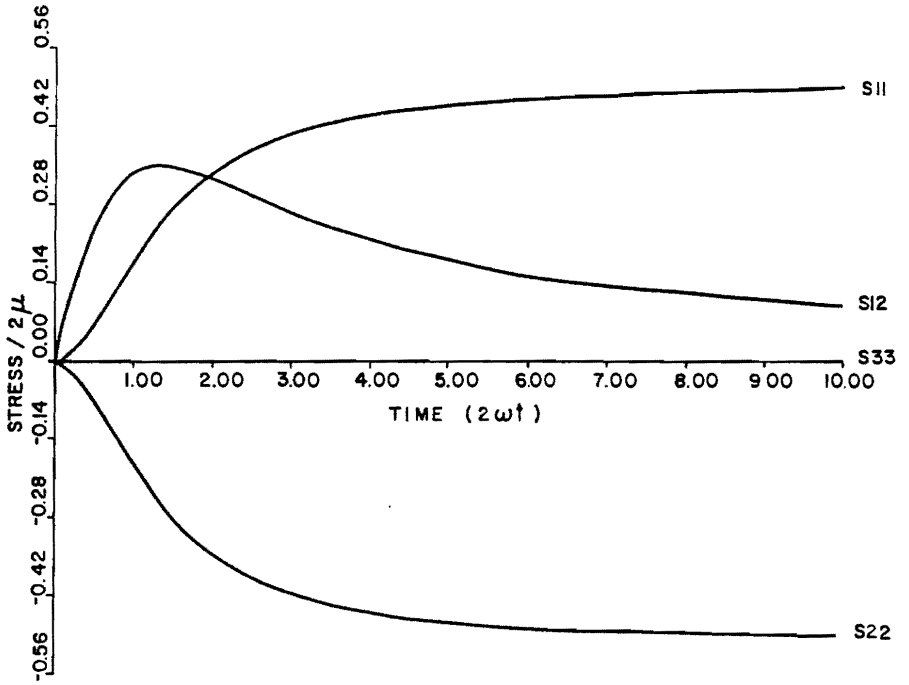

Fig. 3. Stress variations in simple shear: elasto-plastic isotropic-hardening material ($c = \frac{1}{2}$, $\mu_7 = 0$).

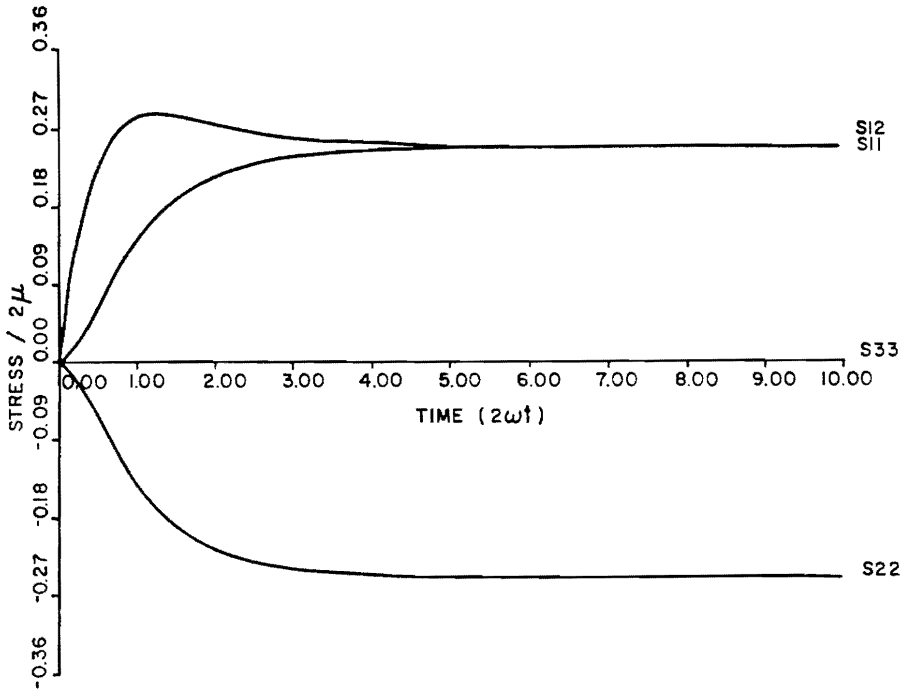

Fig. 4. Stress variations in simple shear: elasto-plastic isotropic-hardening material ($c = \frac{1}{4}$, $\mu_7 = 0$).

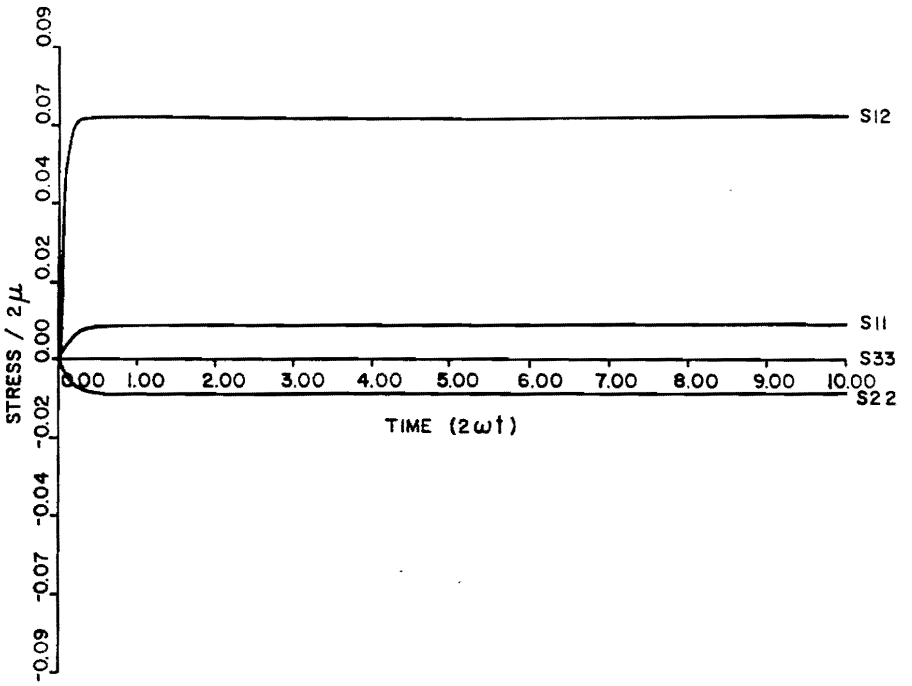

Fig. 5. Stress variations in simple shear: elasto-plastic isotropic-hardening material ($c = \frac{1}{100}$, $\mu_7 = 0$).

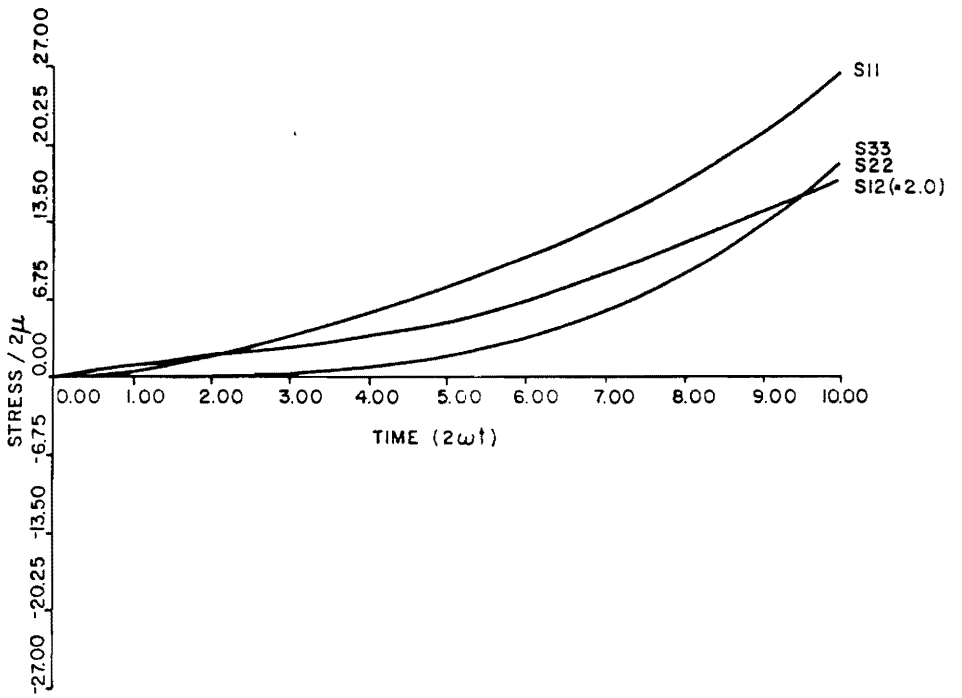

Fig. 6. Stress variations in simple shear: elasto-plastic isotropic-hardening material ($c = 4.0$, $\mu_7 = +1.0$).

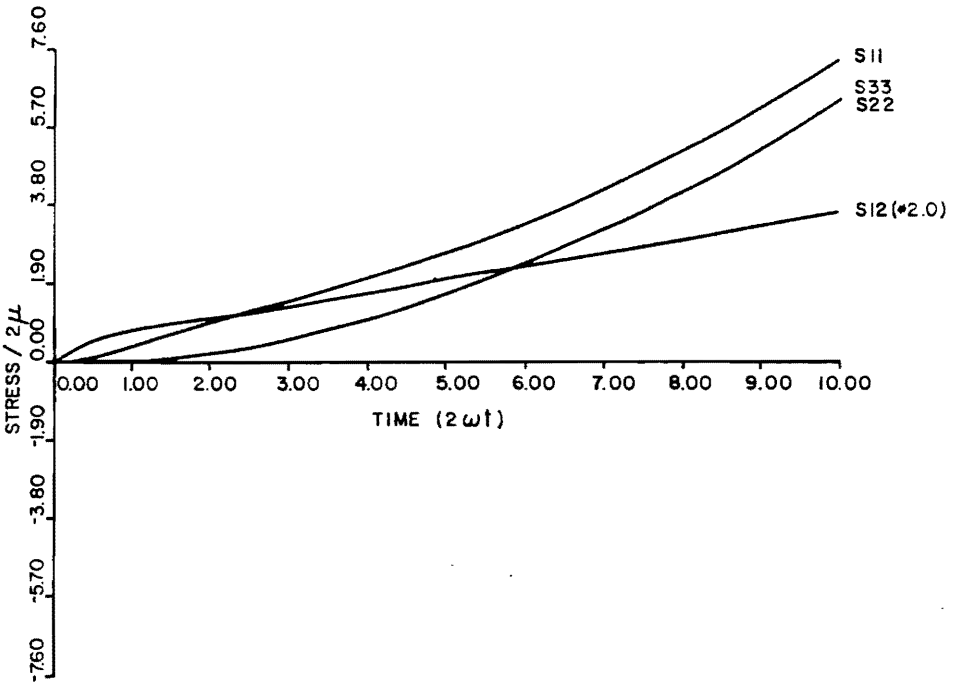

Fig. 7. Stress variations in simple shear: elasto-plastic isotropic-hardening material ($c = \frac{1}{2}$, $\mu_7 = +1.0$).

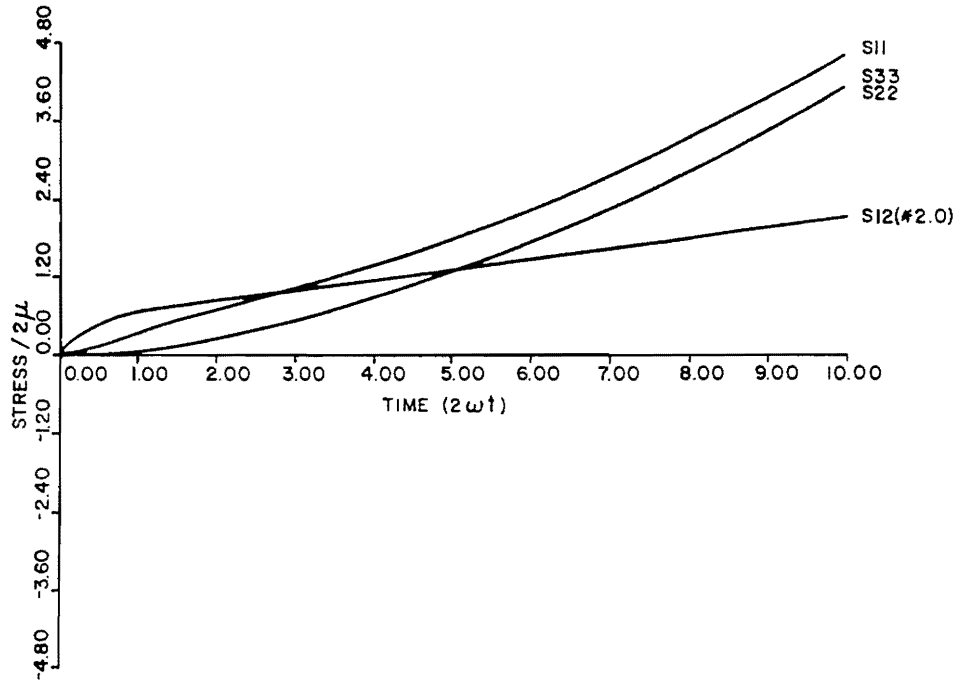

Fig. 8. Stress variations in simple shear: elasto-plastic isotropic-hardening material ($c = \frac{1}{4}$, $\mu_7 = +1.0$).

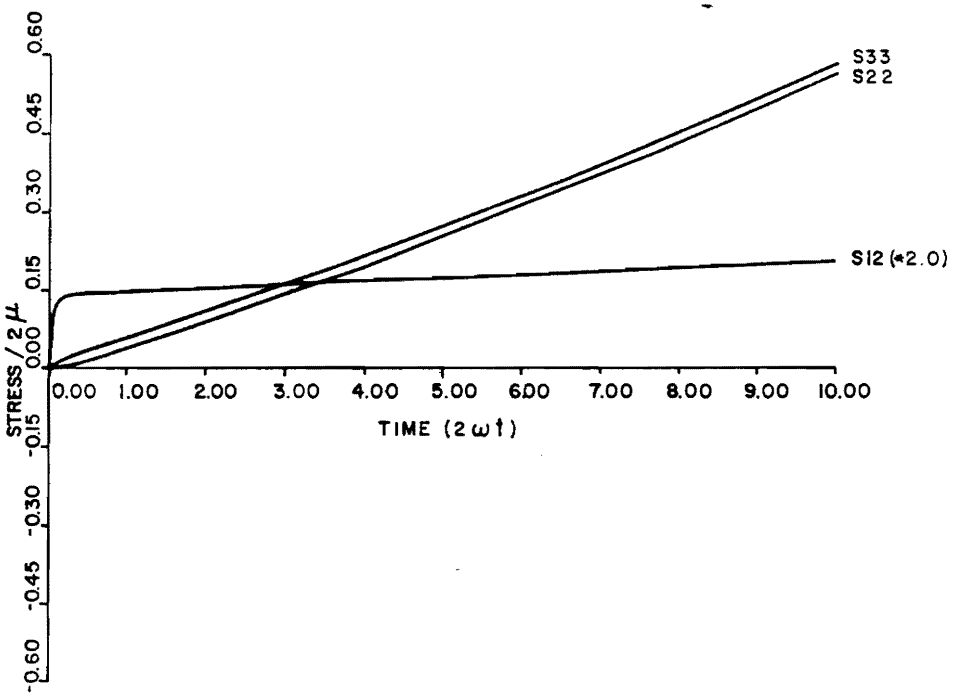

Fig. 9. Stress variations in simple shear: elasto-plastic isotropic-hardening material ($c = \frac{1}{100}$, $\mu_7 = +1.0$).

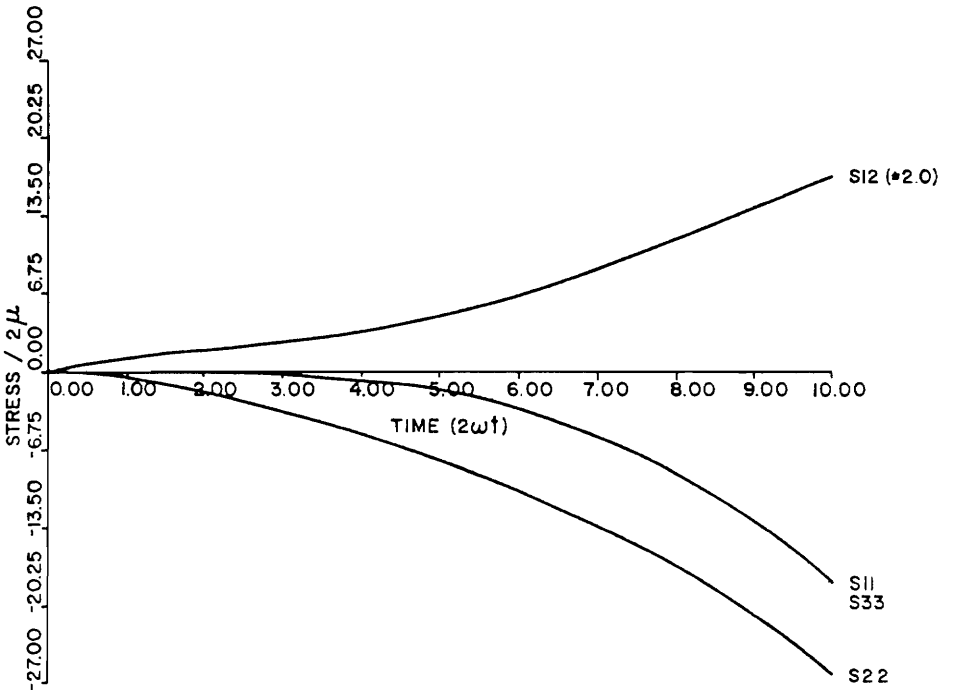

Fig. 10. Stress variations in simple shear: elasto-plastic isotropic-hardening material ($c = 4.0$, $\mu_7 = -1.0$).

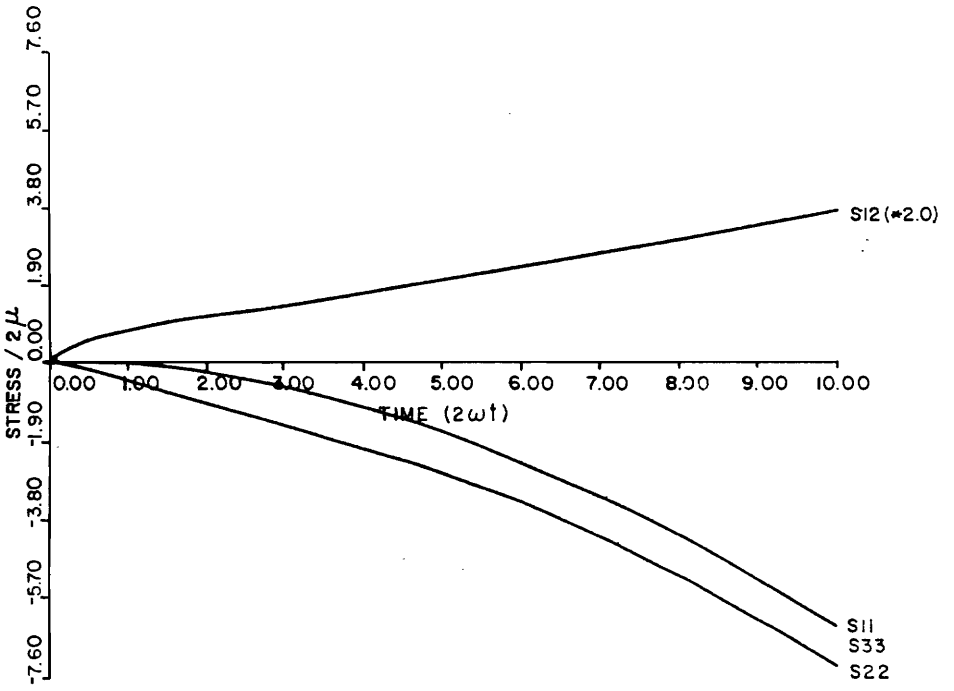

Fig. 11. Stress variations in simple shear: elasto-plastic isotropic-hardening material ($c = \frac{1}{2}$, $\mu_7 = -1.0$).

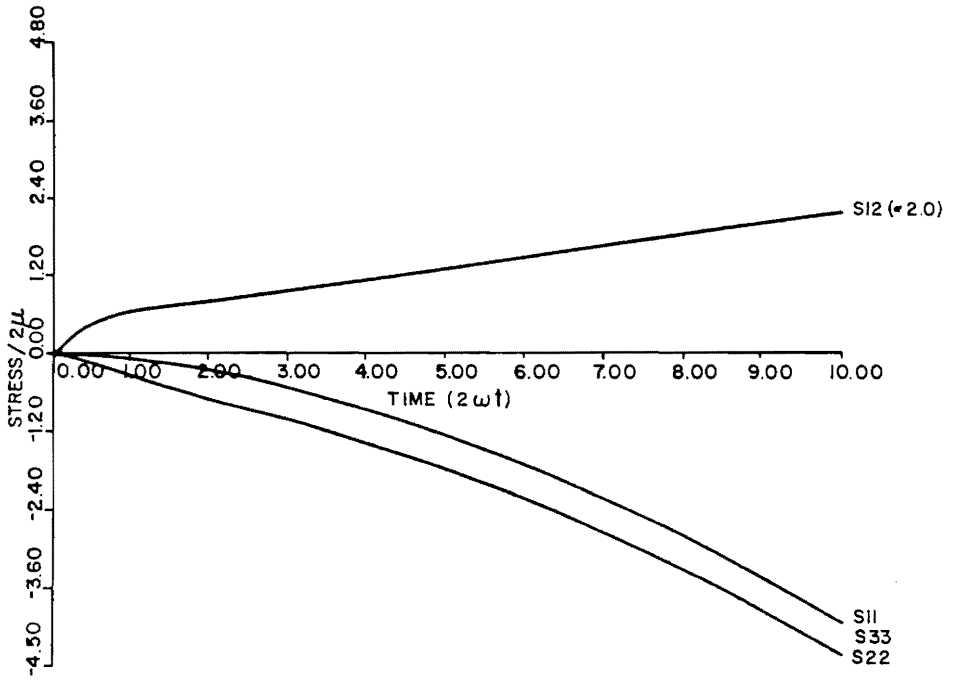

Fig. 12. Stress variations in simple shear: elasto-plastic strain-hardening material ($c = \frac{1}{4}$, $\mu_7 = -1.0$).

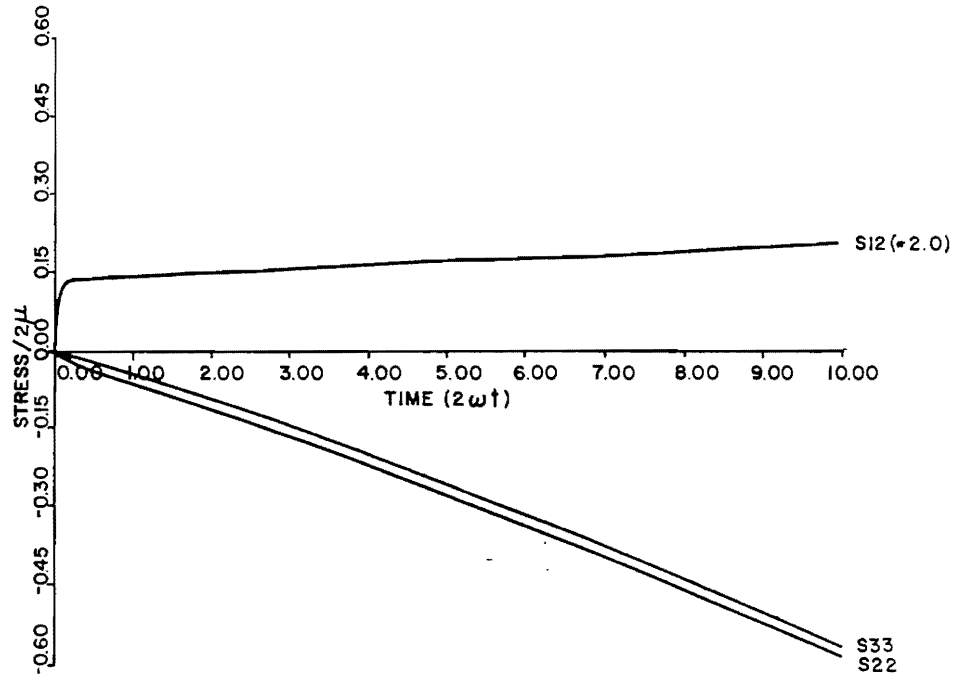

Fig. 13. Stress variations in simple shear: elasto-plastic strain-hardening material ($c = \frac{1}{100}$, $\mu_7 = -1.0$).

It should also be evident that even though the values $\mu_7 = \pm 1$ or $|\mu_7| > 1$ produce *non-oscillatory* results, these values can be used in conjunction with *any stress-rate* (cf. (4.22), (3.11)–(3.15)) *provided that the definition of the generalized stress-rate as in* (4.22) *is used.* Thus, no one stress-rate is preferable to others. However, it should be noted that the simple generalization as in McMeeking and Rice [16] may lead to erroneous results when large elastic strains are present.

We now consider finite strain plasticity with anisotropic hardening.

5. Classical elasto-plasticity: kinematic hardening

We consider the simple kinematic-hardening theory as suggested by Prager [18], in which the current yield surface is defined by

$$f = (\boldsymbol{\sigma}' - \boldsymbol{\alpha}') : (\boldsymbol{\sigma}' - \boldsymbol{\alpha}') - \tfrac{2}{3}\bar{\sigma}^2 = 0 . \tag{5.1}$$

The normality condition is

$$\boldsymbol{\varepsilon}^{\mathrm{p}} = \lambda \frac{\partial f}{\partial \boldsymbol{\sigma}} . \tag{5.2}$$

We will consider pure kinematic hardening, i.e. $\bar{\sigma}$ = constant. The consistency condition then becomes

$$\dot{f} = 0 = \frac{\partial f}{\partial \boldsymbol{\sigma}} : \dot{\boldsymbol{\sigma}}^* - \frac{\partial f}{\partial \boldsymbol{\sigma}} : \dot{\boldsymbol{\alpha}}^* = 0 . \tag{5.3}$$

The linear kinematic-hardening theory of Prager [18], as generalized to finite deformations, states that

$$\dot{\boldsymbol{\alpha}}^* = c\boldsymbol{\varepsilon}^{\mathrm{p}} \tag{5.4}$$

where c is a constant.

Use of (5.4) and (5.2) in (5.3) results in

$$\lambda = \left[\left(\frac{\partial f}{\partial \boldsymbol{\sigma}}\right) : \dot{\boldsymbol{\sigma}}^*\right] \Big/ c\left[\frac{\partial f}{\partial \boldsymbol{\sigma}} : \frac{\partial f}{\partial \boldsymbol{\sigma}}\right] . \tag{5.5}$$

Note that in the present generalizations to finite strain, $\dot{\boldsymbol{\sigma}}^*$ and $\dot{\boldsymbol{\alpha}}^*$ are generalized objective stress-rates such that, as in Section 4,

$$\dot{\boldsymbol{\sigma}}^* = \dot{\boldsymbol{\sigma}}^0 - \gamma_7(\boldsymbol{\sigma} \cdot \boldsymbol{\varepsilon}) - \gamma_8(\boldsymbol{\varepsilon} \cdot \boldsymbol{\sigma}) , \tag{5.6}$$

$$\dot{\boldsymbol{\alpha}}^* = \dot{\boldsymbol{\alpha}}^0 - \gamma_7(\boldsymbol{\alpha} \cdot \boldsymbol{\varepsilon}) - \gamma_8(\boldsymbol{\varepsilon} \cdot \boldsymbol{\alpha}) \tag{5.7}$$

where $\dot{\boldsymbol{\sigma}}^0$ and $\dot{\boldsymbol{\alpha}}^0$ can be any one of the rates $[(\hat{\mathrm{d}}\boldsymbol{\sigma}/\mathrm{d}t),\ \mathrm{D}^i\boldsymbol{\sigma}/\mathrm{D}t,\ i=1,\ldots,4]$ and $[(\hat{\mathrm{d}}\boldsymbol{\alpha}/\mathrm{d}t),\ \mathrm{D}^i\boldsymbol{\alpha}/\mathrm{D}t,\ i=1,\ldots,4]$; and γ_7 and γ_8 are defined as in (3.11)–(3.15).

It can easily be seen from (5.1) that

$$\frac{\partial f}{\partial \boldsymbol{\sigma}} : \frac{\partial f}{\partial \boldsymbol{\sigma}} = \tfrac{8}{3}\bar{\sigma}^2 , \tag{5.8}$$

and hence (5.4) becomes

$$\lambda = \frac{3}{(4c\bar{\sigma}^2)}[(\boldsymbol{\sigma}' - \boldsymbol{\alpha}') : \dot{\boldsymbol{\sigma}}^*] \tag{5.9}$$

and

$$\boldsymbol{\varepsilon}^{\mathrm{p}} = \frac{3}{2c\bar{\sigma}^2}[(\boldsymbol{\sigma}' - \boldsymbol{\alpha}') : \dot{\boldsymbol{\sigma}}^*](\boldsymbol{\sigma}' - \boldsymbol{\alpha}') . \tag{5.10}$$

We first consider the *rigid-plastic* case, as was done by Lee et al. [2, 3], and consider pure kinematic hardening, i.e. $\bar{\sigma}$ = constant. In this case, it follows from (5.3) that

$$2(\boldsymbol{\sigma}' - \boldsymbol{\alpha}') : (\dot{\boldsymbol{\sigma}}^* - \dot{\boldsymbol{\alpha}}^*) = 0 \tag{5.11}$$

or

$$(\boldsymbol{\sigma}' - \boldsymbol{\alpha}') : \dot{\boldsymbol{\sigma}}^* = (\boldsymbol{\sigma}' - \boldsymbol{\alpha}') : \dot{\boldsymbol{\alpha}}^* . \tag{5.12}$$

Thus, in rigid-plastic, *pure kinematic hardening*, we have from (5.10) and (5.12) that

$$\boldsymbol{\varepsilon}^{\mathrm{p}} = \frac{3}{(2c\bar{\sigma}^2)}[(\boldsymbol{\sigma}' - \boldsymbol{\alpha}') : \dot{\boldsymbol{\alpha}}^*](\boldsymbol{\sigma}' - \boldsymbol{\alpha}') . \tag{5.13}$$

Now we consider the example of *finite simple shear*, as described in (2.3) and (2.4). Because of the assumed rigid plasticity, in this example, $\boldsymbol{\varepsilon}^{\mathrm{p}} = \boldsymbol{\varepsilon}$. Thus, for the example,

$$\boldsymbol{\varepsilon}^{\mathrm{p}} = \boldsymbol{\varepsilon} = \begin{bmatrix} 0 & \omega & 0 \\ \omega & 0 & 0 \\ 0 & 0 & 0 \end{bmatrix} .$$

Since $(\boldsymbol{\sigma}' - \boldsymbol{\alpha}') : \dot{\boldsymbol{\alpha}}^* \neq 0$, we obtain from (5.13) that

$$\sigma'_{11} = \alpha'_{11} , \tag{5.14}$$

$$\sigma'_{22} = \alpha'_{22} , \tag{5.15}$$

$$\omega = \left(\frac{3}{2c\bar{\sigma}^2}\right)[(\boldsymbol{\sigma}' - \boldsymbol{\alpha}') : \dot{\boldsymbol{\alpha}}^*](\sigma_{12} - \alpha_{12}) . \tag{5.16}$$

Using (5.14) and (5.15) in (5.16), we find that

$$\frac{3}{(c\bar{\sigma}^2)}(\sigma_{12} - \alpha_{12})^2 \dot{\alpha}^*_{12} = \omega . \tag{5.17}$$

Now we consider the evolution of $\boldsymbol{\alpha}$ for the present rigid-plastic finite shear case. From (5.4), (5.7) and (3.11)–(3.15), we see that

$$\dot{\boldsymbol{\alpha}}^{\mathrm{m}} = c\boldsymbol{\varepsilon} + \boldsymbol{\omega}\cdot\boldsymbol{\alpha} - \boldsymbol{\alpha}\cdot\boldsymbol{\omega} + \mu_7(\boldsymbol{\alpha}\cdot\boldsymbol{\varepsilon} + \boldsymbol{\varepsilon}\cdot\boldsymbol{\alpha}) \tag{5.18}$$

where $\boldsymbol{\varepsilon}$ is given earlier and $\boldsymbol{\omega}$ is given by

$$\boldsymbol{\omega} = \begin{bmatrix} 0 & \omega & 0 \\ \omega & 0 & 0 \\ 0 & 0 & 0 \end{bmatrix}. \tag{5.19}$$

Thus, (5.18) can be written as

$$\frac{\mathrm{D}\alpha_{11}}{\mathrm{D}t} = \dot{\alpha}^{\mathrm{m}}_{11} = 2\omega\alpha_{12}(1+\mu_7), \tag{5.20}$$

$$\frac{\mathrm{D}\alpha_{12}}{\mathrm{D}t} = \omega[c + (\alpha_{22}-\alpha_{11}) + \mu_7(\alpha_{11}+\alpha_{22})], \tag{5.21}$$

$$\frac{\mathrm{D}\alpha_{22}}{\mathrm{D}t} = 2\omega\alpha_{12}(\mu_7 - 1), \tag{5.22}$$

$$\frac{\mathrm{D}\alpha_{33}}{\mathrm{D}t} = 0. \tag{5.23}$$

The system (5.20)–(5.23) is analogous to the system in (3.18)–(3.21) when, in the latter, one sets $\gamma_3 = \gamma_6 = 0$ and $\gamma_5 = c$. Thus, we may define a constant β such that

$$\beta = (\mu_7^2 - 1). \tag{5.24}$$

Assuming $\boldsymbol{\alpha} = \mathbf{0}$ at $t = 0$, we have the solution (cf. (3.27)–(3.32)):

$$\alpha_{12} = \begin{cases} c\omega t, & \beta = 0, \quad (5.25) \\ (c/2|\beta|^{1/2})\sin 2\omega|\beta|^{1/2}t, & \beta < 0, \quad (5.26) \\ (c/4\beta^{1/2})(\exp(2\omega\beta^{1/2}t) - \exp(-2\omega\beta^{1/2}t)), & \beta > 0, \quad (5.27) \end{cases}$$

$$\alpha_{11} = 2\omega(1+\mu_7)\int_t \alpha_{12}(\tau)\mathrm{d}\tau, \tag{5.28}$$

$$\alpha_{22} = 2\omega(\mu_7 - 1)\int_t \alpha_{12}(\tau)\mathrm{d}\tau, \tag{5.29}$$

$$\alpha_{33} = 0. \tag{5.30}$$

It may be seen that Nagtegaal and de Jong [1] and Lee [2] considered the case when $\mu_7 = 0$ or $\beta = -1$. Thus, from (5.26), (5.28) and (5.29), it is seen that in [1, 2], one has

$$\alpha_{12} = \tfrac{1}{2}\sin 2\omega t\,, \tag{5.31}$$

$$\alpha_{11} = -\alpha_{22} = \tfrac{1}{2}c[1-\cos 2\omega t]\,, \tag{5.32}$$

$$\alpha_{33} = 0\,. \tag{5.33}$$

Now, for the rigid-plastic finite shear problem, since

$$(\boldsymbol{\sigma}' - \boldsymbol{\alpha}') : \dot{\boldsymbol{\alpha}}^* = (\boldsymbol{\sigma}' - \boldsymbol{\alpha}') : c\boldsymbol{\varepsilon}^{\mathrm{p}} = 2(\sigma_{12} - \alpha_{12})\omega c\,, \tag{5.34}$$

it is seen that (5.16) leads to

$$\omega = \left(\frac{3\omega}{\bar{\sigma}^2}\right)(\sigma_{12} - \alpha_{12})^2 \tag{5.35}$$

or

$$(\sigma_{12} - \alpha_{12}) = \bar{\sigma}/\sqrt{3}\,. \tag{5.36}$$

From (5.14), (5.15), (5.36) and (5.31)–(5.33), it follows that

$$\sigma_{12} = \frac{\bar{\sigma}}{\sqrt{3}} + \tfrac{1}{2}c\sin 2\omega t \tag{5.37}$$

and

$$\sigma_{11} = -\sigma_{22} = \tfrac{1}{2}c(1-\cos 2\omega t)\,. \tag{5.38}$$

The solution for stresses for finite shear, as in (5.37), (5.58), is clearly unacceptable on physical grounds. It may also be seen from (5.14), (5.15), (5.16) and (5.31)–(5.36) that the reason for oscillatory solutions for $\boldsymbol{\sigma}$ is the oscillatory nature of 'back-stress' $\boldsymbol{\alpha}$ when $\mu_7 = 0$ or $\beta = -1$ in (5.24). This 'anomaly', first reported in [1], has prompted a series of investigations by Lee and his colleagues [2, 3].

In order to remedy the above 'anomaly', Lee et al. [2, 3] proposed a 'modified' Zaremba–Jaumann–Noll rate. This 'modified rate' has a form analogous to that of $\hat{\mathrm{d}}\boldsymbol{\tau}/\mathrm{d}t$ of (1.13), except it is based on the "spin of the specific material directions associated with the kinematic hardening" rather than the spin $\boldsymbol{\omega}$ of the material particle (which is physically the angular velocity of the principal directions of the strain-rate $\boldsymbol{\varepsilon}$). Lee et al. have so far aimed at deriving such a modified rate for the specific problem of finite shear, while such a 'modified rate' for general non-homogeneous three-dimensional deformations appears, as yet, to be vague.

However, it can be seen from the present theory that if $\beta = 0$ (i.e., $\mu_7 = \pm 1$, in (5.18) and (5.24)), we have, from (5.25)–(5.30) that the solution for $\boldsymbol{\alpha}$ is

$$\alpha_{12} = c\omega t\,, \quad \mu_7 = \pm 1\,, \tag{5.39}$$

$$\alpha_{11} = \begin{cases} 2c(\omega t)^2\,, & \mu_7 = +1\,, \\ 0\,, & \mu_7 = -1\,, \end{cases} \tag{5.40a, 5.40b}$$

$$\alpha_{22} = \begin{cases} 0\,, & \mu_7 = +1\,, \\ -2c(\omega t)^2\,, & \mu_7 = -1\,. \end{cases} \tag{5.41a, 5.41b}$$

Hence, it follows from (5.14)–(5.16) and (5.34)–(5.36) that

$$\sigma_{11} = \begin{cases} 2c(\omega t)^2, & \mu_7 = +1, \\ 0, & \mu_7 = (-1), \end{cases} \tag{5.42a}$$
(5.42b)

$$\sigma_{22} = \begin{cases} 0, & \mu_7 = +1, \\ -2(\omega t)^2, & \mu_7 = -1, \end{cases} \tag{5.43a}$$
(5.43b)

$$\sigma_{12} = \frac{\bar{\sigma}}{\sqrt{3}} + c\omega t, \quad \mu_7 = \pm 1. \tag{5.44}$$

Thus, the solution in (5.42a)–(5.44) are non-oscillatory and are physically plausible for structural metals. Which pair of solutions, corresponding to $\mu_7 = (+1)$ or (-1), respectively, is more realistic depends on an actual experiment on the material.

It should be noted that the present theory based on 'generalized' objective rates $\dot{\boldsymbol{\alpha}}^*$ and $\dot{\boldsymbol{\sigma}}^*$ is applicable, clearly, to general non-homogeneous three-dimensional deformations. Moreover, the condition $\mu_7 = \pm 1$ can be achieved in (5.18) for *any one* of the objective rates $(\hat{\mathrm{d}}/\mathrm{d}t)$ or $\mathrm{D}^i/\mathrm{D}t$ through defining γ_7 and γ_8 in (5.6), (5.7), as per (3.11)–(3.15).

We have so far seen that: (i) there are no oscillations in a rigid-plastic isotropic-hardening theory; (ii) there may be oscillations in an *elastic*-plastic isotropic hardening theory, due to an improper 'elastic' constitutive law; (iii) there may be oscillations in a rigid-plastic kinematic-hardening theory due to an 'improper' equation for the rate of $\boldsymbol{\alpha}$. We conclude the present paper by considering an *elastic-plastic* theory with *kinematic* hardening.

Here we postulate an elastic-plastic constitutive law of the type in (4.27), (4.28) except that $\boldsymbol{\varepsilon}^{\mathrm{p}}$ is determined from (5.10) instead of (4.16). Thus, in terms of the 'generalized rates' $\dot{\boldsymbol{\sigma}}^*$ and $\dot{\boldsymbol{\alpha}}^*$, we have the elastic-plastic kinematic-hardening constitutive law

$$\dot{\boldsymbol{\sigma}}^* = 2\mu\boldsymbol{\varepsilon} + \lambda(\boldsymbol{\varepsilon} : \boldsymbol{I})\boldsymbol{I} - 2\mu\left[\frac{3\mu}{(c+2\mu)\bar{\sigma}_0^2}[\boldsymbol{\varepsilon} : (\boldsymbol{\sigma}' - \boldsymbol{\alpha}')](\boldsymbol{\sigma}' - \boldsymbol{\alpha}')\right] \tag{5.45}$$

and

$$\dot{\boldsymbol{\alpha}}^* = c\boldsymbol{\varepsilon}^{\mathrm{p}}. \tag{5.46}$$

In the above, $\dot{\boldsymbol{\sigma}}^*$ and $\dot{\boldsymbol{\alpha}}^*$ are as in (5.6), (5.7) and, hence, are related to material rates as

$$\frac{\mathrm{D}\boldsymbol{\sigma}}{\mathrm{D}t} = \dot{\boldsymbol{\sigma}}^{\mathrm{m}} = \dot{\boldsymbol{\sigma}}^* + \boldsymbol{\omega}\cdot\boldsymbol{\sigma} - \boldsymbol{\sigma}\cdot\boldsymbol{\omega} + \mu_7(\boldsymbol{\sigma}\cdot\boldsymbol{\varepsilon} + \boldsymbol{\varepsilon}\cdot\boldsymbol{\sigma}) \tag{5.47}$$

and

$$\dot{\boldsymbol{\alpha}}^{\mathrm{m}} = \dot{\boldsymbol{\alpha}}^* + \boldsymbol{\omega}\cdot\boldsymbol{\alpha} - \boldsymbol{\alpha}\cdot\boldsymbol{\omega} + \mu_7(\boldsymbol{\alpha}\cdot\boldsymbol{\varepsilon} + \boldsymbol{\varepsilon}\cdot\boldsymbol{\alpha}), \tag{5.48}$$

and μ_7 is defined for various rates as in (3.11)–(3.15). We consider the finite shear problem of (2.3), (2.4) and define a change in variables as

$$\frac{\mathrm{D}s}{\mathrm{D}\tau} = \left(\frac{\mathrm{D}\boldsymbol{\sigma}}{\mathrm{D}t}\right)\left(\frac{1}{2\mu}\right)\left(\frac{1}{2\omega}\right), \qquad \frac{\mathrm{D}\boldsymbol{\beta}}{\mathrm{D}\tau} = \left(\frac{\mathrm{D}\boldsymbol{\alpha}}{\mathrm{D}t}\right)\left(\frac{1}{2\mu}\right)\left(\frac{1}{2\omega}\right). \tag{5.49}$$

Using (5.45)–(5.49), we obtain the following differential equations[4] for the present elastic

[4]For simplicity, we set $\boldsymbol{\varepsilon}^{\mathrm{p}} = \boldsymbol{\varepsilon}$ in the evolution equation for $\boldsymbol{\alpha}$. For large strains, this assumption has been found to be inconsequential.

kinematic-hardening plastic finite shear problem:

$$\frac{D\beta_{11}}{D\tau} = \beta_{12}(1+\mu_7)\,, \tag{5.50}$$

$$\frac{D\beta_{22}}{D\tau} = \beta_{12}(\mu_7-1)\,, \tag{5.51}$$

$$\frac{D\beta_{12}}{D\tau} = \tfrac{1}{2}[c^* + (\beta_{22}-\beta_{11}) + \mu_7(\beta_{11}+\beta_{22})]\,, \tag{5.52}$$

$$\frac{D\beta_{33}}{D\tau} = 0\,, \tag{5.53}$$

$$\frac{Ds_{11}}{D\tau} = [-c_3(s_{12}-\beta_{12})(s'_{11}-\beta'_{11}) + s_{12}(1+\mu_7)]\,, \tag{5.54}$$

$$\frac{Ds_{22}}{D\tau} = [-c_3(s_{12}-\beta_{12})(s'_{22}-\beta'_{22}) + s_{12}(\mu_7-1)\,, \tag{5.55}$$

$$\frac{Ds_{12}}{D\tau} = \tfrac{1}{2}[1+\mu_7(s_{11}+s_{22}) + (s_{22}-s_{11}) - 2c_3(s_{12}-\beta_{12})^2]\,, \tag{5.56}$$

$$\frac{Ds_{33}}{D\tau} = -c_3(s_{12}-\beta_{12})(s'_{33}-\alpha'_{33}) \tag{5.57}$$

where

$$c_3 = \frac{6\mu^2}{\bar{\sigma}^2(c^*+1)} \equiv \frac{1}{K^2(c^*+1)}\,, \tag{5.58}$$

$$c^* = (c/2\mu)\,. \tag{5.59}$$

We present, in the following, numerical solutions of the differential system (5.50)–(5.57) for the case when $c = \frac{2}{3}\bar{\sigma}$, i.e.,

$$c^* = \frac{\bar{\sigma}}{3\mu} = \sqrt{\tfrac{2}{3}}\,K\,. \tag{5.60}$$

It is noted that the present results are for the elastic purely kinematic-hardening case ($\bar{\sigma}$ = constant). In all the results to follow, $K^2 = (\bar{\sigma}^2/6\mu^2) = \frac{1}{400}$. Figs. 14 and 15 show the solutions for the non-dimensional back-stress β_{ij} and true stress s_{ij} for the case $\mu_7 = 0$. From Fig. 14 it is seen that β_{ij} is oscillatory and, as in the rigid kinematic-hardening plastic case, this causes s_{ij} to oscillate as in Fig. 15. Figs. 16 and 17 show the results for β_{ij} and s_{ij}, respectively, for the case when $\mu_7 = +1.0$. Here all the components of β_{ij} and s_{ij} are non-oscillatory and thus are physically plausible for structural metals. Finally, Figs. 18 and 19 show the results for β_{ij} and s_{ij}, respectively, when $\mu_7 = -1.0$. Even though the results for s_{12} in both the cases $\mu_7 = (+1)$ or (-1) are physically plausible, those for s_{11} and s_{22}, while also non-oscillatory, are quite different when $\mu_7 = +1$ from those when μ_7 is (-1). An experiment must be used as an ultimate guide in deciding which of these behaviours is correct. Once again, the value of μ_7 can be set to be ± 1 when any one of the stress-rates $\hat{d}/dt$, D^i/Dt is used as noted earlier.

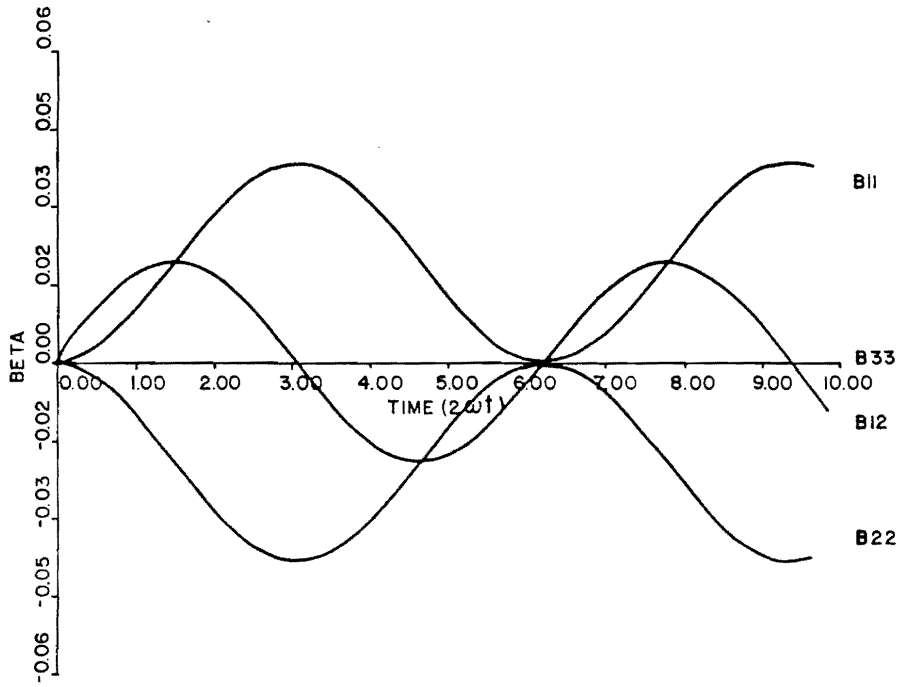

Fig. 14. Variation of back-stresses ($\alpha/2\mu$) in simple shear: elasto-plastic kinematic-hardening material ($K^2 = \frac{1}{400}$, $\mu_7 = 0$).

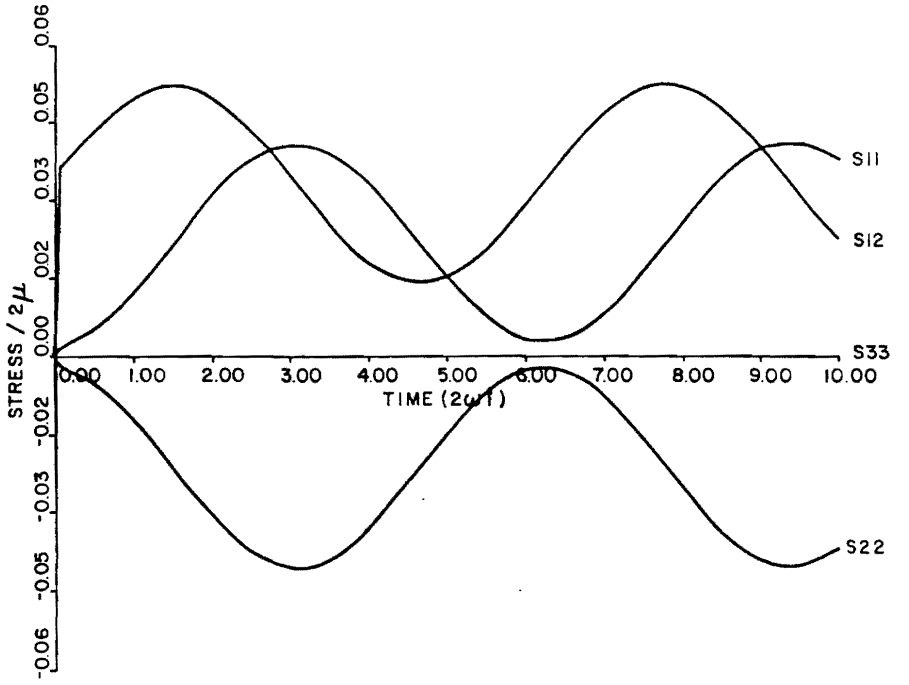

Fig. 15. Variation of stresses in simple shear: elasto-plastic kinematic-hardening material ($K^2 = \frac{1}{400}$, $\mu_7 = 0$).

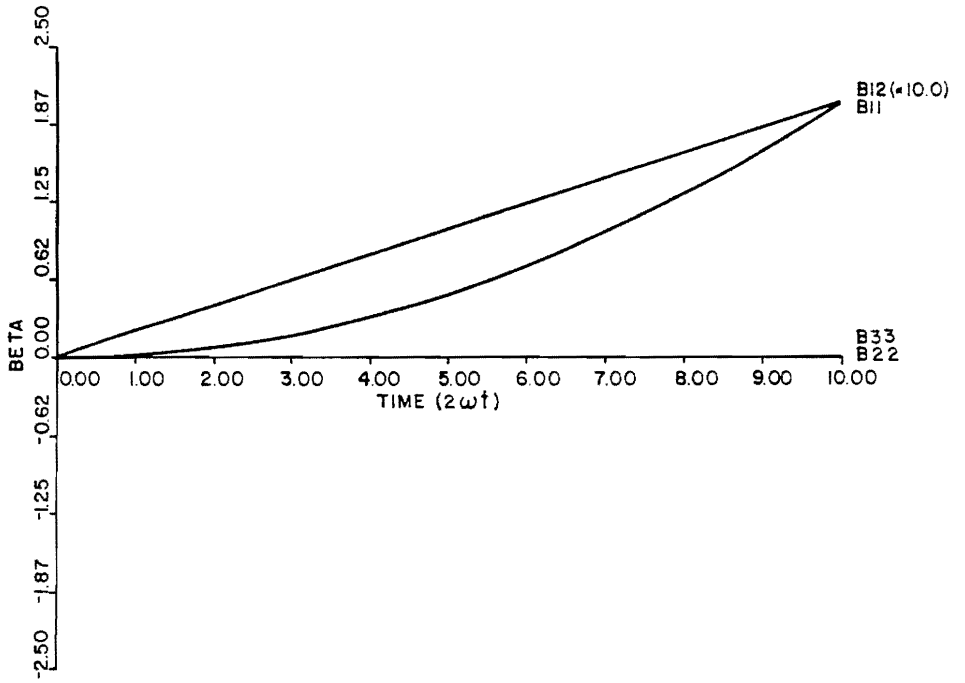

Fig. 16. Variation of back-stresses ($\alpha/2\mu$) in simple shear: elasto-plastic kinematic-hardening material ($K^2 = \frac{1}{400}$, $\mu_7 = 1.0$).

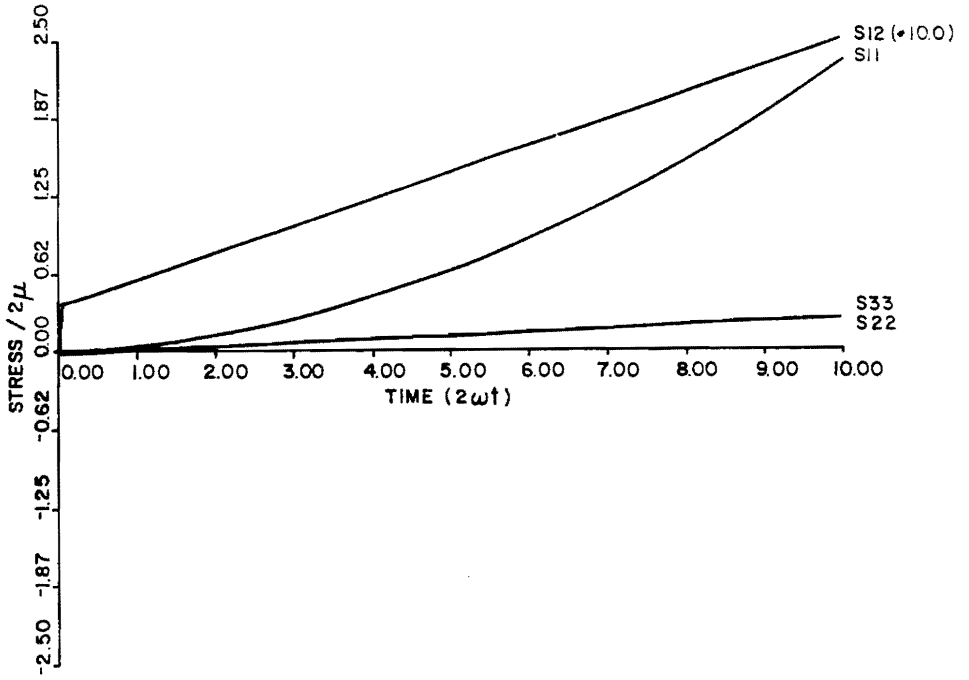

Fig. 17. Variation of stresses in simple shear: elasto-plastic kinematic-hardening material ($K^2 = \frac{1}{400}$, $\mu_7 = 1.0$).

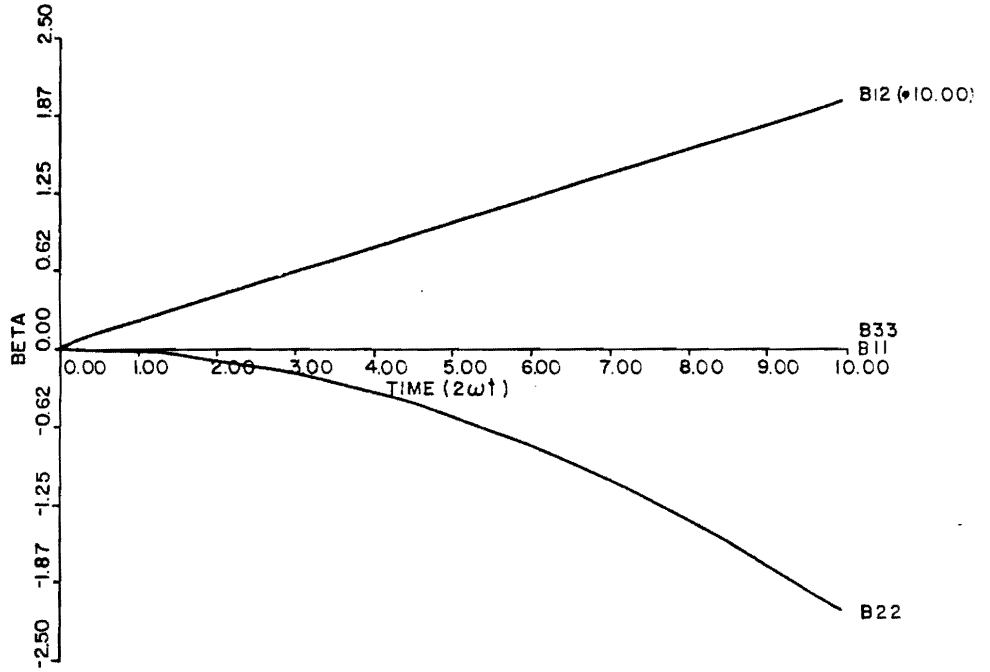

Fig. 18. Variation of back-stresses ($\alpha/2\mu$) in simple shear: elasto-plastic kinematic-hardening material ($K^2 = \frac{1}{400}$, $\mu_7 = -1.0$).

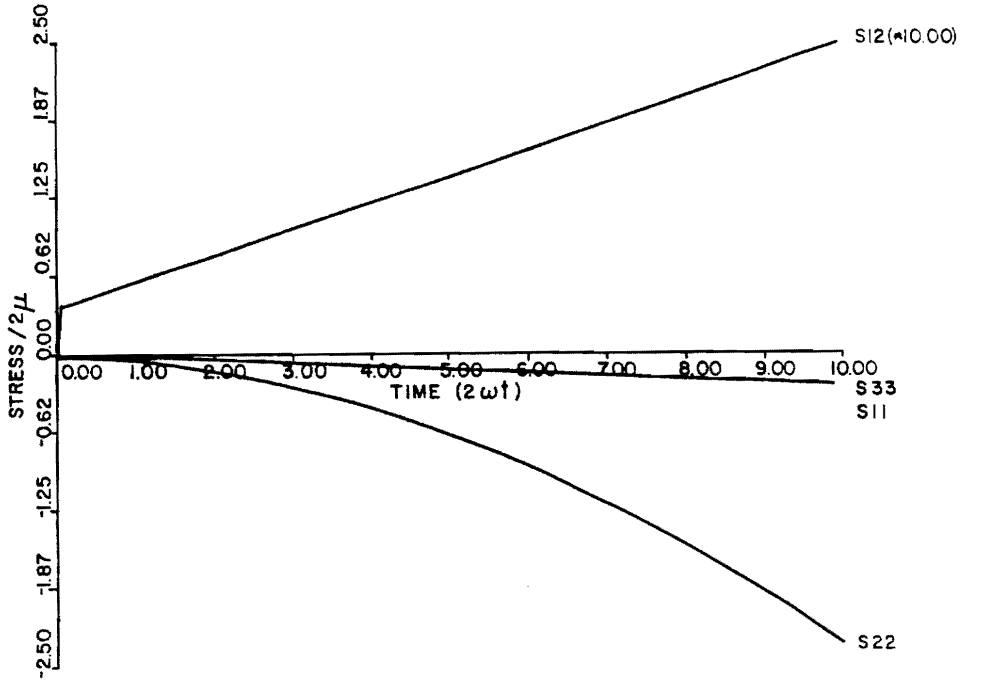

Fig. 19. Variation of stresses in simple shear: elasto-plastic kinematic-hardening material ($K^2 = \frac{1}{400}$, $\mu_7 = -1.0$).

6. Closure

It has been demonstrated that the recent controversies in the choices of stress-rates, in postulating constitutive laws, are largely without basis. More importantly, the anomalies in the finite strain kinematic-hardening plasticity disappear when the generalized stress-rates $\dot{\sigma}^*$ and $\dot{\alpha}^*$ are used.

Acknowledgment

The results presented above were obtained during the course of investigations supported under a grant from the NASA Lewis Research Center, Cleveland, to the Georgia Institute of Technology. The author gratefully acknowledges this support. The assistance of Mr. C.-T. Yang in obtaining the numerical solutions presented herein is thankfully acknowledged. It is a pleasure to acknowledge the assistance of Ms. J. Webb in the preparation of this manuscript.

References

[1] J.C. Nagtegaal and J.E. de Jong, Some aspects of non-isotropic workhardening in finite strain plasticity, in: E.H. Lee and R.L. Mallett, eds., Plasticity of Metals at Finite Strain: Theory, Experiment and Computation, (Div. Appl. Mech. Stanford University and Dept. Mech. Engrg. R.P.I. 1982) 65–102.
[2] E.H. Lee, R.L. Mallett and T.B. Wertheimer, Stress analysis for anisotropic hardening in finite-deformation plasticity, Rept., 1982.
[3] E.H. Lee, Finite deformation effects in plasticity theory, in: Developments in Theoretical and Applied Mechanics (The University of Alabama in Huntsville, 1982) 75–90.
[4] R. Rubinstein and S.N. Atluri, Objectivity of incremental constitutive relations over finite time steps in computational finite deformation analysis, Comput. Meths. Appl. Mech. Engrg. 36 (1983) 277–290.
[5] S.N. Atluri, Lecture Notes (Georgia Institute of Technology, Atlanta, 1980).
[6] C. Truesdell, The simplest rate theory of pure elasticity, Comm. Pure Appl. Math. 8 (1955) 123–132.
[7] J.G. Oldroyd, On the formulation of rheological equations of state, Proc. Roy. Soc. London Ser. A 200 (1950) 523–541.
[8] B.A. Cotter and R.S. Rivlin, Tensors associated with time-dependent stress, Quart. Appl. Math 13 (1955) 177–182.
[9] C. Truesdell and W. Noll, The nonlinear field theories of mechanics, in: S. Flugge, ed., Encyclopedia of Physics (Springer, Berlin, 1965).
[10] J.K. Dienes, On the analysis of rotation and stress rate in deforming bodies, Acta Mech. 32 (1979) 217–232.
[11] S.N. Atluri, On some new general and complementary energy theorems for the rate problem of classical, finite strain elastoplasticity, J. Structural Mech. 8(1) (1980) 36–66.
[12] C. Truesdell, Hypo-elasticity, J. Rational Mech. Anal. 4 (1955) 83–133 (see some corrections, 1019–1020).
[13] C. Truesdell, Hypo-elastic shear, J. Appl. Phys. 27 (1956) 441–447.
[14] R.S. Rivlin, Further remarks on the stress-deformation relations for isotropic materials, J. Rational Mech. Anal. 4 (1955) 681–702.
[15] R. Hill, On the classical constitutive relations for elastic/plastic solids in: B. Broberg et al., eds., Recent Progress in Applied Mechanics (The Folke Odquist Volume) (Wiley, New York, 1967) 241.
[16] R.M. McMeeking and J.R. Rice, Finite element formulations for problems of large elastic-plastic deformation, Internat. J. Solids and Structures 11 (1975) 601–616.

[17] T.Y. Thomas, On the structure of stress-strain relations, and Combined elastic and Prandtl–Reuss stress-strain relations, Proc. Nat. Acad. Sci. U.S.A. 41 (1955) 716–720 and 720–726, resp.
[18] W. Prager, A new method of analyzing stresses and strains in work-hardening plastic solids, J. Appl. Mech. 23 (1956) 493–496.
[19] J.H. Arygris and J.St. Doltsinis, On the large strain inelastic analysis in natural formulation—Part I. Quasistatic problems, Comput. Meths. Appl. Mech. Engrg. 20 (1980) 213–251.
[20] J.H. Argyris, J.St. Doltsinis, P.M. Pimenta and H. Wüstenberg, Thermomechanical response of solids at high strains—natural approach, Comput. Meths. Appl. Mech. Engrg. 32 (1982) 3–57.

212

EXISTENCE AND STABILITY, AND DISCRETE BB AND RANK CONDITIONS, FOR GENERAL MIXED-HYBRID FINITE ELEMENTS IN ELASTICITY

W-M. Xue[1] and S. N. Atluri[2]
Center for the Advancement of Computational Mechanics
Georgia Institute of Technology
Atlanta, Georgia

RACT

In this paper, all possible forms of mixed-hybrid te element methods that are based on multi-field ational principles are examined as to the condi- s for existence, stability, and uniqueness of r solutions. The reasons as to why certain "sim- ied hybrid-mixed methods" in general, and the alled "simplified hybrid-displacement method" in icular (based on the so-called simplified ational principles), become unstable, are ussed. A comprehensive discussion of the crete" BB-conditions, and the rank conditions, of natrices arising in mixed-hybrid methods, is n. Some recent studies aimed at the assurance of rank conditions, and the related problem of the lance of spurious kinematic modes, are presented.

NTS

DUCTION

arly finite element researchers were beleaguered rtain fourth-order problems, such as plate bend- wherein the basis functions in a "compatible- lacement" approach were required to be C^1 nuous. This has generally lead to the search lternate finite element methods in elasticity, ein discontinuous displacements and/or iprocated traction fields are allowable as basis ions, with a suitably reformulated variational framework. Much of this work is summarized in (1-4). Amongst the first such alternate methods is the now so-called "hybrid-stress" method (5,6). The mathematical analyses of these methods is only of recent origin. While the early alternate methods mixed-hybrid methods) were developed on more or less heuristic bases, a firm mathematical analysis of the existence, uniqueness, and stability of solutions based on these methods is hitherto lacking in general; and such an analysis is of primary concern in this paper.

Some of the earliest mathematical studies of the hybrid-mixed methods are due to Babuska and his colleagues (7-12). In 1974, Brezzi (13) presented an interesting study of the existence and stability conditions for solutions to a saddle-point problem with a single Lagrange multiplier. These conditions are labeled, for purposes of this paper, as "BB-conditions" (Babuska-Brezzi conditions). The BB-conditions have been explored recently in a variety of problems. In the study of "penalty methods" for finite element approximation of incompressibility, Oden (14,15) pointed out that the BB-condition plays a fundamental role in stability and convergence considerations. In the study of a "hybrid-stress" finite element method for Stokes flow, in which there are three fields involved in the variational equation, Ying and Atluri (16,17) pointed out the need for satisfying two BB-conditions simultaneously. The skill of the analyst is challenged by the need to choose basis functions for each field in each element such that the discrete BB-conditions are satisfied a priori. On a physical basis, the satisfaction of the discrete BB-conditions is, sometimes, synonymous with the need for the avoidance of the so-called "kinematic" or "zero-energy" modes in mixed-hybrid finite element methods (18-22).

The BB-conditions may be viewed as strategies for analyzing such approximation methods: the approximation methods are characterized by certain bilinear forms, norms (spaces), and families of finite dimensional approximations. Then the error estimates of these norms follow directly. If the BB-conditions

-Doctoral Fellow; currently on the faculty of the of Mech., Tsing-Hua University, Beijing, PRC
nts' Professor of Mechanics

in Hybrid and Mixed FEM, AMD Vol. 73 (Ed. R. Spilker), pp. 91-102, 1985

are not satisfied for some approximation methods, then the methods are not stable. Thus, the strategy for a successful finite element algorithm based on multi-field variational principles consists of two essential steps: (1) knowing the form of the BB-conditions to be satisfied globally, as well as locally (at the element level), and (2) a modus operandi for choosing the basis functions for each of the fields in each element such that the local BB-conditions are satisfied ab initio. Such strategies are the main topics of concern in this paper, in the context of linear solid mechanics.

In Section 3, we present an abstract statement of the Hu-Washizu principle in linear elasticity. In Section 4, we present four types of multi-field principles in linear elasticity, suitable for use in conjunction with discontinuous displacement fields and unreciprocated traction fields. In Section 4, we present the theoretical results concerning the BB-conditions for various mixed-hybrid finite element methods based on multi-field variational principles. Section 5 deals with the so-called "simplified variational principles" and the reasons as to why the so-called "simplified hybrid-displacement method" is, in fact, unstable. Section 6 contains a discussion on the rank condition, i.e. discrete BB-conditions for various mixed-hybrid methods. Specifically, the relation between the rank condition and the singular value of the "BB matrix" is established. The latter will provide, for practical applications, a simple method to check the discrete BB-condition and give a "measure" of the BB-condition to select better hybrid-mixed elements.

ABSTRACT STATEMENT OF HU-WASHIZU PRINCIPLE IN LINEAR ELASTICITY

We consider a linear elastic solid undergoing infinitesimal deformation. Cartesian coordinates x_i identify material particles in the solid; ε_{ij} are the components of the strain tensor; σ_{ij} are components of the stress tensor; u_i are components of the displacement vector; $\bar{f}_i$ are body forces prescribed in the domain Ω of the solid; $\bar{t}_i$ are tractions prescribed at the boundary S_t of the solid Ω; $\bar{u}_i$ are displacements prescribed at the boundary S_u of the solid; and $(.)_{,i}$ denotes a partial derivative with respect to x_i.

The governing equations and boundary conditions of linear elastostatics are well known:

Find $(\sigma, \varepsilon, u) \in T \times E \times V$, s.t.

$$\sigma_{ij} = a_{ijk\ell}\varepsilon_{k\ell} \quad \text{in } \Omega \quad (a)$$

$$\varepsilon_{ij} = u_{(i,j)} \quad \text{in } \Omega \quad (b)$$

$$u_i = \bar{u}_i \quad \text{at } S_u \quad (c)$$

$$\sigma_{ij,j} + \bar{f}_i = 0 \quad \text{in } \Omega \quad (d)$$

$$\sigma_{ij}n_j \equiv t_i = \bar{t}_i \quad \text{at } S_t \quad (e) \qquad (3.1)$$

If the material is isotropic, the coefficients of elasticity $a_{ijk\ell}$ have the properties of symmetry and of ellipticity:

$$a_{ijk\ell} = a_{ij\ell k} = a_{k\ell ij} \qquad (3.2a)$$

$$a_{ijk\ell}\varepsilon_{ij}\varepsilon_{k\ell} \geq \alpha\, \varepsilon_{ij}\varepsilon_{ij} \quad \forall\, \varepsilon_{ij} \qquad (3.2b)$$

where the positive number α depends only upon the property of material. The weak form of (3.1) leads to the following multi-field variational problem:

Find $(\varepsilon, \sigma, u) \in E \times T \times V$, s.t.

$$a(\varepsilon,e) - \ell(e,\sigma) = 0 \qquad \forall\, e \in E$$

$$\ell(\varepsilon,\tau) - p(\tau,u) = \langle g,\tau\rangle \qquad \forall\, \tau \in T$$

$$p(\sigma,v) = \langle f,v\rangle \qquad \forall\, v \in V \qquad (3.3)$$

where the bilinear forms a, ℓ, p and the linear functionals $\langle g,.\rangle$ and $\langle f,.\rangle$ are defined by

$$a(\varepsilon,e) = \int_\Omega a_{ijk\ell}\,\varepsilon_{k\ell}\,\varepsilon_{ij}\,d\Omega$$

$$\ell(\varepsilon,\tau) = \int_\Omega \varepsilon_{ij}\,\tau_{ij}\,d\Omega$$

$$p(\tau,v) = \int_\Omega \tau_{ij}\,v_{(i,j)}\,d\Omega - \int_{S_u} \tau_{ij}\,n_j\,u_i\,ds$$

$$\langle f,v\rangle = \int_\Omega \bar{f}_i\,v_i\,d\Omega + \int_{S_t} \bar{t}_i\,v_i\,ds$$

$$\langle g,\tau\rangle = \int_{S_u} \tau_{ij}\,n_j\,\bar{u}_i\,ds \qquad (3.4)$$

For deriving the last equation in (3.3), we use the first Green's formula in space $H^1(\Omega)$. Therefore, T and V should belong to space $H^1(\Omega)$.

As reported in (24) (Theorem 4.1), the abstract form (3.3) is equivalent to the following simultaneous saddle-point problem:

Find $(\varepsilon,\sigma,u) \in E \times T \times V$, s.t.

$$\mathcal{L}(\varepsilon,\tau,u) \leq \mathcal{L}(\varepsilon,\sigma,u) \leq \mathcal{L}(e,\sigma,u) \qquad \forall\, (e,\tau)$$

$$\mathcal{L}(\varepsilon,\sigma,v) \leq \mathcal{L}(\varepsilon,\sigma,u) \leq \mathcal{L}(e,\sigma,u) \qquad \forall\, (e,v)$$

(3.5)

if the bilinear form a(.,.) is symmetric and positive definite. Due to the properties (3.2a) and (3.2b), these requirements are satisfied. In the saddle-point problem (3.5), the functional $\mathcal{L}(.,.,.)$ is given by

$$\mathcal{L}(\varepsilon,\sigma,u) = \tfrac{1}{2}\,a(\varepsilon,\varepsilon) - \ell(\varepsilon,\sigma) + \langle g,\sigma\rangle + p(\sigma,u) - \langle f,u\rangle\,, \qquad (3.6a)$$

i.e.

$$\mathcal{L}(\varepsilon,\sigma,u) = \int_\Omega \left[\tfrac{1}{2}\,a_{ijk\ell}\,\varepsilon_{k\ell}\,\varepsilon_{ij} + \sigma_{ij}\left(u_{(i,j)} - \varepsilon_{ij}\right) - \bar{f}_i\,u_i\right] d\Omega + \int_{S_u} \sigma_{ij}n_j\,(\bar{u}_i - u_i)\,dS - \int_{S_t} \bar{t}_i\,u_i\,ds \qquad (3.6b)$$

The functional (3.6b) is exactly the same as that employed in the Hu-Washizu principle.

According to the theory of multi-field variational problems developed in (13), (16), and (24), the abstract form (3.3) has a unique and stable solu-

ion, if the following elliptic condition and sta-
ility conditions are satisfied:

$$\sup_{\forall \tau \in T} \frac{\int_\Omega \tau_{ij} v_{(i,j)} d\Omega - \int_{S_u} \tau_{ij} n_j v_i ds}{\|\tau\|_T} \geq \beta \|v\|_V \quad \forall v \in V \tag{3.7a}$$

$$\sup_{\forall e \in E} \frac{\int_\Omega e_{ij} \tau_{ij} d\Omega}{\|e\|_E} \geq \beta \|\tau\|_T \quad \forall \tau \in \mathrm{Ker}(P) \tag{3.7b}$$

$$\int_\Omega a_{ijk\ell}\, e_{ij}\, e_{k\ell}\, d\Omega \geq \alpha \|e\|_E \quad \forall e \in \mathrm{Ker}(L) \tag{3.7c}$$

ıere

$$\mathrm{Ker}(P) = \{\tau \in T,\ \int_\Omega \tau_{ij}\, v_{(i,j)}\, d\Omega - \int_{S_u} \tau_{ij}\, n_j\, v_i\, ds = 0 \quad \forall v \in V\} \tag{3.8a}$$

$$\mathrm{Ker}(L) = \{e \in E,\ \int_\Omega e_{ij} \tau_{ij} dx = 0 \quad \forall \tau \in \mathrm{Ker}(P)\} \tag{3.8b}$$

LTI-FIELD PRINCIPLES IN ELASTICITY, WITH DISCON-
NUOUS DISPLACEMENT FIELDS AND UNRECIPROCATED
ACTION FIELDS

Now we consider the case when a solid is dis-
etized, for purposes of generating an approximate
lution, into a number of finite elements. Let

$$\Omega = \sum_m \Omega_m$$

ere Ω_m is the mth element, with a boundary $\partial\Omega_m$. In
ıeral,

$$\partial\Omega_m = \rho_m + S_{tm} + S_{um}$$

erein, ρ_m is the interelement boundary, and S_{tm} and
n are those segments of $\partial\Omega_m$ which are in common
th the external boundary segments S_t and S_u,
pectively. The field equations (3.1a), (3.1b),
(3.1d) for the elasticity problem may be stated
the finite element assembly as well. Evidently,
each Ω_m, equations (3.1c) and (3.1e) should be
yed at S_{um} and S_{tm}, respectively. In addition, at
interelement boundaries, the following conditions
t be satisfied:

$$u_i^+ = u_i^- \quad \text{at } \rho_m \tag{4.1a}$$

$$(\sigma_{ij} n_i)^+ + (\sigma_{ij} n_i)^- = 0 \quad \text{at } \rho_m \tag{4.1b}$$

(4.1a) and (4.1b), the superscripts (+) and (-)
ıote, arbitrarily, the two "sides" of ρ_m.
ıations (4.1a,b) are called the conditions of
splacement compatibility" and "traction
iprocity", respectively.

As reported in the early work (1) and a recent
atment (24), the weak forms of (4.1a) and (4.1b)
be represented, respectively, by

$$0 = \sum_m \int_{\rho_m} u_i\, \tilde{\tau}_{i\rho}\, ds \tag{4.1A)*}$$

$$0 = \sum_m \int_{\rho_m} \sigma_{ij}\, n_j\, \tilde{v}_{i\rho}\, ds \tag{4.2A)*}$$

or

$$0 = \sum_m \int_{\rho_m} (u_i - \tilde{u}_{i\rho})\, \tau_{i\rho}\, ds \tag{4.1B)*}$$

$$0 = \sum_m \int_{\rho_m} (\sigma_{ij}\, n_j - \tilde{t}_{i\rho})\, v_{i\rho}\, ds \tag{4.2B)*}$$

which may be labeled as the A type weak forms and the
B type weak forms, respectively. In the A type weak
forms, (4.1A)* and (4.2A)*, the Lagrange multipliers
$\tilde{\tau}_{i\rho}$ and $\tilde{v}_{i\rho}$ must be continuous along the interelement
boundary ρ_m. In the B type weak forms (4.1B)* and
(4.2B)*, the Lagrange multipliers $\tau_{i\rho}$ and $v_{i\rho}$ are not
necessarily continuous; but two additional unknown
continuous functions $\tilde{u}_{i\rho}$ and $\tilde{t}_{i\rho}$ are introduced.

Among various applications of modified vari-
ational principles in linear elasticity, based on
which various hybrid-mixed finite element models are
constructed, there are four possibilities for writing
a combined weak form of (3.3) and (4.1). The four
ways in which the weak forms of (4.1A and 4.1B) may
be written are:

Case 1: $u \in V_c$ and (4.2A)*

Case 2: (4.1A)* and (4.2B)*

Case 3: (4.1B)* and (4.2A)*

Case 4: (4.1A)* and (4.2A)*

In the first case, the displacement u is assumed
to be a continous function in V_c. The combined weak
forms of (3.3) and Case 1 above will lead to an
"unmodified" variational principle. The second case
and third case will lead to the so-called first and
second versions (1,3) of modified variational princi-
ples, respectively. Finally, the case 4 will lead,
in fact, to the variational principle for the so-
called simplified hybrid-mixed model. However, it is
important to note that some of the simplified models,
e.g. the simplified displacement method, are
unstable, as shown later in this paper.

To avoid repetition, the lists for all of the
abstract forms, expressions and functionals, and
stability conditions of various hybrid-mixed models
based on modified potential energy, complementary
energy, Reissner type, and Hu-Washizu type principles
in linear elasticity are given in Appendices A, B,
and C. Hereon, we analyze only the case 3, i.e. the
second version of modified Hu-Washizu principle.

Upon using a finite element discretization, the
abstract form (3.3) becomes

$$\begin{aligned} a(\varepsilon,e) - \ell(e,\sigma) &= 0 \quad && \forall e \in E \\ \ell(\varepsilon,\tau) - p(\tau,u) &= \langle g,\tau\rangle && \forall \tau \in T \\ p(\sigma,v) - q(\sigma,v) &= \langle f,v\rangle && \forall v \in V \end{aligned} \tag{4.2}$$

where

$$(\varepsilon,e) = \sum_m \int_{\Omega_m} a_{ijk\ell}\varepsilon_{k\ell}\, e_{ij}\, d\Omega \qquad (4.3a)$$

$$(\varepsilon,\tau) = \sum_m \int_{\Omega_m} \varepsilon_{ij}\, \tau_{ij}\, d\Omega \qquad (4.3b)$$

$$(\tau,u) = \sum_m \{\int_{\Omega_m} \tau_{ij}\, u_{(i,j)}\, d\Omega - \int_{S_{um}} \tau_{ij}\, n_j\, u_i\, ds\} \qquad (4.3c)$$

$$(\tau,u) = \sum_m \int_{\rho_m} \tau_{ij}\, n_j\, u_i\, ds \qquad (4.3d)$$

$$g,\tau> = \sum_m \int_{S_{um}} \bar{u}_i\, \tau_{ij}\, n_j\, ds \qquad (4.3e)$$

$$f,v> = \sum_m \{\int_{\Omega_m} \bar{f}_i\, v_i\, d\Omega + \int_{S_{tm}} \bar{t}_i\, v_i\, ds\} \qquad (4.3f)$$

dditional term $q(\sigma,v)$ comes from the boundary ral in the first Green's formula in $H_1(\Omega_m)$. Let

$$[v,\tilde{t}_\rho) = \sum_m \int_{\rho_m} v_i\, \tilde{t}_{i\rho}\, ds\ , \qquad (4.3g)$$

$$[t_\rho,\tilde{v}_\rho) = \sum_m \int_{\rho_m} t_{i\rho}\, \tilde{v}_{i\rho}\, ds\ . \qquad (4.3g)$$

the weak forms (4.1B)* and (4.2A)* in case 3 e

$$[u,\tau_\rho) - d(\tau_\rho,\tilde{u}_\rho) = 0$$

$$d(\sigma_{ij}\, n_j,\ \tilde{v}_\rho) = 0 \qquad (4.4)$$

g that $q(\sigma,v) = c(v,t_\rho)$, we combine easily the act form (4.2) and weak form (4.4) in this on:

ind $(\varepsilon,\sigma,u,t_\rho,\tilde{u}_\rho) \in E \times T \times V \times T(\rho) \times \tilde{V}(\rho)$, s.t.

$$[\varepsilon,e) - \ell(e,\sigma) = 0 \qquad \forall\ e\in E$$

$$[\varepsilon,\tau) - p(\tau,u) = <g,\tau> \qquad \forall\ \tau\in T$$

$$[\sigma,v) - c(v,t_\rho) = <f,v> \qquad \forall\ v\in V$$

$$[u,\tau_\rho) - d(\tau_\rho,\tilde{u}_\rho) = 0 \qquad \forall\ \tau_\rho\in T(\rho)$$

$$d(t_\rho,\tilde{v}_\rho) = 0 \qquad \forall\ \tilde{v}_\rho\in \tilde{V}(\rho) \qquad (4.5)$$

oved in (24), the multi-field variational em (4.5) is equivalent to a simultaneous e-point problem similar to (3.5) in which the onal $\mathcal{L}(.,.,.,.,.)$ is given by

$$\mathcal{L}(\varepsilon,\sigma,u,t_\rho,\tilde{u}_\rho)$$

$$\tfrac{1}{2}\, a(\varepsilon,\varepsilon) - \ell(\varepsilon,\sigma) + <g,\sigma> + p(\sigma,u)$$

$$- <f,u> - c(u,t_\rho) + d(t_\rho,\tilde{u}) \qquad (4.6)$$

ituting the definitions (4.3a,..h) into (4.6), y derive that

$$\mathcal{L} = \sum_m \{\int_{\Omega_m} [\tfrac{1}{2}\, a_{ijk\ell}\varepsilon_{k\ell}\varepsilon_{ij} + \sigma_{ij}(u_{(i,j)} - \varepsilon_{ij}) - \bar{f}_i u_i]d\Omega$$
$$+ \int_{S_{um}} \sigma_{ij}\, n_j(\bar{u}_i - u_i)ds - \int_{S_{tm}} \bar{t}_i\, d_i\, ds$$
$$+ \int_{\rho_m} \sigma_{ij}\, n_j\, (\tilde{u}_{i\rho} - u_i)ds\} \qquad (4.7)$$

According to the general theory of multi-field variational problem developed in (13), (16), (24), and (25), the problem (4.5), i.e. the second version of modified Hu-Washizu principle, has a unique and stable solution if the following ellipticity and stability conditions are satisfied:

$$\sup_{\forall t_\rho\in T(\rho)} \frac{\sum_m \int_{\rho_m} t_{i\rho}\tilde{v}_{i\rho}ds}{\|t_\rho\|_{\tau(\rho)}} \geq \beta\, \|\tilde{u}_\rho\|_{\tilde{V}(\rho)} \qquad \forall\ \tilde{v}_\rho\in\tilde{V}(\rho) \qquad (4.8a)$$

$$\sup_{\forall\ v\in V} \frac{\sum_m \int_{\rho_m} v_i\, t_{i\rho}ds}{\|v\|_V} \geq \beta\, \|t_\rho\|_{\tau(\rho)} \qquad \forall\ t_\rho\in \mathrm{Ker}(D) \qquad (4.8b)$$

$$\sup_{\forall\ \tau\in T} \frac{\sum_m \{\int_{\Omega_m} \tau_{ij}v_{(i,j)}d\Omega - \int_{S_{um}} \tau_{ij}n_i v_i ds\}}{} \geq \beta\, \|v\|_V \qquad \forall\ v\in \mathrm{Ker}\ (C) \qquad (4.8c)$$

$$\sup_{\forall\ e\in E} \frac{\sum_m \int_{\Omega_m} e_{ij}\tau_{ij}d\Omega}{\|e\|_E} \geq \beta\, \|\tau\|_T \qquad \forall\ \tau\in \mathrm{Ker}(P) \qquad (4.8d)$$

$$\sum_m \int_{\Omega_m} a_{ij}\, e_{k\ell}\, e_{ij}\, d\Omega \geq \alpha\, \|e\|_E \qquad \forall\ e\in \mathrm{Ker}(L) \qquad (4.8e)$$

where

$$\mathrm{Ker}(D) = \{t_\rho\in T(\rho),\ \sum_m \int_{\rho_m} t_{i\rho}\tilde{v}_{i\rho}ds = 0\ \ \forall\ \tilde{v}_\rho\in\tilde{V}(\rho)\}$$

$$\mathrm{Ker}(C) = \{v\in V,\ \sum_m \int_{\rho_m} v_i t_{i\rho}ds = 0 \qquad \forall\ t_\rho\in \mathrm{Ker}(D)\}$$

$$\mathrm{Ker}(P) = \{\tau\in T,\ \sum_m \{\int_{\Omega_m} \tau_{ij}v_{(i,j)}d\Omega - \int_{S_{um}} \tau_{ij}n_j v_i ds\} = 0 \quad \forall\ v\in \mathrm{Ker}(C)\}$$

$$\mathrm{Ker}(L) = \{e\in E,\ \sum_m \int_{\Omega_m} e_{ij}\tau_{ij}d\Omega = 0 \qquad \forall\ \tau\in \mathrm{Ker}(C)\} \qquad (4.9)$$

THEORY OF MULTI-FIELD VARIATIONAL PROBLEM

In this section, we present the major theoretical results in order to obtain the stability conditions for various hybrid-mixed models which are stated in the form of multi-field variational problems. Some of our results are extensions to those of Brezzi (13)

io presented the conditions for existence, unique-
ess, and stability of solutions to a variational
oblem with a single constraint, and to those of
ng and Atluri (16) who presented the variational
eory for a problem, with two constraints, arising
Stokes flow. However, the proofs of the theorems
this paper are formally different from those of
ezzi (13) and may be systematically extended to the
ses with more than two Lagrange multipliers, such
problem (4.5). For the sake of convenience, we
ove the theorems for problem (3.3). The details of
tension to problems with more than two constraints,
ch as (4.5), may be found in (25).

We use T, V, P to denote the Hilbert spaces with
e norms $\|.\|_T$, $\|.\|_V$, and $\|.\|_P$. Let a(.,.), b(.,.),
i c(.,.) be continuous bilinear forms. For a given
linear form b(.,.) V x P → R, we define the associ-
d linear operator B and its dual operator B* by

$$\langle Bv,p\rangle = \langle v,B^*p\rangle = b(v,p) \quad \forall\ (v,p)\in V\times P \tag{5.1}$$

kernel of a linear operator B is defined by

$$\mathrm{Ker}(B) = \{v \in V,\ \langle Bv,p\rangle = 0 \quad \forall\ p\in P\} \tag{5.2}$$

orem 5.1 (Brezzi)
The dual variational problem

Find $(u,q) \in V \times P$, s.t.

$$a(u,v) - b(v,q) = \langle f,v\rangle \quad \forall\ v\in V$$

$$b(u,p) = \langle g,p\rangle \quad \forall\ p\in P \tag{5.3}$$

a unique solution, if the following conditions
satisfied:

$$\sup_{\forall\ v\in V} \frac{b(v,p)}{\|v\|_V} \geq \beta\|p\|_P \quad \forall\ p\in P \tag{5.4a}$$

$$a(v,v) \geq \alpha\|v\|_V^2 \quad \forall\ v\in \mathrm{Ker}(B)$$

e α and β are positive numbers. Moreover, one
the following estimate:

$$\|u\|_V + \|q\|_P \leq C_1(\|f\|_{V^*} + \|g\|_{P^*}) \tag{5.5}$$

C_1 is a positive number.

1 [Girault and Raviart (26)]
he following three properties are equivalent:

ondition (5.4a)

he operator B* is an isomorphism from P onto
$\mathrm{Ker}(B))^\circ$. Therefore,

$$\|B^*p\|_{V^*} \geq \beta\|p\|_P \quad \forall\ p\in P$$

he operator B is an isomorphism from $(\mathrm{Ker}(B))_\perp$
nto P*. Therefore,

$$\|Bv\|_{P^*} \geq \beta\|v\|_V \quad \forall\ v\in (\mathrm{Ker}(B))_\perp ,$$

$(\mathrm{Ker}(B))_\perp$ and $(\mathrm{Ker}(B))^\circ$ are defined by

$$\mathrm{Ker}(B))_\perp = \{v\in V,\ (v,v_o) = 0 \quad \forall\ v_o \in \mathrm{Ker}(B)\} \tag{5.6a}$$

$$(\mathrm{Ker}(B))^\circ = \{f\in V^*,\ \langle f,v_o\rangle = 0 \quad \forall\ v_o \in \mathrm{Ker}(B)\} \tag{5.6b}$$

and (u,v) denotes the inner product of u and v, and
$\langle f,.\rangle$ denotes the continuous linear operator in V*.

Theorem 5.2 [Ying and Atluri (16)]
The three-field variational problem is stated by

Find $(\sigma,u,q)\in T \times V \times P$, s.t.

$$a(\sigma,\tau) - b(\tau,u) = \langle f,\tau\rangle \quad \forall\ \tau\in T$$

$$b(\sigma,v) - c(v,q) = \langle g,v\rangle \quad \forall\ v\in V$$

$$c(u,p) = \langle h,p\rangle \quad \forall\ p\in P \tag{5.7}$$

Suppose that the following conditions are satisfied.

$$\text{(a)}\quad \sup_{\forall\ v\in V} \frac{c(v,p)}{\|v\|_V} \geq \beta\|p\|_P \quad \forall\ p\in P \tag{5.8a}$$

$$\text{(b)}\quad \sup_{\forall\ \tau\in T} \frac{b(\tau,v)}{\|\tau\|_T} \geq \beta\|v\|_V \quad \forall\ v\in \mathrm{Ker}(C) \tag{5.8b}$$

$$\text{(c)}\quad a(\tau,\tau) \geq \alpha\|\tau\|_T^2 \quad \forall\ \tau\in \mathrm{Ker}(B) \tag{5.8c}$$

where

$$\mathrm{Ker}(B) = \{\tau\in T,\ b(\tau,v) = 0 \quad \forall\ v\in \mathrm{Ker}(C)\} .$$

Then we have the following results:

(1) problem (5.7) has a unique solution
$(\sigma,u,q)\in T \times V \times P$,

(2) the mapping ν: $(f,g,h) \to (\sigma,u,q)$ is an isomorphism from $T^* \times V^* \times P^*$ onto $T \times V \times P$,

(3) there exists a positive number C_2 such that

$$\|\sigma\|_T + \|u\|_V + \|q\|_P \leq C_2\{\|f\|_{T^*} + \|g\|_{V^*} + \|h\|_{P^*}\} . \tag{5.9}$$

Proof
Part I: (existence and uniqueness)

According to condition (5.8a) and Lemma 1(b), there exists a unique $u_\perp \in (\mathrm{Ker}(C))_\perp$ such that

$$C\,u_\perp = h \quad \text{in } P^* .$$

Let u_o be arbitrary element in set Ker(C) and denote $u_\perp + u_o = u$. Then we have

$$C\,u = (C\,u_\perp + u_o) = C\,u_\perp = h \quad \text{in } P^* .$$

It remains to find an appropriate $u_o \in \mathrm{Ker}(C)$ such that the first two equations in (5.7) are satisfied, i.e.,

$$A\sigma - B^*\,u_o = F \quad \text{in } T^*$$

$$B\sigma - C^* q = g \qquad \text{in } V^* ,$$

where $F = f + B^* u_\perp$. Due to assumption (5.8a) and Lemma 1(c), the equation $C^*q = B\sigma - g$ has a unique solution q if, and only if, $B\sigma - q$ belongs to $(\mathrm{Ker}(C))^\circ$, i.e. $B\sigma - g = 0$ in $(\mathrm{Ker}(C))^*$. Therefore, it suffices to solve the following problem:

Find $(\sigma, u_o) \in T \times \mathrm{Ker}(C)$, s.t.

$$A\sigma - B^* u_o = F \qquad \text{in } T^*$$

$$B\sigma = g \qquad \text{in } (\mathrm{Ker}(C))^* .$$

According to Theorem (5.1), there is a unique (σ, u_o) if conditions (5.8b) and (5.8c) are satisfied.

Part II: (isomophism property)

According to (5.5) in Theorem (5.1) one may have the following estimate:

$$\|\sigma\|_T + \|u_o\|_V \le C_1 \{\|F\|_{T^*} + \|g\|_{V^*}\}$$

$$\le C_1 \{\|f\|_{T^*} + \|g\|_{V^*}\} + C_1 \|B^*\| \, \|u_\perp\|_V$$

Noting that $\|u_\perp\|_V \le \beta^{-1} \|Cu_\perp\|_{P^*} = \beta^{-1} \|h\|_{P^*}$, one may get that

$$\|\sigma\|_T + \|u\|_V$$

$$\le C_1 \{\|f\|_{T^*} + \|g\|_{V^*}\} + (C_1 \|B^*\| + 1) \beta^{-1} \|h\|_{P^*}$$

$$\le C_2 \{\|f\|_{T^*} + \|g\|_{V^*} + \|h\|_{P^*}\} .$$

Moreover, one has

$$\|q\|_P \le \beta^{-1} \|C^* q\|_{V^*} = \beta^{-1} \|B\sigma - g\|_V \le \beta^{-1} \{\|B\| \, \|\sigma\|_T + \|g\|_{V^*}\}$$

The above inequalities lead immediately to estimate (5.9). It is easy to get the "inverse" of inequality (5.9). Then the mapping ν: $(f,g,h) \to (\sigma,u,q)$ is an isomorphism from $T^* \times V^* \times P^*$ onto $T \times V \times P$. The proof is completed.

As is well known, a finite element approach consists in finding the solution (σ_h, u_h, q_h) in a finite dimensional subspace $T_h \times V_h \times P_h$ instead of the finite dimensional Hilbert space $T \times V \times P$. Thus, the finite element approximation of (5.7) may be stated in the following problem:

Find $(\sigma_h, u_h, q_h) \in T_h \times V_h \times P_h$, s.t.

$$a(\sigma_h, \tau_h) - b(\tau_h, u_h) = \langle f, \tau_h \rangle \quad \forall \ \tau_h \in T_h$$

$$b(\sigma_h, v_h) - c(v_h, g_h) = \langle g, v_h \rangle \quad \forall \ v_h \in V_h$$

$$c(u_h, p_h) = \langle h, p_h \rangle \quad \forall \ p_h \in P_h \qquad (5.10)$$

where the h is the discretization parameter which depends only on the geometric discretization of the domain Ω, T_h, V_h, and P_h are finite dimensional subspaces of T, V, and P, respectively.

Theorem 5.3 (Convergence property)
In addition to assumptions (a), (b), and (c) in Theorem (5.2), we assume that

$$\text{(d)} \quad \sup_{\forall\, v_h \in V_h} \frac{c(v_h, p_h)}{\|v_h\|_V} \ge \beta \|p_h\|_P \quad \forall \ p_h \in P_h \qquad (5.11a)$$

$$\text{(e)} \quad \sup_{\forall\, \tau_h \in T_h} \frac{b(\tau_h, v_h)}{\|\tau_h\|_T} \ge \beta \|v_h\|_V \quad \forall \ v_h \in \mathrm{Ker}_h(C) \qquad (5.11b)$$

$$\text{(f)} \quad a(\tau_h, \tau_h) \ge \alpha \|\tau_h\|_T^2 \quad \forall \ \tau_h \in \mathrm{Ker}_h(B) \qquad (5.11c)$$

Then we have the following properties:

(1) problem (5.7) and (5.10) have unique solutions (σ,u,q) and (σ_h,u_h,q_h), respectively.

(2) there exists a positive number $C_3 > 0$ such that

$$\|\sigma - \sigma_h\|_T + \|u - u_h\|_V + \|q - q_h\|_P$$

$$\le C_3 \{ \inf_{\tau_h \in T_h} \|\sigma - \tau_h\|_T + \inf_{v_h \in V_h} \|u - v_h\|_V$$

$$+ \inf_{P_h \in P_h} \|q - p_h\|_P \} = C_3 \ \mathrm{dis}\{(\sigma,u,q); T_h \times V_h \times P_h\} . \qquad (5.12)$$

where dis{a;A} denotes the distance between element a and space A.

Proof
Due to Theorem (5.2), the existence and uniqueness of solutions (σ,u,q) and (σ_h,u_h,q_h) are already established. It remains to prove the estimate of the error (5.12). It is easy to know that

$$A\sigma_h - B^* u_h = A\sigma - B^* u \qquad \text{in } T_h^*$$

$$B\sigma_h - C^* q_h = B\sigma - C^* q \qquad \text{in } V_h^*$$

$$C u_h = C u \qquad \text{in } P_h^*$$

Taking arbitrary but fixed element $(\tau_h, v_h, p_h) \in T_h \times V_h \times P_h$, one may derive that

$$A(\sigma_h - \tau_h) - B^*(u_h - v_h) = A(\sigma - \tau_h) - B^*(u - v_h) \text{ in } T_h^*$$

$$B(\sigma_h - \tau_h) - C^*(q_h - p_h) = B(\sigma - \tau_h) - C^*(q - p_h) \quad \text{in } V_h^*$$

$$C(u_h - v_h) = C(u - v_h) \quad \text{in } P_h^*$$

According to estimate (5.9), we get that

$$\|\sigma_h - \tau_h\|_T + \|u_h - v_h\|_V + \|q_h - p_h\|_P$$

$$\le C_2 \{(\|A\| + \|B\|)\|\sigma - \tau_h\|_T$$

$$+ (\|B^*\| + \|C\|)\|u - v_h\|_V + \|C^*\| \|q - p_h\|_P\}$$

Therefore, we have

$$\|\sigma - \sigma_h\|_T + \|u - u_h\|_V + \|q - q_h\|_P$$

$$\le \|\sigma - \tau_h\|_T + \|u - v_h\|_V + \|q - p_h\|_P$$

$$+ \|\sigma_h - \tau_h\|_T + \|u_h - v_h\|_V + \|q_h - p_h\|_P$$

$$\le (C_2 \max\{\|A\| + \|B\|, \|B\| + \|C\|\} + 1)$$

$$(\|\sigma - \tau_h\|_T + \|u - v_h\|_V + \|q - p_h\|_P)$$

Since (τ_h, v_h, p_h) is arbitrary, the above inequality leads to estimate (5.12). The proof is completed.

The inference of numerical integration is another interesting topic. The bilinear forms in (5.7) are defined by some kind of energy integrals. If we introduce numerical integration during the finite element procedure, the bilinear forms $\tilde{a}(.,.)$, $\tilde{b}(.,.)$, and $\tilde{c}(.,.)$ will change to be new bilinear forms denoted by $a(.,.)$, $b(.,.)$, and $c(.,.)$. Then the finite element approach (5.10) is changed to be

Find $(\tilde{\sigma}_h, \tilde{u}_h, \tilde{q}_h) \in T_h \times V_h \times P_h$, s.t.

$$\tilde{a}(\tilde{\sigma}_h, \tau_h) - \tilde{b}(\tau_h, \tilde{u}_h) = \langle f, \tau_h \rangle \qquad \forall\ \tau_h \in T_h$$

$$\tilde{b}(\tilde{\sigma}_h, v_h) - \tilde{c}(v_h, \tilde{q}_h) = \langle g, v_h \rangle \qquad \forall\ v_h \in V_h$$

$$\tilde{c}(\tilde{u}_h, p_h) = \langle h, p_h \rangle \qquad \forall\ p_h \in P_h \tag{5.13}$$

Theorem 5.4 (Numerical integration)

In addition to the assumptions (a), (b), ... (f) Theorem 5.2 and Theorem 5.3, we assume that the linear forms $\tilde{a}(.,.)$, $\tilde{b}(.,.)$, and $\tilde{c}(.,.)$ satisfy the condition (d), (e), (f) also. Then we have the following results:

(1) both of problems (5.7) and (5.13) have unique solutions (σ,u,q) and $(\tilde{\sigma}_h,\tilde{u}_h,\tilde{q}_h)$ respectively

(2) there exists constant $C_4 > 0$ such that

$$\|\sigma - \tilde{\sigma}_h\|_T + \|u - \tilde{u}_h\|_V + \|q - \tilde{q}_h\|_P$$

$$\le C_4 \operatorname{dis}\{(\sigma,u,q), T_h \times V_h \times V_h\}$$

$$+ C_4 (\|A - \tilde{A}\| + \|B - \tilde{B}\| + \|C - \tilde{C}\|)$$

$$(\|f\|_{T^*} + \|g\|_{V^*} + \|h\|_{P^*}) \tag{5.14}$$

Proof

It remains to prove the estimate (5.14). Taking arbitrary but fixed $(\tau_h, v_h, p_h) \in T_h \times V_h \times P_h$, one may derive that

$$\tilde{A}(\tilde{\sigma}_h, \tau_h) - \tilde{B}^*(\tilde{u}_h, v_h) = A\sigma - \tilde{A}\tau_h - B^*u + \tilde{B}^*v_h \quad \text{in } T_h^*$$

$$\tilde{B}(\tilde{\sigma}_h, \tau_h) - \tilde{C}^*(\tilde{q}_h - p_h) = B\sigma - \tilde{B}\tau_h - C^*q + \tilde{C}^*p_h \quad \text{in } V_h^*$$

$$\tilde{C}(\tilde{u}_h - v_h) = Cu - \tilde{C}v_h \quad \text{in } P_h^*$$

Thus, we have

$$\|\tilde{\sigma}_h - \tau_h\|_T + \|\tilde{u}_h - v_h\|_V + \|\tilde{q}_h - p_h\|_P$$

$$\le C_2\{\|A - \tilde{A}\| \|\sigma\|_T + \|B - \tilde{B}\| (\|u\|_V + \|\sigma\|_T)$$

$$+ \|C - \tilde{C}\| (\|u\|_V + \|q\|_P)$$

$$+ (\|\tilde{A}\| \pm \|\tilde{B}\|)\|\sigma - \tau_h\|_T + (\|\tilde{B}\| + \|\tilde{C}\|)\|u - v_h\|_V$$

$$+ \|\tilde{C}\| \|q - p_h\|_P\}$$

$$\le C_2^2(\|A - \tilde{A}\| + \|B - \tilde{B}\| + \|C - \tilde{C}\|)$$

$$(\|f\|_{T^*} + \|g\|_{V^*} + \|h\|_{P^*})$$

$$+ C_2(\|\tilde{A}\| + \|\tilde{B}\| + \|\tilde{C}\|)$$

$$(\|\sigma - \tau_h\|_T + \|u - v_h\|_V + \|q - p_h\|_P).$$

This inequality leads to estimate (5.14). The proof is completed.

ON THE SIMPLIFIED VARIATIONAL PRINCIPLES AND THE HYBRID-DISPLACEMENT METHOD

As mentioned in Section 4, Case 4 of the general modified variational principle therein is a simplification of Case 3, that is the second version of modified Hu-Washizu principle. These simplified methods

are sometimes useful in reducing the number of independent variables in a formulation. Actually, the assumed-stress hybrid method can be thought of as being a simplification of modified complementary energy principle.

Unfortunately, several of the simplified variation principles, especially the simplified hybrid-displacement method, which is based on modified potential energy principle, are not stable methods since the ellipticity of bilinear form a(u,v) is destroyed. We shall investigate this problem in detail from either the abstract form or the functional formula.

The second version of modified potential energy principle may be described in the following abstract multi-field variational problem:

$$\text{Find } (u,t_\rho,\tilde{u}_\rho) \in V_o \times T(\rho) \times \tilde{V}(\rho), \text{ s.t.}$$

$$a(u,v) - c(v,t_\rho) = \langle f,v\rangle \qquad \forall\, v\in V_o$$

$$c(u,\tau_\rho) - d(\tau_\rho,\tilde{u}_\rho) = 0 \qquad \forall\, \tau_\rho\in T(\rho)$$

$$d(t_\rho,\tilde{v}_\rho) = 0 \qquad \forall\, \tilde{v}_\rho\in \tilde{V}(\rho)\ , \tag{6.1}$$

where v is the displacement, τ_ρ is independent boundary traction, and $\tilde{v}_\rho$ is continuous boundary displacement. This method was first introduced by Tong in 1970 [see (27)]. At the same time, Tong introduced a so-called "simplified" hybrid-displacement model by assuming the space T(ρ) in the following fashion:

$$T(\rho) = \{\tau_\rho = \sigma_{ij}(v)n_j\ ,\ \text{where } v\in V_o\}\ . \tag{6.2}$$

Then the variational problem (6.1) becomes

$$\text{Find } (u,u^*,\tilde{u}_\rho) \in V_o \times V_o \times \tilde{V}(\rho), \text{ s.t.}$$

$$a(u,v) - c(v,t_\rho(u^*)) = \langle f,v\rangle \qquad \forall\, v\in V_o$$

$$c(u,\tau_\rho(v)) - d(\tau_\rho(v),\tilde{u}_\rho) = 0 \qquad \forall\, v\in V_o$$

$$d(t_\rho(u^*),\tilde{v}_\rho) = 0 \qquad \forall\, \tilde{v}_\rho\in \tilde{V}(\rho)\ . \tag{6.3}$$

This is still a problem involving three unknown variables, i.e. u, $\tilde{u}_\rho$, and u*. As a theoretical result one should have u* = u; but in a finite element approximation, one cannot guarantee that u* is the same as u. Let u* = u + Δu. Then the problem (6.3) may be written as

$$\text{Find } (u,\tilde{u}_\rho) \in V_o \times \tilde{V}(\rho), \text{ s.t.}$$

$$a(u,v) - c(v,t_\rho(u)) = \langle f^*,v\rangle \qquad \forall\, v\in V_o$$

$$c(u,\tau_\rho(v)) - d(\tau_\rho(v),\tilde{u}_\rho) = 0 \qquad \forall\, v\in V_o$$

$$d(t_\rho(u),\tilde{v}_\rho) = \langle g^*,\tilde{v}_\rho\rangle \qquad \forall\, \tilde{v}_\rho\in \tilde{V}(\rho)\ , \tag{6.4}$$

where f* and g* are regarded to be perturbations from f and zero, respectively, i.e.

$$f^* = f + C^*\, t_\rho(\Delta u)$$

$$g^* = -D\, t_\rho(\Delta u) \tag{6.5}$$

All of the above assumptions and procedures are kept on the right track, but it is a mistake if we combine the first two equations of (6.4) to be one. If we do so, the problem (6.4) becomes

$$\text{Find } (u,\tilde{u}_\rho) \in V_o \times \tilde{V}(\rho), \text{ s.t.}$$

$$\hat{a}(u,v) + \hat{b}(v,\tilde{u}_\rho) = \langle f,v\rangle \qquad \forall\, v\in V_o$$

$$\hat{b}(u,\tilde{v}_\rho) = 0 \qquad \forall\, \tilde{v}_\rho\in \tilde{V}(\rho) \tag{6.6}$$

where

$$\hat{a}(u,v) = \sum_m \Big\{\int_{\Omega_m} \sigma_{ij}(u)\varepsilon_{ij}(v)d\Omega - \int_{\rho_m} (u_i\sigma_{ij}(v)n_j + v_i\sigma_{ij}(u)n_j)ds\Big\} \tag{6.7a}$$

$$\hat{b}(u,\tilde{v}_\rho) = \sum_m \int_{\rho_m} \sigma_{ij}(u)n_j\,\tilde{v}_{i\rho}\, ds\ . \tag{6.7b}$$

The associated functional of problem (6.6) is given by

$$\mathcal{L}(u,\tilde{u}_\rho) = \tfrac{1}{2}\hat{a}(u,u) - \langle f,u\rangle + \hat{b}(u,\tilde{u}_\rho)$$

$$= \sum_m \Big\{\int_{\Omega_m} (\tfrac{1}{2}\sigma_{ij}(u)\varepsilon_{ij}(u) - \bar{f}_i\, u_i)d\Omega - \int_{\rho_m} \sigma_{ij}(u)n_j\,(u_i - \tilde{u}_{i\rho})ds - \int_{S_{tm}} \bar{t}_i\, u_i\, ds\Big\} \tag{6.8}$$

This is the same functional employed by Tong in the "simplified" hybrid displacement method [see Eq. (1) and assumption (16) in (27)]. Now this method can be seen to be unstable, since the bilinear form $\hat{a}(u,v)$ is not elliptic anymore. Since the ellipticity condition is violated, the functional (6.8) has even no minimization property. To see that, let us assume that u and $\tilde{u}_\rho$ are the solution of the elasticity problem, i.e.

$$\sigma_{ij,j}(u) + \bar{f}_i = 0 \qquad \text{in } \Omega_m$$

$$\sigma_{ij}(u)n_j = \bar{t}_i \qquad \text{in } S_{tm}$$

$$[\sigma_{ij}(u)n_j]^+ + [\sigma_{ij}(u)n_j]^- = 0 \qquad \text{at } \rho_m$$

$$u_i = \tilde{u}_{i\rho} \qquad \text{at } \rho_m$$

ıen one may have

$$\mathcal{L}(u + \delta u, \tilde{u}_\rho) - \mathcal{L}(u, \tilde{u}_\rho)$$

$$= \sum_m \{ \int_{\Omega_m} \tfrac{1}{2}\, \sigma_{ij}(\delta u)\varepsilon_{ij}(\delta u)\, d\Omega$$

$$- \int_{\rho_m} \sigma_{ij}(\delta u)n_j\, \delta u_i\, ds \}$$

is term is not necessarily always positive. Thus, cannot get a minimization problem from the functional (6.8).

Finally we check the matrix form given by Tong 7) for the "simplified" hybrid-displacement method, ich is shown below:

$$\Pi = \sum_m \{ \tfrac{1}{2}\beta^T H \beta - \beta^T P \beta - \hat{\beta}^T \hat{P} \beta - \beta^T \bar{F}_1$$

$$- \hat{\beta}^T \bar{F}_2 + \beta^T G g - S_o^T g \}$$

i. (17) in (6)]. We have

$$\Pi(\beta + \delta\beta) - \Pi(\beta)$$

$$= \sum \{ \tfrac{1}{2}\delta\beta^T H\, \delta\beta - \delta\beta^T P\, \delta\beta + \delta\beta^T (H\beta - (\rho - P^T)\beta$$

$$- \hat{P}^T \hat{\beta} - F_1 + Gg) \} .$$

ıce the terms of order $(\delta\beta)$ are set to zero in er to find the solution for β, we have

$$\Pi(\beta + \delta\beta) - \Pi(\beta) = \sum_m \delta\beta^T (\tfrac{1}{2}H - P)\delta\beta .$$

all that H, by definition, is positive definite has a rank of dimension same as that of β. How- r, the rank of P is not, in general, assured. ı if P has the same rank as that of H, it is not, general, possible to guarantee that $[\frac{1}{2}H-P]$ will ı the same rank. Therefore, we cannot guarantee above difference is always positive. There is no imization property for the functional (6.8) oyed in simplified displacement method.

DISCRETE BB-CONDITIONS AND RANK CONDITIONS

Discrete BB-Condition in Finite Dimensional Subspace

As is well known, the finite element method is an approach to find the approximate solutions in finite dimensional space instead of the infinite dimensional Hilbert space. Referring to the results in Sections 4 and 5, the key condition for existence, uniqueness, convergence, and stability of the finite element solution of a multi-saddle point problem is the BB-condition in finite dimensional sub-spaces as shown below:

$$\forall\, v \in V_m \quad \sup \frac{b(v,p)}{\|v\|_V} \geq \beta \|p\|_P \qquad \forall\, p \in P_n$$

Since P is arbitrary, the above statement is equivalent to the following inf-sup condition:

$$\forall\, p \in P_n \quad \inf \quad \forall\, v \in V_m \quad \sup \frac{b(v,p)}{\|v\|_V \|p\|_P} \geq \beta > 0 , \qquad (7.1.1)$$

where $b(.,.)$ is a continuous bilinear form, P_n and V_m are finite dimensional subspaces of Hilbert spaces P and V, respectively; and the $\|.\|_V$ and $\|.\|_P$ are norms defined on spaces V and P. The dimensions of V_m and P_n are supposed to be m and n, respectively.

$$\begin{aligned} \dim V_m &= m \\ \dim P_n &= n \end{aligned} \qquad (7.1.2)$$

As defined before we introduce an operator B such that

$$\langle Bv, p \rangle = b(v,p) \triangleq p^T B v \qquad \forall (v,p) \in V_m \times P_n \qquad (7.1.3)$$

Since B is a linear operator from V_m to P_n, B should have an nxm matrix representation. We still denote this matrix by B. Since B^TB is obviously a symmetric non-negative matrix, there exists an orthogonal matrix C such that

$$C^T(B^TB)C = \begin{bmatrix} \mu_1^2 & & & & \\ & \mu_2^2 & & & \\ & & \ddots & & \\ & & & \mu_k^2 & \\ & & & & 0 \\ & & & & & \ddots \end{bmatrix} \qquad (0 \leq k \leq m) \qquad (7.1.4)$$

where μ_i^2 are non-zero eigenvalues of matrix B^TB, k is the rank of B^TB. We rewrite (7.1.4) by

$$(BC)^T(BC) = \begin{bmatrix} \mu_1^2 & & & & \\ & \mu_2^2 & & & \\ & & \ddots & & \\ & & & \mu_k^2 & \\ & & & & 0 \\ & & & & & \ddots \end{bmatrix} \qquad (7.1.5)$$

and denote that

$$(BC) = (C_1, C_2, \ldots C_m) \quad , \tag{7.1.6}$$

here C_j is the jth column vector of matrix BC. It s easy to see from (7.1.5) that

$$C_i^T C_i = \mu_i^2 \neq 0 \qquad (i = 1,2,\ldots k)$$

$$C_i^T C_i = 0 \qquad (i = k+1,\ldots m)$$

$$C_i^T C_j = 0 \qquad (\text{if } i \neq j)$$

e define that

$$d_i = c_i/\mu_i \quad (\text{for each } i = 1,2,\ldots k)(\text{no sum on } i). \tag{7.1.7}$$

ıen we have

$$d_i^T d_j = \delta_{ij} \qquad (i,j = 1,2,\ldots k) \tag{7.1.8}$$

ıe set of vectors $d_1, d_2, \ldots d_k$ may be extended to a andard orthogonal basis $d_1, d_2, \ldots d_m$ so that

$$d_i^T d_j = \delta_{ij} \qquad (i,j = 1,2,\ldots m) \tag{7.1.9}$$

ıen we have

$$(BC) = (c_1, c_2, \ldots c_m)$$

$$= (c_1, c_2, \ldots c_k, 0, \ldots 0) \quad (C_i^T C_i = 0 \text{ for } i \geq k+1)$$

$$= (d_1, d_2, \ldots d_k, 0, \ldots 0) \begin{bmatrix} \mu_1 & & & & \\ & \mu_2 & & & \\ & & \ddots & & \\ & & & \mu_k & \\ & & & & 0 \\ & & & & & \ddots \end{bmatrix}$$

$$= (d_1, d_2, \ldots d_m) \begin{bmatrix} \mu_1 & & & \\ & \ddots & & \\ & & \mu_k & \\ & & & 0 \\ & & & & \ddots \end{bmatrix}$$

$$D^T BC = \begin{bmatrix} \mu_1 & & & \\ & \ddots & & \\ & & \mu_k & \\ & & & 0 \\ & & & & \ddots \end{bmatrix} \triangleq \Sigma \tag{7.1.10}$$

or

$$B = D\Sigma C^T \quad , \tag{7.1.11}$$

where μ_i are the singular values of matrix B, formula (7.1.11) is the singular value decompositon of matrix B, and the orthogonal matrices D and C are defined as ealier. Thus,

$$\mu_i = \left(\lambda_i(B^T B)\right)^{1/2} \quad (i = 1,2,\ldots k) \tag{7.1.12}$$

$$k = \text{rank } (B) \quad , \tag{7.1.13}$$

where λ_i denotes the ith eigenvalue of matrix $B^T B$. Under the singular value decomposition, the BB-condition (7.1.1) becomes that

$$\inf_{\forall\, p \in P_n} \sup_{\forall\, v \in V_m} \frac{b(v,p)}{\|v\|_V \|p\|_P}$$

$$= \inf_{\forall\, p \in P_n} \sup_{\forall\, v \in V_m} \frac{\langle D\Sigma C^T v, p\rangle}{\|v\|_V \|p\|_P}$$

$$= \inf_{\forall\, p \in P_n} \sup_{\forall\, v \in V_m} \frac{\langle \Sigma(C^T v), D^T p\rangle}{\|C^T v\|_V \|D^T p\|_P} \quad (\|C^T v\|_V = \|v\|_V \text{ for orthogonal matrix C})$$

$$\geq \beta > 0$$

i.e.

$$\inf_{\forall\, p \in P_n} \sup_{\forall\, v \in V_m} \frac{\langle \Sigma v, p\rangle}{\|v\|_V \|p\|_P} \geq \beta > 0 \tag{7.1.14}$$

Theorem 7.1.1

The discrete BB-condition (7.1.1) holds if, and only if, the following rank condition is satisfied.

$$\text{rank}(B) = n \leq m \quad . \tag{7.1.15}$$

Remark

In condition (7.1.15), the rank requirement $n \leq m$ comes directly from the BB-condition. In fact, if

$$m = \dim V_m < \dim P_n = n$$

one may find a vector p such that

$$(DP)^T v = 0 \quad ,$$

which is a contradiction to (7.1.1).

Proof

Sufficiency:

Suppose that the rank condition (7.1.15) holds. Then the matrix Σ in singular value decomposition (7.1.11) should have the following form:

$$\Sigma = \begin{bmatrix} \mu_1 & & & \\ & \mu_2 & & \\ & & \ddots & \\ & & & \mu_n \; 0 \ldots 0 \end{bmatrix}_{n \times m} \triangleq (\Sigma_n, o)$$

e the singular values μ_i are positive numbers. any given $p \in P_n$, we choose a special element $v_p \in V_m$ that

$$v_p = \begin{bmatrix} p \\ 0 \\ \vdots \\ \end{bmatrix}_{m \times 1} .$$

, we have the following inequalities:

$$\inf_{\forall\, p \in P_n} \sup_{\forall\, v \in V_m} \frac{\langle \Sigma v, p \rangle}{\|v\| \|p\|}$$

$$\geq \inf_{\forall\, p \in P_n} \frac{\langle \Sigma v_p, p \rangle}{\|v_p\| \|p\|}$$

$$\inf_{\forall\, p \in P_n} \frac{\langle \Sigma_n p, p \rangle}{\|p\| \|p\|}$$

$$\min_{1 \leq i \leq n} \mu_i .$$

ke $\beta = \min_{1 \leq i \leq n} \mu_i$. Thus, we have

sity: $$\inf_{\forall\, p \in P_n} \sup_{\forall\, v \in V_m} \frac{\langle \Sigma v, p \rangle}{\|v\| \|p\|} \geq \beta > 0 .$$

se that the discrete BB-condition (7.1.1) holds. e rank of (B) is less than n, i.e.

ank (B) = k < n .

the matrix Σ in the singular value decomposition 1) should have the following form:

$$= \begin{bmatrix} \mu_1 & & & \\ & \ddots & & \\ & & \mu_k & \\ & & & 0 \\ & & & & \ddots \end{bmatrix} \triangleq \begin{pmatrix} \Sigma_k & 0 \\ 0 & 0 \end{pmatrix} ,$$

the singular values μ_i are positive numbers. e choose the special element $\tilde{p}$ in P_n as the ing.

$$= \begin{pmatrix} 0 \\ \vdots \\ 0 \\ p_n \end{pmatrix}$$

$p_n \neq 0$. Thus, we have $\|\tilde{p}\| \neq 0$, but we get

$$\inf_{\forall\, p \in V_n} \sup_{\forall\, v \in V_m} \frac{\langle \Sigma v, p \rangle}{\|v\| \|p\|}$$

$$\geq \sup_{\forall\, v \in V_m} \frac{\langle \Sigma v, \tilde{p} \rangle}{\|v\| \|\tilde{p}\|}$$

$$= \sup_{\forall\, v \in V_m} \frac{\langle v, \Sigma^T \tilde{p} \rangle}{\|v\| \|\tilde{p}\|}$$

$$= 0 ,$$

since $\Sigma^T \tilde{p} = 0$. It is a contradiction to the BB-condition (7.1.11). Thus, we must have rank (B) = n. Moreover, the fact that m ≥ rank (B) leads to the result that

$$\text{rank } (B) = n \leq m .$$

The proof is completed.

Theorem 7.1.2

Suppose that the rank condition (7.1.15) holds. Then the optimal constant β in discrete BB-condition is equal to the smallest singular value of matrix B. That means

$$\inf_{\forall\, p \in P_n} \sup_{\forall\, v \in V_m} \frac{\langle Bv, p \rangle}{\|v\| \|p\|} = \min_i (\mu_i) , \qquad (7.1.16)$$

where

$$\mu_i = \left(\lambda_i (B^T B)\right)^{1/2} \qquad \text{(for each i)} ,$$

and $\lambda_i(B^T B)$ is the ith eigenvalue of matrix $(B^T B)$.

Proof

According to the proof of Theorem 7.1.1, we have proved that

$$\inf_{\forall\, p \in P_n} \sup_{\forall\, v \in V_m} \frac{\langle Bv, p \rangle}{\|v\| \|p\|} \geq \min_i (\mu_i) .$$

To prove (7.1.16) it suffices to prove that the inverse of the above inequality is also true.

We take a p such that

$$p_v = (I_n 0) \cdot v \in P_n \qquad \forall\, v \in V_m ,$$

where I_n is an identity matrix. It is easy to see that

$$\|p_v\|_p \leq \|v\|_V .$$

Then we have

$$\sup_{\forall\, v\in V_m} \frac{\langle \Sigma v, p\rangle}{\|v\|_V \|p\|_P} = \sup_{\forall\, v\in V_m} \frac{\langle \Sigma_n p_v, p\rangle}{\|v\|_V \|p\|_P}$$

$$\leq \sup_{\forall\, v\in V_m} \frac{\langle \Sigma_n p_v, p\rangle}{\|p_v\|_P \|p\|_P} = \sup_{\forall\, p_v\in P} \frac{\langle \Sigma_n p_v, p\rangle}{\|p_v\|_P \|p\|_P}$$

This result leads to the following inequalities:

$$\inf_{\forall\, p\in P_n} \sup_{\forall\, v\in V_m} \frac{\langle \Sigma v, p\rangle}{\|v\|_V \|p\|_P}$$

$$\leq \inf_{\forall\, p\in P_n} \sup_{\forall\, w\in P} \frac{\langle \Sigma_n w, p\rangle}{\|w\|_P \|p\|_P}$$

$$= \inf_{\forall\, p\in P_n} \sup_{\forall\, w\in P} \frac{\langle w, \Sigma_n p\rangle}{\|w\|_P \|p\|_P}$$

$$\leq \sup_{\forall\, w\in P_n} \frac{\langle w, \mu_i e_i\rangle}{\|w\|_P}$$

$$\text{(taking } v = e_i = \begin{pmatrix} 0 \\ \vdots \\ 1 \\ \vdots \\ 0 \end{pmatrix} \text{ ith component in } P_n)$$

$$= \sup_{\forall\, w\in P_n} \frac{(w_i \mu_i)}{(\Sigma w_1^2)^{1/2}} \qquad (w_i \text{ is the ith component of vector } w)$$

$$\leq \sup_{\forall\, w\in P_n} \frac{w_i \mu_i}{|w_i|}$$

$$= \mu_i \ .$$

ince i is arbitrary, we derive the inequality that

$$\inf_{\forall\, p\in P_n} \sup_{\forall\, v\in V_m} \frac{\langle \Sigma v, p\rangle}{\|v\|_V \|p\|_P} \leq \min_i (\mu_i)$$

ıe proof of (7.1.16) is thus completed.

emark

This result suggests that, in addition to the ınsiderations of representations of the cardinal ates of stress or displacement fields such as ten- .on, bending, torsion, etc., it is preferable to ınstruct a hybrid-mixed finite element model such ıat the smallest singular value is as large as ssible.

Rank Condition of Hybrid Stress Model

Consider the hybrid stress model of second version. Referring to Appendix D, the BB-condition is that

$$\sup_{\forall\, \tau\in T_o} \frac{\Sigma_m \int_{\rho_m} \tau_{ij} n_j \tilde{v}_{i\rho} ds}{\|\tau\|_T} \geq \beta \|\tilde{v}_\rho\|_{\tilde{V}(\rho)} \quad \forall\, \tilde{v}_\rho \in V(\tilde{\rho}) \ , \tag{7.2.1}$$

where the space T_o is defined by

$$T_o = \{\tau_{ij} \in H^1(\Omega_m);\ \tau_{ij,j} = 0 \text{ in } \Omega_m,\ \tau_{ij} n_j = 0 \text{ on } S_{tm}, \forall m\} \tag{7.2.2}$$

Notice that

$$\sum_m \int_{\rho_m} \tau_{ij} n_j \tilde{v}_{i\rho}\, ds$$

$$= \sum_m \{ \int_{\Omega_m} (\tau_{ij,j} \tilde{v}_i + \tau_{ij} \tilde{v}_{(i,j)})\, dx$$

$$- \int_{S_{um}} \tau_{ij} n_j \tilde{v}_{i\rho}\, ds - \int_{S_{tm}} \tau_{ij} n_j \tilde{v}_{i\rho} ds \}$$

$$= \sum_m \{ \int_{\Omega_m} \tau_{ij} \tilde{v}_{(i,j)} dx - \int_{S_{um}} \tau_{ij} n_j \tilde{v}_{i\rho} ds \}$$

$$\forall\, \tau \in T_o \ ,$$

where the function $\tilde{v}$ is an extension of $\tilde{v}_\rho$ in Sobolev space $H^1(\Omega_m)$. We assume that

$$\tilde{v}_{i\rho} = 0 \quad \text{on} \quad S_{um} \ . \tag{7.2.3}$$

Then we get that

$$\sum_m \int_{\rho_m} \tau_{ij} n_j \tilde{v}_{i\rho} ds = \sum_m \int_{\Omega_m} \tau_{ij} \varepsilon_{ij}(\tilde{v}) dx \quad \forall\, \tau \in T_o \tag{7.2.4}$$

According to the trace theorem in the theory of Sobolev space, we know that

$$\|\tilde{v}_\rho\|_{\tilde{V}(\rho)} \leq \alpha \|\tilde{v}\|_{\tilde{V}}$$

where $\tilde{V}$ is defined by

$$\tilde{V} = \{\tilde{v}_i \in H^1(\Omega_m) \cap C_o(\Omega),\ \tilde{v}_i|_{\rho_m} = \tilde{v}_{i\rho} \ , \forall m\} \ . \tag{7.2.5}$$

Then the BB-condition (7.2.1) becomes

$$\sup_{\forall\, \tau\in T_o} \frac{\sum_m \int_{\Omega_m} \tau_{ij}\varepsilon_{ij}(\bar{v})dx}{\|\tau\|_T} \geq \beta \|\bar{v}\|_{\bar{V}} \quad \forall\, \bar{v}\in V \qquad (7.2.6)$$

is global condition is difficult to be investigated or to obtaining a computational solution. Thus, reduce (7.2.6) to a necessary condition

$$\sup_{\forall\, \tau\in T_o} \sum_m \int_{\Omega_m} \tau_{ij}\varepsilon_{ij}(\bar{v})dx > 0 \qquad \forall\, v\in \bar{V}\ ,$$

$$\varepsilon_{ij}(\bar{v}) \neq 0\ . \qquad (7.2.7)$$

satisfy the condition (7.2.7), it suffices to isfy

$$\sup_{\tau\in T_o(\Omega_m)} \int_{\Omega_m} \tau_{ij}\varepsilon_{ij}(\bar{v})dx > 0$$

$$\forall\, \bar{v}\in \bar{V}(\Omega_m),\ \varepsilon_{ij}(\bar{v}) \neq 0\ . \qquad (7.2.8)$$

pose that

$$\tau = P\,\beta \quad \text{in } \Omega_m \qquad (7.2.9)$$

$$\bar{v}_\rho = L\,q \quad \text{in } \Omega_m \qquad (7.2.10)$$

re P is the interpolation function of stress field n element Ω_m, L is the interpolation function of ndary displacement $\bar{v}_\rho$ on boundary Ω_m, and we have

$$\dim(\tau)_m = n_\beta$$
$$\dim(\bar{v}_\rho)_m = n_q\ . \qquad (7.2.11)$$

efore one may derive that

$$\varepsilon(\bar{v}) = (DL)q \triangleq A\alpha\ , \qquad (7.2.12)$$

re D is a differential operator. According to the c concept in solid mechanics, we have

$$\dim(\varepsilon) \triangleq n_\alpha = n_q - r\ ,$$

re r is the number of rigid motions of the element Thus, we may derive that

$$\int_{\Omega_m} \tau_{ij}\varepsilon_{ij}(\bar{v})dx = \beta^T B_m \alpha = \langle B_m^T\beta, \alpha\rangle \qquad (7.2.13)$$

e B_m is a n_β x n_α matrix. According to Theorem 1, the condition (7.2.8) holds if and only if the owing rank condition is satisfied:

$$\text{rank}\,(B_m^T) = n_\alpha \leq n_\beta$$

i.e.

$$\text{rank}\,(B_m) = \dim(\bar{v}_\rho)_m - r \leq \dim(\tau)_m \qquad (7.2.14)$$

Among these finite element models which satisfy the rank condition (7.1.14), the least-order finite element models are defined to be those which satisfy the following rank condition:

$$\text{rank}\,(B_m) = \dim(\bar{v}_\rho)_m - r = \dim(\tau)_m\ . \qquad (7.2.15)$$

The theory of symmetry groups is applied by Rubinstein, Punch, and Atluri [18,19, 20] to develop the least-order, stable, invariant hybrid-stress models. A 20-node cubic element, an 8-node cubic element, a 4-node square, and an 8-node square, based on assumed equilibrated stress within the element and compatible displacements at the boundary of the element, may be found in these references. The following is a brief remark on the method of creating elements to satisfy the condition (7.2.15) for the simple example of a 4-node element.

The strain field in a 4-node element is assumed as

$$\varepsilon_{xx} = A_1 + A_2 y$$

$$\varepsilon_{yy} = A_3 + A_4 x$$

$$\varepsilon_{xy} = A_5 + \tfrac{1}{2}(A_2 x + A_4 y)\ .$$

Equivalently, the strain field may be expressed in matrix form as below:

$$\varepsilon = A_1\begin{bmatrix}1 & 0\\ 0 & 0\end{bmatrix} + A_2\begin{bmatrix}y & \frac{1}{2}x\\ \frac{1}{2}x & 0\end{bmatrix} + A_3\begin{bmatrix}0 & 0\\ 0 & 1\end{bmatrix}$$
$$A_4\begin{bmatrix}0 & \frac{1}{2}y\\ \frac{1}{2}y & x\end{bmatrix} + A_5\begin{bmatrix}0 & 1\\ 1 & 0\end{bmatrix} \qquad (7.2.16)$$

According to the group theory, one may get another decomposition of strain field ε as the following:

$$\varepsilon = \sum_{i=1}^{5} \mu_i\varepsilon_i\ , \qquad (7.2.17)$$

where ε_i belongs to invariant irreducible subspaces Γ_j:

$$\Gamma_1 : \{\varepsilon_1 = \begin{bmatrix}1 & 0\\ 0 & 1\end{bmatrix}\}$$

$$\Gamma_2 : \{\varepsilon_2 = \begin{bmatrix}1 & 0\\ 0 & -1\end{bmatrix}\}$$

$$\Gamma_3 : \{\varepsilon_3 = \begin{bmatrix}0 & 1\\ 1 & 0\end{bmatrix}\}$$

$$\Gamma_5 : \{\varepsilon_4 = \begin{bmatrix} y & \frac{1}{2}x \\ \frac{1}{2}x & 0 \end{bmatrix} ; \quad \varepsilon_5 = \begin{bmatrix} 0 & \frac{1}{2}y \\ \frac{1}{2}y & x \end{bmatrix}\}. \quad (7.2.18)$$

The 7-parameter stress field σ is assumed as

$$\sigma_{xx} = a_1 + a_2 x + a_3 y$$

$$\sigma_{yy} = a_4 + a_5 + a_6 y$$

$$\sigma_{xy} = a_7 - a_6 x - a_2 y \quad \text{i.e.}$$

$$\sigma = a_1\begin{bmatrix}1 & 0\\ 0 & 0\end{bmatrix} + a_2\begin{bmatrix}x & -y\\ -y & 0\end{bmatrix} + A_3\begin{bmatrix}y & 0\\ 0 & 0\end{bmatrix}$$

$$a_4\begin{bmatrix}0 & 0\\ 0 & 1\end{bmatrix} + a_5\begin{bmatrix}0 & 0\\ 0 & x\end{bmatrix} + A_6\begin{bmatrix}0 & -x\\ -x & y\end{bmatrix} + a_y\begin{bmatrix}0 & 1\\ 1 & 0\end{bmatrix} \quad (7.2.19)$$

e may also get a decomposition of stress field as

$$\sigma = \sum_{i=1}^{7} \gamma_i \sigma_i ,$$

ere the stress σ_i belongs to invariant irreducible ɔspaces Γ_j as shown below:

$$\Gamma_1 : \{\sigma_1 = \begin{bmatrix}1 & 0\\ 0 & 1\end{bmatrix}\}$$

$$\Gamma_2 : \{\sigma_2 = \begin{bmatrix}1 & 0\\ 0 & -1\end{bmatrix}\}$$

$$\Gamma_3 : \{\sigma_3 = \begin{bmatrix}0 & 1\\ 1 & 0\end{bmatrix}\}$$

$$\Gamma_5 : \{\sigma_4 = \begin{bmatrix}0 & -x\\ -x & y\end{bmatrix}, \quad \sigma_5 = \begin{bmatrix}x & -y\\ -y & 0\end{bmatrix};$$

$$\sigma_6 = \begin{bmatrix}y & 0\\ 0 & 0\end{bmatrix}, \ \sigma_7 = \begin{bmatrix}0 & 0\\ 0 & x\end{bmatrix}\} . \quad (7.2.20)$$

ice that we have the following orthogonality prop-y of the assumed stress field and strain field:

$$\int_{\hat{\Omega}} \sigma_i : \varepsilon_j dx = 0 \quad \forall \sigma_i \varepsilon \Gamma_i, \varepsilon_i \varepsilon \Gamma_j ; \ i \neq j , \quad (7.2.21)$$

ere $\hat{\Omega}$ is the reference element $\{-1 \le x,y \le 1\}$. Then matrix B_m is easily assembled as

	ε_1	ε_2	ε_3	ε_4	ε_5
σ_1	NZ				
σ_2		NZ			
σ_3			NZ		
σ_4				NZ	
σ_5					NZ
σ_6				NZ	
σ_7					NZ

where NZ represents "non-zero". Regarding the invariant requirement, there are only two possibilities to choose two stress modes in Γ_5 in order to construct stable, invariant and least-order hybrid-stress model, i.e.

$$\sigma_5^{(1)} = \gamma_4\sigma_4 + \gamma_5\sigma_5$$

$$\sigma_5^{(2)} = \gamma_6\sigma_6 + \gamma_7\sigma_7 \ . \quad (7.2.21)$$

Each of these choices satisfies the rank condition (7.2.15). It is eacy to know that the lowest singular value, i.e. the lowest eigenvalue in case of least-order model, is 1/3.

Rank Conditions of Hybrid Displacement Model

Consider the second version of hybrid displacement model. Referring to Appendix D, two BB-conditions should be examined, i.e.

$$\sup_{\forall t_\rho \varepsilon T(\rho)} \frac{\sum_m \int_{\rho_m} t_{i\rho}\tilde{v}_{i\rho} ds}{\|t_\rho\|_{T(\rho)}} \ge \beta \|\tilde{v}_\rho\|_{\tilde{V}(\rho)} \qquad \forall \tilde{v}_\rho \varepsilon \tilde{V}(\rho)$$

$$\sup_{\forall v \varepsilon V_o} \frac{\sum_m \int_{\rho_m} v_i t_{i\rho} ds}{\|v\|_V} \ge \beta \|t_\rho\|_{T(\rho)} \qquad \forall t_\rho \varepsilon Ker(D) , \quad (7.3.1)$$

where

$$Ker(D) = \{t_\rho \varepsilon T(\rho), \ \sum_m \int_{\rho_m} t_{i\rho}\tilde{v}_{i\rho} ds = 0 \quad \forall \tilde{v}_\rho \varepsilon \tilde{V}(\rho)\} .$$

For the sake of convenience, the boundary traction $t_{i\rho}$, which is not necessary to be reciprocated at ρ_m, is given by a stress field, i.e.

$$T(\rho) = \{t_{i\rho} = \tau_{ij} n_j \ \text{ at } \ \rho_m , \ \tau \varepsilon T_o\} , \quad (7.3.2)$$

where the space T is the same as in 7.2, (7.2.2). Assume that

$$\|t_\rho\|^2_{T(\rho)} = \sum_m \|t_\rho\|^2_{H^{\frac{1}{2}}(\rho_m)} . \quad (7.3.3)$$

Then we have

$$\|t_\rho\|^2_{T(\rho)} = \sum_m \|\tau_{ij} n_j\|^2_{H^{\frac{1}{2}}(\rho_m)}$$

$$\le \sum_m |n_j| \, \|\tau_{ij}\|^2_{H^{\frac{1}{2}}(\rho_m)}$$

$$\le \sum_m |n_j| \, k \, \|\tau_{ij}\|^2_{H^1(\Omega_m)} \quad \text{(trace theorem)}$$

$$\le k \sum |\tau_{ij}|^2_{H^1(\Omega_m)} \qquad (|n_j| \le 1)$$

$$= \alpha^2 \|\tau\|_T^2 ,$$

$$\|t_\rho\|_{T(\rho)} \leq \alpha \|\tau\|_T .$$

lowing the same procedure shown in section 7.2, BB-conditions (7.3.1) may be reformed as

$$\frac{\sum_m \int_{\Omega_m} \tau_{ij}\varepsilon_{ij}(\tilde{v})dx}{\|\tau\|_T} \geq \beta\|\tilde{v}\|_{\tilde{V}} \qquad \forall \tilde{v}\in\tilde{V} \qquad (7.3.4a)$$

o

$$\frac{\sum_m \int_{\Omega_m} \varepsilon_{ij}(v)\tau_{ij}dx}{\|v\|_V} \geq \beta\|\tau\|_T \qquad \forall \tau\in Ker(D) \quad (7.3.4b)$$

o

e $\tilde{V}$ is defined by (6.3.5), V and Ker(D) are de- d by

$$V = \{v_i\in H^1(\Omega_m)\cap H^0(\Omega),\ v_{i\rho} = 0 \quad \text{on } s_{um}\}$$

$$Ker(D) = \{\tau\in T_o,\ \sum_m \int_{\Omega_m} \tau_{ij}\varepsilon_{ij}(\tilde{v})dx = 0 \quad \forall \tilde{v}\in\tilde{V}\} . \qquad (7.3.5)$$

The first BB-condition (7.3.4a) is the same as .6). Thus, the rank condition is

$$\text{rank}\,(D_m) = \dim\,(\tilde{v}_\rho)_m - r \leq \dim\,(t_\rho)_m , \qquad (7.3.6)$$

the matrix D_m is given by

$$\int_{\Omega_m} \tau_{ij}(t_\rho)\varepsilon_{ij}(\tilde{v})dx = \beta^T D_m \alpha . \qquad (7.3.7)$$

second BB-condition is essentially a global tion, since the space Ker(D) has meaning only in lobal sense,i.e. the orthogonality property

$$\int_{\Omega_m} \tau_{ij}\varepsilon_{ij}(\tilde{v})dx = 0$$

ncerned on whole domain Ω. According to Theorem , the BB-condition is satisfied if and only if

$$\text{rank}\,(C) = \dim\,(\tau^o) \leq \dim\,(v) - r , \qquad (7.3.8)$$

$\tau^o\in$ Ker(D) and C is given by

$$\int_{\Omega_m} \varepsilon_{ij}(v)\tau^o_{ij}dx = q^T C\beta . \qquad (7.3.9)$$

denote that

- the number of elements in the whole domain Ω

n_p - the number of nodes in the whole domain Ω

k_e - the number of nodes per element (7.3.10)

Then the inequality in (7.3.8) becomes

$$n_e(\dim(v)_m - r) \geq \dim\,(\tau^o) . \qquad (7.3.11)$$

Notice that the dimension of space T_o is $n_e\cdot\dim(\tau)_m$, and the dimension of space $\tilde{V}$ is $n_p\cdot\dim(\tilde{v}_\rho)$ | node. Therefore, the dimension of Ker(D) satisfies

$$\dim\,(\tau^o) \triangleq \dim\,[Ker(D)]$$

$$\leq \dim\,(T_o) - [\dim\,(\tilde{V}) - r]$$

$$= n_e\left[\dim\,(\tau)_m - \frac{n_p}{n_e k_e}\dim\,(\tilde{v}_\rho)_m + \frac{r}{n_e}\right] .$$

Thus, a sufficient conditon of (7.3.11) becomes

$$\dim\,(v)_m - r \geq \dim\,(\tau)_m - \frac{n_p}{n_e k_e}\dim\,(\tilde{v}_\rho)_m + \frac{r}{n_e}$$

Since we usually have

$$\frac{r}{n_e} << 1$$

$$\frac{n_p}{n_p} > 1 ,$$

we may get a sufficient condition of (7.3.12) as shown below

$$\dim\,(v_m) - r \geq \dim\,(\tau)_m - \frac{1}{k_e}\dim(\tilde{v}_\rho)_m , \qquad (7.3.13)$$

or simply

$$\dim\,(v_m) - r \geq \dim\,(\tau)_m . \qquad (7.3.14)$$

The rank condition (7.3.14) is only the sufficient condition for global condition (7.3.11), but not necessary. We are required only to avoid the global kinematic modes. However, one may take a local condition to guarantee the global condition.

On the other hand, the condition (7.3.14) is also necessary if we are going to eliminate the variable v and τ in element level as is usually done in practical computation.

We recall the dual problem statement of hybrid displacement model, that is

$$A_m u - C_m^T T_\rho = f \qquad \text{in } (V_o)^*$$

$$C_m u - D_m^T \tilde{u}_\rho = 0 \qquad \text{in } [T(\rho)]^*$$

$$D_m T_\rho = 0 \qquad \text{in } (\tilde{V}(\rho))^* \ . \tag{7.3.15}$$

n order to eliminate the variables u and T, we must olve the equation

$$A_m u - C_m^T T_\rho = f \qquad \text{in } (V_o)^*$$

$$C_m u = D_m^T \tilde{u}_\rho \qquad \text{in } (T(\rho))^* \tag{7.3.16}$$

o get the expressions of u and T_ρ in terms of $\tilde{u}_\rho$. he necessary and sufficient condition to get a ique solution (u,T_ρ) is that

$$\sup_{\forall v \in V_o} \frac{b_m(v,t_\rho)}{\|v\|_{\Omega_m}} \geq \beta \|t_\rho\|_{\Omega} \qquad \forall t_\rho \in T(\rho) \ ,$$

.e.

$$\sup_{\forall \varepsilon V_o} \frac{\int_{\Omega_m} \varepsilon_{ij}(v)\tau_{ij}(t_\rho)dx}{\|v\|_{\Omega_m}} \geq \beta \|t_\rho\|_{\Omega_m} \qquad \forall t_\rho \in T(\rho) \ . \tag{7.3.17}$$

ie associated rank condition is that

$$\dim (\tau)_m \leq \dim (v)_m - r \ .$$

ierefore, the rank conditions of hybrid-displacement thod are

$$\dim (\tilde{v}_\rho)_m - r \leq \dim (\tau)_m \leq \dim (v)_m - r \ . \tag{7.3.18}$$

nk Conditions of Hybrid Mixed Model

We consider the second version of hybrid-mixed del which is based on the modified Reissner inciple. Referring to Appendix D, there are three -conditions required, i.e.

$$\sup_{\forall t_\rho \in T(\rho)} \frac{\sum_m \int_{\rho_m} t_{i\rho}\tilde{v}_{i\rho} ds}{\|t_\rho\|_{T(\rho)}} \geq \beta \|\tilde{v}_\rho\|_{\tilde{V}(\rho)} \qquad \forall \tilde{v}_\rho \in \tilde{V}(\rho)$$

$$\sup_{\forall v \in V_o} \frac{\sum_m \int_{\rho_m} v_i t_{i\rho} ds}{\|v\|_V} \geq \beta \|t_\rho\|_{T(\rho)} \qquad \forall t_\rho \in Ker(D)$$

$$\sup_{\forall \tau \in T} \frac{\sum_m \int_{\Omega_m} \tau_{ij} v_{(i,j)} dx}{\|\tau\|_T} \geq \beta \|v\|_V \qquad \forall v \in Ker^*(C) \ , \tag{7.4.1}$$

re Ker(D) is the same as in 6.4, and Ker*(C) is ined by

$$Ker^*(C) = \{v \in V_o, \ \sum_m \int_{\rho_m} v_i t_{i\rho} ds = 0 \quad \forall t_\rho \in Ker(D)\}. \tag{7.4.2}$$

For the sake of convenience, the interelement boundary traction t_ρ is defined by a stress field, i.e.

$$T(\rho) = \{t_{i\rho} = \tau_{ij} n_j \ \text{ at } \ \rho_m \ , \ \tau \in T_o\} \ , \tag{7.4.3}$$

where the space T_o is the same as in 7.2. Following the same procedure shown in 7.3, the BB-conditions (7.4.1) may be reformed as following:

$$\sup_{\forall \tau \in T_o} \frac{\sum_m \int_{\Omega_m} \tau_{ij} \varepsilon_{ij}(\tilde{v}) dx}{\|\tau\|_T} \geq \beta \|\tilde{v}\|_{\tilde{V}} \qquad \forall \tilde{v} \in \tilde{V}$$

$$\sup_{\forall v \in V_o} \frac{\sum_m \int_{\Omega_m} \varepsilon_{ij}(v) \tau_{ij} dx}{\|v\|_V} \geq \beta \|\tau\|_T \qquad \forall \tau \in Ker(D)$$

$$\sup_{\forall \tau \in T} \frac{\sum_m \int_{\Omega_m} \tau_{ij} \varepsilon_{ij}(v) dx}{\|\tau\|_T} \geq \beta \|v\|_V \qquad \forall v \in Ker^*(D) \ , \tag{7.4.4}$$

where

$$\tilde{V} = \{\tilde{v}_i \in H^1(\Omega_m) \cap C_o(\Omega), \ \tilde{v}_i|_{\rho_m} = \tilde{v}_{i\rho}, \ \forall m\}$$

$$Ker(D) = \{\tau \in T_o, \ \sum_m \int_{\Omega_m} \sigma_{ij} \tilde{v}_{(i,j)} dx = 0 \quad \forall \tilde{v} \in \tilde{V}\}$$

$$Ker^*(C) = \{v \in V_o, \ \sum_m \int_{\Omega_m} v_{(i,j)} \ \tau_{ij} dx = 0 \ \forall \tau \in Ker(D)\} \tag{7.4.5}$$

Following the same discussion in 6.4, three rank conditions are required:

$$\dim (\tilde{v})_m - r \leq \dim (\tau_o)_m$$

$$\dim (\tau_o)_m \leq \dim (v)_m - r$$

$$\dim (v)_m - r \leq \dim (\tau)_m \ ,$$

i.e.

$$\dim (\tilde{v})_m - r \leq \dim (\tau_o)_m \leq \dim (v)_m - r \leq \dim (\tau)_m \ . \tag{7.4.6}$$

ACKNOWLEDGMENTS

The financial support for this work, from NASA-Lewis Research Center under grant NAG-3-346, is gratefully acknowledged. The encouragement of Drs. C. C. Chamis and L. Berke is sincerely appreciated. The assistance of Ms. Joyce Webb in the preparation of this typescript is acknowledged with thanks.

RENCES

Atluri, S.N., "On Hybrid Finite Element Models in Solid Mechanics" in Advances in Computer Methods for Partial Differential Equations (R. Vichnevetsky, Ed.), AICA, Rutgers University, 1975, pp. 346-356.

Atluri, S.N., Tong, P., and Murakawa, H., "Recent Studies in Hybrid and Mixed Finite Element Methods in Mechanics" in Hybrid & Mixed Finite Element Methods (S.N. Atluri, et al., Eds.), J. Wiley & Sons, 1983, pp. 51-71.

Atluri, S.N., Gallagher, R.H., and Zienkiewicz, O.C. (Eds.), Hybrid & Mixed Finite Element Methods, J. Wiley & Sons, 1983.

Atluri, S.N. and Murakawa, H., "On Hybrid Finite Element Methods in Nonlinear Solid Mechanics" in Finite Elements in Nonlinear Mechanics, Vol. 1 (P.G. Bergan, et al., Eds.), Tapir Press, Norway, 1977, pp. 3-41.

Pian, T.H.H. and Tong, P., "Finite Element Methods in Continuum Mechanics" in Advances in Applied Mechanics, Vol. 1 (C-S.Yih, Ed.), Academic Press, 1972.

Pian, T.H.H., Chen, D.P., and Kang, D., "A New Formulation of Hybrid/Mixed Finite Elements", Computers & Structures, Vol. 16, 1983, pp. 81-87.

Babuska, I., "The Finite Element Method with Lagrange Multipliers", Numer. Math., Vol. 20, 1973, pp. 179-192.

Babuska, I., "Error Bounds for the Finite Element Method", Numer. Math., Vol. 16, 1971, pp. 322-333.

Babuska, I. and Ariz, A., "Survey Lectures on the Mathematical Foundations of the Finite Element Method" in The Mathematical Foundations of the Finite Element Method with Applications to Partial Differential Equations (A.K. Ariz, Ed.), Academic Press, 1973, pp. 5-239.

Babuska, I., Osborn, J., and Pitkaranta, J., "Analysis of Mixed Methods Using Mesh Dependent Norms", Maths. of Computation, Vol. 35, No. 152, 1980, pp. 1039-1062.

Babuska, I., Oden, J.T., and Lee, J.K., "Mixed-Hybrid Finite Element Approximations of Second-Order Elliptic Boundary-Value Problems, Part I", Comp. Meth. Appl. Mech. and Engg., Vol. 11, 1977, pp. 175-206.

Babuska, I., Oden, J.T., and Lee, J.K., "Mixed-Hybrid Finite Element Approximations of Second-Order Elliptic Boundary-Value Problems, Part II", Comp. Meth. Appl. Mech. and Engg., Vol. 14, 1978, pp.1-22.

Brezzi, F., "On the Existence, Uniqueness, and Approximation of Saddle-Point Problems Arising from Lagrange Multipliers", R.A.I.R.O. 8-R2, 1974, pp. 129-151.

(14) Oden, J.T. and Jacquotte, O., "Stable and Unstable Rip/Perturbed Lagrangian Methods for Two-Dimensional Viscous Flow Problems" in Finite Elements in Fluids, Vol. 5 (R.H. Gallagher, et al., Eds.), J. Wiley & Sons, 1984, pp. 127-145.

(15) Oden, J.T. Kikuchi, N. and Song, Y., "Penalty-Finite Element Methods for Analysis of Stokesian Flows", Comp. Meth. Appl. Mech. and Engg., Vol. 31, 1982, pp. 297-329.

(16) Ying, L-A. and Atluri, S.N., "A Hybrid Finite Element Method for Stokes Flow: Part II: Stability and Convergence Studies", Comp. Meth. Appl. Mech. and Engg., Vol. 36, 1983, pp 39-60.

(17) Bratianu, C., Atluri, S.N., and Ying, L-A., "Analysis of Stokes' Flow by a Hybrid Method" in Finite Elements in Fluids, Vol. 5 (R.H. Gallagher et al., Eds.), J. Wiley & Sons, 1984, pp. 27-43.

(18) Rubinstein, R., Punch, E.F., and Atluri, S.N., "An Analysis of, and Remedies for, Kinematic Modes in Hybrid-Stress Finite Elements: Selection of Stable, Invariant Stress Fields", Comp. Meth. Appl. Mech. and Engg., Vol. 38, 1983, pp. 63-92.

(19) Punch, E.F. and Atluri, S.N., "Applications of Isoparametric Three-Dimensional Hybrid-Stress Finite Elements with Least-Order Stress Fields", Comp. & Struct., Vol. 19, No. 3, 1984, pp. 409-430.

(20) Punch, E.F. and Atluri, S.N., "Development and Testing of Stable, Invariant, Isoparametric Curvilinear 2- and 3-D Hybrid Stress Elements", Comp. Meth. Appl. Mech. and Engg., Vol. 47, 1984, pp. 331-356.

(21) Yang, C-T. and Atluri, S.N., "An 'Assumed Deviatoric Stress-Pressure-Velocity' Mixed Finite Element Method for Unsteady, Convective, Incompressible Viscous Flow: Part I - Theoretical Development", Int. Jrl. for Num. Meth. in Fluids, Vol. 3, 1983, pp. 377-398.

(22) Yang, C-T. and Atluri, S.N., "An 'Assumed Deviatoric Stress-Pressure-Velocity' Mixed Finite Element Method for Unsteady, Convective, Incompressible Viscous Flow: Part II - Computational Studies", Int. Jrl. for Num. Meth. in Fluids, Vol. 4, 1984, pp. 43-69.

(23) Punch, E.F., "Stable Invariant, Least-Order Isoparametric Mixed-Hybrid Stress Elements: Linear Elastic Continua and Finitely Deformed Plates and Shells", Ph.D Thesis, Georgia Institute of Technology, 1983.

(24) Xue, W-M., Karlovitz, L.A., and Atluri, S.N., "On the Existence and Stability Conditins for Mixed-Hybrid Finite Element Solutions Based on Reissner's Variational Principle", Int. Jrl. Solids & Struct., Vol. 21, No. 1, 1985, pp. 97-116.

5) Xue, W-M., "Existence, Uniqueness, and Stability Conditions for General Finite Element Methods in Linear Elasticity", Ph.D Thesis, Georgia Institute of Technology, 1984.

6) Girault, V. and Raviart, P.A., "Finite Element Approximation of Navier-Stokes Equations", Lecture Notes in Mathematics No. 749, Springer-Verlag, 1979.

7) Tong, P., "New Displacement Hybrid Finite Element Models for Solid Continua", Int. Jrl. Num. Meth. in Engg., Vol 2, 1970, pp. 73-83.

APPENDIX A

Definitions of Functionals and Bilinear Forms

$$a(u,v) = \sum_m \int_{\Omega_m} a_{ijk\ell}\varepsilon_{k\ell}(u)\varepsilon_{ij}(v)\, dx$$

$$a(\sigma,\tau) = \sum_m \int_{\Omega_m} A_{ijk\ell}\sigma_{k\ell}\tau_{ij}\, dx$$

$$b(\tau,v) = \sum_m \int_{\Omega_m} \tau_{ij}\, v_{(i,j)}\, dx$$

$$c(v,t_\rho) = \sum_m \int_{\rho_m} v_i t_{i\rho}\, ds$$

$$(t_\rho,\tilde{v}_\rho) = \sum_m \int_{\rho_m} t_{i\rho}\tilde{v}_{i\rho}\, ds$$

$$l(\tau,\tilde{v}_\rho) = \sum_m \int_{\rho_m} t_{ij}n_j\tilde{v}_{i\rho}\, ds$$

$$l(\varepsilon,\tau) = \sum_m \int_{\Omega_m} \varepsilon_{ij}\, \tau_{ij}\, dx$$

$$p(\tau,v) = \sum_m \left\{\int_{\Omega_m} \tau_{ij}\, v_{(i,j)}\, dx - \int_{S_{um}} \tau_{ij}n_j v_i\, ds\right\}$$

$$\langle f,v\rangle = \sum_m \left\{\int_{\Omega_m} \bar{F}_i\, v_i\, dx + \int_{S_{tm}} \bar{t}_i\, v_i\, ds\right\}$$

$$\langle g,\tau\rangle = \sum_m \int_{S_{tm}} \bar{t}_i\, \tau_{ij}n_j\, ds$$

Modified Variational Principles

	continuous form	modified form (first version)	modified form (second version)
Hu-Washizu Principle	$HW(\varepsilon,\sigma,u)$ $= \int_\Omega [\tfrac{1}{2} a_{ijk\ell}\varepsilon_{k\ell}\varepsilon_{ij} + \sigma_{ij}(u_{(i,j)} - \varepsilon_{ij}) - \bar{F}_i u_i]dx - \int_{S_t} \bar{t}_i u_i ds + \int_{S_u} \sigma_{ij} n_j (\bar{u}_i - u_i) ds$	$MHW1(\varepsilon,\sigma,u,\tilde{T}_\rho)$ $= \sum_m \{\int_{\Omega_m} \tfrac{1}{2} a_{ijk\ell}\varepsilon_{k\ell}\varepsilon_{ij} + \sigma_{ij}(u_{(i,j)} - \varepsilon_{ij}) - \bar{F}_i u_i]dx - \int_{S_{tm}} \bar{t}_i u_i ds + \int_{S_{um}} \sigma_{ij} n_j (\bar{u}_i - u_i) ds - \int_{\rho_m} u_i \tilde{T}_{i\rho} ds\}$	$MHW2(\varepsilon,\sigma,u,T_\rho,\tilde{u}_\rho)$ $= \sum_m \{\int_{\Omega_m} \tfrac{1}{2} a_{ijk\ell}\varepsilon_{k\ell}\varepsilon_{ij} + \sigma_{ij}(u_{(i,j)} - \varepsilon_{ij}) - \bar{F}_i u_i]dx - \int_{S_{tm}} \bar{t}_i u_i ds + \int_{S_{um}} \sigma_{ij} n_j (\bar{u}_i - u_i) ds + \int_{\rho_m} T_{i\rho}(\tilde{u}_{i\rho} - u_i) ds\}$
Reissner Principle $(\sigma_{ij} = a_{ijk\ell}\varepsilon_{k\ell})$	$HR(\sigma,u)$ $= \int_\Omega [-\tfrac{1}{2} A_{ijk\ell}\sigma_{ij}\sigma_{k\ell} + \sigma_{ij} u_{(i,j)} - \bar{F}_i u_i]dx - \int_{S_t} \bar{t}_i u_i ds + \int_{S_u} \sigma_{ij} n_j (\bar{u}_i - u_i) ds$	$MHR1(\sigma,u,\tilde{T}_\rho)$ $= \sum_m \{\int_{\Omega_m} [-\tfrac{1}{2} A_{ijk\ell}\sigma_{ij}\sigma_{k\ell} + \sigma_{ij} u_{(i,j)} - \bar{F}_i u_i]dx - \int_{S_{tm}} \bar{t}_i u_i ds + \int_{S_{um}} \sigma_{ij} n_j (\bar{u}_i - u_i) ds - \int_{\rho_m} u_i \tilde{T}_{i\rho} ds\}$	$MHW2(\sigma,u,T_\rho,\tilde{u}_\rho)$ $= \sum_m \{\int_{\Omega_m} [-\tfrac{1}{2} A_{ijk\ell}\sigma_{k\ell}\sigma_{ij} + \sigma_{ij} u_{(i,j)} - \bar{F}_i u_i]dx - \int_{S_{tm}} \bar{t}_i u_i ds + \int_{S_{um}} \sigma_{ij} n_j (\bar{u}_i - u_i) ds + \int_{\rho_m} T_{i\rho}(\tilde{u}_{i\rho} - u_i) ds\}$
Potential Energy Principle $\left(\begin{matrix}\varepsilon_{ij} = u_{(i,j)} \\ u_i = \bar{u}_i \text{ on } S_u\end{matrix}\right)$	$PE(u)$ $= \int_\Omega [\tfrac{1}{2} a_{ijk\ell}\varepsilon_{k\ell}(u)\varepsilon_{ij}(u) - \bar{F}_i u_i]dx - \int_{S_t} \bar{t}_i u_i ds$	$MPE1(u,\tilde{T}_\rho)$ $= \sum_m \{\int_{\Omega_m} [\tfrac{1}{2} a_{ijk\ell}\varepsilon_{k\ell}(u)\varepsilon_{ij}(u) - \bar{F}_i u_i]dx - \int_{S_{tm}} \bar{t}_i u_i ds - \int_{\rho_m} u_i \tilde{T}_{i\rho} ds\}$	$MPE2(u,T_\rho,\tilde{u}_\rho)$ $= \sum_m \{\int_{\Omega_m} [\tfrac{1}{2} a_{ijk\ell}\varepsilon_{k\ell}(u)\varepsilon_{ij}(u) - \bar{F}_i u_i]dx - \int_{S_{tm}} \bar{t}_i u_i ds + \int_{\rho_m} T_{i\rho}(\tilde{u}_{i\rho} - u_i) ds$
Complementary Energy Principle $\left(\begin{matrix}\varepsilon_{ij} = A_{ijk\ell}\sigma_{k\ell} \\ \sigma_{ij,j} + \bar{F}_i = 0 \\ \sigma_{ij} n_i = t_i \text{ on } S_t\end{matrix}\right)$	$CE(\sigma)$ $= \int_\Omega [-\tfrac{1}{2} A_{ijk\ell}\sigma_{ij}\sigma_{k\ell}]dx + \int_{S_u} \sigma_{ij} n_j \bar{u}_i ds$	$MCE1(\sigma,u_\rho,\tilde{T}_\rho)$ $= \sum_m \{\int_{\Omega_m} -\tfrac{1}{2} A_{ijk\ell}\sigma_{ij}\sigma_{k\ell} dx + \int_{S_{um}} \sigma_{ij} n_j \bar{u}_i ds - \int_{\rho_m} u_{i\rho}(\tilde{T}_{i\rho} - \sigma_{ij} n_j) ds\}$	$MCE^*(\sigma,\tilde{u}_\rho)$ $= \sum_m \{\int_{\Omega_m} -\tfrac{1}{2} A_{ijk\ell}\sigma_{ij}\sigma_{k\ell} dx + \int_{S_{um}} \sigma_{ij} n_j \bar{u}_i ds + \int_{\rho_m} T_{i\rho}\tilde{u}_{i\rho} ds\}$

	continuous form	modified form (first version)	modified form (second version)
Hu-Washizu Principle	find $(\varepsilon,\sigma,u) \in E\times T\times V$, s.t. $a(\varepsilon,e) - \ell(e,\sigma) = 0 \quad \forall e\in E$ $\ell(t,\tau) - p(\tau,u) = \langle g,\tau\rangle \quad \forall \tau\in T$ $p(\sigma,v) = \langle f,v\rangle \quad \forall v\in V$	find $(\varepsilon,\sigma,u,\tilde{T}_\rho) \in E\times T\times V\times\tilde{T}(\rho)$, s.t. $a(\varepsilon,e) - \ell(e,\sigma) = 0 \quad \forall e\in E$ $\ell(\varepsilon,\tau) - p(\tau,u) = \langle g,\tau\rangle \quad \forall \tau\in T$ $p(\sigma,v) - c(v,\tilde{T}_\rho) = \langle f,v\rangle \quad \forall v\in V$ $c(u,\tilde{t}_\rho) = 0 \quad \forall \tilde{t}_\rho\in\tilde{T}(\rho)$	find $(\varepsilon,\sigma,u,T_\rho,\tilde{u}_\rho) \in E\times T\times V\times T(\rho)\times\tilde{V}(\rho)$, s.t. $a(\varepsilon,e) - \ell(e,\sigma) = 0 \quad \forall e\in E$ $\ell(\varepsilon,\tau) - p(\tau,u) = \langle g,\tau\rangle \quad \forall \tau\in T$ $p(\sigma,v) - c(v,T_\rho) = \langle f,v\rangle \quad \forall v\in V$ $c(u,t_\rho) - d(t_\rho,\tilde{u}_\rho) = 0 \quad \forall t_\rho\in T(\rho)$ $d(T_\rho,\tilde{v}_\rho) = 0 \quad \forall \tilde{v}_\rho\in\tilde{V}(\rho)$
Reissner Principle $\sigma_{ij} = a_{ijk\ell}\varepsilon_{k\ell}$ $u_i = \bar{u}_i$ on S_u	find $(\sigma,u) \in T\times V_o$, s.t. $a(\sigma,\tau) - b(\tau,u) = 0 \quad \forall \tau\in T$ $b(\sigma,v) = \langle f,v\rangle \quad \forall v\in V_o$	find $(\sigma,u,\tilde{T}_\rho) \in T\times V_o\times\tilde{T}(\rho)$, s.t. $a(\sigma,\tau) - b(\tau,u) = 0 \quad \forall \tau\in T$ $b(\sigma,v) - c(v,\tilde{T}_\rho) = \langle f,v\rangle \quad \forall v\in V_o$ $c(u,\tilde{t}_\rho) = 0 \quad \forall \tilde{t}_\rho\in\tilde{T}(\rho)$	find $(\sigma,u,T_\rho,\tilde{u}_\rho) \in T\times V_o\times T(\rho)\times V(\tilde{\rho})$, s.t. $a(\sigma,\tau) - b(\tau,u) = 0 \quad \forall \tau\in T$ $b(\sigma,v) - c(v,T_\rho) = \langle f,v\rangle \quad \forall v\in V_o$ $c(u,t_\rho) - d(t_\rho,\tilde{u}_\rho) = 0 \quad \forall t_\rho\in T(\rho)$ $d(T_\rho,\tilde{v}_\rho) = 0 \quad \forall \tilde{v}_\rho\in V(\rho)$
Potential Energy Principle $\varepsilon_{ij} = u_{(i,j)}$ $u_i = \bar{u}_i$ on S_u	find $u \in V_o$, s.t. $a(u,v) = \langle f,v\rangle \quad \forall v\in V_o$	find $(u,\tilde{T}_\rho) \in V_o\times\tilde{T}(\rho)$, s.t. $a(u,v) - c(v,\tilde{T}_\rho) = \langle f,v\rangle \quad \forall v\in V_o$ $c(u,\tilde{t}_\rho) = 0 \quad \forall \tilde{t}_\rho\in\tilde{T}(\rho)$	find $(u,T_\rho,\tilde{u}_\rho) \in V_o\times T(\rho)\times\tilde{V}(\rho)$, s.t. $a(u,v) - c(v,T_\rho) = \langle f,v\rangle \quad \forall v\in V_o$ $c(u,t_\rho) - d(t_\rho,\tilde{u}_\rho) = 0 \quad \forall t_\rho\in T(\rho)$ $d(T_\rho,\tilde{v}_\rho) = 0 \quad \forall \tilde{v}_\rho\in\tilde{V}(\rho)$
Complementary Energy Principle $\varepsilon_{ij} = A_{ijk\ell}\sigma_{k\ell}$ $\sigma_{ij,j} + \bar{F}_i = 0$ $\sigma_{ij}n_j = t_i$ on S_t	find $\sigma \in T_o$, s.t. $a(\sigma,\tau) = \langle g,\tau\rangle \quad \forall \tau\in T_o$	find $(\sigma,u_\rho,\tilde{T}_\rho) \in T_o\times V(\rho)\times\tilde{T}(\rho)$, s.t. $a(\sigma,\tau) - d(\tau,u_\rho) = \langle g,\tau\rangle \quad \forall \tau\in T_o$ $d(\sigma,v_\rho) - c(v_\rho,\tilde{T}_\rho) = 0 \quad \forall v_\rho\in V(\rho)$ $c(u_\rho,\tilde{T}_\rho) = 0 \quad \forall \tilde{t}_\rho\in\tilde{T}(\rho)$	find $(\sigma,\tilde{u}_\rho) \in T_o\times\tilde{V}(\rho)$, s.t. $a(\sigma,\tau) - d(\tau,\tilde{u}_\rho) = \langle g,\tau\rangle \quad \forall \tau\in T_o$ $d(\sigma,\tilde{v}_\rho) = 0 \quad \forall \tilde{v}_\rho\in\tilde{V}(\rho)$

	continuous form	modified form (first version)	modified form (second version)
Hu-Washizu Principle $(u_i = \bar{u}_i \text{ on } S_u)$	$\int_\Omega a_{ijk\ell}\epsilon_{ij}\epsilon_{kj}dx \geq \alpha\|\epsilon\|_E^2 \quad \forall \epsilon \in \mathrm{Ker}(L)$ $\sup_{\forall\tau} \frac{\int_\Omega \tau_{ij} v_{(i,j)}dx}{\|\tau\|_T} \geq \beta\|v\|_V \quad \forall v\in V_o$ $\sup_{\forall e} \frac{\int_\Omega e_{ij}\tau_{ij}dx}{\|e\|_E} \geq \beta\|\tau\|_T \quad \forall \tau \in \mathrm{Ker}(p)$	$\Sigma_m \int_{\Omega_m} a_{ijk\ell}\epsilon_{ij}\epsilon_{k\ell}dx \geq \alpha\|\epsilon\|_E^2 \quad \forall \epsilon \in \mathrm{Ker}(L)$ $\sup_{\forall v\in V_o} \frac{\Sigma_m \int_{\rho_m} v_i \tilde{t}_{i\rho}ds}{\|v\|_V} \geq \beta\|\tilde{t}_\rho\|_{\tilde{T}(\rho)} \quad \forall \tilde{t}_\rho \in \tilde{T}(\rho)$ $\sup_{\forall\tau} \frac{\Sigma_m \int_{\Omega_m} \tau_{ij} v_{(i,j)}ds}{\|\tau\|_T} \geq \beta\|v\|_V \quad \forall v\in \mathrm{Ker}(C)$ $\sup_{\forall e} \frac{\Sigma_m \int_{\Omega_m} e_{ij}\tau_{ij}dx}{\|e\|_E} \geq \beta\|\tau\|_T \quad \forall \tau\in \mathrm{Ker}^*(P)$	$\Sigma_m \int_{\Omega_m} a_{ijk\ell}\epsilon_{ij}\epsilon_{k\ell}dx \geq \alpha\|\epsilon\|_E^2 \quad \forall \epsilon \in \mathrm{Ker}(L)$ $\sup_{\forall t_\rho} \frac{\Sigma_m \int_{\rho_m} t_{i\rho}\tilde{v}_{i\rho}ds}{\|t_\rho\|_{T(\rho)}} \geq \beta\|\tilde{v}_\rho\|_{\tilde{V}(\rho)} \quad \forall \tilde{v}_\rho \in \tilde{V}(\rho)$ $\sup_{\forall v\in V_o} \frac{\Sigma_m \int_{\rho_m} v_i t_{i\rho}ds}{\|v\|_V} \geq \beta\|t_\rho\|_{T(\rho)} \quad \forall t_\rho \in \mathrm{Ker}(D)$ $\sup_{\forall\tau} \frac{\Sigma_m \int_{\Omega_m} \tau_{ij} v_{(i,j)}dx}{\|\tau\|_T} \geq \beta\|v\|_V \quad \forall v\in \mathrm{Ker}^*(C)$ $\sup_{\forall e} \frac{\Sigma_m \int_{\Omega_m} e_{ij}\tau_{ij}dx}{\|e\|_E} \geq \beta\|\tau\|_T \quad \forall \tau\in \mathrm{Ker}^*(P)$
Reissner Principle $\begin{pmatrix}\sigma_{ij} = a_{ijk\ell}\epsilon_{k\ell} \\ u_i = \bar{u}_i \text{ on } S_u\end{pmatrix}$	$\int_\Omega A_{ijk\ell}\tau_{ij}\tau_{k\ell}dx \geq \alpha\|\tau\|_T^2 \quad \forall \tau \in \mathrm{Ker}(B)$ $\sup_{\forall\tau} \frac{\int_\Omega \tau_{ij} v_{(i,j)}dx}{\|\tau\|_T} \geq \beta\|v\|_V \quad \forall v\in V_o$	$\Sigma_m \int_{\Omega_m} A_{ijk\ell}\tau_{ij}\tau_{k\ell}dx \geq \alpha\|\tau\|_T^2 \quad \forall \tau \in \mathrm{Ker}(B)$ $\sup_{\forall v\in V_o} \frac{\Sigma_m \int_{\rho_m} v_i \tilde{t}_{i\rho}ds}{\|v\|_V} \geq \beta\|\tilde{t}_\rho\|_{\tilde{T}(\rho)} \quad \forall \tilde{t}_\rho \in \tilde{T}(\rho)$ $\sup_{\forall\tau} \frac{\Sigma_m \int_{\Omega_m} \tau_{ij} v_{(i,j)}ds}{\|\tau\|_T} \geq \beta\|v\|_V \quad \forall v\in \mathrm{Ker}(C)$	$\Sigma_m \int_{\Omega_m} A_{ijk\ell}\tau_{ij}\tau_{k\ell}dx \geq \alpha\|\tau\|_T^2 \quad \forall \tau \in \mathrm{Ker}(B)$ $\sup_{\forall t_\rho} \frac{\Sigma_m \int_{\rho_m} t_{i\rho}\tilde{v}_{i\rho}ds}{\|t_\rho\|_{T(\rho)}} \geq \beta\|\tilde{v}_\rho\|_{\tilde{V}(\rho)} \quad \forall \tilde{v}_\rho \in \tilde{V}(\rho)$ $\sup_{\forall v\in V_o} \frac{\Sigma_m \int_{\rho_m} v_i t_{i\rho}ds}{\|v\|_V} \geq \beta\|t_\rho\|_{T(\rho)} \quad \forall t_\rho \in \mathrm{Ker}(D)$ $\sup_{\forall\tau} \frac{\Sigma_m \int_{\Omega_m} \tau_{ij} v_{(i,j)}dx}{\|\tau\|_T} \geq \beta\|v\|_V \quad \forall v\in \mathrm{Ker}^*(C)$

APPENDIX D (continued)

	continuous form	modified form (first version)	modified form (second version)
Potential Energy	$\int_\Omega a_{ijk\ell}\varepsilon_{k\ell}(v)\varepsilon_{ij}(v)dx \geq \alpha\|v\|_V \quad \forall v\in V_o$	$\Sigma_m \int_{\Omega_m} a_{ijk\ell}\varepsilon_{k\ell}(v)\varepsilon_{ij}(v)dx \geq \alpha\|v\|_V \quad \forall v\in Ker(C)$	$\Sigma_m \int_{\Omega_m} a_{ijk\ell}\varepsilon_{k\ell}(v)\varepsilon_{ij}(v)dx \geq \alpha\|v\|_V \quad \forall v\in Ker(C)$
Principle	(no BB-condition)	$\sup_{\forall v\in V_o} \frac{\Sigma_m \int_{\rho_m} v_i \tilde{t}_{i\rho} ds}{\|v\|_V} \geq \beta\|\tilde{t}_\rho\|_{\tilde{T}(\rho)} \quad \forall \tilde{t}_\rho \in \tilde{T}(\rho)$	$\sup_{\forall t_\rho} \frac{\Sigma_m \int_{\rho_m} t_{i\rho}\tilde{v}_{i\rho} ds}{\|t_\rho\|_{T(\rho)}} \geq \beta\|\tilde{v}_\rho\|_{\tilde{V}(\rho)} \quad \forall \tilde{v}_\rho \in \tilde{V}(\rho)$
$\varepsilon_{ij} = u_{(i,j)}$			$\sup_{\forall v\in V_o} \frac{\Sigma_m \int_{\rho_m} v_i t_{i\rho} ds}{\|v\|_V} \geq \beta\|t_\rho\|_{T(\rho)} \quad \forall t_\rho \in Ker(D)$
$u_i = \bar{u}_i$ on S_u			
Complementary	$\int_\Omega A_{ijk\ell}\tau_{ij}\tau_{k\ell}dx \geq \alpha\|\tau\|_T \quad \forall \tau\in T_o$	$\Sigma_m \int_{\Omega_m} A_{ijk\ell}\tau_{ij}\tau_{k\ell}dx \geq \alpha\|\tau\|_T \quad \forall \tau \in Ker(D)$	$\Sigma_m \int_{\Omega_m} A_{ijk\ell}\tau_{ij}\tau_{k\ell}dx \geq \alpha\|\tau\|_T \quad \forall \tau \in Ker(D)$
Energy Principle	(no BB-condition)	$\sup_{\forall v_\rho} \frac{\Sigma_m \int_{\rho_m} v_{i\rho} t_{i\rho} ds}{\|v_\rho\|_{V(\rho)}} \geq \beta\|\tilde{t}_\rho\|_{\tilde{T}(\rho)} \quad \forall \tilde{t}_\rho \in \tilde{T}(\rho)$	$\sup_{\forall \tau\in T_o} \frac{\Sigma_m \int_{\rho_m} \tau_{ij} n_j \tilde{v}_{i\rho} ds}{\|\tau\|_T} \geq \beta\|\tilde{v}_\rho\|_{\tilde{V}(\rho)} \quad \forall \tilde{v}_\rho \in \tilde{V}(\rho)$
$\varepsilon_{ij} = A_{ijk\ell}\sigma_{k\ell}$		$\sup_{\forall \tau\in T_o} \frac{\Sigma_m \int_{\rho_m} \tau_{ij} n_j v_{i\rho} ds}{\|\tau\|_T} \geq \beta\|v_\rho\|_{V(\rho)} \quad \forall v_\rho \in Ker(C)$	
$\sigma_{ij,j} + \bar{F}_i = 0$			
$\sigma_{ij} n_i = \bar{t}_i$ on S_t			

International Journal of Plasticity, Vol. 2, No. 2, pp. 107–134, 1986
Printed in the U.S.A.

0749-6419/86 $3.00 + .00

CONSTITUTIVE MODELING OF CYCLIC PLASTICITY AND CREEP, USING AN INTERNAL TIME CONCEPT

O. WATANABE and S. N. ATLURI

Georgia Institute of Technology

Abstract—Using the concept of an internal time as related to plastic strains, a differential stress–strain relation for elastoplasticity is rederived, such that (i) the concept of a yield-surface is retained; (ii) the definitions of elastic and plastic processes are analogous to those in classical plasticity theory; and (iii) its computational implementation, via a "tangent-stiffness" finite element method and a "generalized-midpoint-radial-return" stress-integration algorithm, is simple and efficient. Also, using the concept of an internal time, as related to both the inelastic strains as well as the Newtonian time, a constitutive model for creep-plasticity interaction, is discussed. The problem of modeling experimental data for plasticity and creep, by the present analytical relations, as accurately as desired, is discussed. Numerical examples which illustrate the validity of the present relations are presented for the cases of cyclic plasticity and creep.

I. INTRODUCTION

The characterization of material behavior at elevated temperatures plays an important role in the design of structures such as in hot sections of modern jet engines and other power plants. The ASME Code [1974] defines acceptable levels of stress and strain in critical components of power plants operating at elevated temperatures. The severe mechanical environment may often cause these structures to operate near or beyond the yield limit of the material. Consequently, a unified theory of creep and plasticity, applicable to cyclic loading, is often desirable.

Typical constitutive relations for creep reported and used in literature include the modified strain hardening rule developed by researchers at the Oak Ridge National Lab (PUGH *et al.* [1972], CORUM *et al.* [1974]), dislocation models (LAGNEBORG [1971], GITTUS [1976]) based on metal physics, nonlinear viscoelasticity theory (BESSELING [1958]); and the kinematic hardening model (MALININ & KHADJINSKY [1972]) using an analogy to plasticity. However, recent efforts in material-constitutive-model development reveal a trend toward unifying creep and plasticity. Some experimental results (CORUM *et al.* [1974], JASKE *et al.* [1975]) have been reported concerning the interaction between creep and plasticity. These unifying theories may be roughly divided into the three categories of (i) potential theories, (ii) microphenomenological theories and (iii) nonlinear viscoplastic theories. Most studies employ these theories either individually or in combination. In the first category, one may cite the theories using time-dependent parameters (KRATOCHVIL & DILLON [1970]), the concept of kinematic hardening (KUJAWSKI & MROZ [1980]), micromechanical considerations (PONTER & LECKIE [1976]), and a combination of viscoplastic theory (CHABOCHE [1977]). The phenomenological theories (BODNER & PARTOM [1975], HART [1976], HART *et al.* [1976], MILLER [1976a, 1976b], KRIEG *et al.* [1978], LEE & ZAVERL [1978], ROBINSON [1978], BODNER *et al.* [1979], STOUFFER & BODNER [1979]) employ certain internal variables to reflect the micromechanics of deformation, such as involving dislocations. Most of these theories assume that the plastic strains are also time-dependent, as are creep strains, and

that the creep surface will translate and expand in the stress-space in a manner similar to that of isotropic and kinematic hardening used in classical plasticity theory. The nonlinear viscoplasticity theories have the variations, in which: the coefficients of the linear viscoelastic theory (CERNOCKY & KREMPLE [1980]) are expressed as a function of stresses and strains, the inelastic strains are divided into viscous and viscoelastic components (FINDLEY & LAI [1978]), and the internal time is measured by the (total) *strain* history (VALANIS [1971a,1971b,1980], BAZANT & BHAT [1976], BAZANT [1978], WU & YIP [1980,1981], VALANIS & FAN [1983]). Of course, the fundamental aspects of inelastic deformation are also studied (RICE [1970,1975], HILL & RICE [1972]) based on micromechanical considerations.

The intrinsic time theory, labeled "the endochronic theory" was presented by VALANIS [1971a,1971b]. This theory held out the prospect of explaining the experimental phenomena of cross-hardening, cyclic hardening, and initial strain problems—the situations that classical plasticity theory could not cope with. BAZANT & BHAT [1976] also showed that the "endochronic" theory is effective in dealing with problems of inelasticity and failure in concrete, and that the Maxwell chain model can describe the creep behavior.

VALANIS [1980] later presented a slightly modified intrinsic time model, wherein the internal time is related to the *inelastic* strain. Recently, VALANIS & FAN [1983] presented an incremental or differential form of the integral relation of stress and strain (VALANIS [1980]) for plasticity. This differential relation (VALANIS & FAN [1983]) is of a fundamentally different form as compared to that of the classical plasticity theory and does not employ the notion of a yield surface nor the attendant concepts of "elastic" and "plastic" processes. Based on such a differential relation, VALANIS & FAN [1983] developed an "initial strain" type iterative finite element approach. In this approach, the determination of stress history (or the stress rate) from a given strain history (or the strain rate) is also highly iterative in nature.

While using the concept of an intrinsic time, which depends on plastic strains, and the integral relations of stress and strain (VALANIS [1980]), we rederive here a differential stress–strain relation, such that (i) the concept of a yield surface is retained; (ii) the definitions of "elastic" and "plastic" processes are analogous to those in classical plasticity theories; and (iii) it can be implemented in a computationally simple and efficient manner, via a "tangent-stiffness" finite element method, and a "generalized-midpoint-radial-return" algorithm for determining the stress history (or the stress rate) for a given strain history (or strain rate). The details of analytically modeling the test data, for monotonic or cyclic plasticity, as accurately as desired, through these differential relations, are discussed.

This paper also presents a simple theory for creep, using the concept of intrinsic time which is measured by the inelastic strain as well as Newtonian time, both of which are irreversible. Further, the present theory makes it possible to incorporate the effect of interaction between creep and plasticity in a simple fashion.

Numerical results are presented for cyclic plasticity and creep, in order to verify the validity of the present theories. It is shown that the present constitutive relations are simple in form, and the material constants involved are few in number. Thus they may be useful in practical analyses of inelastic behavior.

In Section II, we present the nomenclature; Section III contains theoretical developments for plasticity based on an intrinsic time measure; Section IV contains discussion of the issues related to the determination of material constants, characterization of monotonic and cyclic hardening plasticity, and certain pertinent numerical results; and Section V contains a unified theory for creep and plasticity, and pertinent numerical results.

II. NOMENCLATURE

Considerations in the present work are restricted to small strains and infinitesimal deformations. For simplicity, we use a Cartesian system of coordinates x_i, with basis $\mathbf{e}_i$. The stress and strain tensors are represented by $\boldsymbol{\sigma} = \sigma_{ij}\mathbf{e}_i\mathbf{e}_j$ and $\boldsymbol{\epsilon} = \epsilon_{ij}\mathbf{e}_i\mathbf{e}_j$, respectively. The stress and strain deviators are represented by $\mathbf{s} = s_{ij}\mathbf{e}_i\mathbf{e}_j$ and $\mathbf{e} = e_{ij}\mathbf{e}_i\mathbf{e}_j$, respectively. If $\mathbf{A}(A_{ij}\mathbf{e}_i\mathbf{e}_j)$ and $\mathbf{B}(B_{mn}\mathbf{e}_m\mathbf{e}_n)$ are two second-order tensors, the notation: $\mathbf{A}\cdot\mathbf{B} = A_{im}B_{mn}\mathbf{e}_i\mathbf{e}_n$ and $\mathbf{A}:\mathbf{B} = A_{ij}B_{ij}$ is employed.

III. PLASTICITY: THEORETICAL DEVELOPMENT

Let $\mathrm{d}\boldsymbol{\epsilon}$ be the strain rate and $\mathrm{d}\mathbf{e}$ its deviator; $\mathrm{d}\epsilon_m$ the mean strain; $\mathrm{d}\mathbf{e} = \mathrm{d}\mathbf{e}^p + \mathrm{d}\mathbf{e}^e$; the plastic strain rate $\mathrm{d}\boldsymbol{\epsilon}^p$ is purely deviatoric, i.e. $\mathrm{d}\boldsymbol{\epsilon}^p \equiv \mathrm{d}\mathbf{e}^p$; and thus, $\mathrm{d}\epsilon_m$ is purely elastic, i.e. $\mathrm{d}\epsilon_m = \mathrm{d}\epsilon_m^e$. We consider the solid to be elastically isotropic. Thus we have

$$\mathrm{d}\mathbf{e}^p = \mathrm{d}\mathbf{e} - \mathrm{d}\mathbf{s}/2\mu_0 \ . \tag{1}$$

Following VALANIS [1980], we define an endochronic (internal) time ζ (which is a Newtonian time-like parameter), such that

$$\mathrm{d}\zeta = (\mathrm{d}\mathbf{e}^p:\mathrm{d}\mathbf{e}^p)^{1/2} \ , \quad \mathrm{d}z = \mathrm{d}\zeta/f(\zeta) \ , \quad f(0) = 1 \ , \quad \mathrm{d}\zeta \geqq 0 \ , \tag{2}$$

where $f(\zeta)$ is monotonically increasing.

As in VALANIS [1980], the stress in the elastic plastic solid is represented through the integral

$$\mathbf{s} = 2\mu_0 \int_0^z \rho(z - z') \frac{\partial \mathbf{e}^p}{\mathrm{d}z'} \ , \tag{3}$$

where μ_0 is the initial (elastic) shear modulus, and $\rho(z)$ is a material-specific kernel. Equation (3) thus appears to circumvent the need for a yield surface as well as for the flow rules of classical plasticity theory. Differentiation of (3) leads to

$$\mathrm{d}\mathbf{s} = 2\mu_p \left\{ \mathrm{d}\mathbf{e} + \frac{\mathbf{h}(z)}{\rho(0) f(\zeta)} \left[\left(\mathrm{d}\mathbf{e} - \frac{\mathrm{d}\mathbf{s}}{2\mu} \right) : \left(\mathrm{d}\mathbf{e} - \frac{\mathrm{d}\mathbf{s}}{2\mu} \right) \right]^{1/2} \right\} \ , \tag{4}$$

$$\rho(0) = \rho \text{ at } z = 0 \ , \quad \mu_p = \mu_0[1 + \rho(0)]^{-1} \ , \quad \mathbf{h}(z) = \int_0^z \frac{\partial \rho}{\partial z}(z - z') \frac{\partial \mathbf{e}^p}{\partial z'} \mathrm{d}z \ . \tag{5}$$

While the classical loading/unloading criteria (or criteria for elastic or plastic processes) are apparently bypassed in eqn (4), there are, nevertheless, prices extracted for this seeming simplicity. Some of these counterbalancing difficulties of the above endochronic approach, as compared to a classical plasticity theory, are as follows:(i) The determination of stress history (and $\mathrm{d}\boldsymbol{\sigma}$) for a given strain history (or $\mathrm{d}\boldsymbol{\epsilon}$) at each material point becomes highly iterative in nature, as seen from (4). (ii) In a finite element/boundary-element/or other weak solution of the boundary value problem, the trial solution de is derived by differentiation of trial displacements du. To determine the trial stresses ds and yet retain a piecewise-linear-equation solution strategy, there is no recourse other than to approximate eqn (4) as $\mathrm{d}\mathbf{s} = 2\mu_p\mathrm{d}\mathbf{e}$. Thus the stiffness matrix at any stage of loading is essentially the linear-elastic stiffness matrix; and the

elastic-plastic solution method becomes the so-called "initial-strain" method. (iii) To model the uniaxial stress–strain curve of a material that does exhibit a sharp "knee" near the elastic limit, the kernel $\rho(z)$ has to be weakly singular at $z = 0$. These drawbacks notwithstanding, VALANIS & FAN [1983] have recently presented a series of papers dealing with a direct computational implementation of an iterative, initial strain method based on eqn (4) and using exponential functions for the kernel $\rho(z)$ in eqn (3). Details of computational times for achieving convergence of plasticity iterations of the global finite element equations, or of the iterations for stress integration, are not readily available in the work of VALANIS & FAN [1983].

Here we present a rederivation of rate-type elastic-plastic constitutive relations using the essential concepts of an endochronic theory, *but* with the following features: (i) The notion of a yield-surface, and the demarcation in the definitions of the elastic processes and plastic processes, are retained. (ii) The stress history (or $d\sigma$), for a given strain history (or $d\epsilon$), can be determined quite easily, as in a classical plasticity theory, by using a "generalized-midpoint-radial-return" algorithm. (iii) The finite-element formulation can be based on a piecewise linear "tangent-stiffness" approach, wherein the material constitutive law at each point can be chosen differently depending on whether an elastic process or a plastic process is postulated at each point during the current "load" increment. The starting point here is the representation of the kernel $\rho(z)$ in eqn (3) in the form (as also suggested by VALANIS [1980])

$$\rho(z) = \rho_0 \delta(z) + \rho_1(z) \ , \tag{6}$$

where $\delta(z)$ is a Dirac function and $\rho_1(z)$ is a nonsingular function. It is seen in the sequel that the term $\rho_0\delta(z)$ in eqn (6) leads to the notion of a yield surface; the function $f(\zeta)$ in (2) leads to the notion of yield-surface-expansion (isotropic hardening); and the function $\rho_1(z)$ in (6) leads to the notion of yield-surface translation (kinematic hardening). Use of (6) in (3) leads to

$$\mathbf{s} = 2\mu_0\rho_0 \frac{d\mathbf{e}^p}{dz} + 2\mu_0 \int_0^z \rho_1(z - z') \frac{d\mathbf{e}^p}{dz'} dz' \tag{7a}$$

$$\equiv \tau_y^0 \frac{d\mathbf{e}^p}{dz} + \mathbf{r}(z) \ , \tag{7b}$$

wherein the definitions of τ_y^0 and $\mathbf{r}(z)$ (the "back stress") are apparent. Equation (7b) can be written as

$$d\epsilon^p = \frac{(\mathbf{s} - \mathbf{r})}{\tau_y^0 f} \cdot d\zeta \ , \quad d\zeta \geqq 0 \ . \tag{8}$$

Of course, eqn (8) is entirely reminiscent of the classical flow-rule and normality relation for plastic strain-rate using a Mises' yield criterion. However, at this point, this similarity is purely formal.

From the very definition of $d\zeta$ as in (2), it follows that, *during plastic flow*,

$$\frac{d\mathbf{e}^p}{d\zeta} : \frac{d\mathbf{e}^p}{d\zeta} = 1 \ , \quad \text{i.e. } (\mathbf{s} - \mathbf{r}) : (\mathbf{s} - \mathbf{r}) = [\tau_y^0 f(\zeta)]^2 \ . \tag{9a,b}$$

Equation (9b) clearly indicates that during plastic flow, the stress point, in the deviatoric stress space, remains on a Mises-cylinder of radius $\tau_y^0 f(\zeta)$, with the center of the surface at $\mathbf{r}$.

By differentiating (8) with respect to ζ, one obtains the following relation which holds during plastic flow:

$$\left(\frac{\mathrm{d}^2\mathbf{e}^p}{\mathrm{d}\zeta^2} + \frac{\mathrm{d}\mathbf{e}^p}{\mathrm{d}\zeta}\frac{\mathrm{d}f}{\mathrm{d}\zeta}\right) = \left(\frac{\mathrm{d}\mathbf{s}}{\mathrm{d}\zeta} - \frac{\mathrm{d}\mathbf{r}}{\mathrm{d}\zeta}\right)\frac{1}{\tau_y^0} \ . \tag{10}$$

From (1), and the definition of $\mathbf{r}$ as in (7), respectively, we see that:

$$\frac{\mathrm{d}\mathbf{s}}{\mathrm{d}\zeta} = 2\mu_0\left(\frac{\mathrm{d}\mathbf{e}}{\mathrm{d}\zeta} - \frac{\mathrm{d}\mathbf{e}^p}{\mathrm{d}\zeta}\right) \tag{11}$$

and

$$\frac{\mathrm{d}\mathbf{r}}{\mathrm{d}\zeta} = 2\mu_0\left[\rho_1(0)\frac{\mathrm{d}\mathbf{e}^p}{\mathrm{d}\zeta} + \frac{\mathbf{h}^*}{f}\right] \ , \tag{12a}$$

where

$$\mathbf{h}^* = \int_0^z \frac{\mathrm{d}\rho_1}{\mathrm{d}z}(z-z')\frac{\partial \mathbf{e}^p}{\partial z'}\,\mathrm{d}z' \ . \tag{12b}$$

Use of (11) and (12a) in (10) results in

$$\mathrm{d}\mathbf{e} = \left[1 + \rho_1(0) + \tau_y^0\frac{(\mathrm{d}f/\mathrm{d}\zeta)}{2\mu_0}\right]\mathrm{d}\mathbf{e}^p + \frac{\mathbf{h}^*\mathrm{d}\zeta}{f} + \frac{\tau_y^0 f}{2\mu_0}\left(\frac{\mathrm{d}^2\mathbf{e}^p}{\mathrm{d}\zeta^2}\right)\mathrm{d}\zeta \ . \tag{13}$$

Also, during plastic flow, it follows from (9a) and (8) that

$$\frac{\mathrm{d}^2\mathbf{e}^p}{\mathrm{d}\zeta^2} : \frac{\mathrm{d}\mathbf{e}^p}{\mathrm{d}\zeta} = 0 = \left(\frac{\mathrm{d}^2\mathbf{e}^p}{\mathrm{d}\zeta^2}\right) : \left(\frac{\mathbf{s}-\mathbf{r}}{\tau_y^0 f}\right) \ . \tag{14}$$

Taking the trace of both sides of (13) with $[(\mathbf{s}-\mathbf{r})/(\tau_y^0 f)]$ [or which is also equal to $(\mathrm{d}\mathbf{e}^p/\mathrm{d}\zeta)$] and using (14), one obtains

$$\mathrm{d}\mathbf{e} : \frac{(\mathbf{s}-\mathbf{r})}{\tau_y^0 f} = \left[1 + \rho_1(0) + \frac{\tau_y^0(\mathrm{d}f/\mathrm{d}\zeta)}{2\mu_0} + \frac{\mathbf{h}^* : (\mathbf{s}-\mathbf{r})}{\tau_y^0 f}\right]\mathrm{d}\zeta \equiv C\,\mathrm{d}\zeta \ , \tag{15}$$

wherein the definition of C is apparent. Equation (15) can be rewritten as

$$\mathrm{d}\zeta = \frac{1}{C}\left[\frac{(\mathrm{d}\mathbf{e}) : (\mathbf{s}-\mathbf{r})}{\tau_y^0 f}\right] \equiv \frac{1}{C}\,\mathrm{d}\mathbf{e} : \mathbf{N} \ , \tag{16}$$

where $\mathbf{N} = (\mathbf{s}-\mathbf{r})/\tau_y^0 f$ is a unit "Normal." Now, by definition, during a "Plastic Process," i.e. when $\mathrm{d}\mathbf{e}^p \neq 0$, we have $\mathrm{d}\zeta > 0$. Thus (16) clearly indicates:

(A) *Definition of a plastic process* (*P*): $d\zeta > 0$

$$(P) \text{ if (i) } (\mathbf{s}-\mathbf{r}):(\mathbf{s}-\mathbf{r}) = (\tau_y^0 f)^2 \text{ and } d\mathbf{e}:\mathbf{N} > 0 \ . \tag{17}$$

Equation (16) also indicates that a "plastic process" is not possible if $\mathbf{N}:d\mathbf{e} \leqq 0$. In confirmity with this, we define an "elastic process" as follows:

(B) *Definition of an elastic process* (*E*): $d\zeta = 0$

$$(E) \text{ (i) if } (\mathbf{s}-\mathbf{r}):(\mathbf{s}-\mathbf{r}) < (\tau_y^0 f)^2 \tag{18a}$$

or

$$\text{(ii) if } (\mathbf{s}-\mathbf{r}):(\mathbf{s}-\mathbf{r}) = (\tau_y^0 f)^2 \text{ and } \mathbf{N}:d\mathbf{e} \leqq 0 \ . \tag{18b}$$

It is interesting to observe that the (Elastic) and (Plastic) processes defined above, for the present endochronic theory, depend directly on whether $(\mathbf{N}:d\boldsymbol{\epsilon}) \gtrless 0$; while in the classical plasticity theory these processes depend, *ab initio*, on whether $(\mathbf{N}:d\boldsymbol{\sigma}) \gtrless 0$. In computational mechanics, the central problem of plasticity is to determine $d\boldsymbol{\sigma}$, for a given $d\boldsymbol{\epsilon}$. In this context, the (E) and (P) criteria of (17) and (18) are more direct and more meaningful. Using (16) in (8), we obtain:

During (P):

$$d\boldsymbol{\epsilon}^p = \frac{1}{C}\mathbf{N}(\mathbf{N}:d\mathbf{e}) \equiv \frac{1}{C}\mathbf{N}(\mathbf{N}:d\boldsymbol{\epsilon}) \ , \tag{19}$$

since $\mathbf{N}$ is deviatoric. Recall that $\mathbf{r}$ [see (7)] and $\mathbf{h}^*$ [see (12b)], and through them, the coefficient C [see (15)] depend on the kernel $\rho_1(z)$.

A convenient choice for the kernel $\rho_1(z)$ is

$$\rho_1(z) = \sum_i \rho_{1i} \exp(-\beta_i z) \ , \tag{20}$$

such that, from (7) it follows that

$$\mathbf{r} = \sum_i 2\mu_0 \int_0^z \left\{ \rho_{1i} \exp[-\beta_i(z-z')] \frac{d\boldsymbol{\epsilon}^p}{dz'} dz' \right\} \equiv \sum_i \mathbf{r}^{(i)} \tag{21a}$$

and

$$\mathbf{h}^* = \sum_i \left(\frac{-\beta_i}{2\mu_0} \right) \mathbf{r}^{(i)} \ , \tag{21b}$$

with $\mathbf{r}^{(i)}$ being defined in an apparent fashion. From (21) it follows that

$$d\mathbf{r} = 2\mu_0 \rho_1(0)\, d\boldsymbol{\epsilon}^p - \left\{ \sum_i \frac{\beta_i \mathbf{r}^{(i)}}{f} \right\} (d\boldsymbol{\epsilon}^p : d\boldsymbol{\epsilon}^p)^{1/2} \ . \tag{22}$$

Thus the evolution equation for $\mathbf{r}$ is *nonlinear* in $\mathrm{d}\mathbf{e}^p$ and thus is similar to a nonlinear-kinematic-hardening relation. It has been discussed in detail by WATANABE & ATLURI [1986] that the present theory, with the translation of the yield surface as in (21), and the expansion of the yield surface as specified by

$$f = (1 + \gamma\zeta) \quad \text{[linear]} \ , \tag{23a}$$

or

$$f = a + (1 - a)\exp(-\psi\zeta) \quad \text{[saturated]} \ , \tag{23b}$$

where γ and ψ are constants, and $\zeta = \int \mathrm{d}\zeta$, includes the multiple-yield-surface theories of MROZ [1969], KRIEG [1975] and DAFALIAS & POPOV [1976] as special cases.

Based on (19), the stress-strain relation in the present theory may be written as

$$\mathrm{d}\mathbf{s} = 2\mu_0[\mathrm{d}\mathbf{e} - \Gamma(1/C)\mathbf{N}(\mathbf{N}:\mathrm{d}\mathbf{e})] \ , \tag{24a}$$

$$(\mathrm{d}\boldsymbol{\sigma}:\mathbf{I}) = (2\mu + 3\lambda)(\mathrm{d}\boldsymbol{\epsilon}:\mathbf{I}) \ , \tag{24b}$$

where $\Gamma = 1$ in (P) and $\Gamma = 0$ in (E).

It is worth noting that VALANIS [1980] presents an entirely different derivation for $\mathrm{d}\zeta$ and obtains an equation similar to the present eqn (16). However, his result for the coefficient C given in his eqn (3.34) (VALANIS [1980]), which contains certain algebraic errors, differs from the value of C given in the present eqn (15), even after the algebraic errors of VALANIS [1980] are corrected. Specifically, the constant C in Valanis' work does not contain the term $[\tau_y^0(\mathrm{d}f/\mathrm{d}\zeta)]/2\mu_0$ as in the present eqn (15). It will be shown later in this paper that the present eqn (15) is in fact correct.

It is interesting to compare the present stress-strain relations with the familiar classical plasticity theory relations for isotropic and kinematic hardening (ATLURI [1984]).

III.1. *Classical isotropic hardening*

$$\mathrm{d}\mathbf{s} = 2\mu_0\left[\mathrm{d}\mathbf{e} - 3\mu_0\frac{\mathbf{N}(\mathbf{N}:\mathrm{d}\mathbf{e})}{1 + (1/3\mu_0)H}\right] \ , \tag{25a}$$

$$\mathbf{N} = \mathbf{s}/\sigma_0(\epsilon^p) \ , \tag{25b}$$

where $\sigma_0(\epsilon^p)$ is the uniaxial equivalent stress as a function of the equivalent plastic strain, and H is the slope of the true stress vs the logarithmic strain relation.

III.2. *Classical linear kinematic hardening*

$$\mathrm{d}\mathbf{s} = 2\mu_0\left[\mathrm{d}\mathbf{e} - \frac{3\mu_0}{(\hat{c} + 2\mu_0)}\mathbf{N}(\mathbf{N}:\mathrm{d}\mathbf{e})\right] \ , \tag{26a}$$

where

$$\mathbf{N} = (\mathbf{s} - \mathbf{r})/\sigma_y^0 \ , \quad \mathrm{d}\mathbf{r} = \hat{c}\,\mathrm{d}\boldsymbol{\epsilon}^p \ . \tag{26b}$$

Thus the present endochronic relations (24a,b) are entirely analogous to those of classical plasticity theory (25a,b) and (26a,b).

By assuming $\Gamma = 1$ or 0 appropriately, one may proceed to develop a tangent-stiffness finite-element method in the usual fashion. If the stress $\boldsymbol{\sigma}_n$ at state $\mathbf{C}_n$, in an incremental solution, is known, the incremental stresses $\Delta\boldsymbol{\sigma}$ corresponding to the trial-solutions $\Delta\boldsymbol{\epsilon}$ for incremental strains are determined in the usual fashion. We assume that $\boldsymbol{\sigma}_n$ is on the yield surface and further assume that the process had been plastic†; i.e. $\|(\sigma'_n + 2\mu\Delta\epsilon') - r_n\| > (\tau_y^0 f_n)$. Then, for any θ such that $0 < \theta < 1$, the algorithm for determining the actual stress-increment $\Delta\boldsymbol{\sigma}$ in the plastic process proceeds as follows:

$$\mathbf{N}_\theta = \frac{(\mathbf{s}_n + 2\mu\theta\,\Delta\mathbf{e}) - \mathbf{r}_n}{\|(\mathbf{s}_n + 2\mu\theta\,\Delta\mathbf{e}) - \mathbf{r}_n\|} \ , \tag{27a}$$

$$\Delta\mathbf{e}^p = (1/C_n)(\mathbf{N}_\theta : \Delta\boldsymbol{\epsilon})\mathbf{N}_\theta \tag{27b}$$

$$\left\{\text{where } C_n = \left[1 + \rho_1(0) + \frac{\tau_y^0(\mathrm{d}f/\mathrm{d}\zeta)}{2\mu_0} + \frac{\mathbf{h}^* : (\mathbf{s} - \mathbf{r})}{\tau_y^0 f}\right]_n\right\} \ ,$$

$$\Delta\mathbf{S} = 2\mu[\Delta\boldsymbol{\epsilon}' - (1/C_n)(\mathbf{N}_\theta : \Delta\boldsymbol{\epsilon})\mathbf{N}_\theta] \ , \tag{27c}$$

$$\Delta\boldsymbol{\sigma} : \mathbf{I} = (2\mu + 3\lambda)(\Delta\boldsymbol{\epsilon} : \mathbf{I}) \ , \tag{27d}$$

$$\Delta\zeta = (\Delta\boldsymbol{\epsilon}^p : \Delta\boldsymbol{\epsilon}^p)^{1/2} \ , \quad f_{n+1} = f_n + \Delta f \ , \tag{27e}$$

$$\mathbf{r}_{n+1} = \mathbf{r}_n + \left\{2\mu_0\rho_1(0)\Delta\boldsymbol{\epsilon}^p - \left(\sum_i \frac{\beta_i\sigma_n^{(i)}}{f_n}\right)\Delta\zeta\right\} \ . \tag{27f}$$

Of course, several variants of the above algorithm, such as subincremental ones, are possible. The above tangent-stiffness finite-element, and generalized midpoint-radial-return-stress integration, algorithm has been used by WATANABE & ATLURI [1984b] to solve several problems of cyclic plasticity and nonproportional biaxial loading. It has been found that the present models capture the experimentally observed phenomena of cyclic hardening, cross-hardening, ratcheting, etc.

Because of the superior predictive capabilities of the present model and the fact that it is no more difficult to implement than the usual (classical) plasticity models, it may be a candidate for further exploitation in general purpose computational programs.

IV. DETERMINATION OF MATERIAL CONSTANTS AND REPRESENTATION OF MONOTONIC AND CYCLIC HARDENING PLASTICITY

IV.1. *General considerations*

We develop here the stress–strain relations for uniaxial tension so as to be *consistent* with the presently developed alternative three-dimensional relations given in eqns (7) and (24) in integral and differential forms, respectively. We define the uniaxial tension

†For a discussion of a general plasticity algorithm, covering both elastic and plastic processes, see ATLURI [1985].

response through the relations: $\sigma_{11} \neq 0$ otherwise $\sigma_{ij} = 0$; $de^p_{22} = de^p_{33} = -\frac{1}{2} de^p_{11}$, $de^p_{ij} = 0$ $(i \neq j)$. Using (2), we obtain

$$d\zeta^2 = \tfrac{3}{2}(de^p_{11})^2 = \tfrac{3}{2}(d\epsilon^p_{11})^2 \ ,$$

or

$$d\zeta = \sqrt{\tfrac{3}{2}}\, |d\epsilon^p_{11}| \tag{28a}$$

and

$$\zeta = \sqrt{\tfrac{3}{2}} \int \|d\epsilon^p_{11}\| \ . \tag{28b}$$

We also introduce

$$dz = d\zeta / f(\zeta) \ , \quad f(\zeta) = 1 + \beta\zeta \ , \tag{29}$$

$$E_0 \rho(z) = E_0 \rho_0 \delta(z) + E_1 \, e^{-\alpha_1 z} + E_2 \ , \tag{30a}$$

and

$$\mu_0 \rho(z) = \mu_0 \rho_0 \delta(z) + \left(\frac{\mu_0}{E_0}\right) E_1 \, e^{-\alpha_1 z} + \left(\frac{\mu_0}{E_0}\right) E_2 \ . \tag{30b}$$

The stress–strain relation under uniaxial tension that was used by Wu & Yip [1980,1981] is

$$\sigma_{11} = E_0 \int_0^z \rho(z - z') \frac{de^p_{11}}{dz} \, dz' \ , \quad \text{for } \zeta \geq 0^+ \ . \tag{31}$$

Using (28) to (30a,b) in (31), we obtain, for *monotonic uniaxial* tension ($\|d\epsilon^p_{11}\| = d\epsilon^p_{11}$),

$$\sigma_{11} = E_0 \rho_0 \sqrt{\frac{2}{3}} \left(1 + \beta \sqrt{\frac{3}{2}}\, \epsilon^p_{11}\right) + \sqrt{\frac{2}{3}} \left(\frac{E_1}{n_1 \beta}\right) \left(1 + \beta \sqrt{\frac{3}{2}}\, \epsilon^p_{11}\right)$$
$$\times \left\{1 - \left(1 + \beta \sqrt{\frac{3}{2}}\, \epsilon^p_{11}\right)^{-n_1}\right\} + E_2 \epsilon^p_{11} \ , \quad \text{for } \epsilon^p_{11} \geq 0 \ , \tag{32a}$$

where

$$n_1 = 1 + (\alpha_1 / \beta) \ . \tag{32b}$$

It may be worth mentioning that Wu & Yip [1980,1981] use the definition that $d\zeta = |d\epsilon^p_{11}|$ instead of the one in (28b). Hence the result in Wu & Yip [1980,1981] would agree with the present (32) if the constants ρ_0, E_0, E_1, E_2, β_1 and α_1 as used in Wu & Yip [1980,1981] are identified, instead, to be $(\rho_0\sqrt{2/3})$, E_0, E_1, E_2, $(\beta\sqrt{3/2})$ and $(\alpha_1\sqrt{3/2})$, respectively.

On the other hand, the present three-dimensional integral relation, eqn (7), reduces, for the uniaxial tension case, to

$$\sigma_{11} = 3\mu_0\rho_0 \frac{d\epsilon_{11}^p}{dz} + 3\mu_0 \int_0^z \rho_1(z-z') \frac{d\epsilon_{11}^p}{dz'}\, dz' \tag{33}$$

$$= \sqrt{6}\mu_0\rho_0\left(1+\beta\sqrt{\frac{3}{2}}\,\epsilon_{11}^p\right) + \sqrt{\frac{2}{3}}\left(\frac{3\mu_0}{E_0}\right)\frac{E_1}{\beta n_1}\left(1+\beta\sqrt{\frac{3}{2}}\,\epsilon_{11}^p\right)$$

$$\times\left\{1-\left(1+\beta\sqrt{\frac{3}{2}}\,\epsilon_{11}^p\right)^{-n_1}\right\} + \left(\frac{3\mu_0}{E_0}\right)E_2\epsilon_{11}^p\ , \quad \text{for } \epsilon_{11}^p \geq 0\ . \tag{34}$$

In writing (34), monotonic loading has been assumed. By comparing (32) and (34), it may be seen that the WU-YIP [1980,1981] relation agrees with the present, provided $E_0 = 3\mu_0$, i.e. the Poisson's ratio $\nu_0 = 1/2$, even in the elastic region. This is due to the fact that the integral relation used in WU & YIP [1980,1981], which results in (31) and (32), is based on the assumption that the Poisson's ratio is constant through deformation.

We shall henceforth use (34) to evaluate material properties, for use in conjunction with the three-dimensional relations (7) and (24). We will assume that the *elastic* properties are related as $\mu_0 = E_0/2(1+\nu_0)$, $\lambda_0 = 2\mu_0\nu_0/(1-2\nu_0)$, $3k_0 = (3\lambda_0 + 2\mu_0)$.

For large values of ϵ_{11}^p, the asymptotic value of stress, denoted as σ_{11}^∞, may be obtained from (33) to be

$$\sigma_{11}^\infty = \sqrt{6}\mu_0\rho_0\left(1+\beta\sqrt{\frac{3}{2}}\,\epsilon_{11}^p\right) + \sqrt{\frac{2}{3}}\left(\frac{E_1}{\beta n_1}\right)\left(1+\beta\sqrt{\frac{3}{2}}\,\epsilon_{11}^p\right)\left(\frac{3\mu_0}{E_0}\right) + \left(\frac{3\mu_0}{E_0}\right)E_2\epsilon_{11}^p\ . \tag{35}$$

Assuming that the *elastic constants* (E_0, μ_0) are known for the material, it is seen from (34) that the stress-plastic strain response of the material, given in (34), is governed by the five parameters: ρ_0, β, α_1, E_1 and E_2. We now discuss the determination of these five parameters from given *test data* for the material under monotonic uniaxial tension. To this end, first note that

$$\frac{d\sigma_{11}}{d\epsilon_{11}^p} = 3\mu_0\rho_0\beta + \left(\frac{3\mu_0}{E_0}\right)\frac{E_1}{n_1}\left\{1+(n_1-1)\left(1+\beta\sqrt{\frac{3}{2}}\,\epsilon_{11}^p\right)^{-n_1}\right\} + \left(\frac{3\mu_0}{E_0}\right)E_2 \tag{36}$$

and

$$\frac{d\sigma_{11}^\infty}{d\epsilon_{11}^p} = 3\mu_0\rho_0\beta + \left(\frac{3\mu_0}{E_0}\right)\frac{E_1}{n_1} + \left(\frac{3\mu_0}{E_0}\right)E_2\ . \tag{37}$$

We now define parameters σ_0^0, E_p, σ_0^∞ and E_t as may be determined† from the test data as shown in Fig. 1(a), to be

†Here it is to be noted that the "knee" portion (near the "elastic" limit point) of the stress-strain test data is approximated by a straight line $\sigma_{11} = \sigma_0^0 + E_p\epsilon_{11}^p$ for $\epsilon_{11}^p \ll 1$; and for *large values* of ϵ_{11}^p, the stress-strain test data is approximated by a straight line $\sigma_{11} = \sigma_0^\infty + E_t\epsilon_{11}^p$ as shown in Fig. 1(a). Thus the parameters of σ_0^0, E_p, σ_0^∞ and E_t are "read-off" from the test data for uniaxial tension.

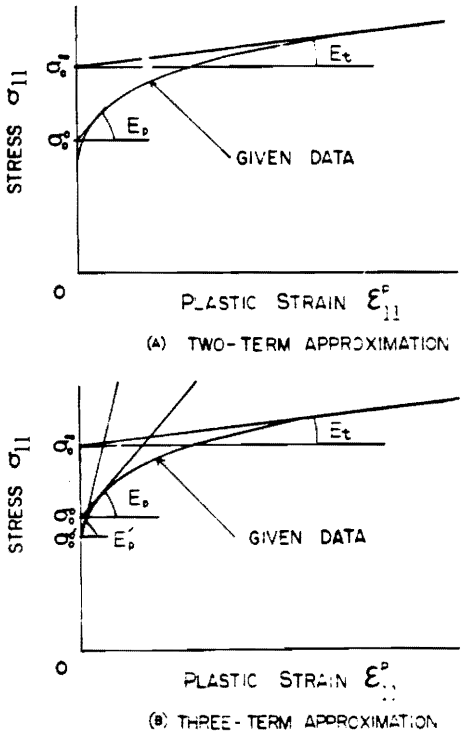

Fig. 1. Nomenclature used in analytical modeling of test data.

$$\sigma_0^0 = \sigma_{11}|_{\epsilon_{11}^p=0} = \sqrt{6}\mu_0\rho_0 \ , \tag{38a}$$

$$E_p = \mathrm{d}\sigma_{11}/\mathrm{d}\epsilon_{11}^p|_{\epsilon_{11}^p=0} = 3\mu_0\rho_0\beta + \left(\frac{3\mu_0}{E_0}\right)E_1 + \left(\frac{3\mu_0}{E_0}\right)E_2 \ , \tag{38b}$$

$$\sigma_0^\infty = \sigma_{11}^\infty|_{\epsilon_{11}^p=0} = \sqrt{6}\mu_0\rho_0 + \sqrt{\frac{2}{3}}\left(\frac{3\mu_0}{E_0}\right)\frac{E_1}{\beta n_1} \ , \tag{38c}$$

and

$$E_t = \frac{\mathrm{d}\sigma_{11}^\infty}{\mathrm{d}\epsilon_{11}^p} = 3\mu_0\rho_0\beta + \left(\frac{3\mu_0}{E_0}\right)\frac{E_1}{n_1} + \left(\frac{3\mu_0}{E_0}\right)E_2 \ . \tag{38d}$$

The four equations (38a)–(38d) are obviously not sufficient to determine the five constants ρ_0, β, α_1, E_1 and E_2. To uniquely determine the five constants, the missing fifth relation may be arrived at by first noting that $\rho_1(z)$ (involving E_1 and E_2) describes the translation of the yield surface, and $f(\zeta)$ (involving β) describes the enlargement (or contraction, as the case may be) of the yield surface. Specifically, by integrating (33) for a loading-unloading-reloading case, assuming that $f(\zeta) = 1 + \beta\zeta$, it may be shown that the stress-drop $\Delta\sigma$ during the elastic part of the first unloading is $2\sigma_0^0(1 + \beta\sqrt{\frac{3}{2}}|\epsilon_{11}^p|^*)$ (see Fig. 3) where $|\epsilon_{11}^p|^*$ is the plastic strain at the beginning of elastic

unloading. Thus material constant β may be determined. Now eqns (38a)–(38d) may be solved for the remaining four unknowns, as

$$n_1 \equiv (1 + \alpha_1/\beta) = 1 + \sqrt{\frac{2}{3}} \left(\frac{E_p - E_t}{\sigma_0^\infty - \sigma_0^0} \right) \frac{1}{\beta} \ , \tag{39a}$$

$$\rho_0 = (\sigma_0^0/\sqrt{6}\mu_0) \ , \tag{39b}$$

$$E_1 = \left(\frac{E_0}{3\mu_0} \right) \left[(E_p - E_t) + \sqrt{\frac{3}{2}} \, (\sigma_0^\infty - \sigma_0^0)\beta \right] \ , \tag{39c}$$

and

$$E_2 = \left(\frac{E_0}{3\mu_0} \right) \left(E_t - \sqrt{\frac{3}{2}} \, \sigma_0^\infty \beta \right) \ . \tag{39d}$$

If a more accurate approximation near the "knee" of the stresss-strain curve (at $\epsilon_{11}^p = 0$) is needed, one may use, instead of (30b), the assumption

$$\mu_0 \rho(z) = \mu_0 \rho_0' \delta(z) + \left(\frac{\mu_0}{E_0} \right) E_1 \, e^{-\alpha_1 z} + \left(\frac{\mu_0}{E_0} \right) E_2 + \left(\frac{\mu_0}{E_0} \right) E_3 \, e^{-\alpha_3 z} \ . \tag{40}$$

The corresponding solution becomes

$$\begin{aligned} \sigma_{11} = {} & \sqrt{6}\mu_0 \rho_0' \left(1 + \beta \sqrt{\frac{3}{2}} \, \epsilon_{11}^p \right) + \sqrt{\frac{2}{3}} \left(\frac{3\mu_0}{E_0} \right) \frac{E_1}{\beta n_1} \left(1 + \beta \sqrt{\frac{3}{2}} \, \epsilon_{11}^p \right) \\ & \times \left\{ 1 - \left(1 + \beta \sqrt{\frac{3}{2}} \, \epsilon_{11}^p \right)^{-n_1} \right\} + \sqrt{\frac{2}{3}} \left(\frac{3\mu_0}{E_0} \right) \frac{E_3}{\beta n_3} \left(1 + \beta \sqrt{\frac{3}{2}} \, \epsilon_{11}^p \right) \\ & \times \left\{ 1 - \left(1 + \beta \sqrt{\frac{3}{2}} \, \epsilon_{11}^p \right)^{-n_3} \right\} + \left(\frac{3\mu_0}{E_0} \right) E_2 \epsilon_{11}^p \ , \end{aligned}$$

where

$$n_3 = 1 + (\alpha_3/\beta) \ . \tag{41}$$

The parameters from the test data,† as shown in Fig. 1(b), are now related as

$$E_t = 3\mu_0 \rho_0' \beta + \left(\frac{3\mu_0}{E_0} \right) \frac{E_1}{n_1} + \left(\frac{3\mu_0}{E_0} \right) \frac{E_3}{n_3} + \left(\frac{3\mu_0}{E_0} \right) E_2 \ , \tag{42a}$$

†In this improved representation, the "knee" portion of the test data is approximated by a straight line $\sigma_{11} = (\sigma_0^0)' + (E_p)' \epsilon_{11}^p$ for $\sigma_{11}^p \ll 1$, as shown in Fig. 1(b). However, for large values of ϵ_{11}^p, the test data is approximated by the same straight line as in the earlier representation [shown in Fig. 1(a)], i.e. $\sigma_{11} = \sigma_0^\infty + E_t \epsilon_{11}^p$. Note also that the definitions of (σ_0^0) and (E_p), shown in Fig. 1(b), remain the same as before, i.e. $\sigma_0^0 = \sqrt{6}\,\mu_0 \rho_0$, and $E_p = 3\mu_0 \rho_0 \beta + (3\mu_0/E_0)E_1$.

$$\sigma_0^\infty = \sqrt{6}\mu_0\rho_0' + \sqrt{\frac{2}{3}}\left(\frac{3\mu_0}{E_0}\right)\frac{E_1}{\beta n_1} + \sqrt{\frac{2}{3}}\left(\frac{3\mu_0}{E_0}\right)\frac{E_3}{\beta n_3} \ , \tag{42b}$$

$$(\sigma_0^0)' = \sqrt{6}\mu_0\rho_0' \ , \tag{42c}$$

$$(E_p)' = 3\mu_0\rho_0'\beta + \left(\frac{3\mu_0}{E_0}\right)E_1 + \left(\frac{3\mu_0}{E_0}\right)E_3 + \left(\frac{3\mu_0}{E_0}\right)E_2 \ . \tag{42d}$$

With β, E_1 and E_2 being as before, the additional constants in the improved approximation are determined as

$$n_3 = \sqrt{\frac{2}{3}}\,\frac{1}{\beta}\left(\frac{E_p' - E_p}{\sigma_0^0 - (\sigma_0^0)'}\right) + 1 \tag{43a}$$

and

$$E_3 = \left(\frac{E_0}{3\mu_0}\right)\left[(E_p' - E_p) + \sqrt{\frac{3}{2}}\,(\sigma_0^0 - \sigma_0^{0\prime})\beta\right] \ . \tag{43b}$$

Similar procedures may be employed when an arbitrary number of terms are used in the expansion

$$E_0\rho(z) = E_0\rho_0\delta(z) + \sum_i E_i\, \mathrm{e}^{-\alpha_i z} \ , \tag{44}$$

which makes it possible to represent the knee portion more and more accurately.

We now consider the presently derived differential form of the stress–strain relation, (24). For the uniaxial tension problem, eqn (24) becomes

$$\mathrm{d}S_{11} = 2\mu_0\left\{\mathrm{d}e_{11} - \frac{(S_{11} - r_{11})^2}{Cf^2S_y^{02}}\,\mathrm{d}e_{11} - \frac{(S_{11} - r_{11})(S_{22} - r_{22})}{Cf^2S_y^{02}}\,\mathrm{d}e_{22} - \frac{(S_{11} - r_{11})(S_{33} - r_{33})}{Cf^2S_y^{02}}\,\mathrm{d}e_{33}\right\} \ . \tag{45}$$

For uniaxial tension,

$$S_{11} = \tfrac{2}{3}\sigma_{11} \ , \quad S_{22} = S_{33} = -\tfrac{1}{3}\sigma_{11} \ , \quad r_{22} = r_{33} = -\tfrac{1}{2}r_{11} \ ,$$

$$\mathrm{d}e_{11} = \mathrm{d}\epsilon_{11} - \frac{\mathrm{d}\sigma_{11}}{9K_0} \ , \quad \mathrm{d}e_{22} = -\tfrac{1}{2}\mathrm{d}\epsilon_{11} + \frac{\mathrm{d}\sigma_{11}}{18K_0} = \mathrm{d}e_{33} \ ,$$

$$r_{11} = 2\mu_0\int_0^z \rho_1(z - z')\,\frac{\mathrm{d}e_{11}^p}{\mathrm{d}z'}\,\mathrm{d}z' \ . \tag{46}$$

Use of (46) in (45) results, for the *monotonic* uniaxial tension problem, in

$$d\sigma_{11} = \frac{2\mu_0[1-(1/C)]}{(2/3)+(2\mu_0/9K_0)[1-(1/C)]}\, d\epsilon_{11} \ , \tag{47}$$

where

$$C = 1 + \rho_1(0) + \frac{S_y^0 f'}{2\mu_0} + \sqrt{\frac{3}{2}}\,\frac{h_{11}^*}{f} \ . \tag{48}$$

For the presently assumed $\rho_1(z)$ and f, as in (30a) and (29), respectively, we have

$$\rho_1(0) = \left(\frac{E_0}{E_1}\right) + \left(\frac{E_2}{E_0}\right) \ , \tag{49a}$$

$$\frac{h_{11}^*}{f} = \frac{1}{f}\int_0^z \frac{\partial \rho_1}{\partial z}(z-z')\frac{de_{11}^p}{dz'}\,dz' = -\sqrt{\frac{2}{3}}\left(\frac{E_1}{E_0}\right)\left(\frac{n_1-1}{n_1}\right)\{1-f^{-n_1}\} \tag{49b}$$

and

$$C = 1 + \left(\frac{E_2}{E_0}\right) + \left(\frac{E_1}{E_0}\right)\frac{1}{n_1}[1+(n_1-1)f^{-n_1}] + \rho_0\beta \ . \tag{49c}$$

Since

$$d\epsilon_{11} = d\epsilon_{11}^p + \frac{d\sigma_{11}}{E_0} \ , \tag{50}$$

it may be easily shown, by using (50) in (47), that

$$\begin{aligned}\frac{d\sigma_{11}}{d\epsilon_{11}^p} &= 3\mu_0(C-1) \\ &= 3\mu_0\rho_0\beta + \left(\frac{3\mu_0}{E_0}\right)\frac{E_1}{n_1}[1+(n_1-1)f^{-n_1}] + \left(\frac{3\mu_0}{E_0}\right)E_2 \ ,\end{aligned} \tag{51}$$

which agrees with (36) derived from the integral relation. This agreement of (51) with (36) is then a confirmation of the validity of the differential stress-strain relations (24a) and (24b), as well as the correctness of the presently derived expression for C as in (15).

IV.2. *Numerical results*

IV.2.1. *Plasticity: monotonic loading.* The applications that we address here pertain to *inelastic deformation at elevated temperatures.* In this subsection, we will consider plasticity; and later in this paper, we deal with the problem of plasticity-creep interaction. Here we make use of experimental data for type-304 stainless steel at high temperatures, produced by the Power Reactor and Nuclear Fuel Development Corporation (hereafter denoted as PNC) in Japan (JSME [1981]). First we study the *monotonic stress-strain curve at 550°C*, for which the PNC data (JSME [1981]) is shown in

Fig. 2. The constitutive equation adopted by PNC (JSME [1981]) may be considered to be a modified version of BLACKBURN's [1972] equation, in which an increment of plastic strain is expressed by a power law in terms of stress. This makes the "knee" portion of the stress vs plastic strain curve to have a very steep initial slope, as shown in Fig. 2.

We now approximate the above PNC data by three different types of the present "intrinsic-time-plasticity" models, eqns (33) or (45). These three modes are designated as Cases A, B and C, respectively, in Tables 1 and 2. In Case A, a two-term approxi-

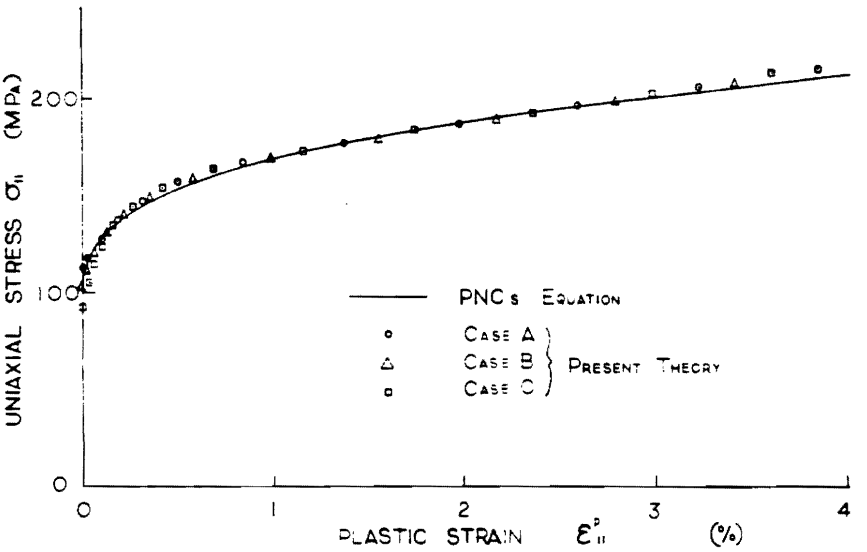

Fig. 2. Modeling of test data for 304 stainless steel to various degrees of approximation.

Table 1. Material constants "read-off" from test data

	σ_0^0 (MPa)	E_p (GPa)	σ_0^{∞} (MPa)	E_r (GPa)	$\sigma_0^{0\prime}$ (MPa)	E_p' (GPa)	E_0 (GPa)
Case A	112.8	17.8	155.0	1.57	—	—	153.8
Case B	112.8	17.8	155.0	1.57	103.0	44.4	153.8
Case C	112.8	17.8	155.0	1.57	92.1	49.0	153.8

Table 2. Material constants "derived" for present analytical modeling

	E_1 (GPa)	α_1	E_2 (GPa)	E_3 (GPa)	α_3	β	σ_y^0 (MPa)
Case A	14.3	314	0.054	—	—	5	112.8
Case B	14.3	314	0.054	23.1	2212	5	103.0
Case C	14.3	314	0.054	27.2	1232	5	92.1

mation for $\rho_1(z)$ as in (36) is used, and the yield-stress (in this case, $\sigma_y^0 = \sigma_0^0$) is the highest among all the cases. In Cases B and C, a three-term approximation for $\rho_1(z)$ as in (40) is used. The yield stress σ_y^0 is now equal to $(\sigma_0^0)'$ in Cases B and C. Note that $(\sigma_0^0)'$ in Case B is chosen to be higher than that in Case C. Material constants (σ_0^0), $(\sigma_0^0)'$, (σ_0^∞), E_t, E_p and E', as inferred from the test data are given in Table 1. Modeling parameters E_1, E_2, E_3, α_1, α_3 and β as calculated from eqns (39a)–(39d) and (43a,b) are given in Table 2. The value $\beta = 5$ is taken from WU & YIP [1981] who base it on their analysis of experimental data for type-304 stainless steel at room temperature.

Figure 2 shows the comparison between the PNC data and the present modeling through eqns (33) or (45). The present results for each of the Cases A, B and C may be seen to agree excellently with experimental data, with the only differences between the three cases being in the knee region, as anticipated.

IV.2.2. *Plasticity: cyclic loading.* A typical cyclic loading, under tension–compression straining, is sketched in Fig. 3. The stress under this cyclic history of loading is calculated by using the *differential* stress–strain relation, (45). Note that now, $d\zeta = \sqrt{\frac{3}{2}}\,|d\epsilon_{11}^p|$, $\zeta = \sqrt{\frac{3}{2}}\int |d\epsilon_{11}^p|$, $dz = d\zeta/f(\zeta)$. Note also that the procedure for the present calculation using (45) or (47) is operationally very similar to that in classical plasticity theory, in that (17) and (18) apply. Referring to Fig. 3, the stress and strain are increased elastically from the "free state" point 0 to the yield point denoted by 1. From point 1 the material is subject to plastic deformation, and until the strain of magnitude $\bar{\epsilon}_{11}$ (see Fig. 3) the yield surface *translates* and *expands*. At point 2, the material is unloaded. During unloading the material behaves elastically, and the stress-state reaches a point on the opposite side of the yield surface. The stress drop, $\Delta\sigma$ in Fig. 3, from point 2 to the elastic limit point 3 is given by $2\sigma_y^0 f_2$ where f_2 is the value of f at point 2. Note that the increments of $\Delta\epsilon_{11}$ between various points in the strain-path, defined, for instance, as $\Delta\epsilon_{11}^{P24} = \int_2^4 \|d\epsilon_{11}^p\|$, are as shown in Fig. 3. We now discuss the *quantitative* features of the hysteresis loops under cyclic loading for *two different types* of functions $f(\zeta)$.

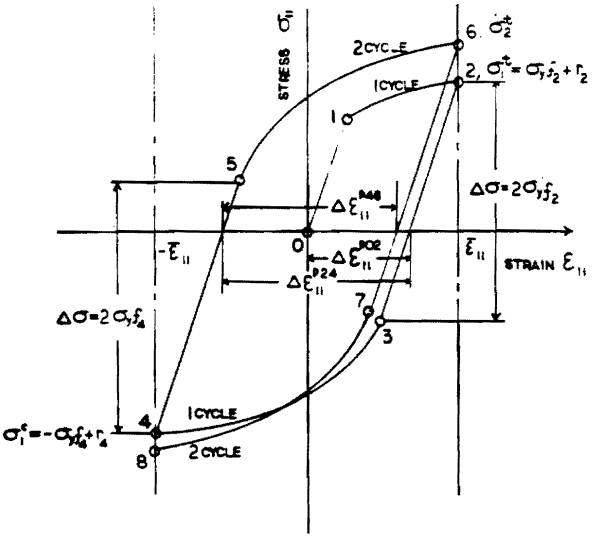

Fig. 3. Schematic of cyclic hardening of elastic-plastic materials.

(i) $f(\zeta) = (1 + \beta\zeta)$, $\zeta = \sqrt{\frac{3}{2}} \int |d\epsilon_{11}^p|$

The analysis of cyclic loading is carried out for material data designated as Case B in Tables 1 and 2, along with the linear function $f(\zeta) = (1 + \beta\zeta)$. Figure 4 shows the calculated results for the σ–ϵ relation for the strain range of $\bar{\epsilon} = \pm 0.5\%$. Peak stresses at the loading–unloading points are denoted by σ_N^t and σ_N^c, where the superscripts t and c imply tension and compression, respectively, while the subsctript N implies the Nth cycle of loading. It is observed from Fig. 4 that these peak stresses increase monotonically with N, and do not reach a stable value as is normally observed in experiments. An examination of Fig. 3 clearly shows that the reason for this monotonic increase of the peak stress is the *linearity* of f with respect to ζ.

(ii) $f(\zeta) = \{a + (1 - a)\exp(-\gamma\zeta)\}$, a and γ constants

Instead of a linear function, the above *saturated* function f will be employed, wherein a and γ are appropriate material parameters. Note that such an f has also been used by Wu & Yip [1981] so as to obtain certain analytical solutions in explicit form. In the

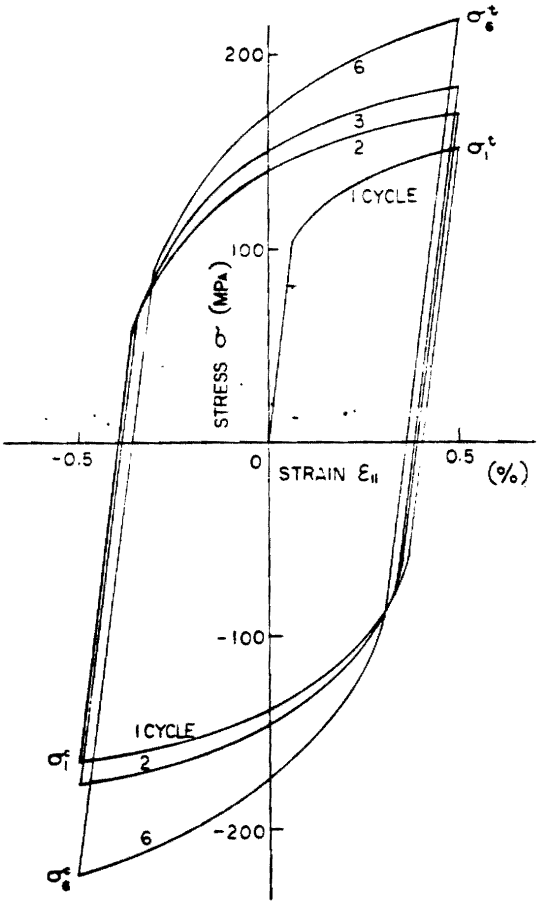

Fig. 4. Analytical modeling of cyclic plasticity using a linear yield function f (Case B).

above, the parameter a represents a *saturated* magnitude of the yield surface. If the initial slope at $\zeta = 0$ is equated for both the linear and saturated functions, the following relation is obtained:

$$(a-1)\nu = \beta \ . \tag{52}$$

Even if a saturated function f is used, we may determine the other material parameter $\rho_1(z)$ as if using a linear f, because a saturated function $f(\zeta)$ can be expected to have an influence only for large values of $\zeta (= \sqrt{\frac{3}{2}} \int |d\epsilon^p_{11}|)$ such as in cyclic loading.

Appropriate experimental data for plasticity for cyclic loading of type-304 stainless steel at elevated temperatures does not appear to be readily available. However, as far as room temperature cyclic loading is concerned, data exists (JSME [1981]) for saturated peak stress σ^l_∞ and initial yield stress σ^0_y for type-304 stainless steel, as

$$\sigma^0_y \simeq 196 \text{ MPa} \ , \quad \sigma^l_\infty = 265 \text{ MPa} \ .$$

Ignoring the kinematic hardening for the time being, one may obtain the following rough *over*estimation, a_0 for a

$$a_0 \simeq \sigma^l_\infty / \sigma^0_y \simeq 1.35 \ .$$

We will henceforth assume that $a = 1.2$. We estimate γ from (52) to be

$$\nu = 5/(0.2) = 25 \ .$$

Of course, if one can easily identify the point of departure from unloading to reloading, such as point 3 in Fig. 3, in the experimental data, one may estimate the values of a and γ more accurately. However, in general, point 3 cannot be so unambiguously identified from experimental data.

Figure 5 shows the presently computed results using the saturated function f. As may be seen, the hysteresis loops saturate after a few cycles of loading. The peak stresses σ^l_N and σ^c_N converge to stable values as shown in Fig. 6. Figure 7 shows the enlargement of the yield surface, i.e. $f(\zeta)$, as a function of $\zeta = \int |d\epsilon^p_{11}|$. The corresponding values at each peak of the tension–compression loading-cycles are also depicted in Fig. 7. The increment between the peak of tension and the peak of compression points can be seen, from Fig. 7, to be almost the same regardless of the number of cycles of loading.

V. CREEP AND PLASTICITY

V.1. *Theoretical development*

In Section III, we employed an intrinsic time measure related, in a differential sense, to the norm of the differential plastic strain, to describe rate-independent plasticity. To characterize the creep and plasticity-creep interaction behavior, we now employ an intrinsic time measure as well as Newtonian time, both of which are nonnegative and irreversible quantities, as was initially suggested by VALANIS [1975]. Specifically, the internal time increment, dz, is expressed as

$$(dz)^2 = \frac{(d\zeta)^2}{f^2(\zeta)} + \frac{(dt)^2}{g^2} \ , \tag{53}$$

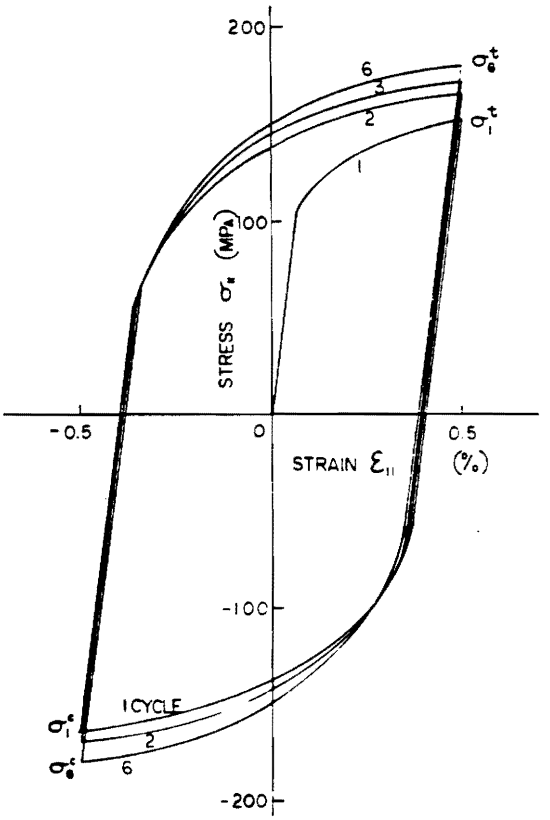

Fig. 5. Analytical modeling of cyclic plasticity using a saturated yield function f (Case B, $a = 1.2$).

where

$$d\zeta^2 = d\boldsymbol{\eta} : d\boldsymbol{\eta} \ , \tag{54a}$$

$$d\boldsymbol{\eta} = \text{inelastic strain differential} \tag{54b}$$

$$\text{(plastic as well as creep, i.e. } d\boldsymbol{\eta} = d\boldsymbol{\eta}^c + d\boldsymbol{\eta}^p\text{)}$$

and

$$g = \text{a scaling function} \ . \tag{54c}$$

As before, assuming elastic isotropy, we have

$$d\boldsymbol{\eta} = \left(d\mathbf{e} - \frac{d\mathbf{s}}{2\mu_0} \right) \ . \tag{55}$$

We will henceforth consider $\alpha = 1$. We assume that the governing equation for creep (and plasticity) is the same as (7), i.e.

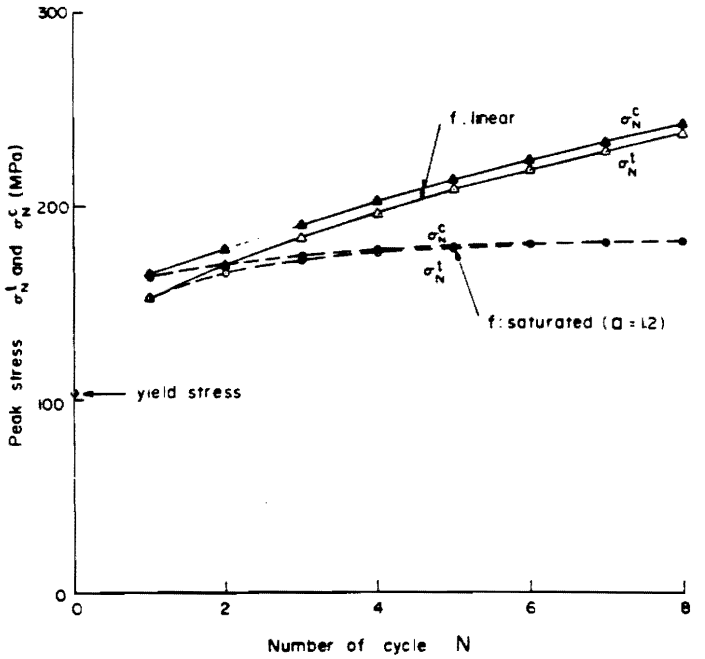

Fig. 6. Convergence of peak stress with the number of cycles (Case B).

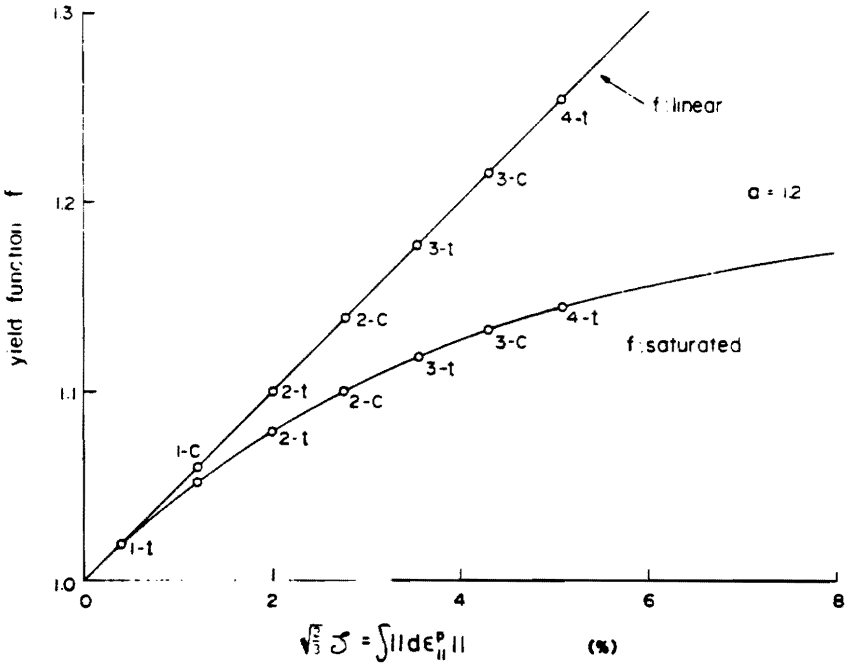

Fig. 7. The function $f(\xi)$.

$$\mathbf{s} = \tau_y^0 \frac{\mathrm{d}\boldsymbol{\eta}}{\mathrm{d}z} + \mathbf{r}(z) \ , \quad \mathbf{r}(z) = \int_0^z \rho_1(z - z') \frac{\mathrm{d}\boldsymbol{\eta}}{\mathrm{d}z'} \, \mathrm{d}z' \ . \tag{56a,b}$$

From (56a) it follows that

$$\frac{\|\mathbf{s} - \mathbf{r}\|^2}{(\tau_y^0)^2} \, \mathrm{d}z^2 = \mathrm{d}\boldsymbol{\eta} : \mathrm{d}\boldsymbol{\eta} = \mathrm{d}\zeta^2 \ , \tag{57}$$

i.e.

$$\frac{\|\mathbf{s} - \mathbf{r}\|^2}{(\tau_y^0)^2 f^2(\zeta)} = \frac{1}{f^2(\zeta)} \frac{(\mathrm{d}\zeta)^2}{(\mathrm{d}z)^2} + \frac{1}{g^2} \frac{(\mathrm{d}t)^2}{(\mathrm{d}z)^2} \ . \tag{58}$$

Using (57) in (53), we have

$$\mathrm{d}z = \frac{1}{\sqrt{1 - \{(\|\mathbf{s} - \mathbf{r}\|)/\tau_y^0 f(\zeta)\}^2}} \left(\frac{\mathrm{d}t}{g}\right) \ . \tag{59}$$

The total inelastic strain-increment, $\mathrm{d}\boldsymbol{\eta}$, is given from (56a) and (59) as

$$\mathrm{d}\boldsymbol{\eta} = \frac{(\mathbf{s} - \mathbf{r})}{\tau_y^0} \frac{1}{\sqrt{1 - \{(\|\mathbf{s} - \mathbf{r}\|)/\tau_y^0 f(\zeta)\}^2}} \left(\frac{\mathrm{d}t}{g}\right) \ . \tag{60}$$

Finally we obtain the differential stress-strain relation in the presence of creep, by using (60) in (55) as

$$\mathrm{d}\mathbf{s} = 2\mu_0 \left\{ \mathrm{d}\mathbf{e} - \frac{(\mathbf{s} - \mathbf{r})}{\tau_y^0} \frac{1}{\sqrt{1 - \{(\|\mathbf{s} - \mathbf{r}\|)/\tau_y^0 f(\zeta)\}^2}} \left(\frac{\mathrm{d}t}{g}\right) \right\} \ . \tag{61}$$

We will postulate, as did BAZANT [1978] and SCHAPERY [1968] in different contexts, that the scaling function g is a function of stress σ and the intrinsic time variable ζ, i.e. $g = g(\sigma, \zeta)$. Specifically, we assume here that

$$g = \frac{f(\zeta)}{B} \left(\frac{\|\mathbf{s} - \mathbf{r}\|}{\tau_y^0 f(\zeta)}\right)^{1-m} \ , \tag{62}$$

where B and m are constants, so that (61) becomes

$$\mathrm{d}\mathbf{s} = 2\mu_0 \left\{ \mathrm{d}\mathbf{e} - B \left(\frac{|\mathbf{s} - \mathbf{r}|}{\tau_y^0 f(\zeta)}\right)^m \frac{(\mathbf{s} - \mathbf{r})}{|\mathbf{s} - \mathbf{r}|} \frac{\mathrm{d}t}{\sqrt{1 - \{(|\mathbf{s} - \mathbf{r}|)/\tau_y^0 f(\zeta)\}^2}} \right\} \ . \tag{63}$$

When the magnitude of stress is small compared to the yield stress, we have

$$\sqrt{1 - \left\{\frac{|\mathbf{s} - \mathbf{r}|}{\tau_y^0 f(\zeta)}\right\}^2} \simeq 1 \ . \tag{64}$$

Then eqn (63) becomes

$$\mathrm{d}\mathbf{s} = 2\mu_0 \left\{ \mathrm{d}\mathbf{e} - B \left(\frac{\|\mathbf{s}-\mathbf{r}\|}{\tau_y^0 f(\zeta)} \right)^m \frac{(\mathbf{s}-\mathbf{r})}{\|\mathbf{s}-\mathbf{r}\|} \, \mathrm{d}t \right\} . \tag{65}$$

V.2. *Determination of material constants and numerical results*

Following the details in Section IV, for uniaxial tension, eqn (63) becomes

$$\mathrm{d}\sigma_{11} = E_0 \left\{ \mathrm{d}\epsilon_{11} - \sqrt{\frac{2}{3}} B \left(\frac{|\sigma_{11} - \frac{3}{2} r_{11}|}{\sigma_y^0 f} \right)^m \frac{\mathrm{d}t}{\sqrt{1 - [(\sigma_{11} - \frac{3}{2} r_{11})/\sigma_y^0 f]^2}} \right\} . \tag{66}$$

Under constant external load, i.e. $\mathrm{d}\sigma_{11} = 0$, the creep strain rate is thus given by

$$\frac{\mathrm{d}\epsilon_{11}}{\mathrm{d}t} = B \sqrt{\frac{2}{3}} \left(\frac{|\sigma_{11} - \frac{3}{2} r_{11}|}{\sigma_y^0 f} \right)^m \frac{1}{\sqrt{1 - [(\sigma_{11} - \frac{3}{2} r_{11})/\sigma_y^0 f]^2}} . \tag{67}$$

For small values of σ_{11} as compared to σ_y^0, (67) may be approximated as

$$\frac{\mathrm{d}\epsilon_{11}}{\mathrm{d}t} \simeq B \sqrt{\frac{2}{3}} \left(\frac{|\sigma_{11} - \frac{3}{2} r_{11}|}{\sigma_y^0 f} \right)^m , \tag{68}$$

which is similar to the well-known Norton's power law for steady-state creep.

We assume that material parameters E_0, E_1, E_2, ρ_0 (or σ_y^0) and β are determined as discussed in Section IV. We now discuss ways of determining material constants B and m. When $\sigma_{11} < \sigma_y^0$, the yield surface retains its initial shape at $t = 0$, which implies that $f = 1$ and $r_{11} = 0$. More specifically, if (67) is evaluated at $t = 0$, we obtain

$$\dot{\epsilon}_{11}^0 = \left. \frac{\mathrm{d}\epsilon_{11}}{\mathrm{d}t} \right|_{t=0} = \sqrt{\frac{2}{3}} B \left(\frac{\sigma_{11}}{\sigma_y^0} \right)^m \frac{1}{\sqrt{1 - (\sigma_{11}/\sigma_y^0)^2}} . \tag{69}$$

Thus we obtain

$$\log \left[\dot{\epsilon}_{11}^0 \sqrt{1 - \left(\frac{\sigma_{11}}{\sigma_y^0} \right)^2} \right] = \log \sqrt{\frac{2}{3}} B + m \log \left(\frac{\sigma_{11}}{\sigma_y^0} \right) . \tag{70}$$

Experimental data for $\dot{\epsilon}_{11}^0 [1 - (\sigma_{11}/\sigma_y^0)^2]^{1/2}$ vs (σ_{11}/σ_y) may be plotted in a logarithmic scale. A straight line may be used to represent the test data in a least-square sense; and from this, B and m may be determined.

We will henceforth refer to the equation of PNC (JSME [1981]) for the elevated temperature (550°C) behavior of type-304 stainless steel, as a basis for comparison of the present creep relation (67) under constant load. As mentioned earlier, the PNC equation (JSME [1981]) is based on BLACKBURN's equation [1972] and is capable of representing test data over a wide range of stress; however, the equations of JSME [1981] and BLACKBURN [1972] do not consider the interaction between creep and plasticity.

We first choose material parameters B and m at 550°C, according to (70). Figure 8 shows the $\dot{\epsilon}_{11}^0$ vs σ_{11} data in logarithmic scale, where the initial rate of creep strain, $\dot{\epsilon}_{11}^0$

is taken according to the PNC equation (JSME [1981]). The results obtained, by a straightline curve fitting, for B and m for the cases A, B and C (with $\sigma_y^0 = 112.8$, 103.0, and 92.1 MPa, respectively, as shown in Table 1) are recorded here in Table 3.

We now present results for creep behavior under constant uniaxial loading. When the prescribed stress is less than the yield stress σ_y^0, the creep analysis is carried out after first raising the stress elastically to the given value. A linear function for f, vis., $f(\zeta) = 1 + \beta\zeta$, is employed, and the increment of internal time, Δz, is assumed to be 0.5×10^{-4}. Figure 9 shows the presently computed results for creep strain for values of σ_{11}, in each of the cases A, B and C, respectively, along with PNC's results (JSME [1981]). A good agreement may be noted between the present and PNC results for $\sigma = 58.8$ MPa. However, for larger magnitudes of σ_{11} and for longer times, the results for case A overestimate and those for C underestimate the creep strain as compared to the PNC equation.

When the prescribed stress level in uniaxial tension is higher than the yield stress, a plasticity analysis is first performed prior to a creep analysis. The steady state as observed in creep experiments may then be regarded as the case when the yield-surface ceases to translate and enlarge.

Figure 10 shows the presently computed creep strain variation with time, along with

Table 3. Material constants B and m derived for present analytical modeling of creep

	B	m
Case A	4.87×10^{-6}	5.2
Case B	2.74×10^{-6}	5.16
Case C	1.23×10^{-6}	4.9

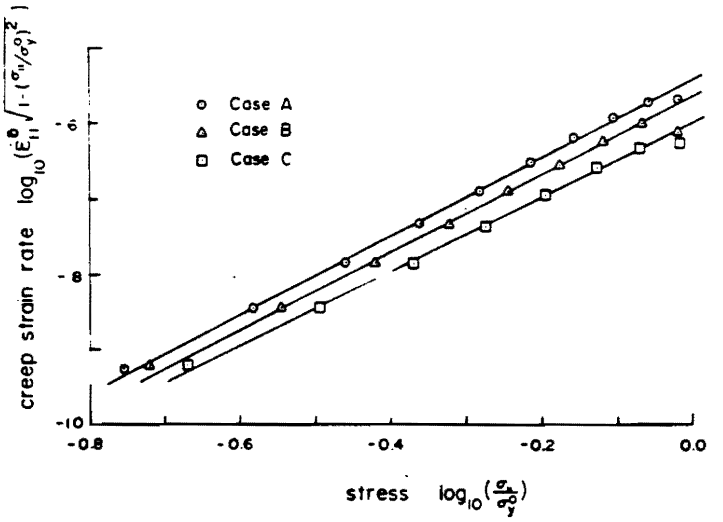

Fig. 8. Determination of material constants B and m.

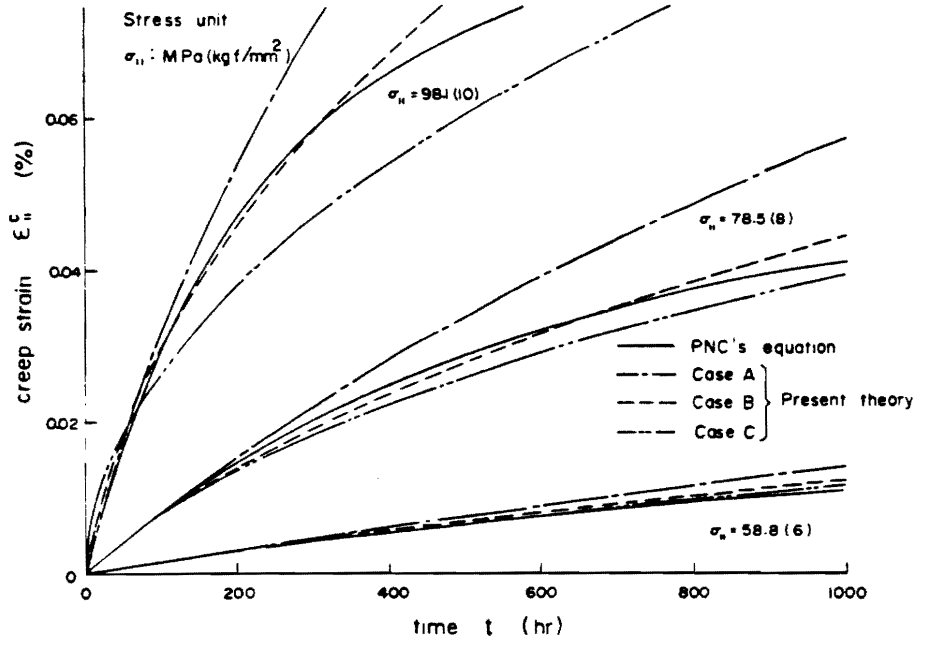

Fig. 9. Prediction of creep strains, for lower magnitudes of stress, using a linear yield function f.

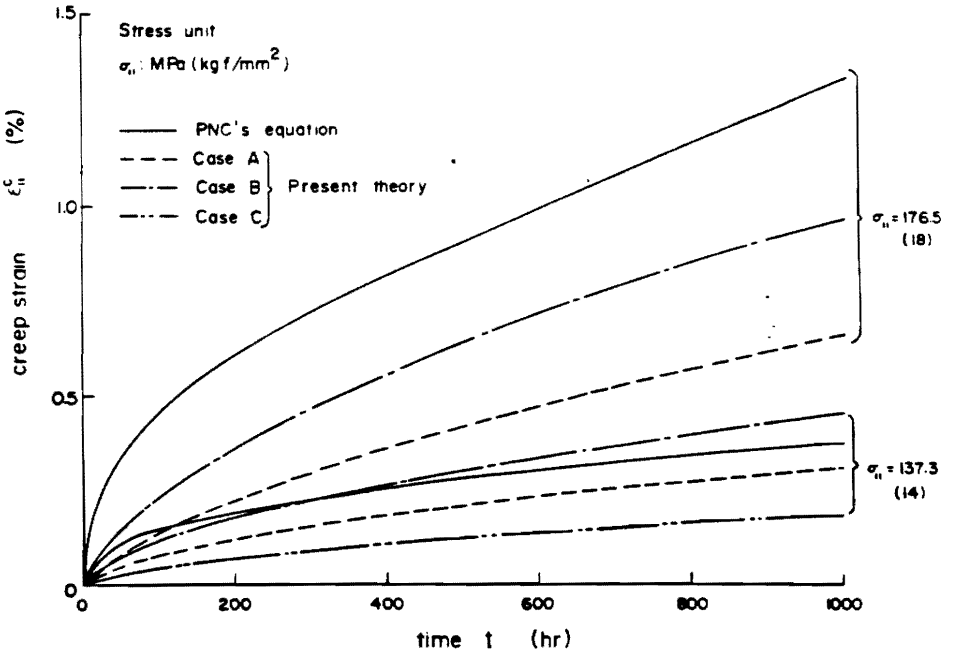

Fig. 10. Prediction of creep strains, for higher magnitudes of stress, using a linear yield function f.

PNC [38] data, for two values of $\sigma_{11} > \sigma_y^0$, for cases A, B and C, respectively. In this set of results, a linear function f is used. The present results are lower than the PNC data, and the discrepancy becomes larger as σ_{11} increases. Next, we consider the effect of using a saturated function f as discussed in subsection IV.1.2.(ii). Figure 11 shows the presently computed results for Case A, when the parameter a in the saturated function f is assigned two different values, $a = 1.2$ and 1.1, respectively. It is observed that the smaller is the value of a, the larger is the creep strain as σ_{11} becomes higher. This is due to the fact that even a small difference between the linear and saturated yield functions f will be magnified due to the power law as in Norton's equation, or eqn (67). It may also be noted that a saturated function f has little or no effect on creep strain for lower values of σ_{11}, since the saturated function f is almost identical to the linear f_1 for small values of ζ.

Figure 12 shows the calculated results for creep strain for Case A, with the value of a being assigned 1.1, for various levels of σ_{11} (from 117.7–176.5 MPa). The experimental results as well as those from the PNC equation (JSME [1981]) are also shown in Fig. 12. Reasonably good agreement is noted between the three sets of data for all stress levels. It is seen that the discrepancies in analytical modeling are somewhat pronounced in the primary stages of creep, while the discrepancies tend to vanish in the steady state. It may be seen that the yield surface in the present theory tends to translate and expand from the initial state to the steady state more rapidly than it should, but the yield surface in the steady state is modeled rather accurately.

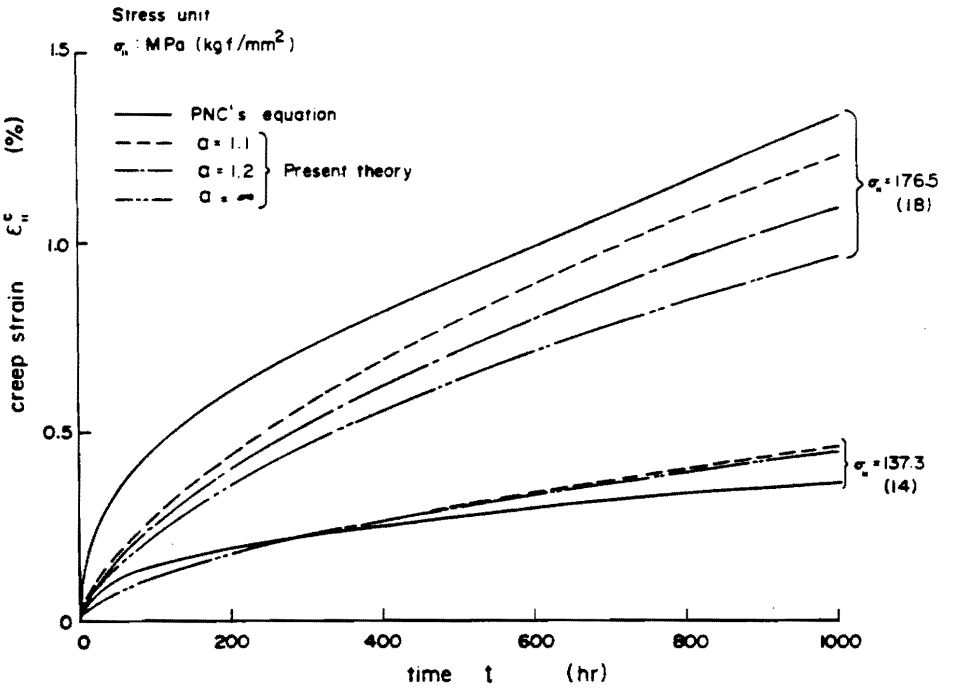

Fig. 11. Effects of using a saturated yield function f, at higher magnitudes of stress.

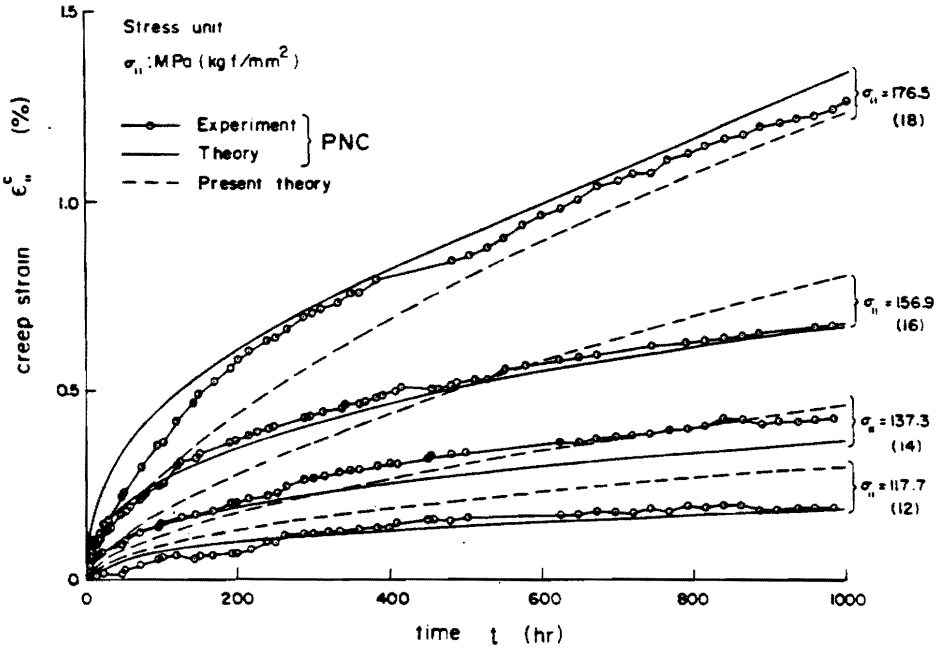

Fig. 12. Comparison of results with PNC's theory and experiment.

VI. CONCLUSIONS

This paper presents a differential stress-strain relation for plasticity, based on an intrinsic-time theory, which is analogous to the classical plasticity relation. Therefore, the present relation may be incorporated readily into existing numerical algorithms. The presently derived equation can approximate the test data for stress-strain curve as accurately as desired.

This paper also presents a simple theory for creep based also on an "internal time" concept, wherein the "internal time" is characterized by both the inelastic strain and Newtonian time. The thus-derived equation employs the concept of a yield surface for plasticity, and makes it possible to incorporate the effects of interaction between creep and plasticity. The presently obtained numerical results may be considered to be reasonable, if the scarcity of available experimental data is kept in mind.

The unified theory presented herein results in constitutive relations that are simple in form; the material constants are few in number and can be easily determined as shown in the paper. It is, therefore, hoped that the present theory may be useful for a practical estimation of inelastic material behavior.

Acknowledgements—This work was supported by the National Aeronautics & Space Administration, Lewis Research Center, under a grant, No. NAG-346 to Georgia Institute of Technology. The authors acknowledge this support as well as the encouragement of Drs. L. Berke and C. Chamis. It is a pleasure to record here our thanks to Ms. J. Webb for her careful assistance in the preparation of this paper.

REFERENCES

1958 BESSELING, J.F., "Theory of Elastic, Plastic, and Creep Deformations of an Initially Isotropic Material Showing Anisotropic Strain-Hardening, Creep Recovery, and Secondary Creep," J. Appl. Mech., **25**, 529.

1968 SCHAPERY, R.A., "On a Thermodynamic Constitutive Theory and Its Application to Various Nonlinear Materials," IUTAM Symp. Thermoinelasticity, East Kilbride (Boley, B.A., ed.), Springer-Verlag, 259.
1969 MROZ, Z., "An Attempt to Describe the Behavior of Metals Under Cyclic Loads Using a More General Workhardening Model," Acta Mech., **7**, 199.
1970 KRATOCHVIL, J. and DILLON, O.W., Jr., "Thermodynamics of Crystalline Elastic-Visco-Plastic Materials," J. Appl. Phys., **41**, 1470.
1970 RICE, J.R., "On the Structure of Stress-Strain Relations for Time-Dependent Plastic Deformation in Metals," J. Appl. Mech., **37**, 728.
1971 LAGNEBORG, R., "A Theoretical Approach to Creep Deformation During Intermittent Load," J. Basic Engng, **93**, 205.
1971a VALANIS, K.C., "A Theory of Viscoplasticity without a Yield Surface, Part I. General Theory," Arch. Mech., **23**, 517.
1971b VALANIS, K.C., "A Theory of Viscoplasticity without a Yield Surface, Part II. Application to Mechanical Behavior of Metals," Arch. Mech., **23**, 535.
1972 BLACKBURN, L.D., "Isochronous Stress-Strain Curves for Austenitic Stainless Steels," The Generation of Isochronous Stress-Strain Curves (Schaefer, A.O., ed.), ASME Winter Annual Meeting, 15.
1972 HILL, R. and RICE, J.R., "Constitutive Analysis of Elastic-Plastic Crystals at Arbitrary Strain," J. Mech. Phys. Solids, **20**, 401.
1972 MALININ, N.N. and KHADJINSKY, G.M., "Theory of Creep with Anisotropic Hardening," Int. J. Mech. Sci., **14**, 235.
1972 PUGH, C.E., CORUM, J.M., LIN, K.C. and GREENSTREET, W.L., "Currently Recommended Constitutive Equations for Inelastic Design Analysis of FFTF Components," ORNL TM-3602.
1974 ASME Boiler and Pressure Vessel Code, Sec. III, Case Interpretations, Code Case N-47-17, ASME.
1974 CORUM, J.M., GREENSTREET, W.L., LIU, K.C., PUGH, C.E. and SWINDEMAN, R.W., "Interim Guidelines for Detailed Inelastic Analysis of High-Temperature Reactor System Components," ORNL-5014.
1975 BODNER, S.R. and PARTOM, Y., "Constitutive Equations for Elastic-Viscoplastic Strain-Hardening Materials," J. Appl. Mech., **42**, 385.
1975 JASKE, C.E., LEIS, B.N. and PUGH, C.E., "Monotonic and Cyclic Stress-Strain Response of Annealed 2 ¼ Cr – 1 Mo Steel," Symposium on Structural Materials for Service at Elevated Temperatures in Nuclear Power Generation (Schaefer, ed.), ASME Winter Annual Meeting, 191.
1975 KRIEG, R.D., "A Practical Two Surface Plasticity Theory," J. Appl. Mech., **42**, 641.
1975 RICE, J.R., "Continuum Mechanics and Thermodynamics of Plasticity in Relation to Microscale Deformation Mechanics," Constitutive Equations in Plasticity (Argon, A.S., ed.), M.I.T. Press, 23.
1975 VALANIS, K.C., "On the Foundations of the Endochronic Theory of Plasticity," Arch. Mech., **27**, 857.
1976 BAZANT, Z.P. and BHAT, P.D., "Endochronic Theory of Inelasticity and Failure of Concrete," J. Engng Mech. Div., Proc. ASCE, **102**, EM4, 701.
1976 DAFALIAS, Y.F. and POPOV, E.P., "Plastic Internal Variables Formalism of Cyclic Plasticity," J. Appl. Mech., **43**, 645.
1976 GITTUS, J.H., "Development of Constitutive Relation for Plastic Deformation from a Dislocation Model," J. Engng Mater. Technol., **98**, 52.
1976 HART, E.W., "Constitutive Relations for the Nonelastic Deformation of Metals," J. Engng Mater. Technol., **98**, 193.
1976 HART, E.W., LI, C.Y., YAMADA, H. and WIRE, G.L., "Phenomenological Theory: A Guide to Constitutive Relations and Fundamental Deformation Properties," Constitutive Equations in Plasticity (Argon, A.S., ed.), M.I.T. Press, 149.
1976a MILLER, A., "An Inelastic Constitutive Model for Monotonic, Cyclic and Creep Deformation: Part I – Equations Development and Analytical Procedures," J. Engng Mater. Technol., **98**, 97.
1976b MILLER, A., "An Inelastic Constitutive Model for Monotonic, Cyclic and Creep Deformation: Part II – Application to Type 304 Stainless Steel," J. Engng Mater. Technol., **98**, 106.
1976 PONTER, A.R.S. and LECKIE, F.A., "Constitutive Relations for the Time Dependent Deformation of Metals," J. Engng Mater. Technol., **98**, 47.
1977 CHABOCHE, J.L., "Viscoplastic Constitutive Equations for the Description of Cyclic and Anisotropic Behavior of Metals," Bull. L'Aca. Polo. Sci., Ser. Sci. Tech., **XXV**, 33.
1978 BAZANT, Z.P., "Endochronic Inelasticity and Incremental Plasticity," Int. J. Solids Struct., **14**, 691.
1978 FINDLEY, W.N. and LAI, J.S., "Creep and Recovery of 2618 Aluminum Alloy Under Combined Stress with a Representation by a Viscous-Viscoelastic Model," J. Appl. Mech., **45**, 507.
1978 KRIEG, R.D., SWEARENGEN, J.C. and ROHDE, R.W., "A Physically-Based Internal Variable Model for Rate-Dependent Plasticity," Inelastic Behavior of Pressure Vessel and Piping Components, ASME PVP-PB-028 (Chang, T.Y. and Kremple, E., eds.), 15.
1978 LEE, D. and ZAVERL, F., Jr., "A Generalized Strain Rate Dependent Constitutive Equation for Anisotropic Metals," Acta Met., **26**, 1771.
1978 ROBINSON, D.N., "A Unified Creep-Plasticity Model for Structural Metals at High Temperatures," ORNL TM-5969.

1979 BODNER, S.R., PARTOM, I. and PARTOM, Y., "Uniaxial Cyclic Loading of Elastic-Viscoplastic Materials," J. Appl. Mech., **46**, 805.
1979 STOUFFER, D.C. and BODNER, S.R., "A Constitutive Model for the Deformation Induced Anisotropic Plastic Flow of Metals," Int. J. Engng Sci., **17**, 757.
1980 CERNOCKY, E.P. and KREMPLE, E., "A Theory of Viscoplasticity Based on Infinitesimal Total Strain," Acta Mech., **36**, 263.
1980 KUJAWSKI, D. and MROZ, Z., "A Viscoplastic Material Model and Its Application to Cyclic Loading," Acta Mech., **36**, 213.
1980 VALANIS, K.C., "Fundamental Consequence of a New Intrinsic Time Measure-Plasticity as a Limit of the Endochronic Theory," Arch. Mech., **32**, 171.
1980 WU, H.C. and YIP, M.C., "Strain Rate and Strain Rate History Effects on the Dynamic Behavior of Metallic Materials," Int. J. Solids Struct., **16**, 515.
1981 Report of Research Cooperation Subcommittee 55 on Design Application Procedure of Inelastic Analysis (II) (Chairman, Yamada, Y.), Japan Society of Mechanical Engineers (in Japanese).
1981 WU, H.C. and YIP, M.C., "Endochronic Description of Cyclic Hardening Behavior for Metallic Materials," J. Engng Mater. Technol., **103**, 212.
1983 VALANIS, K.C. and FAN, J., "Endochronic Analysis of Cyclic Elastoplastic Strain Fields in a Notched Plate," J. Appl. Mech., **50**, 789.
1984 ATLURI, S.N., "On Constitutiive Relations at Finite Strain: Hypo-Elasticity and Elastoplasticity with Isotropic or Kinematic Hardening," Commun. Meth. Appl. Mech. Eng., **43**, 137.
1984b WATANABE, O. and ATLURI, S.N., "A New Endochronic Approach to Computational Elastoplasticity: An Example of a Cyclically Loaded Cracked Plate," J. Appl. Mech., **52**, 857.
1985 ATLURI, S.N., "Notes and Comments on Computational Elasto-Plasticity: Some New Models and Their Numerical Implementation," Int. Conf. on FEICOM, Bombay, India, Dec. 1985.
1986 WATANABE, O. and ATLURI, S.N., "Internal Time, General Internal Variable, and Multi-Yield-Surface Theories of Plasticity and Creep: A Unification of Concept," Int. J. Plastic, **2**, 37.

Center for the Advancement of Computational Mechanics
School of Civil Engineering
Georgia Institute of Technology
Atlanta, Georgia 30332

(*Received* 5 *October* 1984; *in final revised form* 4 *August* 1985)

International Journal of Plasticity, Vol. 1, pp. 63–87, 1985
Printed in the U.S.A.

0749-6419/85 $3.00 + .00

CONSTITUTIVE MODELING AND COMPUTATIONAL IMPLEMENTATION FOR FINITE STRAIN PLASTICITY

KENNETH W. REED* and SATYA N. ATLURI†

*Southwest Research Institute and †Georgia Institute of Technology

(Communicated by George J. Dvorak, Rensselaer Polytechnic Institute)

Abstract—This paper describes a simple alternate approach to the difficult problem of modeling material behavior. Starting from a general representation for a rate-type constitutive equation, it is shown by example how sets of test data may be used to derive restrictions on the scalar functions appearing in the representation. It is not possible to determine these functions from experimental data, but the aforementioned restrictions serve as a guide in their eventual definition. The implications are examined for hypo-elastic, isotropically hardening plastic, and kinematically hardening plastic materials. A simple model for the evolution of the "back-stress," in a kinematic-hardening plasticity theory, that is entirely analogous to a hypoelastic stress-strain relation is postulated and examined in detail in modeling a finitely plastic tension-torsion test. The implementation of rate-type material models in finite element algorithms is also discussed.

I. PRELIMINARIES

We denote the true stress by $\mathbf{s}$, its deviator by $\mathbf{s}'$, and its material derivative by $\dot{\mathbf{s}}$. Invariants p_i of the tensor are defined as

$$p_1 := \mathbf{s}:\mathbf{I} \quad p_2 := (1/2)\mathbf{s}'\mathbf{s}':\mathbf{I} \quad p_3 := (1/3)\mathbf{s}'\mathbf{s}'\mathbf{s}':\mathbf{I}$$

where $(\mathbf{A}:\mathbf{B}) = \mathrm{tr}(\mathbf{A}'\mathbf{B})$ denotes the usual scalar product of two second order tensors, $\mathbf{AB}$ the tensor product, and $\mathbf{A}'$ denotes the transpose of $\mathbf{A}$. We write $\mathbf{e}$ for the stretching, the symmetric part of the velocity gradient, and $\dot{J}$ for its trace. We let $\mathbf{E}$ denote the infinitesimal strain tensor. Finally, by an objective stress rate, of which several exist, we shall mean a stress rate $\mathbf{s}^\bullet$ which transforms between frames by the rule

$$\bar{\mathbf{s}}^\bullet = \mathbf{Q}\mathbf{s}^\bullet\mathbf{Q}'$$

when $\bar{\mathbf{e}} = \mathbf{Q}\mathbf{e}\mathbf{Q}'$ and $\bar{\mathbf{w}} = \mathbf{Q}\mathbf{w}\mathbf{Q}' + \dot{\mathbf{Q}}\mathbf{Q}'$, $\mathbf{w}$ being a general spin tensor and $\mathbf{Q}$ being the rotation between the frames. When $\mathbf{w}$ is chosen as the skew-symmetric part of the velocity gradient, we recover "classical" stress rates; other definitions result in "non-classical" stress rates.

It will occasionally be necessary to emphasize the non-invariant character of certain stress rates. As a convention, we use direct notation for invariant rates and index notation for non-invariant rates.

II. INTRODUCTION

The deficiencies of currently used hypo-elastic and kinematically hardening plastic material laws are briefly discussed below.

Since the time of Cauchy, elasticians have used a material law of the form

$$\mathbf{s} = 2\mu\mathbf{E} + \lambda(\mathbf{I}:\mathbf{E})\mathbf{I} \ . \qquad (1)$$

When used in the analysis of stress in infinitesimally deforming bodies, it predicts shear stresses which vary linearly with the shear strains and no normal stress effects. The stress exhibits no path-dependence.

In recognition of the Principle of Objectivity of material properties, eqn (1) has usually been replaced by the hypo-elastic material law

$$\mathbf{s}^{\circ} = 2\mu\mathbf{e} + \lambda(\mathbf{I}:\mathbf{e})\mathbf{I} \qquad (2)$$

in finite element algorithms when finite deformation analyses were anticipated. It seems to have been presumed that the same sort of idealized material response at finite strain would be predicted by eqn (2) as was predicted by eqn (1) for infinitesimal strains.

DIENES [1979] was the first to demonstrate in the computational mechanics literature the fallacy of this presumption. When $\mathbf{s}^{\circ}$ is identified as the Jaumann stress rate, eqn (2) predicts shear and normal stresses which oscillate as the shear strain increases monotonically (see Fig. 1), a result hardly to be expected by one familiar with eqn (1). His work did serve to emphasize the need for a more rigorous method of arriving at rate-type constitutive equations than then in vogue: A mere replacement of the inobjective material stress rate by an objective rate.

However, Dienes also set a precedent which the present authors regard as unfortunate: he 'blamed' the deficiency of eqn (2) on the Jaumann stress rate and showed that a less objectionable material response could be obtained in the particular problem of rectilinear shearing by introducing a different stress rate. The results obtained by Dienes for the so-called "Green McInnis" rate are shown in Fig. 2.

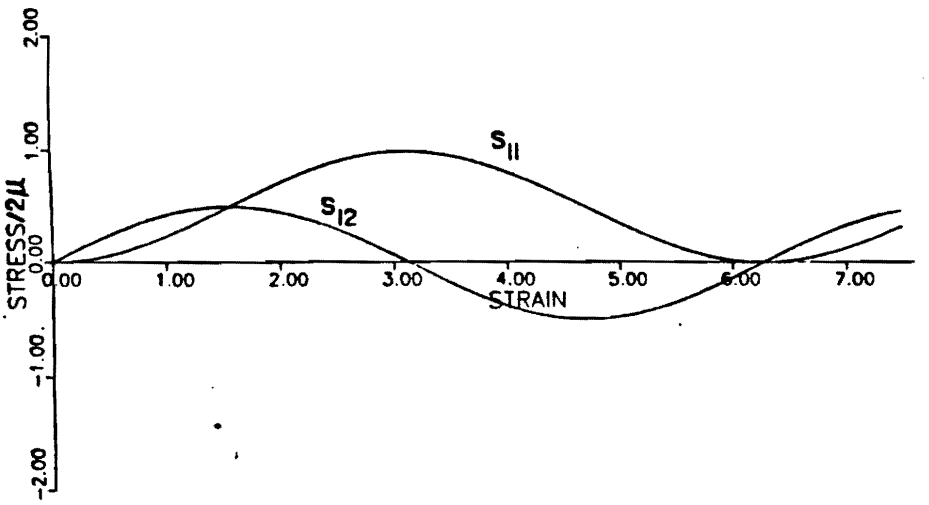

Fig. 1. Rectilinear shearing of the material $(\dot{\boldsymbol{\sigma}}^{\circ}/2\mu) = \boldsymbol{\epsilon} + \left(\frac{\lambda}{2\mu}\right)(\mathbf{I}:\boldsymbol{\epsilon})\mathbf{I}$. $\dot{\boldsymbol{\sigma}}^{\circ}$ = Jaumann Corotational Rate.

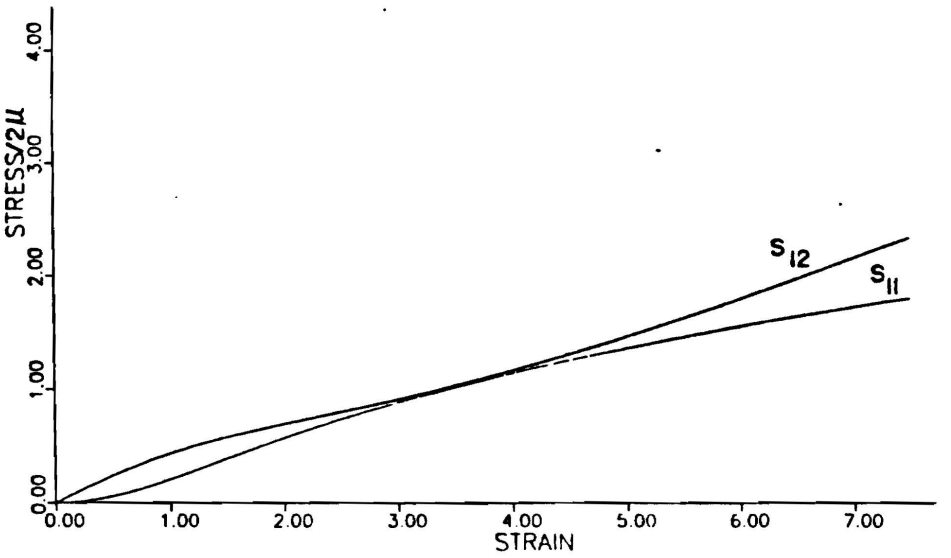

Fig. 2. Rectilinear shearing of the material $(\mathring{\boldsymbol{\sigma}}^{*}/2\mu) = \boldsymbol{\epsilon} + \left(\frac{\lambda}{2\mu}\right)(\mathbf{I}:\boldsymbol{\epsilon})\mathbf{I}$. $\mathring{\boldsymbol{\sigma}}^{*}$ = Green-McInnis Rate.

Two years later, NAGTEGAAL & DE JONG [1981] found that MELAN's [1938] kinematic hardening rule

$$\dot{a}_{ij} = 2h\dot{E}^{p}_{ij}\,, \tag{3}$$

which predicts linear back-stress-strain variation and no path dependence, again led to periodic shear and normal stresses when it is generalized, for finite deformations, to a hypo-elastic-type rule

$$\mathbf{a}^{*} = 2h\mathbf{e}^{p} \tag{4}$$

and $\mathbf{a}^{*}$ is taken to be the Jaumann rate of the back stress. This result is shown in Fig. 3 (We note that the same result had been discussed nearly ten years earlier by LEHMANN [1972]). The non-physical material response was at first attributed to the hardening rule, but eventually "blamed" on the Jaumann stress rate (c.f. LEE *et al.* [1983]). To date, no fewer than four non-classical stress rates have been suggested for use in place of $\mathbf{a}^{*}$ in Melan's equation (LEE *et al.* [1981], LEE *et al.* [1983]), JOHNSON & BAMMANN [1982], DAFALIAS [1983], and NAGTEGAAL [1983]. The shear and normal stresses arising when the Green-McInnis rate and the rate of LEE *et al.* [1983] are used in eqn (4) are shown in Figs. 4 and 5.

We do not believe the present search for an "ideal" stress rate for these problems to be well founded. Our dissatisfaction with the models based on the new stress rates stems from the fact that they cannot be brought into agreement with any realistic idealization of material behavior, much less with experimental data. None guarantees stable material behavior in rectilinear shearing. Normal stresses and normal strains predicted

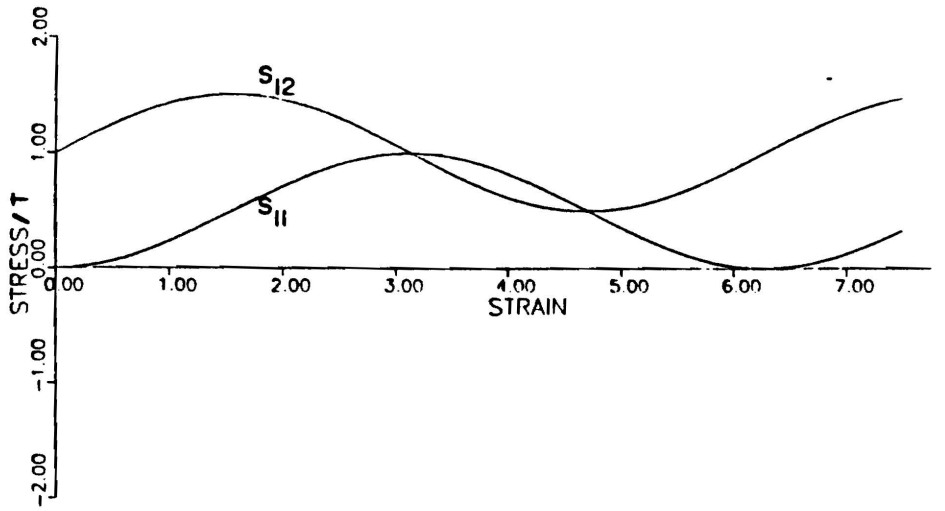

Fig. 3. Rectilinear shearing of the kinematically hardening plastic material (eqn 4).

$\frac{S_{12}}{T} = \frac{a_{12}}{T} + 1$; $\frac{S_{11}}{T} = \frac{a_{11}}{T}$; $\mathbf{a}^\circ = 2h\epsilon^p$; $\mathbf{a}^\circ$ = Jaumann Rate ; $2h = 1$.

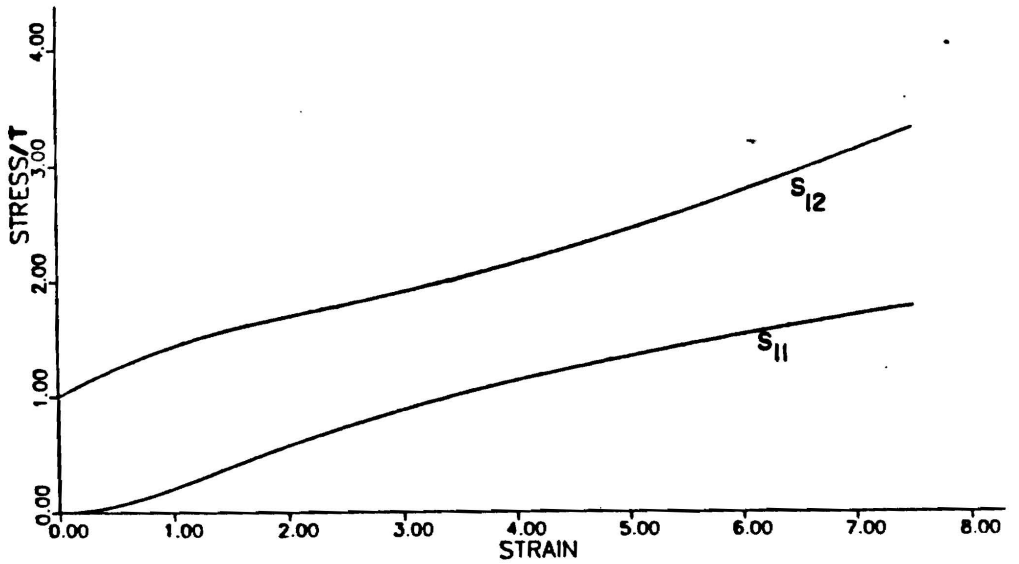

Fig. 4. Rectilinear shearing of the kinematically hardening plastic material (eqn 4).

$\frac{S_{12}}{T} = \frac{a_{12}}{T} + 1$; $\frac{S_{11}}{T} = \frac{a_{11}}{T}$; $\mathbf{a}^\circ = 2h\epsilon^p$; $\mathbf{a}^\circ$ = Green-McInnis Rate ; $2h = 1$.

by the models are generally one or two orders of magnitude larger than have been reported in the experimental literature (c.f. SWIFT [1947], FREUDENTHAL & RONAY [1966], ROSE & STUEWE [1968], BILLINGTON [1977], BELL & KHAN [1980]). In Fig. 6, normal strains obtained by using several alternative definitions for $\mathbf{a}^\circ$ in eqn (4) are plotted against the average shear strain in the thin-walled tube torsion test.

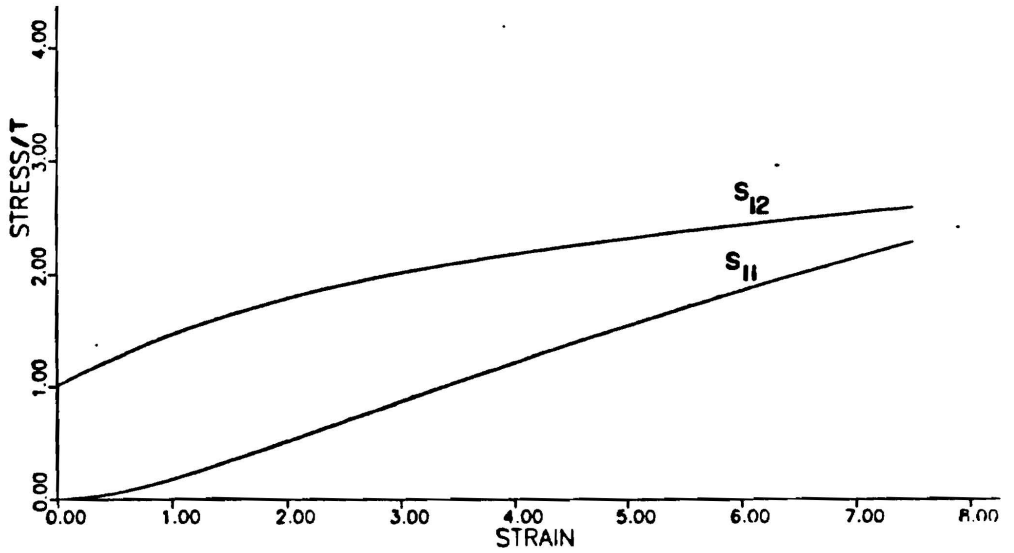

Fig. 5. Rectilinear shearing of the kinematically hardening plastic material (eqn 4).

$\frac{S_{12}}{T} = \frac{a_{12}}{T} + 1$; $\frac{S_{11}}{T} = \frac{a_{11}}{T}$; $\mathbf{a}^\circ = 2h\epsilon^p$; $\mathbf{a}^\circ$ = Lee's Rate ; $2h = 1$.

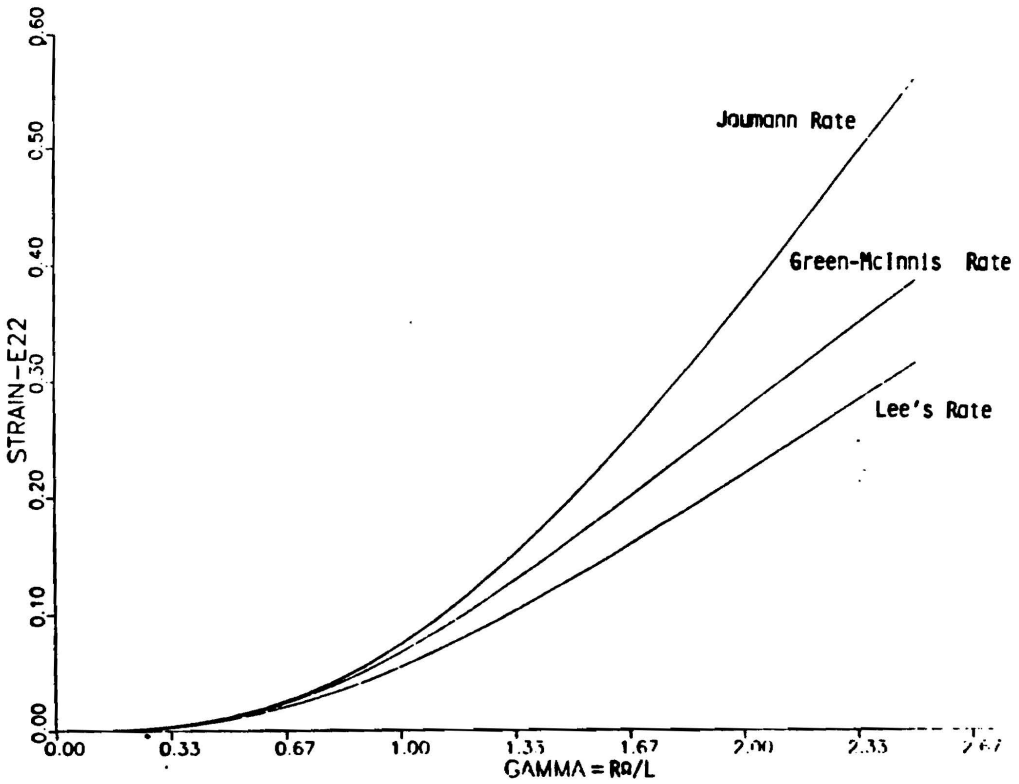

Fig. 6. Normal strains in thin-walled tube torsion test; kinematically hardening plastic material (eqn 4) $(\mathbf{a}^\circ/2h) = \epsilon^p$; $T/2h = 207\text{MPa}/(\sqrt{3}\,310\text{ MPa})$ (cf. LEE *et al.* [1981]).

The goal of this paper is to discuss the relation of certain experimental results to the theory of finitely deforming kinematically hardening plastic material.

In the present treatment of kinematic-hardening plasticity, we consider the objective rate of the back stress, i.e. $\mathbf{a}^*$, to be a general tensor function of the plastic stretching $\mathbf{e}^p$ as well as the current back stress, $\mathbf{a}$. Thus, the present relation represents a generalization of those used by NAGTEGAAL & DE JONG [1981], LEE *et al.* [1981,1983] and ATLURI [1983] in which $\mathbf{a}^*$ is simply related linearly to $\mathbf{e}^p$. The first two authors invoke the rather artificial constraint that the back stress $\mathbf{a}$ must be purely deviatoric and claim, inadvertently, that this requirement necessitates the exclusion of non-corotational type stress rates from use in eqn (4). On the other hand, ATLURI [1983] has shown, in essence, that if $\mathbf{a}^*$ in eqn (4) is taken to be a convective stress-rate of Truesdell or Cotter-Rivlin, then non-oscillatory shear-stresses may be obtained without recourse to the problematical non-classical stress rates (see Fig. 7). This result of Atluri, and the well-known classical solutions (as summarized, for instance in ATLURI [1983]) for the hypo-elastic stress-strain law:

$$\mathbf{s}^* = L(\mathbf{e},\mathbf{s}) - \text{linear w.r.t. } \mathbf{e} \ , \tag{5}$$

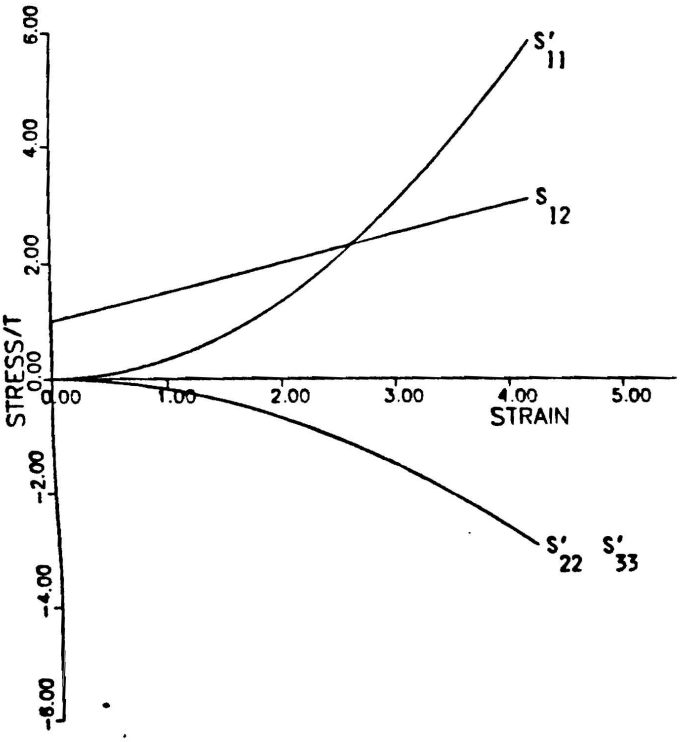

Fig. 7(a). Rectinlinear shearing of the kinematically hardening plastic material (eqn 4).
$\frac{S_{12}}{T} = \frac{a_{12}}{T} + 1$; $\frac{S'_{ii}}{T}\frac{a'_{ii}}{T}$ (no sum) ; $\mathbf{a}^* = 2h\mathbf{e}^p$; $\mathbf{a}^* =$ Truesdell Rate ; $2h = 1$.

suggest that if eqn (4) were to be replaced by:

$$\mathbf{a}^{\circ} = G(\mathbf{e}^{p}, \mathbf{a}) - \text{linear w.r.t. } \mathbf{e}^{p} , \tag{6}$$

then, non-oscillatory results for a can be obtained for any objective stress rate $\mathbf{a}^{\circ}$ by properly adjusting the terms in the function G on the right-hand side. Moreover, the constants in function G may be chosen so as to model the test data, as demonstrated later in this paper. Note that the back-stress $\mathbf{a}$ as determined from the evolution eqn (6) is not necessarily deviatoric; only the deviatoric component of $\mathbf{a}$ may be used in modeling the classical pressure-insensitive metal plasticity. We observe that eqn (6) belongs to the general class of internal-variable-type evolution equations suggested by ONAT & FARDSHISHEH [1973].

From the one-to-one correspondence of the present kinematic hardening plasticity model and the classical hypo-elasticity stems an immediate advantage: from solutions of eqn (5) can be found solutions of eqn (6) by a mere change of variables.

Our plan is to discuss in the next section the relation of experiment to hypo-elastic models for a particular class of loadings. Some specific restrictions on material functions are found. Guided by these restrictions, a new "ideal" hypo-elastic material model is constructed. We then propose a new ideal kinematically hardening plastic material as an analogue to the new ideal hypo-elastic material. The behaviors of the new models are discussed, as well as the problem of modeling non-ideal material behavior.

The paper is concluded with some brief notes on "objective" numerical integration schemes which may be applied to rate-type constitutive equations.

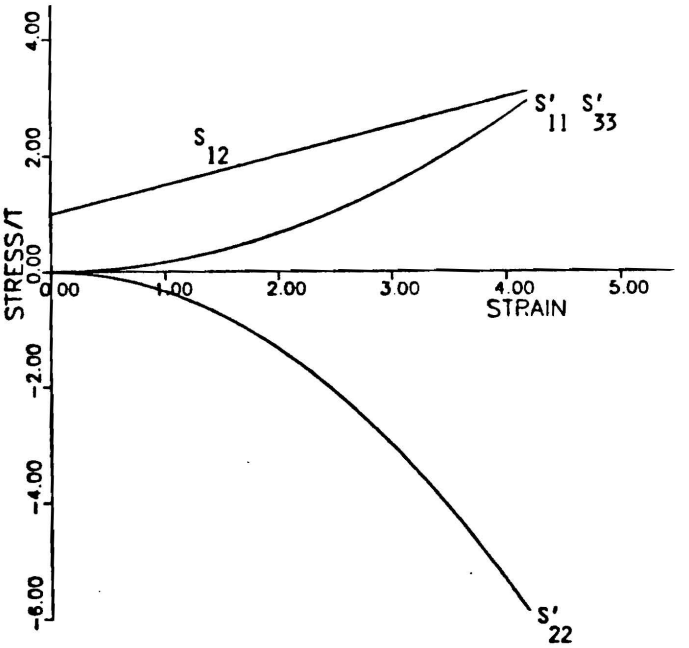

Fig. 7(b). Same as Fig 7(a) except that $\mathbf{a}^{\circ}$ = Cotter-Rivlin Rate.

III. MODELING THE RESPONSE OF THIN-WALLED HYPO-ELASTIC TUBES IN A TENSION-TORSION-INTERNAL PRESSURE TEST

We consider the response of a thin-walled hypo-elastic tube to a certain class of loadings. By hypo-elastic we mean materials whose mechanical response is adequately represented by a constitutive equation of the form

$$\mathbf{s}^* = L(\mathbf{e},\mathbf{s}) - \text{linear w.r.t. } \mathbf{e} \ , \tag{7}$$

where $\mathbf{s}^*$ is corotational: $\mathbf{s}^* = \dot{\mathbf{s}} - \mathbf{w}\mathbf{s} + \mathbf{s}\mathbf{w}$. Since the difference between various acceptable stress rates (e.g. Truesdell, Cotter-Rivlin rates) and corotational rates may be "absorbed" by the right hand side of eqn (7), we have lost no generality by restricting $\mathbf{s}^*$ in eqn (7) to be corotational. We shall also assume that L is invertible:

$$\mathbf{e} = L^{-1}(\mathbf{s}^*,\mathbf{s}) \ . \tag{8}$$

It follows as a special case of WANG's [1970] representation theorem that eqn (8) may be set down as

$$\begin{aligned}\mathbf{e} = {} & [\Lambda^{11}\dot{p}_1 + \Lambda^{12}\dot{p}_2 + \Lambda^{13}(\dot{p}_3 + 2/3\dot{p}_1\dot{p}_2)]\mathbf{I} \\ & + [\Lambda^{21}\dot{p}_1 + \Lambda^{22}\dot{p}_2 + \Lambda^{23}(\dot{p}_3 + 2/3\dot{p}_1\dot{p}_2)]\mathbf{s}' \\ & + [\Lambda^{31}\dot{p}_1 + \Lambda^{32}\dot{p}_2 + \Lambda^{33}(\dot{p}_3 + 2/3\dot{p}_1\dot{p}_2)]\mathbf{s}'\mathbf{s}' \\ & + 2M^1\mathbf{s}^* + M^2(\mathbf{s}'\mathbf{s}^* + \mathbf{s}^*\mathbf{s}') + M^3(\mathbf{s}'\mathbf{s}'\mathbf{s}^* + \mathbf{s}^*\mathbf{s}'\mathbf{s}') \ .\end{aligned} \tag{9}$$

The scalars Λ^{IJ} and M^I generally depend on p_1, p_2, and p_3. The states of stress achieved in the tension-torsion-internal pressure test, when the tube's wall is sufficiently thin, are of the form:

$$\mathbf{s} = \begin{bmatrix} s_{\phi\phi} & s_{\phi z} & 0 \\ s_{\phi z} & s_{zz} & 0 \\ 0 & 0 & 0 \end{bmatrix}. \tag{10}$$

We require that the tension and internal pressure be adjusted so that $s_{\phi\phi} = -s_{zz}$ throughout a test. As a consequence, $\mathbf{s}$ may be written as:

$$\mathbf{s} = \mathbf{s}' = \bar{s}\begin{bmatrix} \cos 2\theta & \sin 2\theta & 0 \\ \sin 2\theta & -\cos 2\theta & 0 \\ 0 & 0 & 0 \end{bmatrix} \tag{11}$$

so that $p_1 = 0$, $p_2 = \bar{s}^2$, and $p_3 = 0$. Likewise, we write $\mathbf{s}^*$ as:

$$\mathbf{s}^* = \begin{bmatrix} \dot{\bar{s}}\cos 2\theta + 2\bar{s}(w - \dot{\theta})\sin 2\theta & \dot{\bar{s}}\sin 2\theta - 2\bar{s}(w - \dot{\theta})\cos 2\theta & 0 \\ \dot{\bar{s}}\sin 2\theta - 2\bar{s}(w - \dot{\theta})\cos 2\theta & -\dot{\bar{s}}\cos 2\theta - 2\bar{s}(w - \dot{\theta})\sin 2\theta & 0 \\ 0 & 0 & 0 \end{bmatrix} . \tag{12}$$

The angle between the tube axis and principal axes of stress in the plane of the tube wall are given by θ and $\theta + \pi/2$. Since only the second stress invariant $p_2 = \bar{s}^2$ is non-zero the Λ^{IJ} and M^I depend only upon p_2 for any load producing a stress system of type eqn (11).

Substitution of eqns (11) and (12) into (9) gives, after straightforward algebra,

$$e_{rr} = 2\bar{s}\dot{\bar{s}}\Lambda^{12} \tag{13}$$

$$j = 2\bar{s}\dot{\bar{s}}(3\Lambda^{12} + 2M^2 + 2\bar{s}^2\Lambda^{32}) \tag{14}$$

$$\begin{bmatrix} \cos 2\theta & \sin 2\theta \\ -\sin 2\theta & \cos 2\theta \end{bmatrix} \begin{bmatrix} (e_{\phi\phi} - e_{zz})/2\dot{\bar{s}} \\ e_{\phi z}/\dot{\bar{s}} \end{bmatrix} = \begin{bmatrix} 1 & 1 \\ -2\bar{s}(w - \dot{\theta})/\dot{\bar{s}} & 0 \end{bmatrix} \begin{Bmatrix} 2M^1 + 2\bar{s}^2 M^3 \\ 2\bar{s}^2\Lambda^{22} \end{Bmatrix} . \tag{15, 16}$$

In these equations, the stress is to be regarded as given, the stretching components as observable, and w as defined (e.g. for the Jaumann rate $w := -e_{\phi z}$). The Λ^{IJ} and M^I depend only upon p_2 since p_1 and p_3 vanish for the loadings considered.

The analysis may be continued by considering $\bar{s} \neq 0$. Then eqns (13) through (16) predict

$$\Lambda^{12} = e_{rr}/\dot{p}_2 \ , \tag{17}$$

which determines Λ^{12} for p_1, $p_3 = 0$, and

$$2M^2 + 2p_2\Lambda^{32} = (e_{zz} - e_{rr})/\dot{p}_2 + (e_{\phi\phi} - e_{rr})/\dot{p}_2 \ , \tag{18}$$

which restricts M^2 and Λ^{32}. When $w = \dot{\theta}$ (at an instant or continuously), eqns (9), (11), and (12) predict also

$$2M^1 + 2p_2M^3 + 2p_2\Lambda^{22} = (e_{\phi\phi} - e_{zz})\cos 2\theta/2\dot{\bar{s}} + (e_{\phi z}/\dot{\bar{s}})\sin 2\theta \tag{19}$$

$$2e_{\phi z}/(e_{\phi\phi} - e_{zz}) = \tan 2\theta = 2s_{\phi z}/(s_{\phi\phi} - s_{zz}) \ . \tag{20}$$

In the first three equations above, the right hand sides are known as either functions of the stress, which was controlled in the test, or the deformation which was observed. Thus, Λ^{12} is determined on the line $p_1 = p_3 = 0$, and Λ^{22}, Λ^{32}, and the M^I are quantitatively restricted. The fourth equation expresses the precise coaxiality of $\mathbf{e}$ with $\mathbf{s}$ necessary when $w = \dot{\theta}$ (see Appendix B). This condition is fulfilled continuously in a proportional loading with $\theta = 0$:

$$s_{\phi\phi} = -s_{zz} \ , \quad s_{\phi z} = 0 \ .$$

Otherwise (when $w \neq \dot{\theta}$) eqns (13) through (16) predict (17), (18), and

$$\begin{Bmatrix} 2M^1 + 2p_2M^3 \\ 2p_2\Lambda^{22} \end{Bmatrix}$$

$$= \begin{bmatrix} \cdot \\ \dot{\bar{s}}/(2\bar{s}(w - \dot{\theta})) \end{bmatrix} \begin{bmatrix} \sin 2\theta & -\cos 2\theta \\ -\sin 2\theta & \cos 2\theta \end{bmatrix} + \begin{bmatrix} 0 & 0 \\ \cos 2\theta & \sin 2\theta \end{bmatrix} \begin{Bmatrix} (e_{\phi\phi} - e_{zz})/2\dot{\bar{s}} \\ (e_{\phi z}/\dot{\bar{s}}) \end{Bmatrix} . \tag{21, 22}$$

Entries on the right-hand side of these equations are known, either because they were prescribed (the stress), observed (the deformation), or defined (the spin). Thus, Λ^{22} may be determined along the line p_1, $p_3 = 0$ and M^1 and M^3 are quantitatively restricted.

Since in eqns (17), (18), (19), (21), and (22) the left-hand sides depend only upon the invariant p_2, it follows that the right-hand sides of those equations must also depend only upon p_2 for loads of the type, (11). This comprises a very severe test to be passed by any genuinely hypo-elastic material.

In general, a series of tests producing stress-systems of the type (11) may be conducted. There result from eqns (17) through (22) restrictions for each test. The material functions may then be defined so as to minimize some invariant measure of the modeling error. Note that loadings need not be proportional.

IV. EXAMPLE: PURE TORSION

If we are willing to take it for granted that a particular material is hypo-elastic then Λ^{12} and Λ^{22} can be found from the results of a single test. As an illustration, we consider the response to pure torsion, $\theta = \pi/4$, $\dot{\theta} = 0$. We shall assume volume and wall-thickness changes to be ignorable in this test, so Λ^{12}, M^2, and Λ^{32} may all be set to zero (under these assumptions the above mentioned material functions can play no role in the description of the material behavior for this loading). Furthermore, we shall use the ordinary Jaumann stress rate, so $w := -e_{\phi z}$. Equations (21) and (22) then give

$$\begin{Bmatrix} 2M^1 + 2p_2M^3 \\ 2p_2\Lambda^{22} \end{Bmatrix} = \begin{bmatrix} (e_{zz} - e_{\phi\phi})/4\bar{s}e_{\phi z} \\ (e_{\phi z}/\bar{s}) - (e_{zz} - e_{\phi\phi})/4\bar{s}e_{\phi z} \end{bmatrix} \quad (23)$$

$$(24)$$

At this juncture, we pause to make the following fascinating observation: in eqns (23) and (24), which are fully general for the loading considered, the observed shear behavior, $(e_{\phi z}/\dot{\bar{s}})$, is associated with the material function Λ^{22}, not with $2M^1$, which is usually called the shear compliance. Only when $p_2 = 0$ is the statement $2M^1 = (e_{\phi z}/\dot{\bar{s}})$ valid. Generally $2M^1$ is associated with the phenomenon studied by POYNTING [1909] and SWIFT [1947].

Consistent with our earlier assumption that e_{rr} and $\dot{J}$ both vanish, we put $e_{\phi\phi} = -e_{zz}$ in eqns (23) and (24). Defining the "tangent shear modulus" $2\mu_t := (\dot{\bar{s}}/e_{\phi z})$ and writing ϵ for $\ln(1/L)$, we get

$$2M^1 + 2p_2M^3 = 2\mu_t(d\epsilon/dp_2) \quad (25)$$

$$\Lambda^{22} = [(1/2\mu_t) - 2\mu_t(d\epsilon/dp_2)]/2p_2 \quad (26)$$

A value for Λ^{22} in the limit $p_2 \to 0$ (if one exists) can be found by application of l'Hôpital's rule. Thus, we have shown that the material's behavior for this loading depends upon only two observable functions of p_2, namely $2\mu_t(p_2)$ and $\epsilon(p_2)$.

In order to continue the example further, we shall assume forms for $2\mu_t$ and ϵ. It should be emphasized that we are not claiming that these functional forms have special physically significant attributes; they are merely the simplest forms which do not lead us to a trivial result, and were chosen for that reason only. We assume for $2\mu_t$ and ϵ:

$$2\mu_t = 2\mu_0 \text{ (a constant with the dimensions of stress)} , \tag{27}$$

$$\epsilon = \ln[1 + 2cp_2/(2\mu_0)^2]^{1/2c} \text{ (c is a dimensionless constant)} . \tag{28}$$

According to eqn (27), the shear stress rate should be linearly related to the shear strain rate for this loading, as in Cauchy elasticity. It is apparent from eqn (28) that the normal strain can be made arbitrarily small at any given value of p_2 simply by choosing a large enough positive value for c. This is an important point, for the parameter c gives us direct control over the magnitude of the normal strains in the torsion test, and, as shall be seen, indirect control over the magnitude of the normal stresses in rectilinear shearing. This is not a feature offered by any other model known to the authors. We can show that for $p_2/(2\mu_0)^2 \ll 1$ eqn (28) reduces to POYNTING's [1909] result.

Putting eqns (27) and (28) into (25) and (26) gives

$$2M^1 + 2p_2M^3 = (1/2\mu_0)[1 + 2cp_2/(2\mu_0)^2]^{-1} \tag{29}$$

$$A^{22} = c(1/2\mu_0)^3[1 + 2cp_2/(2\mu_0)^2]^{-1} , \tag{30}$$

or, choosing $M^3 = 0$ and recalling eqn (9), we get

$$\begin{aligned}\mathbf{e} = {} & [1 + 2cp_2/(2\mu_0)^2]^{-1}[\underline{\mathbf{I}} + c(\mathbf{s}'/2\mu_0) \otimes (\mathbf{s}'/2\mu_0)]:(\mathbf{s}^*/2\mu_0) \\ & + [\text{terms associated with } A^{I1} \text{ and } A^{I3} , \quad I = 1,2,3] .\end{aligned} \tag{31}$$

The constitutive eqn (31) predicts (27) and (28) exactly. Had we chosen different forms for $2\mu_t$ and ϵ [instead of those given in eqns (27) and (28)], they too would have been predicted exactly by the constitutive equation resulting from application of eqns (25), (26), and (9). The material functions A^{IJ} not restricted by this single test may be used to fit predictions of eqn (9) to data from other sorts of tests. If, for example, the bulk behavior of the material is known to follow a law of the form

$$\dot{J} = (1/3k)\dot{p}_1 , \tag{32}$$

in which k may depend upon p_1, then, by choosing A^{11} as

$$A^{11} = (1/3)\{(1/3k) - (1/2\mu_0)[1 + 2cp_2/(2\mu_0)^2]^{-1}\} \tag{33}$$

and setting the other undetermined terms to zero, eqn (31) becomes

$$\begin{aligned}\mathbf{e} = {} & [1 + 2cp_2/(2\mu_0)^2]^{-1}[\underline{\mathbf{I}} - (1/3)\mathbf{I} \otimes \mathbf{I} + c(\mathbf{s}'/2\mu_0) \otimes (\mathbf{s}'/2\mu_0)]:(\mathbf{s}^*/2\mu_0) \\ & + (2\mu_0/9k)(\mathbf{I} \otimes \mathbf{I}):(\mathbf{s}^*/2\mu_0) .\end{aligned} \tag{34}$$

Equation (34) satisfies each of (27), (28), and (32) exactly.

In Figs. 8, 9, and 10 typical stress-strain curves produced by the model 34 in pure torsion, rectilinear shearing, and uniaxial extension, respectively, are shown. In Fig. 8, the shear stress is plotted against the so-called "average" shear strain $\gamma = R\Omega/L$ which is usually used in experiment (c.f. BELL & KHAN [1980]). As $\dot{\gamma} \geq 2e_{\phi z}$ for a tube which extends during torsion, there is a slight negative curvature apparent in the $s_{\phi z}$-γ curve. As the parameter c increases, the extension of the tube for any given γ is reduced, and

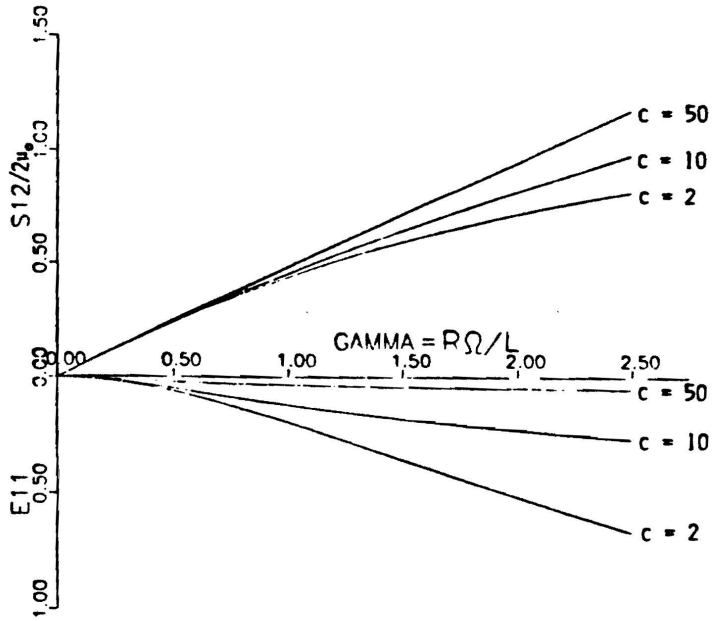

Fig. 8. Thin-walled tube torsion of hypo-elastic material (35). Shear stresses and normal strains w.r.t. variations of the parameter c.

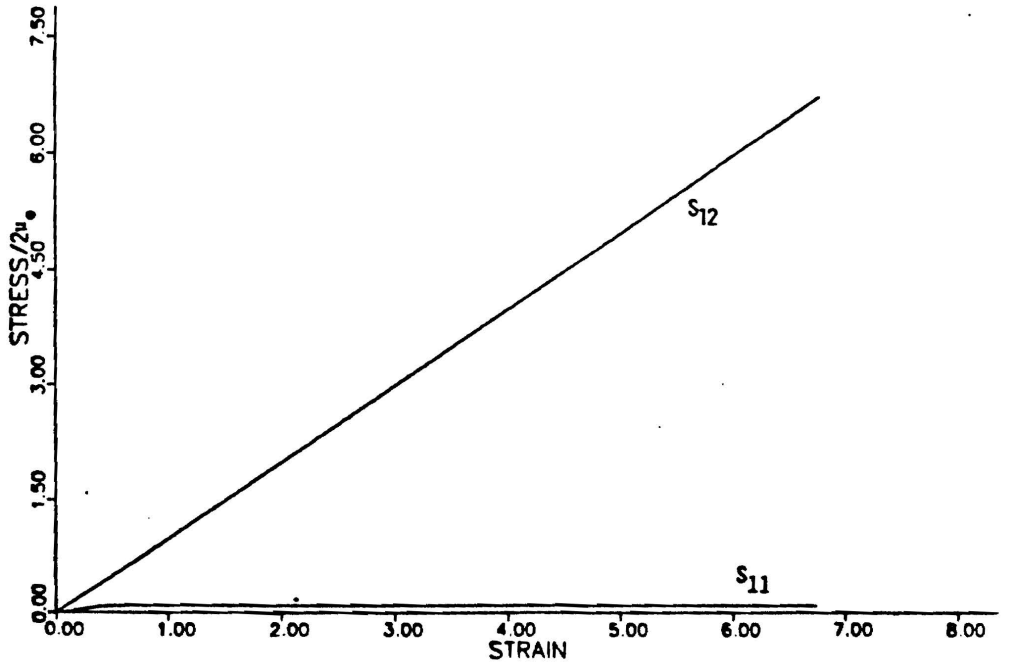

Fig. 9(a). Rectilinear shearing of the hypo-elastic material (35) with $c = 10$.

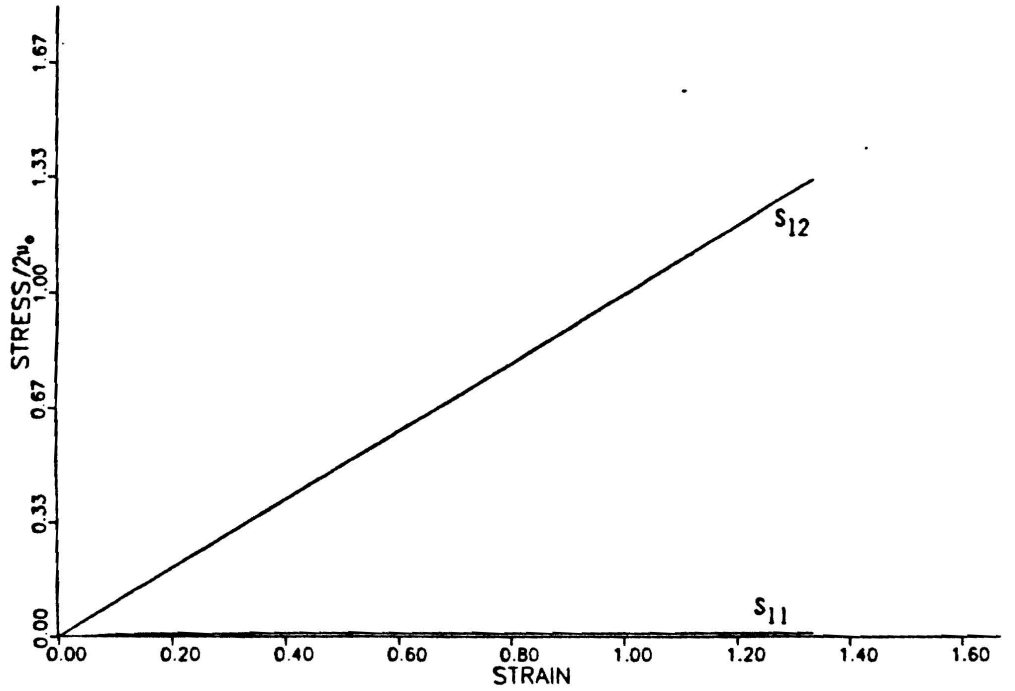

Fig. 9(b). Same as Fig 9(a) except that $c = 100$.

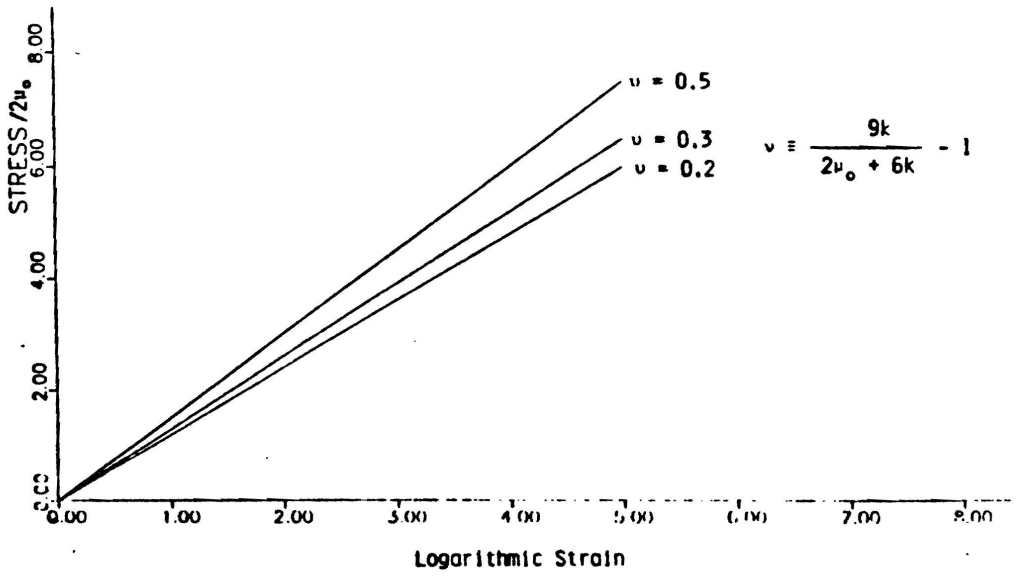

Fig. 10. Uniaxial extension of a hypo-elastic material (35) (independent of parameter c).

hence, the $s_{\phi z}$-γ curve approaches a straight line. In Fig. 9, typical stresses accompanying rectilinear shearing are shown. It is apparent that as the parameter c grows, the ideal Cauchy-type response is approached more and more closely for this load. It can be shown that the magnitude of the normal stress $s_{11}/2\mu_0$ approaches the value $1/c$ asymptotically. In Fig. 10 typical stresses accompanying uniaxial extension are shown, plotted against the 'natural' strain $\epsilon := \ln(1/L)$.

For future reference, we give the inverse of the constitutive eqn (34) in the following uncoupled form:

$$(\mathbf{s}'^{\circ}/2\mu_0) = [(1 + 2cp_2/(2\mu_0)^2)\underline{\mathbf{I}} - c(\mathbf{s}'/2\mu_0) \otimes (\mathbf{s}'/2\mu_0)]:\mathbf{e}' \tag{35}$$

$$\dot{p}_1 = 3k(\mathbf{I}:\mathbf{e}) \ . \tag{36}$$

When rectilinear shearing motions are studied, eqn (35) reduces to

$$\begin{aligned} s_{11} &= -s_{22} \\ (\dot{s}_{11}/2\mu_0)/e_{12} &= 2(s_{12}/2\mu_0)(1 - c(s_{11}/2\mu_0)) \\ (\dot{s}_{12}/2\mu_0)/e_{12} &= 1 - 2(s_{11}/2\mu_0)(1 - c(s_{11}/2\mu_0)) \ . \end{aligned} \tag{37}$$

If we stipulate that $(\dot{s}_{12}/2\mu_0)/e_{12}$ be unconditionally positive, a "stability" condition other workers have sought to fulfill by introduction of new stress rates, we are led by eqn (37) immediately to the restriction:

$$c > 1/2 \ . \tag{38}$$

Thus, when the condition (38) is fulfilled, there will be no unstable behavior in rectilinear shearing for any initial stress of the type (11) + a superposed pressure.

We close this section by remarking that a test for path independence in hypo-elastic materials has been devised by BERNSTEIN [1960].

V. A MODEL OF AN IDEAL KINEMATICALLY HARDENING RIGID-PLASTIC MATERIAL

In view of the formal correspondence between hypo-elasticity and the present kinematically hardening plasticity, we adopt eqn (35) as a model for an ideal kinematically hardening rigid-plastic material. Accordingly, we replace the tangent shear modulus $2\mu_0$ by Melan's hardening modulus $2h$, the stress $\mathbf{s}$ by the back-stress $\mathbf{a}$, the second invariant of the stress p_2 by the second invariant of the back-stress q_2, and finally the stretching $\mathbf{e}'$ by the plastic stretching $\mathbf{e}^p$:

$$(\mathbf{a}'^{\circ}/2h) = [(1 + 2cq_2/(2h)^2\underline{\mathbf{I}} - c(\mathbf{a}'/2h) \otimes (\mathbf{a}'/2h)]:\mathbf{e}^p \ . \tag{39}$$

The path-independence shown by this model may be investigated by application of BERNSTEIN's [1960] result. Inasmuch as eqn (35) gave results very close to the ideal of Cauchy elasticity, we expect eqn (39) to give results approaching the ideal Melan plasticity.

So that we may work a few examples illustrating the behavior of this model, we adopt a Mises-type description of the loading surface and associated flow rule:

$$f(\mathbf{s}', \mathbf{a}') := (\mathbf{s}' - \mathbf{a}'):(\mathbf{s}' - \mathbf{a}')/2 - T^2 = 0 \ , \tag{40}$$

$$\mathbf{e}^p = \dot{\lambda} \mathrm{d}f/\mathrm{d}\mathbf{s} \tag{41}$$

in which T is the radius of the surface. In Fig. 11 are shown the normal strains predicted by the model in pure torsion and the data of Swift. As can be seen, the agreement is excellent for monotonic loading. Agreement is less satisfactory once there has been a reversal, but nevertheless we continue to obtain results of the proper order of magnitude, in contrast to other models which overestimate normal strains by one to two orders of magnitude. Moreover, the magnitude of the Swift effect exhibited by the model can be adjusted independently through the parameter c, without affecting the rate of hardening. In Fig. 12, we show the prediction of the rigid-plastic model for the shear stress–average shear strain curve against the data of Swift. Within the obvious limitations of the rigid-plastic idealization, the agreement is excellent. In Fig. 13, the response of the model in rectilinear shearing is shown. We have not found data to which such data as this could be compared, but the normal stresses are small enough to be regarded as the second-order effect, as they are suspected to be. The shear stress does not oscillate for any initial value of $\mathbf{a}$ of the type (11) so long as $c > 1/2$. In Fig. 14 is shown the uniaxial stress-strain curve predicted by the model. Finally, in Fig. 15 is shown the response of the model to several reversed loadings in torsion.

VI. REMARKS ON MODELING ELASTIC-KINEMATICALLY HARDENING ELASTIC MATERIAL BEHAVIOR

There are both practical and theoretical reasons for not making the rigid-plastic idealization, even when there can be no doubt that plastic strains are much the larger. First of all, rigid-plastic models provide no information about the stresses in the non-plastic

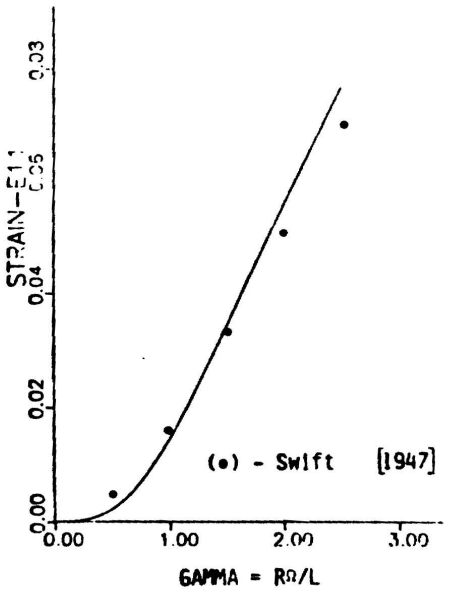

Fig. 11. Thin-walled tube torsion test, kinematically hardening plastic material (39). $T = 15$ tons/in.^{2}; $2h = 7.5$ tons/in.^{2}; $c = 3.7$.

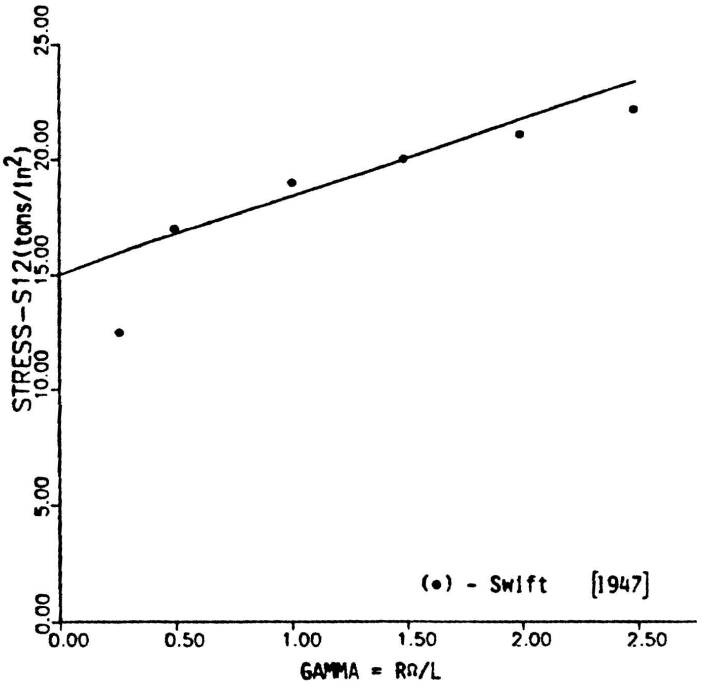

Fig. 12. Same as Fig. 11; Shear-stress-average strain curve.

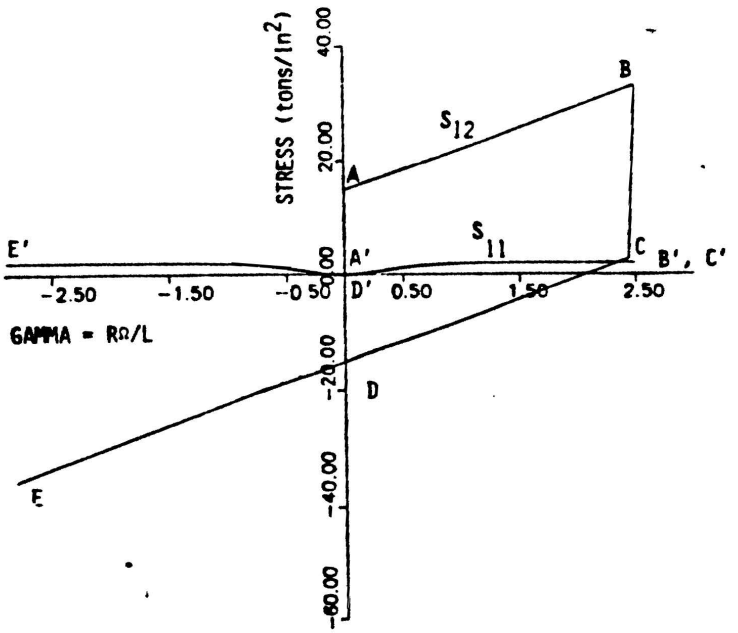

Fig. 13. Rectilinear shearing of a kinematically hardening plastic material (39) with load reversal. Same material as Fig. 11. S_{12} follows *A-B-C-D-E*; S_{11} follows *A'-B'-C'-D'-E'*.

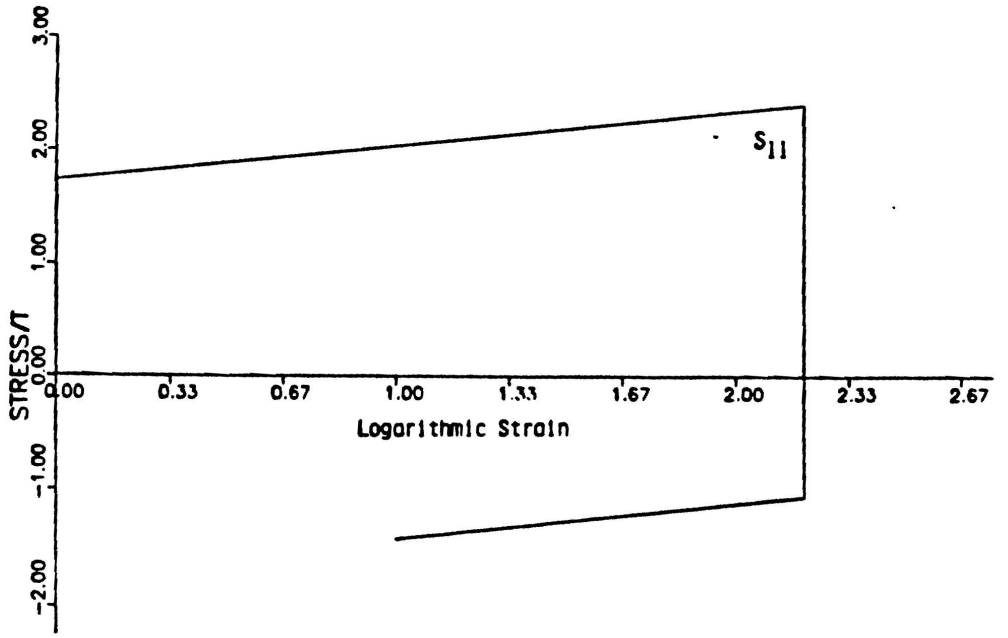

Fig. 14. Uniaxial extension of a kinematically hardening material (39) (independent of parameter c); $2h = 1$.

regions of a deforming body. Secondly, it is known that elastic-plastic structures may become unstable when, under the same loads, the corresponding rigid-plastic structure remains stable (c.f. RICE & RUDNICKI [1980]). The more useful material model incorporates elastic and combined isotropic-kinematic hardening plastic behavior. We discuss very briefly the basis for describing material behavior by such a "combined" model.

Without making any constitutive assumption at all we can express the true stress as a sum of two stress-like tensors:

$$\mathbf{s} = \langle \mathbf{s} - \mathbf{a} \rangle + \mathbf{a} \ . \tag{42}$$

When $\mathbf{s}$ and $\mathbf{a}$ are coaxial, it is possible to represent them as ordinary vectors in the principal-stress-space. The loading surface (40) becomes a circular cylinder with orientation (1,1,1) and diameter $2T$ in that space.

The back-stress $\mathbf{a}'$ lies in the π-plane and serves to locate the center of the loading surface. If only T changes as the material deforms then the hardening is described as "isotropic." If only $\mathbf{a}'$ changes as the material deforms then the hardening is described as "kinematic." When both change during deformation, the hardening is described as "combined isotropic-kinematic." It is clear that the isotropic part of the hardening (the growth of the vector $\langle \mathbf{s}-\mathbf{a} \rangle$) must be tied to the growth of T, but it is not necessarily related to the growth of $\mathbf{a}$. Thus, the simplest possible model incorporating both isotropic and kinematic hardening leaves the two "uncoupled." Mathematically:

$$\langle \mathbf{s} - \mathbf{a} \rangle^{\circ} = L(\mathbf{e}, \langle \mathbf{s} - \mathbf{a} \rangle) \tag{43}$$

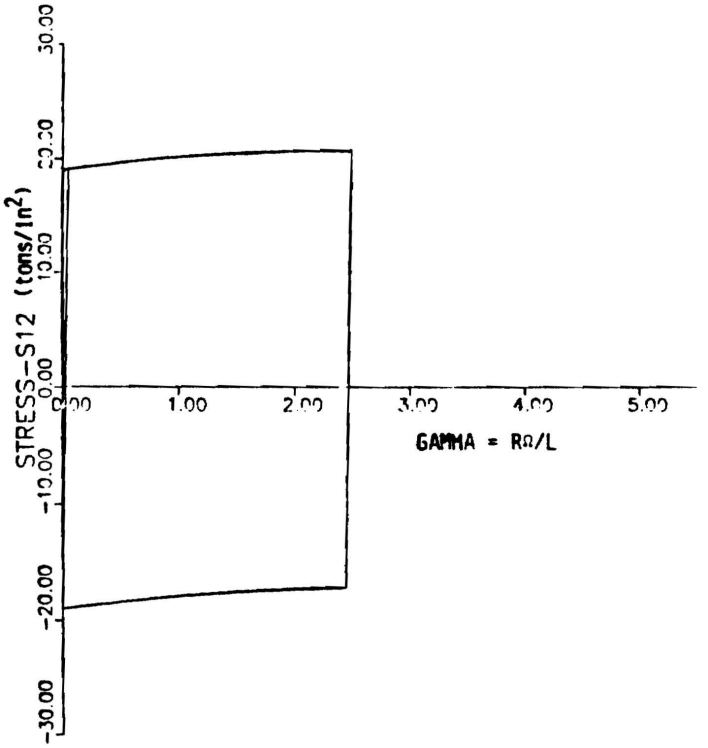

Fig. 15. Thin-walled tube torsion test; kinematically hardening plastic material (39). Three complete cycles between $\gamma = 0$ and $\gamma = 2.4$. Curves are coincident. Accumulated axial strain $E_{11} \approx 19\%$. $c = 0.55$; $T = 19$; $2h = 1$.

$$\mathbf{a}^* = G(\mathbf{e}^p, \mathbf{a}) \ . \tag{44}$$

This is different from the usually encountered model because of the appearance of $\mathbf{a}^*$ on the left-hand side of eqn (43). However its omission would spoil the uncoupled character of the model. Technically, eqn (43) would be styled after ordinary isotropically hardening plasticity and eqn (44) after a model of the type discussed in the previous sections.

VII. NUMERICAL INTEGRATION: STABILITY AND OBJECTIVITY

Stability

A stress-dependent critical strain increment $E := |\mathbf{e}H|$ can be found for the constitutive eqn (5) and hence eqn (6), as

$$E \leq 2/|\mathrm{d}\mathbf{s}^*/\mathrm{d}\mathbf{s}| \tag{45}$$

in which H is the time step, and $|\mathrm{d}\mathbf{s}^*/\mathrm{d}\mathbf{s}|$ signifies the max over $\mathbf{e}$ of $[|\{d(\underline{\mathbf{L}}:\mathbf{e})/\mathrm{d}\mathbf{s}\}|/|\mathbf{e}|]$. The critical strain increment decreases in magnitude as $|\mathbf{s}|$ grows. Critical strain increments for eqns (35) and (39) are found in Appendix C.

Objectivity

In order to be called objective, a numerical approximation for a physical entity must transform between frames of reference by the same rule as the entity itself. The true stress s, for example, transforms between frames according to the rule

$$\bar{\mathbf{s}} = \mathbf{Q}\mathbf{s}\mathbf{Q}' \tag{46}$$

(where Q is an orthogonal tensor), and we thus require any objective approximation for s to transform by the same rule (46). The advantage of this definition of numerical objectivity is that it may be applied directly to any invariant entity; it is not intrinsically bound to any particular stress tensor, constitutive equation, or numerical technique. This is an important point because the potential exists for confusion between the presently discussed "preservation of invariance" and the Principal of Objectivity of material properties (c.f. HUGHES & LIU [1981]).

Unfortunately, we can only achieve degrees of objectivity in numerical analysis, and thus the absolute errors present in an approximate solution depend, to put it crudely, on the choice of coordinates (REED & ATLURI [1983]). This point has not been brought out by other discussors (HUGHES & WINGET [1980], PINSKY *et al.* [1983], RUBENSTEIN & ATLURI [1983]).

The key to the construction of objective algorithms is the recognition of the fact that, just as in time-differentiation of tensors, in their time-integration it is necessary to specify the "group" of reference frames in which the integration is to be carried out, whether that integration is numerical or not. The property which distinguishes an acceptable group of frames is that the relative rotation between any two members of the group is constant w.r.t. time. This in itself does not suffice to determine any unique group; examples of groups of frames possessing this property are (i) the group of all inertial frames; (ii) the group of all Lagrangian frames; and (iii) groups of corotational frames. Groups of the latter two types are regarded as the significant ones with regard to constitutive equations.

If we specify that integration be carried out in a corotational frame then we may apply the "Jaumann integral" of GODDARD & MILLER [1966]:

$$\mathbf{s}(t) = \mathbf{Q}(t)\mathbf{s}(\tau)\mathbf{Q}(t) + \int_\tau^t \mathbf{Q}'(t)\mathbf{Q}(x)\mathbf{s}^*(x)\mathbf{Q}'(x)\mathbf{Q}(t)\,dx \ . \tag{47}$$

In eqn (47) Q is the orthogonal tensor relating quantities in the working frame to their counterparts in the corotational frame. We have previously shown (REED & ATLURI [1983]) that Q is defined through the initial value problem

$$\dot{\mathbf{Q}}(t) = -\mathbf{Q}(t)\mathbf{w}(t) \ , \quad \mathbf{Q}(\tau) = \mathbf{I} \ , \tag{48}$$

in which $\mathbf{w}(t)$ is the ordinary spin tensor. Any of the standard formulae for approximation of definite integrals may be applied to eqn (47) and the result is an "objective" integration rule. When $\mathbf{Q}(t)$ can be found exactly within the interval of interest then the result is precisely objective; that is eqn (47) will yield the same result no matter what frame it is applied in.

However, in practice it is generally only possible to approximate the solution of eqn (48). The "degree" to which our numerical result may be called objective is then directly

related to the degree of accuracy with which $\mathbf{Q}$ has been found. The initial value problem (48) may easily be reduced to a scalar problem by introduction of "angles of rotation":

$$(d\mathbf{Q}/d\theta_i)\theta_i = -\mathbf{Q}(\theta_i)\mathbf{w}(t) \ , \quad \theta_i(\tau) = 0 \ , \tag{49}$$

$$\mathbf{Q}(\theta_1,\theta_2,\theta_3) = \begin{bmatrix} c\theta_2 c\theta_3 & c\theta_1 s\theta_3 + s\theta_1 s\theta_2 c\theta_3 & s\theta_1 s\theta_3 - c\theta_1 s\theta_2 c\theta_3 \\ -c\theta_2 s\theta_3 & c\theta_1 c\theta_3 - s\theta_1 s\theta_2 s\theta_3 & s\theta_1 c\theta_3 + c\theta_1 s\theta_2 s\theta_3 \\ s\theta_2 & -s\theta_1 c\theta_2 & c\theta_1 c\theta_2 \end{bmatrix} \tag{50}$$

in which the abbreviations $s\theta_i = \sin\theta_i$ and $c\theta_i = \cos\theta_i$ have been used. The angles are absolute scalars and may thus be integrated objectively by standard numerical schemes. The error of such schemes is usually expressed in the form

$$|\theta(t_k) - \theta_k| \leq CH^{N+1}\theta^{(N+1)}(t_k) \tag{51}$$

where $\theta^{(N+1)}$ is the $(N+1)$th time derivative of θ and H is the time step size. When eqn (47) is used in conjunction with a $\mathbf{Q}$ of N^{th}-order accuracy, eqn (46) will be exactly satisfied only for those $\mathbf{Q}$ whose angles are N^{th}-order polynomials w.r.t. time. Hence, numerical objectivity cannot be absolute.

As an example, we derive an objective midpoint rule by approximation of eqn (47). By inspection, we can write:

$$\mathbf{s}_{N+1} = \mathbf{Q}^t(t_{N+1})\mathbf{s}_N\mathbf{Q}(t_{N+1}) + H\mathbf{Q}_t(t_{N+1})\mathbf{Q}(t_{N+K})\mathbf{s}^*_{N+K}\mathbf{Q}_t(t_{N+K})\mathbf{Q}(t_{N+1}) \ . \tag{52}$$

When $\mathbf{s}^*$ is eliminated by use of the constitutive equation and K set to 1/2 then eqn (52) reduces to the formulate of KEY *et al.* [1981] & RUBENSTEIN & ATLURI [1983]. The essential point to be made is that through eqn (47) much more general objective schemes may be easily and accurately constructed (see REED & ATLURI [1983]).

Acknowledgements—The results presented herein were obtained during the course of investigations supported by NASA-Lewis Research Center under a grant, NAG-3-346 to Georgia Institute of Technology. This support as well as the encouragement of Drs. C. Chamis and L. Berke are gratefully acknowledged. Appreciation is also expressed to Ms. Joyce Webb and Ms. Tanya Jackson for their assistance in the preparation of the manuscript.

REFERENCES

1909 POYNTING, J.H., "On Pressure Perpendicular to the Shear Planes in Finite Pure Shears and on the Lengthening of Loaded Wires when Twisted," Proc. Roy. Soc. (Lon.) A82, 546.
1938 MELAN, E., "Zur Plastizität des räumlichen Kontinuums," Ing.-Arch., 9, 116.
1947 SWIFT, H.W., "Length Changes in Metals Under Torsional Overstrain," Engineering, 163, 253.
1960 BERNSTEIN, B., "Hypo-Elasticity and Elasticity," Arch. Rat. Mech. Anal., 6, 89.
1966 FREUDENTHAL, A.M. and RONAY, M., "Second Order Effects in Dissipative Media," Proc. Roy. Soc. (Lon.), A292, 14.
1966 GODDARD, J.D. and MILLER, C., "An Inverse for the Jaumann Derivative and Some Applications to the Rheology of Viscoelastic Fluids," Rheologica Acta, 5, 177.
1968 ROSE, W. and STÜWE, H.-P., "Der Einfluss der Textur auf die Längänderung im Torsionversuch," Z. Metallkde, 59, 396.
1970 WANG, C.-C., "A New Representation Theorem for Isotropic Functions," Arch. Rat. Mech. Anal., 36, 198.
1972 LEHMANN, TH., "Einige Bemerkungen zu einer allgemeinen Klasse von Stoffgesetzen für grosse elastoplastische Formänderungen," Ing.-Arch., 41, 297.

1973 ONAT, E.T. and FARDSHISHEH, F., "Representation of Creep, Rate Sensitivity, and Plasticity," SIAM J. Appl. Math., 25, 522.
1977 BILLINGTON, E.W., "Non-linear Mechanical Response of Various Metals I, II, III," J. Phys. D: Appl. Phys., 10, 519.
1977 HARNOY, A., "Three Dimensional Analysis of the Elastico-viscous Lubrication in Short Journal Bearings," Rheologica Acta, 16, 51.
1979 DIENES, J.K., "On the Analysis of Rotation and Stress Rate in Deforming Bodies," Acta Mech., 32, 217.
1979 ASTIN, J and JONES, R.S., "A Note on Harnoy's Equations of State," J. Non-Newtonian Fluid Mech. 4, 359
1980 BELL, J.F. and KHAN, A.S., "Finite Plastic Strain in Annealed Copper During Non-proportional Loading," Int. J. Sol. Struct., 16, 683.
1980 RICE, J.R. and RUDNICKI, J.W., "A Note on Some Features of the Theory of Localization of Deformation," Int. J. Sol. Structu., 16, 597.
1980 HUGHES, T.J.R. and WINGET, J., "Finite Rotation Effects in Numerical Integration of Rate Constitutive Equations Arising in Large-deformation Analysis," Int. J. Numer. Meth. Eng., 15, 1862.
1981 NAGTEGAAL, J.C. and DE JONG, J.E., "Some Aspects of Non-Isotropic Workhardening in Finite Strain Plasticity," Proceedings of the Workshop on Plasticity of Metals at Finite Strain: Theory, Experiment and Computation, eds. LEE, E.H. and MALLETT, R.L., Stanford University, 65.
1981 LEE, E.H., MALLETT, R.L., and WERTHEIMER, T.B., "Stress Analysis for Kinematic Hardening of Finite Deformation Plasticity," Scientific Rept. to the Office of Naval Research, Dept. of Navy.
1981 HUGHES, T.J.R. and LIU, W.K., "Nonlinear Finite Element Analysis of Shells: Part I. Three-dimensional Shells," Comput. Meth. Appl. Mech. Eng., 26, 331.
1981 KEY, S.W., STONE, C.M., and KREIG, R.D., "Dynamic Relaxation Applied to the Quasistatic Large Deformation Inelastic Response of Axisymmetric Solids," in Nonlinear Finite Element Analysis in Structures, Springer, Berlin, 585.
1982 JOHNSON, G.C. and BAMMANN, D.J., "A Discussion of Stress Rates in Finite Deformation Problems," Rept. No. SAND-82-8821, Sandia National Laboratories, Alburquerque, New Mexico.
1983 LEE, E.H., MALLETT, R.L., and WERTHEIMER, T.B., "Stress Analysis for Anisotropic Hardening in Finite-Deformation Plasticity," J. Appl. Mech., 50, 554.
1983 DAFALIAS, Y.F., "Corotational Rates for Kinematic Hardening at Large Plastic Deformations," J. Appl. Mech., 50, 561.
1983 ATLURI, S.N., "On Constitutive Relations at Finite Strain: Hypo-Elasticity and Elasto-Plasticity with Isotropic or Kinematic Hardening," Rept. No. GIT-CACM-SNA-83-16, Ga. Inst. Tech., also Comp. Meth. Appl. Mech. & Eng. (In press).
1983 REED, K.W. and ATLURI, S.N., "Analysis of Large Quasistatic Deformations on Inelastic Bodies by a New Hybrid-Stress Finite Element Algorithm," Comput. Meth. Appl. Mech. Eng., 39, 254.
1983 NAGTEGAAL, J.C., "A Note on the Construction of Spin Tensors," as discussed by T.J.R. Hughes at the Workshop on the Theoretical Foundations for Large-Scale Computations of Nonlinear Material Behavior, Northwestern Univ., Evanston, Illinois, Oct. 24-26.
1983 PINSKY, P.M., ORTIZ, M., and PISTER, K.S., "Rate Constitutive Equations in Finite Deformation Analysis: Theoretical Aspects and Numerical Integration," Comput. Meth. Appl. Mech. Eng., 39.
1983 RUBENSTEIN, R. and ATLURI, S.N., "Objectivity of Incremental Constitutive Equations Over Finite Time Steps in Computational Finite Deformation Analysis," Computer Meth. Appl. Mech. Eng., 36, 277.

APPENDIX A

ON THE SOLUTION OF LEE *ET AL.* [1983] TO THE RECTILINEAR SHEARING PROBLEM

We may represent the back-stress $\mathbf{a}$ in this problem as in eqn (11) in the text above. When Lee's stress rate is used $w = 2e_{12}\sin^2\theta$ for this problem, which, together with Melan's rule (4) yields

$$(\bar{a}'/h) = \sin 2\theta \tag{A1}$$

$$2\theta' = [(1 + (\bar{a}/h))/(\bar{a}/h)]\cos 2\theta - 1 \ . \tag{A2}$$

We assume h to be a constant, as in the published examples. When θ lies in the range $0 < \theta < \pi/2$ then $(\bar{a}'/h) > 0$, so we may divide eqn (A2) by (A1) to obtain

$$\mathrm{d}2\theta/\mathrm{d}\hat{a} = [(1 + \hat{a})\cos 2\theta - \hat{a}]/\hat{a}\sin 2\theta \ , \tag{A3}$$

in which $\hat{a} := (\bar{a}/h)$. Equation (A3) may be integrated for $\hat{a} \neq 0$ as

$$\cos 2\theta = (\hat{a} - 1)/\hat{a} - [\hat{a}_0(1 - \cos 2\theta_0) - 1](1/\hat{a})\exp\{-(\hat{a} - \hat{a}_0)\} \ . \tag{A4}$$

The stress-strain curves published by LEE *et al.* [1983] correspond to a singular solution of eqn (A3). Although Lee's numerical results agree reasonably well with our own for a range of strain, the present result indicates that θ approaches an asymptote of 0 degrees for large strains. This is in conflict with the numerical result of LEE *et al.* [1983], which approached 15° asymptotically.

The stability condition which motivated Lee to introduce a new stress rate may be written as

$$(s'_{12}/h) = (\hat{a}\sin 2\theta)' = \hat{a}'\sin 2\theta + \hat{a}(2\theta')\cos 2\theta > 0 \ , \tag{A5}$$

or, after using eqns (A1) and (A2) to eliminate $\hat{a}'$ and $2\theta'$,

$$1 - \hat{a}\cos 2\theta(1 - \cos 2\theta) > 0 \ . \tag{A6}$$

In Fig. A1 we have plotted eqn (A6) as well as (A4) for various initial $\hat{a}$ and 2θ. As can be seen there is a zone in the $\hat{a} - 2\theta$ plane inside of which the stability condition (A6)

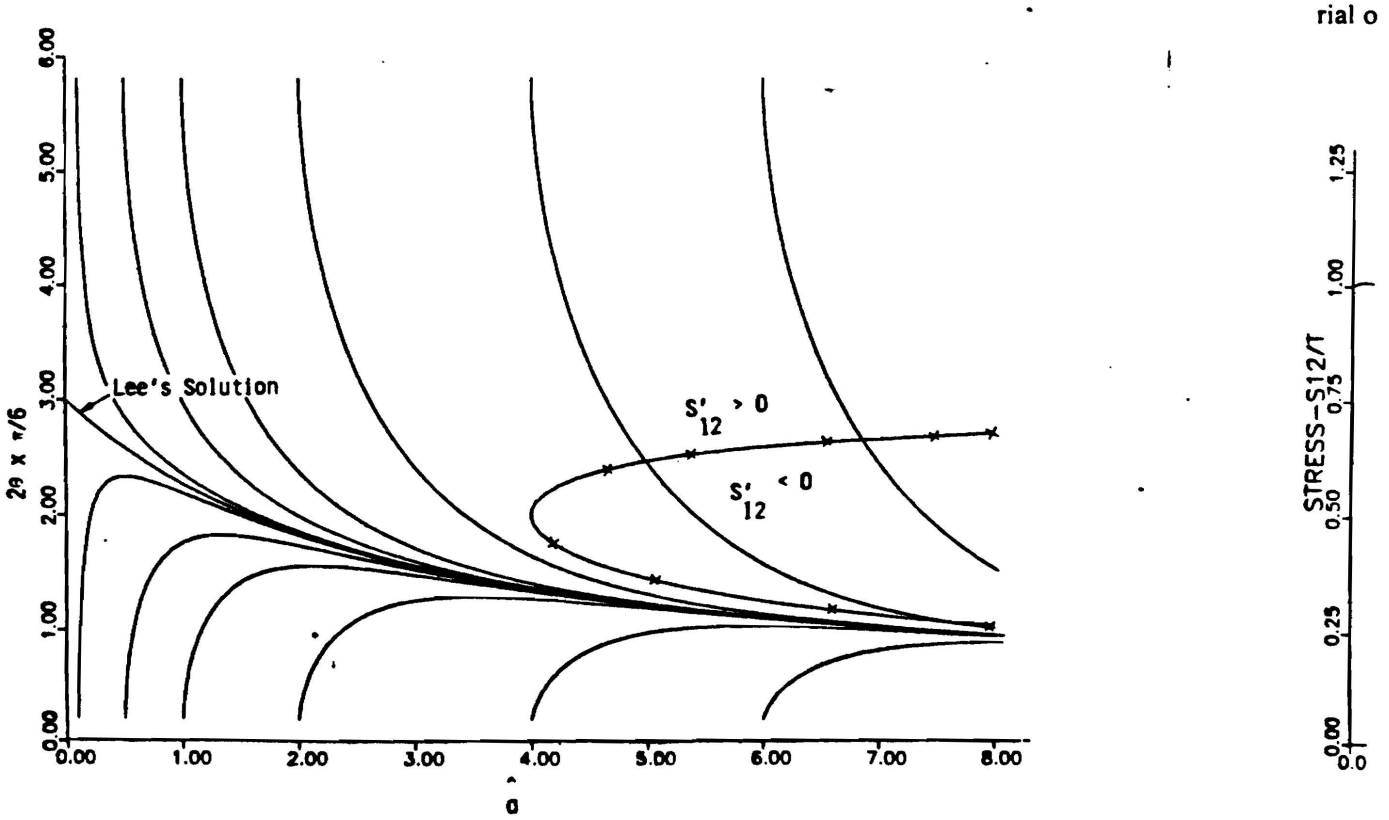

Fig. A1. Solutions of the eqn (A3).

is not satisfied. In Fig. A2 we show a typical shear stress–shear strain curve corresponding to a solution (A4) which passes through this zone. We note that DAFALIAS [1983] has shown that the Green-McInnis rate leads to analogous stress-strain curves for non-vanishing initial $\hat{a}$.

We close by remarking that our solution to this problem is in no way pathological. It also indicates, and we have found numerically, that when the hardening modulus h decreases with strain, as would be required to describe uniaxial strain softening, the use of Lee's rate can then lead to unstable behavior even in infinitesimal shearing.

APPENDIX B
HARNOY'S STRESS RATE

HARNOY [1977] & LEE *et al.* [1981] have proposed that a corotational stress rate be based on the spin of the eigenvector triad of the stress and on the spin of the material elements instantaneously coincident with the eigenvector associated with the maximum eigenvalue of the back-stress, respectively. ASTIN & JONES [1979] have observed correctly that Harnoy's rate must always be coaxial with the stress itself. This is also made evident by defining $w := \dot{\theta}$ in eqn (12). We now recall a constitutive postulate which encompasses a very wide class of rate-type materials, including hypo-elasticity, ordinary plasticity, and some engineering theories of creep and viscoelasticity:

$$\mathbf{e} = F(\mathbf{s}^*, \mathbf{s}) \ , \tag{B1}$$

in which F is not necessarily linear w.r.t. $\mathbf{s}^*$. The coaxiality of $\mathbf{s}$ and $\mathbf{s}^*$ in any material of class (B1) clearly implies that $\mathbf{s}$ and $\mathbf{e}$ are also necessarily coaxial. All solutions

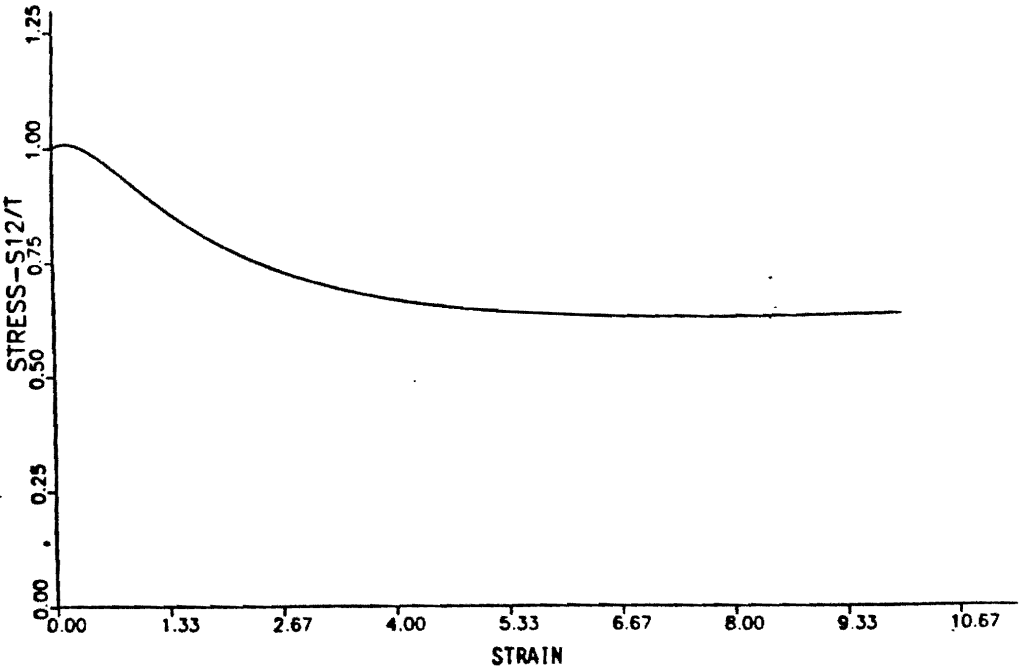

Fig. A2. Stress-strain curve for LEE's [1983] rate; initial values $\hat{a} = 8$, $2\theta = \pi/2$.

of eqn (B1) must have this character, leading us to conclude that this corotational rate is unsuitable for use in this class of constitutive equations.

APPENDIX C
CRITICAL STRAIN INCREMENTS

Evaluation of the matrix norm $|ds^*/ds|$ in the stability condition (45) is equivalent to finding the maximum over e of $|[d(\underline{L}:e)/ds]|/|e|$, i.e., an eigenvalue problem. For the constitutive eqn (35) $d(L:e)/ds$ is given by

$$d(\underline{L}:e)/ds = -cw(\underline{I}) - c(s' \otimes e') + 2c(e' \otimes s') \tag{C1}$$

in which the stress has been normalized by $2\mu_0$ and $w := s':e'$. This is an unsymmetric fourth-order tensor, whose least eigenvalue for $|e| = 1$ and fixed s' will determine the critical strain increment E. [Material stability in the ordinary sense requires that all of these eigenvalues be less than or equal to zero; it is not shown here that this condition is fulfilled by eqn (35).] So that we do not have to work with an unsymmetric tensor, we pre-multiply eqn (C1) by its transpose, obtaining the positive-indefinite fourth-order tensor:

$$c^2[4(e':e')(s' \otimes s') - 3w(s' \otimes e' + e' \otimes s) + (s':s')(e' \otimes e') + w^2(\underline{I})] \ . \tag{C2}$$

The trace D of this tensor is the sum of its eigenvalues, and since all of these are necessarily non-negative, D must be greater than or equal to the greatest eigenvalue R. Hence

$$R \leq c^2[5(s':s')(e':e') + 3w^2] \ , \tag{C3}$$

which we must maximize for $|e'| = 1$. It is clear that this is accomplished by choosing e' parallel to s'; then (C3) yields

$$R \leq 8c^2(s':s') \ . \tag{C4}$$

It follows that the least eigenvalue r of the original matrix (C1), which is necessarily negative, is bounded from below by

$$r \geq -2\sqrt{2}\, c|s'| \ , \tag{C5}$$

so the critical strain increment E must be (in terms of un-normalized stress)

$$E \leq (2\mu_0)/[\sqrt{2}\, c|s'|] \ . \tag{C6}$$

It is noteworthy that this restriction becomes more acute as c and $|s'|$ grow.

In view of the correspondence between the ideal hypo-elastic and kinematically hardening plastic models, we may also establish the following critical plastic strain increment E^p for the latter (39) as

$$E^p = (2h)/[\sqrt{2}\, c|a'|] \ . \tag{C7}$$

We suspect that these bounds are not sharp because no use has been made of the fact that $\mathbf{e}'$ and $\mathbf{s}'$ are traceless. Nevertheless, they are of the proper order of magnitude: when the ideal hypo-elastic model (35) is specialized to the case of rectilinear shearing a critical strain increment may be found independently from the above analysis as $E \leq 2\mu_0/cs_{12}$, which is only about twice as large as that given by eqn (C6).

Southwest Research Institute
San Antonio, TX 78284, USA

Georgia Instiute of Technology
Atlanta, GA 30332, USA

(*Received* 15 *June* 1984)

ineering Fracture Mechanics Vol. 16, No. 6, pp. 769–782, 1982
ed in Great Britain.

0013-7944/82/060769-14$03.00/0
Pergamon Press Ltd.

MOVING SINGULARITY CREEP CRACK GROWTH ANALYSIS WITH THE $(\Delta T)_c$ AND C^* INTEGRALS

R. B. STONESIFER† and S. N. ATLURI‡
Center for the Advancement of Computational Mechanics, School of Civil Engineering, Georgia Institute of Technology, Atlanta, GA 30332, U.S.A.

Abstract—The physical meaning of $(\Delta T)_c$ and its applicability to creep crack growth are reviewed. Numerical evaluation of $(\Delta T)_c$ and C^* is discussed with results being given for compact specimen and strip geometries. A moving crack-tip singularity, creep crack growth simulation procedure is described and demonstrated. The results of several crack growth simulation analyses indicate that creep crack growth in 304 stainless steel occurs under essentially steady-state conditions. Based on this result, a simple methodology for predicting creep crack growth behavior is summarized.

INTRODUCTION

UMEROUS experimental studies have been undertaken with the purpose of finding a parameter which orrelates with creep crack propagation rate. Most of these investigations consider as condidate arameters, K_I, some form of net section (or reference) stress or in more recent studies C^*. See, for xample [1–4]. Since the introduction of C^*, there appears to be less emphasis on K_I as a parameter, owever, there are apparently real materials and conditions for which either net section stress or K_I provide etter correlation with crack growth rate than C^*.

As illustrated in Fig. 1, the above three parameters might be expected to correlate three distinctly ifferent creep crack growth situations. In Fig. 1(a), a crack and its associated ligament are shown for a iaterial and geometry which results in negligible creep strains everywhere except in the vicinity of the rack-tip. This condition is analogous to that of small scale yielding in elastic–plastic fracture.

Figure 1(b) represents a situation in which C^* might be considered an appropriate parameter. This ituation is characterized (i) by the body being essentially at steady-state creep conditions (which implies ery slow crack propagation) and (ii) by the creep-damage process-zone being local to and therefore ontrolled by the crack-tip field. Figure 1(c) illustrates the type of situation for which net section stress might e expected to control crack growth. In this case, the main feature is the widespread creep damage zone.

It is seen from Fig. 1 that intermediate situations can occur. For example, suppose a particular material nd geometry results in a crack propagation rate such that elastic strain rates are not negligible compared to reep rates (i.e. non-steady creep) and at the same time, creep strains are no longer localized to the crack-tip egion. While neither K_I nor C^* could be valid parameters for this case, it appears reasonable to expect that rack growth rate is still determined by the local crack-tip field since the creep damage process zone is still ssumed to be local to the crack-tip.

In the present study, we are concerned primarily with behavior bounded by that illustrated in Fig. 1(a,b). hat is, we consider conditions in which the creep damage zone and presumably crack propagation speed are ontrolled by the crack-tip field. Therefore, if we have a parameter which characterizes the crack-tip fields uring such behavior we presumably have a parameter which will characterize creep crack propagation rate. A parameter which spans the gap between K_I controlled growth and C^* controlled growth has been ntroduced in [5] and subjected to initial scrutiny in [6]. This parameter is referred to as $(\Delta T)_c$ and is defined y a path-independent, vector integral. For stationary cracks, it has been shown [5, 6] that the related uantity $(\dot{T})_c$ is a measure of the amplitude of the HRR crack-tip field which presumably exists for both ion-steady and steady-state creep. It has also been shown that $(\dot{T}_1)_c$ has the energy interpretation $\dot{T}_1)_c = -(\mathrm{d}\dot{U}/\mathrm{d}a)$ for non-steady as well as steady-state creep.

In the process of exploring this new parameter, it has been found [6] that despite C^* being a valid crack-tip arameter for strictly steady-state creep conditions, it is not equivalent to the $(\dot{T}_1)_c$ parameter under any conditions and therefore does not have the energy interpretation commonly attributed to it. Since experimentalists use the energy interpretation as a means of "measuring" C^* it seems more appropriate to refer to these experimental results as $(\dot{T}_1)_c$.

†Doctoral candidate.
‡Regents' Professor of Mechanics.

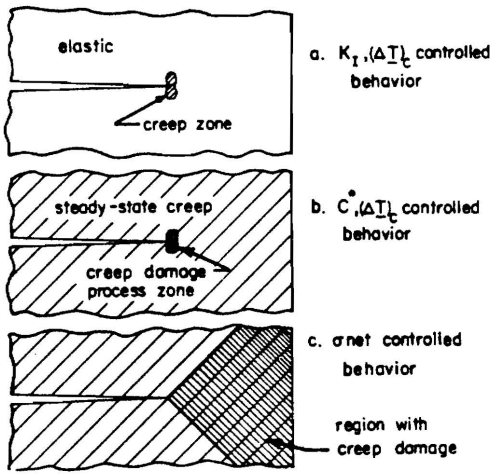

Fig. 1. Conditions for which creep crack growth parameters are expected to be valid.

In the first portion of this paper, we define $(\Delta T)_c$ and a generalized C^* and also summarize the properties and the relationship of these parameters. The remainder of the paper discusses several finite element calculations for both stationary cracks and propagating cracks. The crack propagation study uses a combination of analytical, numerical and experimental results to show that creep crack growth in 304 stainless steel at 650°C occurs under essentially steady-state creep conditions. Finally, based on this observation, a simple crack growth prediction methodology is outlined.

CONSTITUTIVE EQUATIONS

In this study we assume strains are infinitesimal and the deformations small. Furthermore, we assume material behavior of the type:

$$\dot{\epsilon}_{ij} = \dot{\epsilon}^e_{ij} + \dot{\epsilon}^c_{ij} = C_{ijkl}\dot{\tau}_{kl} + \frac{3}{2}\gamma(\bar{\sigma})^{n-1}\tau'_{ij} \tag{1}$$

where $\dot{\epsilon}^e_{ij}$ and $\dot{\epsilon}^c_{ij}$ are the elastic and creep strain rates, respectively, C_{ijkl} is the tensor of elastic moduli, $\dot{\tau}_{kl}$ is the stress rate, τ'_{ij} is the deviatoric stress ($\tau'_{ij} = \tau_{ij} - 1/3\tau_{kk}\delta_{ij}$), and $\bar{\sigma}$ is the equivalent stress given by $\bar{\sigma} = (3/2)(\tau'_{ij}\tau'_{ij})^{1/2}$. The parameters γ and n are those of the familiar Norton power law:

$$\dot{\bar{\epsilon}} = \gamma(\bar{\sigma})^n \tag{2}$$

where

$$\dot{\bar{\epsilon}} = [(2/3)\dot{\epsilon}_{ij}\dot{\epsilon}_{ij}]^{1/2}.$$

The constitutive law (1) can result in steady-state creep response (i.e. $\dot{\tau}_{ij} = 0$) after some preiod of time provided the boundary conditions are some combination of time invariant tractions or time invariant displacement rates.

FRACTURE PARAMETERS $(\Delta T)_c$ and C^*

We now define two vector quantities which have applications to fracture analysis under creep conditions. The first quantity is $(\Delta T)_c$ as recently defined by Atluri[5] and subsequently examined in greater detail in [6]. In [5], $(\Delta T)_c$ is defined in the context of finite strains and large deformations. Here we give the corresponding definition for infinitesimal strains and small deformations.

$$(\Delta T_i)_c \equiv \underset{\epsilon\to 0}{\text{Lt}} \int_{\Gamma_\epsilon} \left[n_i \Delta W - n_j(\tau_{jk} + \Delta\tau_{jk}) \frac{\partial \Delta u_k}{\partial x_i} \right] dS \tag{3}$$

$$= \int_{\Gamma_{234}} \left[n_i \Delta W - n_j(\tau_{jk} + \Delta\tau_{jk}) \frac{\partial \Delta u_k}{\partial x_i} \right] dS$$

$$+\operatorname*{Lt}_{\epsilon\to 0}\left\{\int_{V-V_\epsilon}\left[\rho(a_k-f_k)\frac{\partial\Delta u_k}{\partial x_i}-\frac{\partial\tau_{jk}}{\partial x_i}\Delta\epsilon_{jk}\right]dV\right.$$
$$+\int_{\Gamma_{12}} n_i\Delta W\,dS+\int_{\Gamma_{45}} n_i\Delta W\,dS-\int_{S_t}\bar{t}_k\frac{\partial\Delta u_k}{\partial x_i}dS$$
$$\left.-\int_{S_\epsilon} n_i(\tau_{jk}+\Delta\tau_{jk})\frac{\partial\Delta\bar{u}_k}{\partial x_i}dS\right\}.$$

The various contour integral paths and their outward unit normals n as well as V and V_ϵ are illustrated in Fig. 2 for a two-dimensional, cracked body. In writing (3) it has been assumed that $S_\epsilon + S_t = \Gamma_{12} + \Gamma_{45}$ where S_ϵ and S_t are the portions of the crack surfaces with applied incremental displacements, $\Delta\bar{u}_k$, and applied tractions $\bar{t}_k$, respectively. The initial stress for the increment is denoted τ_{jk}. The mass density is ρ and the acceleration and body force components at the end of the increment are a_k and f_k, respectively. The quantity ΔW is the incremental stress-working density and is given by

$$\Delta W=\left(\tau_{ij}+\frac{1}{2}\Delta\tau_{ij}\right)\Delta\epsilon_{ij}. \tag{4}$$

The right equality of (3) shows that $(\Delta T_i)_c$ is independent of the selection of Γ_{234} (provided the fields within $V-V_\epsilon$ are sufficiently well behaved for the divergence theorem to be applicable). It is important to note that this path-independence exists during non-steady as well as steady-state creep.

In the present study we consider cracks along the x_1 axis and symmetrical, Mode I type deformations. Furthermore, we consider traction-free crack surfaces and assume body forces and accelerations are negligible. Under these conditions, only $(\Delta T_1)_c$ is of interest and we have

$$(\Delta T_1)_c=\int_{\Gamma_{234}}\left[n_1\Delta W-n_j(\tau_{jk}+\Delta\tau_{jk})\frac{\partial\Delta u_k}{\partial x_1}\right]dS-\int_V\frac{\partial\tau_{jk}}{\partial x_1}\Delta\epsilon_{jk}\,dV \tag{5}$$

where we have now taken the limit of the volume integral.

It has been shown in [5] that $(\Delta T_i)_c$ has the physical meaning†

$$(\Delta T_1)_c=-\left(\frac{\Delta U_2-\Delta U_1}{dc_1}\right) \tag{6}$$

where ΔU_2 and ΔU_1 are the incremental potential energies for two cracked bodies which are identical in loading history and geometry except that the second body has an incrementally longer crack by the amount dc_1. In creep applications, it is convenient to define the quantity

$$(\dot{T}_1)_c\equiv\operatorname*{Lt}_{\Delta t\to 0}\frac{(\Delta T_1)_c}{\Delta t}\approx\frac{(\Delta T_1)_c}{\Delta t} \tag{7}$$

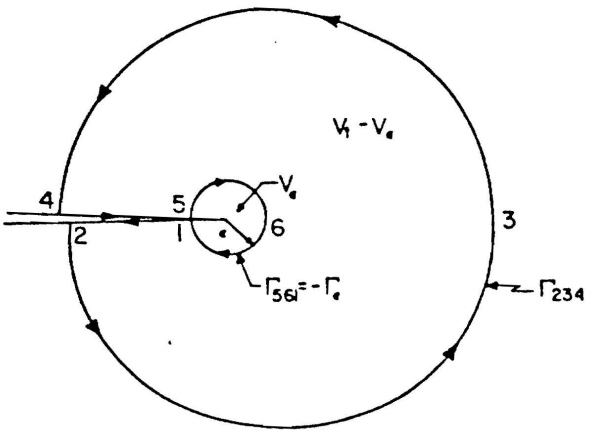

Fig. 2. Contours for applying the conservation law to a two-dimensional, cracked body.

†The sign convention for ΔU_1 and ΔU_2 is reversed from that of [5, 6] to reflect the conventional definition of potential energy.

where Δt is the time increment. Comparing (7) and (6) it can be seen that $(\dot{T}_1)_c$ has the physical meaning which is commonly attributed to $C\dagger$, i.e.

$$(\dot{T}_1)_c = -\frac{d\dot{U}}{dc_1}. \tag{8}$$

We now state a generalized definition for the C^* parameter which has been derived in [6]:

$$\begin{aligned} C\dagger &\equiv \operatorname*{Lt}_{\epsilon\to 0}\int_{\Gamma_\epsilon}\left[n_i W^* - \eta_j\tau_{jk}\frac{\partial \dot{u}_k}{\partial x_i}\right]dS \\ &= \int_{\Gamma_{234}}\left[n_i W^* - \eta_j\tau_{jk}\frac{\partial \dot{u}_k}{\partial x_i}\right]dS \\ &\quad + \operatorname*{Lt}_{\epsilon\to 0}\left\{\int_{V-V_\epsilon}\rho(a_k - f_k)\frac{\partial \dot{u}_k}{\partial x_i}dV + \int_{\Gamma_{12}} n_i W^* dS + \int_{\Gamma_{45}} n_i W^* dS\right. \\ &\quad \left. - \int_{S_t}\bar{t}_k\frac{\partial \dot{u}_k}{\partial x_i}dS - \int_{S_\epsilon} n_j\tau_{jk}\frac{\partial \bar{\dot{u}}_k}{\partial x_i}dS\right\}. \end{aligned} \tag{9}$$

Based on the same simplifying conditions used in obtaining (5) we have

$$C\dagger = \int_{\Gamma_{234}}\left[n_1 W^* - \eta_j\tau_{jk}\frac{\partial \dot{u}_k}{\partial x_1}\right]dS \tag{10}$$

where it is seen that the volume integral no longer is present.

The quantity W^* which appears in (9) and (10) is usually defined as [2]:

$$W^* = \int_0^{\dot{\epsilon}_{ij}} \tau_{ij}\, d\dot{\epsilon}_{ij}. \tag{11}$$

Using the steady-state case of (1) and the associated incompressibility condition, the following more useful expressions can be derived [6]:

$$W^* = \frac{n}{1+n}(\gamma)^{1/n}(\dot{\bar{\epsilon}})^{1+n/n} \tag{12}$$

$$W^* = \frac{n}{1+n}\gamma(\bar{\sigma})^{1+n}. \tag{13}$$

As noted previously, $C\dagger$ is often stated to have the energy interpretation which was given for $(\dot{T}_1)_c$ in (8). It has been shown in [6] that this is incorrect. The relationship of the steady-state value of $(\dot{T}_1)_c$ (i.e. $(\dot{T}_1)_{css}$) and $C\dagger$ is given in [6] as:

$$(\dot{T}_1)_{css} = C\dagger + \left(\frac{\gamma}{n+1}\right)\operatorname*{Lt}_{\epsilon\to 0}\int_{\Gamma_\epsilon} n_1(\bar{\sigma})^{n+1}\, dS. \tag{14}$$

approximate numerical evaluation of (14) in [6] has shown that $(\dot{T}_1)_{css}$ and $C^*_\dagger$ agree to within 2% for plane strain and differ by as much as 14% for plane stress.

From the above discussion it is clear that C^* and $(\dot{T})_c$ are not equivalent quantities under any condition despite their being derived from the same conservation law. The quantity $(\dot{T})_c$ follows more directly from the conservation law and is the more general quantity not only in that it is applicable to non-steady as well as steady-state creep but also in that it is applicable to constitutive laws which are more general than (1) [5]. The quantity C^* relies on the special property of (1) which allows the existence of a potential W^* for the deviatoric stresses, τ'_{ij}. Furthermore, since W^* does not have a physical meaning whereas $\dot{W}$ has the meaning of rate of stress-working density, it is understandable that $(\dot{T})_c$ has an energy interpretation whereas C^* does not. In light of this conclusion, it seems more appropriate to refer to experimental measurements of "$-(d\dot{U}/da)$" as measurements of $(\dot{T}_1)_c$ as opposed to measurements of $C\dagger$ or $\dot{J}_1$, etc.

FINITE ELEMENT EQUATIONS

The following summarizes the finite element model. For a more complete description see [6]. The model is based on the principle of virtual work:

$$\int_V \tau_{ij}\delta\epsilon_{ij}\,dV - \int_{S_t} \bar{t}_i\delta u_i\,dS = 0. \tag{15}$$

By substituting the following incremental stress-strain relation

$$\{\tau\}_I = \{\tau\}_{I-1} + [E]\{\Delta\epsilon\}_I - [E]\{\Delta\epsilon^c\}_I \tag{16}$$

into (15) and applying customary procedures we have the final equation:

$$[K]\{\Delta Q\}_I = \{T\}_I + \{S_c\}_I - \{R\}_{I-1}. \tag{17}$$

In the above, $\{(\ )\}_I$ indicates the quantity at the end of the Ith increment and $(\Delta(\ ))_I$ the increment in the quantity for the Ith increment. The incremental node displacements are denoted $\{\Delta Q\}_I$. The remaining terms of (17) are as follows:

$$[K] = \sum_e \int_{V_e} [B]^T[E][B]\,dV \tag{18}$$

$$\{T\}_I = \sum_e \oint_{S_{t_e}} [N]^T\{\bar{t}\}_I\,dS \tag{19}$$

$$\{S_c\}_I = \sum_e \int_{V_e} [B]^T[E]\{\Delta\epsilon^c\}_I\,dV \tag{20}$$

$$\{R\}_{I-1} = \sum_e \int_{V_e} [B]^T\{\tau\}_{I-1}\,dV. \tag{21}$$

The form of (17) makes this an initial strain formulation. It can be seen that $[K]$ is the elastic stiffness matrix and remains unchanged throughout the time incrementing process. The quantities $\{\Delta\epsilon^c\}_I$ in (20) are predicted prior to the solution of (17) using (1) and $\{\tau\}_{I-1}$. Having solved (17), and thus obtained $\{\Delta\epsilon\}_I$, the actual values of $\{\Delta\epsilon^c\}_I$ and $\{\Delta\tau\}_I$ are obtained by subdividing the time step and performing an Eulerian integration based on subincrements of $\{\Delta\epsilon\}_I$. As a result of this integration procedure, better adherence to the postulated constitutive law (1) is achieved but at the price of introducing some disequilibrium (i.e. $\{R\}_I \neq \{T\}_I$). This disequilibrium is corrected, however, in the next time step as a consequence of $\{R\}_{I-1}$ appearing in (17).

The time step size for the calculations is automatically regulated based on two criteria. The first criteria is the maximum error in the predicted creep strain increments used in solving (17) as compared to the creep strain increments from the subsequent integration procedure. The second criteria is the maximum creep strain increment compared to the total elastic strain. In the present study, the criterion for maximum error in predicted creep strain is 20% and the criterion for maximum creep strain increment is 100%. For problems which have been considered, it appears that the above model and criteria give accurate transient solutions and converged steady-state solutions with time step size comparable to those used with more expensive tangent stiffness methods.

VERIFICATION OF MODEL

A compact specimen has been chosen for verifying the model. The particular geometry and materials were chosen to coincide with those used by Ehlers and Riedel[7] and are illustrated in Fig. 3 along with the two finite element meshes used in the verification. Both meshes consist entirely of eight-noded isoparametric elements, assume plane strain conditions and use collapsed (i.e. triangular) elements at the crack-tip. For the 102 element model these crack-tip elements are given a singular strain field ($r^{-1/2}$) by shifting the appropriate midside nodes to their quarter-points. The 300 element model uses a non-singular crack-tip.

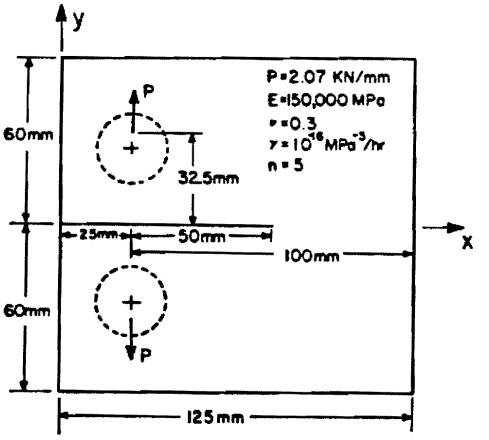

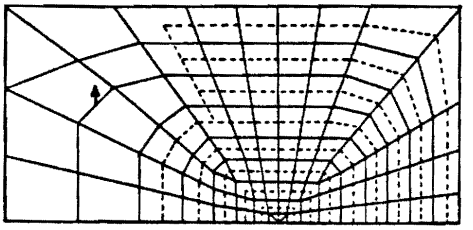

The 102 element mesh (331 nodes; 642 d.o.f.)

The 300 element mesh (941 nodes; 1840 d.o.f.)

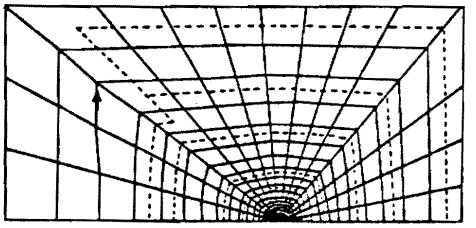

Fig. 3. Summary of geometry, loading, material properties and finite element meshes for the compact specimen.

The elastic J_1 for the 300 and 102 element meshes are 24.1 and 24.3 N/mm, respectively and agree with the value 24.2 N/mm from Srawley[8] to well within 1%. The steady-state ($t = 600$ hr) values of C† for the 300 and 12 element meshes are 131 and 130 N/m · hr, respectively, and agree well with 134 N/m · hr from Shih and Kumar[9] and 137 N/m · hr ($t \approx 300$ hr) from Ehlers and Riedel[7]. Based on these results it is concluded that the numerical procedure in general and the quarter-point crack-tip elements in particular, are accurate and efficient tools for creep fracture analysis.

CALCULATIONS OF $(\dot{T}_1)_C$ AND $(\dot{T}_1)_c^\delta$

Now we consider calculations of $(\dot{T}_1)_c$ (i.e. $(\Delta T_1)_c/\Delta t$). The 300 element mesh results for $(\dot{T}_1)_c$, as computed from (5), are shown in Fig. 4 as the solid curve. This curve shows the time dependence of $(\dot{T}_1)_c$ during the non-steady portion of the creep calculation. The steady-state value of $(\dot{T}_1)_c$ is 130 N/m · hr and thus is in agreement with the previously mentioned relationship between $(\dot{T}_1)_{ss}$ and C†. In [6] it was found that the evaluation of (5) using the 102 element mesh gave values of $(\dot{T}_1)_c$ which were generally in poor agreement with those of the 300 element mesh.The volume integral of (5) was determined to be the cause of this behavior and it was supposed that the origin of the problem was the use of the $r^{-1/2}$ strain singularity as opposed to the HRR type singularity (i.e. $r^{-n/(1+n)}$). However, several calculations with special conforming elements which impose the HRR type radial dependence of strain[10], have shown that this is not the case.

It now seems that the difficulty experienced in computing $(\dot{T}_1)_c$ when using singular crack-tip

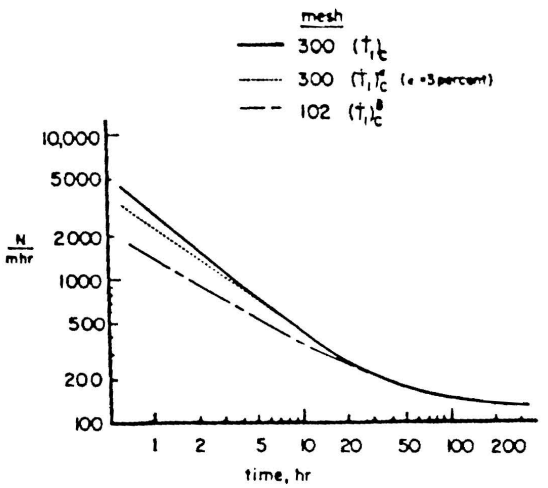

Fig. 4. Comparison of $(\dot{T}_1)_c$ and $(\dot{T}_1)_c^{\delta}$ for the compact specimen.

elements is related to the existence argument for the limit of the volume integral in (3). For the case when the asymptotic field has singular radial dependence but does not identically satisfy the following condition on angular behavior,

$$\operatorname*{Lt}_{\epsilon \to 0} \int_{-\pi}^{\pi} \frac{\partial \tau_{ij}(\epsilon, \theta)}{\partial x_1} \Delta \epsilon_{ij}(\epsilon, \theta)\, \mathrm{d}\theta = 0 \tag{22}$$

the subject limit in (3) does not exist (as discussed in Appendix A of [6]). The condition (22) need not be satisfied exactly if one does not have a singular radial dependence as is demonstrated by the results from the 300 element mesh.

The efficiency, simplicity and general accuracy of the quarter-point element procedure makes it a very attractive alternative to the use of very refined nonsingular meshes or the derivation of singular crack-tip elements which satisfy (22) *a priori*. Therefore, a practical solution to this problem is sought. As noted above, the difficulty is associated with the volume integral over the singular elements. Therefore, calculations were made in which the volume integral over the crack-tip elements was omitted. The resulting quantity, which we call $(\dot{T}_1)_c^{\delta}$, can be written

$$(\dot{T}_1)_c^{\delta} = \int_{\Gamma_{234}} \left[n_1 \Delta W - n_j (\tau_{jk} + \Delta \tau_{jk}) \frac{\partial \Delta u_k}{\partial x_1} \right] \mathrm{d}S - \int_{V - V_{\delta}} \frac{\partial \tau_{jk}}{\partial x_1} \Delta \epsilon_{jk}\, \mathrm{d}V \tag{23}$$

where V_{δ} consists of the singular crack-tip elements. The dashed curve of Fig. 4 is $(\dot{T}_1)_c^{\delta}$ from the 102 element mesh. It can be seen that $(\dot{T}_1)_c^{\delta}$ coincides with the solid curve for times after about 30 hr. For this mesh and problem it can therefore be said that $(\dot{T}_1)_c^{\delta}$ is a valid path-independent, crack-tip parameter for times after 30 hr and for values of $(\dot{T}_1)_c$ beginning at approx. 1.6 of the steady-state value. The steady-state parameter $C^{\dagger}$ is still significantly path-dependent at 30 hr.

For the 102 element mesh, the crack-tip elements are 5% of the ligament size. We therefore assign δ a value of 0.05. A quantity similar to $(\dot{T}_1)_c^{\delta}$ was computed using the 300 element mesh. In this case, a semi-circular region of radius approx. 3% of the ligament was omitted from the evalution of the volume integral of (5). This result which we denote $(\dot{T}_1)_c^{\epsilon}$ with $\epsilon = 3\%$ is also shown in Fig. 4. This curve seems to indicate that the validity of $(\dot{T}_1)_c^{\delta}$ can be expanded to earlier times with rather moderate reductions in the crack-tip, quarter-point element size. For example, the results of Fig. 4 indicate that a δ of 3% of the ligament would result in $(\dot{T}_1)_c^{\delta}$ being valid as early as seven hours and for $(\dot{T}_1)_c$ as large as 4.3 its steady-state value.

CREEP CRACK GROWTH IN A STRIP

We now consider the problem of a finite height ($2h$) infinitely wide strip, with a semi-infinite crack. Loading consists of uniformly applied displacement rates ($\dot{\delta}$) at the top and bottom edges ($y = \pm h$) such

that Mode I behavior results. This problem has been chosen for two reasons. First, since the strip is infinitely wide and the boundary conditions do not change with time, the propagating crack-tip fields can be expected to reach a "convecting steady-state" creep condition. Here we use the phrase "convecting steady-state" to mean that the field remains unchanged in time with respect to a coordinate system which is centered at and moving with the crack-tip. This terminology is used so as not to confuse this condition with the usual steady-state creep condition in which material stress rates are zero.

The second reason for choosing this problem is that C^*† can be evaluated analytically for the special case of steady-state creep (stationary crack). The analytical evaluation of (10) follows easily if one chooses a rectangular contour in which the horizontal portions coincide with the top and bottom edges of the strip (i.e. $y = \pm h$) and the vertical portions are at $x = \pm\infty$. In such a contour one finds only the vertical portion at $x = +\infty$ is non-zero and therefore

$$C^* = 2hW^*_{\infty}. \tag{24}$$

For the corresponding elastic problem with applied displacement δ, one finds a similar relation.

$$J_1 = 2hW_{\infty}. \tag{25}$$

It has been noted that $(\dot{T}_1)_{ss}$ and C^*† are related and therefore it is possible to obtain $(\dot{T}_1)_{ss}$ from (14) and (24). The direct evaluation of $(\dot{T}_1)_c$ in terms of either its integral representation (5) or its energy representation (6) requires knowledge of the stresses in the region of the strip adjacent to the crack-tip and therefore is not a trivial task.

The material properties used in this problem are representative of 304 stainless steel at 650°C. These material properties and the finite element discretization are given in Fig. 5. Note that collapsed, eight-noded, quarter-point elements are used at the crack-tip.

The mesh for this problem may at first appear rather coarse; however, elastic and steady-state creep solutions obtained with this mesh are sufficiently accurate to justify its use for the study at hand. The comparison of computed elastic J_1 values and steady-state C^*† values with their analytic values is given in Table 1.

The first step in this numerical study is to select three values of C^*† which span the range of values reported in the literature for 304 stainless steel at 650°C.† The values which have been chosen are 0.05, 5.0 and 50.0 N/mm · hr. Having these values, the remote ($x = \infty$) steady-state τ_{yy} are determined as well as the edge displacement which results in the same remote elastic τ_{yy}. These displacements are applied to the model elastically at $t = 0$. Next, the steady-state edge displacement rates are determined analytically.

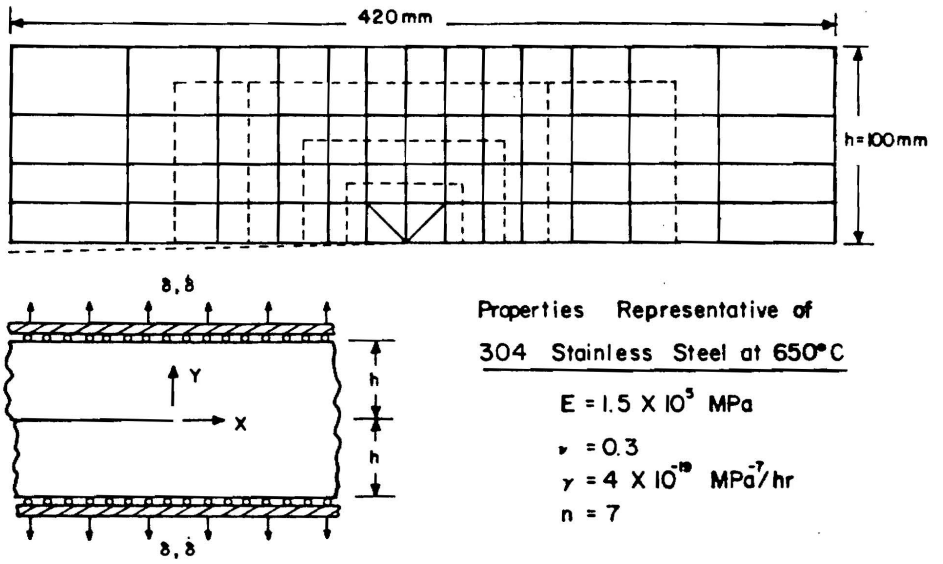

Fig. 5. Summary of geometry, loading, material properties and finite element mesh for the strip problem.

†The use of C^*† rather than $(\dot{T}_1)_c$ is due to the existence of the analytical expression (24) and is justified by the numerical similarity to $(\dot{T}_1)_c$ for plane strain conditions.

Table 1. Summary of analysis parameters for creep crack growth in the plane strain strip of Fig. 5.

Analytical Results					Computed Results		$\frac{da}{dt}$ from (6.4) (mm/hr)	
C_1^* (N/mm·hr)	remote τ_{yy} (MPa)	$\dot{\delta}$ (mm/hr)	δ (elastic) (mm)	J_1 (N/mm)	C_1^* (N/mm·hr)	J_1 (N/mm)	average	upper bound
0.05	83	3.44×10^{-4}	5.04×10^{-2}	4.18	4.99×10^{-2}	4.19	1.00×10^{-4}	5.00×10^{-4}
5.0	148	1.94×10^{-2}	8.95×10^{-2}	13.2	4.99	13.2	2.22×10^{-2}	1.11×10^{-1}
50	197	1.45×10^{-1}	1.19×10^{-1}	23.5	49.8	23.5	3.30×10^{-1}	1.65

Using the elastic solution as an initial state, the displacement rate, $\dot{\delta}$, is applied until the model reaches steady-state.

The next step in this study involves the selection of upper bound crack velocities for the three chosen values of C_1^*. The following formula is based on the experimental data reported in [3, 4] and represents data from center-crack, double-edge-crack, compact, and round bar specimen types.

$$\frac{da}{dt} = \alpha [C_1^*]^{1.173} \tag{26}$$

$$\text{where } \alpha = \begin{cases} 1.68 \times 10^{2} \text{ (upper bound)} \\ 3.36 \times 10^{-3} \text{ (average)} \end{cases}$$

Having reached steady-state, the crack is propagated at the upper bound velocity of (26) until it is determined that a convecting steady-state has been reached.

The crack growth simulation is accomplished through a combination of mesh shifting and periodic remeshing as illustrated in Fig. 6. The region A represents the quarter-point elements which remain centered about the crack-tip. The B type elements are standard eight-noded isoparametric elements which distort during mesh shifting so as to keep region A centered at the crack-tip. The procedure is to shift the region A (and thus the crack-tip) by shifting appropriate nodes of the region A and type B elements. This shifting is done without altering element connectivity. Eventually the type B elements become overly distorted at which time the element connectivities are redefined in the vicinity of the crack-tip so that additional shifting is possible.

Each occurrence of shifting or remeshing requires that shifted nodes have their displacements interpolated and that shifted elements have their 2×2 Gauss point stresses interpolated. The displacement interpolation is by the usual isoparametric shape functions. The stress interpolation uses linear, two-dimensional Lagrangian polynomials in element local coordinates. In the following calculations, the nominal size of the crack growth increments is 0.4 mm or 2% of the crack-tip element width. For the

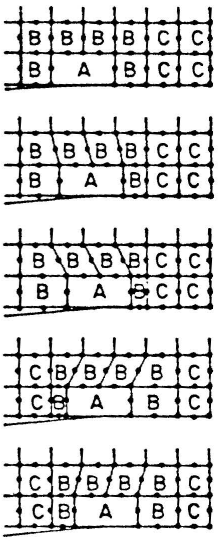

Fig. 6. Illustration of mesh shifting/remeshing procedure for simulation of crack growth.

highest velocity case ($C\dagger = 50$ N/mm · hr), this results in crack growth at approximately every fifth solution step.

RESULTS FOR A PLANE STRAIN STRIP

The results of the plane strain strip calculation with $C\dagger = 50$ N/mm · hr and $(da/dt) = 1.65$ mm/hr are given in Fig. 7. The values of $(\dot{T}_1)_c^{\delta}$ and C_1^* are given for the portion of the calculation prior to steady-state as well as during the crack propagation portion. The band represents the range of values obtained from the four contours illustrated in Fig. 5. Both $(\dot{T}_1)_c^{\delta}$ and $C\dagger$ converge to the 50 N/mm · hr value at steady-state. During the crack propagation, it is seen that $(\dot{T}_1)_c^{\delta}$ and $C\dagger$ do not depart significantly from their steady-state value. This means that this combination of loading and crack speed results in the crack-tip fields being essentially at steady-state conditions. This in turn means that both $(\dot{T}_1)_c^{\delta}$ (or $(\dot{T}_1)_c$) and C_1^* are valid crack-tip field parameters during crack growth.

A closer view of the crack propagation portion of these curves is given in Fig. 8. The dashed curves bracketing the initial portion of the solid curves represent the degree of path-independence and continue to be representative of the path-independence observed during the crack propagation steps. For both $(\dot{T}_1)_c^{\delta}$ and $C\dagger$, it is seen that the strip has essentially returned to its steady-state condition prior to each crack growth increment. It is thought that the larger departure of $(\dot{T}_1)_c^{\delta}$ from steady-state (as compared to $C\dagger$) is more representative of the non-steadiness of the crack-tip field since the validity of $C\dagger$ in general and the numerical evaluation of W^* (13) in particular, are based on the existence of steady-state conditions.

The effect of remeshing is seen at approximately eight hours. The first two steps after the remeshing were found to result in rather erratic contour integral values and are not indicated in these figures. The equilibrium correction feature of the present model and the automatic time step regulation procedure both act to quickly restore equilibrium at the crack-tip.

The propagation portion of the calculation with $C\dagger = 5$ N/mm · hr and $(da/dt) = 0.111$ mm/hr is given in Fig. 9. Here again it is seen that both $(\dot{T}_1)_c^{\delta}$ and $C\dagger$ have converged to the analytical value of $C\dagger$ (to within 2%, which is also about the degree of path-independence). Comparing these results with those in Fig. 8 for the higher $C\dagger$ and crack speed it is seen that steady-state creep conditions were not reached until 12 hr as opposed to approximately two hours in previous cases. Also, the return to the steady-state value after mesh shifting takes more time (two hours compared to 0.25 hr). However, when compared to the time between crack growth steps (both use 0.4 mm) it is seen that the lower velocity case returns to steady-state well before the next growth step occurs. This result indicates that lower load levels and crack speeds are inherently closer to steady-state conditions. While this behavior seems intuitively correct, it should be kept in mind that these results depend on the empirical formula (26) which is valid only for 304 stainless steel. It remains to be seen if similar behavior occurs in other materials.

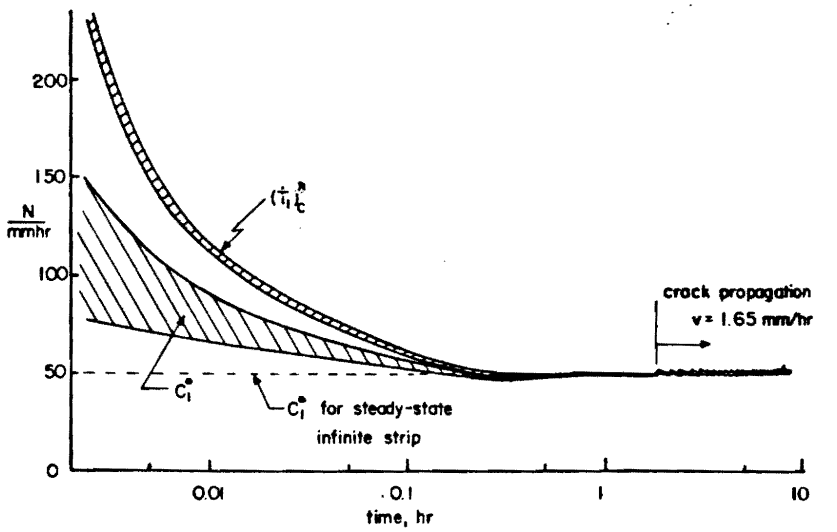

Fig. 7. History of $(\dot{T}_1)_c^{\delta}$ and $C\dagger$ for creep crack growth in a plane strain strip (steady-state $C\dagger$ = 50 N/mm · hr, $da/dt = 1.65$ mm/hr).

as close agreement between C^* and $(\dot{T}_1)_c$ in the case of plane stress. The primary purpose of this analysis is to verify this predicted behavior.

For this plane stress analysis, C^* was chosen to be 50 N/mm · hr and the crack was again propagated at 1.65 mm/hr. The remote τ_{yy}, the steady-state displacement rate, $\dot{\delta}$, and the elastic displacement, δ, are 171 MPa, 0.168 mm/hr and 0.114 mm, respectively.

The results of this calculation are given in Fig. 10 and 11. It is seen from these figures that $(\dot{T}_1)_c^{\delta}$ does converge to a somewhat higher value at steady-state than C^*. The steady-state value is seen from Fig. 11 to be approximately 52 N/mm · hr which is higher than C^* by four percent. While this is a somewhat smaller difference than suggested in [6], the sign of the difference is the same. In light of the approximate integration used in obtaining the numeric values in [6], this discrepancy is within reason. As expected, the general behavior for plane stress conditions is essentially the same as for the previous plane strain analyses. Therefore, previous observations concerning the steady-state nature of the crack-tip fields during crack propagation are unchanged by the shift to plane stress conditions.

SUMMARY AND CONCLUSIONS

It has been noted that despite the fact that C^* characterizes the crack-tip fields under steady-state creep conditions, it does not have an energy or energy rate interpretation. A related path-independent integral parameter $(\dot{T}_1)_c$, however, does have the energy rate interpretation commonly attributed to C^*. The derivation of $(\dot{T}_1)_c$ does not rely on the existence of steady-state creep conditions and thus is a valid crack-tip parameter for non-steady creep conditions as well as for steady-state creep.

An initial strain finite element approach which provides for improved adherence to postulated constitutive behavior and for equilibrium correction has been summarized. The accuracy and efficiency of this model with eight-node isoparametric elements and the quarter-point crack-tip element approach have been verified through several calculations for a compact specimen geometry and a strip geometry. Also, a method of simulating crack growth through shifting of the quarter-point singularity elements and periodic remeshing has been described and demonstrated.

A creep crack growth simulation for 304 stainless steel has shown that for realistic load levels and corresponding crack speeds the crack-tip field is essentially at a steady-state creep condition. This means that for this material the propagating crack-tip field is largely unaffected by the history of crack-growth or the history of loading. This feature can greatly reduce the analysis required for predicting creep crack growth behavior in a component as can be seen from the following suggested methodology.

We assume that the crack propagation speed (da/dt) is related to $(\dot{T}_1)_{ss}$ (i.e. $-(d\dot{U}/dt)$) through the power law suggested by experimental data [3, 4].

$$\frac{da}{dt} = \alpha[(\dot{T}_1)_{ss}]^{\beta}. \tag{27}$$

Next we determine (e.g. by steady-state creep finite element analysis) $(\dot{T}_1)_{ss}$ as a funcion of crack length. Because of the assumed steady-state crack-tip behavior, this can be accomplished by considering several discrete crack lengths and then fitting a curve. No crack growth simulation procedures are necessary. Combining (27) with this result provides the following relationship between time and crack length

$$t = \int_{a_0}^{a(t)} \frac{[(\dot{T}_1)_{ss}]^{-\beta}}{\alpha}\, da + t_i \tag{28}$$

where a_0 is the initial crack length and t_i is the time when crack growth initiates. The only unknown quantity in (28) is the initiation time t_i.

Vitek [11] has simulated several experiments (compact and double-edge-crack specimens) on two CrMoV steels using a dislocation model and has concluded that COD correlated well with the initiation of crack growth in these experiments. If the same conclusion is valid for 304 stainless steel, then one can presumably predict a t_i based on a transient finite element analysis of the initial flawed configuration and a critical value of COD. If initiation occurs long after steady-state conditions are reached, it is then reasonable to estimate t_i using the rate of COD obtained from a steady-state finite element solution. At this time, the validity of (28) and of the critical COD concept has not been investigated by the authors.

Acknowledgements—The support for this work provided by NASA-Lewis Research Center under grant NAG 3-38 is gratefully acknowledged. Ms. M. Eibeman deserves a note of thanks for her assistance in the preparation of this manuscript.

REFERENCES

[1] L. S. Fu, Creep crack growth in technical alloys at elevated temperature-a review. *Engng Fracture Mech.* **13**, pp. 207–330. (1980).
[2] J. D. Landes and J. A. Begley, A fracture mechanics approach to creep crack growth. *Mechanics of Crack Growth*, ASTM STP 590, pp. 128–148 (1976).
[3] J. Ohji, K. Ogura and S. Kubo, The application of modified J-Integral to creep crack growth in austenitic stainless steel and Co-Mo-V steel. *Engng Aspects of Creep*, Proc. Conf. at Univ. Sheffield, I. Mech. E., pp. 9–16 (1980).
[4] R. Koterazawa and T. Mori, Applicability of fracture mechanics parameters to crack propagation under creep conditions. *J. Engng Materials and Technol.* Series H, **99**, pp. 298–305 (1977).
[5] S. N. Atluri, Path-independent integrals in finite elasticity and inelasticity, with body forces, inertia, and arbitrary crack-face conditions. Rep. GIT-CACM-SNA-81-8, Georgia Institute of Technology, March, 1981, also *Engng Fracture Mech.* (in press).
[6] R. B. Stonesifer and S. N. Atluri, On a study of the $(\Delta T)_c$ and C^* integrals for fractue analysis under non-steady creep. Rep. GIT-CACM-SNA-81-21, Georgia Institute of Technology, July 1981, also *Engng Fracture Mech.* (in press).
[7] R. Ehlers and H. Riedel, A finite element analysis of creep deformation in a specimen containing a macroscopic crack. *Advances in Fracture Research*, Vol 2, (Edited by D. Francois) Fifth Intl. Conf. on Fracture, Cannes, pp. 691–698 (1981).
[8] J. F. Srawley, Wide range stress intensity factor expressions for ASTM E399 standard fracture toughness specimens. *Int. J. Fracture* **12**, pp. 475–476 (1976).
[9] C. F. Shih and V. Kumar, Estimation technique for the prediction of elastic-plastic fracture of structural components of nuclear systems. Contract RP 1237-1, First Semiannular Report for Electric Power Research Institute, General Electric Co., Report, 1979.
[10] R. B. Stonesifer, Fast brittle fracture and creep crack growth: moving singularity finite element analysis Ph.D. Dissertation, Dept. of Civil Engineering, Georgia Institute of Technology, 1981.
[11] V. Vitek, A theory of the initiation of creep crack growth. *Int. J. Fracture* **13** pp. 39–50 (1977).

(*Received* 30 *September* 1981; *received for publication* 11 *November* 1981)

Engineering Fracture Mechanics Vol. 16, No. 5, pp. 625–643, 1982
Printed in Great Britain.

0013-7944/82/050625-19$03.00/0
Pergamon Press Ltd.

124

ON A STUDY OF THE $(\Delta \underline{T})_c$ AND C^* INTEGRALS FOR FRACTURE ANALYSIS UNDER NON-STEADY CREEP†

R. B. STONESIFER and S. N. ATLURI
Center for the Advancement of Computational Mechanics, School of Civil Engineering, Georgia Institute of Technology, Atlanta, GA 30332, U.S.A.

Abstract—The validity of the parameter $(\Delta \underline{T})_c$ (which was previously introduced by one of the authors), its meaning, and its calculation, in the analysis of cracked bodies under non-steady creep conditions, are studied. Comparisons are made with the widely used parameter C^*, which is valid for steady-state creep. An efficient finite element method for general, small-strain, elastic/viscoplastic analyses is described and the results of an example calculation for a standard compact specimen are presented and discussed.

INTRODUCTION

METHODS for improved accuracy of life predictions of components subjected to low-cycle creep-fatigue are currently in great demand. Present procedures too often require a component to be resigned from service at a time when a significant portion of its useful life still remains. A contributing factor to this state of affairs is the lack of a parameter which correlates well with a wide range of crack growth data. The most common parameters which have been studied are the elastic stress intensity factor K_I, the net section stress σ_{net}, and in the case of steady-state creep, a path-independent integral C^* (see [1] for a review). Whereas, K_I and C^* are parameters applicable to geometries with macroscopic cracks, σ_{net} seems mostly applicable to geometries where large portions of the body are subjected to stress levels of a magnitude to induce void growth and the formation of micro-cracks.

The parameters K_I and C^* are clearly related to opposite extremes of the creep cracking phenomena. That is, very localized creep behavior and/or fast propagation rates would imply that the crack-tip region is controlled by an elastic field which is characterized by K_I, whereas widespread creep and very slow propagation speeds would imply that the crack-tip field is essentially at steady-state and therefore characterized by C^*. If the crack behavior lies between these extremes, then it is doubtful if either parameter is applicable.

In the present study we consider a new parameter $(\Delta \underline{T})_c$ which has recently been developed by Atluri[2]. This parameter which is a path-independent integral, vector quantity has the attractive feature that it characterizes the crack-tip field for both the extreme cases discussed above, as well as all behavior between. In addition to its role as a crack-tip field characterizing parameter, $(\Delta \underline{T})_c$ also has an energy interpretation‡[2].

In as much as $(\Delta \underline{T})_c$ is a new parameter, the present study is primarily intended to further explore the parameter, its meaning, its calculation, and finally to give the results of an example calculation for a standard compact specimen. In the process of doing this, an efficient finite element method for general elastic/viscoplastic analysis is also described.

PRELIMINARIES

We shall consider problems of creep wherein

$$\dot{\epsilon}_{ij} = \epsilon^e_{ij} + \epsilon^c_{ij} = L_{ijkl}\dot{\sigma}^*_{kl} + (3/2)\gamma(\sigma_{eq})^{n-1}\sigma'_{ij}. \tag{1}$$

If we denote $\dot{u}_i$ as the rate of displacement from the current configuration, then $\dot{\epsilon}_{ij}$ is the symmetric part of the rate of displacment gradient $\dot{e}_{ij} \equiv (\underset{\sim}{\nabla}_t \dot{u})^T = (\partial \dot{u}_i/\partial y_j) \equiv \dot{\epsilon}_{ij} + \dot{\omega}_{ij}$. The gradient operator $\underset{\sim}{\nabla}_t$ is with respect to the current coordinates y_i (as opposed to the coordinates of the underformed body x_i). L_{ijkl} is the tensor of instantaneous elastic moduli. We let $\dot{\sigma}^*_{kl}$ denote the corotational rate (or "Zaremba–Jaumann rate") of the Kirchhoff stress σ_{ij} where σ_{ij} is related to the Cauchy stress τ_{ij} by $\sigma_{ij} = J\tau_{ij}(J = \det[\partial y_m/\partial x_n])$. The equivalent Kirchhoff stress σ_{eq} is related to the deviatoric Kirchhoff stress

†This paper is based on a part of a Ph.D. thesis to be submitted by the first author.

‡Since C^* does not have a similar energy interpretation (even at steady-state), it seems that experimental efforts to measure C^* are most likely resulting in the measurement of $(\Delta \underline{T})_c$ instead.

$\sigma'_{ij}(=\sigma_{ij}-1/3\sigma_{kk}\delta_{ij})$ by $\sigma_{eq}=(3/2)(\sigma'_{ij}\sigma'_{ij})^{1/2}$. The parameters γ and n are those of the familiar Norton's law

$$\dot{\epsilon}_{eq}=\gamma(\sigma_{eq})^n$$

where

$$\dot{\epsilon}_{eq}=[(2/3)\dot{\epsilon}_{ij}\dot{\epsilon}_{ij}]^{1/2}.$$

In the following, we use the notation: $(\underline{\ })$ denotes a second order tensor; $(\underline{\ })$ implies a vector; $\underline{a}=\underline{B}\cdot\underline{c}$ implies $a_i=B_{ij}c_j$; $\underline{A}=\underline{B}\cdot\underline{C}$ implies $A_{ij}=B_{ik}C_{kj}$; $\underline{A}:\underline{B}=A_{ij}B_{ij}$.

A CONSERVATION LAW AND $(\Delta T)_c$

A conservation integral relation given by Atluri[2], for a closed volume V_t (at the current time, t), which is free from singularities and any other defects (which would preclude the application of the divergence theorem), for the special case of material behavior characterized by (1), is:

$$\begin{aligned}\underline{0}=\int_{V_t}\{&\nabla_t\Delta W-(\nabla_t\underline{\tau}):\Delta\underline{e}-\nabla_t\cdot[(\underline{\tau}+\Delta\underline{t})\cdot\Delta\underline{e}]\\&-\rho_t(\underline{f}-\underline{a})\cdot\Delta\underline{e}\}\,dV+\int_{S_t}[\underline{n}_t\cdot(\underline{\tau}+\Delta\underline{t})-\bar{\underline{t}}]\cdot\Delta\underline{e}\,dS\\&+\int_{S_c}\underline{n}_t\cdot(\underline{\tau}+\Delta\underline{t})\cdot(\Delta\underline{e}-\Delta\bar{\underline{e}})\,dS.\end{aligned}\tag{2}$$†

In (2), $\Delta\underline{t}$ is the incremental first-Piola–Kirchhoff (nonsymmetric) stress ($\Delta\underline{t}=[\Delta\underline{\sigma}-\Delta\underline{e}\cdot\underline{\sigma}]/J$, where $\Delta\underline{\sigma}$ is the material increment of Kirchhoff stress. The current mass density is denoted ρ_t, and $\underline{f}$, and $\underline{a}$ are the body force and acceleration vectors at time $t+\Delta t$, respectively. The current outward normal to V_t is $\underline{n}_t$. The quantity ΔW, discussed in detail in[2], is the incremental stress-working density in time Δt, and is given by:

$$\Delta W=\underline{\tau}:\Delta\underline{e}+\frac{1}{2}\Delta\underline{t}^T:\Delta\underline{e}\equiv\underline{\tau}:\Delta\underline{e}+\Delta U\tag{3}$$

where

$$\Delta U=\frac{1}{2}\Delta\underline{t}^T:\Delta\underline{e},\text{ such that, }\Delta\underline{t}^T=\frac{\partial\Delta U}{\partial\Delta\underline{e}}.\tag{4}$$

The validity of (2) is readily verified through the two identities[2]:

$$\begin{aligned}\nabla_t\Delta W=\nabla_t(\underline{\tau}:\Delta\underline{e})+\nabla_t(\Delta U)=\nabla_t\underline{\tau}:\Delta\underline{e}+[\underline{\tau}:(\Delta\underline{e});{}_m\underline{g}^m]\\+[\Delta\underline{t}^T:(\Delta\underline{e});m\underline{g}^m]\end{aligned}\tag{5}$$

and

$$\nabla_t\cdot[(\underline{\tau}+\Delta\underline{t})\cdot\Delta\underline{e}]=[\nabla_t\cdot(\underline{\tau}+\Delta\underline{t})]\cdot\Delta\underline{e}+[(\underline{\tau}+\Delta\underline{t})^T:(\Delta\underline{e});{}_m\underline{g}^m]\tag{6}$$

the satisfaction of linear momentum balance in V_t:

$$\nabla_t\cdot[\underline{\tau}+\Delta\underline{t}]+\rho_t(\underline{f}-\underline{a})=0\tag{7}$$

and the satisfaction of the boundary conditions:

$$\underline{n}_t\cdot[\underline{\tau}+\Delta\underline{t}]=\bar{\underline{t}}\text{ on }S_t\tag{8}$$

$$\Delta\underline{e}=\Delta\bar{\underline{e}}\text{ on }S_c\tag{9}$$

†The validity of (2) does *not* require $S_t+S_c=\partial V_t$ where ∂V_t denotes the surface bounding V_t.

Note that identity (5) assumes that $\underline{\tau}$ (the initial stress for the increment) is an explicit function of its position in V_t. The existence of ΔU is discussed in the work of Atluri[3, 4].

The conservation integral (2) is used[2] to obtain a "path-independent integral" which is applicable to the analysis of cracks by considering a volume $V_t - V_\epsilon$ such as illustrated in Fig. 1. (Note that a two-dimensional case is illustrated for simplicity.) The use of the divergence theorem for the region depicted in Fig. 1 results in (2) being rewritten

$$\int_{\Gamma_{234}} \{\underline{n}_t \Delta W - \underline{n}_t \cdot [(\underline{\tau} + \Delta \underline{t}) \cdot \Delta \underline{e}]\} \, dS + \int_{V_t - V_\epsilon} [(-\underline{\nabla}_t \underline{\tau}) : \Delta \underline{e} - \rho_t (\underline{f} - \underline{a}) \cdot \Delta \underline{e}] \, dV$$
$$+ \int_{\Gamma_{12}} \underline{n}_t \Delta W \, dS + \int_{\Gamma_{45}} \underline{n}_t \Delta W \, dS - \int_{S_t} \bar{\underline{t}} \cdot \Delta \underline{e} \, dS - \int_{S_\epsilon} \underline{n}_t \cdot [(\underline{\tau} + \Delta \underline{t}) \cdot \Delta \bar{\underline{e}}] \, dS$$
$$= \int_{\Gamma_\epsilon} \{\underline{n}_t \Delta W - \underline{n}_t \cdot [(\underline{\tau} + \Delta \underline{t}) \cdot \Delta \underline{e}]\} \, dS \equiv (\Delta \underline{T})_c^\epsilon. \tag{10}$$

In writing (10) it has been assumed that $S_\epsilon + S_t = \Gamma_{12} + \Gamma_{45}$ (so as to have a well posed boundary value problem) but that S_t and S_ϵ do not include any of the contour Γ_{234}. Equation (10) is used to define the quantity $(\Delta \underline{T})_c$ where it can be assumed without loss of generality that $\Gamma_\epsilon = \Gamma_{165}$ is a circle of radius ϵ centered at the crack-tip. Clearly, $(\Delta \underline{T})_c^\epsilon$ will depend on ϵ but not on the selection of Γ_{234}.

Following the reasoning of Atluri[2], we define $(\Delta \underline{T})_c$ as the limit of $(\Delta \underline{T})_c^\epsilon$ as ϵ goes to zero.†

$$(\Delta \underline{T})_c = \operatorname*{Lt}_{\epsilon \to 0} \int_{\Gamma_\epsilon} \{\underline{n}_t \Delta W - \underline{n}_t \cdot [(\underline{\tau} + \Delta \underline{t}) \cdot \Delta \underline{e}]\} \, dS \equiv \int_{\Gamma_{234}} \{\underline{n}_t \Delta W - \underline{n}_t \cdot [(\underline{\tau} + \Delta \underline{t}) \cdot \Delta \underline{e}]\} \, dS$$
$$+ \operatorname*{Lt}_{\epsilon \to 0} \left\{ \int_{V_t - V_\epsilon} (-\underline{\nabla}_t \underline{\tau}) : \Delta \underline{e} - \rho_t (\underline{f} - \underline{a}) \cdot \Delta \underline{e}] \, dS \right. \tag{11}$$
$$\left. + \int_{\Gamma_{12}} \underline{n}_t \Delta W \, dS + \int_{\Gamma_{45}} \underline{n}_t \Delta W \, dS - \int_{S_t} \bar{\underline{t}} \cdot \Delta \underline{e} \, dS - \int_{S_\epsilon} \underline{n}_t \cdot [(\underline{\tau} + \Delta \underline{t}) \cdot \Delta \bar{\underline{e}}] \, dS \right\}.$$

It is clear that $(\Delta \underline{T})_c$ as defined by (11):

(i) Characterizes the crack-tip field.

(ii) Can be evaluated via the arbitrary contour integral Γ_{234} and the volume integral over the region bounded by Γ_{234}.

For symmetrical deformation about the x_1 axis and cracks oriented along the x_1 axis with traction free

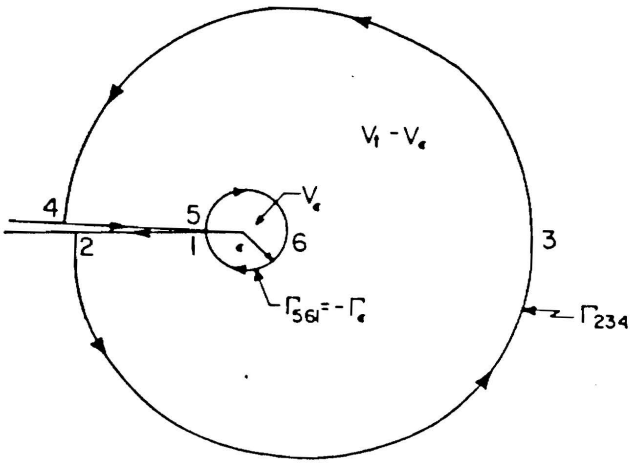

Fig. 1. Contours for applying the conservation integral to a two-dimensional, cracked body.

†The existence of the limit is discussed in Appendix A.

crack surfaces, no body forces and negligible inertial effects, the first component of $(\Delta \underline{T})_c$ is:

$$(\Delta \underline{T}_1)_c = \operatorname*{Lt}_{\epsilon \to 0} \int_{\Gamma_\epsilon} (n_1 \Delta W - n_j(\tau_{ji} + \Delta t_{ji}) \Delta e_{i1}] \, dS$$

$$\equiv \int_{\Gamma_{234}} [n_1 \Delta W - n_j(\tau_{ji} + \Delta t_{ji}) \Delta e_{il}] \, dS - \int_{V_t} \frac{\partial \tau_{ij}}{\partial y_1} \Delta e_{ij} \, dV. \tag{12}$$

Note that the limit of the volume integral has been written in its explicit form as a result of the existence arguments of Appendix A.

It has been shown by Atluri[2], that the vector $(\Delta \underline{T})_c$ has the following physical meaning. Let two cracked bodies be identical except for the second body having an additional, arbitrarily directed, infinitesimal increment in crack length characterized by the vector $d\underline{c}$. It is assumed that both bodies experience identical load histories. Define total potential energy increments corresponding to the time increment Δt as

$$\Delta E_1 = -\Delta \psi_1 - \Delta W_1^* - \Delta K_1^* \tag{13}$$

$$\Delta E_2 = -\Delta \psi_2 - \Delta W_2^* - \Delta K_2^* \tag{14}$$

for the first and second bodies, respectively. In (13), $-\Delta\psi$ is the incremental work of external forces, ΔW^* is the incremental stress-work and ΔK^* is the increment in the kinetic energy. (It should be noted that ΔW^* includes the inelastically dissipated energy.) Then

$$(\Delta T_i)_c dc_i = \Delta E_2 - \Delta E_1. \tag{15}$$

If one is only interested in self-similar crack extension in the x_1-direction, then $dc_2 = dc_3 = 0$ and

$$(\Delta T_1)_c = \frac{\Delta E_2 - \Delta E_1}{dc_1} \tag{16}$$

Therefore, $(\Delta \underline{T})_c$ can be related to the incremental total potential energy difference between two bodies which are identical except for an incremental crack length difference $d\underline{c}$.

It is worth emphasizing, as noted in[2], that the conservation law (2), and the attendant path-independent integral (10) or (11), are valid: (i) even when both elastic as well as creep strains are present, (ii) under steady as well as non-steady creep conditions, and (iii) when finite deformations are accounted for.

We now consider the special case of steady-state, pure creep behavior.

STEADY STATE CREEP AND C^*

It has been shown that $(\Delta \underline{T})_c$ characterizes the crack-tip field for materials which exhibit creep behavior such as in (1). It is known that under certain conditions of applied loading, the constitutive relation (1) can (after long times) result in a steady-state. This steady-state is primarily characterized by the time independence of the stresses (i.e. $\Delta U = \Delta t_{ji} = 0$). Specializing (11) and (12) to steady-state conditions, we define the steady-state value of $(\Delta \underline{T}_1)_c$.

$$(\Delta T_1)_{css} = \operatorname*{Lt}_{\epsilon \to 0} \int_{\Gamma_\epsilon} \{n_1 \tau_{ij} \Delta e_{ij} - n_j \tau_{ji} \Delta e_{i1}\} \, dS$$

$$= \int_{\Gamma_{234}} [n_1 \tau_{ij} \Delta e_{ij} - n_j \tau_{ji} \Delta e_{i1}] \, dS - \int_{V_t} \frac{\partial \tau_{ij}}{\partial y_1} \Delta e_{ij} \, dV. \tag{17}$$

Because (1) results in a power-law relation at steady-state, which is analogous to the power law deformation-theory plasticity (or essentially nonlinear elasticity), Goldman and Hutchinson[5] have suggested a path-independent C_1^* integral,

$$C_1^* = \int_\Gamma \left[n_1 W^* - n_j \tau_{ij} \frac{\partial \dot{u}_i}{\partial x_1} \right] dS \tag{18}$$

ere

$$W^* = \int_0^{\dot{\epsilon}_{ij}} \tau_{ij}\, \mathrm{d}\dot{\epsilon}_{ij} \tag{19}$$

ch that

$$\tau'_{mn} = \partial W^* / \partial \dot{\epsilon}_{mn}. \tag{19b}$$

ie question of how $C^\dagger$ and $(\Delta T_1)_{css}$ are related, is a natural one. Before obtaining an equation relating † to $(\Delta T_1)_{css}$, however, the conservation integral (2) will be used to derive a generalized *vector* integral *.

In specializing (2) to steady-state we note that now stress is a function of the strain-rate, and that ress-increments are zero. Thus, $\Delta W \equiv \underline{\tau}: \Delta \underline{e}$. Also we may write:

$$\int_{V_t} \{\underline{\nabla}_t \Delta W - (\underline{\nabla}_t \underline{\tau}): \Delta \underline{e}\}\, \mathrm{d}V = \int_{V_t} \underline{\tau}: \underline{\nabla}_t \Delta \underline{e}\, \mathrm{d}V \equiv \int_{V_t} [\underline{\tau}: (\Delta \underline{e}); {}_m\underline{g}^m]\, \mathrm{d}V. \tag{20}$$

ius, at steady-state, we may write (2) as:

$$\underline{0} = \int_{V_t} \{\underline{\tau}: (\underline{\nabla}_t \Delta \underline{e}) - \underline{\nabla}_t \cdot [\underline{\tau} \cdot \Delta \underline{e}] - \rho_t (\underline{f} - \underline{a}) \cdot \Delta \underline{e}\}\, \mathrm{d}V$$

$$+ \int_{S_t} [\underline{n}_t \cdot \underline{\tau} - \underline{\bar{t}}] \cdot \Delta \underline{e}\, \mathrm{d}S + \int_{S_\epsilon} \underline{n}_t \cdot \underline{\tau} \cdot (\Delta \underline{e} - \Delta \underline{\bar{e}})\, \mathrm{d}S \tag{21}$$

r equivalently, in rate form,

$$\underline{0} = \int_{V_t} \{\underline{\tau}: (\underline{\nabla}_t \dot{\underline{e}}) - \underline{\nabla}_t \cdot (\underline{\tau} \cdot \dot{\underline{e}}) - \rho_t (\underline{f} - \underline{a}) \cdot \dot{\underline{e}}\}\, \mathrm{d}V$$

$$+ \int_{S_t} [\underline{n}_t \cdot \underline{\tau} - \underline{\bar{t}}] \cdot \dot{\underline{e}}\, \mathrm{d}S + \int_{S_\epsilon} \underline{n}_t \cdot \underline{\tau} \cdot (\dot{\underline{e}} - \dot{\bar{\underline{e}}})\, \mathrm{d}S. \tag{22}$$

Since, at steady-state, stress is a single-valued function of the strain-rate, we note that (using the ymmetry of τ):

$$\underline{\tau}: \underline{\nabla}_t \dot{\underline{e}} = \underline{\tau}: [(\dot{\underline{e}}); {}_m\underline{g}^m] \equiv \underline{\tau}: \left[\frac{1}{2}(\dot{\underline{e}} + \dot{\underline{e}}^T); {}_m\underline{g}^m\right]$$

$$\equiv \underline{\tau}: \underline{\nabla}_t \dot{\underline{\epsilon}} \equiv \underline{\nabla}_t W^*. \tag{23}$$

We can then observe that the mathematical potential W^*, under steady-state conditions, has the form:

$$W^* = \int_0^{\dot{\epsilon}_{mn}} \tau_{ij}\, \mathrm{d}\dot{\epsilon}_{ij} \tag{24}$$

such that

$$\frac{\partial W^*}{\partial y_k} = \frac{\partial W^*}{\partial \dot{\epsilon}_{mn}} \frac{\partial \dot{\epsilon}_{mn}}{\partial y_k} = \tau'_{mn} \dot{\epsilon}_{mn;k} \tag{25}$$

or

$$\underline{\nabla}_t W^* = \underline{\tau}: \underline{\nabla}_t \dot{\underline{\epsilon}}. \tag{26}$$

In particular, we note that for steady-state creep law of type $\dot{\epsilon}_{eq} = \gamma(\sigma_{eq})^n$, (24) becomes

$$W^* = \frac{n}{n+1}\left(\frac{1}{\gamma}\right)^{1/n}(\dot{\epsilon}_{eq})^{(n+1)/n}.$$

Applying (22) to $V_t - V_\epsilon$ and using the divergence theorem, we define the vector quantity $(\underline{C}^*)^\epsilon$.

$$\int_{\Gamma_{234}} \{\underline{n}_t W^* - \underline{n}_t \cdot (\underline{\tau} \cdot \underline{\dot{e}})\}\, dS - \int_{V_t - V_\epsilon} \rho_t(\underline{f} - \underline{a}) \cdot \underline{\dot{e}}\, dV$$
$$+ \int_{\Gamma_{12}} \underline{n}_t W^*\, dS + \int_{\Gamma_{45}} \underline{n}_t W^*\, dS - \int_{S_t} \bar{\underline{t}} \cdot \underline{\dot{e}}\, dS - \int_{S_\epsilon} \underline{n}_t \cdot \underline{\tau} \cdot \bar{\underline{\dot{e}}}\, dS$$
$$= \int_{\Gamma_\epsilon} [\underline{n}_t W^* - \underline{n}_t \cdot (\tau \cdot \dot{e})]\, dS \equiv (\underline{C}^*)^\epsilon. \tag{27}$$

If we define the limit of $(\underline{C}^*)^\epsilon$ as $\epsilon \to 0$ to be $\underline{C}^*$, we have a quantity which characterizes the crack-tip field and is independent of the selection of Γ_{234}. Restricting our attention to problems involving symmetric deformations about the x_1 axis and cracks oriented along the x_1 axis, with traction free crack-faces, no body forces and negligible inertia effects, we find that

$$C_1^* = \operatorname*{Lt}_{\epsilon \to 0} \int_{\Gamma_\epsilon} \left[n_1 W^* - n_j \tau_{ji} \frac{\partial \dot{u}_i}{\partial y_1}\right] dS \equiv \int_{\Gamma_{234}} \left[n_1 W^* - n_j \tau_{ji} \frac{\partial \dot{u}_i}{\partial y_1}\right] dS. \tag{28}$$

Now, we will relate C_1^* of (28) to the steady-state value of $(\Delta T_1)_c$ of (17). First, we may rewrite (17) in rate form as

$$(\dot{T}_1)_{css} = \operatorname*{Lt}_{\epsilon \to 0} \int_{\Gamma_\epsilon} (n_1 \tau_{ij} \dot{e}_{ij} - n_j \tau_{ji} \dot{e}_{i1})\, dS \equiv \int_{\Gamma_{234}} [n_1 \tau_{ij} \dot{e}_{ij} - n_j \tau_{ji} \dot{e}_{i1}]\, dS$$
$$- \int_{V_t} \frac{\partial \tau_{ij}}{\partial y_1} \dot{e}_{ij}\, dV \tag{29}$$
$$\equiv \int_{\Gamma_{234}} (n_1 \dot{W} - n_j \tau_{ji} \dot{e}_{i1})\, dS - \int_{V_t} \frac{\partial \tau_{ij}}{\partial y_1} \dot{e}_{ij}\, dV. \tag{29b}$$

Thus, $\dot{W}$ in (29) is the rate of *stress-working density*, while $\overset{*}{W}$ of (28) is just a mathematical potential for τ'_{ij}. In particular,

$$\dot{W} = \tau_{ij}\dot{e}_{ij} = \tau_{ij}\frac{1}{2}(\dot{e}_{ij} + \dot{e}_{ji}) = \tau_{ij}\dot{e}_{ij} = \sigma_{eq}\dot{e}_{eq} = \gamma\sigma_{eq}^{n+1} = \left(\frac{1}{\gamma}\right)^{1/n}(\dot{e}_{eq})^{([n+1]/n)} \tag{30}$$

as contrasted with W^*:

$$W^* = \left(\frac{n}{n+1}\right)\left(\frac{1}{\gamma}\right)^{1/n}(\dot{e}_{eq})^{([n+1]/n)}.$$

Comparing the left equalities of (28) and (29), it is seen that $(\dot{T}_1)_{css}$ and C_1^* are related by:

$$(\dot{T}_1)_{css} = C_1^* + \operatorname*{Lt}_{\epsilon \to 0} \int_{\Gamma_\epsilon} n_1(\dot{W} - W^*)\, dS \tag{31a}$$
$$= C_1^* + \frac{\gamma}{n+1} \operatorname*{Lt}_{\epsilon \to 0} \int_{\Gamma_\epsilon} n_1(\sigma_{eq})^{n+1}\, dS. \tag{31b}$$

Appendix B gives several numerical examples of relation (31) for two rather extreme values of n.

We now give the HRR field in terms of $(\Delta T_1)_c$. Whereas similar relations have been written in terms of C^*† for steady-state creep [6], the relations in terms of $(\Delta T_1)_c$ will be valid for non-steady creep as well as steady-state creep. The HRR field as given in [5] but modified for creep by replacing ϵ_{ij} and u_i by $\dot{\epsilon}_{ij}$ and $\dot{u}_i$ respectively, is:

$$[\tau_{ij}, \sigma_{eq}] = K_\sigma r^{-1/(n+1)}[\tilde{\sigma}_{ij}(\theta), \tilde{\sigma}_{eq}(\theta)] \tag{32a}$$

$$\dot{\epsilon}_{ij} = \gamma K_\epsilon r^{-n/(n+1)}\tilde{\epsilon}_{ij}(\theta) \tag{32b}$$

$$\dot{u}_i = \gamma K_\epsilon r^{1/(n+1)}\tilde{u}_i(\theta) \tag{32c}$$

where $\tilde{\sigma}_{eq}(\theta)$ has a maximum value of unity and

$$K_\epsilon = (K_\sigma)^n. \tag{32d}$$

Substituting (32a–c) into the left equality of (12), using (32d) and rearranging, gives:

$$K_\sigma \simeq \left(\frac{(\Delta T_1)_c}{\gamma I^* \Delta t}\right)^{(1/[n+1])} = \left(\frac{(\dot{T}_1)_c}{\gamma I^*}\right)^{(1/[n+1])} \tag{33}$$

where I^* is analogous to I defined by eqn (24) of [7] except for the factor $n/(n+1)$ multiplying the energy density term. To be explicit,

$$I^* = I + \frac{1}{n+1}\int_{-\Pi}^{\Pi} [\tilde{\sigma}_{eq}(\theta)]^{n+1} \cos\theta \, d\theta. \tag{34}$$

To summarize, we have presented a path-independent integral which is valid for non-steady creep as well as steady-state creep. The parameter $(\Delta T)_c$ defined by the integral therefore characterizes the crack-tip field for all time. Also, the C^* parameter has been derived from the general conservation law (2), and has been related to the parameter $(\Delta T)_c$ for self-similar crack growth under mode I conditions.

A FINITE ELEMENT MODEL FOR ELASTIC/VISCOPLASTIC MATERIALS

We now describe a finite element model, which is applicable to problems of elastic/viscoplasticity as defined by Perzyna [8]. This model accomodates the material's nonlinear behavior through a step-wise time integration procedure. In the following, it is assumed that strains are infinitesimal and displacements are small. The finite element model is based on the principle of virtual work:

$$\int_V \tau_{ij}\delta\epsilon_{ij} \, dV - \int_{S_\sigma} \bar{t}_i \delta u_i \, dS = 0 \tag{35}$$

where τ_{ij} are current stresses, $\bar{t}_i$ are current prescribed tractions on the surface S_σ, and $\delta u_i[\delta\epsilon_{ij} = 1/2(\delta u_{i,j} + \delta u_{j,i})]$ are arbitrary compatible virtual displacements. Following customary procedures we introduce the element displacement shape functions which relate element displacements u_i to element nodal displacements $\{q\}$

$$u_i = \{u\} = [N]\{q\}; \; \delta u_i = \{\delta u\} = [N]\{\delta q\}. \tag{36}$$

We also use the customary notation wherein strain (and stress) components are placed in one-dimensional arrays

$$\{\epsilon\} = [B]\{q\}; \{\delta\epsilon\} = [B]\{\delta q\}. \tag{37}$$

Substituting (36) and (37) into (35) and applying conventional element summation procedures we have

$$\sum_{\text{elements}} \left\{\int_{V_e} \{\tau\}^T[B] \, dV - \int_{S_{\sigma_e}} \{\bar{t}\}^T[N] \, dS\right\} \times \sum_{\text{elements}} \{\{\delta q\}\} = \{F\}^T\{\delta Q\} = 0.$$

Since $\{\delta Q\}$ are arbitrary virtual nodal displacements, it follows that

$$\sum_{\text{elements}} \left\{ \int_{V_e} \{\tau\}^T [B] \, dV - \int_{S_{\sigma_e}} \{\bar{t}\}^T [N] \, dS \right\} \equiv \{F\}^T = \{0\}^T. \tag{38}$$

We now write the current stress array in the form

$$\{\tau\} \equiv \{\tau\}_I = \{\tau\}_{I-1} + \{\Delta\tau\}_I \tag{39}$$

where the subscript "I" indicates the current time step (or increment) and $I-1$ indicates the previous time step. Application of the incremental elastic constitutive law results in

$$\{\tau\}_I = \{\tau\}_{I-1} + [E]\{\Delta\epsilon\}_I - [E]\{\Delta\epsilon_{vp}\}_I \tag{40}$$

where $\{\Delta\epsilon_{vp}\}_I$ are the incremental viscoplastic strains and $[E]$ is the matrix of elastic constants. Substituting (40) into (38), taking the transpose, and placing the known terms on the right hand side we have the final form of the finite element equations:

$$[K]\{\Delta Q\}_I = \{T\}_I + \{S_{vp}\}_I - \{R\}_{I-1} \tag{41}$$

where

$$[K] = \sum_{\text{elements}} \int_{V_e} [B]^T [E][B] \, dV \tag{42}$$

$$\{T\}_I = \sum_{\text{elements}} \int_{S_{\sigma_e}} [N]^T \{\bar{t}\}_I \, dS \tag{43}$$

$$\{S_{vp}\}_I = \sum_{\text{elements}} \int_{V_e} [B]^T [E]\{\Delta\epsilon_{vp}\}_I \, dV \tag{44}$$

$$\{R\}_{I-1} - \sum_{\text{elements}} \int_{V_e} [B]^T \{\tau\}_{I-1} \, dV. \tag{45}$$

It should be noted that $[K]$ is just the elastic stiffness and therefore only needs to be formed and decomposed† once. This results in significant savings in the number of computations per time step as compared to methods using stiffness matrics which must be reformed at each step (i.e. tangent stiffness methods). It should also be noted that the term $\{S_{vp}\}_I$ is computed from incremental viscoplastic strains $\{\Delta\epsilon_{vp}\}$ which are estimated using $\{\tau\}_{I-1}$ in conjunction with the material constitutive law (i.e. (1) for the present case of creep). Only for the special situation when the stresses do not change with time will this estimate be exact. Having obtained the incremental nodal displacements $\{\Delta Q\}_I$ by solving (41), one can easily find the total incremental strains $\{\Delta\epsilon\}_I$ via the incremental analogue of (37). We now describe two procedures for obtaining $\{\tau\}_I$.

The first and simpler method to obtain $\{\tau\}_I$ is to substitute the estimated $\{\Delta\epsilon_{vp}\}$ used in solving for $\{\Delta Q\}_I$ into (40). If one does this, then it happens that

$$\{R\}_I = \{T\}_I \tag{46}$$

and therefore (41) becomes for the next step‡

$$[K]\{\Delta Q\}_{I+1} = \{T\}_{I+1} + \{S_{vp}\}_{I+1} - \{T\}_I = \{\Delta T\}_{I+1} + \{S_{vp}\}_{I+1}. \tag{47}$$

This method was compared to the following method and was found to require smaller time steps to achieve similar results.

†The eqns (41) are solved in the current work by the decomposition $[K] = [L][D][L]^T$; see, e.g.[9].
‡This procedure results in the current model reducing to that of Zienkiewicz and Cormeau[11].

Rather than using the estimated values of $\{\Delta\epsilon_{vp}\}$ and the constitutive relation (i.e. (1) for the creep problem), the constitutive relation is integrated over the current time step at each Gaussian quadrature point with the condition that the total strain $\{\epsilon\}$ varies linearly with respect to time from $\{\epsilon\}_{I-1}$ to $\{\epsilon\}_I$. (While any number of integration schemes could be adopted for this purpose, the present study uses an Eulerian scheme with each time step being divided into five subincrements.) The result of this procedure is better adherance to the postulated constitutive law at the expense of introducing a somewhat unequilibrated stress state. The amount of disequilibrium depends on the accuracy of the original estimate for the incremental viscoplastic strains and thus on the time step size.

At this point one has two alternatives. The first is to use the viscoplastic strain increments obtained through the time integration procedure as an improved estimate and to re-solve (41) for the current time step. This procedure would, after several iterations, result in a stress state which is equilibrated to within some small user specified tolerance. With this type of procedure the time steps could be as large as those used with tangent stiffness methods. Further, it appears reasonable to expect the solution to be at least as accurate as if a tangent stiffness method were used.†

The second alternative is to go immediately to the next time step with the understanding that the terms $\{R\}_{I-1}$ in (41) results in the disequilibrium from the $I-1$ step being corrected in the Ith step. This feature is the result of the virtual work statement (35), being written in terms of total stress and tractions rather than incremental quantities. Owing to this corrective nature and to the diminishing returns one obtains from additional iterations, the second alternative is used in the present study.

Non-Steady Creep Calculations for a Compact Specimen

We now will discuss the application of the model to the analysis of a plane strain compact specimen. The dimensions of the ASTM standard specimen as well as the material properties and applied loading were chosen to coincide with those used by Ehlers and Riedel[12]. These are illustrated in Fig. 2.

Several finite element meshes have been used in the analysis. All of these meshes employ two-dimensional, eight-noded, isoparametric elements. The element integrations are accomplished with 2×2 Gauss quadrature and therefore only elements with straight sides are employed. The pin-loading-hole is not modeled. In all models the horizontal placement of the point load corresponds with the load line of the ASTM standard geometry ($x = 25.0$ mm). The vertical position is $y = 32.5$ mm. A sensitivity

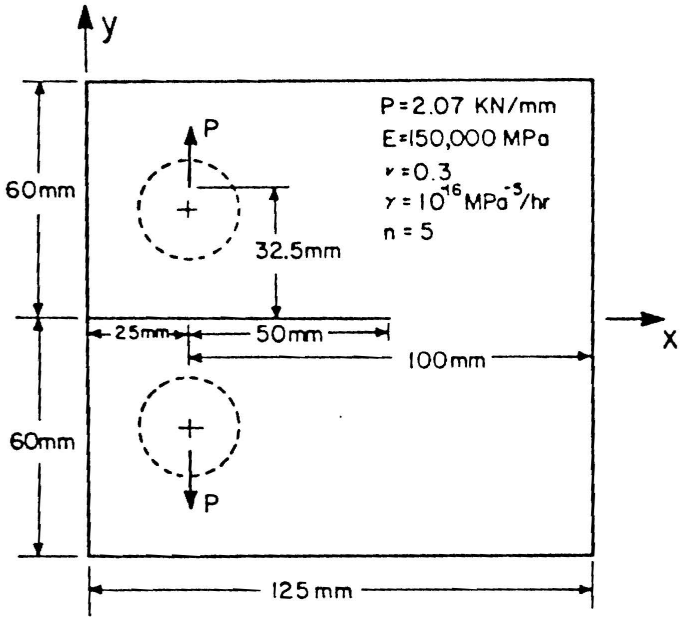

Fig. 2. Compact specimen geometry, loading condition, and material properties which are used in the calculations.

†This procedure could actually be more accurate if similar constitutive law integration procedures and equilibrium iterations are not performed with the tangent stiffness procedure. Also, it has been shown[11] that many element types are not suitable for modeling constitutive behavior approaching incompressibility when using tangent stiffness procedures. This problem of incompressibility constraints is not encountered with the current method.

study showed that shifting the load to $y = 40$ mm had virtually no effect on the pertinent aspects of the solution.

Most of the meshes contain collapsed quadrilateral elements at the crack tip as illustrated in Fig. 3. In several calculations, the midside nodes of these crack-tip elements were shifted to their quarter-points so as to produce a singular ($r^{-1/2}$) strain field at the crack tip. Table 1 identifies the meshes for which calculations have been made and also gives the load point displacement and J_1 for the elastic solution. These J_1 values are compared to those based on the expression given by Srawley[13] and are seen to be in good agreement.

These elastic solutions are assumed to exist at time $t = 0$ so that the creep analyses then proceed from this initial elastic state. The creep calculations use a variable time step size which is automatically regulated by the finite element program based on two criteria. The first criterion is the maximum percent difference between the incremental equivalent estimated creep strain and the incremental equivalent integrated creep strain for all the Gauss points in the mesh:

$$C_1 = \text{Max} \left| \frac{\Delta \bar{\epsilon}_{\text{EST}} - \Delta \bar{\epsilon}_{\text{INT}}}{\Delta \bar{\epsilon}_{\text{INT}}} \right|. \tag{48}$$

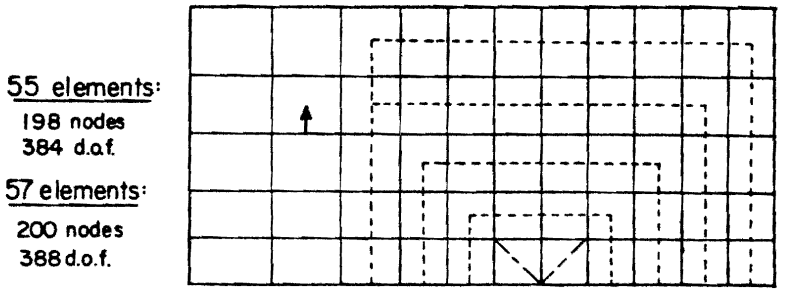

a. The 55 (square crack tip elements) and 57 (triangular crack tip elements) element meshes

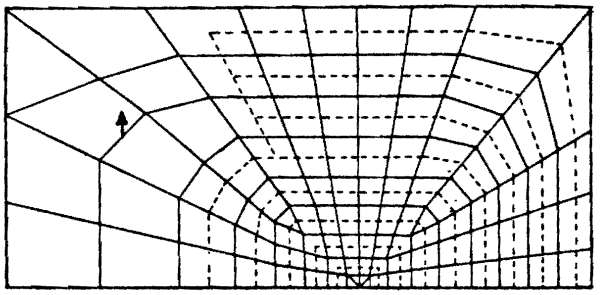

b. The 102 element mesh (331 nodes; 642 d.o.f.)

c. The 300 element mesh (941 nodes; 1840 d.o.f.)

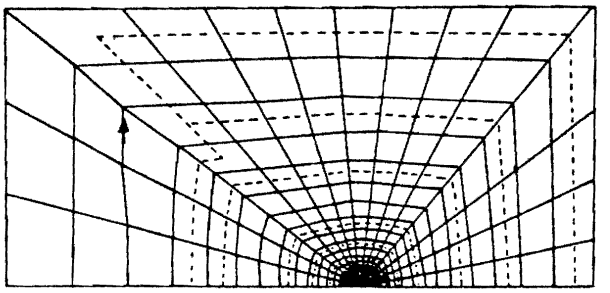

Fig. 3. Finite element meshes used for modeling the compact specimen.

Table 1. Summary of computational aspects and comparison with results from the literature

mesh description (see Figure 3)	Elastic Solution: load point displacement (mm)	J_1 (N/mm)	difference from 24.2 [13](%)	CP time* (sec)	Creep Solution: Δt (hours) initial/final†	number of steps†	CP time* per step (sec)	quasi steady state† $\dot{C}$ (N/mm hr)	difference from 134 [13](%)
55 elements (non-singular)	0.224	22.8	(-5.8)	15	1.0 /34	40	5	90.	(-32.8)
57 elements (1/4-point singular)	0.234	24.2	(0.0)	15	0.009 /17	61	5	121.	(- 9.7)
102 elements (non-singular)	0.231	24.0	(-0.8)	34	0.02 /24	50	8	116.	(-13.4)
102 elements p @ y=40 mm (non-singular)	0.232	24.0	(-0.8)	34	0.02 /24	50	8	116.	(-13.4)
102 elements (1/4-point singular)	0.233	24.3	(0.4)	34	0.0004/6	143	8	130.	(- 3.0)
300 elements (non-singular)	0.234	24.1	(-0.4)	276	0.0008/7	121	32	131.	(- 2.2)

* Control Data CYBER 74
† Quasi steady-state exists and calculation is stopped at t=600 hours

The second criterion is the maximum ratio of incremental equivalent integrated creep strain to the equivalent elastic strain:

$$C_2 = \text{Max}\left[\Delta\bar{\epsilon}_{\text{INT}}\left(\frac{E}{\bar{\sigma}}\right)\right]. \tag{49}$$

The user specified, maximum permissible values for C_1 and C_2 are $\bar{C}_1$ and $\bar{C}_2$, respectively. The size of the next step is then obtained from

$$\Delta t_{I+1} = \Delta t_I X \text{ Min}\left[\frac{\bar{C}_1}{C_1}, \frac{\bar{C}_2}{C_2}\right]. \tag{50}$$

In the present study, the values of $\bar{C}_1$ and $\bar{C}_2$ are 0.2 and 1.0, respectively. With these values, it has been found that the initial time steps are controlled by $\bar{C}_1$ while later time steps are controlled by $\bar{C}_2$. The values of C_1 and C_2 are strongly affected by the mesh refinement since a finer mesh results in Gauss points being closer to the crack tip and therefore having larger stresses and strain rates. The initial time increment cannot be determined from (50) and must be specified by the user so as to satisfy the two step size criteria. Table 1 gives approximate initial time step sizes which satisfy $\bar{C}_1 \le 0.2$ and quasi steady-state time step sizes which satisfy $C_2 \le 1.0$. The initial time step size used by Ehlers and Riedel[12] with their tangent stiffness method was 10^{-5} hr. For times approaching steady-state, they note that this step size was increased by a factor of 100.

To determine the sensitivity of the solution to the selection of $\bar{C}_1$ and $\bar{C}_2$, a calculation was done using the 57 element model (quarter-point singularity with $\bar{C}_1$ and $\bar{C}_2$ being halved (i.e. $\bar{C}_1 = 0.1$ and $\bar{C}_2 = 0.5$). It was found that the load point displacement differed by less than 0.5% for all time and that the steady-state solutions were essentially identical in terms of contour integral evaluations. It therefore appears that $\bar{C}_1$ and $\bar{C}_2$ are small enough to ensure that the solutions to be discussed do not depend on these step size criteria.

NUMERICAL EVALUATION OF CONTOUR INTEGRALS $(\dot{T}_1)_\epsilon$ AND C_1^*

We now describe the evaluation of the previously defined contour integrals. The $\overset{*}{C}_1$ integral is evaluated using (18 or 28) with $\overset{*}{W} = (n/n+1)\gamma\sigma_{eq}^{n+1}$. Despite $\overset{*}{C}_1$ being well defined and path-independent only for steady-state conditions, a quantity we will designate $(\overset{*}{C}_1)'$ was evaluated during all stages of creep. The ϵ superscript designates the particular contour which is used, with ϵ being the nondimensional distance from the crack tip to the point where the contour crosses the crack plane. Therefore, ϵ is zero at the crack tip and has a maximum value of unity when the contour is at the boundary of the specimen. The stress used in the evaluation are the stresses at the end of the time step. The

displacment gradient rates are approximated by

$$\frac{\partial \dot{u}_i}{\partial y_1} \approx \frac{1}{\Delta t} \frac{\partial \Delta u_i}{\partial y_1}.$$

The contours, which are indicated in Fig. 3 by dashed lines, pass through the elements as opposed to along their boundaries so as to benefit from the presumably more accurate solution within the element. Each element contour is divided into two segments with the integration on each segment being accomplished by two point Gaussian quadrature. Stresses within the element are interpolated to the required quadrature points by using the 2×2 element Gauss point values and bilinear interpolation.

The evaluation of the $(\Delta \underline{T})_c$ related integrals will now be described. In (10), we defined the vector quantity $(\Delta \underline{T})_c^\epsilon$ where ϵ is the same non-dimensional parameter as in $(\overset{*}{C}_1)^\epsilon$. The parameter $(\dot{T}_1)_c$ describes the crack tip field during non-steady creep and therefore is the parameter of primary interest. Based on previous discussions we have

$$(\dot{T}_1)_c = \operatorname*{Lt}_{\epsilon \to 0} (\dot{T}_1)_c^\epsilon \approx \operatorname*{Lt}_{\epsilon \to 0} \frac{(\Delta T_1)_c^\epsilon}{\Delta t} \tag{51}$$

where for infinitesimal strains and small deformations

$$(\Delta T_1)_c^\epsilon \equiv \int_{\Gamma_\epsilon} \left[n_1 \Delta W - n_j (\tau_{ij} + \Delta \tau_{ij}) \frac{\partial \Delta u_i}{\partial x_1} \right] \mathrm{d}S \tag{52}$$

$$= \int_{\Gamma_{234}} \left[n_1 \Delta W - n_j (\tau_{ij} + \Delta \tau_{ij}) \frac{\partial \Delta u_i}{\partial x_1} \right] \mathrm{d}S - \int_{V_t - V_\epsilon} \frac{\partial \tau_{ij}}{\partial x_1} \Delta \epsilon_{ij} \, \mathrm{d}V \tag{53}$$

and

$$\Delta W = \left(\tau_{ij} + \frac{1}{2} \Delta \tau_{ij} \right) \Delta \epsilon_{ij}. \tag{54}$$

In the evaluation of (52)–(54), it is to be understood that τ_{ij} is the stress at the beginning of the current step. The contour integrals are evaluated in a similar manner to the $(\overset{*}{C}_1)^\epsilon$ contour integrals already described. The stress derivative appearing in the area integral is evaluated based on the 2×2 element Gauss point values and the assumption that the stressed are distributed bilinearly with respect to element local coordinates. Elements which are entirely within $V_t - V_\epsilon$ are integrated with the usual 2×2 Gauss quadrature. Elements which are only partially within $V_t - V_\epsilon$ have each applicable quadrant integrated by one point Gauss quadrature.

DISCUSSION OF RESULTS

The path-dependence of $(\overset{*}{C}_1)^\epsilon$ during non-steady creep is illustrated in Fig. 4 using results from the 300 element mesh. Values of $(\overset{*}{C}_1)^\epsilon$ are plotted as a function of time for nine values of ϵ ranging from 0.03 to 0.92. It is seen that $(\overset{*}{C}_1)^\epsilon$ is largest for contours close to the crack tip (small ϵ) and that as steady-state is approached, the values from all contours converge to $\overset{*}{C}_1$. The solution has essentially reached steady-state at 300 hr. After 300 hr, the values of $(\overset{*}{C}_1)$ for all nine contours are within 1.5% of their average value. The value of $\overset{*}{C}_1$, as well as values from calculations with the other meshes, is given in Table 1.

Now we consider the evaluation of $(\dot{T}_1)_c$ as given by (51). Since we are interested in the limit of $(\dot{T}_1)_c^\epsilon$ as ϵ goes to zero, we have plotted $(\dot{T}_1)_c^\epsilon$ as a function of ϵ for several times (see Fig. 5). The open points are the values of $(\dot{T}_1)_c^\epsilon$, as computed by (52), for nine contours in the 300 element model. The value of the crack-tip parameter $(\dot{T}_1)_c$ is given by the intersection of each respective curve with the $\epsilon = 0$ axis. Due to the large gradient in $(\dot{T}_1)_c^\epsilon$ for small ϵ (except near steady-state) it is seen that the accuracy of any extrapolation based solely on the evaluation of (52) (i.e. open points) would be of questionable accuracy.

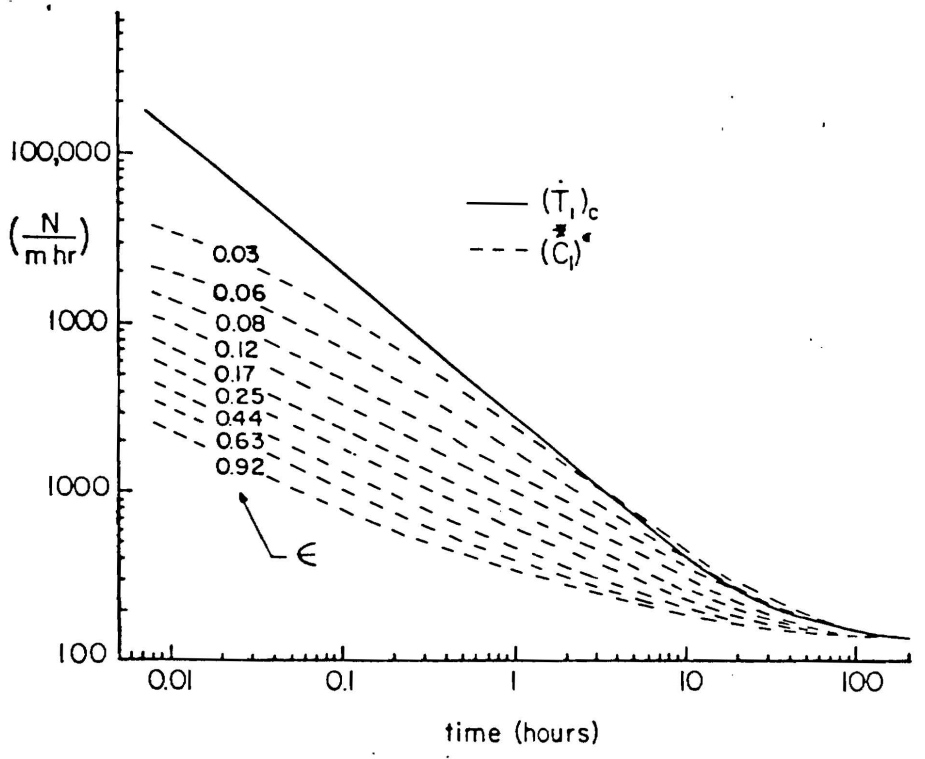

Fig. 4. $(\dot{T}_1)_c$ and $(\overset{*}{C}_1)^\epsilon$ as a function of time for several paths (results from 300 element mesh).

At this point the advantage of the alternative equation (53) for evaluating $(T_1)_c^\epsilon$ can be more fully appreciated. By taking the limit of (53) as ϵ goes to zero, we obtain an explicit formula for $(\Delta T_1)_c$ which does not involve ϵ:

$$(\Delta T_1)_c = \int_{\Gamma_{234}} n_1 \Delta W - n_j(\tau_{ij} + \Delta\tau_{ij}) \frac{\partial \Delta u_i}{\partial x_1} \, dS - \int_{V_t} \frac{\partial \tau_{ij}}{\partial x_1} \Delta\epsilon_{ij} \, dV. \tag{55}$$

The solid points at $\epsilon = 0$ in Fig. 5 have been obtained using (55). It is seen that these values of $(\dot{T}_1)_c$ appear to be reasonable extrapolations of the curves of $(T_1)_c^\epsilon$ computed through (52) thus giving some degree of confidence in their accuracy.

Based on arguments put forth in earlier portions of this paper, the value of $(\dot{T}_1)_c$ obtained through (55) should be independent of the path which is used in its computation. This path-independence is illustrated in Fig. 6a. We have plotted $(\dot{T}_1)_c$ as a function of the nondimensional distance of Γ_{234} from the crack-tip, ξ, for several times. Generally, the path-independence is seen to be quite good. The largest deviation from path-independence in this figure is for the intermediate time of 10.8 hr with the difference between the extreme contour values being less than 3%. To further emphasize this path-independence, we have plotted $(\dot{T}_1)_c$ as a function of time in Fig. 4. As a result of its path-independence, $(\dot{T}_1)_c$ is represented by a single curve. Interestingly, this curve is a straight line for times before approx. 10 hr.

Riedel and Rice[6] have arrived at the following approximation for K_σ [which they call $A(t)$] based on the assumed approximate path-independence of J_1 during the initial portion of non-steady creep.

$$K_\sigma \approx \left[\frac{K_I^2(1-\nu^2)/E}{(n+1)\gamma I t}\right]^{(1/[n+1])}. \tag{56}$$

Comparing (56) with (33) one concludes that $(\dot{T}_1)_c$ should behave like $1/t$ for times when (56) is valid. In a log-log plot of $(\dot{T}_1)_c$ versus time this would result in a straight line with a slope of -1. The straight line shown in Fig. 4 is inclined from the horizontal by 40° and therefore has a slope of -0.84. The current work has resulted in some evidence that J_1 is approximately path-independent during initial non-steady creep but that its value tends to increase with time. The tendency for J_1 to increase with time could explain the rather significant departure of the current results from the behavior of (56).

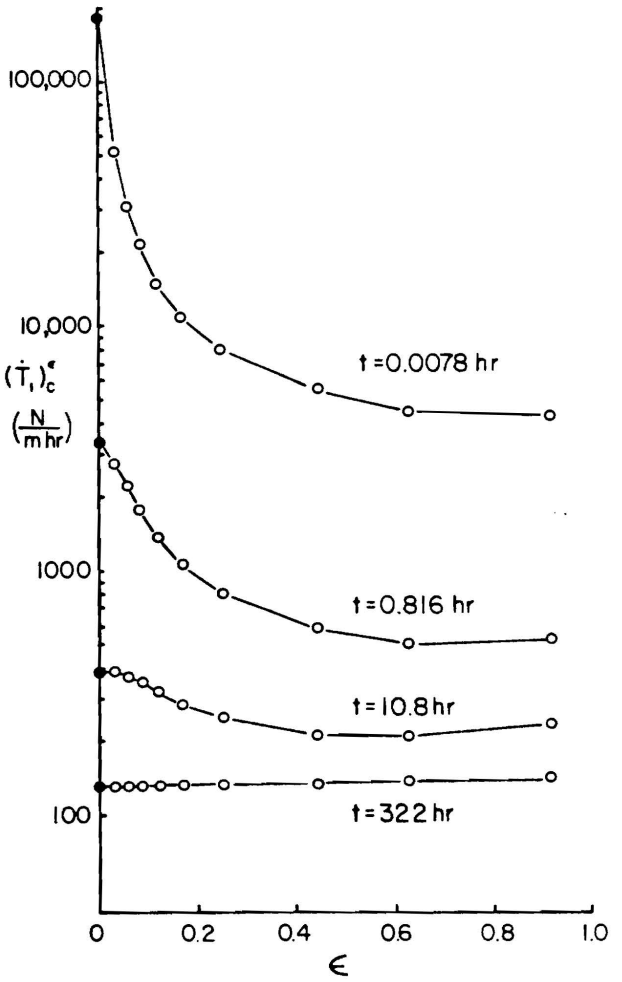

Fig. 5. $(\dot{T}_1)_c^\epsilon$ as a function of ϵ for several times during non-steady creep (results from 300 element mesh).

We next consider the results of computations using the 57 and 102 element meshes with quarter-point singularities. The purpose of considering these coarse meshes is to determine if the expense and effort in using the 300 element model is necessary for obtaining accurate results. Table 1 summarizes the results of these coarser meshes for the limiting cases of purely elastic behavior and steady-state creep behavior. For the elastic problem it is seen that the results from the coarser meshes agree with the 300 element mesh results to within 1 percent. At steady-state the 102 element model still agrees with the 300 element mesh (in terms of $\overset{*}{C}_1$) to within 1 percent while the 57 element model now differs by approximately 8%.

The contours used for the 57 and 102 element mesh are indicated in Fig. 3. It is seen that the 57 element mesh has four contours while the 102 element mesh has eight. The path independence of $(\dot{T}_1)_c$, as computed from (55), is illustrated for these two meshes in Fig. 6(b), 6(c). It is seen that the degree of path-independence in both is similar to that observed for the 300 element mesh. In as much as we have evidence that the 57 element mesh is less accurate than the other meshes at steady-state, it appears that the high quality of the path-independence cannot be interpreted as meaning the solution is accurate. Put more precisely, it seems that while poor path independence of $(\dot{T}_1)_c$ would imply the solution is inaccurate, the converse is not generally true.

To determine the adequancy of the 57 and 102 element meshes for the non-steady creep problem we now compare their $(\dot{T}_1)_c$ histories with that obtained with the 300 element mesh (see Fig. 7). The curve appearing in this figure has been placed through computed points from the 300 element mesh. The results of the 102 element mesh agree almost perfectly with this curve for times between 0.2 and 16 hr. Prior to this period and after this period the results fall below the curve by as much as 20%. While little can be said about the absolute accuracy of the calculations for the early portions of non-steady creep, we know (based on appendix B) that $(\dot{T}_1)_c$ should agree numerically with $\overset{*}{C}_1$ at steady-state to within a few

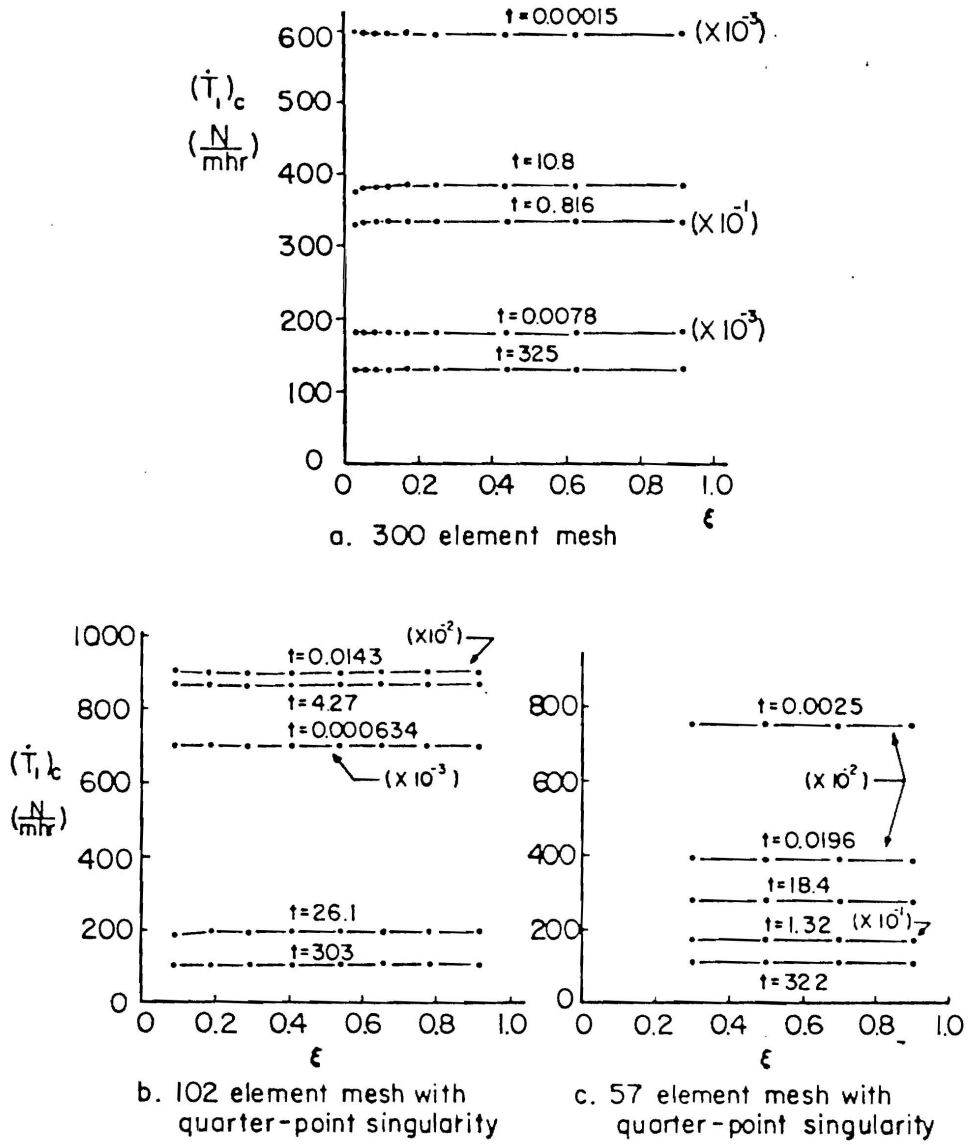

Fig. 6. Path-independence of $(\dot{T}_1)_c$ for several times during non-steady creep (ξ is the non-dimensional size of Γ_{234}).

percent. Therefore it can be said that the 102 element results are significantly in error at steady-state. The 57 element results do not compare favorably with the curve of Fig. 7 for any significant portion of the solution. For most times the values of $(\dot{T}_1)_c$ fall below the curve with the percent difference ranging from 50% at $t = 0.02$ hr to 15% at steady state.

Based on the discrepancy of $\overset{*}{C}_1$ indicated in Table 1 and in the generally bad comparison of $(\dot{T}_1)_c$ in Fig. 7, it appears that the 57 element mesh with quarter-point singularity is not sufficiently refined for accurate creep calculations. The conclusion is perhaps a bit unexpected considering the degree of accuracy which this mesh displayed for the elastic problem (see Table 1). The reason for this drastic change of accuracy in going from elastic to creep behavior may be the result of the crack tip strain singularity being appropriate for the elastic problem (i.e. $r^{-1/2}$) but inappropriate for the $r^{-n/n+1}$ type singularity which is expected to exist during creep.

In considering the suitability of the 102 element mesh with quarter-point singularity for modeling the present creep problem it seems that the apparent discrepancy for times less than 0.2 hr should be less of a concern than the discrepancy as steady-state is approached. This is due in part to the general inaccuracy of the Norton type creep law during the primary stage of creep and in part to the experimental evidence that creep crack growth occurs at rates which would make the later portion of this curve more important. Recalling that this model gave a steady-state value of $\overset{*}{C}_1$ which agreed quite

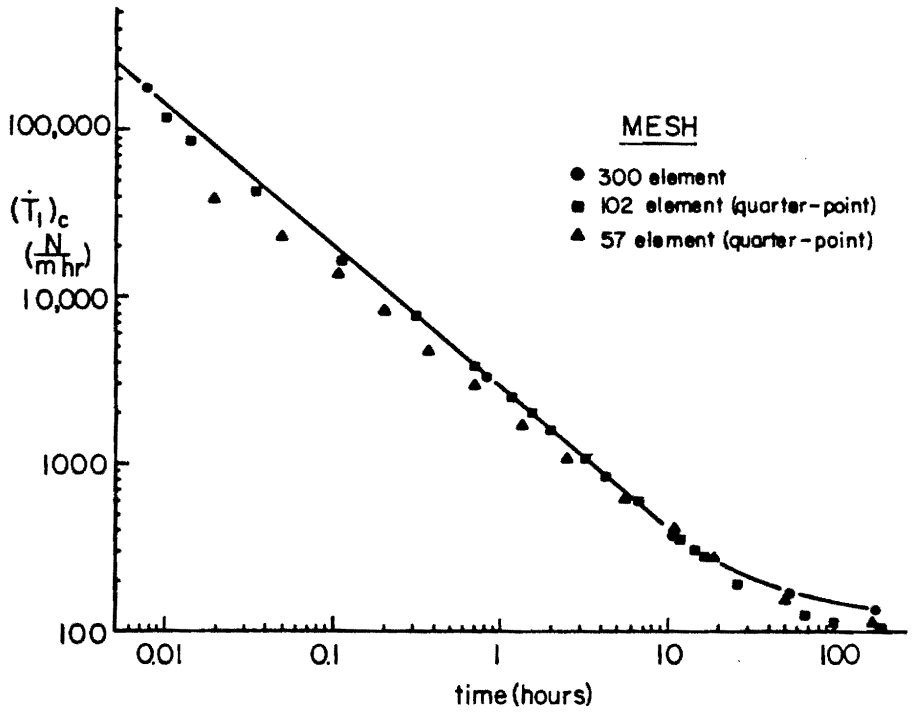

Fig. 7. Comparison of $(\dot{T}_1)_c$ from calculations with three meshes.

well with the 300 element mesh results (see Table 1) it is perhaps surprising that such a significant difference in $(\dot{T}_1)_c$ can exist. To better understand the results of this model we therefore plot $(\dot{T}_1)_c^\epsilon$ as a function of ϵ in Fig. 8. It is noted from this figure that the value of $(\dot{T}_1)_c$ based on (55) (i.e. the solid points) appear to be reasonable extrapolations for times when the results are in agreement with the 300 element mesh results. However, as steady-state is approached, it is seen that these solid points no longer appear reasonable. If one crudely extrapolates the values of $(\dot{T}_1)_c^\epsilon$ to $\epsilon = 0$ for the bottom two curves of Fig. 8, it is found that these values of $(\dot{T}_1)_c$ are in much better agreement with the 300 element mesh results.

In comparing the equations for evaluating $\overset{*}{C}_1$, $(\dot{T}_1)_c^\epsilon$ and $(\dot{T}_1)_c$ it is seen that $(\dot{T}_1)_c$ is the only one of the three which involves an integration over the crack-tip quarter-point elements. Based on this and the apparently good accuracy of $\overset{*}{C}_1$ and $(\dot{T}_1)_c^\epsilon$ it is believed that the solution within these elements is the major cause of discrepancy between the 102 and 300 element mesh results (at least for times approaching steady-state). Again, it appears that forcing the crack tip field to have a $r^{-1/2}$ strain singularity when the natural singularity is $r^{-n/n+1}$, may be the cause of difficulty.

CONCLUSION

This study shows that $\Delta \underline{T}$, a general path-independent integral given by Atluri[2], is easily applied to problems of non-steady creep as well as steady-state creep. In as much as the time rate of the first term of this vector quantity, $(\dot{T}_1)_c$, characterizes a mode I crack-tip field for non-steady as well as steady creep, has an energy interpretation and is still readily calculated within numerical models, it seems that it has some advantage over the more common $\overset{*}{C}_1$.

A finite element model has been derived which is generally applicable to viscoplastic material models. This model uses an initial strain approach which reduces computation time spent in forming the decomposing stiffness matrices and also circumvents the problem of element incompressibility constraints. Through special features including a correction term in the finite element equation, it appears that this model allows time steps which approach in size those used in tangent stiffness methods.

Finally, the finite element model has been used to model creep in a compact specimen. The model resulted in an elastic solution and a steady-state solution which agrees quite well with other solutions reported in the literature. Based on calculations with several meshes (some including quarter-point

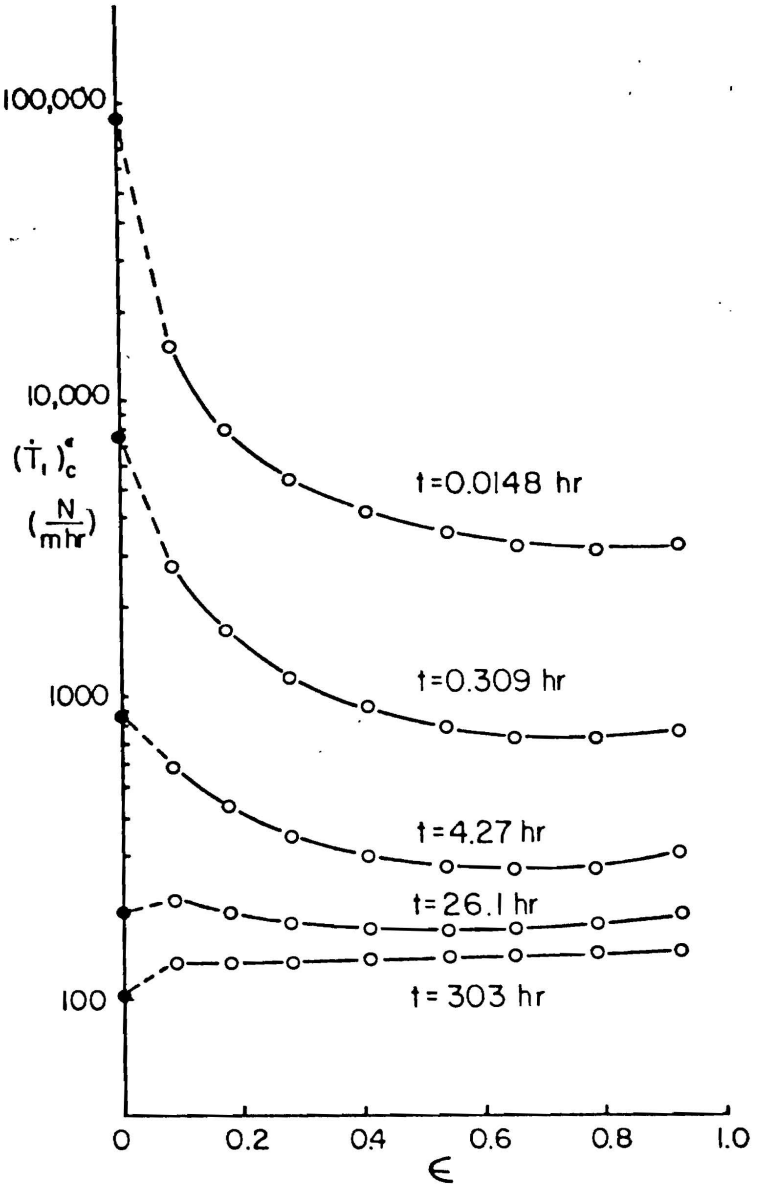

Fig. 8. $(\dot{T}_1)_c^*$ as a function of ϵ for several times during non-steady creep (results from 102 element mesh with quarter-point singularity).

element singularities) it appears that the presence of an area integral in the equation for $(\dot{T}_1)_c$ makes the accurate simulation of the crack-tip field more critical than for strictly far-field contours such as J_1 and C_1^*. Further work will include a study on the effectiveness of special crack-tip elements (which induce the "correct", $r^{-n/n+1}$, crack-tip strain field) in improving the accuracy of the model.

Acknowledgements—The above results were obtained during the course of investigation supported by NASA-Lewis Research Center, under grant NASANAG 3-38, and by AFOSR under grant AFOSR-81-0057. These supports, and encouragement of Drs. L. Berke, and A. Amos are gratefully acknowledged. The authors thank Ms. Margarete Eiteman for her care and assistance in the preparation of this manuscript.

REFERENCES

[1] K. Ohji, Nonlinear fracture mechanics approach to creep crack growth problems. *27th Japan Nat. Cong. for Appl. Mech.*, Tokyo Japan, pp. 3–20 (1977).

[2] S. N. Atluri, Path-independent integrals in finite elasticity and inelasticity, with body forces, inertia and arbitrary crack-face conditions. Report No. GIT-CACM-SNA-81-8, Georgia Institute of Technology March 1981, also *Engng Fracture Mech.* **16**, 341–364 (1982).

[3] S. N. Atluri, On rate principles for finite strain analysis of elastic and inelastic nonlinear solids. *Recent Research on Mechanical Behavior of Solids* (Prof. H. Miyamoto's 60th Anniversary Volume), pp. 79–107. Univ. of Tokyo Press, Tokyo, Japan (1979).

[4] S. N. Atluri and H. Murakawa, New general and complementary energy theorems, finite strain, rate sensitive inelasticity and finite element: some computational studies. *Nonlinear Finite Element Analysis in Structural Mechanics*, Proc. Europe-U.S. Workshop Ruhr-University Bochum, Germany, July, 1980, (Ed. Wunderlich, Stein and Bathe), Springer-Verlag, pp. 28–47, (1981).
[5] N. L. Goldman, J. W. Hutchinson, Fully-plastic crack problems: The center cracked strip under plane strain. *Int. J. Solids Structures* **11**, 575–592 (1975).
[6] H. Riedel and J. R. Rice, Tensile cracks in creeping solids. Brown University Rep. E(11-1) 3084/64 to U.S. Dept. of Energy (1979).
[7] J. W. Hutchinson, Singular behavior at the end of a tensile crack in a hardening material. *J. Mech. Phys. Solids* **16**, 13–31 (1968).
[8] P. Perzyna, Fundamental problems in viscoplasticity. *Adv. Appl. Mech.* **9**, 243–377 (1966).
[9] K. Bathe and E. L. Wilson, *Numerical Methods in Finite Element Analysis*. Prentice-Hall, Englewood Cliffs, New Jersey (1976).
[10] J. C. Nagtegaal, D. M. Parks and J. R. Rice, On numerically accurate finite element solutions in the fully plastic range. *Comput. Meth. Appl. Mech. Engng* **4**, 153–177 (1974).
[11] O. C. Zienkiewicz and I. C. Cormeau, Visco-plasticity-plasticity and creep in elastic solids—a unified numerical solution approach. *Int. J. Num. Meth. Engng* **8**, 821–845 (1974).
[12] R. Ehlers and H. Riedel, A finite element analysis of creep deformation in a specimen containing a macroscopic crack. *Advances in Fracture Research Vol.* 2, (Edited by D. Francois) Fifth Int. Conf. on Fracture, Cannes, pp. 691–698 (1981).
[13] J. F. Srawley, Wide range stress intensity factor expressions for ASTM E399 standard fracture toughness specimens. *Int. J. Fracture* **12**, 475–476 (1976).
[14] C. F. Shih and V. Kumar, Estimation technique for the prediction of elastic-plastic fracture of structural components of nuclear systems. Contract RP 1237-1, First Semiannual Report for Electric Power Research Institute, General Electric Co. Rep. (1979).

(*Received* 27 *July* 1981; *received for publication* 26 *August* 1981)

APPENDIX A

This appendix discusses the existence of the various limits which have been taken in defining $(\Delta \underline{T})_c$, $(\bar{T})_c$ and $\overset{*}{C}$. In considering these limits, we make use of the generally accepted result (see, e.g.[7]) that strain energy density quantities ΔW and $\dot{W}$ as well as the quantity $\overset{*}{W}$ behave as $1/r$ in the vicinity of the crack tip. This is assumed to be valid for non-steady as well as steady-state creep and also for the elastic state existing at $t = 0$.

Based on the known asymptotic behavior at the crack tip (i.e. the HRR field) the limits of Γ_ϵ contour integrals for eqns (11), (12), (17) and (28) can be written in the following form provided one takes Γ_ϵ as being a circular contour centered at the crack tip.

$$\operatorname*{Lt}_{\epsilon \to 0} \int_{\Gamma_\epsilon} \left(\frac{1}{\epsilon}\right) f(\theta) \epsilon \, d\theta = \int_{-\Pi}^{\Pi} f(\theta) \, d\theta. \tag{A1}$$

It is clear therefore that all the limits of this type exist.

We next consider the limits taken of $V_t - V_\epsilon$ type integrals. Inspection of these integrals show that they can all be put into the form

$$C + \operatorname*{Lt}_{\epsilon \to 0} \int_{V_t' - V_\epsilon} \left(\frac{1}{r^2}\right) g(\theta) r \, dr \, d\theta = C + \operatorname*{Lt}_{\epsilon \to 0} \int_{\epsilon}^{R} \left(\frac{1}{r}\right) \int_{-\Pi}^{\Pi} g(\theta) \, d\theta \, dr \tag{A2}$$

where V_t' is a small volume in the vicinity of the crack tip and C is the integral over the region $V_t - V_t'$. A first inspection of (A2) results in the conclusion that the limit does not exist since the integrand has a non-integrable singularity. If , however, we look at the right equality of (11), it is seen that this conclusion results in a contradication. That is, we have shown that the limit of the integral on Γ_ϵ does exist and therefore (11) requires that the limit of the integral over $V_t - V_\epsilon$ must exist. A re-inspection of (A2) shows that the only way for this apparent contradiction to be resolved is if the $g(\theta)$ of (A2) has the following property

$$\operatorname*{Lt}_{\epsilon \to 0} \int_{-\Pi}^{\Pi} g(\theta) \, d\theta = 0. \tag{A3}$$

The function $g(\theta)$ is known explicitly for the linear elastic case and therefore (A3) can be directly verified. For the HRR field, $g(\theta)$ is not known explicitly and therefore (A3) can only be verified numerically.

For infinitesimal strain, nonlinear elasticity, the following relation provides an alternative to verifying (A3) directly.

$$\int_{V - V_\epsilon} \frac{\partial \sigma_{ij}}{\partial x_1} \Delta \epsilon_{ij} \, dV = \int_{\Gamma} n_j \Delta \sigma_{ij} \frac{\partial u_i}{\partial x_1} \, dS - \int_{\Gamma_\epsilon} n_j \Delta \sigma_{ij} \frac{\partial u_i}{\partial x_1} \, dS. \tag{A4}$$

The relation (A4) (which assumes zero crack surface tractions and no body forces) illustrates that this volume integral of type (A2) can be expressed in terms of the contour integral of type (A1). The relation (A4) can be verified through the divergence theorem, the linear momentum balance condition and the following identities.

$$\frac{\partial \sigma_{ij}}{\partial x_1} = \frac{\partial}{\partial x_1}\left(\frac{\partial W}{\partial \epsilon_{ij}}\right) = \frac{\partial}{\partial \epsilon_{ij}}\left(\sigma_{mn} \frac{\partial \epsilon_{mn}}{\partial x_1}\right) = \frac{\partial \sigma_{mn}}{\partial \epsilon_{ij}} \frac{\partial \epsilon_{mn}}{\partial x_1}$$

$$\frac{\partial \sigma_{mn}}{\partial \epsilon_{ij}} \Delta \epsilon_{ij} = \Delta \sigma_{mn}$$

$$\frac{\partial}{\partial x_n}\left(\Delta \sigma_{mn} \frac{\partial u_m}{\partial x_1}\right) = \Delta \sigma_{mn} \frac{\partial \epsilon_{mn}}{\partial x_1}.$$

APPENDIX B

The purpose of this appendix is to give some examples to illustrate the numerical difference between $(\dot{T})_{css}$ and $\overset{*}{C}_1$ as given by (31). Using (33), (32a) and (34), we have

$$\frac{(\dot{T}_1)_{css}}{\overset{*}{C}_1} = \frac{I^*}{I} = 1 + \frac{1}{(n+1)I}\int_{-\pi}^{\pi} \tilde{\sigma}_{eq}^{n+1}(\theta)\cos\theta\, d\theta. \tag{B1}$$

The values tabulated in Table B1 were computed *approximately* from values of I and plots of $\tilde{\sigma}_{eq}(\theta)$ given in [7] and should be viewed accordingly. It is seen that for the range of n commonly encountered, $(\dot{T}_1)_{css}$ and $\overset{*}{C}_1$ are numerically ver similar for plane strain and only slightly less so for plane stress.

Table B. 1 Comparison of $(\dot{T}_1)_{css}$ and $\overset{*}{C}_1$

	Plane Strain		*Plane Stress*	
$\frac{(\dot{T}_1)_{css}}{\overset{*}{C}_1}$	$n = 3$	$n = 13$	$n = 3$	$n = 13$
	0.98	0.00	1.11	1.14

Computers & Structures Vol. 19, No. 1-2, pp. 175–182, 1984
Printed in the U.S.A.

0045-7949/84 $3.00 + .00

160

HYBRID STRESS FINITE ELEMENTS FOR LARGE DEFORMATIONS OF INELASTIC SOLIDS

K. W. REED† and S. N. ATLURI‡
Center for the Advancement of Computational Mechanics, School of Civil Engineering, Georgia Institute of Technology, Atlanta, GA 30332, U.S.A.

Abstract—A new hybrid stress finite element algorithm, based on a generalization of Fraeijs de Veubeke's complementary energy principle is presented. Analyses of large quasistatic deformation of inelastic solids (hypoelastic, plastic, viscoplastic) are within its capability.

Principal variables in the formulation are the nominal stress rate and spin. A brief account is given of the boundary value problem in these variables, and the 'equivalent' variational principle. The finite element equation, along with initial positions and stresses, comprise an initial value problem. Factors affecting the choice of time integration schemes are discussed. Results found by application of the new algorithm are compared to those obtained by a velocity based finite element algorithm.

NOTATION

$C(\tau)$	configuration (image of the body in space at time τ)
$\mathbf{X}$	position vector in space at time τ
$\mathbf{x}$	position vector in space at (present) time t
∇	$e^i\partial/\partial x^i$; $\nabla_X = e^I\partial/\partial X^I$; $\dot{a} = \partial a/\partial t + \mathbf{V}\cdot\nabla a$ (material derivative of 'a')
χ_τ	deformation function; maps $C(\tau)$ to $C(t)$ as $\mathbf{x} = \chi_\tau(\mathbf{X}, t)$
$\mathbf{V}$	velocity function; related to deformation function as $\mathbf{V}(\chi_\tau(\mathbf{X}, t), t) = \partial/\partial t\chi_\tau(\mathbf{X}, t)$
E_τ	$\equiv(\nabla_X\chi_\tau(\mathbf{X}, t))^T$ deformation gradient
J_τ	$=\det F_\tau$
L	$=(\nabla\mathbf{V}(\mathbf{x}, t))^T$ velocity gradient
J	$=\nabla\cdot\mathbf{V}(\mathbf{x}, t)$ *dilatation*
ϵ	$=\frac{1}{2}(L + L^T)$ stretching
ω	$=\frac{1}{2}(L - L^T)$ spin
$\mathbf{T}$	true traction; $\mathbf{T}_\tau$ nominal traction relative to $C(\tau)$
τ	true stress; $\sigma_\tau = J_\tau\tau$ Kirchhoff stress relative to $C(\tau)$
t_τ	$=F_\tau^{-1}\sigma_\tau$ nominal stress relative to $C(\tau)$
$\dot{\mathbf{T}}$	true traction rate; $\dot{\mathbf{T}}_\tau$ nominal traction rate
$\dot{\sigma}$	$=\dot{J}\tau + \dot{\tau}$ Kirchhoff stress rate
$\dot{t}$	$=-(\epsilon + \omega)\cdot\tau + \dot{\sigma}$ nominal stress rate
$\dot{\sigma}^*$	$=\dot{\sigma} - \omega\cdot\tau + \tau\cdot\omega$ 'corotational' stress rate
$\underline{\underline{\mathcal{W}}}$	=material stiffness tensor

INTRODUCTION

The research which produced the present hybrid stress finite element algorithm was motivated by the observation that hybrid stress algorithms consistently outperform those using velocity (or displacement) as the sole variable. Hybrid stress models for infinitesimal deformation of shells and incompressible solids have been topics of intense research since Pian's first presentation of such a model in 1964[1]. However, hybrid stress models for finite deformations have only been researched since Fraeijs de Veubeke's[2] presentation of a complementary energy principle for finite elastic deformations, and Atluri's[3, 4] generalization of that principle for inelastic solids. A hybrid stress model for finite elastic deformation was presented by Murakawa[5]. In this report a hybrid stress model for finite inelastic deformation is presented.

THE BOUNDARY VALUE PROBLEM

Compatibility

$$\nabla X(\epsilon - \omega) = \mathbf{0};\quad \epsilon - \epsilon^T = \mathbf{0};\quad \omega + \omega^T = \mathbf{0}. \tag{1}$$

Linear Momentum Balance (LMB)

$$\nabla\cdot\dot{t} + \rho\dot{\mathbf{b}} = \mathbf{0}. \tag{2}$$

Angular Momentum Balance (AMB)

$$[(\epsilon + \omega)\cdot\tau + \dot{t}] - [(\epsilon + \omega)\cdot\tau + \dot{t}]^T = \mathbf{0}. \tag{3}$$

Constitutive Equation

$$\epsilon = \underline{\underline{\mathcal{W}}}^{-1}:(\dot{r} - \Sigma);\quad \dot{r} = \frac{1}{2}(\dot{t} + \tau\cdot\omega - \omega\cdot\tau + \dot{t}^T). \tag{4}$$

Velocity Boundary Condition (VBC)

$$\delta\mathbf{s}\cdot(-\epsilon + \omega + \nabla\dot{\mathbf{V}}) = \mathbf{0} \text{ on } S_v$$
($\delta\mathbf{s}$ is any tangent on S_v). (5)

Traction Boundary Condition (TBC)

$$\mathbf{n}\cdot\dot{t} = \dot{\mathbf{T}}_\tau \text{ on } S_\sigma. \tag{6}$$

Above are listed the equations of the general boundary value problem associated with quasistatic deformations of inelastic solids.§ From (1) to (4) one may obtain 18 scalar equations for the 9 unknown stress rate components $\dot{t}^{ij}$, 3 unknown spin components ω^{ij}, and 6 unknown stretching components ϵ^{ij}. In conventional approaches one resets (1)–(6) so that only velocity components V^i appear as variables. Alternatively one may use (4) to eliminate ϵ as a variable in (1), (3) and (5), thus obtaining a boundary value problem involving only the components of stress rate and spin. Any solution of this latter boundary value problem necessarily satisfies the vari-

†Post-Doctoral Research Fellow.
‡Regents' Professor of Mechanics.
§The eqns (1) and (3)–(6) are exact. The constitutive equation (4) encompasses many of the material models found in the engineering literature.

ational problem,

$$\int_V \{[(\epsilon+\omega)\cdot\tau+\dot{t}]:\delta\omega\}=0; \tag{7}$$

$$\int_V \{[-\epsilon+\omega]:\delta\dot{t}\}\,dV+\int_{S_V}\mathbf{n}\cdot\delta\dot{t}\cdot\nabla\,dS=0; \tag{8}$$

$$\int_{S_\sigma}(\mathbf{n}\cdot\dot{t}-\dot{\mathbf{T}}_t)\cdot\delta\mathbf{V}\,dS=0; \tag{9}$$

$$\omega+\omega^T=0; \tag{10}$$

$$\nabla\cdot\dot{t}+\rho\dot{\mathbf{b}}=0; \tag{11}$$

provided that only stress rate variations $\delta\dot{t}$ such that

$$\nabla\cdot\delta\dot{t}=0 \tag{12}$$

and spin variations $\delta\omega$ such that

$$\delta\omega+\delta\omega^T=0 \tag{13}$$

are admitted to the functionals. In (7) and (8) ϵ is supposed to be expressed as a function of $\dot{t}$ and ω, via (4). Equations (7)–(13) are counterpart to the complementary virtual work principle of infinitesimal deformation theories, and form the basis for the finite element algorithm presented here.

As may be surmised from eqns (4) above, the present approach necessitates reformulation of the constitutive equation. In applications one typically is given or may find a constitutive equation of the form

$$\dot{\sigma}^*=\underline{\mathbf{Y}}:\epsilon+\Sigma, \tag{14}$$

where $\underline{\mathbf{Y}}$ and Σ may depend upon the stress but not on ϵ. The form (4) is easily obtained if one first notes the relation between the corotational stress rate $\dot{\sigma}^*$ and the symmetrical Luré stress rate $\dot{r}$:

$$\dot{r}=\dot{\sigma}^*-\underline{\mathbf{T}}:\epsilon; \qquad \mathcal{T}_{ijkl}=\frac{1}{2}(\tau_{ik}\delta_{lj}+\delta_{ik}\tau_{lj}). \tag{15}$$

Using (14) to eliminate $\dot{\sigma}^*$ from (15), we get

$$\dot{r}=\underline{\mathbf{W}}:\epsilon+\Sigma: \qquad \underline{\mathbf{W}}\equiv\underline{\mathbf{Y}}-\underline{\mathbf{T}}. \tag{16}$$

The form (4) follows immediately by inversion of (16). Since no new constitutive postulate was made, the 'reformulation' is really no more than a change of variable.

THE FINITE ELEMENT ALGORITHM

Equations (7)–(13) are the basis for the finite element algorithm presented here. The finite element equations are obtained by introduction of polynomial representations for V, ω, and $\dot{t}$ (satisfying 10–13 *a priori*) to (7)–(9), and performing the assigned integrations.† On the Nth element let V, ω, and $\dot{t}$ be represented as

$$\mathbf{V}=\sum_{i=1}^{NQ}\mathbf{N}_i\tilde{q}_N^i \quad \mathbf{N}_i\text{: isoparametric shape functions} \tag{17}$$

$$\omega=\sum_{i=1}^{NW}QW_i\alpha_N^i \quad \text{where } QW_i+QW_i^T=0 \tag{18}$$

$$\dot{t}=\sum_{i}^{NT=1}QT_i\beta_N^i+\dot{t}^b \quad \text{where } QT_i=\nabla\times\Phi_i \tag{19}$$

$$\nabla\cdot\dot{t}^b=-\rho\dot{\mathbf{b}}.$$

The representation for the stress rate $\dot{t}$ is independent on each element, so to (9) we append a statement of 'interelement traction reciprocity', obtaining:

$$\sum_{N=1}^{NELM}\left\{\int_{S_N\sim(S_N\cap S_V)}(\mathbf{n}\cdot\dot{t}\cdot\delta\mathbf{V})\,dS-\int_{(S_N\cap S_\sigma)}\dot{\mathbf{T}}_t\cdot\delta\mathbf{V}\,dS\right\}=0, \tag{20}$$

(which includes 9). The finite element counterparts to (7), (8) and (20) are listed below (the element index 'N' has been suppressed on the spin and stress rate parameters α^i and β^i).

$$\{\delta\alpha\}^T\left\{-[H^{11}\quad H^{12}]\begin{Bmatrix}\alpha\\ \beta\end{Bmatrix}+\{P^{\alpha b}\}+\{P^{\alpha\Sigma}\}\right\}=0 \tag{21}$$

$$\{\delta\beta\}^T\left\{-[H^{21}\quad H^{22}]\begin{Bmatrix}\alpha\\ \beta\end{Bmatrix}+\{P^{\beta b}\}+\{P^{\beta\Sigma}\}+[G]\{\tilde{q}_N\}\right\}=0 \tag{22}$$

$$\sum_{N=1}^{NELM}\left\{\{\delta q_N\}^T[0\quad G_N^T]\begin{Bmatrix}\alpha\\ \beta\end{Bmatrix}-\{\delta q_n\}^T\{F_N\}\right\}=0. \tag{23}$$

Henceforth we refer to (21) as AMB, to (22) as compatibility, and to (23) as TBC. The individual matrices are defined below:

$$H_{ij}^{11}=\int_{V_N}\{(\tau\cdot QW_i):\underline{\mathbf{D}}:(\tau.QW_j)+\tau:(QW_i\quad QW_j)\}\,dV \tag{24}$$

$$H_{ij}^{12}=\int_{V_N}\{(\tau\cdot QW_i):\underline{\mathbf{D}}:(QT_j)-QW_i:QT_j\}\,dV \tag{25}$$

$$H_{ij}^{21}=\int_{V_N}\{(QT_i):\underline{\mathbf{D}}:(\tau\cdot QW_j)-QT_i:QW_j\}\,dV \tag{26}$$

$$H_{ij}^{22}=\int_{V_N}(QT_i):\underline{\mathbf{D}}:(QT_j)\,dV \tag{27}$$

$$G_{ij}=\int_{S_N}\mathbf{n}\cdot(QT_i)\cdot(\mathbf{N}_j)\,dS \tag{28}$$

$$F_i=\int_{(S_N\cap S_\sigma)}\dot{\mathbf{T}}_t(\mathbf{N}_i)\,dS \tag{29}$$

$$P_i^{\alpha b}=\int_{V_N}\left\{(QW_i):\dot{t}^b+(\underline{\mathbf{D}}:\dot{t}^b)\cdot\tau+\frac{1}{h}\tau\right\}dV \tag{30}$$§

†Gaussian quadrature rules are used.

‡Mathematical "rank" conditions require that $NT=NQ-T$, where T is the number of translational degrees of freedom of an element. Moreover, the $[QW]$ and $[QT]$ should be of the same polynomial degree. See [6] for further discussion. The shape functions used in the example accompanying this paper are given in Appendix A.

§The last term in the integrand is an "angular momentum imbalance"; h is the time step size; see [6].

$$P_I^{b,b} = \int \{(QT_I):(-\underline{D}:\mathring{t}^b)\}\,dV \tag{31}$$

$$P_I^{\sigma,\Sigma} = \int \{(\tau \cdot QW_I):\underline{D}:\Sigma\}\,dV \tag{32}$$

$$P_I^{b,\Sigma} = \int \{(QT_I):\underline{D}:\Sigma\}\,dV \tag{33}$$

and $\underline{D}$ is obtained from $\underline{W}^{-1}$ by symmetrization:

$$D_{ijkl} = \frac{1}{4}(W^{-1}_{ijkl} + W^{-1}_{jikl} + W^{-1}_{ijlk} + W^{-1}_{jilk}). \tag{34}$$

This symmetrization is easily done *after* $\underline{W}^{-1}$ is computed, and serves to reduce by a factor of four the number of multiplications required to compute the H matrices (24)–(27).

The procedure which leads one from (21) to (23) to the approximate solution of the boundary problem involves little beyond ordinary algebra. We remark that (21) and (22) may be used to eliminate the spin and stress rate parameters from (23), so that *the final system of equations involves only the nodal velocities as unknowns*. Details may be found in [6].

INTEGRATION OF THE MOTION OF THE BODY

The finite element algorithm just described produces an approximation for the stress rate $\mathring{t}$ and velocity $\mathbf{V}$, as opposed to stress increments and displacement increments. Thus, considerably more freedom of choice of time integration schemes is afforded by the present approach than by incremental approaches (which are predisposed to integration by the relatively inefficient Euler's method). In this section we (i) formally state an initial value problem, (ii) discuss numerical integration of that problem, and (iii) present a "forward gradient scheme" which stabilizes numerical solutions of that problem (for bodies which exhibit stress relaxation).

Let $\{\mathbf{x}\} = \{\mathbf{x}^1, \mathbf{x}^2, \ldots, \mathbf{x}^{ND}\}$ be the vector of *nodal positions*, and let $\{\mathbf{v}\} = \{\mathbf{v}^1, \mathbf{v}^2, \ldots, \mathbf{v}^{ND}\}$ be the vector of *nodal velocities*, where ND is the total number of nodes. Similarly, let $\{\tau\} = \{\tau^1, \tau^2, \ldots, \tau^G\}$ and $\{\mathring{t}\} = \{\mathring{t}^1, \mathring{t}^2, \ldots, \mathring{t}^G\}$ be the *quadrature point stresses* and *stress rates*, respectively, where G is the total number of quadrature points in the body. To indicate the dependence of $\{\mathbf{v}\}$ and $\{\mathring{t}\}$ on $\{\mathbf{x}\}$, $\{\tau\}$, and the time dependent prescribed loads, we write†

$$\{\mathbf{v}\} = f[\{\mathbf{x}\}, \{\tau\}, t] \tag{35}$$

$$\{\mathring{t}\} = g[\{\mathbf{x}\}, \{\tau\}, t]. \tag{36}$$

Since each element node is associated with the same material point $\mathbf{X}^I$ throughout a deformation, and likewise for each quadrature point, we may write each component of $\{\mathbf{x}\}$, $\{\tau\}$, $\{\mathbf{v}\}$, and $\{\mathring{t}\}$ as

$$\mathbf{x}^I = \chi_t(\mathbf{X}^I, t) \tag{37}$$

$$\tau^I = (1/J_t^I)F_t^I \cdot t_t(\mathbf{X}^I, t) \tag{38}$$

$$\mathbf{V}^I = \dot{\chi}_t(\mathbf{X}^I, t) \tag{39}$$

$$\mathring{t}^I = (1/J_t^I)F^I \cdot \mathring{t}_t(\mathbf{X}^I, t). \tag{40}$$

Introduction of (37)–(40) to (35) and (36) gives

$$\{\dot{\chi}_t\} = f_t[\{\chi_t\}, \{t_t\}, t]; \tag{41}$$

$$\{\mathring{t}_t\} = g_t[\{\chi_t\}, \{\tau_t\}, t]; \tag{42}$$

the definitions of f_t and g_t being clear. Equations (41) and (42) and appropriate initial values comprise an initial value problem.

It is clear that this initial value problem is predisposed to numerical integration. In principle, any time stepping scheme in the literature may be used. Three important factors affecting the choice of a particular scheme are:

(1) The solution vector $\langle\{\chi_t(t_N)\}, \{t_t(t_N)\}\rangle$ at the time $t = t_N$ is of scalar dimension $NDOF + 9G$, where $NDOF$ is the number of kinematic degrees of freedom of the mesh and G is the total number of quadrature points. Storage required for implementation of different integration schemes can vary appreciably.

(2) Evaluation of $\langle f_t, g_t\rangle$ is expensive since it involves forming and solving the finite element equations.

(3) The functions f_t and g_t are generally discontinuous at points $\langle\{\chi_t\}, \{t_t\}\rangle$ which correspond to material yield surfaces.

The multistep methods (implicit and explicit) require relatively few evaluations of $\langle f_t, g_t\rangle$ per step; this is an attractive feature. However, multistep methods are not self starting, the time step is not easily changed, and they have relatively large storage requirements (since several past values of $\langle f_t, g_t\rangle$ must be carried along). Moreover, they cannot be expected to be accurate when the solution crosses a yield surface (since they are based on smooth polynomial interpolation of the solution over several time steps). On the other hand, the single step methods (implicit and explicit) are easily started, the time step size is easily adjusted, and they have relatively small storage requirements. They can be expected to perform more favorably than the multistep methods when the solution crosses a yield surface since smoothing over several time steps is not "built in". The disadvantage of the single step methods is that a relatively larger number of evaluations of $\langle f_t, g_t\rangle$ are required per step to achieve a given accuracy when a yield surface is not crossed. The scheme used may be varied from problem to problem, and it is often advantageous to vary it within a single problem.

In the example accompanying this report the Euler and classical second order Runge–Kutta (RK2) methods were used. Details of these methods may be found in many textbooks. Errors of the Euler method were gauged (qualitatively) by step-halving and by comparison to results of second order integration for randomly selected time steps.

It is worthy of special note that complementary work and energy principles provide no means whatever for checking the satisfaction of LMB‡, so it is of crucial importance that the numerical integration scheme not introduce errors which unbalance the

†The functions f and g are introduced specifically as a "shorthand" for the solution of the finite element equations. In practice integrations may be performed on one element at a time.

‡By formation of a residual.

stress. This maintenance of balanced stress, necessary in stress-based finite element algorithms, is the counterpart of maintenance of compatible deformation, necessary in velocity-based algorithms. It can be shown [6] that LMB is maintained when the stress t_τ is integrated explicitly, but not when other stresses (such as τ) are integrated explicitly. Thus we integrate t_τ (and χ_τ), and find τ (afterwards) by the formula

$$\tau = \mathbf{1}/J_\tau F_\tau \cdot t_\tau. \tag{43}$$

STABILITY OF NUMERICAL TIME INTEGRATION SCHEMES

It is possible that the difference between two supposed numerical solutions of a given initial value problem is much larger than would be expected to arise from discretization error alone. As an example, consider integration of the stress in a material of the type (14) by the Euler method. We suppose, for the sake of simplicity, that $\epsilon(t)$ is given and $\Sigma(\tau) = -2\mu(\frac{3}{2}\gamma\tau')$, so that the difference between two solutions satisfies

$$\Delta\dot{\sigma}^* = [\underline{\mathbf{Y}}(\tau + \Delta\tau) - \underline{\mathbf{Y}}(\tau)]:\epsilon(t) - (3\mu\gamma)\Delta\tau'. \tag{44}$$

If the eleastic matrix and stretching are such that, in the Euclidean norm,

$$\|[\underline{\mathbf{Y}}(\tau + \Delta\tau) - \underline{\mathbf{Y}}(\tau)]:\epsilon(t)\|/\|\Delta\tau \to 0 \tag{45}$$

as $\|\Delta\tau\| \to 0$, then for sufficiently small $\|\Delta\tau\|$, eqn (44) may be replaced by

$$\Delta\dot{\sigma}^* = -(3\mu\gamma)\Delta\tau'. \tag{46}$$

Defining $\Delta\sigma$ as $\Delta\sigma = J_0\sqrt{\frac{3}{2}}\Delta\tau':\Delta\tau'$, we may reduce (46) to a scalar equation in the invariant $\Delta\sigma$:

$$\mathrm{d}/\mathrm{d}t(\Delta\sigma) = -(3\mu\gamma)\Delta\sigma. \tag{47}$$

For an initial value $\Delta\sigma(0)$ (small), the closed form solution of (47) is

$$\Delta\sigma(t) = \Delta\sigma(0)\,\mathrm{e}^{-(3\mu\gamma)t}. \tag{48}$$

Euler's method yields

$$\Delta\sigma_N = \Delta\sigma(0)(1 - 3\mu\gamma h)^N. \tag{49}$$

It is clear from (48) that $\Delta\sigma$ decays to zero as time passes. This means that the closed form solution of the initial value problem

$$\dot{\sigma}^* = \underline{\mathbf{Y}}:\epsilon(t) + \Sigma; \quad \tau(0) = \tau_0 \tag{50}$$

is stable with respect to sufficiently small perturbations of τ_0'. On the other hand, the numerical solution (49) attenuates as time passes only if

$$|(1 - 3\mu\gamma h)| < 1. \tag{51}$$

This means that the numerical solution of (50) is stable with respect to small perturbations of τ_0' only so long as the time step h is bounded as

$$|h| < 2/(3\mu\gamma). \tag{52}$$

This bound is identical to the bound given by Cormeau ([7], see eqns 16 and 54 in this reference).

Time steps such as (52) are necessary stability of numerical solutions of the finite element-initial value problem as presented above. Argyris *et al.* [8] remark that this time step restriction amounts to limiting the inelastic strain increment to be smaller than the elastic strain. Since the elastic strain is usually very small in metals such as those used in structures, this implies that a finite deformation analysis would entail an intolerably large number of steps.

The work of Kanchi *et al.* [9] and Atluri and Murakawa [4] suggest the "forward gradient scheme" now given. To improve the estimate of the inelastic strain increment in a time step, we replace $\epsilon^p(\tau_N)$ by an estimate of the mean value of the inelastic stretching in that time step:

$$\epsilon^p(\tau(t_N + \theta h)) = \epsilon^p(\tau(t_N) + \theta h \left.\frac{\mathrm{d}\epsilon^p}{\mathrm{d}\tau}\right|_{\tau=\tau_N} :\dot{\sigma}^* \tag{53}$$

where the parameter θ, $0 \le \theta \le 1$, serves to locate the time at which the mean value is achieved.

Equation (53) may be introduced to the finite element algorithm through the constitutive equation; (14) becomes

$$\dot{\sigma} = \underline{\mathbf{Y}}_\theta:\epsilon + \Sigma_\theta$$

where

$$\underline{\mathbf{Y}}_\theta = \left[\underline{\mathbf{Y}}^{-1} + \theta h \frac{\mathrm{d}\epsilon^p}{\mathrm{d}\tau}\right]^{-1}; \quad \Sigma_\theta = -\underline{\mathbf{Y}}_\theta:\epsilon^p. \tag{54}$$

From $\underline{\mathbf{Y}}_\theta$ (54) we derive $\underline{\mathbf{W}}_\theta$ just as we derived $\underline{\mathbf{W}}$ from $\underline{\mathbf{Y}}$

$$\underline{\mathbf{W}}_\theta = \underline{\mathbf{Y}}_\theta - \underline{\mathbf{T}}; \quad T_{ijkl} = \frac{1}{2}(\tau_{ik}\delta_{lj} + \delta_{ik}\tau_{lj}); \tag{55}$$

$$\Sigma_\theta = -\underline{\mathbf{Y}}_\theta:\epsilon^p = -(\underline{\mathbf{W}}_\theta + \underline{\mathbf{T}}):\epsilon^p.$$

When a material which exhibits relaxation is to be analyzed, $\underline{\mathbf{W}}_\theta$ and Σ_θ are introduced to the finite element algorithm for $\underline{\mathbf{W}}$ and Σ. The effect on accuracy of so called "gradient schemes" is investigated in [6].

EXAMPLE: GROWTH OF A VOID IN A VISCOPLASTIC MEDIUM

In this example we examine the growth of a void in a hypoelastic/viscoplastic medium. This problem has been studied (numerically) by Burke and Nix [10], who treated the material as rigid/viscoplastic. We present the problem as a demonstration of the performance of the finite element algorithm. The material exhibits stress relaxation, so the forward gradient scheme must be used to stabilize the time integration. The present results agree quite closely with those of Burke and Nix.

The motion is assumed to be plane strain, and throughout the body is a doubly periodic array of cylinderical voids. Due to the symmetry we need analyze only one quadrant of one rectangular cell of the body. The finite element mesh and boundary conditions are described in Fig. 1.

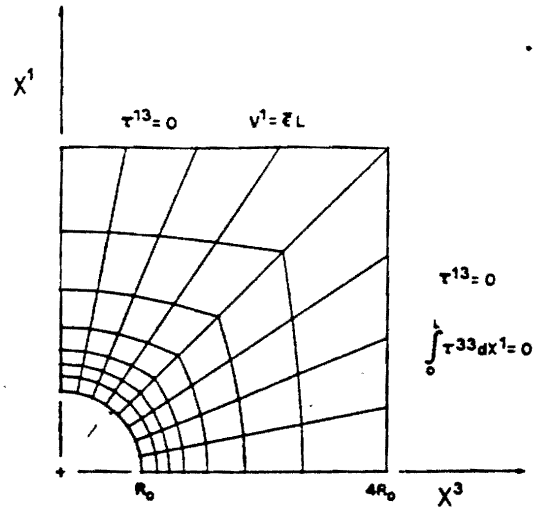

Fig. 1. Finite element mesh and boundary conditions for void growth problem.

Burke and Nix motivate their study by recalling the widely held belief that the initiation of creep fracture is attributable to the coalescence of voids. Some evidence suggests that the growth of voids is governed not by diffusion, but by "inhomogeneous plastic deformation of the surrounding grains." Correlation of a "deformation theory" of creep fracture to experiment could (in principle) be accomplished by finite element analyses of a number of model problems. The example presented here serves to demonstrate; (i) the feasibility of such an analysis and (ii) the performance of the new finite element algorithm.

The problem has been analyzed in three parts. In the first part the cell is brought rapidly from the stress-free state to a state of purely elastic strain. This is accomplished by a single RK2 step. In the second part, relatively small time steps are taken while the stress relaxes from the elastic distribution to a nearly steady creep distribution. In the third part, time steps are taken which produce 1% nominal elongation of the cell in each step. To stabilize time integration in the second and third parts the forward gradient scheme is used, the stability parameter θ set as $\theta = 1/2$ and 3/4, respectively. Only the Euler time stepping scheme has been used in the second and third parts of the problem.

The material model is a special case of (14):

$$\epsilon = \epsilon^e + \epsilon^p$$

$$\epsilon^e = \left(\frac{1+\nu}{E}\right)\dot{\sigma}^* - \left(\frac{\nu}{E}\right)(I:\dot{\sigma}^*)I$$

$$\epsilon^p = \frac{3}{2}\gamma\tau'$$

This model corresponds to that of Burke and Nix with (their) creep exponent $n = 1$. The fluidity γ is set as $\gamma = 1 \times 10^{-19}$ (psi-sec)$^{-1}$. The velocity at the top of the cell (see Fig. 1) was adjusted so that a specimen with no void would experience a homogeneous constant stretching $\epsilon^{11} = \bar{\epsilon} = 0.25 \times 10^{-14}$ sec^{-1}. Since the material was treated as an incompressible viscous fluid by Burke and Nix, our choice of elastic constants is somewhat arbitrary. We have taken Young's modulus $E = 3 \times 10^7$ psi and Poisson's ration $\nu = 0.4$, so the material is somewhat like steel in its elastic response.

In Figs 2–4 the contours of stress τ^{11}, stress τ^{33} and mean stress, have been plotted for L (the elongation of the cell) $L = 1.01$. The stress concentration where the hole edge crosses the x^3 axis is approximately 2.7.† This is quite reasonable since the theoretical value for an isolated void in a purely elastic medium is 3.0. Burke and Nix found an approximate value of 2.66 for the viscous fluid. In Fig. 5 the contours of effective strain rate $\sqrt{\frac{2}{3}\epsilon^p:\epsilon^p}/\bar{\epsilon}$ are plotted for $L = 1.01$. Qualitatively this compares very well to Fig. 7 in [10].

In Fig. 6 the deformation is traced from $L = 1.0$ to $L = 1.5$. These deformations are physically tenable. We remark that no indication of any numerical

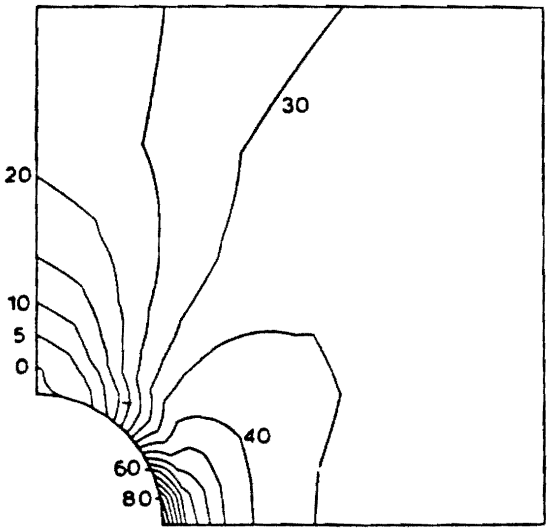

Fig. 2. Contours of true stress τ^{11} ($L = 1.01$).

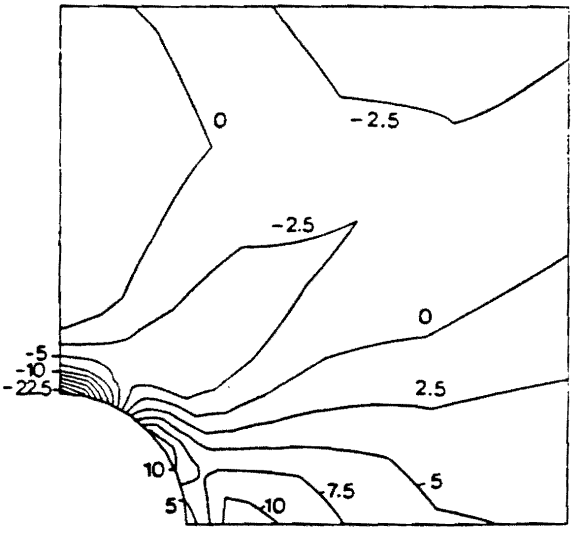

Fig. 3. Contours of true stress τ^{33} ($L = 1.01$).

†A stress concentration of approx. 2.59 was observed for the elastically stressed medium.

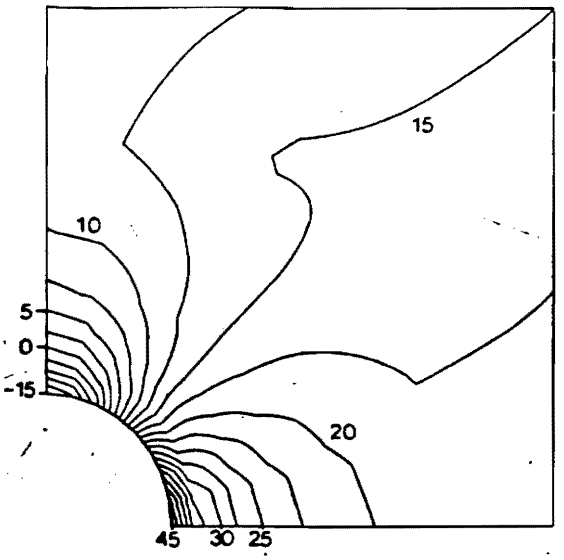

Fig. 4. Contours of mean stress ($L = 1.01$).

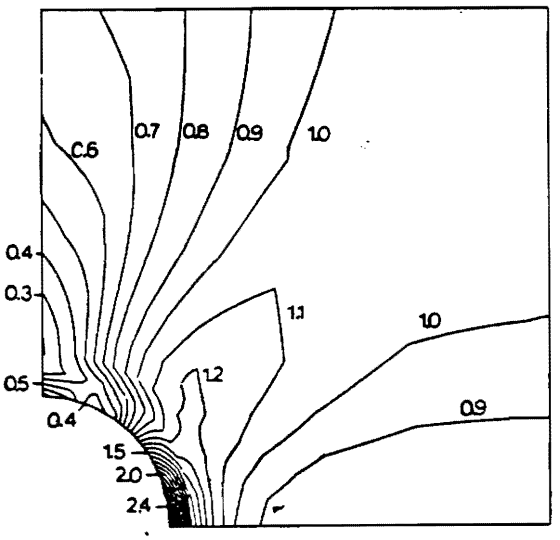

Fig. 5. (a) Contours of effective strain rate ($L = 1.01$).

instability was observed in the of integrating this deformation.

In Figs. 7–9 the contours of stress τ^{11}, τ^{33}, and mean stress, have been plotted for $L = 1.50$. They compare very well to the stresses found in ([10], see Fig. 8 there). We note that the stress concentration has dropped to 1.7i. The stress concentration de-

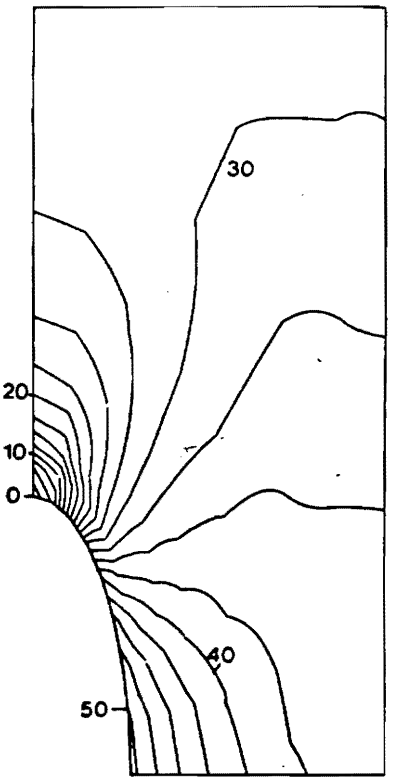

Fig. 7. Contours of true stress τ^{11} ($L = 1.50$).

pends strongly on the geometry of the specimen; as such, it was observed to decline steadily throughout the deformation. In Fig. 10 the contours of effective strain rate are plotted for $L = 1.5$. Again, the qualitative agreement with the results of Burke and Nix [10] is noted (see Fig. 9 there).

We conclude by noting that in the present analysis only 56 four noded elements were used, as compared to 56 eight noded elements used in the analysis of Burke and Nix. Considering the agreement between their results and our own, the present method appears to have performed very well, in spite of the large disparity in the degrees of freedom of the finite element mesh.

CLOSURE

A new hybrid-stress finite element algorithm for the analysis of large, quasi static, inelastic deformations has been developed, and its versatility in analyzing problems of stress-concentration has been demonstrated. The results point to the relative accuracy of

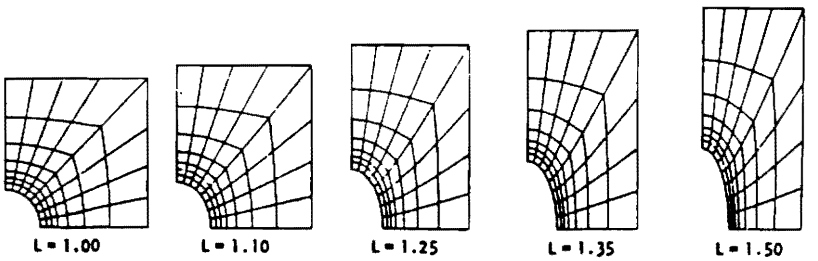

Fig. 6. Deformation history of cell quadrant.

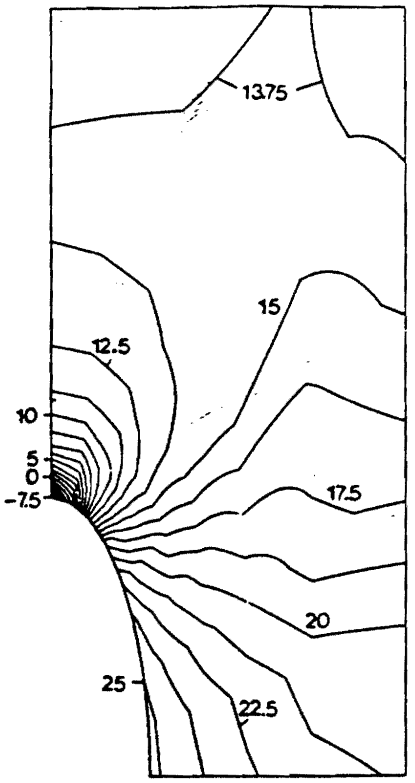

Fig. 8. Contours of true stress τ^{33} ($L = 1.50$).

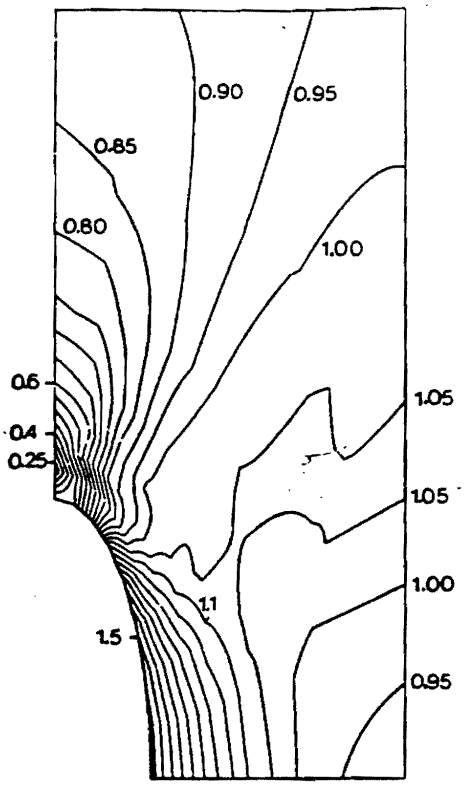

Fig. 10. Contours of effective strain rate ($L = 1.50$).

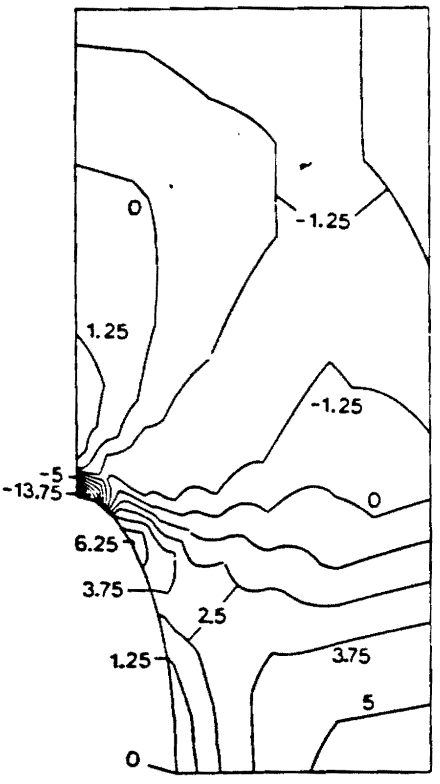

Fig. 9. Contours of mean stress ($L = 1.50$).

the present algorithm as compared to standard assumed velocity formulations commonly reported in literature.

Acknowledgements—This work was supported by the NASA-Lewis Research Center under grant NAG3-38 to Georgia Tech. The authors gratefully acknowledge this support. Appreciation is expressed to Ms. Brenda Bolinger for her help in preparing this manuscript.

REFERENCES

1. T. H. H. Pian, Derivation of element stiffness matrices by assumed stress distributions. *AIAA J.* **2**, 1333–1336 (1964).
2. B. Fraeijs de Veubeke, A new variational principle for finite elastic deformations. *Int. J. Eng. Sci.* **10**, 745–763 (1972).
3. S. N. Atluri, On some new general and complementary energy theorems for the rate problems of finite strain, classical elasto–plasticity. *J. Structural Mech.* **8**, 61–92 (1980).
4. S. N. Atluri and H. Murakawa, New general and complementary energy theorems, finite strain, rate sensitive inelasticity and finite elements: some computational studies. In *Nonlinear Finite Element Analysis in Structural Mechanics* (Edited by W. Wunderlich, E. Stein and K.-J. Bathe). Springer-Verlag, Berlin (1981).
5. H. Murakawa, Incremental hybrid finite element methods for finite deformation problems (with special emphasis on the complementary energy principle). Ph.D. Dissertation, Georgia Institute of Technology, August 1978.
6. K. W. Reed, Analysis of large quasistatic deformations of inelastic solids by a new stress-based finite element method. Ph.D. Dissertation, Center for the Advance-

ment of Computational Mechanics, Georgia Institute of Technology, April 1982.
7. I. Cormeau, Numerical stability in quasistatic elasto–viscoplasticity. *Int. J. Num. Mech. Engng* **9**, 109–127 (1975).
8. J. H. Argyris, L. E. Vaz and K. J. Willam, Improved solution methods for inelastic rate problems. *Comput. Meth. Appl. Mech. Eng.* **16**, 231–277 (1978).
9. M. B. Kanchi, O. C. Zienkiewicz and R. J. Owen, The visco-plastic approach to problems of plasticity and creep involving geometric nonlinear effects. *Int. J. Num. Meth. Engng* **12**, 169–181 (1978).
10. M. A. Burke and W. D. Nix, A numerical analysis of void growth in tension creep. *Int. J. Solids Structures* **15**, 55–71 (1979).

APPENDIX A

Plane strain

The deformation studied in the example accompanying this report is plane strain in the character. Just as for formulations using ordinary stresses, a number of the components of the velocity, spin, and stress rate vanish if a Cartesian Coordinate system is chosen with one axis normal to the plane of deformation. We have chosen the x^2 coordinate line to be normal to the plane of deformation, so that the velocity, spin, stress rate, and stress are of the forms

$$\mathbf{v} = v^1\mathbf{e}_1 + v^3\mathbf{e}_3$$

$$\boldsymbol{\omega} = \omega^{13}\mathbf{e}_1\mathbf{e}_3 + \omega^{31}\mathbf{e}_e\mathbf{e}_1$$

$$\dot{t} = \dot{t}^{11}\mathbf{e}_1\mathbf{e}_1 + \dot{t}^{13}\mathbf{e}_1\mathbf{e}_3 + \dot{t}^{22}\mathbf{e}_2\mathbf{e}_2 + \dot{t}^{31}\mathbf{e}_3\mathbf{e}_1 + \dot{t}^{33}\mathbf{e}_3\mathbf{e}_3$$

$$\boldsymbol{\tau} = \tau^{11}\mathbf{e}_1\mathbf{e}_1 + \tau^{13}\mathbf{e}_1\mathbf{e}_3 + \tau^{22}\mathbf{e}_2\mathbf{e}_2 + \tau^{31}\mathbf{e}_3\mathbf{e}_1 + \tau^{33}\mathbf{e}_3\mathbf{e}_3.$$

None of the components depends upon x^2. The velocity is represented on each element as

$$\mathbf{v} = \sum_{i=1}^{NQ} \mathbf{N}_i q^i.$$

The shape functions $\mathbf{N}_i$ are described below. Similarly the spin and stress rate are represented as

$$\boldsymbol{\omega} = \sum_{i=1}^{NW} QW_i\alpha^i; \quad \dot{t} = \sum_{i=1}^{NT} QT_i\beta^i.$$

We note that the plane strain condition is not satisfied a priori; that is

$$\delta\epsilon_{22} = (\mathbf{e}_2\mathbf{e}_2) : \underline{\mathbf{W}}^{-1} : \delta\dot{t} \neq 0$$

for arbitrary $\delta\dot{t}$. Rather, $\epsilon_{22} = 0$ follows from the stationary condition (a component of (8)):

$$\int_V [-\epsilon_{22}(\dot{t}, \boldsymbol{\omega})]\delta\dot{t}^{22}\,\mathrm{d}V = 0.$$

In using the finite element algorithm the plane strain condition is satisfied only in a mean sense on each element.

Shape functions for velocity, stress rate, and spin

Shape functions for plane strain

$$x^1 = x; \quad x^3 = z.$$

Velocity shape functions

$$\mathbf{N}_i = N_{1,i}\mathbf{e}_1 + N_{3,i}\mathbf{e}_3.$$

Four noded element

$$N_{1,i} = \begin{cases} \frac{1}{4}(1 + \xi\xi_i)(1 + \eta\eta_i) & i = 1, 2, 3, 4 \\ 0 & i = 5, 6, 7, 8 \end{cases}$$

$$N_{3,i} = \begin{cases} 0 & i = 1, 2, 3, 4 \\ \frac{1}{4}(1 + \xi\xi_{i-4})(1 + \eta\eta_{i-4}) & i = 5, 6, 7, 8 \end{cases}$$

$$|\xi| \leq 1, \quad |\eta| \leq 1,$$

$$\xi_1 = -1, \quad \xi_2 = 1, \quad \xi_3 = 1, \quad \xi_4 = -1$$

$$\eta_1 = -1, \quad \eta_2 = -1, \quad \eta_3 = 1, \quad \eta_4 = 1.$$

Shape functions for spin

$$QW_i = QW_{13,i}\mathbf{e}_1\mathbf{e}_3 + QW_{31,i}\mathbf{e}_3\mathbf{e}_1$$

where

$$QW_{13,1} = c$$

$$QW_{31,1} = -c_1$$

$$QW_{13,2} = xc_2$$

$$QW_{13,3} = zc_3$$

$$QW_{31,2} = -xc_2$$

$$QW_{31,3} = -zc_3.$$

The constants were used to improve the condition of $[H]$.

Stress rate shape functions

$$QT_i = QT_{11,i}\mathbf{e}_1\mathbf{e}_1 + 0 + QT_{13,i}\mathbf{e}_1\mathbf{e}_3 + 0 + QT_{22,i}\mathbf{e}_2\mathbf{e}_2 + QT_{31,i}\mathbf{e}_3\mathbf{e}_1 + 0 + QT_{33,i}\mathbf{e}_3\mathbf{e}_3$$

$$QT_{11,1} = 1$$

$$QT_{31,2} = -1$$

$$QT_{22,3} = 1$$

$$QT_{13,4} = -1$$

$$QT_{33,5} = 1.$$

For $NT = 13$ add the following stress shape functions

$$QT_{11,6} = x$$

$$QT_{31,6} = -z$$

$$QT_{31,7} = -x$$

$$QT_{22,8} = x$$

$$QT_{13,9} = -x$$

$$QT_{33,9} = z$$

$$QT_{33,10} = x$$

$$QT_{11,11} = z$$

$$QT_{13,12} = -z$$

$$QT_{22,13} = z.$$

#168

COMPUTER METHODS IN APPLIED MECHANICS AND ENGINEERING 40 (1983) 171–198
NORTH-HOLLAND

168

ANALYSES OF LARGE QUASISTATIC DEFORMATIONS OF INELASTIC BODIES BY A NEW HYBRID-STRESS FINITE ELEMENT ALGORITHM: APPLICATIONS

K.W. REED and S.N. ATLURI

Center for the Advancement of Computational Mechanics, School of Civil Engineering, Georgia Institute of Technology, Atlanta, GA 30332, U.S.A.

Received 14 October 1982

In an earlier paper [1] the authors described a new hybrid-stress finite element algorithm suitable for the analysis of large quasistatic deformations of inelastic bodies. However, that paper focused on the subtleties of the algorithm, and only finite homogeneous deformation problems were presented as examples. The present paper is concerned with the algorithm's implementation and application to problems of technological interest.

0. Nomenclature[1]

$C(\tau)$ configuration (image of the body in space at time τ),
X position vector in space at time τ,
x position vector in space at (present) time t,
$\nabla = e^i \partial/\partial x^i$,
$\nabla_\tau = e^I \partial/\partial X^I$,
$\dot{a} = \partial a/\partial t + v \cdot \nabla a$ (material derivative of 'a'),
χ_τ deformation function, maps $C(\tau)$ to $C(t)$ as $x = \chi_\tau(X, t)$,
v velocity function, related to deformation function as $v(\chi_\tau(X, t), t) = \partial/\partial t\, \chi_\tau(X, t)$,
$\mathbf{F}_\tau \equiv (\nabla_\tau \chi_\tau(X, t))^t$ deformation gradient,
$J_\tau = \det \mathbf{F}_\tau$,
$\mathbf{L} = (\nabla v(x, t))^t$ velocity gradient,
$\dot{J} = \nabla \cdot v(x, t)$ dilitation,
$\boldsymbol{\varepsilon} = \frac{1}{2}(L + L^t)$ stretching,
$\boldsymbol{\omega} = \frac{1}{2}(L - L^t)$ spin,
T true traction,
T_τ nominal traction relative to $C(\tau)$,
$\boldsymbol{\tau}$ true stress,
$\boldsymbol{\sigma}_\tau = J_\tau \boldsymbol{\tau}$ Kirchhoff stress relative to $C(\tau)$,
$\mathbf{t}_\tau = \mathbf{F}_\tau^{-1} \boldsymbol{\sigma}_\tau$ nominal stress relative to $C(\tau)$,
$\dot{T}$ true traction rate,
$\dot{T}_\tau$ nominal traction rate,
$\dot{\boldsymbol{\sigma}} = \dot{J}\boldsymbol{\tau} + \dot{\boldsymbol{\tau}}$ Kirchhoff stress rate,
$\mathbf{t} = -(\boldsymbol{\varepsilon} + \boldsymbol{\omega}) \cdot \boldsymbol{\tau} + \dot{\boldsymbol{\sigma}}$ nominal stress rate,
$\dot{\boldsymbol{\sigma}}^*$ $= \dot{\boldsymbol{\sigma}} - \boldsymbol{\omega} \cdot \boldsymbol{\tau} + \boldsymbol{\tau} \cdot \boldsymbol{\omega}$ 'corotational' rate of Kirchhoff stress.

1. Introduction

It is well known that finite element algorithms in which the stress is one of the principal variables produce significantly better approximations for the stress than do algorithms involv-

[1] A reasonably complete discussion of the fundamental kinematics and dynamics may be found in the authors' earlier article [1].

0045-7825/83/$3.00

on this rate-principle; it takes the form

$$\pi_c(v, \omega, \dot{\mathbf{t}}; \dot{\mathbf{r}}) = \int_V \{-\mathscr{R}(\dot{\mathbf{r}}) - \tfrac{1}{2}\boldsymbol{\tau} : (\boldsymbol{\omega} \cdot \boldsymbol{\omega}) + \dot{\mathbf{t}} : \boldsymbol{\omega}\} \mathrm{d}V + \int_{S_v} \boldsymbol{n} \cdot \dot{\mathbf{t}} \cdot \bar{\boldsymbol{v}} \, \mathrm{d}S + \int_{S_\sigma} (\boldsymbol{n} \cdot \dot{\mathbf{t}} - \dot{\bar{\boldsymbol{T}}}_t) \cdot \boldsymbol{v} \, \mathrm{d}S \tag{2.1}$$

with subsidiary conditions

$$\dot{\mathbf{r}} = \tfrac{1}{2}(\dot{\mathbf{t}} + \boldsymbol{\tau} \cdot \boldsymbol{\omega} - \boldsymbol{\omega} \cdot \boldsymbol{\tau} + \dot{\mathbf{t}}^{\mathrm{t}}),$$
$$\dot{\mathbf{t}} = \dot{\mathbf{t}}^0 + \dot{\mathbf{t}}^b, \qquad \dot{\mathbf{t}}^0 = \nabla \times \boldsymbol{\Phi}, \qquad \nabla \cdot \dot{\mathbf{t}}^b = -\rho \dot{\mathbf{b}},^5 \tag{2.2}$$
$$\boldsymbol{\omega} + \boldsymbol{\omega}^{\mathrm{t}} = \mathbf{0}.$$

The function $\mathscr{R}(\dot{\mathbf{r}})$ is formally counterpart to the complementary energy density of linear elasticity, sharing with it the property

$$\boldsymbol{\varepsilon} = \partial_{\dot{\mathbf{r}}} \mathscr{R}(\dot{\mathbf{r}}). \tag{2.3}$$

When a rate-type constitutive equation of the form

$$\dot{\sigma}^*_{ij} = V_{ijkl}(\varepsilon_{kl} - \varepsilon^\rho_{kl}) \tag{2.4}$$

exists, then using the definitions $\dot{\mathbf{t}} \equiv \dot{\boldsymbol{\sigma}} - (\boldsymbol{\varepsilon} + \boldsymbol{\omega}) \cdot \boldsymbol{\tau}$ and $\dot{\boldsymbol{\sigma}}^* \equiv \dot{\boldsymbol{\sigma}} - \boldsymbol{\omega} \cdot \boldsymbol{\tau} + \boldsymbol{\tau} \cdot \boldsymbol{\omega}$, we can show that

$$\tfrac{1}{2}(\dot{t}_{ij} + \tau_{ik}\omega_{kj} - \omega_{ik}\tau_{kj} + \dot{t}_{ji}) = [V_{ijkl} - \tfrac{1}{2}(\tau_{ik}\delta_{lj} + \delta_{ik}\tau_{lj})]\varepsilon_{kl} - V_{ijkl}\varepsilon^\rho_{kl}$$

or simply, using the definition of $\dot{\mathbf{r}}$,

$$\dot{\mathbf{r}} = \underline{\mathbf{W}} : \boldsymbol{\varepsilon} - \underline{\mathbf{V}} : \boldsymbol{\varepsilon}^\rho. \tag{2.5}$$

If $\underline{\mathbf{W}}$ is invertible then we may solve (2.5) for $\boldsymbol{\varepsilon}$:

$$\boldsymbol{\varepsilon} = \underline{\mathbf{W}}^{-1} : (\dot{\mathbf{r}} + \underline{\mathbf{V}} : \boldsymbol{\varepsilon}^\rho), \tag{2.6}$$

and if $\underline{\mathbf{W}}$ is symmetric (i.e. $W_{ijkl} = W_{klij}$; this is contingent upon the symmetry of V_{ijkl}), then we can define $\mathscr{R}(\dot{\mathbf{r}})$ as:

$$\mathscr{R}(\dot{\mathbf{r}}) \equiv \tfrac{1}{2}(\dot{\mathbf{r}} - \boldsymbol{\Sigma}) : \underline{\mathbf{W}}^{-1} : (\dot{\mathbf{r}} - \boldsymbol{\Sigma}) \tag{2.7}$$

where

$$\boldsymbol{\Sigma} \equiv -\underline{\mathbf{V}} : \boldsymbol{\varepsilon}^\rho.$$

[5] $\dot{\mathbf{t}}^0$ is subject to variation whereas $\dot{\mathbf{t}}^b$ is not.

as S_N. The rate functional π_c (2.1) may now be written

$$\pi_c(v, \omega, \dot{t}; \dot{r}) = \sum_{N=1}^{NELM} \left\{ \int_{V_N} \{-\mathscr{R}(\dot{r}) - \tfrac{1}{2}\tau : (\omega \cdot \omega) + \dot{t} : \omega\} dV + \int_{(S_N \cap S_V)} n \cdot \dot{t} \cdot \bar{v}\, dS + \int_{(S_N \cap S_V)} (n \cdot \dot{t} - \dot{\bar{T}}_t) \cdot v\, dS \right\}. \tag{2.13}$$

Of course the same subsidiary conditions (2.2) apply. This implies that only stress function Φ differentiable over all V are 'admissible' to the variational principle, a condition inconvenient to meet in the actual implementation of finite element algorithms. It is much more convenient to respect Φ independently on each element, enforcing 'traction reciprocity' between elements via a Lagrange multiplier v such that

$$\sum_{N=1}^{NELM} \left\{ \int_{S_N - (S_N \cap S)} n \cdot \dot{t} \cdot \delta v\, dS \right\} = 0. \tag{2.14}$$[6]

Appending (2.14) to (2.13), and treating the velocity boundary condition as subsidiary, we finally get

$$\pi_c^*(v, \omega, \dot{t}; \dot{r}) = \sum_{N=1}^{NELM} \left\{ \int_{V_N} \{-\mathscr{R}(\dot{r}) - \tfrac{1}{2}\tau : (\omega \cdot \omega) + \dot{t} : \omega\} dV + \int_{S_N} n \cdot \dot{t} \cdot v\, dS - \int_{S_N \cap S} \dot{\bar{T}}_t \cdot v\, dS \right\}, \tag{2.15}$$

which admits $\omega, \dot{t}$, and $\dot{r}$ subject to (2.2), but independent between elements, and v that is single-valued over all $(S_N \cap S)$, $(S_N \cap S_M)$, and equal to $\bar{v}$ on S_V. Since we can easily construct representations for $\omega, \dot{t}, \dot{r}$, and v satisfying these conditions of admissibility, π_c^* (2.15) is suitable as a basis for a finite element algorithm.

3. The finite element equations

The finite element equations are obtained by introduction of polynomial representations for v, ω and $\dot{t}$ to π_c^* (2.15) and performing the assigned quadratures. On the Nth element let v, ω and $\dot{t}$ be represented as

$$v = \sum_{i=1}^{NQ} N_i q_N^i = [N]\{q_N\}, \tag{3.1}$$

$$\omega = \sum_{i=1}^{NW} QW_i \alpha_N^i = [QW]\{\alpha_N\}, \tag{3.2}$$

[6] Due to the single-valuedness of δv on interelement boundaries, terms in (2.14) 'pair up' as $\int_{(S_N \cap S_M)} (n_N \cdot \dot{t}_N + n_M \cdot \dot{t}_M) \cdot \delta v\, dS = 0$, which clearly expresses interelement traction reciprocity.

$\{\alpha/\beta\}$ from (3.9) leads to 'global' finite element equations of the form (for details, see [1, 15])

$$\{\delta\mathcal{Q}\}^t\{[\mathcal{K}]\{\mathcal{Q}\}+\{\mathcal{P}\}-\{\mathcal{F}\}\}=0\,. \tag{3.10}$$

Here $[\mathcal{K}]$ is the stiffness matrix, $\{\mathcal{P}\}$ includes effects of relaxation and body force, $\{\mathcal{F}\}$ includes the traction boundary condition, and $\{\mathcal{Q}\}$ is the global nodal velocity vector, satisfying $\mathcal{Q}_I=\bar{\mathcal{Q}}_I$ and $\delta\mathcal{Q}_I=0$ on S_V. Equation (3.10) can be solved by standard methods [17]. It should be noted that the global stiffness matrix changes with time, as in any tangent stiffness formulation. By a process of backsubstitution one may finally recover $\boldsymbol{v}(\boldsymbol{x},t)$, $\boldsymbol{\omega}(\boldsymbol{x},t)$, and $\dot{\mathbf{t}}(\boldsymbol{x},t)$.

4. Definition and numerical treatment of the initial value problem

The finite element algorithm described in the previous section produces approximations for the stress rate $\dot{\mathbf{t}}$ and spin $\boldsymbol{\omega}$ on the interior of each element, and the velocity of the boundary of each element. The velocity on the interior of an element is found by interpolation of its boundary velocity. (The soundness of this procedure is examined in [15].)

Now let us write $\{\boldsymbol{x}\}=\{\boldsymbol{x}^1,\boldsymbol{x}^2,\ldots,\boldsymbol{x}^{\mathrm{ND}}\}$ for the vector of *nodal positions*, and $\{\boldsymbol{v}\}=\{\boldsymbol{v}^1,\boldsymbol{v}^2,\ldots,\boldsymbol{v}^{\mathrm{ND}}\}$ for the vector of *nodal velocities*, ND being the total number of nodes in the finite element mesh. Similarly, let $\{\boldsymbol{\tau}\}=\{\boldsymbol{\tau}^1,\boldsymbol{\tau}^2,\ldots,\boldsymbol{\tau}^G\}$ be the vector of *quadrature point stresses*, and let $\{\dot{\mathbf{t}}\}=\{\dot{\mathbf{t}}^1,\dot{\mathbf{t}}^2,\ldots,\dot{\mathbf{t}}^G\}$ be the vector of *quadrature point stress rates*. As a 'shorthand' for the solution of the finite element equations, which depends upon $\{\boldsymbol{x}\}$, $\{\boldsymbol{\tau}\}$ and the time dependent prescribed loads, we write

$$\{\boldsymbol{v}\}=\mathscr{f}[\{\boldsymbol{x}\},\{\boldsymbol{\tau}\},t]\,, \tag{4.1}$$

$$\{\dot{\mathbf{t}}\}=g[\{\boldsymbol{x}\},\{\boldsymbol{\tau}\},t]\,. \tag{4.2}$$[9]

Putting $\boldsymbol{\chi}_\tau(\boldsymbol{X},t)$ for $\boldsymbol{x}$, $\dot{\boldsymbol{\chi}}_\tau(\boldsymbol{X},t)$ for $\boldsymbol{v}(\boldsymbol{\chi}_\tau(\boldsymbol{X},t),t)$, $J_\tau^{-1}(\boldsymbol{X},t)\mathbf{F}_\tau(\boldsymbol{X},t)\cdot\mathbf{t}_\tau(\boldsymbol{X},t)$ for $\boldsymbol{\tau}(\boldsymbol{\chi}_\tau(\boldsymbol{X},t),t)$, and $J_\tau^{-1}(\boldsymbol{X},t)\mathbf{F}_\tau(\boldsymbol{X},t)\cdot\dot{\mathbf{t}}_\tau(\boldsymbol{X},t)$ for $\dot{\mathbf{t}}(\boldsymbol{\chi}_\tau(\boldsymbol{X},t),t)$ in (4.1) and (4.2), we finally obtain

$$\{\dot{\boldsymbol{\chi}}_\tau\}=\mathscr{f}_\tau[\{\boldsymbol{\chi}_\tau\},\{\mathbf{t}_\tau\},t]\,, \tag{4.3}$$

$$\{\dot{\mathbf{t}}_\tau\}=g_\tau[\{\boldsymbol{\chi}_\tau\},\{\mathbf{t}_\tau\},t]\,. \tag{4.4}$$

Equations (4.3) and (4.4), along with appropriate initial values for $\boldsymbol{\chi}_\tau$ and $\mathbf{t}_\tau$, define an initial value problem of ordinary differential equations. Since the finite element equations must be formed and solved anew for each evaluation of $\mathscr{f}_\tau$ and g_τ (i.e. the boundary value and initial value problems are coupled), we speak of the problem as the *finite element/initial value* problem.

In the examples accompanying this paper Euler and second- and fourth-order Runge–Kutta schemes were used [19, Section 6.5]. Quadrature point values of the true stress $\boldsymbol{\tau}$ were

[9] In practice it is never necessary to construct the 'global' vectors for $\{\boldsymbol{\tau}\}$ or $\{\dot{\mathbf{t}}\}$; their components $\boldsymbol{\tau}^I$, $\dot{\mathbf{t}}^I$ on each element may be treated independently of components on the other elements. The functions $\mathscr{f}$ and g are introduced here only for conceptual clarity.

contrasted to the performance of a velocity-based finite element algorithm, we have chosen particular materials identical to those used in the bifurcation study of Burke and Nix [27]. This appears to be the only other numerical study of bifurcation of classical elastic/plastic materials in plane extension in the literature.[11]

Finally, we investigate the sensitivity of our results to variations in the number, shape and type[12] of elements in the finite element mesh. This latter study serves not only to graphically demonstrate the stability of the finite element algorithm, but also to help characterize the approximation it provides.

5.1. *Bifurcation analysis*

Bifurcation analyses involving elastic/plastic bodies are complicated by the nonlinearity of the constitutive equation. However, Hill [30] has shown that if deformations of a certain 'linear comparison solid' are unique, then, under the same circumstances, deformations of the elastic/plastic solid are necessarily unique. In the present case, bifurcation from configurations of pure extension, bifurcation is possible in the elastic/plastic solid *as soon as it is possible in the linear comparison solid.*[13] Thus, we focus exclusively upon the question of uniqueness for the linear comparison solid.

Deformations of the linear comparison solid are unique if and only if the corresponding homogeneous boundary value problem has but the trivial solution. The finite element approximation for the deformation is unique if and only if the finite element equations (for the linear comparison solid) have only the trivial solution for homogeneous boundary data. The critical configurations are those in which (see (3.20))

$$\{\delta\mathcal{Q}\}^{\mathrm{t}}[\mathcal{K}]\{\mathcal{Q}\}=0\,,\qquad \mathcal{Q}^I=0 \quad\text{and}\quad \delta\mathcal{Q}^I=0 \quad\text{on } S_V\,,$$

does not imply that $\{\mathcal{Q}\}\equiv\{0\}$.

We consider a specimen of initial length $2a_0^3$ and thickness $2a_0^1$. We assume that the bifurcation mode will by symmetric in the sense that the velocity field may be reflected across the x^3-axis (see Fig. 1; this is consistent with usage of the adjective 'symmetric' by Hill and Hutchinson). The finite element mesh covers the region $0\leq x^1\leq a^1$, $0\leq x^3\leq 2a^3$. The specimen is composed of an elastic/plastic material whose loading behavior is defined by [27, (14)–(16)]

$$\boldsymbol{\varepsilon}=\underset{\sim}{\mathbf{V}}^{-1}:\dot{\boldsymbol{\sigma}}^{*}\,, \tag{5.1}$$

$$\underset{\sim}{\mathbf{V}}^{-1}=\left(\frac{1+\nu}{E}\right)\underset{\sim}{\mathbf{I}}-\left(\frac{\nu}{E}\right)\boldsymbol{\Pi}+\left(\frac{9}{4h\bar{\tau}^2}\right)\boldsymbol{\tau}'\boldsymbol{\tau}'\,. \tag{5.2}$$

The constants E and ν are Young's modulus and Poisson's ratio, respectively, and $\boldsymbol{\tau}'$ is the deviatoric stress. The 'effective uniaxial stress' $\bar{\tau}$ is defined as $\bar{\tau}\equiv(\frac{3}{2}\boldsymbol{\tau}':\boldsymbol{\tau}')^{1/2}$, and the 'uniaxial

[11]Other workers consider specimens with geometric imperfections; cf. [28, 29].

[12]The 'type' is determined by the number of boundary nodes, the number of spin parameters and the number of stress-rate parameters.

[13]In fact, an actual bifurcated solution of the elastic/plastic boundary value problem can be constructed by judicious superposition of the 'eigenmodal deformation' and the pure extension of the linear comparison solid.

which (i) (5.4) was a very good approximation, and (ii) the influence of ν on $4\mu^*$ was negligible.

The dimensionless stress $(\tau^{33}/4\mu^*)$ arises naturally in the analysis of Hill and Hutchinson. When the material (5.1)–(5.2) is incompressible, we find that in pure extension

$$\frac{\tau^{33}}{4\mu^*} = \frac{\sqrt{3}N\tau_y}{2E}\left(\frac{\sqrt{3}\tau^{33}}{2\tau_y}\right)^N = -\tfrac{1}{2}N\ln(X/X_0) \tag{5.6}$$

where $X = (a^1/2a^3)$ is the *stubbiness*, and X_0 is the initial stubbiness. It is well known that the maximum load occurs when the plane strain tangent modulus falls to equal the stress; (i.e. when $(\tau^{33}/4\mu^*) = 1$). No bifurcation can occur before this point [31].

The tangent modulus continues to decline after the maximum load, so $4\mu^* < \tau^{33}_{\text{max load}} \ll \mu$; that is, the tangent modulus is much smaller than the shear modulus in the neighborhood of the bifurcations points. As such, the critical stress $(\tau^{33}/4\mu^*)$ may be found by the asymptotic formula [26, (6.8)]

$$(\tau^{33}/4\mu^*) = \tfrac{1}{2} + \frac{\gamma}{\sin 2\gamma} + \frac{2\mu^*}{\mu}\left\{\left(\frac{\gamma}{\sin 2\gamma}\right)^3(1+\cos 2\gamma) - \tfrac{1}{8} - \frac{\gamma}{\sin 2\gamma}(\tfrac{1}{4}+\tfrac{1}{3}\gamma^2)\right\} + O\left(\frac{\mu^*}{\mu}\right)^2 \tag{5.7}$$

where $\gamma = m\pi X$, m an integer. As $(2\mu^*/\mu)\to 0$, this formula reduces to that of Cowper and Onat [32] for a rigid-plastic solid. We could use (5.6) to eliminate either $(\tau^{33}/4\mu^*)$ or X from (5.7) to get eigenvalue equations for X or $(\tau^{33}/4\mu^*)$, respectively, but for clarity it is better to plot (5.6) and (5.7) independently in the X-$(\tau^{33}/4\mu^*)$ plane. The critical configurations in plane extension may then be identified as the points at which the curves intersect. This is the approach we take, marking the critical configurations found by application of the finite element algorithm on the same plot.

For numerical study we take Young's modulus $E = 6.895\times 10^4$ MPa, $\nu = \frac{1}{3}$, and $\tau_y = 344.75$ MPa. Six individual cases are considered, corresponding to values of the hardening exponent $N = 4$ and $N = 8$, for initial slenderness of $1/X_0 = 2, 3$ and 4. These same six cases were studied by Burke and Nix. The problem may be treated in two parts: (i) generation of the solution for homogeneous extension, and (ii) location of the critical configurations through which the specimen passes in the course of homogeneous extension.

To generate the solution for homogeneous extension for all six cases it is only necessary to find the solutions for extensions of a unit cube of the two materials involved. These solutions consist of a sequence of configurations through which the specimen passes in the course of plane extension. It is anticipated that the bifurcation analysis will be sensitive to small variations of the stress and stubbiness, so an accurate integration of the homogeneous extension is essential. We use one element. For the material whose hardening exponent N equals four, a single RK2 step[16] brings the material from the stress free state to the yield surface. This is followed by 30 RK4 steps to bring the specimen out to nominal stretch $l = 1.04$. Subsequent steps are (all RK4) stretch increments $\Delta l = 0.002$ out to $l = 1.10$, followed by

[16]We use the abbreviations 'RK2' and 'RK4' for the second- and fourth-order Runge–Kutta methods, respectively; cf. [19, Section 6.5] for description of these algorithms.

Table 1
Critical configurations in plane extension

	$2a_0^3/a_0^1$	a_c^1	$2a_c^3$	τ_c^{22}	τ_c^{33}
$N = 4$	2	3.6191	13.9342	584.79	1173.34
	3	3.7800	20.0053	564.15	1132.54
	4	3.8388	26.2625	556.25	1116.87
$N = 8$	2	4.0714	12.3385	322.63	646.19
	3	4.2852	17.5819	311.39	623.93
	4	4.3533	23.0741	307.26	615.77

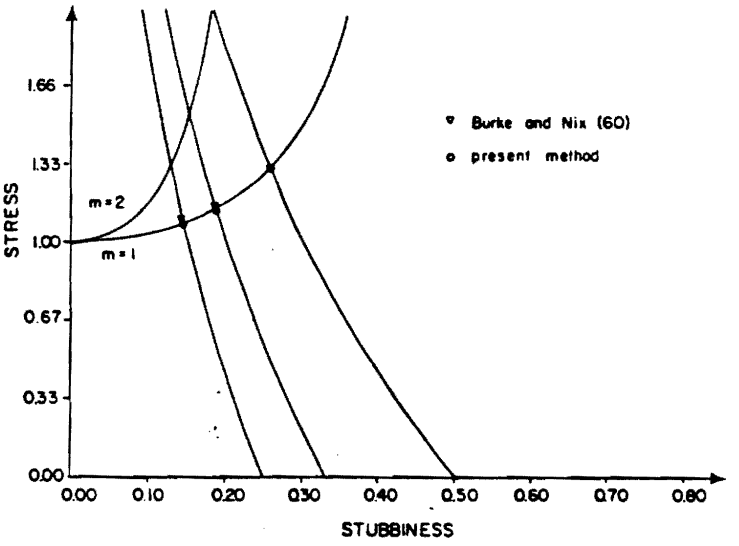

Fig. 2. Results of necking analysis—$N = 4$.

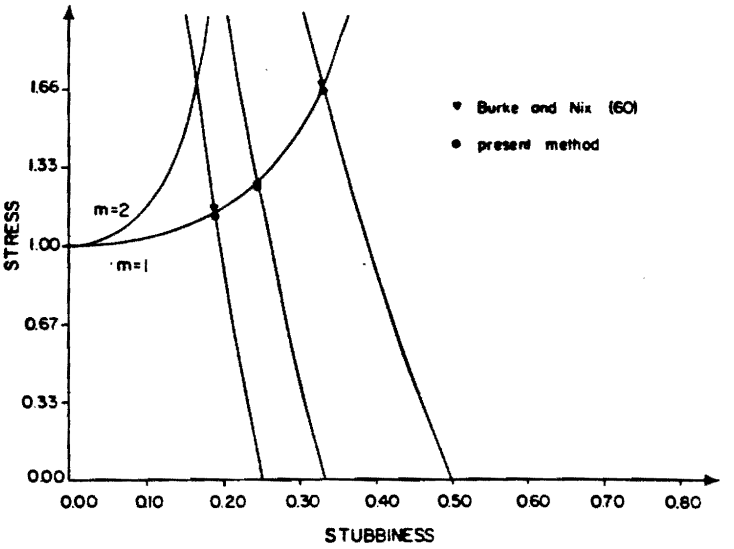

Fig. 3. Results of necking analysis—$N = 8$.

Table 2
Configuration for parameter study

$2a_0^3/a_0^1$	a^1	$2a^3$	τ^{22}	τ^{33}
2	4.0752	12.3271	322.44	645.83

Table 3
Data for Fig. 4 (8 noded element, NT = 21, NW = 6)

Mesh	Symbol	Degrees of freedom	Eigenvalue
1×2	□	15	0.5341
1×3	□	23	0.3221
1×4	□	31	0.2416
1×6	□	47	0.1505
2×4	△	55	0.1850
2×6	△	83	0.1259
2×8	△	111	0.0957
2×10	△	139	0.0772
3×6	○	119	0.0925
3×8	○	159	0.0703
3×10	○	199	0.0568
3×12	○	239	0.0476
4×9	◇	233	0.0495

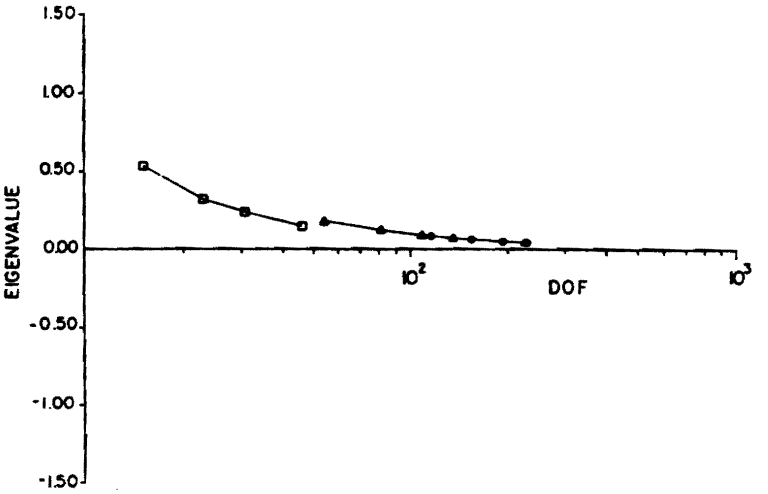

Fig. 4. Necking eigenvalue for various finite element meshes—eight node elements (NT = 21, NW = 6).

Table 4
Data for Fig. 5 (4 noded element, NT = 13, NW = 3)

Mesh	Symbol	Degrees of freedom	Eigenvalue
2×6	□	29	0.3732
2×8	□	39	11.2843
2×10	□	49	22.6500
3×6	△	41	27.1690
3×9	△	62	0.1777
3×12	△	83	2.7302
3×15	△	104	5.4067
4×8	○	71	9.5265
4×12	○	107	0.1059
4×20	○	179	1.8974
5×10	◇	109	4.1738
5×15	◇	164	0.0706
5×20	◇	219	0.4415

opposite effect that decreasing the number of kinematic parameters had—decrease the stiffness [2]. However, we found no difference in the necking eigenvalue for four-noded elements when 13 or 21 stress parameters were used, for either 1, 3, 4 or 6 spin parameters. This result is summarized in Table 6.

As a final example we consider meshes of four-noded elements, each with 5 stress-rate parameters and 1 spin parameter. Each element has two kinematic modes, but when the global stiffness matrix $[\mathcal{K}^*]$ is assembled these modes disappear. The element is interesting because the equations of compatibility and angular momentum balance are satisfied precisely on the

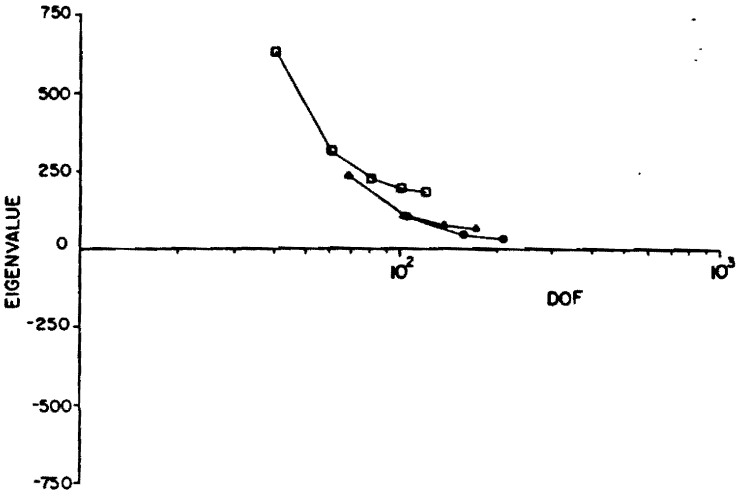

Fig. 6. Necking eigenvalue for various finite element meshes—four node elements (NT = 13, NW = 1).

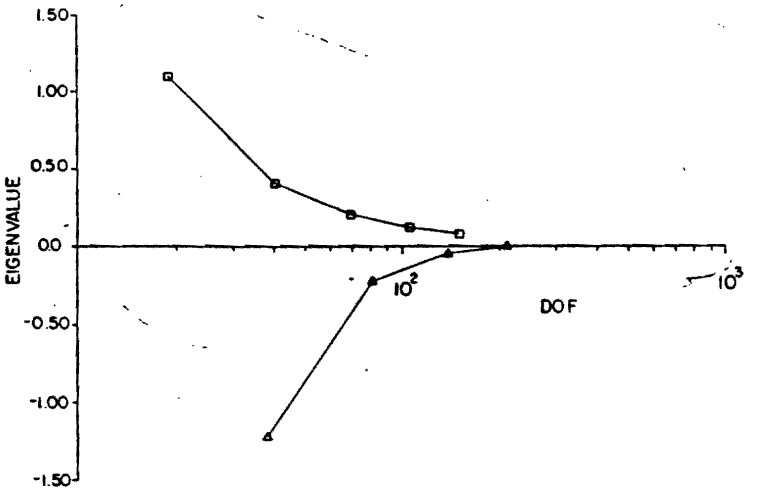

Fig. 7. Necking eigenvalue for various finite element meshes—four node elements (NT = 5, NW = 1).

proximated to any degree of accuracy by continuation of either of these sequences. In Fig. 7 the sequences of eigenvalues corresponding to these two sequences are plotted. These simple elements apparently are converging to the same value as all the other elements at a rate matched only by the eight-noded 'high-order' elements. But the most striking feature is that one of the sequences of approximate eigenvalues is converging from above while the other from below.

The natural tendency would be to attribute this behavior to the presence of kinematic modes on the element level. However, for sufficiently distorted meshes of other-wise well-behaved elements, similar behavior was observed.[26] This example demonstrates that the present method does not necessarily lead to an upper or lower bound for a critical load.

Table 7
Data for Fig. 7 (4 noded element, NT = 5, NW = 1)

Mesh	Symbol	Degrees of freedom	Eigenvalue
2×4	□	19	1.0948
3×6	□	41	0.4043
4×8	□	71	0.2074
5×10	□	109	0.1269
6×12	□	155	0.0862
2×8	△	39	−1.2258
3×12	△	83	−0.2204
4×16	△	143	−0.0426
5×20	△	219	0.0003

[26]For a (1×10) mesh of eight-noded elements an eigenvalue of −30.3368 was found; it was not determined whether this value was simply erratic (due to the irregular element shape), or whether similar negative values could be found for 'nearby' meshes (such as 1×9 or 1×11).

use of the forward gradient scheme [1], only the Euler time stepping scheme was used in the second and third parts of the problem.

Our material model is that of an elastico-viscous fluid:

$$\boldsymbol{\varepsilon} = \boldsymbol{\varepsilon}^e + \boldsymbol{\varepsilon}^p, \qquad \boldsymbol{\varepsilon}^e = \left(\frac{1+\nu}{E}\right)\dot{\boldsymbol{\sigma}}^* - \left(\frac{\nu}{E}\right)(\mathbf{I}:\dot{\boldsymbol{\sigma}}^*)\mathbf{I}, \qquad \boldsymbol{\varepsilon}^p = \tfrac{3}{2}\gamma\boldsymbol{\tau}'.$$

This model corresponds to that of Burke and Nix [34] with (their) creep exponent $n = 1$. The fluidity γ is set as $\gamma = 1 \times 10^{-19}$ (psi-sec)$^{-1}$. The velocity at the top of the cell (see Fig. 8) was adjusted so that a specimen with no void would experience a homogeneous constant stretching $\varepsilon^{11} = \bar{\varepsilon} = 0.25 \times 10^{-14}$ sec^{-1}. Since the material was treated as an incompressible inelastic fluid in [34], our choice of elastic constants is somewhat arbitrary. We have taken Young's modulus $E = 3 \times 10^7$ psi and Poisson's ratio $\nu = 0.4$, so the material is somewhat like mild steel in its elastic response.

In Figs. 9, 10 and 11 the contours of stress τ^{11}, mean stress and stress τ^{33} have been plotted for L (the elongation of the cell) $L = 1.01$. The stress concentration where the hole edge crosses the x^3-axis was approximately 2.7.[27] The theoretical value for an *isolated* void in a purely elastic medium is 3.0 [36]; Burke and Nix found an approximate value of 2.66. In Fig. 12 the contours of effective strain rate $\sqrt{\frac{2}{3}\boldsymbol{\varepsilon}^p:\boldsymbol{\varepsilon}^p}/\bar{\varepsilon}$ are plotted for $L = 1.01$. Qualitatively this compares very well to Fig. 7 in Burke and Nix's paper.

In Fig. 13 the deformation is traced from $L = 1.0$ to $L = 1.5$. These deformations are physically tenable. We remark that no indication of any numerical instability was observed in the course of integrating this deformation.

In Figs. 14, 15 and 16 the contours of stress τ^{11}, mean stress, and τ^{33} have been plotted for $L = 1.50$. They compare very well to the stresses found by Burke and Nix (see Fig. 8 there). We note that the stress concentration dropped to 1.71. The stress concentration depends

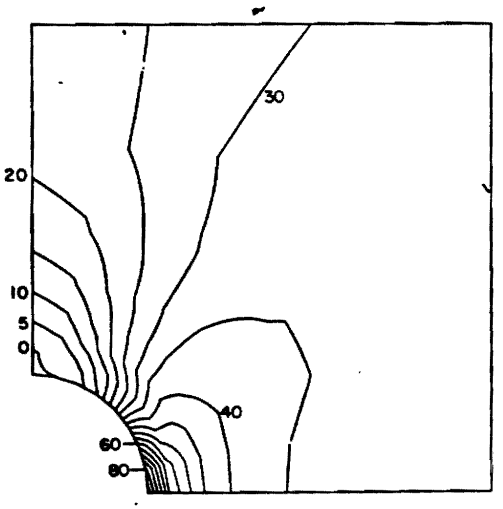

Fig. 9. Contours of stress τ^{11} at $L = 1.01$.

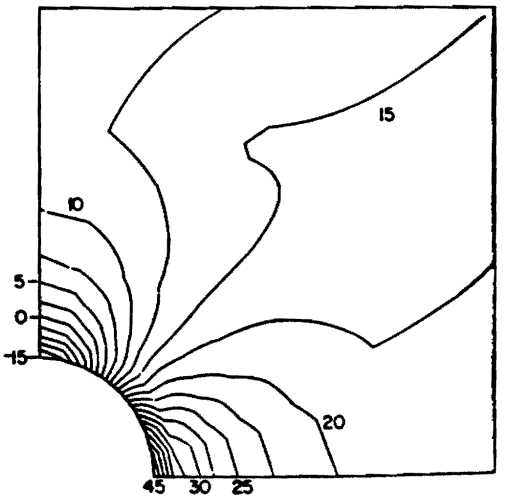

Fig. 10. Contours of mean stress at $L = 1.01$.

[27] A stress concentration of approximately 2.59 was observed for the elastically stressed medium.

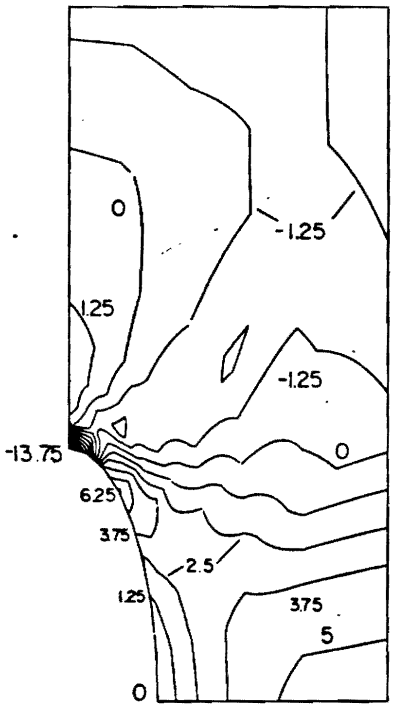

Fig. 16. Contours of stress τ^{33} at $L = 1.5$.

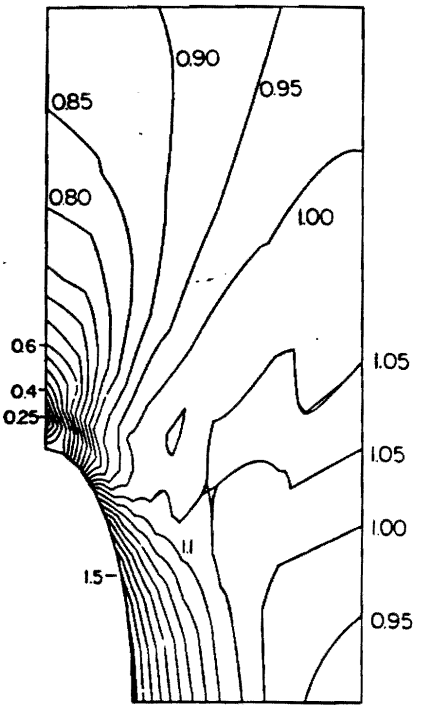

Fig. 17. Contours of effective strain rate $\varepsilon^p/\bar{\varepsilon}$ at $L = 1.5$.

strongly on the geometry of the specimen; such as, it was observed to decline steadily throughout the deformation. In Fig. 17 the contours of effective strain rate are plotted for $L = 1.5$. Again, the qualitative agreement with the results of Burke and Nix is noted (see Fig. 9 there).

The present calculation was terminated at $L = 1.5$ because of the unstable traction boundary condition at $x^3 = 0.0$ and the edge of the hole, and the general breakdown of (total) traction reciprocity conditions on the interior of the cell. This problem is easily avoided by incorporation of traction residuals.

We conclude by noting that in the present analysis only 56 *four-noded* elements were used, as compared to 56 *eight-noded* elements used in the analysis of Burke and Nix. Considering the agreement between their results and our own, the present method appears to have performed very well, in spite of the large disparity in the degrees of freedom of the finite element mesh.

7. Conclusions

A new hybrid-stress finite element algorithm, suitable for analyses of large quasistatic deformations of inelastic solids, has been presented. The feasibility and performance of the algorithm has been demonstrated through examples.

The capability of the stress-based finite element algorithm for extremely accurate bifurcation analysis was demonstrated. Moreover, it was shown that one could expect the

Thus, the plane strain condition $\varepsilon^{22} = 0$ is only satisfied in a mean sense in using the present algorithm.

Shape functions for plane strain

$$x^1 = x, \qquad x^3 = z.$$

Velocity shape functions

$$\boldsymbol{N}_i = N_{1,i}\boldsymbol{e}_1 + N_{3,i}\boldsymbol{e}_3 .$$

Four-noded element

$$N_{1,i} = \begin{cases} \frac{1}{4}(1+\xi\xi_i)(1+\eta\eta_i), & i = 1,2,3,4, \\ 0, & i = 5,6,7,8, \end{cases}$$

$$N_{3,i} = \begin{cases} 0, & i = 1,2,3,4, \\ \frac{1}{4}(1+\xi\xi_{i-4})(1+\eta\eta_{i-4}), & i = 5,6,7,8. \end{cases}$$

$$|\xi| \leqslant 1, \qquad |\eta| \leqslant 1,$$

$$\xi_1 = -1, \quad \xi_2 = 1, \quad \xi_3 = 1, \quad \xi_4 = -1,$$

$$\eta_1 = -1, \quad \eta_2 = -1, \quad \eta_3 = 1, \quad \eta_4 = 1.$$

Eight-noded element

$$N_{1,i} = \begin{cases} H_i, & i = 1,2,\ldots,8, \\ 0, & i = 9,10,\ldots,16, \end{cases}$$

$$N_{3,i} = \begin{cases} 0, & i = 1,2,\ldots,8, \\ H_{i-8}, & i = 9,10,\ldots,16. \end{cases}$$

$$H_i = \begin{cases} \frac{1}{2}(1-\xi^2)(1+\eta\eta_i), & i = 2,6, \\ \frac{1}{2}(1+\xi\xi_i)(1-\eta^2), & i = 4,8, \\ \frac{1}{4}(1+\xi\xi_i)(1+\eta\eta_i)(\xi\xi_i+\eta\eta_i-1), & i = 1,3,5,7. \end{cases}$$

$$\xi_1 = \xi_7 = \xi_8 = -1, \quad \xi_2 = \xi_6 = 0, \quad \xi_3 = \xi_4 = \xi_5 = 1,$$

$$\eta_1 = \eta_2 = \eta_3 = -1, \quad \eta_4 = \eta_8 = 0, \quad \eta_5 = \eta_6 = \eta_7 = 1.$$

Shape functions for spin

$$\mathbf{QW} = QW_{13,i}\boldsymbol{e}_1\boldsymbol{e}_3 + QW_{31,i}\boldsymbol{e}_3\boldsymbol{e}_1$$

where

$$QW_{13,i} = c_1, \qquad QW_{31,1} = -c_1.$$

If NW = 3 add the following shape functions

$$QW_{13,2} = xc_2, \qquad QW_{13,3} = zc_3, \qquad QW_{31,2} = -xc_2, \qquad QW_{31,3} = -zc_3,$$

[8] S.N. Atluri, On some new general and complementary energy theorems for the rate problems of finite strain, classical elasto-plasticity, J. Structural Mech. 8(1) (1980) 61–92.
[9] C. Truesdell and W. Noll, The Nonlinear Field Theories of Mechanics, Handbuch der Physik III/3 (Springer, Berlin, 1965).
[10] R. Hill, Aspects of invariance in solid mechanics, Adv. Appl. Mech. 18 (1978) 1–75.
[11] W. Prager, Introduction to the Mechanics of Continua (Ginn, New York, 1961).
[12] Y.C. Fung, Foundations of Solid Mechanics (Prentice-Hall, Englewood Cliffs, NJ, 1965).
[13] E.H. Dill, The complementary energy principle in nonlinear elasticity, Lett. Appl. Engrg. Sci. 5 (1977) 95–106.
[14] I. Ergatoudis, B.M. Irons and O.C. Zienkiewicz, Curved, isoparametric, quadrilateral elements for finite element analysis, Internat. J. Solids Structures 4 (1968) 31–42.
[15] K.W. Reed, Analysis of large quasistatic deformations of inelastic solids by a new stress based finite element method, Ph.D. Dissertation, Georgia Institute of Technology, Atlanta, GA, 1982.
[16] P. Tong and J.N. Rossettos, Finite Element Method: Basic Technique and Implementation (MIT, Cambridge, MA, 1977).
[17] K.-J. Bathe, Finite Element Procedures in Engineering Analysis (Prentice-Hall, Englewood Cliffs, NJ, 3rd ed., 1982).
[18] P. Tong and T.H.H. Pian, A variational principle and the convergence of a finite element method based on assumed stress distribution, Internat. J. Solids Structures 5 (1969) 463–472.
[19] S.D. Conte and C. de Boor, Elementary Numerical Analysis (McGraw-Hill, New York, 2nd ed., 1972).
[20] I. Cormeau, Numerical stability in quasistatic elasto-visco-plasticity, Internat. J. Numer. Meths. Engrg. 9 (1975) 109–127.
[21] T.J.R. Hughes and R.L. Taylor, Unconditionally stable algorithms for quasi-static elasto-visco-plastic finite element analysis, Comput. & Structures 8 (1978) 169–173.
[22] J.H. Argyris, L.E. Vaz and K.J. Willam, Improved solution methods for inelastic rate problems, Comput. Meths. Appl. Mech. Engrg. 16 (1978) 231–277.
[23] M.B. Kanchi, O.C. Zienkiewicz and D.R.J. Owen, The visco-plastic approach to problems of plasticity and creep involving geometric nonlinear effects, Internat. J. Numer. Meths. Engrg. 12 (1978) 169–181.
[24] J.W. Hutchinson and J.P. Miles, Bifurcation analysis of the onset of necking in an elastic/plastic cylinder under uniaxial tension, J. Mech. Phys. Solids 22 (1974) 61–71.
[25] J.P. Miles, The initiation of necking in rectangular elastic/plastic specimens under uniaxial and biaxial tension, J. Mech. Phys. Solids 23 (1975) 197–213.
[26] R. Hill and J.W. Hutchinson, Bifurcation phenomena in the plane tension test, J. Mech. Phys. Solids 23 (1975) 239–264.
[27] M.A. Burke and W.D. Nix, A numerical study of necking in the plane tension test, Internat. J. Solids Structures 15 (1979) 379–393.
[28] J.R. Osias, Finite deformation of elastic-plastic solids: the example of necking in flat tensile bars, Ph.D. Thesis, Carnegie-Mellon Univ., Pittsburgh, PA, 1972.
[29] R.M. McMeeking and J.R. Rice, Finite element formulations for problems of large elastic-plastic deformation, Internat. J. Solids Structures 11, (1975) 601–616.
[30] R. Hill, A general theory of uniqueness and stability in elastic-plastic solids, J. Mech. Phys. Solids 6 (1958) 236–249.
[31] R. Hill, Some basic principles in the mechanics of solids without a natural time, J. Mech. Phys. Solids 7 (1959) 209–225.
[32] G.R. Cowper and E.T. Onat, The initiation of necking and buckling in plane plastic flow, in: R.M. Rosenberg, ed., Proceedings of the Fourth U.S. National Congress of Applied Mechanics (ASME, New York, 1962).
[33] B.F. de Veubeke and A. Millard, Discretization of stress field in the finite element method, J. Franklin Inst. 302 (5, 6) (1976) 389–412.
[34] M.A. Burke and W.D. Nix, A numerical analysis of void growth in tension creep, Internat. J. Solids Structures 15 (1979) 55–71.
[35] R.B. Bird, R.C. Armstrong and O. Hassager, Dynamics of Polymeric Liquids, Vol. 1 (Wiley, New York, 1977).
[36] S.P. Timoshenko and J.N. Goodier, Theory of Elasticity (McGraw-Hill, New York, 3rd ed., 1970).
[37] J.H. Argyris, J.St. Doltsinis, P.M. Pimenta and H. Wüstenberg, Thermomechanical response of solids at high strains natural approach, Comput. Meths. Appl. Mech. Engrg. 32 (1982) 3–57.

COMPUTER METHODS IN APPLIED MECHANICS AND ENGINEERING 39 (1983) 245–295
NORTH-HOLLAND

ANALYSES OF LARGE QUASISTATIC DEFORMATIONS OF INELASTIC BODIES BY A NEW HYBRID-STRESS FINITE ELEMENT ALGORITHM

K.W. REED and S.N. ATLURI
Center for the Advancement of Computational Mechanics, School of Civil Engineering, Georgia Institute of Technology, Atlanta, GA 30332, U.S.A.

Received 14 October 1982

A new hybrid-stress finite element algorithm, suitable for analyses of large, quasistatic, inelastic deformations, is presented. The algorithm is based upon a generalization of de Veubeke's complementary energy principle. The principal variables in the formulation are the nominal stress rate and spin, and the resulting finite element equations are discrete versions of the equations of compatibility and angular momentum balance.

The algorithm produces true rates, time derivatives, as opposed to 'increments'. There results a complete separation of the boundary value problem (for stress rate and velocity) and the initial value problem (for total stress and deformation); hence, their numerical treatments are essentially independent. After a fairly comprehensive discussion of the numerical treatment of the boundary value problem, we launch into a detailed examination of the numerical treatment of the initial value problem, covering the topics of efficiency, stability and objectivity. The paper is closed with a set of examples, finite homogeneous deformation problems, which serve to bring out important aspects of the algorithm.

1. Introduction

In his 'Treatise on the Mathematical Theory of Elasticity', Love [1, p. 2] observed that "When the general equations had been obtained, all questions of the small strain of elastic bodies were reduced to a matter of mathematical calculation." To this day, that 'matter of mathematical calculation' figures prominently in applied mechanics.

The early mechanicians realized that the general equations of elasticity were too difficult to solve except in a few special cases, so a large part of their effort was focused on methods for finding approximate solutions to problems of technological interest. Some of the techniques they used in deriving approximate theories for rods, plates, and shells are, in fundamental ways, very similar to the finite element technique.

Today it is well understood that the classical theories of rods, plates and shells may all be systematically derived from elasticity theory by introduction of approximations for the displacement to the principle of virtual work. Kirchhoff is the first person mentioned by Love [1] as having used this methodology, and in using it he managed to give a clear interpretation of the boundary conditions in the plate theory with which his name is now associated. In two respects Kirchhoff's methodology is the same as the finite element methodology. First of all, he made kinematic approximations, and secondly, he used an energy principle to maintain 'consistency' between his generalized stresses and strains, and to arrive at the correct boundary conditions. The principal difference between Kirchhoff's methodology and the finite

element methodology lies in the degree to which the kinematic field is approximated. Because of the similarities in the construction of the classical rod, plate and shell theories to the construction of finite element equations, the successes and failures of the classical structural theories reflect, at least qualitatively, upon the performance of the finite element method.

No special theory in the realm of solid mechanics has enjoyed greater success than that of elastic beams, for there the general equations of elasticity are effectively replaced by a single ordinary differential equation. The theory is not only reasonably accurate, but extremely easy to understand because of its displacement based derivation. The classical plate and shell theories provide equations less easy to understand and less easy to solve than the beam equations, but still regarded as simpler than the general equations of elasticity.

A major failing of the classical theories of beams, plates and shells is their inability to account for the effects of 'transverse shear stress'; that is, the shear stress acting on plane sections through the thickness of the structure. As a direct consequence, those theories always give a higher estimate of the stiffness of a structure than does the general theory. Secondly, the twisting moment and shear force are coupled on the edge of such a plate or shell. In spite of these shortcomings, it was not until after Reissner's [2] investigation into the effect of shear stress on the bending of plates that satisfactory alternatives to the classical theory were widely accepted. But Reissner's paper has had as great an impact on the methods used in applied mechanics as did his plate theory of itself. In its derivation, his theory is distinguished from the classical theories by the fact that both assumed stresses and displacements are used. Since that time the use of assumed stresses in the derivation of plate and shell theories has become common.

It is not surprising that the finite element method has evolved along similar lines. The finite element method in which one introduces kinematic approximations to the virtual work principle is the direct counterpart of Kirchhoff's rod and plate theories. The same types of advantages and defects are inherent.

The principal advantage of the displacement based finite element methods is their conceptual simplicity. For application to beams, the simplicity rivals the simplicity of the beam theory itself. In the cases of plates and shells though, it proves difficult to construct 'compatible' shape functions for the displacement. Finite elements for thin plates based on kinematic approximations sometimes overestimate the stiffness of the plate so badly that they are described as 'locking'. As a means of avoiding locking, and just for simpler construction of shape functions, some researchers have presented 'incompatible' plate bending elements, elements which do not satisfy slope continuity at element interfaces. A second drawback of displacement based finite element methods (in general) is their inability only to satisfy traction boundary conditions accurately (analogous to the coupling of moment and shear force at a Kirchhoff plate's edge).

It was Pian's [3] investigation into the derivation of element stiffness matrices that brought widespread attention to the potential advantages of introducing the stress as an independent variable. By his formulation, which was based on the complementary energy principle of linear elasticity, a viable alternative to incompatible elements was made available. Also, as was the case in Reissner's plate theory, the stress formulation made possible considerably more accurate satisfaction of traction boundary conditions. Finally, Pian observed a marked acceleration in the convergence of the components of the stiffness matrix when the stress method was used. Since that time, the study of finite element methods related to Pian's (which have

come to be known as 'hybrid stress methods') has produced a number of special methods which may be applied where conventional displacement based finite elements fail.

One particular class of problems in which the conventional displacement based finite element method fails is composed of problems involving incompressible or nearly incompressible bodies. The constitutive equation for such bodies is nearly or precisely singular for the mode of dilatation. The shape functions for the displacement used in the conventional finite element method are incapable of producing any motion other than pure shearing which does not contain (loosely speaking) 'excessive' dilatation. As a consequence, the conventional finite element method drastically overestimates the resistance to deformation of nearly and precisely incompressible bodies. In a key paper by Herrmann [4], it was shown that the difficulty could be avoided if only the mean stress were introduced as an independent variable.

Problems involving finite deformations of strain-softening bodies resemble problems involving nearly incompressible bodies in the sense that the body's shear compliance is much greater than its bulk compliance. For the most part, finite element analyses of such deformations have been accomplished only at considerable expense, even when the pressure is introduced as an independent variable. No hybrid stress finite element algorithm for finite deformations was known.

The door to stress based finite element analysis of finite deformation problems was opened in 1972 by Fraeijs de Veubeke [5] with his presentation of a complementary energy principle for finite deformation elasticity.[1] The stationary conditions of this principle are both the equations of compatibility and angular momentum balance. To date, variants of the principle have been used by de Veubeke and Millard [6], Sander and Carnoy [7], Koiter [8], Wunderlich and Obrecht [9], Murakawa [10], Murakawa and Atluri [11, 12], Murakawa et al. [13] and Atluri and Murakawa [14], in problems ranging from elastic membrane theory to beam, plate and shell theories.

A considerable generalization of de Veubeke's principle was given by Atluri [15]. His reformulation of de Veubeke's principle for stress rate and spin opened the way for the current work, that of developing a stress-rate based finite element algorithm for analysis of large deformations of inelastic bodies. It appears that the sole other analysis of large deformations of inelastic bodies by any similar algorithm is that presented by Atluri and Murakawa [14], in which necking of an elastic-plastic bar and postbifurcation analysis of a thin elastic-plastic plate was performed. The finite element algorithm used by those researchers was based on stress increments, rather than stress rates, and the motion of the elastic-plastic body was found by summation of increments. It was assumed that the accumulated error in this procedure could be kept small by the method of 'residual loads'. This procedure has a firm foundation for problems involving elastic bodies (whose deformations were the subject of Murakawa's earlier research), but is of questionable validity when the body is not elastic. In their assessment of incremental solution methods for inelastic rate problems, Argyris et al. [19] conclude that:

> "Inelastic rate processes are in general path-dependent; therefore, the drift (i.e. the accumulation of numerical integration errors) cannot be eliminated by residual load iteration, e.g. at the end of each time step."

[1] An invalid principle was presented by Levinson [16], and again by Zubov [17]. The failure of that principle is discussed by Dill [18].

Moreover, when the body exhibits relaxation effects, this solution technique's numerical stability becomes extremely sensitive to the time step size. Hughes and Taylor [20] observe that the time steps required for stability in the explicit time stepping technique are much smaller than required for accuracy when only quasistatic deformations are to be analyzed.

A final objection to 'incremental' finite element formulations may be raised on the grounds that there always results an artificial coupling between the boundary value problem and the initial value problem. When dealing with rate-type constitutive equations it is possible to treat the boundary value problem (for the rates) and the initial value problem (for the total stress and deformation) separately. Typically the boundary value problem for the rates is either precisely linear, or equivalent to a linear problem (without approximation). All of the nonlinearity falls into the initial value problem. Nonlinear initial value problems are, perhaps, of all nonlinear problems, the single type which we are best equipped to treat numerically. In any case, we are better equipped to treat them than we are nonlinear boundary value problems. The incremental approach has the effect of carrying the nonlinearity of the initial value problem into the boundary value problem, where it is dealt with, less efficiently, by some iterative technique.

The objective of the present work is to develop a stress-*rate* based finite element algorithm for analysis of large quasistatic deformations of inelastic bodies. In doing so, we discard the notion of 'increments' entirely. As a direct result, the boundary value problem and the initial value problem may be treated separately. The algorithm which results is applied to analyze large deformations of inelastic bodies.

As is true of 'stress formulations' in general, the development of the boundary value and initial value problems is more complicated than it is in a 'velocity formulation'. The first part of this paper is devoted to presenting, with reasonable completeness, the development of the boundary value problem and associated variational principles. It follows that the finite element algorithm is more complicated, in that it involves more computation, and more attention to detail, than velocity based algorithms. However, from the results it is clear that the improvement in accuracy over velocity based methods is substantial; so much so that, in view of the difficulties encountered in the application of velocity based methods to finite deformation problems, the present stress based algorithm must be regarded as a 'viable alternative'.

2. Kinematics, dynamics, rate-type constitutive equations

2.1. Kinematics

We represent natural space as a three-dimensional Euclidean space $\mathscr{E}$. Consider a motion of a body through space. The image of the body in $\mathscr{E}$ at time t is the *configuration* $C(t)$. As time passes, the configuration changes, and we say that the body *deforms*. Let $\boldsymbol{X}$ be the position in $\mathscr{E}$ that was occupied by a certain particle of the body at time τ, and let $\boldsymbol{x}$ be the position occupied by that same particle at time t; then our notion of deformation relative to the configuration $C(\tau)$ is expressed by

$$\boldsymbol{x} = \boldsymbol{\chi}_\tau(\boldsymbol{X}, t)\,. \tag{2.1.1}$$

The mapping $\boldsymbol{\chi}_\tau$ embodies every aspect of the body's motion.

As is customary, we denote by $\mathbf{F}_\tau$ the *deformation gradient* and by J_τ its determinant:

$$\mathbf{F}_\tau(\boldsymbol{X}, t) \equiv [\nabla_\tau \boldsymbol{\chi}_\tau(\boldsymbol{X}, t)]^t, \qquad J_\tau(\boldsymbol{X}, t) \equiv \det \mathbf{F}_\tau(\boldsymbol{X}, t). \tag{2.1.2}$$[2]

A particle's velocity is given by the time derivative of $\boldsymbol{\chi}_\tau$:

$$\boldsymbol{v}_\tau(\boldsymbol{X}, t) = \frac{\mathrm{d}}{\mathrm{d}t} \boldsymbol{\chi}_\tau(\boldsymbol{X}, t), \tag{2.1.3}$$

and the spatial velocity distribution is found by putting $\boldsymbol{\chi}_\tau^{-1}(\boldsymbol{x}, t)$ for $\boldsymbol{X}$ in $\boldsymbol{v}_\tau(\boldsymbol{X}, t)$:

$$\boldsymbol{v}(\boldsymbol{x}, t) = \boldsymbol{v}_\tau(\boldsymbol{\chi}_\tau^{-1}(\boldsymbol{x}, t), t). \tag{2.1.4}$$

We caution the reader by pointing out that $\boldsymbol{v}_\tau$ and $\boldsymbol{v}$ are entirely different functions. Throughout this paper it is crucially important for the reader to keep such distinctions in mind.

We denote by $\mathbf{L}$ the *velocity gradient* and by $\dot{J}$ its trace:

$$\mathbf{L}(\boldsymbol{x}, t) \equiv [\nabla \boldsymbol{v}(\boldsymbol{x}, t)]^t, \qquad \dot{J}(\boldsymbol{x}, t) \equiv \operatorname{tr} \mathbf{L}(\boldsymbol{x}, t) = \nabla \cdot \boldsymbol{v}(\boldsymbol{x}, t). \tag{2.1.5}$$

J_τ, $\dot{J}_\tau$ and $\dot{J}$ are related by *Euler's expansion formula* (see [21, p. 32])

$$\dot{J} = \dot{J}_\tau / J_\tau. \tag{2.1.6}$$

The symmetric and skew-symmetric parts of $\mathbf{L}$,

$$\boldsymbol{\varepsilon} = \tfrac{1}{2}(\mathbf{L} + \mathbf{L}^t) \quad \text{and} \quad \boldsymbol{\omega} = \tfrac{1}{2}(\mathbf{L} - \mathbf{L}^t), \tag{2.1.7}$$

have the physical significance of *stretching* and *spin*, and are thus named.

Of course not any tensor field $\mathbf{L}$ is the gradient of a velocity field; the condition of integrability (henceforth called *compatibility equation*) is

$$\nabla \times (\mathbf{L}^t) = \mathbf{0}. \tag{2.1.8}$$

Likewise, if $\boldsymbol{\varepsilon}$ is a symmetric tensor field and $\boldsymbol{\omega}$ is a skew-symmetric tensor field, and $(\boldsymbol{\varepsilon} - \boldsymbol{\omega})$ satisfies the compatibility equation

$$\nabla \times (\boldsymbol{\varepsilon} - \boldsymbol{\omega}) = \mathbf{0}, \tag{2.1.9}$$

then there is a twice differentiable vector field $\boldsymbol{v}$ for which

$$\boldsymbol{\varepsilon} = \tfrac{1}{2}(\nabla \boldsymbol{v}^t + \nabla \boldsymbol{v}) \quad \text{and} \quad \boldsymbol{\omega} = \tfrac{1}{2}(\nabla \boldsymbol{v}^t - \nabla \boldsymbol{v}). \tag{2.1.10}$$

It is worthy of special mention that (2.1.9) is *precise* as well as *linear*.

[2] In Appendix A the notations of this paper are explained.

2.2. Dynamics

The two fundamental principles of dynamics are called *balance of linear moment* (LMB) and *balance of angular momentum* (AMB). Under ordinary circumstances, the principles are equivalent to[3]

$$\boldsymbol{T}_\tau(\boldsymbol{n}_\tau) + \boldsymbol{T}_\tau(-\boldsymbol{n}_\tau) = \boldsymbol{0}\,, \tag{2.2.1}$$

$$\boldsymbol{T}_\tau(\boldsymbol{n}_\tau) = \boldsymbol{n}_\tau \cdot \mathbf{t}_\tau\,, \tag{2.2.2}$$

$$\nabla_\tau \cdot \mathbf{t}_\tau + \rho_\tau \boldsymbol{b}_\tau = \rho_\tau \dot{\boldsymbol{v}}_\tau\,, \tag{2.2.3}$$

$$(\mathbf{F}_\tau \cdot \mathbf{t}_\tau) - (\mathbf{F}_\tau \cdot \mathbf{t}_\tau)^{\mathrm{t}} = \mathbf{0}\,. \tag{2.2.4}$$

In (2.2.1) through (2.2.4) $\boldsymbol{T}_\tau$ is the *nominal traction* and $\mathbf{t}_\tau$ is the *nominal stress*[4]; ρ_τ, $\boldsymbol{n}_\tau$ and $\boldsymbol{b}_\tau$ are defined by

$$\rho_\tau(\boldsymbol{X}) = \rho(\boldsymbol{X}, \tau)\,, \tag{2.2.5}$$

$$\boldsymbol{n}_\tau(\boldsymbol{X}) = \boldsymbol{n}(\boldsymbol{X}, \tau)\,, \tag{2.2.6}$$

$$\boldsymbol{b}_\tau(\boldsymbol{X}, t) = \boldsymbol{b}(\boldsymbol{\chi}_\tau(\boldsymbol{X}, t), t) \tag{2.2.7}$$

where $\rho(\cdot, t)$ is the mass density over $C(t)$, $\boldsymbol{n}(\cdot, t)$ the outward-directed normal to a material surface in $C(t)$, and $\boldsymbol{b}(\cdot, t)$ the intensity of body force over $C(t)$. Equations (2.2.1) through (2.2.4) are referred to as 'traction reciprocity', 'the stress principle', 'linear momentum balance' and 'angular momentum balance', respectively.

Using the stress principle (2.2.2) and Nanson's relation (see [21, p. 18])

$$\boldsymbol{n}_\zeta \, \mathrm{d}S_\zeta = J_\tau(\zeta)\, \boldsymbol{n}_\tau \cdot \mathbf{F}_\tau^{-1}(\zeta)\, \mathrm{d}S_\tau\,, \tag{2.2.8}$$

we obtain the equation relating the nominal stresses $\mathbf{t}_\tau(t)$ and $\mathbf{t}_\zeta(t)$:

$$\mathbf{t}_\tau(t) = J_\tau(\zeta)\, \mathbf{F}_\tau^{-1}(\zeta) \cdot \mathbf{t}_\zeta(t)\,. \tag{2.2.9}$$

In the special case that $\zeta = t$, we recover

$$\mathbf{t}_\tau(t) = J_\tau(t)\, \mathbf{F}_\tau^{-1}(t) \cdot \boldsymbol{\tau}(t)\,, \tag{2.2.10}$$

the equation relating $\mathbf{t}_\tau$ to the true stress $\boldsymbol{\tau}$.

[3] A careful account of the derivation of these equations, including qualifications, is given by Truesdell [22].

[4] There are two forms which the stress principle may take: $\boldsymbol{T}_\tau(\boldsymbol{n}_\tau) = \boldsymbol{n}_\tau \cdot \mathbf{t}_\tau$ and $\boldsymbol{T}_\tau(\boldsymbol{n}_\tau) = \mathbf{t}'_\tau \cdot \boldsymbol{n}_\tau$. The "nominal" [23] stress $\mathbf{t}_\tau$ follows from the former, the "first Piola–Kirchhoff" [22] stress $\mathbf{t}'_\tau$ from the latter. The nominal stress is also called the "Lagrange" stress [24, 16, 25], or the "Piola" stress [18, 8, 5, 26, 17].

We now set (2.2.1) through (2.2.4) for traction rates and stress rates[5]. By ordinary differentiation, we obtain

$$\dot{\boldsymbol{T}}_\tau(\boldsymbol{n}_\tau)+\dot{\boldsymbol{T}}_\tau(-\boldsymbol{n}_\tau)=\boldsymbol{0}, \tag{2.2.11}$$

$$\dot{\boldsymbol{T}}_\tau(\boldsymbol{n}_\tau)=\boldsymbol{n}_\tau\cdot\dot{\mathbf{t}}_\tau, \tag{2.2.12}$$

$$\nabla_\tau\cdot\dot{\mathbf{t}}_\tau+\rho_\tau\dot{\boldsymbol{b}}_\tau=\rho_\tau\ddot{\boldsymbol{v}}_\tau, \tag{2.2.13}$$

$$(\dot{\mathbf{F}}_\tau\cdot\mathbf{t}_\tau+\mathbf{F}_\tau\cdot\dot{\mathbf{t}}_\tau)-(\dot{\mathbf{F}}_\tau\cdot\mathbf{t}_\tau+\mathbf{F}_\tau\cdot\dot{\mathbf{t}}_\tau)^{\mathrm{t}}=\mathbf{0}. \tag{2.2.14}$$

From (2.2.9) and (2.2.10) we obtain upon differentiation (and then choosing $\zeta = t$ in (2.2.9) and $\tau = t$ in (2.2.10)),

$$\dot{\mathbf{t}}_\tau=J_\tau\mathbf{F}_\tau^{-1}\cdot\dot{\mathbf{t}} \tag{2.2.15}$$

and

$$\dot{\mathbf{t}}=-(\boldsymbol{\varepsilon}+\boldsymbol{\omega})\cdot\boldsymbol{\tau}+\dot{J}\boldsymbol{\tau}+\dot{\boldsymbol{\tau}}. \tag{2.2.16}$$

Equation (2.2.16), which effectively defines the *nominal stress rate* [23], will be used when we make a 'change of variables' in the constitutive equation; (2.2.15) will prove essential in the eventual integration of the stress rate.

If the motion is quasistatic, (2.2.11) through (2.2.14), for $\zeta = t$, become

$$\dot{\boldsymbol{T}}_t(\boldsymbol{n})+\dot{\boldsymbol{T}}_t(-\boldsymbol{n})=\boldsymbol{0}, \tag{2.2.17}$$

$$\dot{\boldsymbol{T}}_t(\boldsymbol{n})=\boldsymbol{n}\cdot\dot{\mathbf{t}}, \tag{2.2.18}$$

$$\nabla\cdot\dot{\mathbf{t}}+\rho\dot{\boldsymbol{b}}=\boldsymbol{0}, \tag{2.2.19}$$

$$(\boldsymbol{\varepsilon}+\boldsymbol{\omega})\cdot\boldsymbol{\tau}+\dot{\mathbf{t}}-\dot{\mathbf{t}}^{\mathrm{t}}-\boldsymbol{\tau}\cdot(\boldsymbol{\varepsilon}-\boldsymbol{\omega})=\mathbf{0}. \tag{2.2.20}$$

It is this form of the dynamic equations that we use henceforth. The reader should note that (2.2.17) through (2.2.20) are *precise* as well as *linear.*

It is instructive to examine the equation relating the nominal and true traction rates:

$$\dot{\boldsymbol{T}}_t=\dot{\boldsymbol{T}}+(\dot{J}-\boldsymbol{n}\cdot\boldsymbol{\varepsilon}\cdot\boldsymbol{n})\,\boldsymbol{T}. \tag{2.2.21}$$[6]

In rate and incremental type finite element algorithms the (interelement) traction reciprocity equation

$$\dot{\boldsymbol{T}}_t(\boldsymbol{n})+\dot{\boldsymbol{T}}_t(-\boldsymbol{n})=\boldsymbol{0} \tag{2.2.22}$$

[5]We emphasize that 'rate' means 'time derivative'. Emphasis is necessary because some authors use the word 'rate' interchangeably with the word 'increment'.

[6]Hill [23, p. 53] gives the kinematical formulas needed to construct (2.2.21) from $\dot{\boldsymbol{T}}=\dot{\boldsymbol{n}}\cdot\boldsymbol{\tau}+\boldsymbol{n}\cdot\dot{\boldsymbol{\tau}}$. It should be clear that $(\dot{J}-\boldsymbol{n}\cdot\boldsymbol{\varepsilon}\cdot\boldsymbol{n})$ measures the surface expansion or contraction.

is usually solved approximately. According to (2.2.21), this is equivalent to solving

$$\frac{\mathrm{d}}{\mathrm{d}t}[\boldsymbol{T}(\boldsymbol{n})+\boldsymbol{T}(-\boldsymbol{n})]+(\dot{J}-\boldsymbol{n}\cdot\boldsymbol{\varepsilon}\cdot\boldsymbol{n})[\boldsymbol{T}(\boldsymbol{n})+\boldsymbol{T}(-\boldsymbol{n})]=\boldsymbol{0} \tag{2.2.23}$$[7]

in an approximate manner. The traction imbalance grows or attenuates as $(\dot{J}-\boldsymbol{n}\cdot\boldsymbol{\varepsilon}\cdot\boldsymbol{n})$ is negative or positive [27]; that is, as the interelement surface contracts or expands. In practice the traction imbalance may be kept small by addition of a *residual*, $-[\boldsymbol{T}(\boldsymbol{n})+\boldsymbol{T}(-\boldsymbol{n})]/h$, to the right-hand side of (2.2.23), where h is the time step size.

Finally, we note that the general solution of the linear momentum balance (2.2.19) is of the form

$$\dot{\mathbf{t}}=\dot{\mathbf{t}}^0+\dot{\mathbf{t}}^b \tag{2.2.24}$$

where $\dot{\mathbf{t}}^0$ is the solution of the homogeneous equation $\nabla\cdot\dot{\mathbf{t}}=\boldsymbol{0}$,

$$\dot{\mathbf{t}}^0(\boldsymbol{x},t)=\nabla\times\boldsymbol{\Phi}(\boldsymbol{x},t)\,, \tag{2.2.25}$$

and $\dot{\mathbf{t}}^b$ is any particular solution of $\nabla\cdot\dot{\mathbf{t}}=-\rho\dot{\boldsymbol{b}}$. A particular solution $\dot{\mathbf{t}}^b$ may be constructed in cartesian coordinates using indefinite integrals [15]

$$\dot{t}^b_{ij}=-\delta_{ij}\int\left\{\rho\left[\frac{\partial}{\partial t}b_i+\boldsymbol{v}\cdot\nabla b_i\right]\right\}\mathrm{d}x_i\quad\text{(no sum)}\,. \tag{2.2.26}$$

Notice that $\dot{\mathbf{t}}^b$ will depend upon $\boldsymbol{v}$ unless $\boldsymbol{v}\cdot\nabla\boldsymbol{b}=\boldsymbol{0}$. If $\boldsymbol{b}$ is spatially constant, as gravitational force is usually presumed to be, then $\boldsymbol{v}\cdot\nabla\boldsymbol{b}\equiv\boldsymbol{0}$. However, if D'Alembert's principle is used, or if $\boldsymbol{b}$ is due to motion through an electromagnetic field, then $\boldsymbol{v}\cdot\nabla\boldsymbol{b}$ generally does not vanish, and $\dot{\mathbf{t}}^b$ depends upon $\boldsymbol{v}$.

The angular momentum balance (2.2.20) involves the stretching, spin and true stress, as well as $\dot{\mathbf{t}}$. For this reason there are no second-order stress functions analogous to those for the true stress; the function $\boldsymbol{\Phi}$ in equation (2.2.25) is called a "first order stress function" [15].

2.3. *Rate-type constitutive equations*

Our aim in this section is only to discuss a certain 'change of variable' possible in rate-type constitutive equations. We consider only materials whose mechanical behavior may be adequately described[8] by a relation of the form:

$$\dot{\boldsymbol{\sigma}}^*=\underline{\mathbf{V}}:\boldsymbol{\varepsilon}+\boldsymbol{\Sigma}\,, \tag{2.3.1}$$

which we call 'rate-type'. In (2.3.1) $\dot{\boldsymbol{\sigma}}^*$ is the *corotational rate of the Kirchhoff stress*[9], defined by

[7] For isoparametric elements, $(\dot{J}-\boldsymbol{n}\cdot\boldsymbol{\varepsilon}\cdot\boldsymbol{n})$ is continuous across interelement boundaries.

[8] The notion of 'adequacy' of a rate-type equation relative to specific data has been discussed by the authors [28].

[9] This stress rate seems to have been introduced by Hill [29] as a means of making a certain b.v.p. self-adjoint.

$$\dot{\boldsymbol{\sigma}}^* \equiv (\dot{\boldsymbol{\tau}} - \boldsymbol{\omega}\cdot\boldsymbol{\tau} + \boldsymbol{\tau}\cdot\boldsymbol{\omega}) + \dot{J}\boldsymbol{\tau}\,, \tag{2.3.2}$$

and $\underline{\mathbf{V}}$ and $\boldsymbol{\Sigma}$ are independent of $\boldsymbol{\varepsilon}$.[10] If $V_{ijkl} = V_{klij}$, then we describe $\underline{\mathbf{V}}$ as *symmetric*. The parenthecized quantity in (2.3.2) is the well-known Zaremba–Jaumann stress rate.[11]

The following variable change leaves the constitutive equation in the form needed for our discussion of variational principles. According to (2.2.16) and (2.3.2), the symmetric and skew-symmetric parts of $\dot{\mathbf{t}}$ are

$$\tfrac{1}{2}(\dot{\mathbf{t}} + \dot{\mathbf{t}}^{\mathrm{t}}) = \dot{\boldsymbol{\sigma}}^* - \tfrac{1}{2}(\boldsymbol{\varepsilon}\cdot\boldsymbol{\tau} + \boldsymbol{\tau}\cdot\boldsymbol{\varepsilon}) - \tfrac{1}{2}(\boldsymbol{\tau}\cdot\boldsymbol{\omega} - \boldsymbol{\omega}\cdot\boldsymbol{\tau})\,, \tag{2.3.3}$$

$$\tfrac{1}{2}(\dot{\mathbf{t}} - \dot{\mathbf{t}}^{\mathrm{t}}) = -\tfrac{1}{2}[(\boldsymbol{\varepsilon} + \boldsymbol{\omega})\cdot\boldsymbol{\tau} - \boldsymbol{\tau}\cdot(\boldsymbol{\varepsilon} - \boldsymbol{\omega})]\,. \tag{2.3.4}$$

Equation (2.3.4) is merely a rearrangement of the angular momentum condition (2.2.20).[12] Using (2.3.1) to eliminate $\dot{\boldsymbol{\sigma}}^*$ from (2.3.3) yields

$$\begin{aligned} &\dot{\mathbf{r}} = \underline{\mathbf{W}} : \boldsymbol{\varepsilon} + \boldsymbol{\Sigma}\,,\\ &W_{ijkl} \equiv V_{ijkl} - \tfrac{1}{2}(\tau_{ik}\delta_{lj} + \delta_{ik}\tau_{lj})\,,\\ &\dot{\mathbf{r}} \equiv \tfrac{1}{2}(\dot{\mathbf{t}} + \boldsymbol{\tau}\cdot\boldsymbol{\omega} - \boldsymbol{\omega}\cdot\boldsymbol{\tau} + \dot{\mathbf{t}}^{\mathrm{t}})\,. \end{aligned} \tag{2.3.5}$$

According to Hill[13], the stress rate $\dot{\mathbf{r}}$ was introduced by Biot (see [32, p. 62; 33])[14]. We note that if $\underline{\mathbf{V}}$ is symmetric, then $\underline{\mathbf{W}}$ is symmetric also.

When $\underline{\mathbf{W}}$ is symmetric a *rate potential* $\mathcal{W}\hat{}$ exists for $\dot{\mathbf{r}}$:

$$\dot{\mathbf{r}} = \partial_{\boldsymbol{\varepsilon}}\mathcal{W}\hat{}(\boldsymbol{\varepsilon}, \boldsymbol{\tau})\,, \qquad \mathcal{W}\hat{}(\boldsymbol{\varepsilon}, \boldsymbol{\tau}) \equiv \tfrac{1}{2}\boldsymbol{\varepsilon} : \underline{\mathbf{W}} : \boldsymbol{\varepsilon} + \boldsymbol{\varepsilon} : \boldsymbol{\Sigma}\,. \tag{2.3.6}$$

If $\underline{\mathbf{W}}$ is also non-singular[15], then (2.3.5) may be inverted

$$\boldsymbol{\varepsilon} = \underline{\mathbf{W}}^{-1} : (\dot{\mathbf{r}} - \boldsymbol{\Sigma}) \tag{2.3.7}$$

and there exists a rate potential $\mathcal{R}$ for $\boldsymbol{\varepsilon}$:

$$\boldsymbol{\varepsilon} = \partial_{\dot{\mathbf{r}}}\mathcal{R}(\dot{\mathbf{r}}, \boldsymbol{\tau})\,, \qquad \mathcal{R}(\dot{\mathbf{r}}, \boldsymbol{\tau}) \equiv \tfrac{1}{2}(\dot{\mathbf{r}} - \boldsymbol{\Sigma}) : \underline{\mathbf{W}}^{-1} : (\dot{\mathbf{r}} - \boldsymbol{\Sigma})\,. \tag{2.3.8}[16]$$

[10] A particularly simple kind of exception is made to this rule so that (2.3.1) may include classical plasticity.

[11] The work of Key et al. [30] suggests that distinction of the two rates may not be necessary for nearly incompressible materials. However Bazant [31] has shown that esimates of buckling loads can be very sensitive to a change of stress rate.

[12] Biot's [32, p. 59] "alternative" stress, in the present notation, is $(\dot{\mathbf{t}}^{\mathrm{t}} - \boldsymbol{\omega}\cdot\boldsymbol{\tau})$; he gave the same interpretation of the two-dimensional counterpart to (2.3.4).

[13] Hill [23, p. 20], actually credits Biot for introducing a stress, whose rate ($\dot{\mathbf{r}}$) Biot gave.

[14] Hill and Hutchinson [34] refer to it as Biot's "peculiar 'symmetrized stress'".

[15] $\underline{\mathbf{W}}$ is non-singular iff $(\underline{\mathbf{W}} : \boldsymbol{\varepsilon} = \mathbf{0}) \Rightarrow \boldsymbol{\varepsilon} = \mathbf{0}$.

[16] Atluri [15] considers more complicated inverse relations than (2.3.7); $\mathcal{R}$ may still be defined by a Legendre. or contact transformation.

3. Boundary value problems, initial value problems

3.1. Scope of section

Thus far we have treated kinematics, dynamics and material behavior as separate subjects. Presently, we regard the equations of compatibility (2.1.9), linear momentum balance (2.2.19), angular momentum balance (2.2.20) and the constitutive equations (2.3.1) and (2.3.7), as a system of coupled partial differential equations. For ease of reference we collect these equations below:

$$\nabla \times (\boldsymbol{\varepsilon} - \boldsymbol{\omega}) = \mathbf{0} \quad \text{in } V; \qquad \boldsymbol{s} \cdot (-\boldsymbol{\varepsilon} + \boldsymbol{\omega} + \nabla \boldsymbol{v}) = \boldsymbol{0} \quad \text{on } S; \tag{3.1.1}$$[17]

$$\nabla \cdot \dot{\mathbf{t}} + \rho \dot{\boldsymbol{b}} = \boldsymbol{0} \quad \text{in } V; \qquad \boldsymbol{n} \cdot \dot{\mathbf{t}} = \dot{\boldsymbol{T}}_t \quad \text{on } S; \tag{3.1.2}$$

$$\tfrac{1}{2}[(\boldsymbol{\varepsilon} + \boldsymbol{\omega}) \cdot \boldsymbol{\tau} + \dot{\mathbf{t}} - \dot{\mathbf{t}}^{\mathrm{t}} - \boldsymbol{\tau} \cdot (\boldsymbol{\varepsilon} - \boldsymbol{\omega})] = \mathbf{0} \quad \text{in } V; \tag{3.1.3}$$

$$\dot{\mathbf{t}} = \underline{\mathbf{V}} : \boldsymbol{\varepsilon} - \boldsymbol{\varepsilon} \cdot \boldsymbol{\tau} - \boldsymbol{\tau} \cdot \boldsymbol{\omega} + \boldsymbol{\Sigma}; \tag{3.1.4}$$[18]

$$\boldsymbol{\varepsilon} = \underline{\mathbf{W}}^{-1} : [\tfrac{1}{2}(\dot{\mathbf{t}} + \boldsymbol{\tau} \cdot \boldsymbol{\omega} - \boldsymbol{\omega} \cdot \boldsymbol{\tau} + \dot{\mathbf{t}}^{\mathrm{t}}) - \boldsymbol{\Sigma}]; \tag{3.1.5}$$

$$\boldsymbol{v} = \bar{\boldsymbol{v}} \quad \text{on } S_v; \tag{3.1.6}$$

$$\dot{\boldsymbol{T}}_t = \dot{\bar{\boldsymbol{T}}}_t \quad \text{on } S_\sigma. \tag{3.1.7}$$

We call this set of equations *the general boundary value problem.*

In this section we first present and compare the specializations of the general boundary value problem obtained by systematic use of (2.1.10) (the general solution of (3.1.1)) and (2.2.24) (the general solution of (3.1.2)). Then variational statements of the same boundary value problems are derived and discussed. Finally, under the assumption that a solution[19] of the general boundary value problem is known, we show that an initial value problem must be solved to find the total deformation and stress.

3.2. Specializations of the general boundary value problem

If the general solution of the compatibility equation is used to eliminate $\boldsymbol{\varepsilon}$, $\boldsymbol{\omega}$ and $\dot{\mathbf{t}}$ from the general boundary value problem ($\dot{\mathbf{t}}$ by virtue of the constitutive equation 3.1.4), then we obtain a single, second-order, partial differential equation for the velocity field $\boldsymbol{v}$:

$$\nabla \cdot \dot{\mathbf{t}}(\nabla \boldsymbol{v}) + \rho(\partial_t \boldsymbol{b} + \boldsymbol{v} \cdot \nabla \boldsymbol{b}) = \boldsymbol{0} \tag{3.2.1}$$

[17]Throughout this section it is implied, rather than expressly stated, that $\boldsymbol{\varepsilon}$ is symmetric and $\boldsymbol{\omega}$ is skew-symmetric. The vector $\boldsymbol{s}$ is an arbitrary tangent on S. The boundary condition governs in-surface components of $\boldsymbol{\varepsilon}$ and $\boldsymbol{\omega}$ only; it is the formal counterpart to the stress principle.

[18]This equation follows directly from (2.2.16), (2.3.1) and (2.3.2).

[19]A solution is made up of the fields $\boldsymbol{\varepsilon}$, $\boldsymbol{\omega}$ and $\dot{\mathbf{t}}$.

and the boundary conditions:

$$\boldsymbol{v} = \bar{\boldsymbol{v}} \quad \text{on } S_v\,; \qquad \boldsymbol{n}\cdot\dot{\mathbf{t}}(\nabla \boldsymbol{v}) = \dot{\bar{\boldsymbol{T}}}_t \quad \text{on } S_\sigma\,. \tag{3.2.2}$$

In analogy to its counterpart in linear elasticity, we call (3.2.1) "Navier's" equation [24. p. 155]. It is important to note that the angular momentum balance (3.1.3) is satisfied *implicitly* so long as $\underline{\mathbf{V}}$ satisfies

$$(\underline{\mathbf{V}}:\boldsymbol{\varepsilon}) - (\underline{\mathbf{V}}:\boldsymbol{\varepsilon})^{\mathrm{t}} = \mathbf{0} \tag{3.2.3}$$

for all symmetric $\boldsymbol{\varepsilon}$.[20]

By a procedure parallel to that above, we use the general solution of the linear momentum balance to eliminate $\dot{\mathbf{t}}$ and $\boldsymbol{\varepsilon}$ from the general boundary value problem, thereby obtaining

$$\nabla \times [\boldsymbol{\varepsilon}(\dot{\mathbf{t}}^0, \boldsymbol{\omega}) - \boldsymbol{\omega}] = \mathbf{0}\,, \tag{3.2.4}[21]$$

$$[\boldsymbol{\varepsilon}(\dot{\mathbf{t}}^0, \boldsymbol{\omega}) + \boldsymbol{\omega}]\cdot\boldsymbol{\tau} + \dot{\mathbf{t}}^0 + \dot{\mathbf{t}}^b = \text{symmetric}\,, \tag{3.2.5}$$

and the boundary conditions

$$\begin{aligned} &\boldsymbol{s}\cdot[-\boldsymbol{\varepsilon}(\dot{\mathbf{t}}^0, \boldsymbol{\omega}) + \boldsymbol{\omega}] + (\boldsymbol{s}\cdot\nabla)\,\bar{\boldsymbol{v}} = \boldsymbol{0} \quad \text{for all } \boldsymbol{s} \text{ on } S_v\,, \\ &\boldsymbol{n}\cdot\dot{\mathbf{t}} = \dot{\bar{\boldsymbol{T}}}_t \quad \text{on } S_\sigma\,. \end{aligned} \tag{3.2.6}$$

In analogy to its counterpart in linear elasticity, we call (3.2.4) the "Beltrami–Michell" equation [24, p. 160]. In contrast to the situation in linear elasticity, where the general simultaneous solution of linear *and* angular momentum balance equations are known, here the angular momentum balance equation must be retained.[22]

Both Navier's and Beltrami–Michell equations are linear and second-order; the stronger appeal of Navier's equation stems from the clear physical significance of the principal unknown, the velocity field. The boundary conditions are simple, and possess a natural interpretation. In contrast, the significance of a stress function is difficult to grasp; in terms of it, boundary conditions become complicated and defy an easy interpretation. Now, it is a fact that 'semi-inverse' techniques are the most widely understood of all methods of solution, and their use generally requires some intuition. So it is no puzzle as to why Navier's equation is encountered so much more frequently than the Beltrami–Michell equation.

3.3. Variational principles

The first step of the finite element method consists of *generalizing* the equations of the boundary value problem. It is the generalized problem upon which the approximate scheme is

[20]Contrary to the usual claims, $\underline{\mathbf{V}}$ need not satisfy $V_{ijkl} = V_{jikl}$. Consider, for example, the tensor $A_{ijkl} \equiv \delta_{ik}\delta_{jl}$: $\underline{\mathbf{A}}$ certainly satisfies (3.2.3), but still $A_{1212} \neq A_{2112}$.

[21]We write $\dot{\mathbf{t}}^0$ for $\nabla\times\boldsymbol{\Phi}$; $\nabla\cdot\dot{\mathbf{t}}^b = -\rho\dot{\boldsymbol{b}}$.

[22]This has been a stumbling block for a number of workers; cf. [15, 18, 22].

founded.[23] In engineering this generalization is accomplished by finding a variational principle 'equivalent' to the original problem. In solid mechanics, the construction of variational principles was first systemetized by Washizu [26]. The formalism he introduced led not only to unification of the classical energy principles, but also to the abstraction of those principles for inelastic materials.[24] Thus, the variational principles discussed below are called 'virtual work', 'potential energy', etc., so as to remind the reader of the corresponding principle of linear elastostatics.

We begin by deriving the generalization of the linear momentum balance equation (3.1.2). Let us momentarily regard δv as a Lagrange multiplier. Then a stress rate $\dot{\mathbf{t}}$ and a traction rate $\dot{\boldsymbol{T}}_t$ satisfy (3.1.2) if[25]

$$\int_V [-\nabla \cdot \dot{\mathbf{t}} \delta v - \rho \dot{\boldsymbol{b}} \cdot \delta v] \, dV - \int_S (\dot{T}_t - \boldsymbol{n} \cdot \dot{\mathbf{t}}) \cdot \delta v \, dS = 0 , \tag{3.3.1}$$

for arbitrary δv. In this equation $\dot{\mathbf{t}}$ apparently must be differentiable, but δv need not even be continuous. Now, by formally integrating by parts[26], (3.3.1) is transformed to

$$\int_V [\dot{\mathbf{t}} : \nabla \delta v - \rho \dot{\boldsymbol{b}} \cdot \delta v] \, dV - \int_S \dot{T}_t \cdot \delta v \, dS = 0 , \tag{3.3.2}$$

to be satisfied for arbitrary *differentiable* δv. In (3.3.2) the stress rate $\dot{\mathbf{t}}$ need not even be continuous. Any stress rate $\dot{\mathbf{t}}$ admissible to the differential form of LMB (3.1.2) is also admitted by (3.3.2), but the converse is not true.[27] Therefore we call (3.3.2) the 'generalized' linear momentum balance.

A modification of the general boundary value problem is now possible: we simply use (3.3.2) in place of (3.1.2). If we proceed to eliminate $\boldsymbol{\varepsilon}$, $\boldsymbol{\omega}$ and $\dot{\mathbf{t}}$ from this modified boundary value problem, just as we did in deriving Navier's equation, we obtain

$$\begin{aligned} &\int_V [\dot{\mathbf{t}}(\nabla v) : \nabla \delta v - \rho \dot{\boldsymbol{b}} \cdot \delta v] \, dV - \int_S \dot{\boldsymbol{T}}_t \cdot \delta v \, dS = 0 , \\ &v = \bar{v} \quad \text{on } S_v ; \qquad \dot{\boldsymbol{T}}_t = \dot{\bar{\boldsymbol{T}}}_t \quad \text{on } S_\sigma . \end{aligned} \tag{3.3.3}$$

If we admit only $v = \bar{v}$ on S_v, $\dot{\boldsymbol{T}}_t = \dot{\bar{\boldsymbol{T}}}_t$ on S_σ, and $\delta v = \boldsymbol{0}$ on S_v, then (3.3.3) is reduced to a functional of the velocity field alone; that any solution of the general boundary value problem also causes this functional to vanish comprises a statement of the *principle of virtual work*. Most finite element algorithms used in engineering today are founded upon the principle of virtual work.

By a procedure parallel to that above we may derive the generalization of the equation of

[23]This is in sharp contrast to the finite difference method, in which the differential operator plays the fundamental role.

[24]A unified treatment of variational principles for rate-type materials has been given by Atluri [15].

[25]The stress rate $\dot{\mathbf{t}}$ and traction rate $\dot{\boldsymbol{T}}_t$ are independent.

[26]Throughout this section integration by parts is *formal*.

[27]In particular, (3.3.2) admits discontinuous stress rate fields, where as (3.1.2) does not.

compatibility (3.1.1). Let us momentarily regard the stress function $\delta\Phi$ and the surface tangents δs^j as Lagrange multipliers. We write $(\delta s^j \boldsymbol{e}_j)$ as $(\boldsymbol{n} \times \delta\Phi)$. Then the stretching $\boldsymbol{\varepsilon}$, spin $\boldsymbol{\omega}$ and velocity $\boldsymbol{v}$ satisfy (3.1.1) if

$$\int_V [\nabla \times (-\boldsymbol{\varepsilon} + \boldsymbol{\omega})] : \delta\Phi \, dV + \int_S (\boldsymbol{n} \times \delta\Phi) : (-\boldsymbol{\varepsilon} + \boldsymbol{\omega} + \nabla \boldsymbol{v}) \, dS = 0 \tag{3.3.4}$$

for arbitrary $\delta\Phi$. Just as for the linear momentum balance, we formally integrate by parts to relax the smoothness requirements on $\boldsymbol{\varepsilon}$ and $\boldsymbol{\omega}$, obtaining

$$\int_V [-\boldsymbol{\varepsilon} + \boldsymbol{\omega}] : (\nabla \times \delta\Phi) \, dV + \int_S (\boldsymbol{n} \times \delta\Phi) : (\nabla \boldsymbol{v}) \, dS = 0 \,, \tag{3.3.5}$$

to be satisfied for arbitrary *differentiable* $\delta\Phi$. For the same reasons that we called (3.3.2) the generalization of linear momentum balance, we call (3.3.5) the generalization of compatibility. When expressed in this form it is easy to see that the velocity field enters the compatibility equation only so far as to determine the stretching and spin of the bounding surface of the body. This fact is not brought out in the literature,[28] and is obscured by the conventional form for generalized compatibility, which we now give. Using the formula (integration by parts)

$$\int_S (\boldsymbol{n} \times \delta\Phi) : (\nabla \boldsymbol{v}) \, dS = \int_S \boldsymbol{n} \cdot (\nabla \times \delta\Phi) \cdot \boldsymbol{v} \, dS$$

and identifying $(\nabla \times \delta\Phi)$ as $\delta \dot{\mathbf{t}}$ (in accordance with (2.2.24)), equation (3.3.5) becomes

$$\int_V [-\boldsymbol{\varepsilon} + \boldsymbol{\omega}] : \delta \dot{\mathbf{t}} \, dV + \int_S \boldsymbol{n} \cdot \delta \dot{\mathbf{t}} \cdot \boldsymbol{v} \, dS = 0 \,. \tag{3.3.6}$$

It is clear from this derivation that the stress rate variations $\delta \dot{\mathbf{t}}$ are subject to no constraint except $\delta \dot{\mathbf{t}} = \nabla \times \delta\Phi$.[29]

We now consider the general boundary value problem as modified by replacing (3.1.1) with (3.3.6). If we proceed by eliminating $\boldsymbol{\varepsilon}$ from the modified problem just as we did in deriving the Beltrami-Michell equation, then we obtain

$$\begin{aligned}
&\int_V [-\boldsymbol{\varepsilon}(\dot{\mathbf{t}}^0, \boldsymbol{\omega}) + \boldsymbol{\omega}] : \delta \dot{\mathbf{t}} \, dV + \int_S \boldsymbol{n} \cdot \delta \dot{\mathbf{t}} \cdot \boldsymbol{v} \, dS = 0 \quad \text{for all } \delta \dot{\mathbf{t}} = \nabla \times \delta\Phi \,; \\
&[\boldsymbol{\varepsilon}(\dot{\mathbf{t}}^0, \boldsymbol{\omega}) + \boldsymbol{\omega}] \cdot \boldsymbol{\tau} + \dot{\mathbf{t}}^0 + \dot{\mathbf{t}}^b = \text{symmetric} \,; \\
&\boldsymbol{v} = \bar{\boldsymbol{v}} \quad \text{on } S_v \,; \qquad \boldsymbol{n} \cdot (\dot{\mathbf{t}}^0 + \dot{\mathbf{t}}^b) = \dot{\bar{\boldsymbol{T}}}_t \,.
\end{aligned} \tag{3.3.7}$$

If we admit to (3.3.7) only $\boldsymbol{v} = \bar{\boldsymbol{v}}$ on S_v, $\boldsymbol{n} \cdot (\dot{\mathbf{t}}^0 + \dot{\mathbf{t}}^b) = \dot{\bar{\boldsymbol{T}}}_t$ on S_σ, $\boldsymbol{n} \cdot \delta \dot{\mathbf{t}} = \boldsymbol{0}$ on S_σ, and

[28] In fact, we find no counterpart of (3.3.5) in the literature, though our search has not been exhaustive.

[29] In the generalized compatibility equation of infinitesimal strain theories, stress variations must also satisfy AMB.

combinations of $(\dot{\mathbf{t}}^0 + \dot{\mathbf{t}}^b)$ which satisfy AMB, then we can reduce (3.3.7) to a single functional. That any solution of the general boundary value problem also causes this functional to vanish comprises a statement of the principle of complementary virtual work. Except for pathological cases, e.g. $S = S_v$, $\boldsymbol{\tau} = \mathbf{0}$, construction of such $(\dot{\mathbf{t}}^0 + \dot{\mathbf{t}}^b)$ and $\boldsymbol{\omega}$ is impracticable.

The problems associated with use of the complementary virtual work principle in its 'pure' form may be avoided by treating the angular momentum balance and conditions on S_σ as *constraints*. We introduce the Lagrange multipliers $\delta\boldsymbol{\omega}$ (for the angular momentum balance) and $\delta\boldsymbol{v}$ (for the traction boundary condition). Then (3.3.7) may be restated in the form

$$\begin{aligned}
&\int_V [-\boldsymbol{\varepsilon}(\dot{\mathbf{t}}^0, \boldsymbol{\omega}) + \boldsymbol{\omega}] : \delta\dot{\mathbf{t}}\, dV + \int_S \boldsymbol{n} \cdot \delta\dot{\mathbf{t}} \cdot \boldsymbol{v}\, dS = 0 \quad \text{for all } \delta\dot{\mathbf{t}} = \nabla \times \delta\boldsymbol{\Phi}\,, \\
&\int_V [(\boldsymbol{\varepsilon}(\dot{\mathbf{t}}^0, \boldsymbol{\omega}) + \boldsymbol{\omega}) \cdot \boldsymbol{\tau} + \dot{\mathbf{t}}^0 + \dot{\mathbf{t}}^b] : \delta\boldsymbol{\omega}\, dV = 0 \quad \text{for all } \delta\boldsymbol{\omega}\text{:} \quad \delta\boldsymbol{\omega} + \delta\boldsymbol{\omega}^t = \mathbf{0}\,, \\
&\int_{S_\sigma} [\boldsymbol{n} \cdot (\dot{\mathbf{t}}^0 + \dot{\mathbf{t}}^b) - \dot{\bar{\boldsymbol{T}}}_t] \cdot \delta\boldsymbol{v}\, dS = 0 \quad \text{for all } \delta\boldsymbol{v} \text{ on } S_\sigma\,, \\
&\boldsymbol{v} = \bar{\boldsymbol{v}} \quad \text{on } S_v\,.
\end{aligned} \tag{3.3.8}$$

That any solution of the general boundary value problem also satisfies (3.3.8) is the statement of the complementary virtual work principle upon which our finite element algorithm is based.

The most important property of the generalized linear momentum balance and compatibility equations is that they admit functions $\boldsymbol{v}$, $\boldsymbol{\varepsilon}$, $\boldsymbol{\omega}$ and $\dot{\mathbf{t}}$ less smooth than did their partial differential equation counterparts. A second property to be noted is their independence from any constitutive equation. In deriving the generalized Navier's equation (3.3.3) and the generalized Beltrami–Michell equation (3.3.8) we tacitly restricted our attention to materials whose constitutive equations are expressible in the forms $\dot{\mathbf{t}} = \dot{\mathbf{t}}(\nabla\boldsymbol{v})$ and $\boldsymbol{\varepsilon} = \boldsymbol{\varepsilon}(\dot{\mathbf{t}}, \boldsymbol{\omega})$, respectively. Now, by inspection of (3.3.3), we see that an 'energy' principle exists if potentials $\mathcal{U}$, Ψ and ψ exist such that

$$\dot{\mathbf{t}} = \partial_{\mathbf{L}^t}\mathcal{U}\,, \qquad -\dot{\boldsymbol{b}} = \partial_{\boldsymbol{v}}\Psi\,, \qquad -\dot{\bar{\boldsymbol{T}}}_t = \partial_{\boldsymbol{v}}\psi\,.$$

Henceforth we assume that $\partial\dot{\boldsymbol{b}}/\partial\boldsymbol{v} = \mathbf{0}$ and $\partial\dot{\bar{\boldsymbol{T}}}_t/\partial\boldsymbol{v} = \mathbf{0}$ so that $\Psi = -\dot{\boldsymbol{b}} \cdot \boldsymbol{v}$ and $\psi = -\dot{\bar{\boldsymbol{T}}}_t \cdot \boldsymbol{v}$. From (2.1.7) and (2.3.3) through (2.3.5) we see that

$$\dot{\mathbf{t}} : \delta\mathbf{L}^t = \dot{\boldsymbol{\tau}} : \delta\boldsymbol{\varepsilon} - (\delta\boldsymbol{\varepsilon} : \boldsymbol{\tau} \cdot \boldsymbol{\omega} + \boldsymbol{\varepsilon} : \boldsymbol{\tau} \cdot \delta\boldsymbol{\omega}) - \tfrac{1}{2}\boldsymbol{\tau} : (\boldsymbol{\omega} \cdot \delta\boldsymbol{\omega} + \delta\boldsymbol{\omega} \cdot \boldsymbol{\omega})\,, \tag{3.3.9}$$

so the potential $\mathcal{U}$ exists whenever the potential $\mathcal{W}$ (2.3.6) exists; i.e. when $\underset{\sim}{\mathbf{V}}$ is symmetric. Henceforth we shall assume that $\underset{\sim}{\mathbf{V}}$ is symmetric. Then $\mathcal{U}$ may be expressed as

$$\mathcal{U}(\boldsymbol{\varepsilon}, \boldsymbol{\omega}, \boldsymbol{\tau}) = \mathcal{W}(\boldsymbol{\varepsilon}, \boldsymbol{\tau}) - \boldsymbol{\varepsilon} : \boldsymbol{\tau} \cdot \boldsymbol{\omega} - \tfrac{1}{2}\boldsymbol{\tau} : (\boldsymbol{\omega} \cdot \boldsymbol{\omega})\,. \tag{3.3.10}$$

We now introduce the potential $\mathcal{U}$ to (3.3.3) to obtain

$$\boldsymbol{\varepsilon} = \tfrac{1}{2}(\nabla\boldsymbol{v}^t + \nabla\boldsymbol{v})\,, \qquad \boldsymbol{\omega} = \tfrac{1}{2}(\nabla\boldsymbol{v}^t - \nabla\boldsymbol{v})\,, \qquad \boldsymbol{v} = \bar{\boldsymbol{v}} \quad \text{on } S_v\,. \tag{3.3.11}$$

$$\delta\pi(\boldsymbol{v}, \boldsymbol{\varepsilon}, \boldsymbol{\omega}) = 0\,,$$
$$\pi(\boldsymbol{v}, \boldsymbol{\varepsilon}, \boldsymbol{\omega}) \equiv \int_V [\mathcal{U}(\boldsymbol{\varepsilon}, \boldsymbol{\omega}) - \rho \dot{\boldsymbol{b}} \cdot \boldsymbol{v}]\, \mathrm{d}V - \int_{S_\sigma} \dot{\bar{\boldsymbol{T}}}_i \cdot \boldsymbol{v}\, \mathrm{d}S\,. \tag{3.3.12}$$

There are two ways to deal with the subsidiary conditions (3.3.11). It is an easy exercise to reduce (3.3.11) and (3.3.12) to a functional of the velocity field alone. Alternatively we may 'enforce' (3.3.11) by use of Lagrange multipliers.

The first course of action transforms (3.3.11) and (3.3.12) to

$$\delta\pi_{\mathrm{p}}(\boldsymbol{v}) = 0\,, \quad \pi_{\mathrm{p}}(\boldsymbol{v}) \equiv \pi(\boldsymbol{v}, \tfrac{1}{2}(\nabla \boldsymbol{v}^{\mathrm{t}} + \nabla \boldsymbol{v}), \tfrac{1}{2}(\nabla \boldsymbol{v}^{\mathrm{t}} - \nabla \boldsymbol{v}))\,. \tag{3.3.13}$$

Any solution of the general boundary value problem is a solution of (3.3.13): this comprises the *principle of stationary potential energy*.

The alternative course of action leads us to a *Hu–Washizu energy principle*. Let us momentarily regard $\dot{\bar{\boldsymbol{T}}}_i$ and $\dot{\mathbf{t}}$ as Lagrange multipliers. Then equations (3.3.11) and (3.3.12) may be replaced by

$$\delta\pi_{\mathrm{HW}}(\boldsymbol{v}, \boldsymbol{\varepsilon}, \boldsymbol{\omega}, \dot{\bar{\boldsymbol{T}}}_i, \dot{\mathbf{t}}) = 0\,,$$
$$\pi_{\mathrm{HW}}(\boldsymbol{v}, \boldsymbol{\varepsilon}, \boldsymbol{\omega}, \dot{\bar{\boldsymbol{T}}}_i, \dot{\mathbf{t}}) \equiv \pi(\boldsymbol{v}, \boldsymbol{\varepsilon}, \boldsymbol{\omega}) + \int_V \dot{\mathbf{t}} : (\nabla \boldsymbol{v} - (\boldsymbol{\varepsilon} - \boldsymbol{\omega}))\mathrm{d}V - \int_{S_t} \dot{\bar{\boldsymbol{T}}}_i \cdot (\boldsymbol{v} - \bar{\boldsymbol{v}})\mathrm{d}S\,. \tag{3.3.14}$$

Any solution of the general boundary value problem necessarily satisfies (3.3.14). We write out the stationary conditions for future reference:

LMB:

$$\int_V [\dot{\mathbf{t}} : \nabla \delta \boldsymbol{v} - \rho \dot{\boldsymbol{b}} \cdot \delta \boldsymbol{v}]\mathrm{d}V - \int_{S_\sigma} \dot{\bar{\boldsymbol{T}}}_i \cdot \delta \boldsymbol{v}\, \mathrm{d}S - \int_{S_t} \dot{\bar{\boldsymbol{T}}}_i \cdot \delta \boldsymbol{v}\, \mathrm{d}S = 0\,; \tag{3.3.15}$$

constitutive equation:

$$\int_V [(\partial_{\boldsymbol{\varepsilon}} \mathcal{W}) - \tfrac{1}{2}(\dot{\mathbf{t}} + \boldsymbol{\tau} \cdot \boldsymbol{\omega} - \boldsymbol{\omega} \cdot \boldsymbol{\tau} + \dot{\mathbf{t}}^{\mathrm{t}})] : \delta \boldsymbol{\varepsilon}\, \mathrm{d}V = 0\,; \tag{3.3.16}$$

AMB:

$$\int_V [\tfrac{1}{2}(\boldsymbol{\varepsilon} + \boldsymbol{\omega}) \cdot \boldsymbol{\tau} + \dot{\mathbf{t}} - \dot{\mathbf{t}}^{\mathrm{t}} - \boldsymbol{\tau} \cdot (\boldsymbol{\varepsilon} - \boldsymbol{\omega})] : \delta \boldsymbol{\omega}\, \mathrm{d}V = 0\,; \tag{3.3.17}$$

velocity boundary condition:

$$\int_{S_t} \delta \dot{\bar{\boldsymbol{T}}}_i \cdot (\bar{\boldsymbol{v}} - \boldsymbol{v})\mathrm{d}S = 0\,; \tag{3.3.18}$$

compatibility:

$$\int_V [\nabla \boldsymbol{v} - (\boldsymbol{\varepsilon} - \boldsymbol{\omega})] : \delta \dot{\mathbf{t}} \, dV = 0 . \tag{3.3.19}$$

Notice that the stationary condition for $\delta \boldsymbol{v}$ (3.3.15) is the generalized linear momentum balance (3.3.2).

Now, solely by rearrangement of terms, π_{HW} may be written in the form

$$\pi_{HW}(\boldsymbol{v}, \boldsymbol{\varepsilon}, \boldsymbol{\omega}, \dot{\boldsymbol{T}}_t, \dot{\mathbf{t}}) \equiv \int_V \{[\mathscr{U}^*(\boldsymbol{\varepsilon}) - \tfrac{1}{2}(\dot{\mathbf{t}} + \boldsymbol{\tau} \cdot \boldsymbol{\omega} - \boldsymbol{\omega} \cdot \boldsymbol{\tau} + \dot{\mathbf{t}}^t) : \boldsymbol{\varepsilon}] - \tfrac{1}{2}\boldsymbol{\tau} : \boldsymbol{\omega} \cdot \boldsymbol{\omega} + \dot{\mathbf{t}} : \boldsymbol{\omega}\} dV$$
$$+ \int_V \{\dot{\mathbf{t}} : \nabla \boldsymbol{v} - \rho \dot{\boldsymbol{b}} \cdot \boldsymbol{v}\} dV - \int_{S_\sigma} \dot{\bar{\boldsymbol{T}}}_t \cdot \boldsymbol{v} \, dS - \int_{S_t} \dot{\boldsymbol{T}}_t \cdot \boldsymbol{v} \, dS + \int_{S_t} \dot{\boldsymbol{T}}_t \cdot \bar{\boldsymbol{v}} \, dS . \tag{3.3.20}$$

If the constitutive equation (2.3.7) is used to eliminate $\boldsymbol{\varepsilon}$ as a variable from π_{HW}, then, defining

$$-\mathscr{R}(\dot{\mathbf{t}}, \boldsymbol{\omega}) \equiv \mathscr{U}^*(\boldsymbol{\varepsilon}(\dot{\mathbf{t}}, \boldsymbol{\omega})) - \tfrac{1}{2}(\dot{\mathbf{t}} + \boldsymbol{\tau} \cdot \boldsymbol{\omega} - \boldsymbol{\omega} \cdot \boldsymbol{\tau} + \dot{\mathbf{t}}^t) : \boldsymbol{\varepsilon}(\dot{\mathbf{t}}, \boldsymbol{\omega}) ,$$

we obtain a *Hellinger–Reissner energy principle*:

$$\delta \pi_{HR}(\boldsymbol{v}, \boldsymbol{\omega}, \dot{\boldsymbol{T}}_t, \dot{\mathbf{t}}) = 0 , \tag{3.3.21}$$

$$\pi_{HR}(\boldsymbol{v}, \boldsymbol{\omega}, \dot{\boldsymbol{T}}_t, \dot{\mathbf{t}}) \equiv \int_V \{-\mathscr{R}(\dot{\mathbf{t}}, \boldsymbol{\omega}) - \tfrac{1}{2}\boldsymbol{\tau} : (\boldsymbol{\omega} \cdot \boldsymbol{\omega}) + \dot{\mathbf{t}} : \boldsymbol{\omega}\} dV + \int_{S_t} \dot{\boldsymbol{T}}_t \cdot \bar{\boldsymbol{v}} \, dS$$
$$+ \int_V [\dot{\mathbf{t}} : \nabla \boldsymbol{v} - \rho \dot{\boldsymbol{b}} \cdot \boldsymbol{v}] \, dV - \int_{S_\sigma} \dot{\bar{\boldsymbol{T}}}_t \cdot \boldsymbol{v} \, dS - \int_{S_t} \dot{\boldsymbol{T}}_t \cdot \boldsymbol{v} \, dS .$$

Any solution of the general boundary value problem is also a solution of (3.3.21). The stationary conditons are LMB (3.3.15), AMB (3.3.17), velocity boundary condition (3.3.18) and compatibility (3.3.19). In the stationary conditions $\boldsymbol{\varepsilon}$ appears only as a function of the stress rate and spin.

If we admit to π_{HR} only stress rates $\dot{\mathbf{t}}$ and traction rates $\dot{\boldsymbol{T}}_t$ which satisfy the generalized linear momentum balance (3.3.2), then we obtain the *complementary energy principle* of Atluri [15]:

$$\delta \pi_c(\boldsymbol{\omega}, \dot{\mathbf{t}}) = 0 ,$$
$$\pi_c(\boldsymbol{\omega}, \dot{\mathbf{t}}) \equiv \int_V \{-\mathscr{R}(\dot{\mathbf{t}}, \boldsymbol{\omega}) - \tfrac{1}{2}\boldsymbol{\tau} : (\boldsymbol{\omega} \cdot \boldsymbol{\omega}) + \dot{\mathbf{t}} : \boldsymbol{\omega}\} dV + \int_{S_t} \boldsymbol{n} \cdot \dot{\mathbf{t}} \cdot \bar{\boldsymbol{v}} \, dS . \tag{3.3.22}$$

$$\dot{\mathbf{t}} = \nabla \times \boldsymbol{\Phi} + \dot{\mathbf{t}}^b ,$$
$$\boldsymbol{n} \cdot \dot{\mathbf{t}} = \dot{\bar{\boldsymbol{T}}}_t \quad \text{on } S_\sigma . \tag{3.2.23}$$

Any solution of the general boundary value problem is a solution of (3.3.22) and (3.3.23). The stationary conditions are AMB (3.3.17), velocity boundary condition (3.3.18) and compatibility (3.3.19). In the stationary conditions $\boldsymbol{\varepsilon}$ appears only as a function of the stress rate and spin.

It is generally not practicable to construct stress rates satisfying the traction boundary condition (3.3.23). As we have done several times before, we introduce the Lagrange multiplier v on S_σ to 'enforce' (3.3.23). The result is a modified complementary energy principle,

$$\begin{aligned} &\delta\pi_c^*(v, \boldsymbol{\omega}, \dot{\mathbf{t}}) = 0\,, \\ &\pi_c^*(v, \boldsymbol{\omega}, \dot{\mathbf{t}}) \equiv \pi_c(\boldsymbol{\omega}, \dot{\mathbf{t}}) + \int_{S_\sigma} (n \cdot \dot{\mathbf{t}} - \dot{\bar{T}}_i) \cdot v \, dS\,, \qquad \dot{\mathbf{t}} = \nabla \times \boldsymbol{\Phi} + \dot{\mathbf{t}}^b\,. \end{aligned} \tag{3.3.24}$$

Any solution of the general boundary value problem is a solution of (3.3.24). The stationary conditions are the same as those of the 'pure' complementary energy π_c, except that the traction boundary condition follows from $\delta\pi_c^*/\delta v = 0$.

3.4. *Initial value problems*

At this point we assume that a solution of the general boundary value problem can be constructed in any assigned configuration $C(t)$ once the stress $\boldsymbol{\tau}(\boldsymbol{x}, t)$ and boundary conditions are specified. A 'solution' consists of the values of $\boldsymbol{\varepsilon}(\boldsymbol{x}, t)$, $\boldsymbol{\omega}(\boldsymbol{x}, t)$ and $\dot{\mathbf{t}}(\boldsymbol{x}, t)$ over $C(t)$ at the instant t. The velocity may be found by integration:

$$v(\boldsymbol{x}, t) = \bar{v}(\bar{\boldsymbol{x}}, t) + \int_{\bar{\boldsymbol{x}}}^{\boldsymbol{x}} [\boldsymbol{\varepsilon}(\boldsymbol{x}, t) + \boldsymbol{\omega}(\boldsymbol{x}, t)] \, d\boldsymbol{x} \tag{3.4.1}$$

where $\bar{\boldsymbol{x}}$ is a point on S_v. For the purposes of the discussion in this section, we formally indicate the dependence of v and $\dot{\mathbf{t}}$ on $\boldsymbol{x}$, $\boldsymbol{\tau}$, and the time-dependent prescribed loads by introduction of integral operators $\mathcal{F}$ and $\underline{\mathcal{G}}$ such that

$$v = \mathcal{F}\{\boldsymbol{x}, \boldsymbol{\tau}, t\}\,, \tag{3.4.2}$$

$$\dot{\mathbf{t}} = \underline{\mathcal{G}}\{\boldsymbol{x}, \boldsymbol{\tau}, t\}\,. \tag{3.4.3}$$

In principle $\mathcal{F}$ and $\underline{\mathcal{G}}$ could be found by an integral transform method [35][30], since the boundary value problem is linear.

Now consider the following transformation:

$$\begin{aligned} &\boldsymbol{x} = \boldsymbol{\chi}_\tau(\boldsymbol{X}, t)\,, \\ &\boldsymbol{\tau}(\boldsymbol{\chi}_\tau(\boldsymbol{X}, t), t) = J_\tau^{-1}(\boldsymbol{X}, t)\, \mathbf{F}_\tau(\boldsymbol{X}, t) \cdot \mathbf{t}_\tau(\boldsymbol{X}, t)\,, \\ &v(\boldsymbol{\chi}_\tau(\boldsymbol{X}, t), t) = \dot{\boldsymbol{\chi}}_\tau(\boldsymbol{X}, t)\,, \\ &\dot{\mathbf{t}}(\boldsymbol{\chi}_\tau(\boldsymbol{X}, t), t) = J_\tau^{-1}(\boldsymbol{X}, t)\, \mathbf{F}_\tau(\boldsymbol{X}, t) \cdot \dot{\mathbf{t}}_\tau(\boldsymbol{X}, t)\,. \end{aligned} \tag{3.4.4}$$

[30]Fung [24] discusses integral transforms for boundary value problems of linear elasticity.

Introduction of (3.4.4) for $\boldsymbol{x}$, τ, $\boldsymbol{v}$ and $\dot{\mathbf{t}}$ in equations (3.4.2) and (3.4.3) gives

$$\dot{\boldsymbol{\chi}}_\tau = \mathscr{F}_\tau\{\boldsymbol{\chi}_\tau, \mathbf{t}_\tau, t\}, \tag{3.4.5}$$

$$\dot{\mathbf{t}}_\tau = \underline{\mathscr{G}}_\tau\{\boldsymbol{\chi}_\tau, \mathbf{t}_\tau, t\} \tag{3.4.6}$$

where $\mathscr{F}_\tau$ and $\underline{\mathscr{G}}_\tau$ are defined by

$$\mathscr{F}_\tau\{\cdot, \cdot, t\} \equiv \mathscr{F}\{\cdot, J_\tau^{-1}\underline{\mathbf{F}}_\tau \cdot, t\}, \tag{3.4.7}$$

$$\underline{\mathscr{G}}_\tau\{\cdot, \cdot, t\} \equiv J_\tau \mathbf{F}_\tau^{-1} \cdot \underline{\mathscr{G}}\{\cdot, J_\tau^{-1}\mathbf{F}_\tau \cdot, t\}. \tag{3.4.8}$$

Equations (3.4.5) and (3.4.6), along with initial values for $\boldsymbol{\chi}_\tau$ and $\mathbf{t}_\tau$, constitute an initial value problem.

The initial value problem described above is ill-posed for two reasons. First, construction of the operators $\mathscr{F}$ and $\underline{\mathscr{G}}$ is impracticable.[31] Second, $\mathscr{F}_\tau$ and $\underline{\mathscr{G}}_\tau$ govern the evolution of functions defined continuously over $C(\tau)$; excepting cases in which $\mathscr{F}_\tau$ and $\underline{\mathscr{G}}_\tau$ are linear,[32] no analytical methods have been devised for treating such initial value problems. We shall see that neither of these problems cause any difficulty in the numerical treatment of the problem.

4. The finite element algorithm

4.1. Shape functions

Equation (3.3.8) is the basis of the finite element algorithm presented here.[33] The finite element equations are obtained by introduction of polynomial representations for $\boldsymbol{v}$, $\boldsymbol{\omega}$ and $\dot{\mathbf{t}}$ (satisfying $\boldsymbol{\omega} + \boldsymbol{\omega}^t = 0$, $\dot{\mathbf{t}} = \dot{\mathbf{t}}^0 + \dot{\mathbf{t}}^b$, $\boldsymbol{v} = \bar{\boldsymbol{v}}$ and $\delta\boldsymbol{v} = \boldsymbol{0}$ on S_v a priori) to that functional and performing the assigned integrations.[34] On the Nth element let $\boldsymbol{v}$, $\boldsymbol{\omega}$ and $\dot{\mathbf{t}}$ be represented by

$$\boldsymbol{v} = \sum_{i=1}^{NQ} \boldsymbol{N}_i q_N^i, \quad \boldsymbol{N}_i\text{: isoparametric shape functions [38]}, \tag{4.1.1}$$

$$\boldsymbol{\omega} = \sum_{i=1}^{NW} \mathbf{QW}_i \alpha_N^i \quad \text{where } \mathbf{QW}_i + \mathbf{QW}_i^t = \mathbf{0}, \tag{4.1.2}$$

$$\dot{\mathbf{t}} = \sum_{i=1}^{NT} \mathbf{QT}_i \beta_N^i + \dot{\mathbf{t}}^b \quad \text{where } \mathbf{QT}_i = \nabla \times \boldsymbol{\Phi}_i, \quad \nabla \cdot \dot{\mathbf{t}}^b = -\rho \dot{\boldsymbol{b}} \tag{4.1.3}$$

[31] Indeed, their counterparts in linear elasticity are known only for bodies of infinite extent [24].

[32] In infinitesimal strain linear viscoelasticity the boundary value/initial value problem may be solved by successive use of integral transforms.

[33] A more comprehensive exposition may be found in the author's dissertation [36].

[34] Gaussian quadrature rules are used on each element, so the finite element equations depend only on the quadrature-point values of deformation and stress; cf. [37].

where NQ is the number of velocity parameters (on the Nth element). NW is the number of spin parameters (on the Nth element) and NT is the number of stress parameters (on the Nth element). The shape functions used in the examples accompanying this paper are given in Appendix B.

4.2. *The finite element equations*

As is customary for 'hybrid stress' finite elements, the representation of the stress rate $\dot{t}$ is independent on each element, so to (3.3.8) we append the following statement of 'interelement traction reciprocity':

$$\sum_{N=1}^{\mathrm{NELM}} \left\{ \int_{S_N - (S_N \cap S_v)} (\boldsymbol{n} \cdot \dot{\mathbf{t}} \cdot \delta v) \mathrm{d}S - \int_{(S_N \cap S_\sigma)} \dot{\bar{\boldsymbol{T}}}_t \cdot \delta v \, \mathrm{d}S \right\} = 0 \tag{4.2.1}$$[35]

where NELM is the total number of elements. The finite element equations resulting from use of the representations (4.1.1) through (4.1.3) in equations (3.3.8) and (4.2.1) are

$$\{\delta\alpha\}^{\mathrm{t}} \{-[H^{11} \;\; H^{12}]\{\dot{\beta}\} + \{P^{\alpha,b}\} + \{P^{\alpha,\Sigma}\}\} = 0 \,, \tag{4.2.2}$$[36]

$$\{\delta\beta\}^{\mathrm{t}} \{-[H^{21} \;\; H^{22}]\{\dot{\beta}\} + \{P^{\beta,b}\} + \{P^{\beta,\Sigma}\} + [G]\{\dot{q}_N\}\} = 0 \,, \tag{4.2.3}$$

$$\sum_{N=1}^{\mathrm{NELM}} \{\{\delta q_N\}^{\mathrm{t}} [0 \;\; G_N^{\mathrm{t}}]\{\dot{\beta}\} - \{\delta q_N\}^{\mathrm{t}} \{F_N\}\} = 0 \,. \tag{4.2.4}$$

The individual matrices in (4.2.2) through (4.2.4) are defined below:

$$H_{ij}^{11} = \int_{V_N} \{(\boldsymbol{\tau} \cdot \mathbf{QW}_i) : \underline{\mathbf{D}} : (\boldsymbol{\tau} \cdot \mathbf{QW}_j) + \boldsymbol{\tau} : (\mathbf{QW}_i \cdot \boldsymbol{QW}_j)\} \mathrm{d}V \,, \tag{4.2.5}$$

$$H_{ij}^{12} = \int_{V_N} \{(\boldsymbol{\tau} \cdot \mathbf{QW}_i) : \underline{\mathbf{D}} : (\mathbf{QT}_j) - \mathbf{QW}_i : \mathbf{QT}_j\} \mathrm{d}V \,, \tag{4.2.6}$$

$$H_{ij}^{21} = \int_{V_n} \{(\mathbf{QT}_i) : \underline{\mathbf{D}} : (\boldsymbol{\tau} \cdot \mathbf{QW}_j) - \mathbf{QT}_i : \mathbf{QW}_j\} \mathrm{d}V \,, \tag{4.2.7}$$

$$H_{ij}^{22} = \int_{V_N} \{(\mathbf{QT}_i) : \underline{\mathbf{D}} : (\mathbf{QT}_j)\} \mathrm{d}V \,, \tag{4.2.8}$$

$$G_{ij} = \int_{S_N} \boldsymbol{n} \cdot (\mathbf{QT}_i) \cdot (\boldsymbol{N}_j) \mathrm{d}S \,, \tag{4.2.9}$$

$$F_i = \int_{(S_N \cap S_\sigma)} \dot{\bar{\boldsymbol{T}}}_t \cdot (\boldsymbol{N}_i) \, \mathrm{d}S \,, \tag{4.2.10}$$

[35] This equation includes the traction boundary condition.

[36] The element index 'N' has been suppressed on the stress rate and spin parameters.

$$P_i^{\alpha,b} = \int_{V_N} \left\{ (\mathbf{QW}_i) : \left[\dot{\mathbf{t}}^b + (\underline{\mathbf{D}} : \dot{\mathbf{t}}^b) \cdot \boldsymbol{\tau} + \frac{1}{h} \boldsymbol{\tau} \right] \right\} \mathrm{d}V, \tag{4.2.11}$$[37]

$$P_i^{\beta,b} = \int_{V_N} \{ (\mathbf{QT}_i) : (-\underline{\mathbf{D}} : \dot{\mathbf{t}}^b) \} \mathrm{d}V, \tag{4.2.12}$$

$$P_i^{\alpha,\Sigma} = \int_{V_N} \{ (\boldsymbol{\tau} \cdot \mathbf{QW}_i) : \underline{\mathbf{D}} : \boldsymbol{\Sigma} \} \mathrm{d}V, \tag{4.2.13}$$

$$P_i^{\beta,\Sigma} = \int_{V_N} \{ (\mathbf{QT}_i) : \underline{\mathbf{D}} : \boldsymbol{\Sigma} \} \mathrm{d}V. \tag{4.2.14}$$

The tensor $\underline{\mathbf{D}}$ is obtained from $\underline{\mathbf{W}}^{-1}$ by symmetrization

$$D_{ijkl} = \tfrac{1}{4}(W^{-1}_{ijkl} + W^{-1}_{jikl} + W^{-1}_{ijlk} + W^{-1}_{jilk}).$$

and serves to reduce by a factor of four the number of multiplications required to compute the H matrices.

After simultaneous solution of (4.2.2) and (4.2.3), i.e. finding $[H^{-1}G \mid H^{-1}P]$ such that

$$[H]\left[H^{-1}G \middle| H^{-1}P \right] = \left[\begin{matrix} 0 \\ G \end{matrix} \middle| P \right] \tag{4.2.15}$$

where

$$[H] \equiv \begin{bmatrix} H^{11} & H^{12} \\ H^{21} & H^{22} \end{bmatrix}, \qquad [P] \equiv \begin{bmatrix} P^{\alpha,b} + P^{\alpha,\Sigma} \\ P^{\beta,b} + P^{\beta,\Sigma} \end{bmatrix},$$

we may eliminate the stress rate and spin parameters from (4.2.4) to get

$$\sum_{N=1}^{\mathrm{NELM}} \{q_N\}^{\mathrm{t}} \{ [k_N]\{q_N\} + [0 \;\; G_N^{\mathrm{t}}]\{H^{-1}P_N\} - \{F_N\} \} = 0. \tag{4.2.16}$$

Here we have identified the element stiffness matrix $[k_N]$

$$[k_N] \equiv [0 \;\; G_N^{\mathrm{t}}][H^{-1}G_N]. \tag{4.2.17}$$

Now we introduce the global nodal velocity vector

$$\{\mathcal{Q}\}, \qquad \mathcal{Q}_I = \bar{\mathcal{Q}}_I \quad \text{and} \quad \delta\mathcal{Q}_I = 0 \text{ on } S_v,$$

and the 'assembly matrices' $[A_N]$. The $\{q_N\}$ and $\{\delta q_N\}$ are now expressible as

$$\{q_N\} = [A_N]\{\mathcal{Q}\}, \qquad \{\delta q_N\} = [A_N]\{\delta\mathcal{Q}\}.$$

[37]The last term in the integrand provides a residual for any imbalance of angular momentum [36]; h is the time step size.

Elimination of $\{q_N\}$ and $\{\delta q_N\}$ from (4.2.16) gives

$$\{\delta\mathcal{Q}\}^{\mathrm{t}}\{[\mathcal{K}]\{\mathcal{Q}\}+\{\mathcal{P}\}-\{\mathcal{F}\}\}=0\,, \tag{4.2.18}$$

in which the global stiffness $[\mathcal{K}]$, and global load vectors $\{\mathcal{P}\}$ and $\{\mathcal{F}\}$ are defined by

$$[\mathcal{K}]\equiv\sum_{N=1}^{\mathrm{NELM}}[A_N]^{\mathrm{t}}[k_N][A_N]\,,$$

$$\{\mathcal{P}\}\equiv\sum_{N=1}^{\mathrm{NELM}}[A_N]^{\mathrm{t}}[0\;\;G_N^{\mathrm{t}}]\{H^{-1}P_N\}\,,\qquad \{\mathcal{F}\}\equiv\sum_{N=1}^{\mathrm{NELM}}[A_N]^{\mathrm{t}}\{F_N\}\,.$$

The equation (4.2.18) can be solved by standard methods [39]. We note that (4.2.18) involves only the nodal velocities as unknowns. By a process of backsubstitution we may finally recover $\boldsymbol{v}(\boldsymbol{x},t)$, $\boldsymbol{\omega}(\boldsymbol{x},t)$ and $\dot{\boldsymbol{t}}(\boldsymbol{x},t)$ [36].

4.3. Numerical stability criteria

In our presentation of the finite element equations it was tacitly assumed that the following conditions held:

$\underset{\sim}{\mathbf{W}}$ nonsingular at each quadrature point, (4.3.1)

$[H_N]$ singular on each element, (4.3.2)

$[G_N]\{q_N\}\neq\{0\}$ except for rigid translations. (4.3.3)

$\{\delta\mathcal{Q}\}[\mathcal{K}]\{\mathcal{Q}\}\neq\{0\}$ for any $\{\mathcal{Q}\}$ satisfying the velocity boundary conditon. (4.3.4)

The first of these is satisfied by models for solids found in the engineering literature. If the last is not satisfied for some $\{\bar{\mathcal{Q}}\}$, then typically the solution of the initial value problem is at a physically significant bifurcation point. Satisfaction of the second and third conditions depends principally upon the functions $\boldsymbol{N}_i$, $\mathbf{QW}_i$, and $\mathbf{QT}_i$ used in forming the matrices $[H_N]$ and $[G_N]$. In this section we discuss conditions whose fulfillment is necessary for satisfaction of (4.3.2) and (4.3.3); these conditions we call 'numerical stability criteria'.

An analogue to the condition (4.3.3) arises in the hybrid-stress finite element algorithm of linear elastostatics. The analysis of Tong and Pian [40], with a minor modification, applies in the present case. The rank of the matrix $[G]$ is usually

$$\min(\mathrm{NT},\mathrm{NQ}-T)$$

where NT is the number of stress rate parameters, NQ the number of boundary velocity parameters, and T the number of *translational* degrees of freedom of an element. It is well known that if $\mathrm{NT}<\mathrm{NQ}-T$, then 'kinematic modes' (deformations to which the element offers no resistance) will occur. The 'rank' condition which is necessary for the satisfaction of (4.3.3) is

$$NT \geq NQ - T.$$

In the examples accompanying this work, the number of stress rate parameters always equalled or exceeded the number of boundary velocity parameters, and no kinematic mode was encountered.

A second type of kinematic mode is possible in any complementary work or energy based finite element algorithm. If a velocity shape function N_j vanishes everywhere on an element's boundary,[38] then it is easy to see that the jth column of G_{ij} (defined in (4.2.9)) vanishes identically. In practice one must therefore use boundary-noded elements only.[39]

The condition (4.3.2) turns out to be the most troublesome. Even when $[H]$ is not singular, it may be so ill-conditioned that an accurate solution of the matrix equation (4.2.15) can only be found by scaling, that is, adjusting the magnitude of the stress and spin functions to improve the condition of $[H]$. In any case, the problem may be overcome by replacing $\mathbf{QW}_i$ and $\mathbf{QT}_i$ in a trial and error process until nonsingular $[H]$ is found.

After a number of trials, it became apparent that when $[H]$ was singular, the spurious eigenmode consisted of a pure (but inhomogeneous) spin. Moreover, if a combination of functions [QW] and [QT] was found to be acceptable in the stress-free state, it remained so as the deformation progressed. Setting the initial stress to zero, the criterion sufficient for no spin mode to occur follows as

$$[H_0^{21}]\{\delta\alpha\} \neq 0, \quad [H_0^{21}]_{ij} \equiv \int_{V_N} (\mathbf{QT}_i : \mathbf{QW}_j) \mathrm{d}V. \tag{4.3.5}$$

A similar criterion (for a finite element model of an elastic membrane) was given by de Veubeke and Millard [6], but their conclusions differ from our own. A necessary condition for the satisfaction of (4.3.5) is that

$$NT^* \geq NW$$

where NT^* is the number of skew-symmetric tensors $(\mathbf{QT}_i - \mathbf{QT}_i^{\mathrm{t}})$ that are linearly independent, and NW is the number of spin functions $\mathbf{QW}_i$.[40]

De Veubeke and Millard suggest that the polynomial degree of the spin field (m) be related to the polynomial degree of the stress field (n) as $m = n - 1$ ($NT^* > NW$), calling the case $m = n$ ($NT^* = NW$) the 'classical equilibrium model'. However, experience with the present finite element algorithm indicates that if m is less than n, then the angular momentum balance is not satisfied with reasonable (pointwise) accuracy. The degree of the spin field and the degree of the stress rate field were always the same in the examples accompanying this work.

5. Numerical treatment of the initial value problem

5.1. *Definition of the initial value problem*

The finite element algorithm described in the previous section produces an approximation

[38] Examples include shape functions for interior nodes, and 'bubble functions'.

[39] A more general examination of this problem is given in the author's dissertation [36].

[40] It has been tacitly assumed that all of the $\mathbf{QW}_i$ (and $\mathbf{QT}_i$ and N_i) are linearly independent.

for the stress rate $\dot{\mathbf{t}}$ and spin $\boldsymbol{\omega}$ on the interior of each element, and the velocity $\boldsymbol{v}$ on the boundary of each element. The algorithm does not define the velocity on the interior of an element.[41] We have chosen to assign the velocity on the interior of each element simply by interpolation of that element's boundary velocity, and in doing so we effectively discard $(\boldsymbol{\varepsilon}(\dot{\mathbf{t}}, \boldsymbol{\omega}) - \boldsymbol{\omega})$.[42]

Now let us write $\{\boldsymbol{x}\} = \{\boldsymbol{x}^1, \boldsymbol{x}^2, \ldots, \boldsymbol{x}^{ND}\}$ for the vector of *nodal positions*, and $\{\boldsymbol{v}\} = \{\boldsymbol{v}^1, \boldsymbol{v}^2, \ldots, \boldsymbol{v}^{ND}\}$ for the vector of *nodal velocities*, ND being the total number of nodes. Similarly, we write $\{\boldsymbol{\tau}\} = \{\boldsymbol{\tau}^1, \boldsymbol{\tau}^2, \ldots, \boldsymbol{\tau}^G\}$ for the *quadrature point stresses* and $\{\dot{\mathbf{t}}\}$ for the *quadrature point stress rates*, G being the total number of quadrature points in the body. We indicate the dependence of $\{\boldsymbol{v}\}$ and $\{\dot{\mathbf{t}}\}$ on $\{\boldsymbol{x}\}$, $\{\boldsymbol{\tau}\}$, and the time dependent boundary conditions by introduction of functions $\mathcal{f}$ and $\mathcal{g}$ such that

$$\{\boldsymbol{v}\} = \mathcal{f}[\{\boldsymbol{x}\}, \{\boldsymbol{\tau}\}, t], \tag{5.1.1}$$

$$\{\dot{\mathbf{t}}\} = \mathcal{g}[\{\boldsymbol{x}\}, \{\boldsymbol{\tau}\}, t]. \tag{5.1.2}$$

The reader should note that the *integral operators* $\mathcal{F}$ and $\mathcal{G}$ (see (3.4.2) and (3.4.3)) are replaceable by *functions* $\mathcal{f}$ and $\mathcal{g}$ because the finite element equations depend *exclusively* upon the *quadrature point values* of $\boldsymbol{x}$ and $\boldsymbol{\tau}$. Performing the transformation (3.4.4), we finally obtain

$$\{\dot{\boldsymbol{\chi}}_\tau\} = \mathcal{f}_\tau[\{\boldsymbol{\chi}_\tau\}, \{\mathbf{t}_\tau\}, t], \tag{5.1.3}$$

$$\{\dot{\mathbf{t}}_\tau\} = \mathcal{g}_\tau[\{\boldsymbol{\chi}_\tau\}, \{\mathbf{t}_\tau\}, t]. \tag{5.1.4}$$

The functions $\mathcal{f}_\tau$ and $\mathcal{g}_\tau$ govern the evolution of *discrete* values of $\boldsymbol{\chi}_\tau$ and $\mathbf{t}_\tau$, so (5.1.3), (5.1.4) and appropriate initial values of $\{\boldsymbol{\chi}_\tau\}$ and $\{\mathbf{t}_\tau\}$, represent an initial value problem of *ordinary differential equations*.

A great number of 'time-stepping' schemes are presently available for the numerical treatment of such problems.[43] In principle, any scheme in the literature may be used. In practice, three factors, aside from stability, affect the choice of scheme.

(1) *Storage requirements* for implementation of integration schemes can vary appreciably.

(2) *Execution time* depends principally upon the number of evaluations of $\mathcal{f}_\tau$ and $\mathcal{g}_\tau$; the finite element equations must be formed and solved for each evaluation, as in a tangent stiffness formulation.

(3) The functions $\mathcal{f}_\tau$ and $\mathcal{g}_\tau$ will generally be *discontinuous* when the solution lies on a yield surface.

A comparison of five methods by Gear [42, pp. 233–235] indicates that when the number of function evaluations must be kept very small, the classical fourth-order Runge–Kutta method gives lower errors than (implicit and explicit) multistep methods. Single step methods generally

[41] Equation (3.4.1) is of no use since the finite element approximation for $[\boldsymbol{\varepsilon}(\dot{\mathbf{t}}, \boldsymbol{\omega}) - \boldsymbol{\omega}]$ is not compatible.

[42] Outwardly, the very arbitrariness of this procedure would appear to invalidate it; to any velocity field found by interpolation of the element's boundary velocity one could add another velocity field which vanished on the element's boundary. However, one must ask whether or not the addition of such a field would improve the 'order of accuracy' of the velocity representation (cf. [41, p. 169]; when it would not, the procedure of boundary velocity interpolation is apparently sound.

[43] An up-to-date exposition has been given by Gear [42].

have smaller storage requirements, and since smoothing over several time steps is not 'built in' (as it is with multi-step methods), they can be expected to perform more favorably when the solution crosses a yield surface. Finally, in contrast to multistep schemes, single step schemes are easily started and the time step may be easily changed. In the examples accompanying this work the Euler, and second- and fourth-order explicit Runge–Kutta schemes (denoted RK2 and RK4, respectively) were used, cf. [43, Section 6.5]. The accuracy of a result was gauged by step-doubling [42, p. 81], or by comparison to the result found by application of a higher order scheme.

It is crucially important that the time stepping scheme not introduce errors which tend to unbalance the total stress $\mathbf{t}_\tau$ (or τ). This is because the numerical scheme is centered about the (generalized) compatibility equation, not the linear momentum balance equation, so there is no way to form a linear momentum residual to check for or correct an unbalanced stress. This maintenance of balanced stress, necessary in stress-based finite element algorithms, is the counterpart of maintenance of compatible deformation, necessary in velocity-based algorithms. It can be shown [36] that LMB is maintained when the stress $\mathbf{t}_\tau$ is integrated explicitly, but not when other stresses (such as τ) are integrated explicitly. Thus we integrate $\mathbf{t}_\tau$ (and χ_τ), and find τ (afterwards) by the formula

$$\tau = 1/J_\tau \mathbf{F}_\tau \cdot \mathbf{t}_\tau .$$

5.2. Stability of numerical solutions of the initial value problem

It can happen that a small change in the initial condition or time step size leads to a very large change in the numerical approximation to a mathematically stable solution of the initial value problem. Problems involving materials with a relaxation time (or spectrum of relaxation times) are the most susceptible to such *numerical instabilities*, so our attention in this section is focused on them.

Cormeau [37] has shown that Euler's method, when applied to finite element-initial value problems of infinitesimal strain quasistatic elasto/viscoplasticity [44], yields a stable numerical solution only if the time step is within a certain bound. Argyris et al. [19] have noted that Cormeau's bound is the same as the bound necessary for stable integration of the stress if in the rate-type constitutive equation one prescribes the deformation. It seems plausible that a correspondence of time step bounds would also exist between the present finite element-initial value problem and the constitutive equation (2.3.1). Since a direct analysis of the present finite element initial value problem does not appear feasible, we give instead an analysis of the initial value problem

$$\dot{\boldsymbol{\sigma}}^* = \underline{\mathbf{V}} : \boldsymbol{\varepsilon} + \boldsymbol{\Sigma} , \qquad \tau(0) = \tau_0 , \tag{5.2.1}$$[44]

in which $\boldsymbol{\varepsilon}$ is prescribed, and $\underline{\mathbf{V}}$ and $\boldsymbol{\Sigma}$ depend upon τ. We assume that any time step bound thus obtained applies equally well to the finite element-initial value problem. This assumption is borne out by experience.

After application of Euler's method to (5.2.1) to generate two sequences of stresses, $\{\tau_N\}$

[44]It is clear that a time step bound must be invariant with respect to any 'change of variables' of the type described in Section 2.3.

and $\{\boldsymbol{\tau}_N + \Delta\boldsymbol{\tau}_N\}$, $\Delta\boldsymbol{\tau}_0 \neq \mathbf{0}$, we find that their difference $\{\Delta\boldsymbol{\tau}_N\} = \{\boldsymbol{\tau}_N + \Delta\boldsymbol{\tau}_N\} - \{\boldsymbol{\tau}_N\}$ satisfies

$$\|\Delta\boldsymbol{\tau}_{N+1}\| \leq |\rho\{(1 - h\dot{J})\,\underline{\mathbf{I}} + h\partial_\tau(\underline{\mathbf{V}} : \boldsymbol{\varepsilon} + \boldsymbol{\Sigma})|_{\tau=\tau_N}\}| \cdot \|\Delta\boldsymbol{\tau}_N\| . \tag{5.2.2}$$[45]

Here $\rho\{\underline{\mathbf{A}}\}$ signifies the maximum eigenvalue of a fourth-order tensor $\underline{\mathbf{A}}$. The sequence (numerical solution) $\{\boldsymbol{\tau}_N\}$ is stable with respect to perturbations of the initial condition if

$$\|\Delta\boldsymbol{\tau}_{N+1}\| \leq \|\Delta\boldsymbol{\tau}_N\| \tag{5.2.3}$$

[42, pp. 16–18], hence the time step h must be chosen so that

$$|(1 - h\dot{J}) + h\rho\{\partial_\tau(\underline{\mathbf{V}} : \boldsymbol{\varepsilon} + \boldsymbol{\Sigma})|_{\tau=\tau_N}\}| \leq 1 . \tag{5.2.4}$$

In pure relaxation ($\boldsymbol{\varepsilon} = \mathbf{0}$ and $\dot{J} = 0$), or when $\underline{\mathbf{V}}$ is independent of τ and $\dot{J} = 0$, (5.2.4) reduces to Cormeau's result. In most problems of technological interest, the deformation is an unknown, as opposed to prescribed; equation (5.2.4) is inapplicable, so no *least* bound is found.[46] However, satisfaction of the 'pure relaxation' bound is still *necessary* for general stability. Regarding those bounds, Hughes and Taylor [20] have commented:

> "For slowly varying loads, or when equilibrium response is of prime interest, stability requires that time steps be selected which are much smaller than those necessary for accuracy."

Argyris et al. [19] remarked that the time step bound

> "physically infers ... that the inelastic strain increment ... remains smaller than the elastic strain".[47]

Since in metals the elastic strain is always infinitesimal, this implies that an intolerably large number of steps would be required for a finite strain analysis.

As a means of avoiding the stringent time step bounds associated with the use of the Euler method, several generalizations of the trapezoid (or midpoint) rule have been devised [49, 19, 46, 50, 20]. A clear survey of these methods, including discussions of stability and convergence requirements, has been given by Argyris et al. [46].[48] The simplest of these they have called "the forward gradient scheme", and "the linear finite approximation scheme".

[45] Our analysis has been simplified by choosing a 'corotational frame'; see [45, art. 147–148], and by assuming $\underline{\mathbf{V}}$ and $\boldsymbol{\Sigma}$ to be differentiable w.r.t. τ.

[46] Argyris, Doltsinis and Willam [46] claim that in the case of pure relaxation "we obtain the most critical statements for stability."

[47] For a material with a spectrum of relaxation times T_i, the time step bound becomes $h \leq 2T_{\min}$, or $\frac{1}{2} < N^*_{DE}$, where $N^*_{DE} \equiv T_{\min}/h$ amounts to a numerical counterpart to the "Deborah number" [47] (whose precise definition is debated in the rheology literature [48]). The response to a stretching increment is predominantly elastic when $N^*_{DE} > 1$, fluid when $(T_{\max}/h) < 1$.

[48] In an earlier paper, Argyris et al. [19] derived a time step bound which assured $\|\boldsymbol{\tau}_{N+1}\| \leq \|\boldsymbol{\tau}_N\|$ in pure relaxation (see equations (3.22), (3.26) and (3.27) therein). The relevance of this bound to numerical stability is not clear: in fact, if in their equation (3.22) we replace $\frac{1}{2}\Delta t$ by $\zeta\Delta t$, then the critical time step obtained in the limit as $\zeta \to 0$ does not agree with Cormeau's.

In the forward gradient scheme we replace the relaxation term $\boldsymbol{\Sigma}$ in the constitutive equation (2.3.1) by $\boldsymbol{\Sigma} + \theta h(\partial_\tau \boldsymbol{\Sigma}) : \dot{\boldsymbol{\sigma}}^*$,[49] to obtain

$$\dot{\boldsymbol{\sigma}}^* = [\mathbf{I} - \theta h \partial_\tau \boldsymbol{\Sigma}]^{-1} : (\underline{\mathbf{V}} : \boldsymbol{\varepsilon} + \boldsymbol{\Sigma}) \tag{5.2.5}$$

($\boldsymbol{\Sigma}$ and $\partial_\tau \boldsymbol{\Sigma}$ are evaluated at τ_N), or simply

$$\dot{\boldsymbol{\sigma}}^* = \underline{\mathbf{V}}_\theta : \boldsymbol{\varepsilon} + \boldsymbol{\Sigma}_\theta , \tag{5.2.6}$$

in which the definitions of $\underline{\mathbf{V}}_\theta$ and $\boldsymbol{\Sigma}_\theta$ are apparent. Since (5.2.6) is of the same form as the original constitutive equation (3.2.1), we find the stability criterion simply by replacing $\underline{\mathbf{V}}$ and $\boldsymbol{\Sigma}$ with $\underline{\mathbf{V}}_\theta$ and $\boldsymbol{\Sigma}_\theta$ in (5.2.4). In pure relaxation we obtain:

$$|1 + h\rho\{\partial_\tau \boldsymbol{\Sigma}_\theta\}| \leqslant 1 . \tag{5.2.7}$$

In the special case that $\boldsymbol{\Sigma} = -(1/T)\boldsymbol{\tau}'$, T being a constant time of relaxation, $\partial_\tau \boldsymbol{\Sigma} = -(1/T)(\underline{\mathbf{I}} - \frac{1}{3}\mathbf{II})$. From (5.2.7) we get the following time step restriction

$$\left| \frac{1 - (1-\theta)(h/T)}{1 + \theta(h/T)} \right| \leqslant 1 , \tag{5.2.8}$$

so, in this special case, unconditional stability is obtained for $\theta \geqslant \frac{1}{2}$. For $\theta = 0$ we recover Cormeau's bound. To use the forward gradient scheme we derive $\underline{\mathbf{W}}_\theta$ from $\underline{\mathbf{V}}_\theta$ just as we derived $\underline{\mathbf{W}}$ from $\underline{\mathbf{V}}$ (see 2.3.5):

$$\underline{\mathbf{W}}_\theta = \underline{\mathbf{V}}_\theta - \underline{\mathbf{T}} , \quad T_{ijkl} = \tfrac{1}{2}(\tau_{ik}\delta_{lj} + \delta_{ik}\tau_{lj}) . \tag{5.2.9}$$

When a material which exhibits relaxation is to be analyzed, $\underline{\mathbf{W}}_\theta$ and $\boldsymbol{\Sigma}_\theta$ are used in place of $\underline{\mathbf{W}}$ and $\boldsymbol{\Sigma}$ in forming the finite element equations. One effect of the forward gradient scheme is to lengthen all of the characteristic times so that the time step exceeds the least of them by no more than a factor of $(1/\theta)$. In the special case above, T is effectively replaced by $(T + \theta h)$, so for $\theta \geqslant \frac{1}{2}$, $h/(T + \theta h) \leqslant 1/\theta \leqslant 2$.[50]

Two linear finite approximation schemes have been proposed in the literature [20, 19]. In practice both are very similar to the forward gradient scheme, above, differing mainly because of their implicitness. To facilitate their discussion, we introduce the 'plastic stretching' $\boldsymbol{\varepsilon}^p = -\underline{\mathbf{V}}^{-1} : \boldsymbol{\Sigma}$, and the intermediate stress $\boldsymbol{\tau}_\theta$, defined by

$$\boldsymbol{\tau}_\theta \equiv (1-\theta)\boldsymbol{\tau}_N + \theta\boldsymbol{\tau}_{N+1} , \quad 0 \leqslant \theta \leqslant 1 . \tag{5.2.10}$$

We assume that a function $\underline{\mathbf{g}}(\boldsymbol{\tau})$ may be defined such that $\boldsymbol{\varepsilon}^p = \underline{\mathbf{g}} : \boldsymbol{\tau}$, and we write $\underline{\mathbf{G}}$ for $\partial_\tau \boldsymbol{\varepsilon}^p$; finally, $\mathbf{g}_\theta = \mathbf{g}(\boldsymbol{\tau}_\theta)$, and $\underline{\mathbf{G}}_\theta = \underline{\mathbf{G}}(\boldsymbol{\tau}_\theta)$.

[49] A truncated series for $\boldsymbol{\Sigma}$ about $\boldsymbol{\Sigma}(\tau_N)$, in a *corotational* frame, is $\boldsymbol{\Sigma}(\tau_N) + \theta h(\partial_\tau \boldsymbol{\Sigma}) : \dot{\boldsymbol{\tau}}$; using $\dot{\boldsymbol{\sigma}}$ for $\dot{\boldsymbol{\tau}}$ is a further approximation.

[50] Recall Cormeau's bound, $h/T_{\min} \leqslant 2$.

Hughes and Taylor [20] replace $\underline{\mathbf{V}}$ by

$$\underline{\mathbf{V}}'_\theta \equiv [\underline{\mathbf{V}}^{-1} + \theta h \underline{\mathbf{G}}_\theta]^{-1} = [\underline{\mathbf{I}} + \theta h \underline{\mathbf{V}} : \underline{\mathbf{G}}_\theta]^{-1} : \underline{\mathbf{V}}, \tag{5.2.11}$$

and $\boldsymbol{\varepsilon}^p(\tau_N)$ by $\boldsymbol{\varepsilon}^p(\tau_\theta)$ in the finite element equations. The forward gradient scheme is used as a 'predictor', and the Hughes' and Taylors' scheme for a 'corrector'.

Argyris et al. [19] replace $\underline{\mathbf{V}}$ by

$$\underline{\mathbf{V}}''_\theta \equiv [\underline{\mathbf{I}} + \theta h \underline{\mathbf{V}} : \underline{\mathbf{g}}_\theta]^{-1} : \underline{\mathbf{V}} \tag{5.2.12}$$

and $\boldsymbol{\varepsilon}^p(\tau_N)$ by $\underline{\mathbf{g}}_\theta : \boldsymbol{\tau}_N$ in the finite element equations. They do not say how the resulting 'corrector' equation should be started, by a 'guess' (such as $\tau_{N+1} = \tau_N$), by the forward gradient scheme, or by the simple 'initial load' scheme ($\theta = 0$).

We conclude this section by pointing out that for the constitutive equation (2.3.1) with constant $\underline{\mathbf{V}}$ and $\boldsymbol{\Sigma} = -(1/T)\boldsymbol{\tau}'$ (T being a constant relaxation time), the matrices $\underline{\mathbf{G}}$ and $\underline{\mathbf{g}}$ are *constant* and *equal to each other*. As a consequence, the scheme of Argyris et al. reduces *identically* to the forward gradient scheme. The scheme of Hughes and Taylor differs from the forward gradient scheme only in that the 'initial load' depends on τ_θ instead of τ_N. This circumstance is exploited in the sample problems accompanying this paper; when the forward gradient scheme is used to stabilize time integration, *the results characterize the performance of all three integration schemes.*

5.3. Numerical integration and objectivity

In order to be called *objective* a numerical approximation for a physical entity must transform between frames according to the same rule as the entity itself. An algorithm which produces an objective approximation will itself be called objective.

Recently, Hughes and Winget [51] proposed an algorithm whose use, they argued, ensured 'objective' numerical integration of rate-type constitutive equations. Key et al. [52] implemented midstep constitutive evaluation in the algorithm (in two dimensions), at the price of using trigonometric formulas to find the square root of the incremental rotation. Finally, Rubinstein and Atluri [53] gave a representation for the incremental rotation as a function of time, thereby making the evaluation of any root of the rotation increment trivial.[51] The algorithm of Hughes and Winget, and its modifications, all embrace as basic the notion that 'proper invariance', or 'objectivity', of stress increments is achieved by "taking rigid body rotations of a material point relative to the spatial coordinates ... into account" [52].

Our approach to this subject is slightly different from that of previous workers in that numerical objectivity is treated without reference to any constitutive equation. As noted by previous workers, the source of inobjectivity is not the constitutive equation, but the inexactness of the numerical integration scheme. The entanglement of integration schemes and constitutive equations, which characterizes the earlier work, is not only unnecessary, but could very well lead to confusion between general objectivity of physical entities and the

[51] It was recently learned that this representation was also given by Schwerdtfeger [54, p. 238].

Principle of Objectivity of Material Properties.[52] Here we focus on integration schemes which produce 'objective approximations' for physical entities.

Consider the motion of an isolated particle relative to some frame in which we describe its position and velocity by $\boldsymbol{x}'(t)$ and $\dot{\boldsymbol{x}}'(t)$, respectively. For the sake of illustration, let us say that the velocity $\dot{\boldsymbol{x}}'$ is known precisely at each moment of time, and we wish to find the position $\boldsymbol{x}'$ as a function of time. For this purpose we apply Euler's rule, and in the time step from t_N to t_{N+1} we get:

$$\boldsymbol{x}'_{N+1} = \boldsymbol{x}'_N + h\dot{\boldsymbol{x}}'_N \,. \tag{5.3.1}$$

Now a second observer, in a frame whose origin coincides with that of our own, describes the position and velocity of that same particle by $\boldsymbol{x}''(t)$ and $\dot{\boldsymbol{x}}''(t)$. He applies Euler's rule to find the position of the particle, and in the time step from t_N to t_{N+1} he gets:

$$\boldsymbol{x}''_{N+1} = \boldsymbol{x}''_N + h\dot{\boldsymbol{x}}''_N \,. \tag{5.3.2}$$

Between the two frames $\boldsymbol{x}'(t)$ and $\boldsymbol{x}''(t)$ are related by a rotation $\mathbf{Q}(t)$ as

$$\boldsymbol{x}''(t) = \mathbf{Q}(t)\cdot\boldsymbol{x}'(t) \tag{5.3.3}$$

and the velocities as

$$\dot{\boldsymbol{x}}''(t) = \dot{\mathbf{Q}}(t)\cdot\boldsymbol{x}'(t) + \mathbf{Q}(t)\cdot\dot{\boldsymbol{x}}'(t) \,. \tag{5.3.4}$$

If we assume that $\boldsymbol{x}''_N = \mathbf{Q}(t_N)\cdot\boldsymbol{x}'_N$, then, at time t_{N+1}, $\boldsymbol{x}'_{N+1}$ and $\boldsymbol{x}''_{N+1}$ are related as

$$\begin{aligned}\boldsymbol{x}''_{N+1} - \mathbf{Q}(t_{N+1})\cdot\boldsymbol{x}'_{N+1} &= \mathbf{Q}(t_N)\cdot\boldsymbol{x}'_N + h[\dot{\mathbf{Q}}(t_N)\cdot\boldsymbol{x}'_N + \mathbf{Q}(t_N)\cdot\dot{\boldsymbol{x}}'_N] - \mathbf{Q}(t_{N+1})\cdot[\boldsymbol{x}'_N + h\dot{\boldsymbol{x}}'_N] \\ &= [\mathbf{Q}(t_N) + h\dot{\mathbf{Q}}(t_N) - \mathbf{Q}(t_{N+1})]\cdot\boldsymbol{x}'_N + h[\mathbf{Q}(t_N) - \mathbf{Q}(t_{N+1})]\cdot\dot{\boldsymbol{x}}'_N \,.\end{aligned} \tag{5.3.5}$$

Since the right-hand side of (5.3.5) does not vanish identically, $\boldsymbol{x}'_K$ and $\boldsymbol{x}''_K$ do not obey (5.3.3) at times t_K later than t_N, and therefore a result found by application of Euler's rule is *frame dependent*.[53]

At this point we pause to consider the result above, to clarify our objection to it. It is clearly futile to call upon the Principle of Objectivity of Material Properties, for no material property is involved. Our singular objection to the result above is that it is *inobjective*. Hughes and Winget seem to have been first to point this out.

We now ask whether or not Euler's rule can be modified, or restricted in its application, in

[52]Hughes and Liu [55, Introduction], state that the incremental objectivity of their algorithm "is in keeping with the 'objectivity' of well-set finite-deformation constitutive equations".

[53]It *is* worthy of note that the result is objective with respect to all frame changes of the type $\mathbf{Q}'(t)\cdot\dot{\mathbf{Q}}(t) = \mathbf{0}$. Had we not chosen a common origin for the two frames, the result would have been objective only for frame changes of the type $\boldsymbol{x}'' = (\boldsymbol{x}''_0 + \dot{\boldsymbol{x}}''_0 t) + \mathbf{Q}\cdot\boldsymbol{x}'$, $\boldsymbol{x}''_0$, $\dot{\boldsymbol{x}}''_0$ and $\mathbf{Q}$ being constant.

such a way that frame dependent results will be avoided. This may be done by specifying that Euler's method may only be applied in 'special' frames. We might, for example, choose to apply Euler's rule only in those frames whose angular velocity relative to an inertial frame vanishes.[54] Between all such frames $\mathbf{Q}^{\mathrm{t}}(t)\cdot\dot{\mathbf{Q}}(t)=\mathbf{0}$, and it follows immediately that results will be frame independent. In a frame of zero absolute angular velocity, $\boldsymbol{w}=\boldsymbol{0}$, Euler's rule gives us

$$\boldsymbol{x}_{N+1}=\boldsymbol{x}_N+h\dot{\boldsymbol{x}}_N\,. \tag{5.3.6}$$

Now we transform this equation, term by term, to a general frame (distinguishing entities in the general frame by primes)[55]:

$$\boldsymbol{x}_{N+1}=\mathbf{Q}(t_{N+1})\cdot\boldsymbol{x}'_{N+1}\,,\qquad \boldsymbol{x}_N=\boldsymbol{x}'_N\,,$$

$$\dot{\boldsymbol{x}}_N=\dot{\mathbf{Q}}(t_N)\cdot\boldsymbol{x}'_N+\dot{\boldsymbol{x}}'_N,$$

hence

$$\boldsymbol{x}'_{N+1}=\mathbf{Q}^{\mathrm{t}}(t_{N+1})\cdot[\boldsymbol{x}'_N+h\hat{\boldsymbol{x}}'_N]\,,\qquad \hat{\boldsymbol{x}}'=\dot{\boldsymbol{x}}'+\boldsymbol{w}'\times\boldsymbol{x}'\,. \tag{5.3.7}$$

The vector $\boldsymbol{w}'$ is the absolute angular velocity of the general frame. The orthogonal tensor $\mathbf{Q}(t_{N+1})$ is the 'incremental rotation' that occurred between the defining frame ($\boldsymbol{w}=\boldsymbol{0}$) and the general frame ($\boldsymbol{w}'\neq\boldsymbol{0}$) during the time interval (t_N, t_{N+1}). The incremental rotation is found by solving the initial value problem

$$\dot{\mathbf{Q}}(t)=-\mathbf{Q}(t)\cdot\mathbf{W}''(t)\,,\qquad \mathbf{Q}(t_N)=\mathbf{I}\,, \tag{5.3.8}$$

$\mathbf{W}''(t)$ being the skew-symmetric tensor whose dual vector is the angular velocity.[56] A similar formula (to 5.3.7) is found for the generalized trapezoid rule:

$$\boldsymbol{x}_{N+1}=\boldsymbol{x}_N+h[(1-\theta)\,\dot{\boldsymbol{x}}_N+\theta\dot{\boldsymbol{x}}_{N+1}]$$

becomes

$$\boldsymbol{x}_{N+1}=\mathbf{Q}^{\mathrm{t}}(t_{N+1})\cdot[\boldsymbol{x}_N+(1-\theta)\,h\hat{\boldsymbol{x}}_N]+\theta h\hat{\boldsymbol{x}}_{N+1} \tag{5.3.9}$$

(for a general frame, $\boldsymbol{w}\neq\boldsymbol{0}$). As $\theta\to 0$ we recover (5.3.7). Letting $\theta\to 1$ in (5.3.9) we get an implicit 'backward difference' scheme.

We note that (5.3.7) and (5.3.9) are no more than discrete approximations to the 'Jaumann integral' of Goddard and Miller [57][57]

$$\boldsymbol{x}(t)=\mathbf{Q}^{\mathrm{t}}(t)\cdot\boldsymbol{x}(\tau)+\int_\tau^t\mathbf{Q}^{\mathrm{t}}(t)\cdot\mathbf{Q}(\zeta)\cdot\hat{\boldsymbol{x}}(\zeta)\mathrm{d}\zeta \tag{5.3.10}$$

[54]It must be emphasized that *such a choice is arbitrary*. We could just as well choose as special those frames in which the particle's velocity is always radial, $(\boldsymbol{x}\times\dot{\boldsymbol{x}}=\mathbf{0})$. No matter what convention is used, we shall henceforth refer to the special frames as *defining frames*, after Zhong-Heng [56].

[55]We take $\mathbf{Q}(t_N)=\mathbf{I}$ with no loss of generality.

[56]$W_{ij}=-\frac{1}{2}e_{ijk}w_k$ in cartesian tensor index notation.

[57]These authors consider only the case in which $\mathbf{W}$ is put equal to the material spin.

where $\hat{\boldsymbol{x}} = \dot{\boldsymbol{x}} + \boldsymbol{w} \times \boldsymbol{x} = \dot{\boldsymbol{x}} - \mathbf{W} \cdot \boldsymbol{x}$. Putting $\tau = t_N$ and $t = t_{N+1}$, it is easily seen that (5.3.7) results if we approximate the integral

$$\int_{t_N}^{t_{N+1}} \mathbf{Q}(\zeta) \cdot \hat{\boldsymbol{x}}(\zeta) \mathrm{d}\zeta \quad \text{by } h\hat{\boldsymbol{x}}(t_N) \quad (\text{recall } \mathbf{Q}(t_N) = \mathbf{I}) \tag{5.3.11}$$

and (5.3.9) results if we approximate the same integral by

$$h[(1-\theta)\hat{\boldsymbol{x}}(t_N) + \theta \mathbf{Q}(t_{N+1}) \cdot \hat{\boldsymbol{x}}(t_{N+1})] . \tag{5.3.12}$$

The relationship between the Jaumann integral and the objective numerical integration schemes is important because while the 'special' frames do play the role of defining frames for those numerical schemes, the algebra associated with their use can become tedious. The Jaumann integral is the vehicle by which general multistep schemes may be easily cast in an objective form. For example, we may write out, by inspection, the general formula for the objective Adams–Bashforth method:

$$\boldsymbol{x}_{N+1} = \mathbf{Q}^{\mathrm{t}}(t_{N+1}) \cdot [\mathbf{Q}(t_{N-p}) \cdot \boldsymbol{x}_{N-p} + h \sum_{k=0}^{m} \gamma_p^k \Delta^k (\mathbf{Q}(t_{N-k}) \cdot \hat{\boldsymbol{x}}_{N-k})] \tag{5.3.13}$$

where

$$\gamma_p^k \equiv \int_{-p}^{1} (-1)^k \binom{-s}{k} \mathrm{d}s ,$$

$\binom{-s}{k}$ being the binomial function and Δ^k is the kth order forward difference operator.[58] A similar general formula can be given for implicit schemes.

Using the formula $\mathbf{Q}^{\mathrm{t}} \cdot \ddot{\mathbf{Q}} = \mathbf{W} \cdot \mathbf{W} - \dot{\mathbf{W}}$ we can show that the generalized trapezoid rule. when applied to integrate the velocity from the acceleration, takes the objective form

$$\hat{\boldsymbol{x}}_{N+1} = \mathbf{Q}^{\mathrm{t}}(t_{N+1}) \cdot [\hat{\boldsymbol{x}}_N + h(1-\theta)\hat{\dot{\boldsymbol{x}}}_N] + \theta h \hat{\dot{\boldsymbol{x}}}_{N+1} . \tag{5.3.14}$$

By induction it may be shown that the objective generalized trapezoid formulas for higher accelerations are of the same form as (5.3.14).

One more problem must be considered before we can discuss algorithms for integration of the stress. Absolute objectivity is achieved by the schemes above only if we can construct the rotation increment $\mathbf{Q}(t_{N+1})$ precisely.[59] This is generally not possible. In the next few paragraphs we discuss schemes by which the rotation increment may be approximated.

The initial value problem for $\mathbf{Q}$ (5.3.8) may easily be reduced to a scalar problem by introduction of the 'angles of rotation' θ_i:

$$\sum_{i=1}^{3} \left(\frac{\partial}{\partial \theta_i} \mathbf{Q} \right) \dot{\theta}_i = -\mathbf{Q} \cdot \mathbf{W} , \qquad \theta_i(t_N) = 0 , \tag{5.3.15}$$

$$\mathbf{Q}(\theta_1, \theta_2, \theta_3) = \begin{bmatrix} (\mathrm{c}\theta_2 \mathrm{c}\theta_3) & (\mathrm{c}\theta_1 \mathrm{s}\theta_3 + \mathrm{s}\theta_1 \mathrm{s}\theta_2 \mathrm{c}\theta_3) & (\mathrm{s}\theta_1 \mathrm{s}\theta_3 - \mathrm{c}\theta_1 \mathrm{s}\theta_2 \mathrm{c}\theta_3) \\ (-\mathrm{c}\theta_2 \mathrm{s}\theta_3) & (\mathrm{c}\theta_1 \mathrm{c}\theta_3 - \mathrm{s}\theta_1 \mathrm{s}\theta_2 \mathrm{s}\theta_3) & (\mathrm{s}\theta_1 \mathrm{c}\theta_3 + \mathrm{c}\theta_1 \mathrm{s}\theta_2 \mathrm{s}\theta_3) \\ (\mathrm{s}\theta_2) & (-\mathrm{s}\theta_1 \mathrm{c}\theta_2) & (\mathrm{c}\theta_1 \mathrm{c}\theta_2) \end{bmatrix} .$$

[58] Complete details are given by Conte and de Boor [43].

[59] Rubinstein and Atluri have also studied this problem.

in which the abbreviations $s\theta_i = \sin\theta_i$ and $c\theta_i = \cos\theta_i$ have been used [58, p. 106][60]. Though no general solution of (5.3.15) is known, it may be integrated by standard numerical schemes.[61] The local error of such schemes is usually expressed in the form

$$|\theta(t_k) - \theta_k| \leq c h^{N+1} \theta_i^{(N+1)}, \tag{5.3.16}$$

where $\theta_i^{(N+1)}$ is the $(N+1)$th time derivative of θ_i. The scheme whose error term is of the form (5.3.16) we call 'Nth order'. If the θ_i are polynomials in time of degree less than or equal to N, then the angles, and hence the rotation increment, may be integrated precisely. The set of all time dependent rotations whose angles are of degree less than or equal to N we denote by $r(N)$. If an approximate rotation increment (whose angles were found by an Nth order scheme) is used in place of the precise rotation increment in one of the 'objective' schemes, then we describe the modified scheme as 'objective relative to $r(N)$'. For example, the classical Euler's method is objective relative to $r(0)$ (since it is absolutely objective when the θ_i are constant). If Euler's method is used to find approximations for the angles θ_i, and the resulting approximate rotation increment is used in place of $\mathbf{Q}$ in (5.3.7), then the modified scheme is objective relative to $r(1)$. In an Nth order method is used to approximate the angles, then the modification of (5.3.7) which results is objective relative to $r(N)$.

The principal objection to the method above for approximation of rotation increments is that it entails extra numerical work. We now discuss explicit approximation of the rotation increments. Following Gantmacher [59, p. 155], each interval (t_N, t_{N+1}) is divided up into K subintervals $(t^{\kappa-1}, t^{\kappa})$, such that $t^0 = t_N$ and $t^K = t_{N+1}$, and from each subinterval we pick an intermediate time τ^{κ}. We define the subincremental rotation as

$$\mathbf{\Omega}_{\kappa-1}^{\kappa} = \mathbf{Q}(t^{\kappa}) \cdot \mathbf{Q}^{\mathrm{t}}(t^{\kappa-1}). \tag{5.3.17}$$

Then it follows that the rotation increment $\mathbf{Q}$ may be represented as

$$\mathbf{Q}(t_{N+1}) = \mathbf{\Omega}_{K-1}^{K} \cdot \mathbf{\Omega}_{K-2}^{K-1} \cdots \mathbf{\Omega}_{1}^{2} \cdot \mathbf{\Omega}_{0}^{1}. \tag{5.3.18}$$

Now we approximate $\mathbf{\Omega}_{\kappa-1}^{\kappa}$ as

$$\mathbf{\Omega}_{\kappa-1}^{\kappa} = [\exp(\Delta t^{\kappa} \mathbf{W}(\tau^{\kappa}))]^{\mathrm{t}}, \quad \Delta t^{\kappa} = (t^{\kappa} - t^{\kappa-1}). \tag{5.3.19}$$

This is exact when $\mathbf{W}(t) \equiv \mathbf{W}(\tau^{\kappa})$, a constant. The matrix function $\exp(\mathbf{W}t)$ has the representation [54, p. 238; 53]

$$\exp(\mathbf{W}t) = \mathbf{I} + \left(\frac{\sin wt}{w}\right)\mathbf{W} + \left(\frac{1-\cos wt}{w^2}\right)\mathbf{W}^2, \quad w^2 = \tfrac{1}{2}\mathbf{W}:\mathbf{W} \tag{5.3.20}$$

for any constant skew-symmetric $\mathbf{W}$. Hence, we can get an explicit approximation for the rotation increment by use of (5.3.18), (5.3.19) and (5.3.20). This approximation converges to

[60] Euler's angles are less convenient since the precession and spin are not always well-defined; see [58, p. 143].

[61] The rate of the angle between two vectors is an absolute scalar, i.e. has the same value in all frames, so standard numerical integration schemes may be applied to obtain an 'objective' approximation to the angle itself.

the precise rotation increment if we let K, the number of subintervals, approach infinity in such a way that the largest $|\Delta t^\kappa| \to 0$ [59]. Only a partial ordering of these approximate rotation increments appears to be possible.[62]

The discussions above apply to integration schemes for all orders of tensors. Instead of mechanically deriving a plethora of formulas, we shall examine one certain scheme for integration of rate-type constitutive equations. The Jaumann integral for the true stress is given by

$$\boldsymbol{\tau}(t) = J_\tau^{-1}(t)\,\mathbf{Q}^{\mathrm{t}}(t)\cdot\boldsymbol{\tau}(\tau)\cdot\mathbf{Q}(t) + \int_\tau^t J_\tau^{-1}(\zeta)\,\mathbf{Q}^{\mathrm{t}}(t)\cdot\mathbf{Q}(\zeta)\cdot\dot{\boldsymbol{\sigma}}^*(\zeta)\cdot\mathbf{Q}^{\mathrm{t}}(\zeta)\cdot\mathbf{Q}(t)\,\mathrm{d}\zeta\,. \tag{5.3.21}$$

Here $\mathbf{Q}(t)$ is defined as the solution of

$$\dot{\mathbf{Q}}(t) = -\mathbf{Q}(t)\cdot\boldsymbol{\omega}(t)\,, \qquad \mathbf{Q}(\tau) = \mathbf{I}\,, \tag{5.3.22}$$

and may be thought of as an 'integrating factor'.[63] Frames which spin with the principal axes of stretching play the role of defining frames for numerical schemes based on (5.3.21). By inspection we write the objective generalized midpoint rule as

$$\begin{aligned}\boldsymbol{\tau}_{N+1} = {} & J_N^{-1}(t_{N+1})\,\mathbf{Q}^{\mathrm{t}}(t_{N+1})\cdot\boldsymbol{\tau}_N\cdot\mathbf{Q}(t_{N+1}) \\ & + hJ_N^{-1}(t_{N+\theta})\,\mathbf{Q}^{\mathrm{t}}(t_{N+1})\cdot\mathbf{Q}(t_{N+\theta})\cdot\dot{\boldsymbol{\sigma}}^*_{N+\theta}\cdot\mathbf{Q}^{\mathrm{t}}(t_{N+\theta})\cdot\mathbf{Q}(t_{N+1})\,.\end{aligned} \tag{5.3.23}$$

Now suppose that in this formula we use $[\underset{\sim}{\mathbf{V}}:\boldsymbol{\varepsilon}+\boldsymbol{\Sigma}]$ in place of $\dot{\boldsymbol{\sigma}}^*$. Equation (5.3.23) then reduces, in essence, to the formulas of Key et al. [52] and Rubinstein and Atluri [53] for $\theta = \frac{1}{2}$. The formula of Hughes and Winget [51] cannot be recovered since they use midpoint constitutive evaluation but fail to properly rotate the resulting stress increment. An analagous formula has been given by Pinsky et al. [61]. Those workers [52, 53, 61] did not give any schemes other than midpoint schemes, or indicate how other schemes could be obtained.[64] Moreover, their discussions revolve around integration of (rate-type) constitutive equations: this could cause confusion of general physical objectivity with the Principle of Objectivity of Material Properties. Finally, no distinction is made between relative objectivity and absolute objectivity.

The present choice of defining frames, those frames in which the material spin $\boldsymbol{\omega}$ vanishes. is outwardly as arbitrary now as it was before; we could just as well have chosen those frames whose absolute angular velocity $\boldsymbol{w}$ vanishes as defining frames. Intuitively, one would expect the local error to be smallest in the former frames,[65] however, an easy proof is not apparent. This is the only motive we can imagine for choosing corotational frames for defining frames.

[62]Approximate rotation increments constructed over different sets of subintervals appear not to be comparable. in general.

[63]This idea has been exploited by Petrie [60]. His integral may be used as a basis for more general numerical schemes. giving as special cases *all* of the schemes below (including that of Pinsky et al. [61]).

[64]Pinsky et al. [61] do introduce defining frames, so it is apparent that their results may be extended. Hughes and Winget [51] remark that their algorithm may be generalized to a subincremental one. but omit details.

[65]Especially when the deformation consists of a rigid motion.

6. Examples: finite homogeneous deformations

6.1. Introduction

Through the study of homogeneous deformations various important aspects of the performance of the finite element algorithm can be identified and studied. Since closed form solutions to problems of homogeneous deformation are widely available, questions of the accuracy of the finite element solutions can be resolved quickly and absolutely. If we immediately engaged problems complicated by inhomogeneous deformation, the accuracy of any solution we obtained would be no more than a subject for speculation. Homogeneous deformations also make convenient subjects for testing of time step bounds, and in the present case, for study of the effect on accuracy of the forward gradient scheme. Finally, the results serve to underscore the fact that the material models themselves are too idealized to be used in problems of technological interest when strains are very large.

6.2. Finite plane extension

We begin our study of homogeneous deformations by considering finite plane extension of (i) a hypoelastic material and (ii) an elastico-viscous fluid. The geometry of the specimen is given in Fig. 1. In these examples we focus on the relative efficiencies (accuracy/effort) of the Euler, Runge–Kutta second order (RK2) and Runge–Kutta fourth-order (RK4) integration schemes, and the effect on accuracy of the forward gradient scheme.

Consider plane extension of the hypoelastic material defined by

$$\mathring{\boldsymbol{\sigma}}^{*} = 2\mu\boldsymbol{\varepsilon} + \lambda(\mathbf{I}:\boldsymbol{\varepsilon})\mathbf{I}\,. \tag{6.2.1}$$

The closed form solution for the stress is given by

$$s^{11}(L) = 0\,, \qquad s^{22}(L) = \nu s^{33}(L)\,, \qquad s^{33}(L) = \left(\frac{1}{1-2\nu}\right)(1 - L^{-\bar{\nu}}) \tag{6.2.2}$$

where $\mathbf{s} = \boldsymbol{\tau}/2\mu$ and $\bar{\nu} = (1-2\nu)/(1-\nu)$. In Figs. 2, 3 and 4 the stresses found by application of

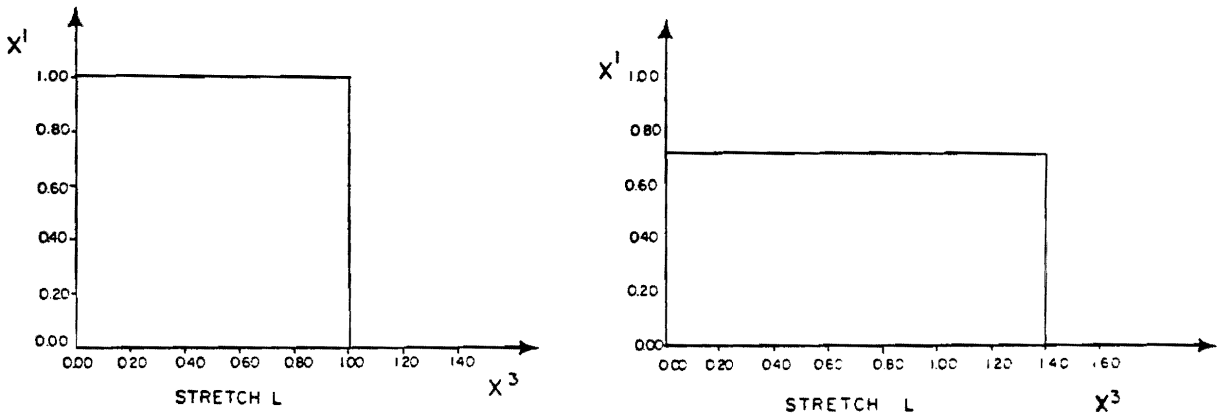

Fig. 1. Plane extension specimen.

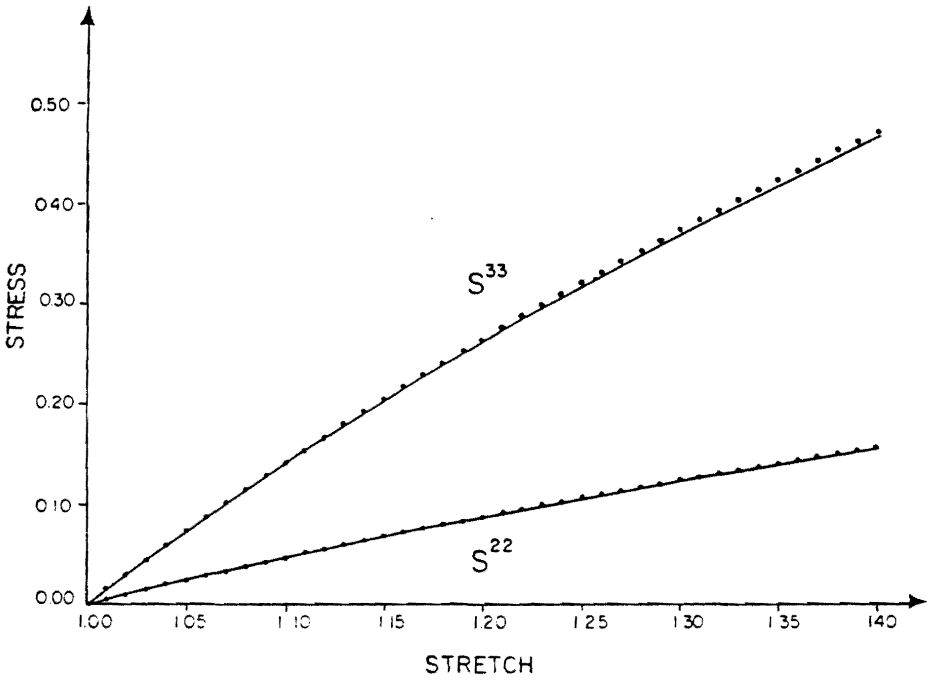

Fig. 2. Stress accompanying plane extension of a hypoelastic material—Euler integration.

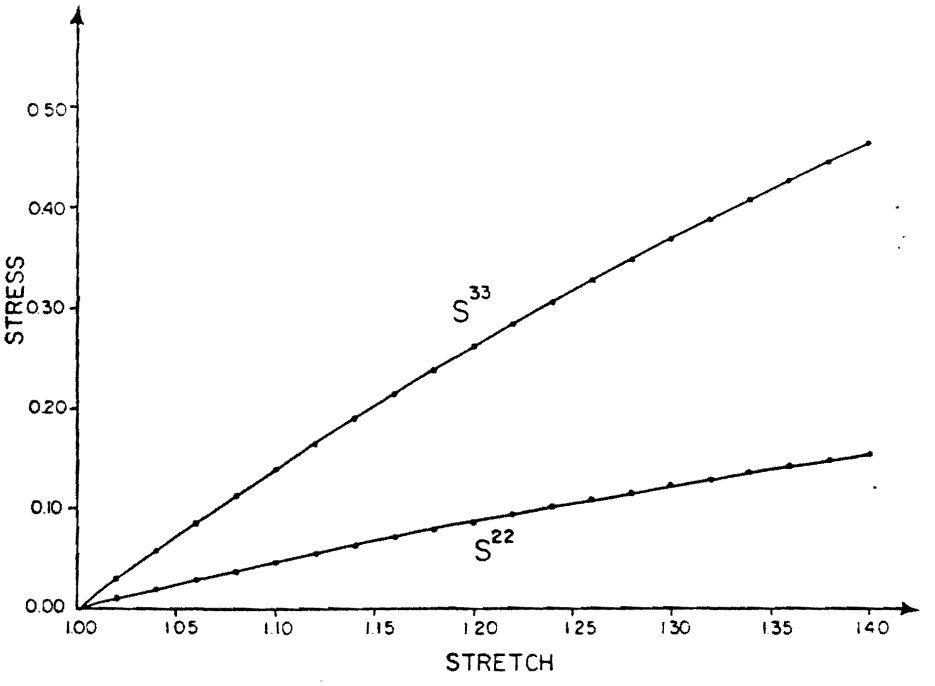

Fig. 3. Stress accompanying plane extension of a hypoelastic material—RK2 integration.

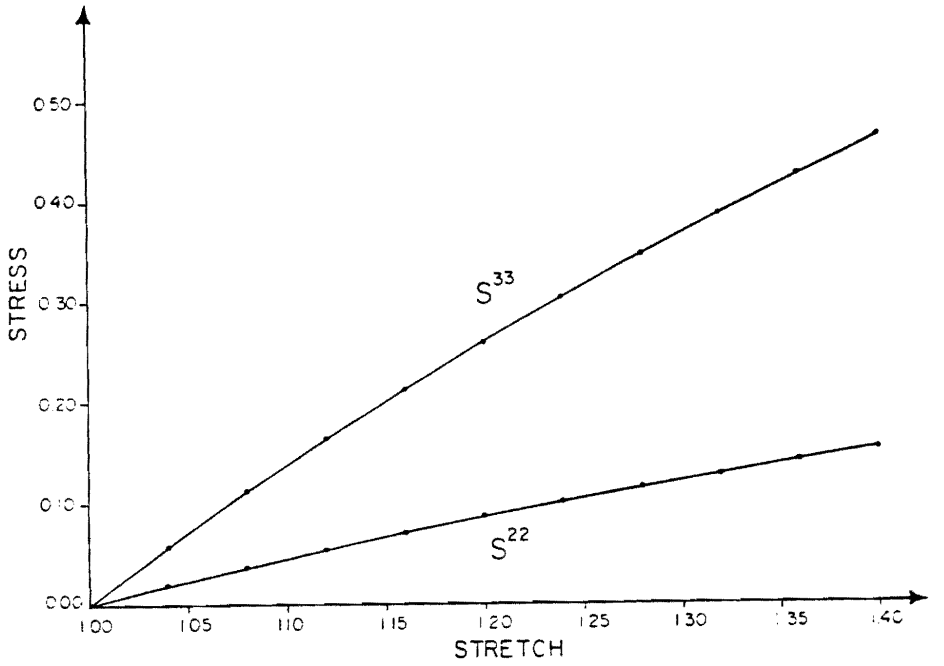

Fig. 4. Stress accompanying plane extension of a hypoelastic material—RK4 integration.

the finite element algorithm are compared to the closed form solution for $\nu = \frac{1}{3}$. The Euler scheme (Fig. 2) leads to an underestimation of the strain-softening, but the RK2 and RK4 schemes (Figs. 3 and 4) give results virtually indistinguishable from the closed form solution. Since the time steps used gave stretch increments of (0.01), (0.02) and (0.04), respectively, the computational effort was the same for each of these three cases. In view of the differences in accuracy attained, we rank the RK4 scheme as most efficient, followed by RK2 and Euler.

Here we pause to remind the reader that 'incremental' finite element algorithms are predisposed to integration by the relatively inefficient Euler scheme.

Now consider plane extension of the elastico-viscous fluid defined by

$$\boldsymbol{\varepsilon} = \dot{\mathbf{s}}^* - \left(\frac{\nu}{1+\nu}\right)(\mathbf{I}:\dot{\mathbf{s}}^*)\,\mathbf{I} + \frac{1}{T}\mathbf{s}', \qquad \dot{\mathbf{s}}^* = \dot{\boldsymbol{\sigma}}^*/2\mu\,, \quad \mathbf{s}' = \boldsymbol{\tau}'/2\mu\,. \tag{6.2.3}$$[66]

The closed form solution for the stress, when $\nu = 0.5$, is given by

$$\begin{aligned} &s^{11}(t) = 0\,, \qquad s^{22}(t) = \tfrac{1}{2}s^{33}(t)\,, \\ &s^{33}(t) = s^{33}(0)\,e^{-t/T} + 2\int_0^t \varepsilon^{33}(\zeta)\,e^{-(t-\zeta)/T}\,\mathrm{d}\zeta\,. \end{aligned} \tag{6.2.4}$$

[60, Appendix A]. For the stretch history $L(t) = 1 + Vt$, the stretching is given by $\varepsilon^{33}(t) =$

[66]For an incompressible fluid we recover from (6.2.3) the model of Zaremba (1903), Fromm (1947, 1948), and Dewitt (1955), according to Bird et al. [62]. The constant T is the relaxation time.

$V/(1+Vt)$, and s^{33} may be expressed as a function of the stretch L as

$$s^{33}(L) = s^{33}(1)\, e^{-(L-1)/VT} + 2e^{-L/VT}\left\{\mathrm{Ei}\left(\frac{L}{VT}\right) - \mathrm{Ei}\left(\frac{1}{VT}\right)\right\}. \tag{6.2.5}$$[67]

In the two cases following we have taken $V = 10^{-14}\,\mathrm{sec}^{-1}$, $\nu = 0.4$, and $T = \frac{1}{2}\cdot\frac{28}{45}\times 10^{12}$ sec. Cormeau's [37] time step bound is $h < h_c = 2T$.

In the first case we assign the initial stress as if nearly-steady conditions existed from the outset: $\dot{\mathbf{s}}(1) = \mathbf{0}$. From (6.2.3) we thus obtain

$$s^{11}(1) = 0\,, \qquad s^{22}(1) = \tfrac{1}{2}s^{33}(1) = VT\,.$$

We take time steps $h = \frac{45}{28}h_c$, $h = 2\cdot\frac{45}{28}h_c$ and $h = 4\cdot\frac{45}{28}h_c$ (corresponding to stretch increments of 0.01, 0.02 and 0.04), applying Euler, RK2 and RK4 schemes, respectively. Since the time steps exceed the critical time step h_c, the forward gradient scheme is used, with θ set to $\frac{1}{2}$. The stresses found by application of the finite element algorithm (for $\nu = 0.4$) are compared to the closed form solution (for $\nu = 0.5$) in Figs. 5, 6 and 7.

It is apparent from these figures that the numerically integrated stress is slightly greater than the actual stress in the incompressible material, which is surprising, for one would expect a *lower* stress in the more compliant material when the deformation was prescribed. We note

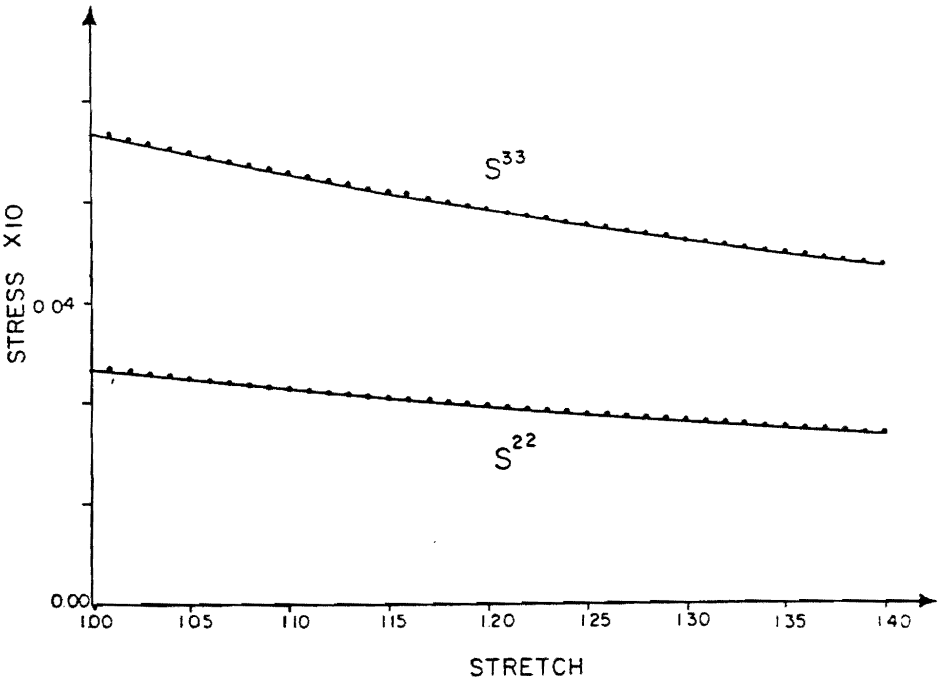

Fig. 5. Stress accompanying plane extension of a elastico-viscous fluid—Euler integration.

[67]Here Ei is the exponential integral $\mathrm{Ei}(x) = \int_{-\infty}^{x}(e^z/z)\mathrm{d}z$, whose values are tabulated [63].

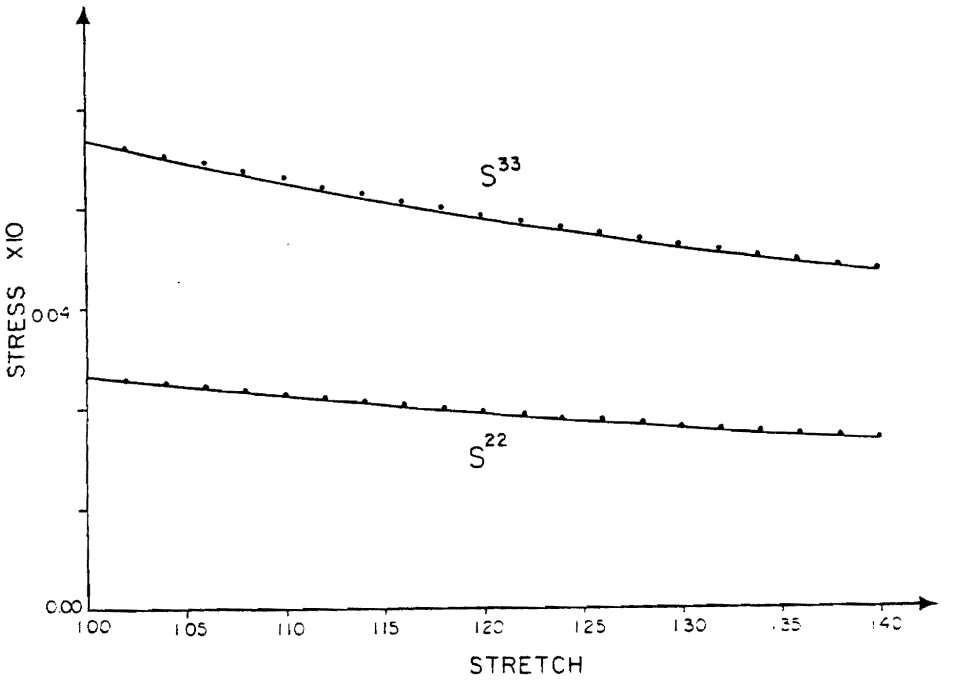

Fig. 6. Stress accompanying plane extension of a elastico-viscous fluid—RK2 integration.

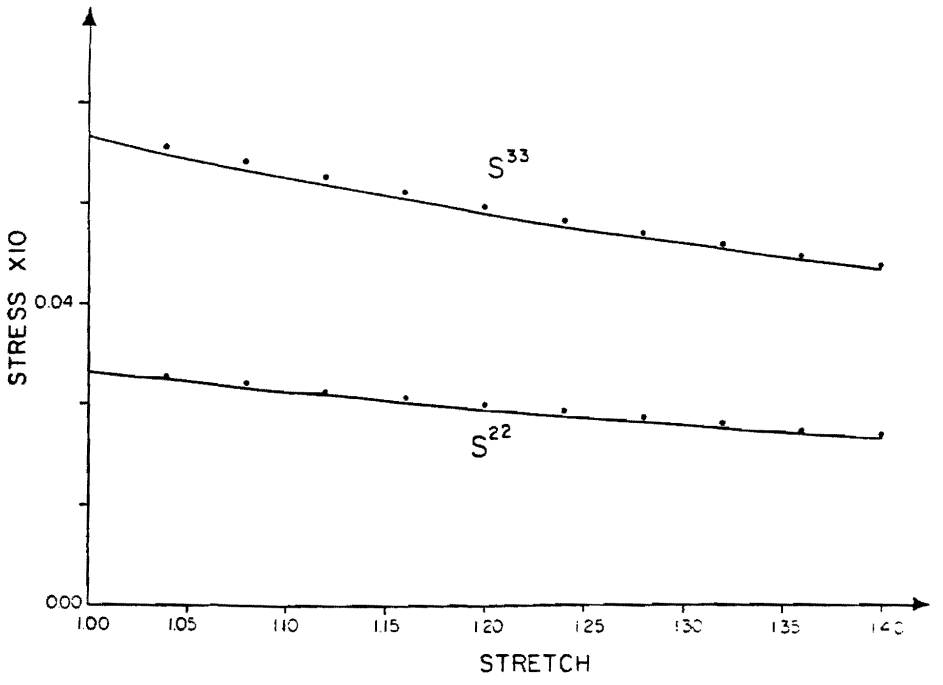

Fig. 7. Stress accompanying plane extension of a elastico-viscous fluid—RK4 integration.

that using the forward gradient scheme is essentially the same as replacing the constitutive equation (6.2.3) by

$$\boldsymbol{\varepsilon} = \left(1+\frac{\theta h}{T}\right)\dot{\mathbf{s}}^* - \left(\frac{\nu}{1+\nu}+\frac{1}{3}\frac{\theta h}{T}\right)(\mathbf{I}:\dot{\mathbf{s}}^*)+\frac{1}{T}\mathbf{s}' .$$

Defining $\mathbf{z} = (1+\theta h/T)\,\mathbf{s}$, $T_\theta = T + \theta h$, and setting $\nu = 0.5$ gives

$$\boldsymbol{\varepsilon} = \dot{\mathbf{z}}^* - \tfrac{1}{3}(\mathbf{I}:\dot{\mathbf{z}}^*)\,\mathbf{I} + (1/T_\theta)\,\mathbf{z}' . \tag{6.2.6}$$

But this equation is of the same form as (6.2.3), which has already been integrated for plane extension; distinguishing the closed form solution of (6.2.6) from that of (6.2.3) with a subscript θ, we write

$$\begin{aligned} &s_\theta^{11}(t) = 0 , \qquad s_\theta^{22}(t) = \tfrac{1}{2}s_\theta^{33}(t) , \\ &s_\theta^{33}(t) = s_0^{33}e^{-t/T_\theta} + \frac{2T}{T_\theta}\int_0^t \varepsilon^{33}(\zeta)e^{-(t-\zeta)/T_\theta}\,\mathrm{d}\zeta . \end{aligned} \tag{6.2.7}$$

Now, to compare $\mathbf{s}$ and $\mathbf{s}_\theta$, we consider the case that $\varepsilon^{33}(t) = \varepsilon_0^{33}$, a constant. From (6.2.4) and (6.2.7) we easily obtain

$$s^{33}(t) = s_0^{33}e^{-t/T} - 2T\varepsilon_0^{33}(1-e^{-t/T})$$

and

$$s_\theta^{33}(t) = s_0^{33}e^{-t/T_\theta} + 2T\varepsilon_0^{33}(1-e^{-t/T_\theta}) .$$

At times much later than T and T_θ, both s^{33} and s_θ^{33} achieve the steady value $2T\varepsilon_0^{33}$. The important difference is the rate at which the stresses approach their steady state value. It is clear that $s_\theta^{33}(t)$ is related to $s^{33}(t)$ as

$$s_\theta^{33}(t) = s^{33}(t - \theta h\, t/T_\theta)$$

so the stress s_θ^{33} lags the actual stress s^{33}. This is exactly what is shown in Figs. 5, 6 and 7. Moreover, that lag becomes more and more apparent as the order of the integration scheme is increased, since the numerical solution tends towards s_θ^{33} (not shown), rather than the actual stress s^{33}.

In the second case of plane extension of the elastico-viscous fluid defined by (6.2.3) we set the initial stress to zero. The stress in this case differs from that of the first case solely because of the different initial condition, and that difference attenuates like $e^{-t/T}$. At times much later than $t = T$, the stress in this case is indistinguishable from that of the first case. We use Euler's method exclusively, taking time steps of $h = \frac{1}{2}\cdot\frac{45}{28}h_c$, $h = \frac{45}{28}h_c$ and $h = 2\cdot\frac{45}{28}h_c$, for stretch increments of 0.005, 0.01 and 0.02, respectively. The parameter θ in the forward gradient scheme is set to unity, $\theta = 1$, giving $T_\theta/T = 2.61$, $T_\theta/T = 4.21$ and $T_\theta/T = 7.43$, respectively. In Figs. 8, 9 and 10 the stress found by application of the finite element algorithm (for $\nu = 0.4$) is plotted alongside the actual stress s^{33} and the stress s_θ^{33} (for $\nu = 0.5$).

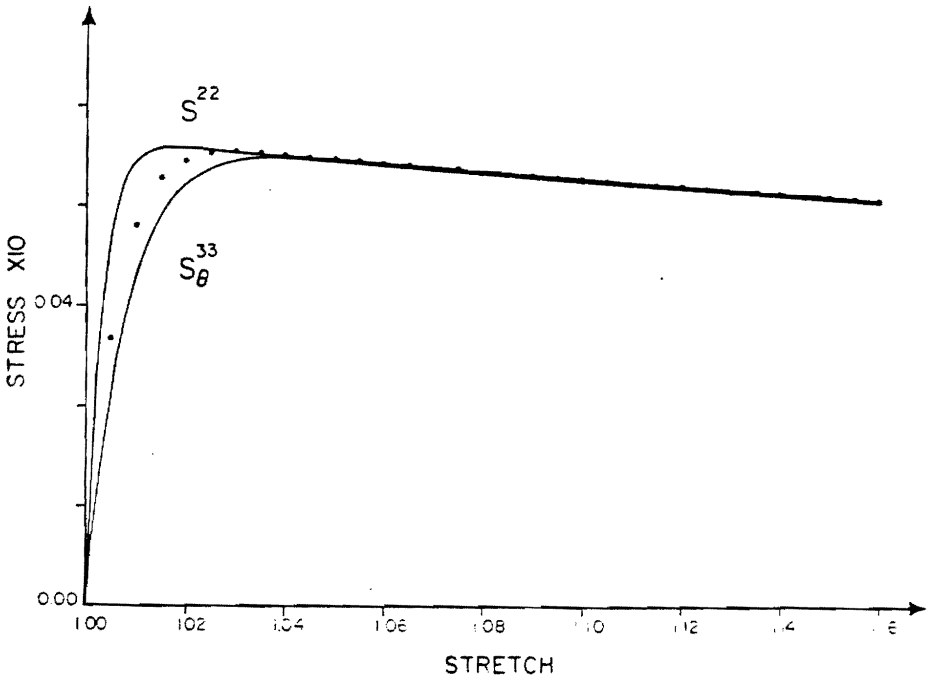

Fig. 8. Stress accompanying plane extension of a elastico-visous fluid—$(T_\theta/T) = 2.61$.

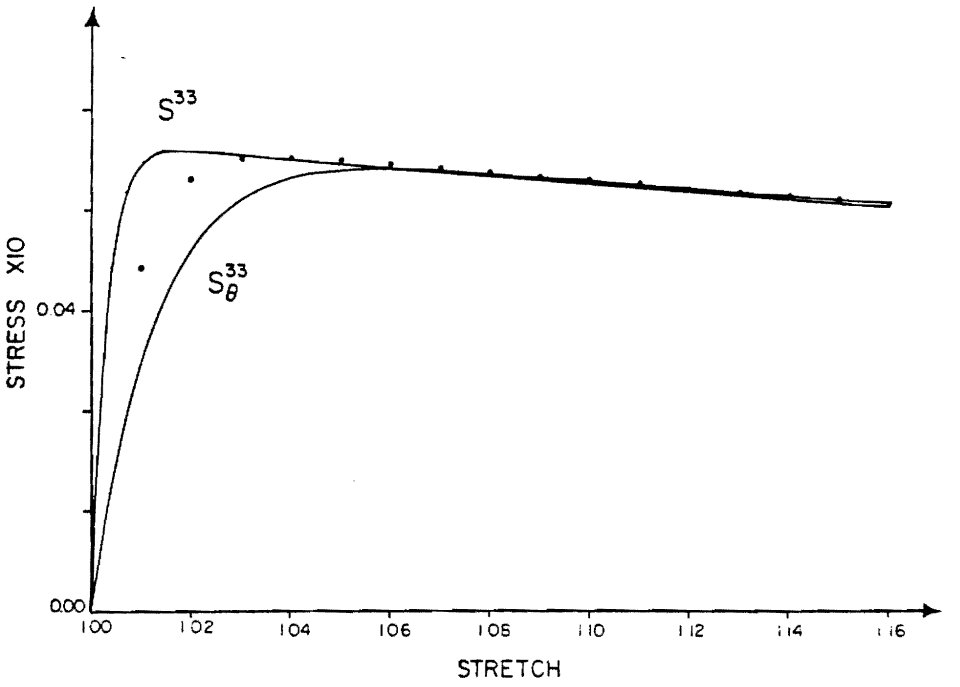

Fig. 9. Stress accompanying plane extension of a elastico-viscous fluid—$(T_\theta/T) = 4.21$.

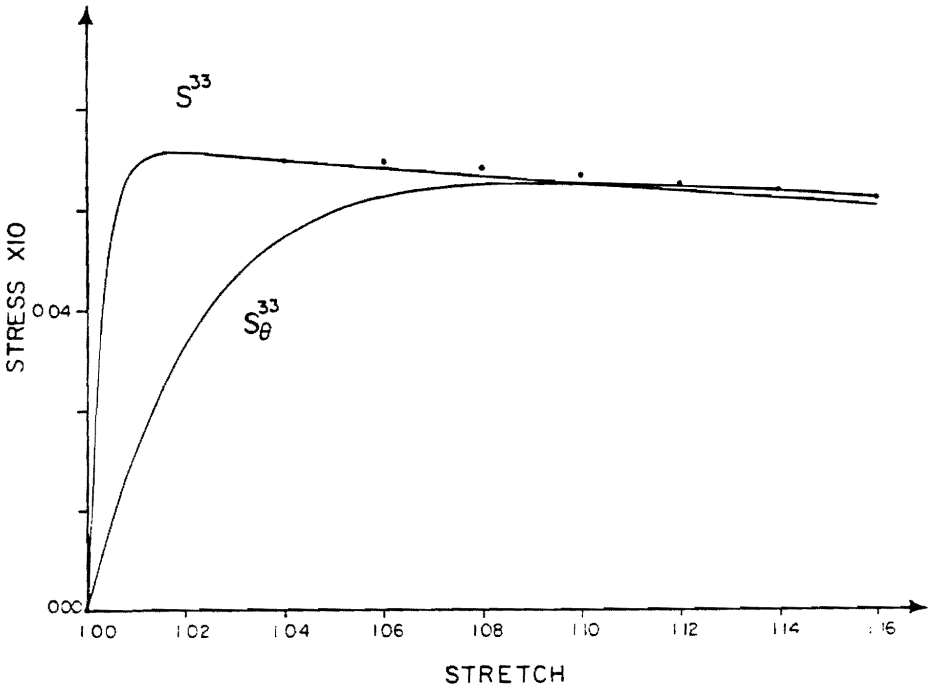

Fig. 10. Stress accompanying plane extension of a elastico-viscous fluid—$(T_\theta/T) = 7.43$.

It is clear that even for $(T_\theta/T) = 2.61$ only a qualitative estimate of the transient response is given by the finite element algorithm, and that estimate is degraded as (T_θ/T) is increased. More important, though, is the fact that use of a higher order integration scheme *cannot* improve the accuracy of the numerical solution, since that solution would be drawn towards s^{33}_θ, not the actual stress s^{33}. It is therefore senseless to use integration schemes other than Euler's in conjunction with the forward gradient scheme.

6.3. Finite plane shear

We conclude our study of homogeneous deformations by considering finite plane shear of (i) the hypoelastic material defined by (6.2.1), (ii) a second hypoelastic material which resembles an elastic-perfectly plastic material and (iii) the elastico-viscous fluid defined by (6.2.3). The geometry of the specimen is given in Fig. 11. These examples serve not only to further demonstrate the performance of the finite element algorithm, but also to portray aspects of the finite deformation behavior of materials themselves. In the third case, involving the elastico-viscous fluid, only time steps smaller than the critical time step are taken, making it possible to compare the numerical results obtained through use of the forward gradient scheme to those obtained without it.

Throughout this section only the second-order Runge–Kutta integration scheme is used.

Consider plane shearing from a stress-free state of the hypoelastic material (6.2.1). The closed form solution for the stress is given by

$$s^{33}(e) = -s^{11}(e) = \tfrac{1}{2}(1 - \cos(e)), \qquad s^{13}(e) = \tfrac{1}{2}\sin(e). \tag{6.3.1}$$

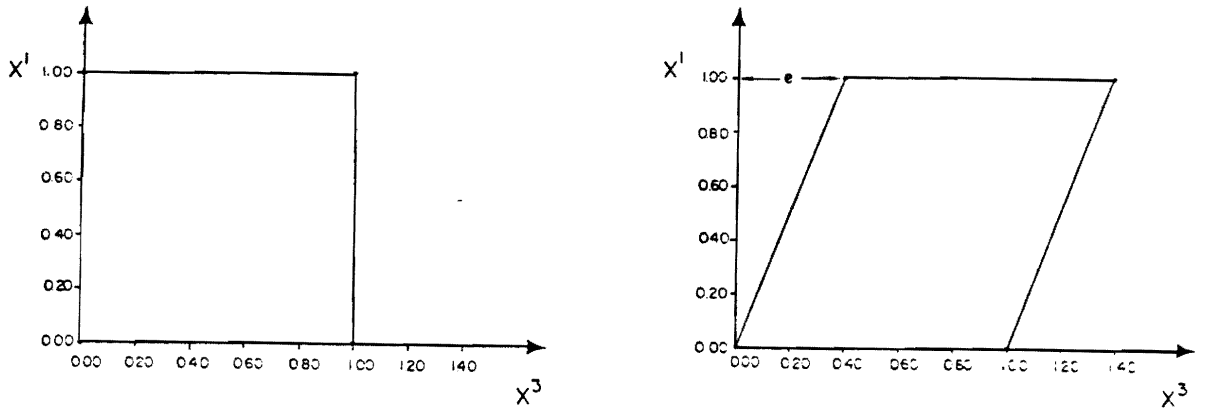

Fig. 11. Rectilinear shear specimen.

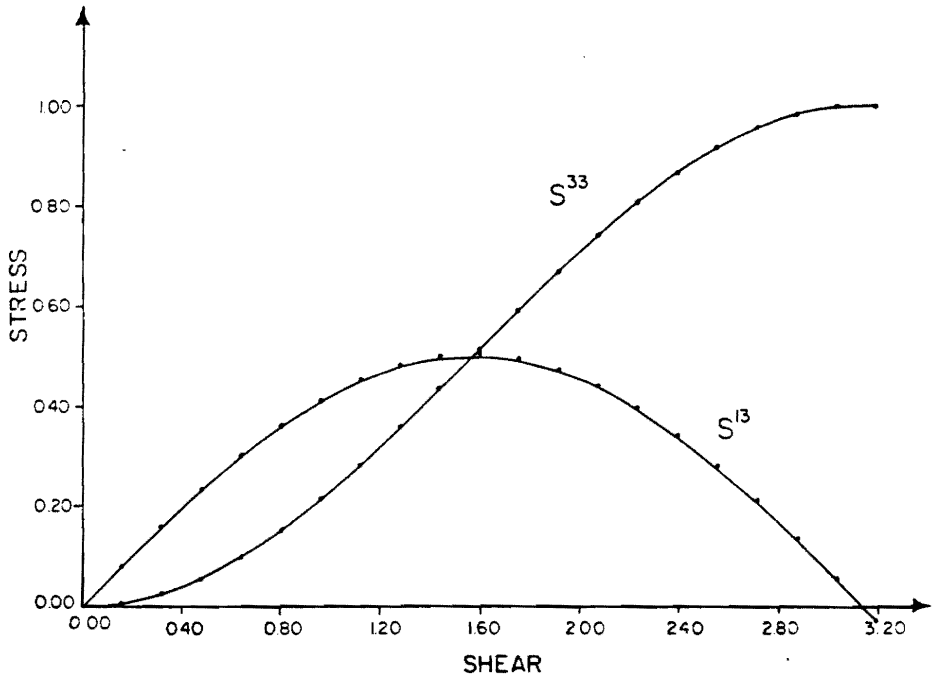

Fig. 12. Stress accompanying rectilinear shear of a hypoelastic material.

The closed form and finite element solutions are plotted in Fig. 12.[68] Though the finite element solution does agree with the closed form solution, it is evident that the predicted large strain behavior is not representative of any real material. The fault, of course, lies with the over-simple constitutive equation (6.2.1). This might seem to be of little consequence if one is interested only in metals such as those used in structures because some mechanism of inelasticity always becomes active long before such large shear strains as $e = \frac{1}{2}\pi$ are reached.

[68]Time steps corresponding to nominal shear strain increments $(e_{N+1} - e_N) = 0.16$ were used in the finite element algorithm.

However, since the constitutive equation (6.2.1) is frequently used as a component in 'superposition' models,[69] it is relevant to ask if similar periodic behavior might be predicted by those models.

Consider plane shearing from a stress-free state of a hypoelastic material of grade two, defined by

$$\dot{\mathbf{s}}^{*} = \boldsymbol{\varepsilon} + \left(\frac{\nu}{1-2\nu}\right)(\mathbf{I}:\boldsymbol{\varepsilon})\,\mathbf{I} - \frac{1}{K^2}(\mathbf{s}':\boldsymbol{\varepsilon})\,\mathbf{s}' . \tag{6.3.2}$$

When K^2 is identified as $\frac{2}{3}(\tau_Y/2\mu)^2$, (6.3.2) is the same as the constitutive equation for an elastic-perfectly plastic material; only the yield surface has been removed. The closed form solution for the stress has been given [22, p. 423] as

$$s^{33}(\phi) = -s^{11}(\phi) = \tfrac{1}{2}c^2(1-\cos(\phi)), \qquad s^{13}(\phi) = \tfrac{1}{2}c\sin(\phi) \tag{6.3.3}$$

where, for $K^2 < \frac{1}{2}$,

$$c^2 \equiv K^2/(\tfrac{1}{2}+K^2), \qquad d^2 = K^2/(\tfrac{1}{2}-K^2),$$
$$\phi \equiv 2\tan^{-1}\{(d/c)\tanh(c/d)\}.$$

The closed form and finite element solutions, for $K = (0.10)$, are plotted in Fig. 13.[70] The shear stress s^{13} reaches its maximum value at a nominal shear strain e_c (for $\phi = \frac{1}{2}\pi$)

$$e_c = d\ln\left(\frac{1}{2K^2}+\frac{1}{cd}\right) \doteq 0.656431,$$

and declines after that, so again the predicted large strain behavior is not representative of any real material.

Finally, consider plane shearing from a stress-free state of the elastico-viscous fluid (6.2.3). The closed form solution for the stress is given by [64, p. 363, 60, Appendix A]

$$\begin{aligned} s^{33}(t) &= -s^{11}(t) = \tfrac{1}{2}C\{E - e^{-t/T}[\sin(\dot{e}t) + E\cos(\dot{e}t)]\}, \\ s^{13}(t) &= \tfrac{1}{2}C\{1 - e^{-t/T}[\cos(\dot{e}t) - E\sin(\dot{e}t)]\} \end{aligned} \tag{6.3.4}$$

where

$$C \equiv E/(1+E^2), \quad E \equiv \dot{e}T,$$

E, of course, is the nominal strain at the instant $t = T$. Three cases are examined, differing only in the strain rate prescribed. We consider values of the strain rate $\dot{e} = \frac{45}{28}10^{-12}\,\mathrm{sec}^{-1}$, $\dot{e} = 2\cdot\frac{45}{28}10^{-12}\,\mathrm{sec}^{-1}$, and $\dot{e} = 4\cdot\frac{45}{28}10^{-12}\,\mathrm{sec}^{-1}$, giving $E = 0.5$, $E = 1.0$ and $E = 2.0$, respectively. The reader should note that these strain rates are indeed very slow. In Figs. 14, 15 and 16 the

[69] The term seems to have been introduced by Truesdell [21]. Superposition models are dominant in the solid mechanics engineering literature.

[70] Time steps corresponding to nominal shear strain increments $(e_{N+1} - e_N) = 0.06$ were used in the finite element algorithm.

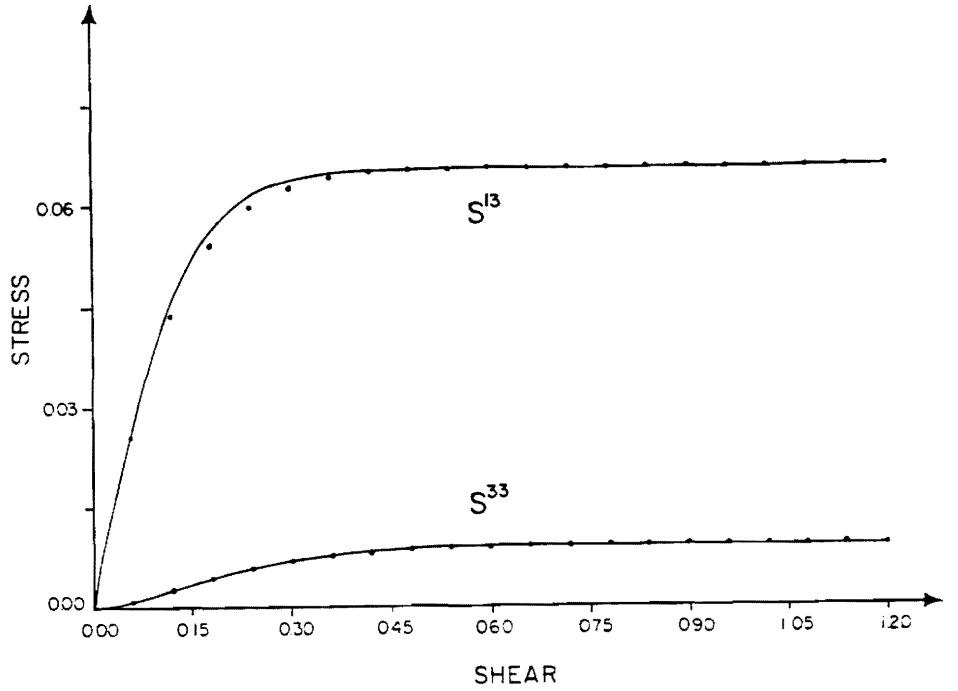

Fig. 13. Stress accompanying recilinear shear of a hypoelastic material of grade 2.

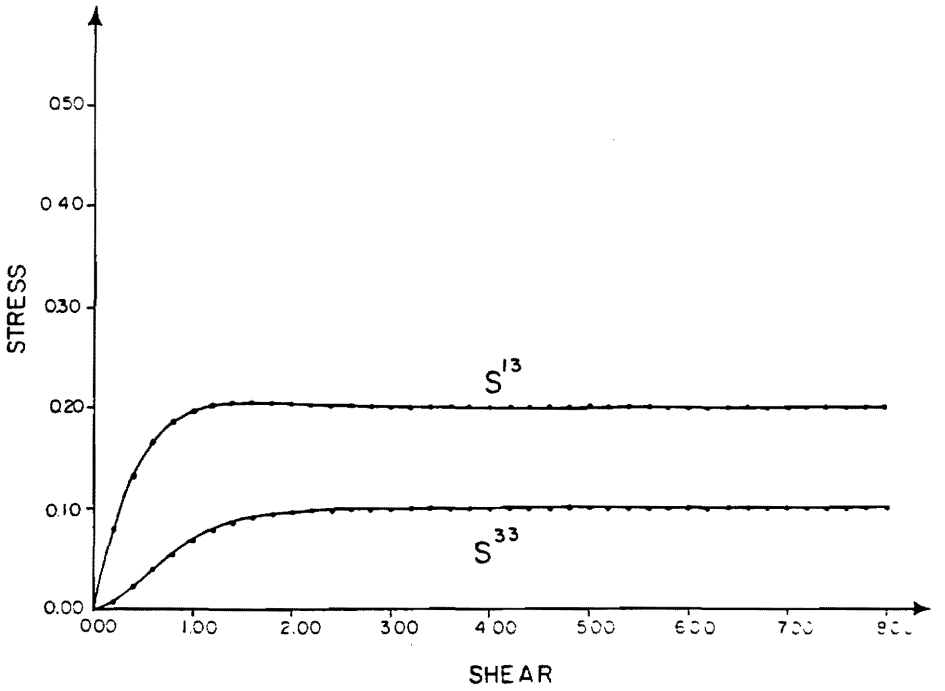

Fig. 14. Stress accompanying recilinear shear of a elastico-viscous fluid—$E = 0.5$.

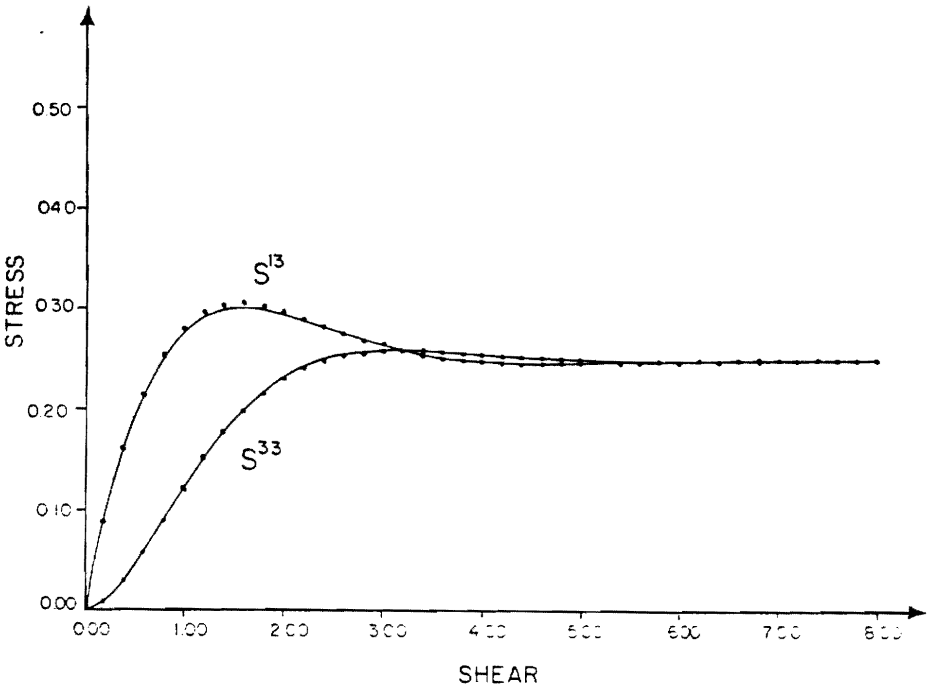

Fig. 15. Stress accompanying rectilinear shear of a elastico-viscous fluid—E = 1.0.

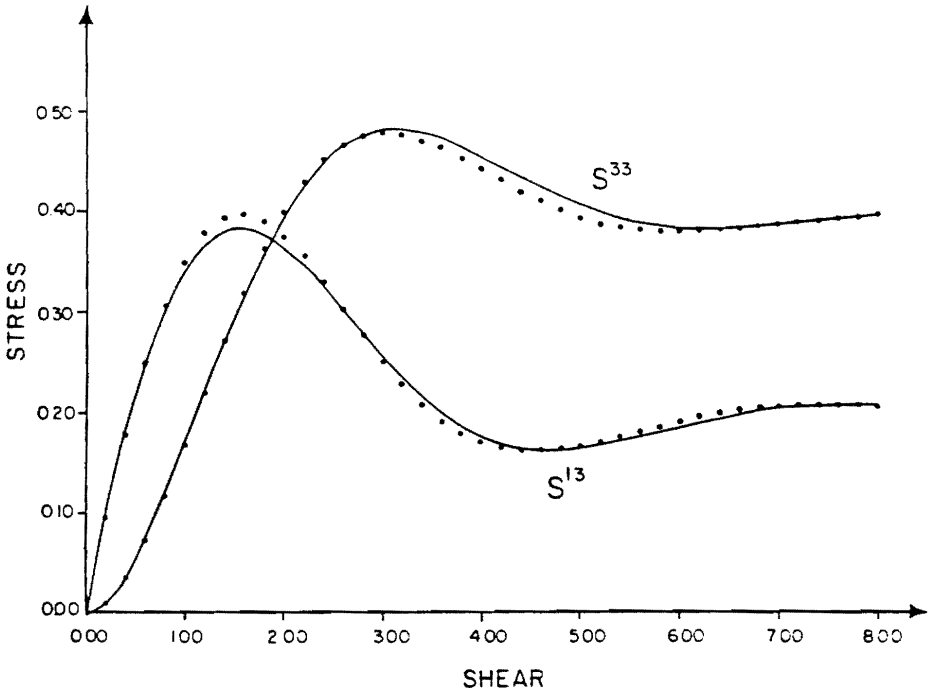

Fig. 16. Stress accompanying rectilinear shear of a elastico-viscous fluid—E = 2.0.

closed form and finite element solutions are plotted.[71] The shear stress reaches its first maximum value at a nominal shear strain $e_c = \frac{1}{2}\pi$. This predicted large strain behavior bears a *qualitative* resemblance to some data for transient stresses in polymer melts [65], but no resemblance at all to stresses observed in metals. Thus, the utility of the constitutive equation is extremely limited in the finite strain range.

Though it was not necessary to use the forward gradient scheme in the three cases above, we may still introduce it to the finite element algorithm just to see what error it causes. Just as for the plane extension examples, it is possible to integrate the modified constitutive equation in closed form. We obtain

$$\begin{aligned} s_\theta^{33}(t) &= -s_\theta^{11}(t) = \tfrac{1}{2}(T/T_\theta)\, C_\theta\{E_\theta - e^{-t/T_\theta}[\sin(\dot{e}t) + E_\theta \cos(\dot{e}t)]\}, \\ s_\theta^{13}(t) &= \tfrac{1}{2}(T/T_\theta)\, C_\theta\{1 - e^{-t/T_\theta}[\cos(\dot{e}t) - E_\theta \sin(\dot{e}t)]\} \end{aligned} \tag{6.3.5}$$

where

$$C_\theta \equiv E_\theta/(1+E_\theta^2), \qquad E_\theta \equiv \dot{e}T_\theta, \qquad T_\theta = T + \theta h .$$

The closed form solutions s and s_θ, and the finite element solution, for $E = 2.0$ and $\theta = 1.$ are plotted in Fig. 17.

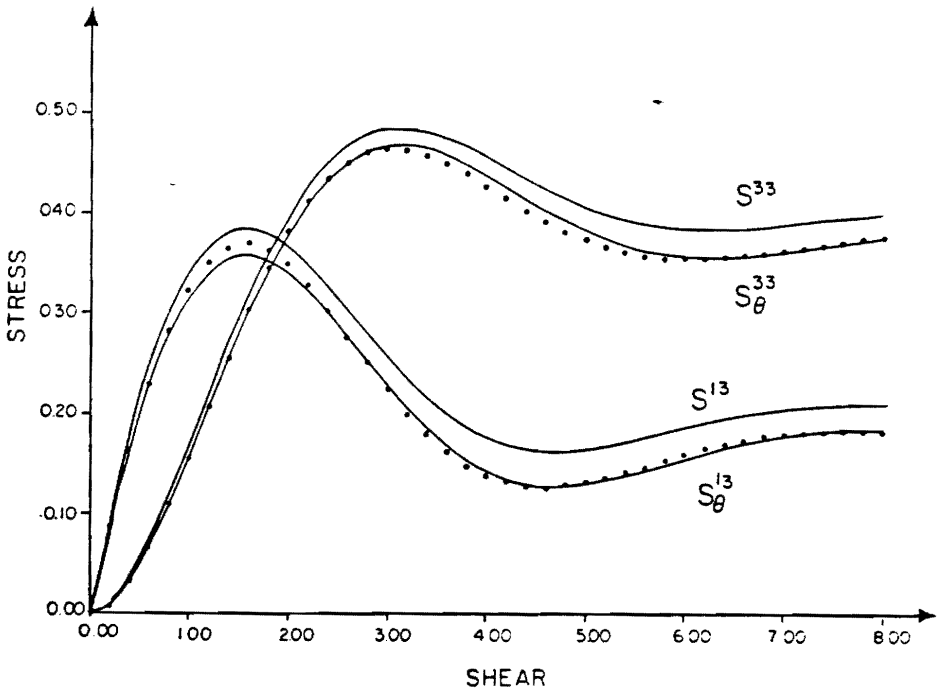

Fig. 17. Stress accompanying rectilinear shear of a elastico-viscous fluid—$E = 2.0$, $\theta = 1$.

[71]Time steps $h = (0.2)\, h_c$, $(0.1)\, h_c$, and $(0.05)\, h_c$ were used (corresponding to nominal strain increments of 0.2), so it was unnecessary to use the forward gradient scheme.

As is apparent, the two solutions $\mathbf{s}$ and $\mathbf{s}_\theta$ do not coincide at late times; rather we get the ratios

$$s_\theta^{13}/s^{13} \to (1+E^2)/(1+E_\theta^2), \qquad s_\theta^{11}/s^{11} \to (s_\theta^{13}/s^{13})(E_\theta/E),$$

which both go to zero as $\theta h \to \infty$. The unconditional stability of the forward gradient scheme is indeed of dubious value!

The source of the error is not hard to find. Equation (6.2.6) may be set in the form

$$(T/T_\theta)\,\boldsymbol{\varepsilon} = \dot{\mathbf{s}}^* - \tfrac{1}{3}(\mathbf{I}:\dot{\mathbf{s}}^*)\,\mathbf{I} + (1/T_\theta)\,\mathbf{s}'. \tag{6.3.6}$$

If, when steady-state conditions are reached, the corotational stress rate vanishes, $\dot{\mathbf{s}}^* = \mathbf{0}$, then *both* the original constitutive equation (6.2.3) and (6.3.6) reduce to

$$\boldsymbol{\varepsilon} = (1/T)\,\mathbf{s}', \tag{6.3.7}$$

and no discrepancy arises. This was the situation in plane extension. However, 'steady-state' generally does not imply that the corotational stress rate vanishes, and when it does not, T_θ cannot 'cancel out' of equation (6.3.6). Of course, if the constitutive equations (6.2.3) and (6.3.6) cannot be reconciled under steady-state conditions, then neither can the stresses.[72] This was the situation in plane shearing.

Deformations (or flows) of technological interest usually are neither pure extension nor pure shear, but somewhere between those two extremes. Petrie [67, p. 2] has remarked that "for polymeric liquids there is strong evidence that in flows involving both shear and elongation, the elongation will have a dominant influence." If we assume that the actual solution to some deformation/flow boundary value problem may be so characterized, then one might still be able to use the forward gradient scheme and get a reasonable approximation to that solution.

7. Conclusions

A new hybrid-stress finite element algorithm for the analysis of large, quasistatic, inelastic deformations has been presented. Principal variables in the formulation are the nominal stress rate and spin.

In contrast to 'incremental' finite element algorithms, whose solutions (displacement increments, stress increments) are predisposed to integration by the relatively inefficient Euler's method, the present 'rate' algorithm permits an independent treatment of the initial value problem. Much of this work is focused on that initial value problem, treating the subjects of numerical stability and numerical objectivity in depth. A new approach to numerical objectivity was proposed, and it was shown that previous 'objective' algorithms were but special cases of new algorithms that could be obtained by this approach. Finally, it was shown that the

[72]For the same reasons, Oldroyd [66] (note) concluded that "an elastico-viscous liquid will in general behave differently from any inelastic viscous liquid, even in steady-state experiments".

forward gradient scheme, and by implication, two 'finite approximation schemes', could lead to significant error.

Appendix A. Special notation

The special notations used in this work are summarized in the formulas below. We write a second-order tensor $\mathbf{T}$ and its transpose $\mathbf{T}^t$ as

$$\begin{aligned}\mathbf{T} &= T^{IJ}\boldsymbol{e}_I\boldsymbol{e}_J = T^I_J\boldsymbol{e}_I\boldsymbol{e}^J = T^J_I\boldsymbol{e}^I\boldsymbol{e}_J = T_{IJ}\boldsymbol{e}^I\boldsymbol{e}^J,\\ \mathbf{T}^t &= T^{IJ}\boldsymbol{e}_J\boldsymbol{e}_I = T^I_J\boldsymbol{e}^J\boldsymbol{e}_I = T^J_I\boldsymbol{e}_J\boldsymbol{e}^I = T_{IJ}\boldsymbol{e}^J\boldsymbol{e}^I\end{aligned} \tag{A.1}$$

where the $\boldsymbol{e}_K$ are the natural base vectors of the x^K coordinates. A fourth-order tensor $\underline{\mathbf{E}}$ may be written out as

$$\underline{\mathbf{E}} = E^{IJKL}\boldsymbol{e}_I\boldsymbol{e}_J\boldsymbol{e}_K\boldsymbol{e}_L\,. \tag{A.2}$$

The scalar product of two second-order tensors $\mathbf{S}$ and $\mathbf{T}$ is

$$\mathbf{S}:\mathbf{T} = S^{IJ}T_{IJ}\,. \tag{A.3}$$

The product of a fourth-order tensor $\underline{\mathbf{E}}$ and a second-order tensor $\mathbf{T}$ is

$$\underline{\mathbf{E}}:\mathbf{T} = E^{IJKL}T_{KL}\boldsymbol{e}_I\boldsymbol{e}_J, \qquad \mathbf{T}:\underline{\mathbf{E}} = T_{KL}E^{KLIJ}\boldsymbol{e}_I\boldsymbol{e}_J\,. \tag{A.4}$$

The product of two fourth-order tensors $\underline{\mathbf{D}}$ and $\underline{\mathbf{E}}$ is

$$\underline{\mathbf{D}}:\underline{\mathbf{E}} = D_{IJKL}E^{KLMN}\boldsymbol{e}^I\boldsymbol{e}^J\boldsymbol{e}_M\boldsymbol{e}_N\,. \tag{A.5}$$

Differentiation by a tensor is defined as

$$\frac{\partial R}{\partial \mathbf{T}} = \frac{\partial R}{\partial T_{IJ}}\boldsymbol{e}_I\boldsymbol{e}_J, \qquad \frac{\partial \mathbf{S}}{\partial \mathbf{T}} = \frac{\partial S^{IJ}}{\partial T_{KL}}\boldsymbol{e}_I\boldsymbol{e}_J\boldsymbol{e}_K\boldsymbol{e}_L\,. \tag{A.6}$$

The operators GRAD, DIV and CURL may be represented as the vector operators

$$\text{GRAD}\,\boldsymbol{v} = \nabla\boldsymbol{v}, \qquad \text{DIV}\,\boldsymbol{v} = \nabla\cdot\boldsymbol{v}, \qquad \text{CURL}\,\boldsymbol{v} = \nabla\times\boldsymbol{v} \tag{A.7}$$

where ∇ is the symbolic gradient operator:

$$\nabla = \boldsymbol{e}^K\frac{\partial}{\partial x^K}\,. \tag{A.8}^a$$

[a] In the text we write ∇_τ for the 'material gradient operator', $\nabla_\tau = \boldsymbol{E}^K\partial/\partial X^K$, $\boldsymbol{E}_K$ being the natural base vectors of the X^I coordinate system at time $t = \tau$.

In dyad notation (A.7) may be written out as

$$\begin{aligned} &\text{GRAD } \boldsymbol{v} = \nabla \boldsymbol{v} = (v^J)_{,I} \boldsymbol{e}^I \boldsymbol{e}_J \\ &\text{DIV } \boldsymbol{v} = \nabla \cdot \boldsymbol{v} = (v^J)_{,J} \\ &\text{CURL } \boldsymbol{v} = \nabla \times \boldsymbol{v} = (v^I)_{,J} e^J_{IK} \boldsymbol{e}^K \end{aligned} \tag{A.9}$$

where $(\ )_{,I}$ denotes the covariant derivative with respect to x^I, and e^I_{JK} is the alternating tensor, defined by

$$e^I_{JK} = (\boldsymbol{e}^I \times \boldsymbol{e}_J) \cdot \boldsymbol{e}_K . \tag{A.10}$$

A convenient summary of formulas of vector analysis is given by Spiegel [68].

Appendix B. Shape functions for velocity, stress rate and spin

Shape functions for plane strain

$$x^1 = x , \quad x^3 = z .$$

Velocity shape functions

$$\boldsymbol{N}_i = N_{1,i} \boldsymbol{e}_1 + N_{3,i} \boldsymbol{e}_3 .$$

Four noded element

$$N_{1,i} = \begin{cases} \frac{1}{4}(1 + \xi\xi_i)(1 + \eta\eta_i) , & i = 1, 2, 3, 4 , \\ 0 , & i = 5, 6, 7, 8 , \end{cases}$$

$$N_{3,i} = \begin{cases} 0 , & i = 1, 2, 3, 4 , \\ \frac{1}{4}(1 + \xi\xi_{i-4})(1 + \eta\eta_{i-4}) , & i = 5, 6, 7, 8 , \end{cases}$$

$$|\xi| \leqslant 1 , \qquad |\eta| \leqslant 1 ,$$

$$\xi_1 = -1 , \quad \xi_2 = 1 , \quad \xi_3 = 1 , \quad \xi_4 = -1 ,$$

$$\eta_1 = -1 , \quad \eta_2 = -1 , \quad \eta_3 = 1 , \quad \eta_4 = 1 .$$

Shape functions for spin

$$\mathbf{QW}_i = QW_{13,i} \boldsymbol{e}_1 \boldsymbol{e}_3 + QW_{31,i} \boldsymbol{e}_3 \boldsymbol{e}_1 ,$$

$$QW_{13,1} = c_1 , \quad QW_{31,2} = x c_2 , \quad QW_{13,3} = z c_3 ,$$

$$QW_{31,1} = -c_1 , \quad QW_{31,2} = -x c_2 , \quad QW_{31,3} = -z c_3 .$$

The constants were used to improve the condition of $[H]$.

Shape functions for stress rate

$$\mathbf{QT}_i = QT_{11,i}\boldsymbol{e}_1\boldsymbol{e}_1 + 0 + QT_{13,i}\boldsymbol{e}_1\boldsymbol{e}_3 + 0 + QT_{22,i}\boldsymbol{e}_2\boldsymbol{e}_2 + QT_{31,i}\boldsymbol{e}_3\boldsymbol{e}_1 + 0 + QT_{33,i}\boldsymbol{e}_3\boldsymbol{e}_3 ,$$

$$QT_{11,1} = 1 , \quad QT_{31,2} = -1 , \quad QT_{22,3} = 1 ,$$

$$QT_{13,4} = -1 , \quad QT_{33,5} = 1 , \quad QT_{11,6} = x ,$$

$$QT_{31,6} = -z , \quad QT_{31,7} = -x , \quad QT_{22,8} = x ,$$

$$QT_{13,9} = -x , \quad QT_{33,9} = z , \quad QT_{33,10} = x ,$$

$$QT_{11,11} = z , \quad QT_{13,12} = -z , \quad QT_{22,13} = z .$$

Acknowledgment

This work was supported by the NASA-Lewis Research Center under grant NAG3-38 to Georgia Tech. The authors gratefully acknowledge this support. Appreciation is expressed to Ms. Brenda Bolinger for her help in preparing this manuscript.

References

[1] A.E.H. Love, A Treatise on the Mathematical Theory of Elasticity (Dover, New York, 4th ed., 1944).
[2] E. Reissner, The effect of transverse shear deformation on the bending of elastic plates, J. Appl. Mech. 12(2) (1945) 69–77.
[3] T.H.H. Pian, Derivation of element stiffness matrices by assumed stress distributions, AIAA J. 2(7) (1964) 1333–1336.
[4] L.R. Herrmann, Elasticity equation for incompressible materials by a variational theorem, AIAA J. 3(10) (1965) 1896–1900.
[5] B.F. de Veubeke, A new variational principle for finite elastic deformations, Internat. J. Engrg. Sci. 10 (1972) 745–763.
[6] B.F. de Veubeke and A. Millard, Discretization of stress field in the finite element method, J. Franklin Inst. 302(5, 6) (1976) 389–412.
[7] G. Sander and E. Carnoy, Equilibrium and mixed formulations in stability analysis, in: Proceedings of the International Conference on Finite Element in Nonlinear Solid and Structural Mechanics, Geilo, Norway (1977) 87–105.
[8] W.T. Koiter, Complementary energy, neutral equilibrium, and buckling, Proc. Kon. Ned. Akad. Wetensch., Ser. B (1977) 183–200.
[9] W. Wunderlich and H. Obrecht, Large spatial deformations of rods using generalized variational principles, in: W. Wunderlich, E. Stein and K.J. Bathe, eds., Nonlinear Finite Element Analysis in Structural Mechanics (Springer, Berlin, 1981) 185–216.
[10] H. Murakawa, Incremental hybrid finite element methods for finite deformation problems (with special emphasis on the complementary energy principle). Ph.D. Dissertation, Georgia Institute of Technology, 1978.

[11] H. Murakawa and S.N. Atluri, Finite elasticity solutions using hybrid finite elements based on a complementary energy principle, J. Appl. Mech. 45 (1978) 539–548.
[12] H. Murakawa and S.N. Atluri, Finite elasticity solutions using hybrid finite elements based on a complementary energy principle—II: Incompressible materials, J. Appl. Mech. 46 (1979) 71–78.
[13] H. Murakawa, K.W. Reed, S.N. Atluri and R. Rubinstein, Stability analysis of structures via a new complementary energy principle, in: A.K. Noor and H.G. McCome, eds. Computational Methods in Nonlinear Structural and Solid Mechanics (Pergamon, London, 1981) 11–19.
[14] S.N. Atluri and H. Murakawa, New general and complementary energy theorems, finite strain, rate sensitive inelasticity and finite elements: Some computational studies, in: W. Wunderlich, E. Stein and K.-J. Bathe, eds., Nonlinear Finite Element Analysis in Structural Mechanics (Springer, Berlin, 1981) 28–48.
[15] S.N. Atluri, On some new general and complementary energy theorems for the rate problems of finite strain, classical elasto-plasticity, J. Structural Mech. 8(1) (1980) 61–92.
[16] M. Levinson, The complementary energy theorem in finite elasticity, J. Appl. Mech. 87 (1965) 826–828.
[17] L.M. Zubov, The stationary principle of complementary work in nonlinear theory of elasticity, J. Appl. Math. Mech. (transl. Prikl. Mat. Meh.) 34 (1970) 228–232.
[18] E.H. Dill, The complementary energy principle in nonlinear elasticity, Lett. Appl. Engrg. Sci. 5 (1977) 95–106.
[19] J.H. Argyris, L.E. Vaz and K.J. Willam, Improved solution methods for inelastic rate problems. Comput. Meth. Appl. Mech. Engrg. 16 (1978) 231–277.
[20] T.R.J. Hughes and R.L. Taylor, Unconditionally stable algorithms for quasi-static elasto-visco-plastic finite element analysis, Comput. Structures 8 (1978) 169–173.
[21] C. Truesdell, The mechanical foundations of elasticity and fluid dynamics, in: C. Truesdell, ed., Continuum Mechanics (Gordon and Breach, New York, 1966).
[22] C. Truesdell and W. Noll, the Nonlinear Field Theories of Mechanics, Handbuch der Physik, III/3 (Springer, Berlin, 1965).
[23] R. Hill, Aspects of invariance in solid mechanics, Adv. Appl. Mech. 18 (1978) 1–75.
[24] Y.C. Fung, Foundations of Solid Mechanics (Prentice-Hall, Englewood Cliffs, NJ, 1965).
[25] W. Prager, Introduction to the Mechanics of Continua (Ginn, New York, 1961).
[26] K. Washizu, Variational Methods in Elasticity and Plasticity (Pergamon, London, 2nd ed., 1975).
[27] R. Bellman, Stability Theory of Differential Equations (McGraw-Hill, New York, 1953).
[28] K.W. Reed and S.N. Atluri, On the generalization of certain rate-type constitutive equations for very large strains, in: Proceedings of the International Conference on Constitutive Laws for Engineering Materials. University of Arizona, Tucson, January 10–14, 1983.
[29] R. Hill, A general theory of uniqueness and stability in elastic-plastic solids, J. Mech. Phys. Solids 6 (1958) 236–249.
[30] S.W. Key, J.H. Biffle and D. Krieg, A study of the computational and theoretical differences of two finite strain elastic-plastic constitutive models, in: K.J. Bathe and J.T. Oden, eds., Formulations and Computational Algorithms in Finite Element Analysis (MIT Press, Cambridge, MA, 1977).
[31] Z.P. Bazant, A correlation study of formulations of incremental deformation and stability of continuous bodies, J. Appl. Mech. 38 (1971) 919–928; discussion; 39 (1972) 632–634.
[32] M.A. Biot, Mechanics of Incremental Deformations (Wiley, New York, 1965).
[33] D. Durban and M. Baruch, Natural stress rate, Quart. Appl. Math. 35 (1977) 55–61.
[34] R. Hill and J.W. Hutchinson, Bifurcation phenomena in the plane tension test, J. Mech. Phys. Solids 23 (1975) 239–264.
[35] R.V. Churchill, Operational Mathematics (McGraw-Hill, New York, 3rd ed. 1972).
[36] K.W. Reed, Analysis of large quasistatic deformations of inelastic solids by a new stress based finite element method, Ph.D. Dissertation, Georgia Institute of Technology, Atlanta, GA, 1982.
[37] I. Cormeau, Numerical stability in quasistatic elasto-visco-plasticity, Internat. J. Numer. Meths. Engrg. 9 (1975) 109–127.
[38] I. Ergatoudis, B.M. Irons and O.C. Zienkiewicz, Curved, isoparametric, quadrilateral elements for finite element analysis, Internat. J. Solids Structures 4 (1968) 31–42.
[39] K.-J. Bathe, Finite Element Procedures in Engineering Analysis (Prentice-Hall, Englewood Cliffs, NJ. 1982).
[40] P. Tong and T.H.H. Pian, A variational principle and the convergence of a finite element method based on assumed stress distribution, Internat. J. Solids Structures 5 (1969) 463–472.

[41] P. Tong and J.N. Rossettos, Finite Element Method; Basic Technique and Implementation (MIT Press, Cambridge, MA, 1977).
[42] C.W. Gear, Numerical Initial Value Problems in Ordinary Differential Equations (Prentice-Hall, Englewood Cliffs, NJ, 1971).
[43] S.D. Conte and C. de Boor, Elementary Numerical Analysis (McGraw-Hill, New York, 2nd ed., 1972).
[44] O.C. Zienkiewicz and I.C. Cormeau, Visco-plasticity and creep in elastic solids—a unified numerical solution approach, Internat. J. Numer. Meths. Engrg. 8 (1974) 821–845.
[45] C. Truesdell and R.A. Toupin, Classical field theories, in: S. Flugge, ed., Encyclopedia of Physics (Springer, Berlin, 1980) 226–790.
[46] J.H. Argyris, J.St. Doltsinis and K.J. Willam, New developments in the inelastic analysis of quasistatic and dynamic problems, Internat. J. Numer. Meths. Engrg. 14 (1979) 1813–1850.
[47] M. Reiner, The Deborah number, Phys. Today 17 (1964) 62.
[48] R.R. Huilgol, On the concept of the Deborah number, Trans. Soc. Rheology 19 (1975) 297–306.
[49] K.J. Willam, Numerical solution of inelastic rate processes, Comput. & Structures 8 (1978) 511–531.
[50] M.B. Kanchi, O.C. Zienkiewicz and D.R.J. Owen, The visco-plastic approach to problems of plasticity and creep involving geometric nonlinear effects, Internat. J. Numer. Meths. Engrg. 12 (1978) 169–181.
[51] T.J.R. Hughes and J. Winget, Finite rotation effects in numerical integration of rate constitutive equations arising in large-deformation analysis, Internat. J. Numer. Meths. Engrg. 15 (1980) 1862–1867.
[52] S.W. Key, C.M. Stone and R.D. Krieg, Dynamics relaxation applied to the quasi-static large deformation, inelastic response of axisymmetric solids, in: W. Wunderlich, E. Stein and K.-J. Bathe, eds., Nonlinear Finite Element Analysis in Structural Mechanics (Springer, Berlin, 1981) 585–620.
[53] R. Rubinstein and S.N. Atluri, Objectivity of incremental constitutive relations over finite time steps in computational finite deformation analysis, Comput. Meths. Appl. Mech. Engrg. 36 (1983) 277–290.
[54] H. Schwerdtfeger, Introduction to Linear Algebra and the Theory of Matrices (Noordhoff, Leyden, 2nd ed., 1961).
[55] T.J.R. Hughes and W.K. Liu, Nonlinear finite element analysis of shells: Part I. Three-dimensional shells, Comput. Meths. Appl. Mech. Engrg. 26 (1981) 331–362.
[56] G. Zhong-Heng, Time derivatives of tensor fields in non-linear continuum mechanics, Arch. Mech. Stos. 15 (1963) 131–163 (English transl.).
[57] J.D. Goddard and C. Miller, An inverse for the Jaumann derivative and some applications to the rheology of viscoelastic fluids, Rheologica Acta 5 (1966) 177–184.
[58] L.M. Meirovitch, Methods of Analytical Dynamics (McGraw-Hill, New York, 1970).
[59] F.R. Gantmacher, Applications of the Theory of Matrices (Interscience, New York, 1959) (transl. of J.L. Brenner).
[60] C.J.S. Petrie, Measures of deformation and convected derivatives, J. Non-Newtonian Fluid Mech. 5 (1979) 147–176.
[61] P.M. Pinsky, M. Ortiz and K.S. Pister, Rate constitutive equations in finite deformation analysis: theoretical aspects and numerical integration, Comput. Meths. Appl. Mech. Engrg. to appear.
[62] R.B. Bird, O. Hassager and S.I. Abdel-Khalik, Co-rotational models and the Goddard expansion, AIChE J. 20 (1974) 1041–1066.
[63] M. Abramowitz and I.A. Stegun, eds., Handbook of Mathematical Functions (Dover, New York, 9th ed., 1970).
[64] R.B. Bird, R.C. Armstrong and O. Hassager, Dynamics of Polymeric Liquids, Vol. 1 (Wiley, New York, 1977).
[65] H.M. Laun, Description of the non-linear shear behavior of a low density polyethylene melt by means of an experimentally determined strain dependent memory function, Rheologica Acta 17 (1978) 1–15.
[66] J.G. Oldroyd, On the formulation of rheological equations of state, Proc. Roy. Soc. London A-200 (1950) 523–541.
[67] C.J.S. Petrie, Elongational Flows (Pitman, London, 1979).
[68] M.R. Spiegel, Vector Analysis (McGraw-Hill, New York, 1959).
[69] J.H. Argyris and J.St. Doltsinis, On the integration of inelastic stress-strain relations. Part 1 and Part 2, Res. Mech. Lett. 1 (1981) 343–355.
[70] J.H. Argyris, An excursion into large rotations, Comput. Meths. Appl. Mech. Engrg. 32 (1982) 85–155.